

Volker Coors · Dirk Pietruschka ·  
Berndt Zeitler *Editors*

---

# iCity. Transformative Research for the Livable, Intelligent, and Sustainable City

Research Findings of University of  
Applied Sciences Stuttgart

OPEN ACCESS

 Springer

---

iCity. Transformative Research for the Livable,  
Intelligent, and Sustainable City

---

Volker Coors • Dirk Pietruschka • Berndt Zeitler  
Editors

# iCity. Transformative Research for the Livable, Intelligent, and Sustainable City

Research Findings of University of Applied  
Sciences Stuttgart

 Springer

### Editors

Volker Coors  
Institute for Applied Research  
University of Applied Sciences Stuttgart  
Stuttgart, Baden-Württemberg  
Germany

Dirk Pietruschka  
Institute for Applied Research  
University of Applied Sciences Stuttgart  
Stuttgart, Baden-Württemberg  
Germany

Berndt Zeitler  
Institute for Applied Research  
University of Applied Sciences Stuttgart  
Stuttgart, Baden-Württemberg  
Germany



ISBN 978-3-030-92095-1      ISBN 978-3-030-92096-8 (eBook)  
<https://doi.org/10.1007/978-3-030-92096-8>

Hochschule für Technik Stuttgart

© The Editor(s) (if applicable) and The Author(s) 2022. This book is an open access publication.

**Open Access** This book is licensed under the terms of the Creative Commons Attribution 4.0 International License (<http://creativecommons.org/licenses/by/4.0/>), which permits use, sharing, adaptation, distribution and reproduction in any medium or format, as long as you give appropriate credit to the original author(s) and the source, provide a link to the Creative Commons license and indicate if changes were made.

The images or other third party material in this book are included in the book's Creative Commons license, unless indicated otherwise in a credit line to the material. If material is not included in the book's Creative Commons license and your intended use is not permitted by statutory regulation or exceeds the permitted use, you will need to obtain permission directly from the copyright holder.

The use of general descriptive names, registered names, trademarks, service marks, etc. in this publication does not imply, even in the absence of a specific statement, that such names are exempt from the relevant protective laws and regulations and therefore free for general use.

The publisher, the authors and the editors are safe to assume that the advice and information in this book are believed to be true and accurate at the date of publication. Neither the publisher nor the authors or the editors give a warranty, expressed or implied, with respect to the material contained herein or for any errors or omissions that may have been made. The publisher remains neutral with regard to jurisdictional claims in published maps and institutional affiliations.

This Springer imprint is published by the registered company Springer Nature Switzerland AG  
The registered company address is: Gewerbestrasse 11, 6330 Cham, Switzerland

*This book is dedicated to all those young-spirited people who care for our cities and are setting out to make them better places.*

---

## Foreword

The more confidence we have in research at universities of applied sciences, the more it grows in its tasks. It is gratifying to see how a concentrated passion for interdisciplinary and sustainable urban and climate research has developed at the Stuttgart University of Applied Sciences in recent years: starting from the two main research areas “energy-efficient buildings and sustainable urban development” and “technologies for spatial data and simulation” to the BMBF funding “FH-Impuls,” which we are grateful to receive.

I wish the research network iCity continued good cooperation with a wealth of research results, partnerships, and follow-up projects that contribute to achieving the global climate goals. May the manifold present research contributions inspire young students and encourage them to participate in our common goals.

President, University of Applied Sciences Stuttgart  
Stuttgart, Germany

Katja Rade

---

## Foreword

### ***They are the cities***

*The city is the first.*

*The city commences.*

*The city begins.*

*The city is the stone.*

*Stone thrown into the lake.*

*Now drawing circles.*

*Over the calm, vast water expanse.*

*Inertia loosens up everywhere.*

*Bringing excitement – freshness.*

*The city begins.*

*The city is the mouth.*

*The city is fist and*

*banner of red color.*

*From here,*

*from the mouth goes  
excitement into the country.*

*The fist and the loosening up.*

*Banner, red, freshness.*

*To everywhere.*

*In many waves.*

*The city is the stone.*

*(Transl. Nina Ehresmann)*

*Es sind die Städte<sup>1</sup>**Die Stadt ist die Erste.**Die Stadt fängt an.**Die Stadt beginnt.**Die Stadt ist der Stein.**In den See geworfener Stein.**Nun Kreise ziehend.**Über die ruhige, weite Fläche Wasser.**Überall Trägheit lockernd.**Erregung bringend – Frische.**Die Stadt beginnt.**Die Stadt ist der Mund.**Die Stadt ist Faust und**Banner roter Farbe.**Von hier geht,**vom Mund geht**die Erregung ins Land.**Die Faust und das Auflockern.**Fahne, Rot, Frische.**Nach Überall.**In vielen Wellen.**Die Stadt ist der Stein.*

---

<sup>1</sup>Günter Kunert, *Wegschilder und Mauerinschriften*, Aufbau-Verlag GmbH, Berlin W8 1950, p. 19.  
© 1950 Günter Kunert. Published by kind permission of Carl Hanser Verlag München.



---

## Editorial

Working in the field of urban research, you have a feel for cities. You know their pulse, and discover their impulses. You listen to what makes them tick. The University of Applied Sciences Stuttgart (HFT) is located in the heart of the city of Stuttgart. Being involved in the iCity project ([www.icity.de](http://www.icity.de)), we consider this very fortunate. Every day we approach the city center from different directions and observe commuter traffic of all kinds, the silhouette of the city's many industries, its residential buildings and neighborhoods that characterize them, as well as the beautifully landscaped squares with the greenery for which we are grateful. We feel the breath, the life returning after the Covid-19 freeze. On campus, we are filled with joy by the motivated students who flock back to the downtown campus from all regions. Students who are inspired by the city and help shaping it in continuous loops. As academic staff, we, too, are part of this community in which we work and get inspiration at the same time.

But the changing climate has noticeably altered the perception of cities. The city is not only an incubator of creativity and ideas but can also be a burden: amplify heat waves, be source of heavy rains and strong winds here and elsewhere, and cause health problems due to constant noise and air pollution. Cities as an abstract whole have their share of climate change. Yet, they certainly are affected by their own destructive forces. Even their oft-cited resilience lately appears overstretched, which is visible and tangible.

This is why the iCity project was coined ([www.icity.de](http://www.icity.de)). iCity is a transdisciplinary project as cooperation of over 50 researchers at HFT and over 45 project partnerships. It is funded by the Federal Ministry of Education and Research (BMBF) in the then newly created funding line FH-Impuls that supports research networks at universities of applied sciences. Coined in 2017, it has focused on methods, services, and products for efficient energy, building, data and mobility systems, so that cities can be run in a renewable, sustainable, and socially acceptable way. The research project involves all types of partners and relevant stakeholders to jointly contribute to the transformation of cities in order to prevent increasing climate change.

As a former technical university and original winter school for building tradesmen, the University of Applied Sciences has a constantly grown focus on teaching and research in

the urban field. With this book, we have summarized the most recent results in the realm of the iCity project regarding sustainable urban research. This publication does not include project results that have already been published elsewhere. For example, we think of the open access book *Quartiersentwicklung und Klimaschutz. Handlungsoptionen für Städte* (*Neighborhood Development and Climate Protection: Options for Cities*) ([https://www.hft-stuttgart.de/fileadmin/Dateien/Allgemeine-Hochschuldaten/Allgemeine\\_Hochschuldaten/HFT\\_Quartiersentwicklung\\_und\\_Klimaschutz.pdf](https://www.hft-stuttgart.de/fileadmin/Dateien/Allgemeine-Hochschuldaten/Allgemeine_Hochschuldaten/HFT_Quartiersentwicklung_und_Klimaschutz.pdf)), published in 2020 from the University of Applied Sciences Stuttgart and formidably edited by Karin Hopfner and Christina Simon-Philipp, a book we recommend to interested reader.

The publication at hand is a result of combined forces. Our great thanks go to all those who have made this book possible. First and foremost is the German Federal Ministry of Education and Research (BMBF), which, with its FH-Impuls funding line, has given universities of applied sciences the opportunity to conduct long-term project research together with partners from industry, local authorities and NGOs. This is how we were able to coin the iCity project. We also heartily thank Dr. Siegfried Schubert and Dr. Lukas Hoehr of VDI Technologiezentrum GmbH, who closely supervise our iCity project as project sponsors of BMBF and provide administrative expertise wherever we fail.

Our partners in the project are providers of ideas and impulses, financial backers, and particularly important critics. Our deep gratitude goes to them, and many of them have been involved in the joint project from the very beginning. Sincere and heartfelt thanks go to Werner Steiner of Robert Bosch GmbH as iCity partnership spokesman for industry. He has helped develop the project from the outset and continues to support it creatively and purposefully, providing the necessary valuable and free scope for maneuver.

Above all, our thanks go to the researchers and academic staff who are at heart of the project. They are committed to an open exchange of ideas, welcoming new ways of thinking and transdisciplinary formats, and putting them on paper. We are thankful to all those who have taken on teaching loads to make research possible for their respective colleagues. We acknowledge an extremely collegial approach that is necessary to enable externally funded research at universities of applied sciences. Also, our thanks go to the HFT rectorate, which strongly supports the research project as a whole. Some articles of this book are results of research projects that did not appear within the iCity project. Whenever this is the case, it has been pointed out in the introduction. We are grateful that they have been made available to us to be included here. Finally, we want to thank all those helping hands that made this book possible and whom we would like to mention by name: Leonie Kinner, Christine Kraus, Vanessa Laane, Dr. Christina Rehm, Vipul Vinod Sarnot, Hans-Jörg Seidler, Fenna Weber, and Ann-Kathrin Wolf.

Nina Ehresmann

---

# Introduction

The research goal of the iCity project at the Stuttgart University of Applied Sciences, and of all associated research presented in this book is to support cities in becoming more livable, intelligent, and sustainable. The research results compiled here propose tools, applications and services in the areas of mobility systems, energy, artificial intelligence, smart data, buildings, and infrastructures. The research relates to the relevant areas as well as to information and communication technologies and acceptance studies. Transdisciplinary research with mutual inspiration characterizes the research teams, which are composed of academia, industry, and municipalities. Different experiences, ways of working, and points of view lead to leaving their own single scientific research field behind and move towards life science-oriented transformative research. We believe that many of the results presented in the following chapters will also be useful in the long run when dealing with complex and multidisciplinary technology cycles in terms of sustainable use. The following contributions are organized into four parts: I Mobility, II Energy, III Simulation and Data, and IV Buildings and Infrastructure.

---

## I Mobility

Mobility and transportation play one of the most important roles in sustainable urban development: they influence the interaction of economy and society and hold great potential for CO<sub>2</sub> savings. The articles presented here deal with offers of a socially acceptable use of existing mobility systems and with digital technologies to get there. They address questions of the design of motorized individual transport (MIT): Which factors influence the choice of mobility offers? How must the offers be designed in order to be used effectively and sustainably? How can we increase sustainable means of transport since supply, participation and use can be highly emotional topics? Many of the papers demonstrate acceptance research methods and analyses of published empirical studies. This is due to the expansion of acceptance research in the university's business psychology department. It goes hand in hand with the structure of the iCity project to

include acceptance research as a cross-cutting field in all research teams and thus to conduct transformative studies with different stakeholders. Sustainable mobility here means efficient mobility offers for the socially compatible use of infrastructures, drive technologies, and services in order to efficiently reduce harmful CO<sub>2</sub> emissions.

The chapter “Mobility and Transport” is opened with “How Innovative Mobility Can Drive Sustainable Development: Conceptual Foundations and Use Cases Using the Example of the iCity Ecosystem for Innovation” by Popovic, Bäumer et al. The authors explain their holistic understanding of sustainability, and the necessity to reduce CO<sub>2</sub> emissions according to the 2030 Agenda. They examine the iCity project in terms of the SDGs and identify it as a living lab. The individual iCity projects involve key stakeholders in the research process, have an interdisciplinary layout, and work according to the six key principles underlying living labs: networking of stakeholders, co-definition of the problem, collaboration, iterative feedback loops, co-creation, and co-production. Popovic et al. describe the iCity project as transformative research with a high potential for sustainable innovation. As an example, they explore the application of key principles for living labs using the tool of the “RouteMeSafe” application for cyclists developed in the iCity project.

The following article “Interests of (In)frequent Bike Users: Analysis of Differing Target Groups’ Needs Concerning the RouteMeSafe Application” (Silberer et al.) describes the process of inventing the RouteMeSafe application. Here, an app was developed that allows bicyclists to identify safety levels of possible routes. The study was motivated by the understanding that safety information from the cycling infrastructure of metropolitan regions can generally make cycling more attractive. The RouteMeSafe app can be developed further by users. At the time of writing, a prototype allowed users to enter, view, and rate dangerous locations to provide future feedback to local governments on their routing and cause for improvement.

In “Artificial Intelligence Supporting Sustainable, Individual Mobility: Development of an Algorithm for Mobility Planning and Choice of Means of Transport,” Heckmann et al. describe the development of an application EmiLa for mobility planning. The research design is based on a route planning algorithm fed by multiple linear regression. In contrast to existing well-known routing apps, users can further develop, influence, and even personalize the app developed here far beyond the usual parameters of date, time, and means of transport: individualized adjustments can be made such as number of travellers and their possible physical limitations and pieces of luggage carried; it differentiates between ownership or rental of the means of transport, mobility subscriptions, and even weather conditions. The app “EmiLa” is indeed available on the market.

“Almost every German citizen owns a bicycle, however roughly 50% [of which] are used less than once a month or not at all”, as Armstroff and Gaspers point out in their paper “Challenges to Turn Transport Behavior into Emission Friendly Use of Means of Transport”. Since the use of emission-friendly cycling as means of transport has hardly increased, they investigate in why this is so. They compare German bicycle use figures with those of the Netherlands and conclude that over there, i.e., roads are wider and separated from car traffic, Dutch people identify with bicycles as part of country’s

branding, and bicycles must be given right of way on roads over cars. From their field tests with pedelecs in the city of Tuttlingen, they conclude that the use of pedelecs can contribute to significantly reducing the amount of passenger cars used in general.

Rawiel, too, investigated in use of pedelecs and comes up with a focus on navigation systems in “Positioning of Pedelecs for a Pedelec Sharing System with Free Floating Bikes.” Since global navigation satellite systems (GNSS) offer limited accuracy while satellite signals are shadowed or reflected, i.e., vehicles in tunnels, he found out that fusing GNSS with the method of dead reckoning (DR) proves to be promising, especially for free-floating pedelec fleets used for sharing systems. While integrating different inertial low-cost sensors to describe the movements of vehicles independently, Rawiel suggests not only a secure tracking method for the fleet but also a low-cost system to compensate for lacking GNSS data accuracy.

Why is it that so many people own a bicycle and do not use it as a means of transportation to work, even though they only have relatively short distances to cover? Weisbeck and Gaspers developed empirical qualitative online studies with students and former students of the Stuttgart University of Applied Sciences (“Behavioral Development of University Graduates in the Area of Work-Related Mobility: A Study Conducted for the University of Applied Sciences Stuttgart”). They brought up an interesting correlation between the use of bicycles as a mode of transportation during college and later in life for commuting to work. Thus, making cycling to college more attractive to students could be another lever to get more people cycling in the long run!

While the six of our mobility-related articles deal with two-wheeled mobility, the last three articles deal with four-wheeled mobility regarding sustainable freight transport (Meyer et al.), battery charging (Herrlich et al.), and use of electric trucks (Stütz et al.). After reading Meyer et al.’s “Cargo-Hitching in Long-Distance Bus Transit: An Acceptance Analysis,” the reader is left wondering why cargo hitching is only hesitantly used in Germany. The junior researchers investigated the transport of parcels by long-distance buses and propose a business model that is economical, could be in demand, and at the same time reduces emissions. They compared the use of this parcel transfer in Germany with that of other countries such as Sweden, the USA, and Canada, where the system is already widely used. We have to give it away here: Meyer et al. developed groundworks for a sustainable business model for FlixBus. Most importantly, however, after cross-checking with research on CO<sub>2</sub> emissions in parcel delivery, they conducted a quantitative online customer acceptance study based on UTAUT2, using seven existing expectation variables as factors and employing sustainable expectation as an additional variable in a way that has not been used before in this context.

In their paper “Promoting Zero-Emission Urban Logistics: Efficient Use of Electric Trucks Through Intelligent Range Estimation,” Stütz et al. describe research results of the project EN-WIN that was funded by the German Federal Ministry for the Environment, Nature Conservation and Nuclear Safety (BMU). The study addressed power range and consumption as critical success factors for use of electric trucks. They develop a model to predict both, arguing that basic information from vehicle dispatching can be used for range

prediction with higher precision than other approaches. The last three chapters of the mobility section by Weißbeck/Gaspers (6), Meyer/Lang/Dehdari (7) and Stütz/Gade/Kirsch (8) were not written in the context of the iCity project. We are glad that we are allowed to include their work here.

---

## II Energy

Preventing or at least limiting man-made climate change, which is mainly caused by the CO<sub>2</sub> emissions of the industrialized world, is one of the greatest challenges facing our society in this century. Globally, cities are growing by 1.5 million people every week<sup>2</sup> and are responsible for nearly 80% of the energy-related global CO<sub>2</sub> emissions.<sup>3</sup> This clearly highlights the significant role of cities in climate change prevention policies. Side effects of cities' high-energy demand include air pollution from hazardous gases and particulate matter, as well as noise pollution. For a livable, intelligent, and sustainable city, a significant reduction in energy demand and the transition to renewable and clean energy technologies are of great importance.

To address these challenges, energy efficiency and the integration of renewable energy systems play a major role in the iCity project. Topics covered range from the development of new simulation tools for planning the energy transition in buildings and urban mobility to technologies and systems for renewable energies and new ICT and IoT technologies. The latter are important for efficient energy data collection and predictive control of entire energy systems depending on the availability of renewable energy and the demand of the power grid. The efficient coupling of different energy sectors is the key to the flexibility required to adapt energy demand to available volatile renewable energy sources such as wind or photovoltaics.

For commercial and industrial sites, highly innovative refurbishment and energy supply concepts are still very limited and only available on a sector-specific basis. Such properties often include own heating and cooling networks to supply the connected buildings and production processes. The energy demand density of such sites is much higher than in residential districts and therefore more complex to transform to CO<sub>2</sub>-neutral energy supply. Within the iCity project, we are placing a special focus on this sector with the analysis of a large research and development center of Robert Bosch GmbH in the community of Schwieberdingen near Stuttgart. This site has a total energy demand of nearly 120 GWh per year. As an example of the work done, the paper by Andres Biesinger et al. analyzes possibilities of using a large-scale absorption chiller to extend the operation time of an

---

<sup>2</sup>PwC analysis of United Nations, Department of Economic and Social Affairs, Population Division (2014).

<sup>3</sup>Seizing the global opportunity partnerships for better growth and a better climate, The 2015 New Climate Economy Report.

existing CHP unit. This unit supplies heat to the heating network and electricity to the local power grid. The absorption chiller uses the heat from the CHP unit to generate cooling energy in summertime. A new simulation tool for analyzing and improving the overall efficiency of heating and cooling networks is also presented.

Another huge challenge in the energy transition is the question of how electricity from PV systems can be seasonally stored to be available in wintertime. Batteries are still far too expensive, but hydrogen technologies could be a solution to transfer this “excess” electricity from summertime to the winter months. However, apart from economic problems, which can be solved in the future mainly by scaling effects, operational reliability problems must also be solved. iCity addresses these challenges by developing special simulation tools for the system planning and by establishing a hydrogen laboratory for system integration testing and control development. For example, the presented paper by Daniel Lust et al. addresses the possible application of a PEM electrolysis, high pressure storage, and a PEM fuel cell to generate electricity and heat for a district heating system in a rural area. It highlights the specific challenges and problems that this technology will face in such future oriented applications.

The boom in electrical cars provides challenges for the energy system that are also being addressed in the iCity project. The rapidly growing number of electric cars requires an intelligent load management at the building and neighborhood level to prevent overloads in the low-voltage power grid. To date, the main focus has been on limiting the electrical power of car charging to the maximum capacity of the building’s power grid connection. However, the lower voltage power grid is not sufficiently sized, if all buildings use their full capacity at the same time. Therefore, in the near future, an interaction between the charging infrastructure in buildings, the local transformer stations, and the higher power grid will be required. The presented paper of Ester Herrlich et al. summarizes the state of the art of e-mobility with respect to the availability of charging infrastructure and the challenges in interaction with the power grid. It highlights that apart from solvable technical challenges, the establishment of legal standards could be a far greater challenge. Their research has not been part of the iCity project. Yet we think that the article fits perfectly into the Energy section. We are thankful that we are allowed to present it here.

---

### **III Simulation and Data**

The Simulation and Data chapter focuses on the role of digital solutions in the transition toward livable, intelligent, and sustainable cities and metropolitan regions. Most solutions to reduce CO<sub>2</sub> emissions in the mobility and energy sector include sophisticated information and communication technology to optimize the use of resources. Data-driven approaches use artificial intelligence to analyze measured data, detect pattern, and predict future demand that supports decision-making. Data acquisition methods from geodesy, photogrammetry, and remote sensing play an essential role especially in urban environments. More and more cities worldwide use urban digital twins as digital

presentation of the built environment as well as a real-time monitoring platform and information system of a city. The selected papers present specific topics of this development with a technological focus, but it also explains how citizens and city administrations benefit from these solutions.

The paper “ARaaS: Context Aware Optimal Charging Distribution Using Deep Reinforcement Learning” by Sharif, Heendeniya, and Lückemeyer presents a new agent-based approach to optimize decision-making in an electro-mobility eco-system. Two use cases – optimization of charging an electric vehicle along a planned route for individuals and short-term electricity demand prediction for local grid operators – illustrate the impact of the proposed algorithm. Both use cases are highly relevant for future mobility scenarios as described in the first chapter of this book, for this reason, we have included the paper, even though the research was not conducted as part of the iCity project. We are thankful to the authors that we were allowed to include their findings.

Maintenance and renovation of existing infrastructure is crucial in urban management. Predictive maintenance can help identify infrastructure malfunctions as early as possible, reduce renovation costs and, above all, prevent the collapse of infrastructure elements—such as bridges and tunnels—and thus save lives. The paper “A Multi-camera Mobile System for Tunnel Inspection” of Alidoost, Austen, and Hahn shows the use of machine vision technologies for maintenance of tunnels. It proposes advanced methods of data acquisition and data analysis resulting in a very dense point cloud and a 3D model of the tunnel. The model can be used for damage detection using machine learning.

The next two papers deal with the urban environment, in particular air quality and fine dust. Gitahi and Hahn evaluate the stability and accuracy of fine dust (PM<sub>2.5</sub>) measurements from low-cost sensors crowdsourced from a citizen science project in Stuttgart. Harbola, Storz, and Coors propose the use of augmented reality to get a better understanding of wind flows in urban environments. A better understanding of wind flows might lead to an improvement of air quality due to natural ventilation. Another application is the identification of suitable buildings and other places to use wind as a renewable energy source and generate power using small wind turbines.

Santhanavanich, Sihombing, Kabiro, Würstle, and Sini are young researchers with backgrounds in photogrammetry, geoinformatics, and software technology. In their paper, they investigated and evaluated three approaches to managing energy-related building data when working with 3D building models such as the SimStadt simulation software developed at HFT. In the absence of a suitable open-source tool or platform to efficiently manage and distribute energy-related data, they created the use case of heat demand and photovoltaic potential analyses using the 3D building models *On-the-Fly*, *PostgreSQL Database*, and *OGC SensorThings* in the cities of Stöckach-Stuttgart, Ludwigsburg, and Grünbühl, resulting in balanced recommendations for smart cities’ applications.

The chapter concludes with a paper on “Deep Learning Methods for Extracting Object-Oriented Models of Building Interiors from Images” by Obrock and Gülch. The aim of the proposed DeepLabv3+ architecture is to extract geometric and semantic information of



building interior and to reconstruct a building information model (BIM). This “BIM as built” will be used for facility management and is a very valuable source for further building simulations. It also connects the indoor and outdoor environment, as discussed in the next chapter.

---

## IV Urban Planning and Buildings

Urban areas and buildings that are planned and designed with their citizens in mind become more livable and thereby more sustainable on whole. These urban areas and buildings thereby get utilized “properly” for much longer periods of time ensuring the targeted energy and CO<sub>2</sub> savings can be met. Incorporating intelligent planning processes and intelligent technologies can also support the sustainability goals, however only if the technologies are accepted by the users and the user’s behavior is considered in the planning process. Therefore, the citizens and the occupants of the buildings play a large role in this chapter on “Urban Planning and Buildings.”

At first glance, it might not be obvious that the outdoor environment (urban areas) and indoor environment (in buildings) have a strong link. The interface between them, which will be discussed here as well, is the façade of the building. The façade has several objectives, among others, to protect the occupants from the outdoor environment (heat/cold, moisture, noise, lighting, etc.) and to allow energy saving or even harvesting. Within the iCity project, several methods were utilized to capture the indoor and outdoor situation (citizen satisfaction and indoor environment) including questionnaires during citizen participation as well as various sensors and prediction tools. Further steps were then carried out after analyzing this data to design and optimize an urban area and building elements. Their approach to sustainability is forward-looking, and some of the results presented here for the first time are being submitted to national and international standardization bodies. All contributions presented in this chapter are results of iCity research.

The chapter “Urban Planning and Building” begins in the outdoor environment with “Cooperative Planning Strategies in Urban Development Processes: The Example Common Space ‘Österreichischer Platz’ in Stuttgart” by Lahode and Schumann and follows through the façade to the indoor environment. Their transdisciplinary study takes a closer look at an urban area with a multistory traffic structure in Stuttgart. As many stakeholders as possible (including politicians and city administration, residents and passers-by) were included in the planning process of “Österreichischer Platz.” At the end of the 2-year planning period, nearly 175 single cooperative events had been organized and carried out. In a preliminary evaluation process, key findings, such as a need for space for the common good, culture, encounter, exercise, and experiments, were established for the further development of the site.

The next article “On the Prospects of the Building Envelope in the Context of Smart Sustainable Cities: A Brief Review” by Liebhart and Cremers is, as the title states, a literature review showing the state of the art in façades and where the journey can go. The

general role of the façade in providing shelter and protection from the outer environmental impacts and the control of energy transport including solar radiation and the flow of air between the inside and outside is explained. Also, the importance of the aesthetic vision of its creators and owners is touched upon. Examples are shown of the façade being utilized to reduce heat transfer into the building by dynamic shading or to generate energy by energy harvesting methods via photovoltaic/photothermic element. Further innovative functionalities presented include air and water purification with green façades. Incorporating the described technologies can have a drastic impact on the sustainability of building façades and is promoted for future use.

A “Monitoring Tool for Improving Indoor Environment Quality and Performance Based on IoT Sensors: State of the Art and Concept” is the next article presented in this chapter by Traboulsi and Knauth. This article discussed the link between human thermal sensation and productivity at work using mechanical heating/ventilation systems. It shows that “new” technologies often do not succeed as planned due to user behavior. To identify this, the indoor and outdoor temperatures were monitored as well as the user interaction with the heat regulators. An IoT monitoring tool was developed to manage the challenges in smart buildings by extracting and processing relevant data. Based on this data, an artificial intelligence methodology was proposed for the development of a simplified regression-based model to forecast indoor temperature and predict the workers’ thermal sensation.

“Box-Type Windows as Means for Better Air Quality and Acoustic Comfort in Urban Areas” by Offtermatt, Lust, and Erhart on the other hand investigates natural ventilation instead of mechanical ventilation. But here, too, an automated operation of the window has been developed, based, among other things, on the levels of CO<sub>2</sub> and temperature in the room. Also, the issue of user behavior and noise transmission through the open window was addressed. Finally, a box-type window with optimized regulation and geometry was developed that can at the same time provide appropriate sound insulation and appropriate air exchange rate utilizing computational fluid dynamics, tracer gas and in situ sound insulation measurement, and user questionnaires.

The following article “Airborne Sound Insulation of Sustainable Building Facades” by Drechsler, Reinhold, Ruff, Schneider, and Zeitler focuses on optimizing several different façade elements (wall linings, windows, and decentralized ventilation) regarding sound insulation and predicting the overall indoor sound levels from different mobility sources such as trains, cars, and trucks. The box-type window investigated in the last article was developed further in the laboratory. Resonant and broadband absorbers were incorporated in the lining of the box-type window to achieve still higher insulation results, thereby reducing the levels in the room at certain frequencies by up to 12 dB. Also, a novel method was developed to drastically reduce the operational sound of and sound transmission through a decentralized ventilator, which in terms of sound insulation can be seen as a hole in the wall. The final investigated façade element is a masonry wall with a lining attached by multiple anchors, which often reduced the sound insulation of the wall in the low frequency range. The sound transmission of these lined walls could be reduced and predicted with a developed engineering model. The importance of the spectra of both the

outdoor sound source and of the façade insulation element is discussed, and suggestions are made as to which normative single number ratings are most appropriate for which situation.

In the last article of this chapter, “Impact Sound Insulation of Thermally Insulated Balconies” by Heidemann, Scheck, and Zeitler, a different kind of noise, namely, impact noise, is addressed. Occupants in units situated diagonally below balconies can be disturbed by impact noise such as footsteps on the balconies. To save energy, balconies are commonly thermally decoupled from the walls and floors on which they stand. This thermal decoupling also provides a reduction of the sound transmitted to the unit. This article answers the questions of how to predict impact sound in the receiving room and how to characterize the acoustic quality of these thermal decoupling elements. Finally, the development of a measurement procedure supported by finite element modeling is also presented. It will be proposed to national and international standardization committees.

Volker Coors  
Nina Ehresmann  
Dirk Pietruschka  
Berndt Zeitler

---

# Contents

## Part I Mobility

<b>1</b>	<b>How Innovative Mobility Can Drive Sustainable Development: Conceptual Foundations and Use Cases Using the Example of the iCity Ecosystem for Innovation</b> . . . . .	<b>3</b>
	Tobias Popovic, Thomas Bäumer, Ezgi Gökdemir, and Jan Silberer	
1.1	Introduction . . . . .	4
1.2	Sustainable Innovation and Mobility . . . . .	4
1.3	Sustainable Mobility and Digitalization . . . . .	7
1.4	Creating a Safer Cycling Infrastructure . . . . .	9
1.5	Conclusion . . . . .	11
	References . . . . .	11
<b>2</b>	<b>Interests of (In)frequent Bike Users: Analysis of Differing Target Groups' Needs Concerning the RouteMeSafe Application</b> . . . . .	<b>15</b>
	Jan Silberer, Greta Dangel, Thomas Bäumer, Patrick Müller, and Georgios Kotziabassis	
2.1	Introduction . . . . .	16
2.2	Study 1: UX Study with Frequent and Infrequent Cyclists . . . . .	18
2.3	Study 2: Technology Acceptance Study with Frequent Cyclists . . . . .	22
2.4	General Discussion . . . . .	24
	Bibliography . . . . .	25
<b>3</b>	<b>Artificial Intelligence Supporting Sustainable and Individual Mobility: Development of an Algorithm for Mobility Planning and Choice of Means of Transport</b> . . . . .	<b>27</b>
	Rebecca Heckmann, Sören Kock, and Lutz Gaspers	
3.1	Introduction . . . . .	28
3.2	Objective . . . . .	29
3.3	Development of the Algorithm for Personalized-Quantified Routing Including Self-Learning Units . . . . .	30
3.4	Testing of the Algorithm . . . . .	35

3.5	Conclusions . . . . .	38
	Bibliography . . . . .	40
<b>4</b>	<b>Challenges to Turn Transport Behavior into Emission-Friendly Use of Means of Transport . . . . .</b>	<b>43</b>
	Torsten Armstroff and Lutz Gaspers	
4.1	Development of Modal Split for Germany . . . . .	44
4.2	Benchmark View of Modal Split for the Netherlands . . . . .	44
4.3	Sharing as Opportunity to Extend Bicycle and Pedelec Use in Germany . . . . .	46
4.4	Necessity for Further Research . . . . .	48
	References . . . . .	48
<b>5</b>	<b>Positioning of Pedelecs for a Pedelec Sharing System with Free-Floating Bikes . . . . .</b>	<b>51</b>
	Paul Rawiel	
5.1	Introduction . . . . .	52
5.2	Materials and Methods . . . . .	53
5.3	Sensor Tests . . . . .	54
5.4	Sensor Calibration and Alignment . . . . .	55
5.5	Kalman Filter . . . . .	57
5.6	Findings and Results . . . . .	59
5.7	Necessity for Further Research . . . . .	62
	References . . . . .	63
<b>6</b>	<b>Behavioural Development of University Graduates in the Area of Work-Related Mobility: A Study Conducted for the University of Applied Sciences, Stuttgart . . . . .</b>	<b>65</b>
	Joschua Weißbeck and Lutz Gaspers	
6.1	Introduction . . . . .	66
6.2	Research Methodology . . . . .	67
6.3	Data Evaluation . . . . .	68
6.4	Conclusion . . . . .	74
	References . . . . .	75
<b>7</b>	<b>Cargo-Hitching in Long-Distance Bus Transit: An Acceptance Analysis . . . . .</b>	<b>77</b>
	Vanessa Meyer, Sarah Lang, and Payam Dehdari	
7.1	Introduction . . . . .	78
7.2	Cargo-Hitching as an Alternative Delivery Concept . . . . .	78
7.3	Adapting an Underlying Acceptance Model . . . . .	80
7.4	Methodology: Acceptance Analysis of a Cargo-Hitching Model . . . . .	81
7.5	Results . . . . .	83
7.6	Discussion and Outlook . . . . .	86
	References . . . . .	87

<b>8</b>	<b>Promoting Zero-Emission Urban Logistics: Efficient Use of Electric Trucks Through Intelligent Range Estimation . . . . .</b>	<b>91</b>
	Sebastian Stütz, Andreas Gade, and Daniela Kirsch	
8.1	Introduction . . . . .	92
8.2	The Need for Precise Energy Consumption and Range Estimation . . . . .	92
8.3	Towards an Intelligent Method for Range Prediction . . . . .	96
8.4	Results and Discussion . . . . .	98
8.5	Conclusion . . . . .	99
	References . . . . .	101
<b>Part II</b>	<b>Energy</b>	
<b>9</b>	<b>Increased Efficiency Through Intelligent Networking of Producers and Consumers in Commercial Areas Using the Example of Robert Bosch GmbH . . . . .</b>	<b>105</b>
	Andreas Biesinger, Ruben Pesch, Mariela Cotrado, and Dirk Pietruschka	
9.1	Introduction . . . . .	106
9.2	Case Study Description . . . . .	107
9.3	Study to Increase the Run Time of a CHP by an Absorption Chiller . . . . .	109
9.4	Development of a Simulation Programme for Modelling and Calculation of a Thermal Local Heat Supply . . . . .	124
	References . . . . .	142
<b>10</b>	<b>Case Study of a Hydrogen-Based District Heating in a Rural Area: Modeling and Evaluation of Prediction and Optimization Methodologies . . . . .</b>	<b>145</b>
	Daniel Lust, Marcus Brennenstuhl, Robert Otto, Tobias Erhart, Dietrich Schneider, and Dirk Pietruschka	
10.1	Introduction . . . . .	146
10.2	Related Work/State of the Art: Research . . . . .	147
10.3	Methodology . . . . .	149
10.4	Hydrogen System: Modeling, Design, and Control . . . . .	156
10.5	Simulation Results and Discussion . . . . .	161
10.6	Conclusions . . . . .	173
10.7	Outlook . . . . .	175
	References . . . . .	179

<b>11</b>	<b>Parking and Charging: New Concepts for the Use of Intelligent Charging Infrastructure in Car Parks</b> . . . . .	183
	Esther Herrlich, Elisabeth Schaich, Stephanie Wagner, and Dieter Uckelmann	
11.1	Introduction . . . . .	184
11.2	State of the Art . . . . .	186
11.3	Pilot Projects . . . . .	188
11.4	Technologies in Intelligent Car Parks . . . . .	189
11.5	Conclusion and Outlook . . . . .	192
	References . . . . .	193
<b>Part III</b>	<b>Simulation and Data</b>	
<b>12</b>	<b>ARaaS: Context-Aware Optimal Charging Distribution Using Deep Reinforcement Learning</b> . . . . .	199
	Muddsair Sharif, Charitha Buddhika Heendeniya, and Gero Lückemeyer	
12.1	Introduction . . . . .	200
12.2	Architecture . . . . .	201
12.3	User Scenario . . . . .	204
12.4	Simulation Environment . . . . .	205
12.5	Conclusion and Future Work . . . . .	207
	References . . . . .	208
<b>13</b>	<b>A Multi-camera Mobile System for Tunnel Inspection</b> . . . . .	211
	Fatemeh Alidoost, Gerrit Austen, and Michael Hahn	
13.1	Introduction . . . . .	212
13.2	Related Work . . . . .	212
13.3	Proposed Method . . . . .	213
13.4	Conclusion . . . . .	220
	References . . . . .	222
<b>14</b>	<b>Evaluation of Crowd-Sourced PM<sub>2.5</sub> Measurements from Low-Cost Sensors for Air Quality Mapping in Stuttgart City</b> . . . . .	225
	Joseph Gitahi and Michael Hahn	
14.1	Introduction . . . . .	226
14.2	Methodology . . . . .	228
14.3	Results and Discussion . . . . .	232
14.4	Conclusions . . . . .	237
	References . . . . .	239

<b>15</b>	<b>Augmented Reality for Windy Cities: 3D Visualization of Future Wind Nature Analysis in City Planning</b> . . . . .	241
	Shubhi Harbola, Martin Storz, and Volker Coors	
15.1	Introduction . . . . .	242
15.2	Methodology . . . . .	243
15.3	Dataset . . . . .	244
15.4	Results . . . . .	245
15.5	Conclusion . . . . .	249
	References . . . . .	250
<b>16</b>	<b>Storing and Visualising Dynamic Data in the Context of Energy Analysis in the Smart Cities</b> . . . . .	251
	Thunyathep Santhanavanich, Rosanny Sihombing, Pithon Macharia Kabiro, Patrick Würstle, and Sabo Kwado Sini	
16.1	Introduction . . . . .	252
16.2	Background . . . . .	253
16.3	Concept . . . . .	255
16.4	Implementation . . . . .	257
16.5	Evaluation . . . . .	261
16.6	Conclusion . . . . .	263
	References . . . . .	264
<b>17</b>	<b>Deep Learning Methods for Extracting Object-Oriented Models of Building Interiors from Images</b> . . . . .	267
	Lars Obrock and Eberhard Gülch	
17.1	Introduction . . . . .	267
17.2	Related Work . . . . .	268
17.3	Methodology . . . . .	269
17.4	Semantic Segmentation of Interiors . . . . .	271
17.5	Classified Point Cloud . . . . .	272
17.6	Reclassifying the Point Cloud . . . . .	273
17.7	Quality Analysis of the Point Clouds . . . . .	274
17.8	Automated Post-processing . . . . .	276
17.9	Conclusions . . . . .	276
	References . . . . .	278
<b>Part IV Urban Planning and Buildings</b>		
<b>18</b>	<b>Cooperative Planning Strategies in Urban Development Processes</b> . . . . .	283
	Carolin Lahode and Elisabeth Schaumann	
18.1	Introduction . . . . .	284
18.2	Participation in Urban Planning Processes . . . . .	284
18.3	Case Study ‘Österreichischer Platz’ . . . . .	286



18.4	Assessment . . . . .	290
18.5	Conclusion . . . . .	291
	References . . . . .	292
<b>19</b>	<b>On the Prospects of the Building Envelope in the Context of Smart Sustainable Cities: A Brief Review . . . . .</b>	<b>295</b>
	Heiko Liebhart and Jan Cremers	
19.1	Emergence of Smart Urban Structures over the Course of Time . . . . .	296
19.2	The Building Envelope: From Skin to Sculpture to Sensor . . . . .	298
19.3	Future Prospects of the Building Envelope: Examples from Research and Commerce . . . . .	299
19.4	Upcoming Investigation Within iCity Phase 2 . . . . .	301
19.5	Conclusion and Outlook on the Necessity for Further Research . . . . .	301
	Bibliography . . . . .	302
<b>20</b>	<b>Monitoring Tool for Improving Indoor Environment Quality and Performance Based on IoT Sensors: State of the Art and Concept . . . . .</b>	<b>307</b>
	Salam Traboulsi and Stefan Knauth	
20.1	Introduction . . . . .	308
20.2	Related Work . . . . .	309
20.3	Setup and Overview of the IoT Monitoring Tool . . . . .	310
20.4	Conclusion . . . . .	313
	References . . . . .	313
<b>21</b>	<b>Box-Type Windows as Means for Better Air Quality and Acoustic Comfort in Urban Areas . . . . .</b>	<b>315</b>
	David Offtermatt, Daniel Lust, and Tobias Erhart	
21.1	Introduction . . . . .	316
21.2	Controlled Natural Ventilation . . . . .	319
21.3	Box-Type Windows . . . . .	320
21.4	Laboratory Set-up . . . . .	321
21.5	Airflow Through Box-Type Windows . . . . .	322
21.6	Architectural Integration . . . . .	327
21.7	Acoustic Comfort . . . . .	330
21.8	Conclusions . . . . .	330
21.9	Outlook . . . . .	333
	References . . . . .	333
<b>22</b>	<b>Airborne Sound Insulation of Sustainable Building Facades . . . . .</b>	<b>335</b>
	Andreas Drechsler, Steffi Reinhold, Andreas Ruff, Martin Schneider, and Berndt Zeitler	
22.1	Introduction . . . . .	336
22.2	Noise Sources . . . . .	337

---

22.3	Sound Insulation . . . . .	341
22.4	Indoor Levels . . . . .	350
22.5	Conclusion and Outlook . . . . .	356
	References . . . . .	356
<b>23</b>	<b>Impact Sound Insulation of Thermally Insulated Balconies . . . . .</b>	<b>359</b>
	Lucas Heidemann, Jochen Scheck, and Berndt Zeitler	
23.1	Introduction . . . . .	360
23.2	Structure-Borne Sound Transmission in Buildings . . . . .	361
23.3	Laboratory Test Set-up . . . . .	362
23.4	Laboratory Test Procedure . . . . .	362
23.5	Experimental Modal Analysis . . . . .	365
23.6	Impact Sound Level Difference . . . . .	367
23.7	Modification of the TIE . . . . .	368
23.8	Finite Element Simulations . . . . .	369
23.9	Conclusion . . . . .	369
	References . . . . .	370

---

## About the Contributors

**Fatemeh Alidoost** is a Research Associate at the University of Applied Sciences (HFT) Stuttgart. She obtained her Ph.D. degree in Photogrammetry from the School of Surveying and Geospatial Engineering, University of Tehran in 2019. From April 2018 until September 2019, she was a researcher at the Technical University of Munich (TUM). Her current project is: “ABOUT: Evaluation procedure for automated BIM-capable object detection in tunnel constructions.” Contact: [fatemeh.alidoost@hft-stuttgart.de](mailto:fatemeh.alidoost@hft-stuttgart.de)

**Gerrit Austen** is a Professor for Applied Geodesy at the University of Applied Sciences (HFT) Stuttgart since 2015. His main research interests are engineering geodesy, UAV applications, and BIM. He obtained his Ph.D. (Dr.-Ing.) degree in Physical Geodesy from the University of Stuttgart in 2008. From 2007 until 2015, he worked in different positions of the surveying administrations of the Federal State of Baden-Württemberg and the city of Stuttgart. Contact: [gerrit.austen@hft-stuttgart.de](mailto:gerrit.austen@hft-stuttgart.de)

**Thomas Bäumer** is a social psychologist with a focus on consumer and decision research. He worked for almost 10 years at GIM (Gesellschaft für Innovative Marktforschung mbH) as a market researcher. Since 2013, he is a professor for psychological market research at the HFT Stuttgart. His expertise lies in the conception, execution, and analysis of surveys with a focus on consumer understanding. He received his Ph.D. (Dr. phil) at the Psychological Institute of the University of Heidelberg. Contact: [thomas.bauemer@hft-stuttgart.de](mailto:thomas.bauemer@hft-stuttgart.de)

**Andreas Biesinger** studied building physics and has worked as a research assistant at the Stuttgart University of Applied Sciences since 2004. Initially he supported hardware research projects in the field of solar cooling and solar drying of food. Since 2010, he has been working in the field of technical building monitoring and operational optimization of technical building equipment systems in non-residential buildings. From numerous

research projects, he has many years of project management experience in cooperation with partners from the industrial environment. Contact: andreas.biesinger@hft-stuttgart.de

**Marcus Brennenstuhl** is a research associate at the University of Applied Sciences Stuttgart and a doctoral candidate at the University of Stuttgart. He studied Sustainable Energy Competence and has work experience in various European and national research projects such as InSun (Industrial Process Heat by Solar Collectors), FLEXYNETS (development of a new generation of intelligent DHC networks), SIM4BLOCKS (demand response in blocks of buildings), EnVisaGe (transformation of a rural municipality into a plus energy settlement), WeBest (automated determination of building refurbishment status), 3% (increasing the refurbishment rate of the residential building stock) as well as a building physics engineer. His main research topics are renewable heat and electricity generation on building and quarter level, demand response, building simulations and optimization. Contact: marcus.brennenstuhl@hft-stuttgart.de

**Volker Coors** studied computer science at the TU Darmstadt and received his doctorate in computer graphics. Since 2002, he has been a Professor of Computer Science and Geo-Informatics at HFT Stuttgart. His research focuses on 3D geospatial data infrastructures and the visualization of spatial data. From 2006 to 2017, he was a Dean of Studies of the Information Logistics course. Since 2019, he is a scientific director of the Institute for Applied Research at HFT Stuttgart. He is a member of the CityGML Standard Working Group (SWG) and a chairman of the 3D Portrayal SWG of the Open Geospatial Consortium (OGC). He is a founding member of the joint commission “3D-Stadtmodelle” of the German Society for Cartography e.V. and the German Society for Photogrammetry, Remote Sensing and Geoinformation e.V., and German representative on the board of the Urban Data Management Society. Contact: Volker.Coors@hft-stuttgart.de

**Mariela Cotrado Sehgelmeble** studied chemical engineering at the Universidad Nacional de Ingeniería in Peru. She completed her master’s (M.Sc.) degree “WASTE” in environmental protection technology at the University of Stuttgart and the master’s degree “SENCE” in renewable energies at the Stuttgart University of Applied Sciences. Since 2012, she has been working at the Competence Center Sustainable Energy Technology zafh.net at the Stuttgart University of Applied Sciences in various national and European research projects. Her expertise lies in conducting simulation studies for the development and optimization of innovative energy systems for the industrial and building sectors. Contact: mariela.cotrado@hft-stuttgart.de

**Jan Cremers** is an architect (Dr.-Ing.) with high expertise on membrane structures. He is a professor for building technology at the University of Applied Sciences Stuttgart since 2008, and was elected dean in 2017. His research interests are innovative and sustainable building typologies, building components, materials and technology. Contact: jan.cremers@hft-stuttgart.de

**Greta Dangel** studied business psychology at the Hochschule für Technik Stuttgart and wrote her bachelor thesis about the optimization and analysis of the User Experience of the RouteMeSafe App. Currently she is studying psychology at the University Ulm with focus on human factors and HRM. Contact: 72dagr1bwp@hft-stuttgart.de

**Payam Dehdari** studied industrial management and specialized in logistics (Dr.-Ing.). For over 10 years, he was responsible for logistics topics in a company stretching across different industries, like automotive and industrial goods. Since 2018, he has been a professor for sustainable logistics and lean methods at the University for Applied Sciences in Stuttgart. His expertise is designing systems and optimizing processes in transport, warehousing, and inventory management. Contact: payam.dehdari@hft-stuttgart.de

**Andreas Drechsler** works part time as a research associate at the Institute of Applied Research at the University of Applied Sciences Stuttgart since 2003. He is a member of the acoustics group. He does research in building acoustics, room acoustic, and urban sound planning. His current projects focus on soundscape studies and citizen science. Contact: andreas.drechsler@hft-stuttgart.de

**Nina Ehresmann** is a project manager of iCity and a research manager at the University of Applied Sciences, Stuttgart since 2018. She was a managing director of Forum Stadt—Netzwerk historischer Städte e.V. and a research associate at the Allensbach Institute for Public Opinion Research. Nina received her Ph.D. (Dr. phil.) at the University of Hamburg in Cultural Studies. She studied at Leuphana University, Lüneburg (M.A.), The University of Lawrence/Kansas, New York University, and Università di Pavia/Italy. Contact: nina.ehresmann@hft-stuttgart.de

**Tobias Erhart** is a Senior Researcher and lecturer in the field of energy and building technologies and has received his Ph.D. (Dr.-Ing.) and master degrees in mechanical Engineering, Sustainable Energy engineering, and electric engineering. He is a project manager of the research project “iCity—Intelligent motor-driven windows for the natural ventilation of building.” Contact: tobias.erhart@hft-stuttgart.de

**Andreas Gade** studied logistics at the Technical University of Dortmund (M.Sc.) and is a research assistant in the Transportation Logistics Department of the Fraunhofer Institute for Material Flow and Logistics IML in Dortmund since 2017. He is an expert for urban logistics with a focus on electromobility in freight transport and last mile concepts. Contact: andreas.gade@iml.fraunhofer.de

**Lutz Gaspers** is Vice-President (Studies and Teaching) in the Department of Transportation Planning and Mobility Solutions at the University of Applied Sciences Stuttgart since 2010. He is involved in numerous research projects and is an international guest speaker. He was a visiting professor at the University of New Brunswick in Canada in 2018. Since 2009, Prof. Gaspers is a head of the Steinbeis Consulting Center “Spatial Planning and Structural Development” and advises municipalities and companies. Before being a professor, he was a planner of mobility, transportation, and urban development in different engineering offices and public authorities. He has received his Ph.D. (Dr.-Ing.) at the University of Stuttgart. Contact: lutz.gaspers@hft-stuttgart.de

**Joseph Gitahi** is a Research Assistant (M.Sc.) in the Faculty of Geomatics, Computer Science, and Mathematics at the University of Applied Sciences Stuttgart. Since 2018, he has been working on urban air quality monitoring using satellite images and low-cost sensor networks. His current research interests are remote sensing techniques for air pollution monitoring, machine learning, and big data analysis techniques in geospatial applications. Contact: joseph.gitahi@hft-stuttgart.de

**Ezgi Gökdemir** is a research associate at the Center of Sustainable Economics and Management (CSEM/ZNWM) at the University of Applied Sciences Stuttgart. Her expertise lies in the fields of Business Model Development and Innovation Management with a focus on sustainability. Contact: ezgi.goekdemir@hft-stuttgart.de

**Eberhard Gülch** is a photogrammetrist (Dr.-Ing.) with a focus on research of image understanding, industrial scene analysis, and AI. Since 2003, he is a professor of Photogrammetry and Geoinformatics at HFT Stuttgart. He was an associate editor of the ISPRS Journal of the International Society for Photogrammetry and Remote Sensing, a Secretary of the German Society for Photogrammetry, Remote Sensing, and Geoinformation (DGPF), a Commission President of EuroSDR (European Spatial Data Research), and a Working Group Chairman of ISPRS and DGPF Working groups. In 2001, he was awarded the Hansa Luftbildpreis together with Thomas Läbe and Hardo Müller. Contact: eberhard.guelch@hft-stuttgart.de

**Michael Hahn** studied Geodesy at the University of Karlsruhe (Dipl.-Ing.) and received the Ph.D. (Dr.-Ing.) degree in Visual Odometry from the University of Stuttgart, in 1994. He was a postdoctoral researcher and ARC (Australian Research Council) fellow with the School of Electrical Engineering, Queensland University of Technology from 1996 to 1997. He joined the University of Applied Sciences (HFT) in Stuttgart in 1998, where he is a professor for Photogrammetry and Geomatics. From 2001 to 2007, he was a vice president at HFT. He chaired working groups of the International Society for Photogrammetry and Remote Sensing for almost two decades. His main research interests include photogrammetry, remote sensing, computer vision, AI, and sensor integration. Contact: michael.hahn@hft-stuttgart.de

**Shubhi Harbola** is a Ph.D. student at the University of Applied Sciences Stuttgart in the field of Computer Science and Information Technology where she has worked as a research scholar. She has received doctoral scholarships under the Postgraduate Scholarships Act of the Land of Baden-Wuerttemberg (LGFG). She is an active IEEE student member. She received a master's degree (M.Tech) from the Indian Institute of Technology Kanpur (IITK) India in Geoinformatics Engineering. Her research interests include LiDAR, data algorithms, remote sensing, geo-spatial data processing, and visual analysis of environmental data. Contact: Shubhi.harbola@hft-stuttgart.de

**Rebecca Heckmann** is an industrial engineer (Dipl.-Ing.) with focus on mobility research and innovations in mobility, working at the University of Applied Sciences and in electric mobility economy in the automotive industry. She has worked internationally for various research institutions and in an engineering office for traffic planning. She has been working at the HFT Stuttgart since 2017 and is doing her doctorate at the Dresden University of Technology at the Institute of Economics and Transport. At the HFT, she is a team leader of the New Mobility Division and responsible for synergies and measures of several research projects. Her main projects are in the field of app development, prototyping, and conception of mobility strategies as well as products and services in Electric Mobility. In a partnership with Sören Kock, she is founding the EmiLa company for sustainable business traveling. Contact: Rebecca.heckmann@hft-stuttgart.de

**Charitha Buddhika Heendeniya** obtained a bachelor's degree (Hons.) in Electrical Engineering at the University of Moratuwa (Sri Lanka) and the master's degree in Renewable Energy Engineering and Management at the University of Freiburg, Germany. Since 2020, he works as a research scientist in the Institute for Applied Sustainability and the Built Environment Group at the University of Applied Sciences and Arts of Southern Switzerland (SUPSI) in Lugano (Switzerland) following his position as a research scientist at the University of Applied Sciences Stuttgart. His research interests are energy communities, smart-grids, smart-mobility, and data-driven management of energy systems. Contact: charitha.heendeniya@supsi.ch

**Lucas Heidemann** is an acoustician with focus on structure-borne sound insulation and musical acoustics. Since his master's degree at the Chalmers University of Technology in 2019, he has been working at the University of Applied Sciences Stuttgart in the research group of Prof. Dr.-Ing. Berndt Zeitler. In 2020, he also started to teach at the Oscar-Walcker School for Musical Instrument building. Contact: lucas.heidemann@hft-stuttgart.de

**Pithon Macharia Kabiro** holds a Master of Science in Photogrammetry and Geoinformatics degree from the University of Applied Sciences Stuttgart. Since 2016, he has been working at his alma mater as a research assistant. Prior to this, he worked in the field of geographic information systems, with a focus on its application in the environmental sciences. His current research interests include 3D spatial data quality and 3D visualization. Contact: pithon.kabiro@hft-stuttgart.de

**Daniela Kirsch** (Dipl.-Logist.) is leading the team "urban logistics and electromobility" in the Transportation Logistics Department at the Fraunhofer Institute for Material Flow and Logistics IML. She worked in the field of multi-modal logistics, urban logistics, and electrified freight delivery for almost 10 years. She was responsible for the research project GeNaLog (Nighttime delivery with electric trucks) and has expertise in the preparation of future studies, last mile delivery, and urban logistics. Contact: daniela.kirsch@iml.fraunhofer.de

**Stefan Knauth** is a Professor of Computer Science at the University of Applied Sciences, Stuttgart, Germany. From 2005 to 2008, he was a Senior Research Assistant and the Deputy Head of the CEESAR Centre (now iHomeLab), Lucerne University of Applied Sciences, Lucerne, Switzerland. His research was focused on ambient-assisted living and smart energy. His earlier stations include a 3GPP System Engineer with Siemens ICM/ICN, Leipzig, and a System Engineer for ISS research payloads in cooperation with ESA and Kayser-Threde (now OHB System AG), Munich, Germany. He holds a Ph.D.-(Dr.-Ing.) with research interests in indoor positioning, the Internet of Things (IoT), low resource embedded systems, building automation, and mobile applications. Contact: stefan.knauth@hft-stuttgart.de

**Sören Kock** B.Eng. is an industrial engineer and information systems specialist, working at Daimler AG in the field of logistics optimization and module planning as well as at the HFT as a research assistant in app development. Since 2013, he is working in the field of logistics at Daimler AG, currently specializing in optimization topics. In connection with HFT, he focuses on sustainability topics and balancing. Until summer 2021, he studies



business informatics in a remote course. His main topics are data management, software technology, business modeling, and IT management. Sören Kock is a head of IT and finances in the start-up EmiLa, developing software and services for business customers to establish green company mobility solutions. Contact: soeren.kock@hft-stuttgart.de

**Georgios Kotziabassis** is a software developer with a focus on the front end. He graduated with a bachelor's degree in Computer Science at the University of Applied Sciences Stuttgart. His expertise lies in the conception and development of web and mobile applications with the latest technologies. Contact: kotziabassis@gmail.com

**Carolin Lahode** is an architect and researcher in the field of urban strategies and co-design processes. She studied architecture at the Tokyo University of Arts and the ABK Stuttgart, where she graduated in 2015 (M.A.). She has gained experience as a practicing architect in several offices and has worked as part of the M4\_LAB project at HFT Stuttgart since 2018. Her research focuses on prerequisites for cooperative development and use of public spaces. She is a member of the Stuttgart-based initiative Stadtlücken e.V. Contact: carolin.lahode@hft-stuttgart.de

**Sarah Lang** is a psychologist (M.Sc.) in the field of social psychology and work- and organizational psychology. After she finished her bachelor's degree in business psychology at the University of Applied Sciences Stuttgart, she graduated in psychology at Universität Ulm in 2018. In the year since, she has worked in the project M4\_LAB at HFT Stuttgart as a researcher and is fulfilling her Ph.D. at Universität Kassel. Her main research field concerns how people react to psychological threats—especially to uncertainty—in organizational and social contexts. Contact: sarah.lang@hft-stuttgart.de

**Heiko Liebhart** is a physicist and research associate at the Hochschule für Technik Stuttgart. Since 2017, he has been working in the field of numerical dynamic building simulation and building energy demand optimization. Since August 2017, he supports the research project "FLEX-G" dealing with dynamic shading by electrochromic elements in the context of membrane structures. Contact: heiko.liebhart@hft-stuttgart.de

**Gero Lückemeyer** is a business process management expert with a focus on service, IT, and development processes. He founded and managed a small business process consulting company for about 13 years and worked for almost 5 years at CapGemini sd&m as a consultant, chief architect, and project manager. Since 2010, he is a professor of business information systems with special focus on business process management at the HFT

Stuttgart. He is involved in several research projects at the Institute of Applied Science Stuttgart. He received his Ph.D. (Dr. rer. nat.) at Cologne University. Contact: [gero.lueckemeyer@hft-stuttgart.de](mailto:gero.lueckemeyer@hft-stuttgart.de)

**Daniel Lust** is a research associate at the University of Applied Sciences Stuttgart and a doctoral candidate at the University of Stuttgart. He studied aerospace engineering at the University of Stuttgart. He is working in the field of energy systems with a focus on hydrogen production and utilization. From April 2017 to October 2020, he supported the research project “iCity—Intelligent motor-driven windows for the natural ventilation of building.” Contact: [daniel.lust@hft-stuttgart.de](mailto:daniel.lust@hft-stuttgart.de)

**Vanessa Meyer** is a student of business administration at the University of Applied Sciences in Stuttgart. She focused her studies on logistics. After her bachelor’s degree, she will pursue a master’s degree in logistics in combination with environmental-oriented fields. Contact: [meyer.vanessa1994@web.de](mailto:meyer.vanessa1994@web.de)

**Patrick Müller** has been a professor of Business Psychology—HRM at the Stuttgart University of Applied Sciences since 2012. He studied psychology and business administration in Mannheim and Waterloo, Canada. He then completed his doctorate at the University of Mannheim (Dr. phil.) on the subject of the formation of fairness judgments and their impact on economic decisions. After completing his doctorate, he researched and taught as an assistant professor at the University of Utrecht in the Netherlands. He then worked in an international HRM consultancy and as a manager in the recruiting department of a large service company. His interests lie in HRM, data analytics, and technology acceptance. Contact: [patrick.mueller@hft-stuttgart.de](mailto:patrick.mueller@hft-stuttgart.de)

**Lars Sören Obrock** is a researcher (M.Eng.) at the HFT Stuttgart. Since 2017, he has been working in the field of photogrammetry, image analysis, and BIM. Focusing on artificial intelligence, he has a lot of experience in the field of image analysis. Since 2019, he also joined the “SensAR” project at HFT Stuttgart and provides deep learning methods for online and offline processing as well as location information for augmented reality applications. Contact: [lars.obrock@hft-stuttgart.de](mailto:lars.obrock@hft-stuttgart.de)

**David Offtermatt** is a research associate at the University of Applied Sciences Stuttgart. He studied climate engineering there and subsequently earned a master’s degree in energy and building systems at the University of Applied Sciences in Biberach. Since 2017, he is working in the field of sustainable building development and urban density. From April

2017 until October 2020, he supported the research project “iCity—Intelligent motor-driven windows for the natural ventilation of building.” Contact: david.offermatt@hft-stuttgart.de

**Robert Otto** is a researcher at the Stuttgart University of Applied Sciences. He studied Sustainable Energy Competence (SENCE) there and is now working in the field of energy optimization of building quarters. He is also engaged in data processing and the application of Machine Learning for the energy optimization of buildings and residential quarters. Contact: robert.otto@hft-stuttgart.de

**Ruben Pesch** has a diploma in building physics and is a Master of Science in SENCE (Sustainable Energy Competence). Since 2007, he has been working as a research assistant at the Stuttgart University of Applied Sciences. His main topics include the simulation and monitoring of geothermal heat exchangers and local heating networks. The programming environments that he has used in the course of his work at the HFT range from COMSOL-Multiphysics to Eclipse (FORTRAN, C++) to graphic programming languages, especially INSEL (Integrated Simulation Environment Language). Contact: ruben.pesch@hft-stuttgart.de

**Dirk Pietruschka** has a diploma in building physics and a Master of Science degree in Sustainable Energy Competence. He holds a Ph.D. (Dr.-Ing.) in building physics in the field of control optimization of renewable driven HVAC systems. Since 2004, he has been working as a researcher at the Stuttgart University of Applied Sciences. Here he is the scientific director of the research center Sustainable Energy Technologies (zafh.net). His main research expertise is in the field of innovative energy systems for buildings and city quarters. Contact: dirk.pietruschka@hft-stuttgart.de

**Tobias Popovic** is a professor of Corporate and Sustainable Finance, Financial Markets & Services, CSR in the business and economics department at HFT Stuttgart as of 2009. He received his Ph.D. in Economics in the field of Customer Capital. Since 2010, he is an ethics officer and until 2017 he also was a sustainability officer of HFT. In 2014, he was assigned a co-director of the Centre for Sustainable Economics and Management (CSEM/ZNWM). Research areas include Living Labs, Cooperatives, Sustainable Innovation and Entrepreneurship and Sustainable Finance. He is a guest lecturer at the Universidad de Oviedo, Tatung University in Taipei and Metropolia University in Helsinki on sustainable finance. He cooperates with UNEP FI. Prior to his professorship, he has worked for DZ BANK in Frankfurt and as a member of the board of Banco Cooperativo Español in Madrid. Contact: tobias.popovic@hft-stuttgart.de

**Paul Rawiel** is a surveying engineer. Before he began working for a software company where he developed business solutions based on the Oracle data base, he worked as a scientific assistant at the Geodetic Institute of the University of Karlsruhe (KIT) where he developed his Ph.D. (Dr.-Ing.) in the field of deformation analysis. Before his time at the KIT, he worked for the Max-Planck-Institute for Limnology in an ecological project in the Gran Pantanal in Brazil with remote sensing with the purpose of vegetation mapping. He has been a professor for surveying engineering at the Hochschule für Technik Stuttgart since 2005 and specializes in adjustment theories and multisensory systems. Contact: paul.rawiel@hft-stuttgart.de

**Steffi Reinhold** currently works as a research associate in the field of building acoustics at the Institute of Applied Research at the University of Applied Sciences Stuttgart. She does research in building acoustics and vibro-acoustics, specialized in the areas of airborne and structure-borne sound as well as prediction models such as FEM and SEA. As a part-time student of the University of Liverpool, supervised by Carl Hopkins, she is finishing her Ph. D. on the characterization of steady-state and time-varying structure-borne sound sources using a reception plate to predict sound pressure levels in buildings. Contact: steffi.reinhold@hft-stuttgart.de

**Andreas Ruff** is a member of the acoustics group at the University of Applied Sciences Stuttgart since 2006. The acoustics group is a part of the Institute of Applied Research (IAF). He works mainly in building acoustics, technical acoustics (service equipment of buildings) and also in room acoustics. Contact: andreas.ruff@hft-stuttgart.de

**Thunyathep Santhanavanich** studied Photogrammetry and Geoinformatics at the University of Applied Sciences Stuttgart and passed his Master of Science degree with distinction. He won in several international competitions in the topic of Smart Cities and received awards from NASA and the United Nations. Since 2018, he has been a researcher at University of Applied Sciences Stuttgart. His research focuses on 3D geodata infrastructures, the visualization of 3D spatial data, and sensor data integration with OGC SensorThings API. Contact: thunyathep.santhanavanich@hft-stuttgart.de

**Elisabeth Schaumann** is a research associate at the Center for Sustainable Urban Development at the HFT Stuttgart. She is part of the project TransZ on transformation processes in district centers. She studied cultural geography and urban planning at FAU Erlangen and HFT Stuttgart and graduated in 2017 (M.Eng.). In the context of her dissertation project, she is currently working on ways to strengthen civil society involvement in urban renewal.

She is a member of the Stuttgart- based initiative Stadtlücken e.V. Contact: elisabeth.schaumann@hft-stuttgart.de

**Jochen Scheck** is an expert in acoustics with focus on building acoustics and technical acoustics and has been working at the University of Applied Sciences Stuttgart since 2001. In 2011, he completed his Ph.D. at the University of Liverpool on measurement methods to characterize structure-borne sound sources in buildings and their application to vibrating lightweight stairs. He also works as a consultant and contributes to various standardization processes in national and international groups. Contact: jochen.scheck@hft-stuttgart.de

**Dietrich Schneider** (Dipl.-Ing.) has more than 25 years of experience as a Senior Researcher at the HFT-Stuttgart in national and international scientific project work, project management, and project coordination in the fields of renewable technology development and system integration. Contact: dietrich.schneider@hft-stuttgart.de

**Martin Schneider** is an academic researcher in the Building Physics department of the Applied University of Sciences Stuttgart (HFT) since 1996. He works in different fields of building acoustics and has managed various research projects with numerous publications. He is involved in building acoustic standardization and is a member in different national and international committees. Contact: martin.schneider@hft-stuttgart.de

**Muddsair Sharif** works as a researcher at the University of Applied Sciences Stuttgart in the M4LAB project. He has experience in optimal resource distribution projects in an IoT environment. His expertise lies in the conception, execution, and analysis with a focus on Context-Aware Optimal Resource in Mixed-Intelligence inside Internet of Things Environment. He has completed his Master's degree in Software Technology with a focus on Information Visualization from Linnaeus University, Sweden. Contact: muddsair.sharif@hft-stuttgart.de

**Rosanny Sihombing** holds a Master of Science degree in Software Technology from the University of Applied Sciences Stuttgart, at which she is a researcher since 2017. She previously worked as a Software Developer for about 5 years in various industries. Her current research focuses on 3D Web Geovisualization. Contact: rosanny.sihombing@hft-stuttgart.de

**Jan Silberer** is a business psychologist with a focus on technology acceptance and sustainability research. He received his M.Sc. works as a research associate at the University of Applied Sciences Stuttgart. His expertise lies in the conception, execution, and

analysis of surveys with a focus on sustainable technologies. Contact: jan.silberer@hft-stuttgart.de

**Sabo Kwada Sini** has a master's degree in Photogrammetry and Geoinformatics at the University of Applied Sciences Stuttgart and has been a researcher there since 2019 with a focus on the visualization of 3D spatial data. His current research interests include 3D geodata infrastructures and open standards such as the CityGML Energy ADE, and the OGC SensorThings API. Contact: sabo.sini@hft-stuttgart.de

**Martin Storz** is a research scientist at the University of Applied Sciences Stuttgart where he received his master's degree in Software Technology. His research is focused on augmented reality, specifically on finding ways to use it in a way that provides additional value over common applications. He has been working in several augmented reality projects in the research group of Professor Volker Coors at the University of Applied Sciences Stuttgart since 2014. contact: martin.Storz@hft-stuttgart.de

**Sebastian Stütz** is a professor for supply chain management at the IU International University of Applied Sciences and a researcher at the Fraunhofer Institute for Material Flow and Logistics IML. After his doctorate in production economics (Dr. rer. pol.), he worked at different positions in revenue management and industrial engineering at United Parcel Service Germany before he joined Fraunhofer as a scientist in the field of transportation logistics. He is an expert for urban logistics, electrified freight delivery, and distribution logistics, notably last mile delivery. Contact: sebastian.stuetz@iu.org or sebastian.stuetz@iml.fraunhofer.de

**Salam Traboulsi** is a research associate at the Centre for Digitization in Research, Education and Business at the University of Applied Sciences Stuttgart. Her expertise lies in distributed systems and conception of surveys. Specialties include statistical methods development and analysis with Rstudio, LINUX systems, database development, Programming languages include C/C++/JAVA/Python and Linux Shell script. She received her Ph.D. in Computer Science at the University of Toulouse, France. Contact: salam.traboulsi@hft-stuttgart.de

**Joschua Weißbeck** is a former student at the University of Applied Sciences Stuttgart. He completed his bachelor's degree in Infrastructure Management in 2019 and his master's degree in Transportation Infrastructure Management in 2020. His studies focused on topics related to sustainable mobility and traffic engineering. After completing his studies, he

---

worked for the city administration in Waiblingen as an engineer with a focus on traffic and road planning. Contact: [joschua.weissbeck@waiblingen.de](mailto:joschua.weissbeck@waiblingen.de)

**Patrick Würstle** studied Photogrammetry and Geoinformatics at the University of Applied Sciences Stuttgart. He won in several international competitions in the field of Smart Cities and received awards from NASA and the United Nations. Since 2018, he has been a researcher at the University of Applied Sciences. His research focuses on 3D geodata infrastructures and the visualization of 3D spatial data. Contact: [patrick.wuerstle@hft-stuttgart.de](mailto:patrick.wuerstle@hft-stuttgart.de)

**Berndt Zeitler** is a professor of Technical Acoustics and Building Acoustics in the Building Physics department of the Applied University of Sciences Stuttgart since 2015. Besides lecturing on acoustics at graduate and under-graduate levels, he is the deputy Academic Director of the Institute of Applied Research of the HFT, and leads the acoustics group, which has its main focus on airborne, impact, and structure-borne sound transmission in construction. These also are the fields of his vast research projects. He is a member of the senate at HFT. He received his Ph.D. (Dr.-Ing.) in acoustics at TU Berlin. He lead the Acoustic Group and pursued research at NRC Canada between 2007 and 2015. Contact: [berndt.zeitler@hft-stuttgart.de](mailto:berndt.zeitler@hft-stuttgart.de)

---

**Part I**

**Mobility**





# How Innovative Mobility Can Drive Sustainable Development: Conceptual Foundations and Use Cases Using the Example of the iCity Ecosystem for Innovation

1

Tobias Popovic, Thomas Bäumer, Ezgi Gökdemir, and Jan Silberer

## Abstract

Economy and society today face a multitude of complex challenges (“grand challenges”) like climate change, demographic change, urbanization, or digitalization, which create a constant demand for new technologies, services, business models, and consequently innovative solutions. In this light, the mobility sector has undergone a great change over the past few years, which is formed by digital technologies on a large scale. Against this background, this article will demonstrate, based on the example of the *iCity* research project, to what extent the research design of transdisciplinary living labs can serve as a basis for the development of innovative and sustainable mobility solutions. At the same time, the influence of digitalization which plays a major role in developing real implementable solutions for such challenges will be examined.

## Keywords

Sustainable mobility · Digital transformation · Ecosystems for innovation · Living labs · SDGs · Sustainable innovation and entrepreneurship · Sustainable urban development · Safety

T. Popovic · T. Bäumer · J. Silberer (✉)  
Hochschule für Technik Stuttgart, Stuttgart, Germany  
e-mail: [jan.silberer@hft-stuttgart.de](mailto:jan.silberer@hft-stuttgart.de)

E. Gökdemir  
KI Professionals GmbH, Stuttgart, Germany

## 1.1 Introduction

Digitalization has led to a transformation of the entire sectors. When its potential is realized, it offers several benefits in different industries (Reichstein et al., 2018; Härting et al., 2017). In the mobility sector, there is a high potential for using digitalization to make the sector more sustainable. For example, using digitalization for smart urban mobility strategies with on-demand electrical automotive fleets could help to significantly lower carbon emissions (Bauer et al., 2020). Innovative and sustainable solutions like the aforementioned that reduce carbon emissions by employing newly invented or further developed (digital) technologies are currently high in demand. There is a worldwide growing interest in the transport sector in lowering carbon emissions because of its development in the past years (Condurat et al., 2017). At the same time, the Covid-19 development has brought along significant challenges for public transport (Tirachini and Cats, 2020). If Covid-19 turns out to be a longer-term crisis, it is possible that innovative sustainable solutions for motorized individual traffic will be needed. Within the *iCity* project at the University of Applied Sciences, Stuttgart, solutions for a sustainable and comfortable transportation in future cities were developed in a living lab environment. One of the foundations in creating this research target was the UN Sustainable Development Goals (SDGs).

This paper aims at providing a conceptual framework for the evaluation of innovative mobility solutions in their potential to drive sustainable development in urban areas. A suitable example to demonstrate the usability of this framework is the concept for a feedback app for cycling infrastructure which resulted from the *iCity* research project and which will be discussed at the end of this paper.

---

## 1.2 Sustainable Innovation and Mobility

### 1.2.1 Need for Sustainable Mobility Against the Background of “Grand Challenges”

Climate change driven by human behavior is the greatest risk to our society and to economic development. The last two issues of the Global Risks Report which is presented annually at the World Economic Forum in Davos state that the greatest risks to the world economy are directly and indirectly related to man-made climate change (World Economic Forum, 2019, 2020).

It is becoming more and more obvious that a fundamental change in the nature of global economic activity in the sense of decoupling economic growth and CO<sub>2</sub> emissions is needed. In view of the scope and complexity of major societal challenges such as climate change, the German Council of Science and Humanities (Wissenschaftsrat) has been speaking of “grand challenges” in this context for some time (Wissenschaftsrat, 2015).

Today, more than 50% of the world's population are living in urban areas, following a continuous trend of urbanization which is expected to result in roughly 70% living in cities by 2050 (United Nations, 2018). Cities are already consuming over two-thirds of the global energy while being responsible for over 70% of global CO<sub>2</sub> emissions (C40 Cities). Furthermore, by 2030, annual passenger traffic is expected to increase by 50% in comparison to 2015 and reach 80 trillion passenger kilometers (Sustainable Mobility for All, 2017, p. 6). These numbers make clear that cities play a major role in driving climate change as well as being able to fuel sustainable development in the long term. Thus, well-managed urbanization could be a key success factor in averting climate change (United Nations, 2018).

Among many other factors, mobility behavior within cities is a major driver of carbon emissions and—if wisely handled—a vital instrument to drive sustainable urbanization. According to Germany's Federal Ministry for the Environment, Nature Conservation, Nuclear Safety and Consumer Protection (BMU), mobility is responsible for up to 19% of the average carbon footprint (BMU, 2020) and is classified as one out of six consumer sectors with the greatest potential for environmental relief (BMU, 2019). In the attempt to work toward a low-carbon urban development, in 2015, the UN has announced several goals as part of their 2030 Agenda for Sustainable Development which includes 17 Sustainable Development Goals (SDGs) (United Nations, 2015). Among which, many goals focus on sustainable mobility and transport—areas considered as fundamental in realizing the SDGs (Sustainable Mobility for All, 2017, p. 15).

The following illustration (Fig. 1.1) gives an overview of the SDGs related directly and indirectly to sustainable urbanization and especially sustainable mobility.

Reaching the SDGs relies on innovations and progress in sustainable mobility, since there are various interdependencies between the different goals. For example, reducing the greenhouse gas emissions in order to achieve SDG 13 will not be possible without working on SDG 7—ensuring access to sustainable and modern energy sources. Resilient infrastructure (SDG 9) is needed to provide access to sustainable and safe transport means for people of all ages and backgrounds (SDG 11) (Sustainable Mobility for All, 2017, p. 15). In a nutshell, sustainable development—especially in urban areas—cannot be achieved without shaping the future of mobility in a holistic way that is at the same time equitable (providing universal access), efficient, safe, and climate responsive (Sustainable Mobility for All, 2017, p. 7).

### **1.2.2 Transdisciplinary Living Labs as a Basis for Ecosystems for Sustainable Innovation**

Transdisciplinary living labs represent an interdisciplinary research design within the scientific system suitable for trying to tackle the grand challenges addressed by the UN SDGs (Popović and Bossert, 2020). Living labs are characterized by involving key stakeholders, going beyond institutional boundaries between research and practice, and

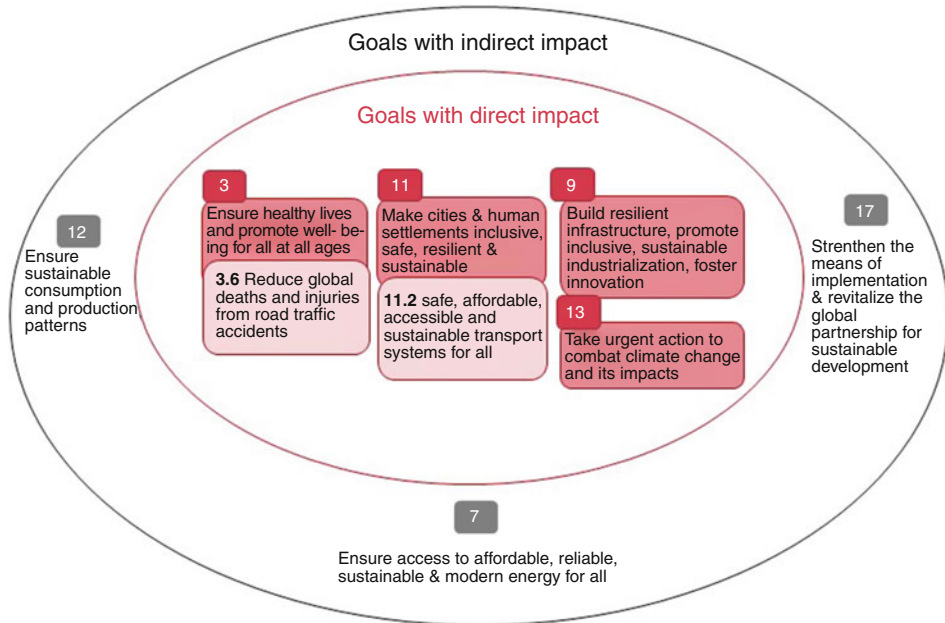


**Fig. 1.1** Sustainable mobility SDGs (United Nations, 2015)

being able to address needs or problems originating from the stakeholders' living environment (e.g., grand challenges) within collaborative and interactive research and development processes. Living labs aim to develop scientifically grounded but also feasible problem solutions in an evolutionary process (Zürcher Hochschule der Künste, 2011; Carayannis et al., 2012; Popović et al., 2020). The key principles of living labs—(1) networking of stakeholders, (2) co-definition of the problem, (3) collaboration, (4) iterative feedback loops, (5) co-creation, and (6) co-production (Popovic and Baumgärtler, 2019; Jahn et al., 2012; Capdevila, 2017; Popović et al., 2020)—suggest that they build a methodological basis for innovation ecosystems. Universities and research institutes can serve as innovation hubs within this network. Through transformative research and education, they can lay the foundation for sustainable innovation and actively contribute to the development of sustainable innovation in response to the grand challenges (Popović and Bossert, 2020, 2–3). The *iCity* research project represents a living lab format which is laying the ground for a holistic view of challenges in urban areas to enable the development of sustainable and innovative solutions for the city of the future. *iCity* addresses all areas of sustainable urban and district development, from energy management and innovative buildings to sustainable mobility, thus actively combating climate change and the climate impact of cities. From the very beginning, *iCity* strives to involve the population (as stakeholders) in all processes in a participatory manner in acceptance research and in the development of new business models (Popovic et al., 2021).

### 1.3 Sustainable Mobility and Digitalization

The future of sustainable mobility will most probably be shaped by digital solutions. Over the past years, developments such as carsharing, bike sharing, mobility as a service, or mobility flat rates, which are all enabled through digital services, made clear that digitalization is a major cornerstone on the path to sustainable mobility solutions.

According to Sustainable Mobility for All (an initiative working toward transforming the mobility sector alongside the SDGs), sustainable mobility is being defined by four global objectives (see Fig. 1.2):

Digital services have the potential to enhance the realization of all four objectives. For instance, driver assistance systems, autonomous vehicles, and other data-driven solutions can make future mobility more comfortable and more efficient. At the same time, these digital tools may also significantly improve road safety (Ministry of Transport Baden-Württemberg, 2018, p. 18). They will contribute to the aforementioned objectives as follows:

**Universal access** In an urban context, this objective focuses on the possibility to grant access to public transport for everybody and is measured by the percentage of jobs and urban service reachable within 60 min by any transport mode (Sustainable Mobility for All, 2017, p. 45). Mobility services fueled by digital technologies such as mobile apps make these goals more feasible. Thus, a shift from providing access to one specific transportation mode to being a full-service mobility provider focusing on mobility as a service (MaaS) is observable. The idea of MaaS is to integrate different transport services into a platform making each transport mode accessible on demand (MaaS Alliance).

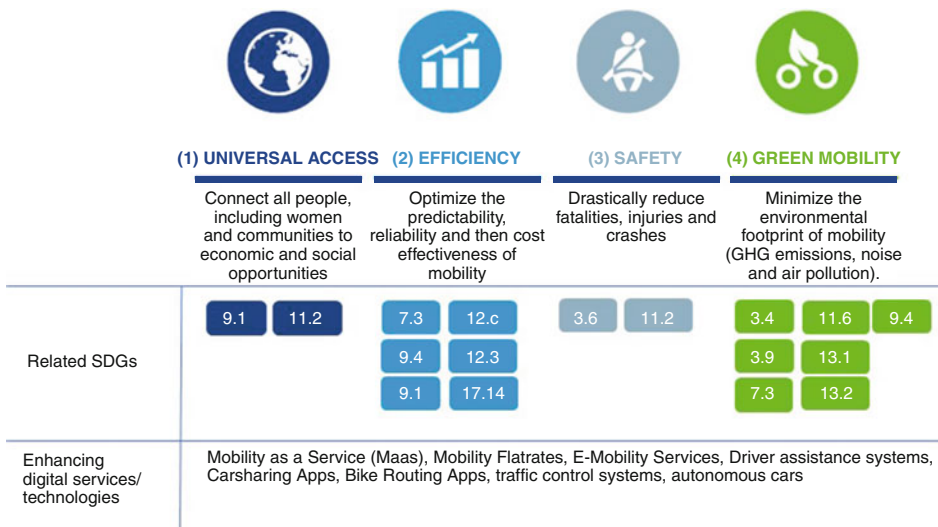


**Fig. 1.2** Global objectives of sustainable mobility (Sustainable Mobility for All, 2017, 2019, p. 16)

**Efficiency** “Efficiency aims to meet the demand for mobility at the least possible cost by 2030” (Sustainable Mobility for All, 2017, p. 58). With regard to the growing urban population (see Chap. 2), mobility systems in urban areas can have a major contribution to this goal. Many technologies focus on efficiency in terms of car transportation or city logistics. However, digital services are also driving the shift to more sustainable mobility forms. A prominent example to describe this shift is the city of Vancouver—a thriving smart and sustainable city known as the third greenest city of the world. Despite the fact that the population is constantly growing, traffic within the city is dominated by pedestrians and cyclists. To achieve this result and driving the trend even further, the city is continuously encouraging walking, cycling, and rolling by building cycling routes accessible for all ages and abilities, enhancing safety for pedestrians, and supporting the transit to these transportation modes. Consequently, Vancouver is focusing on all four objectives of sustainable mobility (City of Vancouver, 2020).

**Safety** Safety relates to the prevention of deaths, injuries, and property damage encompassing all transportation modes. Overall road traffic is responsible for 97% of all deaths related to transportation (European Transport Safety Council, 2003). However, the risk varies largely among different types of road users. Whereas a lot of attention is drawn toward safety for motorist and the entire road infrastructures being constructed with their needs in mind, pedestrians and cyclists have a 7–9 times higher fatality risk compared to motorists (Sustainable Mobility for All, 2017, p. 68). Furthermore, 40–50% of traffic fatalities occur in urban areas (Sustainable Mobility for All, 2017, p. 68), making measures to improve road safety for all traffic participants in urban areas even more important. Digitalization has a great potential to improve road safety. By nature, digital services are data-driven. Obtaining accurate data about road traffic, road conditions, user behavior, and legislation can help not only to improve user experience of all traffic participants but also lay the ground for building safer roads and even vehicles (Sustainable Mobility for All, 2017, p. 70).

**Green Mobility** Green mobility stands for a broad concept which is aiming to reduce the environmental impact of the transport sector in line with the SDGs (Sustainable Mobility for All, 2017, p. 82) and can be enhanced by digital technologies. Digital technologies can contribute to more climate responsiveness in multiple ways. The main focus lies on reducing greenhouse gas emissions (GHG), enhancing climate resilience of transport infrastructures and systems, and reducing air and noise pollution (Sustainable Mobility for All, 2017, p. 82). For example, an intelligent and digital traffic control system could lead to greater efficiency and lower emissions in road traffic (Ministry of Transport Baden-Württemberg, 2018, p. 15) and consequently improve air quality. Any transportation mode and technology related to sustainable mobility can be related to this objective.

Within the *iCity* research project, the objectives of sustainable mobility are addressed by setting the focus on transportation modes with a positive environmental balance, such as public transport, cycling, and pedestrian traffic (HFT Stuttgart, 2020) with a special focus

on the aspect of safety. As a result, the RouteMeSafe application (see Chap. 4) has been developed at the HFT Stuttgart—an innovative, data-based application which aims toward creating a feeling of safety for cyclists by directly addressing the safety obstacle and consequently encouraging the usage of sustainable transportation modes.

---

## 1.4 Creating a Safer Cycling Infrastructure

Despite the risk of road accidents, subjective safety can have an impact on peoples' decision to use the bicycle. Many people feel unsafe while cycling (Singleton, 2019), and feeling unsafe represents a barrier to cycling (Rérat, 2019). An aspect that could help to change this feeling while cycling is the infrastructure. It influences cyclists' feeling of unsafety significantly (Schmidkunz et al., 2019). To reduce this feeling of unsafety while cycling, a prototype of the feedback function of the RouteMeSafe application was developed at the University of Applied Sciences (HFT). This was done in a cooperation of the Departments of Informatics and Business Psychology. A screenshot of the application can be seen in Fig. 1.3.

The function is supposed to generate feedback by cyclists for city and municipal administrations. Obtaining and using feedback from cyclists for the design of infrastructure measures could help to create more user-centered and safer cycling infrastructure. To evaluate if there is an interest in this function by potential future employees of city administrations, an online study with 13 urban planning students was conducted at the HFT. This group of students was chosen because city administrations are possible future employers for them. Participants were contacted directly by employees of the urban planning department at the HFT. The questionnaire was designed on the basis of the Unified Theory of Acceptance and Use of Technology by Venkatesh et al. (2003). All answers were given on a scale of 1 (not at all interested) to 5 (very interested). Table 1.1 provides an overview of the answers given in the survey.

The students indicated a positive intention toward testing (mean = 4) and regularly using the application (mean = 4). They also imagine the application to be useful (mean = 4). Furthermore, they think they would get support in using the application by their possible future organization (mean = 4), as well as their colleagues (mean = 4). The participants were not sure if the application is easy to use (mean = 3). Regarding the sales model of the application, they indicated that they would rather buy a full license once (mean = 4) or a monthly subscription (mean = 4) than a yearly subscription (mean = 3). The study showed that there is generally a positive attitude toward using the application among urban planning students. However, the results have to be replicated based on a larger sample with actual city administration employees. Doing so could help to find out which of the constructs researched has the largest impact on the intention to use the application. This information is essential to determine the focus of user experience research in the further development of the application. Aspects in this matter are, for example, if the focus in the development is on an easy-to-use application or fitting the application to specific work

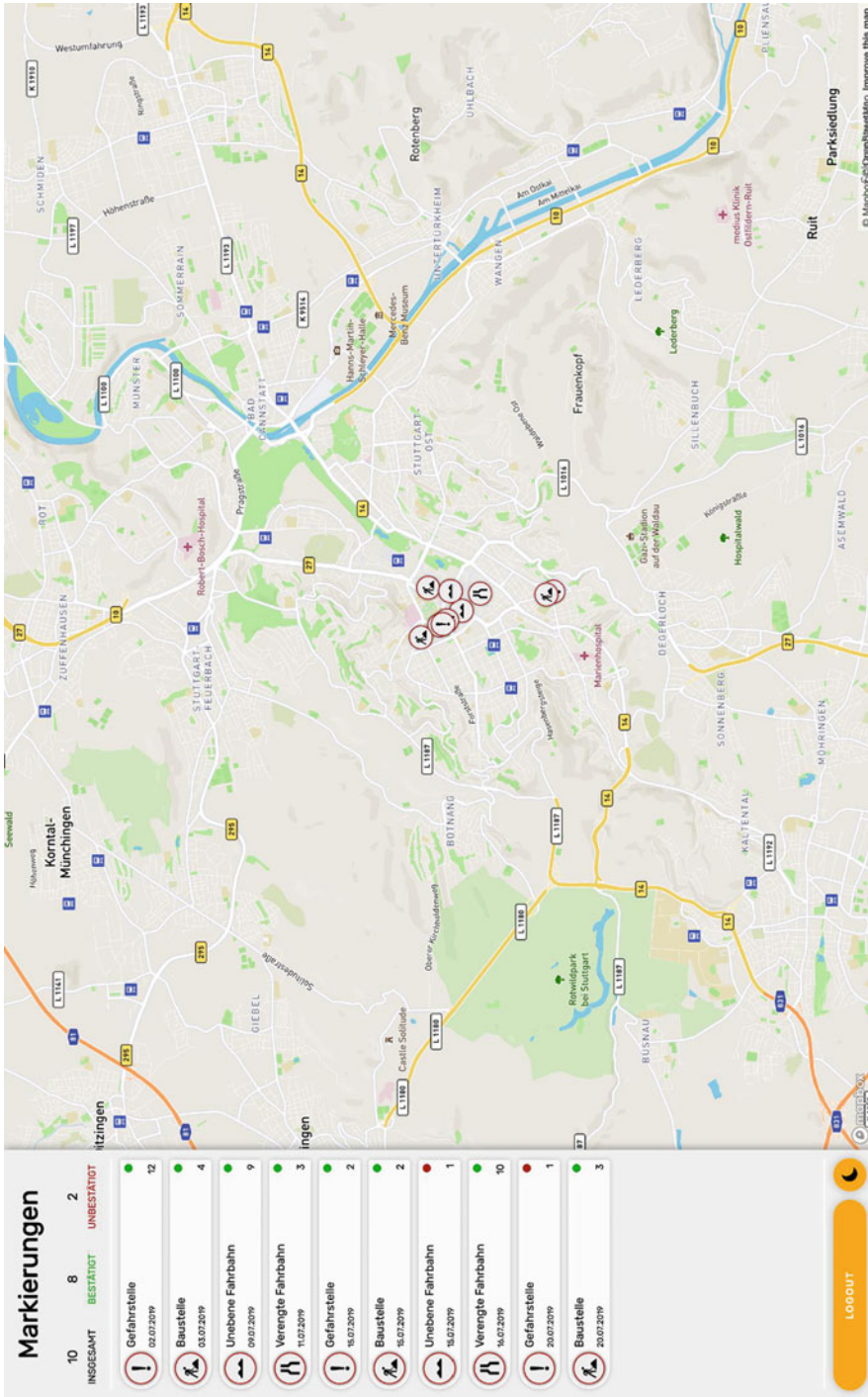


Fig. 1.3 Screenshot of the RouteMcSafe feedback tool



**Table 1.1** Results of the study with urban planners on the RouteMeSafe feedback tool

Variable	Mean	<i>N</i>
Intention test use	4	13
Intention regular use	4	13
Usefulness	4	13
Easy to use	3	13
Support by organization	4	13
Support by colleagues	4	13
Full license	4	13
Monthly subscription	4	13
Yearly subscription	3	13

contexts to make it more useful for city administration employees. If there is a comparably positive attitude toward the application in further studies, the high expectations have to be fulfilled by precise user experience testing in the development of the final application.

---

## 1.5 Conclusion

In the attempt of reducing the risks and the impact of climate change and considering the fact that cities are responsible for over 70% of global CO<sub>2</sub> emissions (C40 Cities), sustainable urban development plays a major role. Thus, smart cities and projects related to smart cities (such as the *iCity* research project) focus on creating a more sustainable living environment which benefits everyone regardless of their social background, by following a holistic approach which drives the transformation of the mobility and the energy sector to a large extent. A deep dive into urban mobility has shown how enormous sustainable urban mobility is and how important a framework addressing all challenges in this context (such as the UN SDGs) can be. Sustainable mobility is also a major part of the *iCity* research project. The project is addressing the manifold aspects of sustainable mobility of which one is safety. To address the safety aspect which is especially high for pedestrians and cyclists and holds back road users from renouncing their cars, the *iCity* research team has developed a solution which enables urban planners to create safer cycling routes for cyclists.

---

## References

- Bauer, G., Zheng, C., Greenblatt, J. B., Shaheen, S., Kammen, D. M. (2020). On-demand automotive fleetelectrification can catalyze global transportation decarbonization and smart urban mobility. *Environmental Science Technology*, 54(12), 7027-7033.
- BMU (2019): Nationales Programm für nachhaltigen Konsum. Gesellschaftlicher Wandel durch einen nachhaltigen Lebensstil. Edited by Bundesministerium für Umwelt, Naturschutz und

- nukleare Sicherheit (BMU). Available online at [https://nachhaltigerkonsum.info/sites/default/files/medien/dokumente/nachhaltiger\\_konsum\\_broschuere\\_bf.pdf](https://nachhaltigerkonsum.info/sites/default/files/medien/dokumente/nachhaltiger_konsum_broschuere_bf.pdf), checked on 8/28/2020.
- BMU (2020): Nachhaltiger Konsum. Edited by Bundesministerium für Umwelt, Naturschutz und nukleare Sicherheit (BMU). Available online at <https://www.bmu.de/themen/wirtschaft-produkte-ressourcen-tourismus/produkte-und-konsum/nachhaltiger-konsum/#c12951>, checked on 8/31/2020.
- C40 Cities: Why Cities? A Global Opportunity for Cities to Lead. Available online at [https://www.c40.org/why\\_cities](https://www.c40.org/why_cities), checked on 10/12/2020.
- Capdevila, Ignasi (2017): A typology of localized spaces of collaborative innovation. In Maarten van Ham, Darja Reuschke, Reinout Kleinhans, Colin M. Mason, Stephen Syrett (Eds.): *Entrepreneurial neighbourhoods. Towards an understanding of the economies of neighbourhoods and communities*. Cheltenham, UK, Northampton, MA: Edward Elgar Publishing (Entrepreneurship, space and place), pp. 80–97.
- Carayannis, Elias G.; Barth, Thorsten D.; Campbell, David F. J. (2012): The Quintuple Helix innovation model: global warming as a challenge and driver for innovation. In *J Innov Entrep* 1 (1), p. 2. DOI: <https://doi.org/10.1186/2192-5372-1-2>.
- City of Vancouver (2020): Walk + bike + roll: Getting around the Vancouver way. Available online at <https://vancouver.ca/streets-transportation/walk-bike-and-transit.aspx>, updated on 10/15/2020.
- Condurat, M., Nicuță, A. M., & Andrei, R. (2017). Environmental impact of road transport traffic. A case study for county of Iași road network. *Procedia Engineering*, 181, 123-130.
- European Transport Safety Council (2003): Transport Safety Performance in the EU – A Statistical Overview, checked on 10/14/2020.
- Härtig, R. C., Reichstein, C., & Jozinovic, P. (2017). The Potential Value of Digitization for Business. *INFORMATIK 2017*.
- HFT Stuttgart (2020): Fields of action. Field of action 5. Sustainable mobility. Hochschule für Technik Stuttgart (HFT). Available online at <https://www.hft-stuttgart.com/research/i-city/fields-of-action#subnavigation>, checked on 10/20/2020.
- Jahn, Thomas; Bergmann, Matthias; Keil, Florian (2012): Transdisciplinarity: Between mainstreaming and marginalization. In *Ecological Economics* 79, pp. 1–10. DOI: <https://doi.org/10.1016/j.ecolecon.2012.04.017>.
- MaaS Alliance: What is MaaS? Available online at <https://maas-alliance.eu/homepage/what-is-maas/>, checked on 9/15/2020.
- Ministry of Transport Baden-Württemberg (2018): Verwegen - Ideenschmiede für Digitale Mobilität. Impulse und Empfehlungen aus der Ideenschmiede. Stuttgart.
- Popovic, Tobias; Baumgärtler, Thomas (2019): Genossenschaftliche Innovationsökosysteme. Transformation aus der Kraft der Gemeinschaft. In *White Paper, Akademie Deutscher Genossenschaften (ADG)* (3), checked on 9/15/2020.
- Popovic, Tobias; Gökdemir, Ezgi; Schwemin, Elias: Innovative Produkte und Dienstleistungen für einen nachhaltigen Konsum an der Schnittstelle von Energie- und Mobilitätswende. (erscheint im Frühjahr 2021). In: *Nachhaltiger privater und öffentlicher Konsum 2021*, o.S. (in Druck).
- Popović, Tobias; Bossert, Michael (2020): Zwischen “Purpose” und “Impact”. Transdisziplinäre Reallabore an Hochschulen als Elemente regionaler Innovationsökosysteme. In Adrian Boos, Mare van den Eeden, Tobias Viere (Eds.): *CSR und Hochschullehre. Transdisziplinäre und innovative Konzepte und Fallbeispiele*. 1. Auflage 2020. Berlin: Springer Berlin; Springer Gabler (Management-Reihe Corporate Social Responsibility), o.S.
- Popović, Tobias; Bossert, Michael; Bronner, Uta (2020): Transdisciplinary Living Labs in a Next Generation Context—Ecosystems for Sustainable Innovation and Entrepreneurship. In Patrick Planing, Patrick Müller, Payam Dehdari, Thomas Bäumer (Eds.): *Innovations for Metropolitan Areas*. Berlin, Heidelberg: Springer Berlin Heidelberg, pp. 199–211.

- Reichstein, C., Härting, R. C., & Neumaier, P. (2018, June). Understanding the Potential Value of Digitization for Business—Quantitative Research Results of European Experts. In KES International Symposium on Agent and Multi-Agent Systems: Technologies and Applications (pp. 287-298). Springer, Cham.
- Rérat, P. (2019). Cycling to work: Meanings and experiences of a sustainable practice. *Transportation research part A: policy and practice*, 123, 91-104.
- Schmidkunz, M., Schroth, O., Zeile, P., & Kias, U. (2019, April). Road Safety from Cyclist's Perspective. In REAL CORP 2019—IS THIS THE REAL WORLD? Perfect Smart Cities vs. Real Emotional Cities. Proceedings of 24th International Conference on Urban Planning, Regional Development and Information Society (pp. 597-604). CORP—Competence Center of Urban and Regional Planning.
- Singleton, P. A. (2019). Walking (and cycling) to well-being: Modal and other determinants of subjective well-being during the commute. *Travel behaviour and society*, 16, 249-261.
- Sustainable Mobility for All (2017): Global Mobility Report. Tracking Sector Performance. Available online at <https://www.sum4all.org/publications/global-mobility-report-2017>, checked on 10/13/2020.
- Sustainable Mobility for All (2019): Global Roadmap of Action. Toward Sustainable Mobility. Washington DC. Available online at <http://pubdocs.worldbank.org/en/350451571411004650/Global-Roadmap-of-Action-Toward-Sustainable-Mobility.pdf>, checked on 10/14/2020.
- Tirachini, A., & Cats, O. (2020). COVID-19 and public transportation: Current assessment, prospects, and research needs. *Journal of Public Transportation*, 22(1), 1.
- United Nations (2015): Transforming our World: The 2030 Agenda for Sustainable Development. Edited by United Nations. Available online at <https://sustainabledevelopment.un.org/post2015/transformingourworld>, checked on 8/28/2020.
- United Nations (2018): World Urbanization Prospects: The 2018 Revision. Key facts. Available online at <https://population.un.org/wup/Publications/Files/WUP2018-KeyFacts.pdf>, checked on 9/21/2020.
- Venkatesh, V., Morris, M. G., Davis, G. B., Davis, F. D. (2003). User acceptance of information technology: Toward a unified view. *MIS quarterly*, 425-478.
- Wissenschaftsrat (2015): Zum wissenschaftspolitischen Diskurs über Große gesellschaftliche Herausforderungen. Positionspapier (Drs. 4594-15), checked on 6/11/2019.
- World Economic Forum (2019): The Global Risks Report 2019. 14th Edition, checked on 6/12/2019.
- World Economic Forum (2020): Global Risks Report 2020. Edited by World Economic Forum. Geneva. Available online at [http://www3.weforum.org/docs/WEF\\_Global\\_Risk\\_Report\\_2020.pdf](http://www3.weforum.org/docs/WEF_Global_Risk_Report_2020.pdf), checked on 10/4/2020.
- Zürcher Hochschule der Künste (2011): Transdisziplinarität. Available online at <https://blog.zhdk.ch/trans/>, checked on 6/13/2019.

**Open Access** This chapter is licensed under the terms of the Creative Commons Attribution 4.0 International License (<http://creativecommons.org/licenses/by/4.0/>), which permits use, sharing, adaptation, distribution and reproduction in any medium or format, as long as you give appropriate credit to the original author(s) and the source, provide a link to the Creative Commons license and indicate if changes were made.

The images or other third party material in this chapter are included in the chapter's Creative Commons license, unless indicated otherwise in a credit line to the material. If material is not included in the chapter's Creative Commons license and your intended use is not permitted by statutory regulation or exceeds the permitted use, you will need to obtain permission directly from the copyright holder.





# Interests of (In)frequent Bike Users: Analysis of Differing Target Groups' Needs Concerning the RouteMeSafe Application

# 2

Jan Silberer, Greta Dangel, Thomas Bäumer, Patrick Müller,  
and Georgios Kotziabassis

## Abstract

Cycling is an emission-free and healthy mode of transportation. However, the share of cycling in the modal split is still low. Perceived safety during cycling could be a reason for that. The *RouteMeSafe application* is developed at Stuttgart University of Applied Sciences with the aim of tackling this issue. A *safety routing function* is supposed to increase the short-term safety of cycling by showing safe paths for cyclists. Long-term safety is supposed to be increased with the *feedback function* enabling cyclists to share their evaluation of the cycling infrastructure with the city administration. The *safety routing function* is currently in the design phase and the *feedback function* in prototype phase. To develop the application user-friendly, target groups for both functions need to be defined and their expectations considered in the development process. Two studies with *infrequent* and *frequent cyclists* have been conducted to do so. Study 1, a user experience study based on a student sample, showed that *infrequent cyclists* could be a target group for the *safety routing function* and *frequent cyclists* could be a target group for the *feedback function*. The latter was confirmed in study 2, a technology acceptance study based on a sample with *frequent cyclists* of Stuttgart. Future studies on the application should investigate the long-term technology acceptance of the two groups.

---

J. Silberer (✉) · T. Bäumer · P. Müller  
Hochschule für Technik Stuttgart, Stuttgart, Germany  
e-mail: [jan.silberer@hft-stuttgart.de](mailto:jan.silberer@hft-stuttgart.de)

G. Dangel  
Universität Ulm, Ulm, Germany

G. Kotziabassis  
SPACEGOATS, Stuttgart, Germany

This could help to find out whether both groups can serve as target groups on the long run.

---

**Keywords**

Target groups · Transportation · Cycling · Safety · Infrastructure · Routing

---

## 2.1 Introduction

As a means of transport, cycling offers several benefits for citizens of urban areas. It is emission-free and healthy for the user. Well-being and physical and mental health are promoted by cycling (Singleton, 2019). Nevertheless, the share of the bicycle in the modal split in Germany is only 12% (Agora Verkehrswende, 2019). One reason for that could be the negative emotional state experienced during cycling. Cycling is perceived as unsafe by many people (Singleton, 2019). This feeling of danger represents a barrier to cycling (Rérat, 2019). Therefore, city administrations should try to improve perceived cycling safety. In this matter, the cycling infrastructure is an important point of reference because it influences perceived cycling safety significantly (Schmidkunz, Schroth, Zeile and Kias, 2019). To improve the cycling infrastructure in metropolitan regions, the *RouteMeSafe application* is being developed at the Stuttgart University of Applied Sciences in the project *i\_city: intelligent city*. Hereby, two main goals are pursued: To improve perceived cycling safety in the long run, the application is supposed to provide city administrations with a *feedback function* on the perceived safety of their cycling infrastructure. This could enable city administrations to implement measures based on the evaluation of the people using the cycling infrastructure. However, the implementation of infrastructure measures often requires a lot of time. Therefore, a *safety routing function*, which illustrates safe routes for cyclists, is additionally being developed to increase the short-term perceived cycling safety. In a bachelor thesis, supervised by the Departments of Computer Science and Business Psychology, a prototype (available for Android and iOS) of the *feedback function* was developed. In the prototype, cyclists can enter, view, and evaluate dangerous spots (Fig. 2.1).

The *safety routing function* is currently still in the conception phase. As a next step in the development process, the *i\_city* development team decided to define the target groups for the *RouteMeSafe application* and to include their expectations in the further development process. Although it might seem logical to address as many users as possible with a product, a different approach is recommended in the literature on user-centered product development. According to Cooper (2004), no one product can satisfy all potential users sufficiently. It is therefore recommended to rather focus on the complete satisfaction of a subgroup of potential users instead of trying to satisfy all potential users only partially. In the case of the *RouteMeSafe application*, there is a need for users who generate data (enter/rate dangerous spots) with the *feedback function* and use the *security routing function*. Users who generate data are important for filling the application's database, which provides the foundation for the *feedback* and *safety routing functions*. The size and quality of the

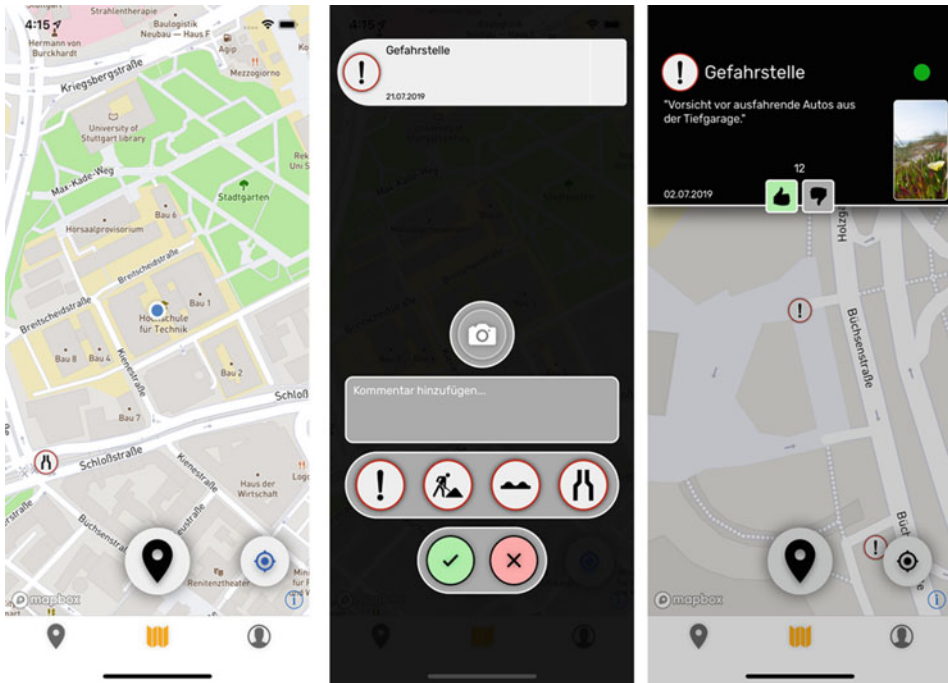


**Fig. 2.1** Features of the crowdsourcing application

database will most likely play a part in how reliably the functions work. Furthermore, a large and high-quality database will make the application more attractive for city administrations because they can thereby generate valid feedback on their infrastructure measures. Users who regularly utilize the *safety routing function* are needed to showcase to city administrations that the application can increase perceived cycling safety and thus motivate other citizens to use the bicycle. This could create an incentive for city administrations to carry the costs of the application in the long run. To identify the abovementioned user groups and their expectations toward the *RouteMeSafe application*, two studies with *frequent* and *infrequent cyclists* were conducted. The two groups are known to have different risk perceptions during cycling according to Lehtonen et al. (2015). Consequently, it was hypothesized that they have different expectations toward the functions of a cycling security application. Study 1 was a user experience study aimed at determining for which functions of the *RouteMeSafe application* *frequent* and *infrequent cyclists* could serve as a target group and what they expect of them based on a student sample from Stuttgart. Study 2 was a technology acceptance study investigating the expectations of *frequent cyclists* regarding the *feedback function* based on a sample with citizens of Stuttgart in more detail. As a basis for study 1, the *Hedonic-Pragmatic Model* by Hassenzahl (2001) and the *Kano Model* by Kano (1984) were used, which will be introduced in the following.

## 2.2 Study 1: UX Study with Frequent and Infrequent Cyclists

### 2.2.1 Hedonic-Pragmatic Model

In the corporate environment, emotional (hedonic) as well as functional (pragmatic) product qualities are becoming increasingly important (Diefenbach & Hassenzahl, 2017). A basic model of hedonic and pragmatic product characteristics is the *Hedonic-Pragmatic Model* by Hassenzahl (2001). The *hedonic quality* of a product describes emotional aspects of the product experience (Hassenzahl, 2001). An example for that is the perception of the product by the customer as beautiful, interesting, or innovative. The *pragmatic quality* of a product describes its utility and usability for the customer (Hassenzahl, 2001). This includes, for example, the customer's perception of the product as practical, simple, or clear. In the model, the *hedonic* as well as the *pragmatic quality* is related to the perceived attractiveness of the product, which in turn is related to the behavioral consequence (e.g., increased use) and the emotional consequence (e.g., joy) (Hassenzahl, 2001). Figure 2.2 illustrates the *Hedonic-Pragmatic Model* by Hassenzahl (2001).

### 2.2.2 Kano Model

In addition to determining expectations toward *hedonic* and *pragmatic qualities* of an application, it can be beneficial to find out which *additional functions* potential users expect. Covering expectations thoroughly is important in product development. According to Michalco et al. (2015), users approximate their product rating to the level of disconfirmation, when their expectations are not met and vice versa. The *Kano Model* by Kano (1984) provides a sound basis for evaluating expectations toward additional functions for the *RouteMeSafe application*.

The *Kano Model* describes the relationship between the fulfillment of expectations and customer satisfaction (Hölzing, 2008). In the model, the attributes (functions) of a product are divided into five categories that have different effects on customer satisfaction: basic attributes, performance attributes, attractive attributes, indifferent attributes, and reverse attributes (Engelhardt & Magerhans, 2019). Table 2.1 shows a description of the product attributes in the *Kano Model*.

In summary, it can be said that the *hedonic-pragmatic model* by Hassenzahl (2001) provides a basis for determining the holistic evaluation with regard to hedonic and pragmatic qualities of a product by potential users. The *Kano Model* by Kano (1984) provides a foundation for understanding whether *additional features* are desired by potential users. Based on these findings in literature, a study of the *RouteMeSafe application* was conducted at Stuttgart University of Applied Sciences.

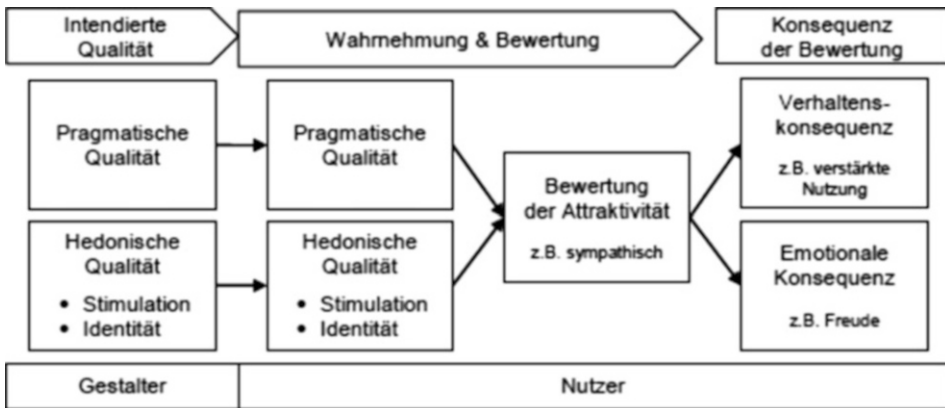


**Fig. 2.2** Representation of the hedonic-pragmatic model according to Hassenzahl (2001)

**Table 2.1** Types and description of product attributes according to Kano (1984)

Type of product attribute	Description
Basic attributes	Trigger particularly high dissatisfaction in case of non-fulfillment, but no satisfaction in case of fulfillment (Engelhardt & Magerhans, 2019)
Performance attributes	Trigger the more satisfaction, the more they meet expectations and vice versa (Hölzing, 2008)
Attractive attributes	Trigger particularly high satisfaction with fulfillment, but no dissatisfaction with non-fulfillment (Engelhardt & Magerhans, 2019)
Indifferent attributes	Have no effect on satisfaction (Hölzing, 2008)
Reverse attributes	Trigger high dissatisfaction when fulfilled (Hölzing, 2008)

### 2.2.3 Methodology

Students were recruited by e-mail and incentivized with course credits. The inclusion criteria were that the participants could operate a smart phone and ride a bicycle. In addition, it was attempted to generate a balanced sample of *frequent* and *infrequent cyclists*. Since the two groups have a different risk perception according to Lehtonen et al. (2015), different expectations toward the *RouteMeSafe* application were hypothesized. The experiment was divided into three parts: a preliminary survey, testing of the application while cycling over a predefined route in Stuttgart, and a follow-up survey. By testing the application in the field, it was intended to create an experimental context as close to reality as possible. In the preliminary survey, general data on the participants and cycling frequency, expectations toward the application, as well as the perceived cycling safety were collected. When testing the application, the participants were instructed to record at least two dangerous spots and to evaluate two existing dangerous spots (entered by other



users). A survey evaluating the application was conducted afterward. The follow-up survey again included the subjects' perceived cycling safety. Furthermore, the user experience of the application was assessed by participants via the short version of the *User Experience Questionnaire Short (UEQ-S)*, which is based on the *Hedonic-Pragmatic Model* by Hassenzahl (2001). The UEQ-S was chosen as a central instrument because the questionnaire allows to measure the user experience reliably and quantitatively with a small number of items (Sarodnick & Brau, 2011). In order to find out whether the target group would like to have *additional functions* for the application, the standard questionnaire of the *Kano Model* by Kano (1984) was used. The following ideas for *additional functions* were evaluated by the participants: a safety routing function (avoiding dangerous spots), a function that includes predefined routes (along popular landscapes and sights), a community function (platform to discuss cycling security), and a function that enables tracking of the cycled routes (environmental impact compared to other modes of transport). Furthermore, the participants were asked which *additional functions* they consider useful in addition to the ones evaluated in the *Kano analysis*.

## 2.2.4 Results

Thirty-one students with an average age of 26 years completed the experiment. Seventy-four percent of the sample were female and 26% male. Forty-eight percent of the participants stated that they used the bicycle at least once a month and were categorized as *frequent cyclists*, and 52% stated that they used the bicycle less than once a month and were categorized as *infrequent cyclists*.

The UEQ-S ratings of the application in terms of pragmatic, hedonic, and overall quality ranged between 0.4 and 0.8. According to Schrepp, Hinderks, and Thomaschewski (2017), this can be interpreted as neutral values. A comparison of the perception of safety before (mean = 2.5, on a scale from 1 (very unsafe) to 5 (very safe)) and after use of the application (mean = 3.5) showed a significant increase. The subjects reported a significantly higher perceived cycling safety ( $z = -2.496, p = 0.013^1$ ) after using the application. In both, the evaluation of the *RouteMeSafe application* in the UEQ-S and the safety perception of cyclists before and after use of the application, no differences were found between *frequent* and *infrequent cyclists*. Accordingly, the application had a positive effect on the perceived safety of both groups. Table 2.2 shows the results of the UEQ-S.

The *Kano analysis* showed that a *security routing function* was categorized as a performance attribute (O) by the participants. Predefined routes and tracking statistics were categorized as attractive attributes (A). The community function was categorized as an indifferent attribute (I). The Fong test checks all four category assignments for significance and becomes significant if the inequality is not true. This was the case for all four

---

<sup>1</sup>A Mann–Whitney U-test has been conducted.

**Table 2.2** Results of the UEQ-S

Scale	<i>M</i>	SD	Confidence interval (95%)	
			Lower limit	Upper limit
Pragmatic quality	0.758	0.956	0.421	1.095
Hedonic quality	0.476	0.918	0.153	0.799
Overall	0.617	0.789	0.339	0.895

**Table 2.3** Results of the Kano analysis

Functions	<i>A</i> (%)	<i>M</i> (%)	<i>O</i> (%)	<i>I</i> (%)	<i>R</i> (%)	Category
Navigation	22.6	25.8	<b>51.6</b>	0	0	O
Predefined routes	<b>74.2</b>	0	6.5	19.4	0	A
Community function	25.8	0	0	<b>67.7</b>	6.5	I
Tracking statistics	<b>77.4</b>	0	9.7	12.9	0	A

functions: Navigation ( $8 < 3.84$ ), predefined routes ( $17 < 6.48$ ), community function ( $13 < 6.48$ ), tracking statistics ( $20 < 6.47$ ). Table 2.3 shows the results of the *Kano analysis*.

The additional features most frequently suggested by the participants were an acoustic notification of nearby dangerous spots (81.50%), automatic map rotation in the direction of cycling (74.10%), and categorization of dangerous spots according to their severity (66.70%). However, *infrequent cyclists* did not expect any additional features in the application.

## 2.2.5 Discussion

The expectations of the participants regarding the application were partially fulfilled. The pre- and post-use analysis of the application shows that it increases perceived cycling safety in the short term. In future studies on the application, it should be examined whether this effect remains after a long-term use. The neutral values on the UEQ-S constructs indicate that the expectation of simplicity and reliability is only partially fulfilled in the current prototype. The implementation of a safety route, an acoustic notification of nearby dangerous spots, the automatic turning of the map in cycling direction, and a categorization of dangerous spots according to their severity could improve the simplicity and reliability of the application. This should be investigated further in a usability test after the implementation of these functions. *Infrequent cyclists* expressed that they expect a security routing function. After the function has been developed, user experience tests with this target group should be conducted in order to check whether they could serve as a target group for it. *Frequent cyclists* indicated that they did not expect any additional functions such as safety routing for the application. This indicates that *frequent cyclists* could be considered as a target group for the feedback function of the *RouteMeSafe* application. To test this hypothesis on a larger sample and further investigate the expectations of *frequent cyclists*

regarding the *feedback function*, study 2 was conducted. The Unified Theory of Technology Acceptance 2 (UTAUT2) was used as a basis.

---

## 2.3 Study 2: Technology Acceptance Study with Frequent Cyclists

### 2.3.1 Unified Theory of Technology Acceptance 2 (UTAUT2)

UTAUT2 is a technology acceptance model designed for the consumer use context, which has been widely used in studies researching various technologies (Tamilmani, Rana and Dwivedi, 2017). The model proposes a direct influence of performance expectancy, effort expectancy, social influence, facilitating conditions, hedonic motivation, habit, and price value on the intention to use a technology, which is the best predictor of the actual use of a technology. Furthermore, moderating effects of age, gender, and experience on the relationships of facilitating conditions, hedonic motivation, habit, and price value with the intention to use a technology are stated. Also, a moderating effect of experience on the relationship of the intention to use a technology with the actual use of a technology is proposed in the model (Venkatesh et al., 2012). Figure 2.3 illustrates the UTAUT2. This model was the basis of study 2.

### 2.3.2 Methodology

Participants were recruited via the newsletter of the General German Bicycle Club (ADFC). This medium was chosen because of the assumption that most of the members of the ADFC would be *frequent cyclists*. In the first part of the online survey, the functions of the *RouteMeSafe application* and its development status were described and illustrated with screenshots. Then the participants were asked to state their opinion on the prototype (*feedback function* only) and then on the overall concept of the application (feedback and security routing function) based on the UTAUT2 constructs. In this, the original items of Venkatesh et al. (2012) with the anchors 1 (*strongly disagree*) and 7 (*strongly agree*) were used. In the last part, questions about possible purposes of use, desired additional functions, demography, and frequency of cycling were asked.

### 2.3.3 Results

A total of 29 members of the General German Bicycle Club (ADFC) with an average age of 50 years were surveyed. Fourteen percent of the sample were female and 86% male. All participants stated that they used their bicycles at least once a month which confirmed the assumption that most of the ADFC members would be *frequent cyclists* and 86% of the sample even several times a week. The participants stated that they could imagine using the

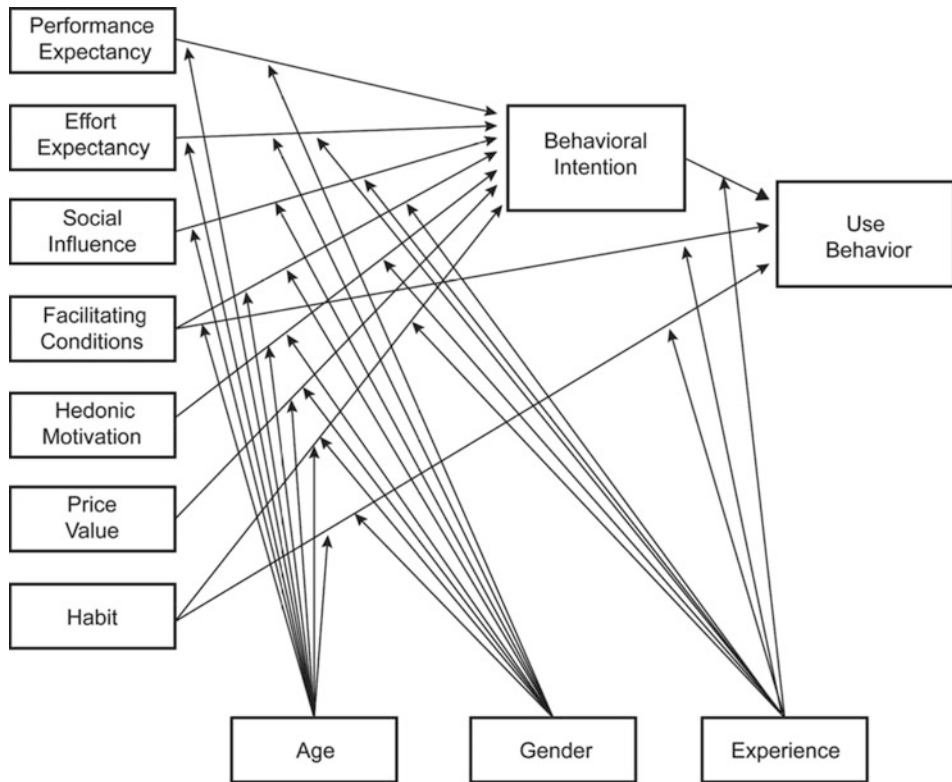


**Fig. 2.3** Illustration of UTAUT 2 according to Venkatesh et al. (2012)

prototype regularly (mean = 5.9). The subjects imagine the prototype to be useful (mean = 6.1), easy to use (mean = 5.6), and even entertaining (mean = 4.9). In addition, they indicate that their social environment would support that they use the prototype of the application (mean = 4.5) and that their smart phone would be suitable for using the prototype (mean = 6.4). The overall concept of the application (feedback and security routing function) portrayed a similar picture. The participants stated that they could imagine using the application regularly (mean = 5.7). Furthermore, they imagine the application to be useful (mean = 5.8), easy to use (mean = 5.4), and entertaining (mean = 5.0). They also indicate that their social environment would support it if they used the application (mean = 4.4) and that their smart phone would be suitable for using the application (mean = 6.4). Participation in cycling infrastructure measures (79%), cycling tours (79%), and the route to leisure activities (76%) were stated as the most likely purposes of use. The majority of the sample could imagine using the application on known as well as on unknown routes (76%). Other desired features were a categorization of dangerous spots according to their severity, a feedback function on measures taken to eliminate reported hazards, and black ice warnings.

### 2.3.4 Discussion

*Frequent cyclists* already state high acceptance of the prototype of the *RouteMeSafe application*. The group shows a high usage intention and imagines the application as useful, easy to use, and entertaining. One of the two most frequently mentioned purposes of use is the *participation in cycling infrastructure measures*. This indicates that *frequent cyclists* could be a target group for the feedback function. Another important motivator for the regular entering of dangerous spots with the application could be a notification function on the status of measures initiated to eliminate reported dangerous spots. After implementation of the function, this assumption should be tested in a further user experience study.

---

## 2.4 General Discussion

Two studies were conducted with the aim to determine the target groups for the functions of the *RouteMeSafe application*. The results of study 1 with 31 students indicated that *infrequent cyclists* could be a target group for the *security routing function* of the *RouteMeSafe application* and *frequent cyclists* could be a target group for the *feedback function*. The former should be checked in a further technology acceptance study based on a large sample with citizens of Stuttgart. The latter was confirmed in study 2 with 29 ADFC members. *Frequent cyclists* already indicate high acceptance of the prototype in its current development state. They could thus serve as the required users who fill the applications database. Functions such as a categorization of dangerous spots according to their severity, a feedback function on measures taken to eliminate reported hazards, and black ice warnings could further increase acceptance in this group. After these functions have been implemented, their user experience should be investigated based on a randomly selected sample with *frequent cyclists* from Stuttgart. Furthermore, diary studies investigating the user experience of the *RouteMeSafe application* should be conducted with *infrequent* and *frequent cyclists* from Stuttgart. Doing so could help to find out whether both groups can serve as target groups of the *security routing* and *feedback function* on the long run.

**Acknowledgments** The project *i\_city: Intelligent City* is funded by the Bundesministerium für Bildung und Forschung (Federal Ministry of Education and Research) under the funding number 13FH9I011A and supervised by the project management agency VDI Technologiezentrum GmbH on behalf of the Bundesministerium für Bildung und Forschung (Federal Ministry of Education and Research).

## Bibliography

- Agora Verkehrswende. (2019). Verteilung genutzter Verkehrsmittel im Personenverkehr in Deutschland nach ökonomischem Status im Jahr 2017 [Graph]. In Statista. Zugriff am 12. Oktober 2020, von <https://de.statista.com/statistik/daten/studie/1074305/umfrage/vergleich-des-modal-splits-nach-oekonomischem-status/>
- Cooper, A. (2004). Why high-tech products drive us crazy and how to restore the sanity. 2nd rev. ed. Indianapolis: Sams Publishing; [distributor] Pearson Education Ltd.
- Diefenbach, S. & Hassenzahl, M. (2017). Psychology in user-centered product design. Berlin, Heidelberg: Springer Berlin Heidelberg. <https://doi.org/10.1007/978-3-662-53026-9>
- Engelhardt, J.-F. & Magerhans, A. (2019). eCommerce klipp et klar (WiWi klipp et klar, 1st ed. 2019). Wiesbaden: Springer Fachmedien Wiesbaden; Springer Gabler.
- Hassenzahl, M. (2001). The effect of perceived hedonic quality on product appealingness. *International Journal of Human-Computer Interaction*, 13(4), 481-499.
- Hinterhuber, H. H. & Matzler, K. (2009). Customer-oriented corporate management: Gabler.
- Hölzing, J. A. (2008). Die Kano-Theorie der Kundenzufriedenheitsmessung. Eine theoretische und empirische Überprüfung (Gabler Edition Wissenschaft, 1. Aufl.). Zugl.: Mannheim, Univ., Diss., 2007. Wiesbaden: Gabler Verlag / GWV Fachverlage GmbH Wiesbaden. <https://doi.org/10.1007/978-3-8349-9864-4>
- Lehtonen, E., Havia, V., Kovanen, A., Leminen, M. Saure, E. (2015). Evaluating bicyclists' risk perception using video clips: Comparison of frequent and infrequent city cyclists. *Transportation Research Part F Traffic Psychology and Behaviour*, 195–203. <https://doi.org/10.1016/j.trf.2015.04.006>
- Kano, N. (1984). Attractive quality and must-be quality. *Hinshitsu (Quality, The Journal of Japanese Society for Quality Control)*, 14, 39-48.
- Michalco, Jaroslav, Simonsen, Jakob Grue, Hornbæk, Kasper (2015): An Exploration of the Relation Between Expectations and User Experience. In: *International Journal of Human-Computer Interaction* 31 (9), S. 603–617. DOI: <https://doi.org/10.1080/10447318.2015.1065696>.
- Rérat, P. (2019). Cycling to work: Meanings and experiences of a sustainable practice. *Transportation research part A: policy and practice*, 123, 91-104.
- Sarodnick, F. Brau, H. (2011). Methoden der Usability Evaluation. *Wissenschaftliche Grundlagen und praktische Anwendung (Wirtschaftspsychologie in Anwendung, 2., überarb. und aktualisierte Aufl.)*. Bern: Huber
- Schallmo, D. R. (2018). *Apply Design Thinking now*. Springer Trade Media Wiesbaden.
- Schmidkunz, M., Schroth, O., Zeile, P., & Kias, U. (2019, April). Road Safety from Cyclist's Perspective. In *REAL CORP 2019-IS THIS THE REAL WORLD? Perfect Smart Cities vs. Real Emotional Cities*. Proceedings of 24th International Conference on Urban Planning, Regional Development and Information Society (pp. 597-604). CORP-Competence Center of Urban and Regional Planning.
- Singleton, P. A. (2019). Walking (and cycling) to well-being: Modal and other determinants of subjective well-being during the commute. *Travel behaviour and society*, 16, 249-261.
- Schrepp, M., Hinderks, A. & Thomaschewski, J. (2017). Design and Evaluation of a Short Version of the User Experience Questionnaire (UEQ-S). *International Journal of Interactive Multimedia and Artificial Intelligence*, 4(6), 103-108. <https://doi.org/10.9781/ijimai.2017.09.001>
- Tamilmani, K., Rana, N. P., & Dwivedi, Y. K. (2017, November). A systematic review of citations of UTAUT2 article and its usage trends. In *Conference on e-Business, e-Services and e-Society* (pp. 38-49). Springer, Cham.

Venkatesh, V., Thong, J. Y., & Xu, X. (2012). Consumer acceptance and use of information technology: extending the unified theory of acceptance and use of technology. *MIS quarterly*, 157-178.

**Open Access** This chapter is licensed under the terms of the Creative Commons Attribution 4.0 International License (<http://creativecommons.org/licenses/by/4.0/>), which permits use, sharing, adaptation, distribution and reproduction in any medium or format, as long as you give appropriate credit to the original author(s) and the source, provide a link to the Creative Commons license and indicate if changes were made.

The images or other third party material in this chapter are included in the chapter's Creative Commons license, unless indicated otherwise in a credit line to the material. If material is not included in the chapter's Creative Commons license and your intended use is not permitted by statutory regulation or exceeds the permitted use, you will need to obtain permission directly from the copyright holder.





# Artificial Intelligence Supporting Sustainable and Individual Mobility: Development of an Algorithm for Mobility Planning and Choice of Means of Transport

Rebecca Heckmann, Sören Kock, and Lutz Gaspers

## Abstract

Mobility planning is rarely individually tailored. Instead people have to make an active effort to adapt standard solutions to their requirements. Routing apps like Google Maps allow for personalization only by saving important places like home and a workplace but do not allow the user to influence the routing suggestions or choice of mode of transport based on preferences, limitations, or situation. It becomes even more difficult when different means of transport are to interact since most routing applications offer very little multimodal optimization aside from the last mile. Thus, the objective of this article is to present a concept for the utilization of artificial intelligence and regression models in order to enable individual and sustainable mobility planning. To achieve this objective, initially existing routing and mobility planning applications are examined and are conceptually expanded in order to outlay the benefits of personalized route planning. The concrete objective alongside with a method for the development of a new solution is summarized. An algorithm fulfilling these objectives based on multiple linear regression is conceptualized. Relevant factors with coefficient are identified, as well as necessary data sources and interfaces. This algorithm is then implemented in a limited prototype as a proof of concept. Finally, this prototype is tested based on a set of mobility scenarios in order to validate the achievement of the defined objective.

---

R. Heckmann (✉)

University of Applied Sciences Stuttgart, Stuttgart, Germany

Hochschule für Technik Stuttgart, Stuttgart, Germany

e-mail: [rebecca.heckmann@hft-stuttgart.de](mailto:rebecca.heckmann@hft-stuttgart.de)

S. Kock · L. Gaspers

Hochschule für Technik Stuttgart, Stuttgart, Germany

© The Author(s) 2022

V. Coors et al. (eds.), *iCity. Transformative Research for the Livable, Intelligent, and Sustainable City*,

[https://doi.org/10.1007/978-3-030-92096-8\\_3](https://doi.org/10.1007/978-3-030-92096-8_3)



---

**Keywords**

Sustainable mobility · Personalized routing · Artificial intelligence · Multiple linear regression

---

### **3.1 Introduction**

Routing apps have a major impact on the choice of mode of transport for most people—especially for non-routine trips and, due to varying conditions and contexts, even for routine trips. Thus, they play a major role in spreading the adoption of sustainable modes of transport. They shall therefore be the starting point of this article: first we take a short look at the state of the art and then we draw a vision of what routing apps could offer. This serves as a guideline for the development of a corresponding method and algorithm for route planning.

#### **3.1.1 Routing Apps: What They Provide Today**

Google Maps is one of the most important services offered by Google (Brandt, 2016). It provides two essential functions: searching routes for different modes of transport and navigation. When looking for a route for an upcoming trip, Google Maps compares a trip by car, public transport (bus and train), walking, cycling, and flight and sometimes includes local offers such as cabs or electric scooters. Users can find out estimated travel times and distances and, in case of multimodal connections, the transfers. If the user wants to travel by car, by bicycle, or by foot, Google Maps provides detailed navigation. It also takes into account current traffic or closures. Since Google evaluates the cell phone data of all users for its route optimization, the navigation is widely considered to be precise, especially with regard to delays and obstacles. A recent confirmation for this has been provided (La Rocco, 2016; Leicht, 2018). The main competitors of Google Maps are Apple Maps, Here WeGo, ReachNow, and OpenStreetMap. The functionality of all these applications and their restrictions in regard to personalization is very similar.

#### **3.1.2 A Vision for Routing Apps: Individually Tailored, Sustainable Mobility**

None of these existing routing apps allow the user to influence process or optimization parameters. The user may only enter a few travel parameters: date, time, and the choice of means of transport. These limited parameters significantly restrict the individualization of travel planning in exchange for a simplistic user experience. For example, there is no way to include physical restrictions, presence or absence of privately owned vehicles, mobility subscriptions, or simply an aversion to or preference for a means of transport. There are no

situation-dependent parameters either, such as weather conditions, luggage, or fellow passengers. However, all these parameters strongly influence the optimal travel option. For example, if the user needs to utilize the travel time for work on a long trip, traveling by train is more advantageous than it would be otherwise. The number of people traveling also has a strong impact on the pros and cons of a means of transport.

Parameters that influence the decision for routing and means of transport are countless. So far, they are not sufficiently covered in any existing application. However, existing technologies could already enable the consideration of person- and situation-dependent parameters. Moreover, artificial intelligence and a self-learning algorithm could be able to learn from past decisions and behavior of each user and independently reflect these results in a profile, which could be considered for future route planning. The advantages thereof can be attributed to three areas:

1. *Significantly increased comfort for the traveler*: By taking into account the personal preferences and situational conditions, recommendations can be made on an individual level. As a result, route planning adapts to the traveler.
2. *Less effort for the traveler*: Until now, a traveler has to independently compare different routes and means of transport (combinations) through different applications and websites. A new route planning application that includes individual context and independently is able to learn can make things easier for the traveler, since it automatically recommends exactly the most suitable option.
3. *Multicriteria optimization is possible*: Until now, optimization according to a single criterion was the rule with routing apps. Their use was associated with a high level of manual effort on the part of travelers when comparing routes and means of transport. At the same time, they only provided little information. The routing apps (or the users themselves) thus tried to find a route or connection that fulfilled one criterion, e.g., as cheap or as fast as possible. However, if the optimization is automated by a new routing app and sufficient information is available, multicriteria optimization is possible. Then an app could, among other factors, simultaneously optimize for sustainability, costs, and travel duration (Scholz, 2018).

Thus, traveling can be more comfortable; the process of planning a trip is less complex, and more sustainable modes of transport are more accessible and useful. This vision of a routing app will be realized, albeit initially in a limited state, in a prototypical routing app called “EmiLa.”

---

## 3.2 Objective

The goal of the future application and therefore the algorithm is to popularize low-emission mobility for a wide range of users by establishing it as an optimization criterion without disregarding other factors. Giving emissions, among other factors, an adequate weight in

the decision-making process is intended to nudge the users toward more environmentally friendly means of transport. Thereby, reducing mobility-induced emissions, a contribution can be made to reduce the impact of climate change.

The algorithm needs to be able to process all these types of information and based on them find an optimal connection, possibly multimodal, on an optimal route for a requested change of location from A to B, possibly including intermediate stops. The objective of the optimization is the fulfillment of a main goal, while secondary goals must be reached and conditions must be fulfilled. For the more limited first prototype of the app EmiLa, the main goal is to minimize the emissions of the journey, while secondary objectives are the shortest possible travel time, the lowest possible travel costs, and taking into account the personal profile and situation-dependent parameters (weather, as few transfers as possible, etc.).

---

### 3.3 Development of the Algorithm for Personalized-Quantified Routing Including Self-Learning Units

Based on the set objective, this chapter will elaborate on the fundamental idea and structure behind the algorithm as well as the process of data integration necessary in order for the algorithm to give informed recommendations.

#### 3.3.1 Concept and Structure of the Algorithm

The requirement of optimizing based on numerous variables without a common metric represents the key challenge for the intended algorithm. First of all, each singular criterion needs a quantified scale standardized to the same dimensions. Additionally, the weighting of the criteria needs to be incorporated in an adaptable way in order to personalize the decision-making process. Also, it allows for a continuous learning process in the prioritization of optimizing a decision that is based on different factors with no existing common metric to assess them. This problem can be formulated similarly to a multiple linear regression, as described, for example, in Draper and Smith (1998):

$$y = (\beta_0) + \beta_1x_1 + \beta_2x_2 + \dots + \beta_nx_n + (u)$$

$y$  = estimated value of the dependent variable, i.e., overall score for a route and mode of transport. For the prototype application EmiLa, this is branded as “EmiQ” (emission quotient).

$\beta_0$  = intercept on the  $y$ -axis, not relevant for this application as there is no baseline score.

$\beta_1$  to  $\beta_n$  = coefficient for each factor, i.e., the weight of the different factors included in the overall score. For the prototype application EmiLa, this is branded as “QuPeR” (quantified personalized routing).

$x_1$  to  $x_n$  = value of the independent variable, i.e., score for each singular factor (emissions, costs, travel time, etc.).

$u$  = remaining error, not relevant for this application as this is not calculated.

Furthermore, the general model for linear regression needs to be extended for this use case (excluded factors from before are omitted):

$$y = (x_1 + \beta_2 x_2 + \dots + \beta_n x_n) \times (p_1 \times p_2 \times \dots \times p_n)$$

$p_1$  to  $p_n$  = prohibitive coefficient, representing (individual) exclusion rules or strong aversions to a certain mode of transport. Examples for this are the exclusion of driving a car without a license or refusal to ride a bike in the snow. This application of multiple linear regression enables weighting the different factors through discrete individual coefficients. The metric and scaling of each factor have to be solved separately as only the result thereof can be processed as the  $x$  variable.

### 3.3.2 Metric and Scaling of the Factors

A central requirement for enabling the optimization of the chosen mode of transport based on the previously stated variety of factors is quantifying the degree of satisfaction for each factor for each available option. Thus, the factors need a common metric and a common scale. The length of the scale is negligible, so long as it is uniform across all factors. A grade system of 1 to 5 has been chosen for the prototype EmiLa, 1 representing the best possible score and 5 the worst possible score. An important requirement regarding the metric that arose during initial tests was to assess the factors relative to the set of available options. For example, the overall duration and the duration per kilometer vary strongly depending on the length of a trip. One unified scale for all trips would distort the score for this metric. For EmiLa, this has already been solved for the first three factors:

- *Duration of the trip*: The fastest available option always receives the best score of 1, regardless of the absolute value overall or per kilometer. Even if an option may be slow by certain standards, it has to be adequately expressed that it is the fastest one available. Based on a small-scale user test, the worst possible score of 5 is given for any duration at least three times as long as the fastest possible option. In between those values is a linear scale. This can be summarized in the following resulting pseudo-formula for each option:

$$x_{\text{duration}} = \text{MIN} \left( 5; 1 + \frac{4 \times (\text{Duration} - \text{Minimum duration across all options})}{2 \times \text{Minimum duration across all options}} \right)$$

- *Cost of the trip*: The assessment of the cost works very similar to the assessment of the travel duration. Unlike the duration, there are options that achieve a value of zero (e.g., walking), requiring an alternative calculation for distances that can be traveled by those means of transport. In these cases, the cost advantage of free options should be reflected with the best score of 1 without ignoring the differences among the other options, whereof the cheapest one receives a score of 3 and values at least three times as high receive a score of 5. Thus, the following two pseudo-formulas for each option have been created, the first without free travel options and the latter with free travel options:

$$x_{\text{cost\_without\_free}} = \text{MIN} \left( 5; 1 + \frac{4 \times (\text{Costs} - \text{Minimum costs across all options})}{2 \times \text{Minimum Costs across all options}} \right)$$

$$x_{\text{cost\_with\_free}} = \text{IF}(\text{costs} = 0) \text{ then } 1;$$

$$\text{else } \text{MIN} \left( 5; 3 + \frac{2 \times (\text{Costs} - \text{Minimum costs across all options})}{2 \times \text{Minimum Costs across all options}} \right)$$

- *Emissions caused by the trip*: The scoring of the emissions has been designed differently from the costs and duration. A universal scale better fulfills the goal of measuring the adequacy of a mode of transport compared to a relative scaling. Especially for overseas trips, flights would receive a perfect emissions rating due to the lack of a more environmentally friendly option. Thus, a universal scale based on the current emission levels of the most widely used modes of transport has been defined, returning the best score of 1 for zero emissions and the worst score of 5 for emissions of 150 grams of CO<sub>2</sub> equivalents per kilometer and above. This threshold for the worst score represents a relatively modern car with only one passenger. Unlike the other two factors, the scale is also separated into two parts from 0 to 30 and from 30 to 150 grams per kilometer. This serves the purpose of adding a slight advantage for modes of transport with very low emissions, thus reducing the elasticity of the scale in the lower range. Again, two pseudo-formulas result from this reasoning:

$$x_{\text{emissions}} = \text{IF}(\text{emissions} \leq 30) \text{ then } \left( 1 + \frac{\text{emissions}}{30} \right);$$

$$\text{else } \text{MIN} \left( 5; 2 + \frac{3 \times (\text{emissions} - 30)}{120} \right)$$

All three of these scales represent merely a starting point and are to be further adjusted based on more large-scale testing and studies. The approach of defining one metric per factor and then adjusting the scale between 1 and 5 based on user studies can be applied to any further factors as well, even qualitative ones with certain adjustments (e.g., comfort based on number of transits and a scoring model for different modes of transport). The prohibitive factors require less intricate scales, as they are only intended to eliminate certain modes of transport in certain conditions or favor them in others. Resulting scales are to be defined on a personal level though, primarily from preferences stored in a user profile. An exemplary factor may look as follows:

$$p_{\text{weather}} = \text{IF}(\text{mode of transport} = \text{walking and weather} = \text{rain}) \text{ then} = 5; \text{ else} = 1$$

Thus, all options including walking in the rain automatically receive the worst possible overall score, if the user has made that choice in their profile.

### 3.3.3 Utilizing Machine Learning for Improving the Algorithm

The two main elements are the metrics for each factor  $x$  and the corresponding coefficients  $\beta$ . While the metrics of the factors are to be refined through empirical studies, the coefficients are intended to be improved continuously and user specific through machine learning. Only an initial calibration for the coefficients is predefined within the algorithm as that is necessary for any results to be calculated before there is any historical data of user choices to use for optimization. Afterward, the comparison between the recommended mode of transport and the one chosen by the user will serve to calculate vectors for each coefficient, similar to the method described in Tao et al. (2006), i.e., if the starting coefficients are  $\beta_{\text{emission}} = 0.5$ ,  $\beta_{\text{duration}} = 0.25$ , and  $\beta_{\text{costs}} = 0.25$  but most users opt for a more expensive faster option, the weight of  $\beta_{\text{duration}}$  and  $\beta_{\text{costs}}$  needs to be adapted accordingly. The coefficient for emissions,  $\beta_{\text{emission}}$ , will not be as dynamically adjusted according to user choices, as one of the main purposes is to encourage the wider usage of sustainable modes of transport whenever the drawbacks are within reasonable bounds.

As stated, the continuous optimization through vector-based machine learning can be conducted on an individual as well as on a global level. When nearly all users demonstrate different priorities in their choice of mode of transport than suggested by the algorithm, the global coefficients will be adjusted. If only an individual repeatedly demonstrates their divergent priorities though, these can be reflected as a user-based coefficient adjustment stored in the user database and retrieved whenever the specific user sends a request.

### 3.3.4 Application of the Algorithm in EmiLa

The first implementation of the previously elaborated concept is a prototype of the aforementioned routing application EmiLa. It serves as a proof of concept for the developed algorithm and also allows the adjustment of the predefined factors and metrics based on a wide sample of real-world user tests.

The routing application EmiLa compares the available means of transport, routes, connections, and combinations thereof in order to find the one that represents the optimum in relation to the multitude of defined factors. In the current first stage, the prototype only includes the comparison of costs, duration, and emissions. It can be expanded further based on the algorithm described in the previous paragraphs. To achieve this, the necessary data on the factors needs to be obtained from third parties (e.g., mobility service providers).

The principle works as shown in Fig. 3.1.

Personal mobility-related data stored in a user profile to derive prohibitive coefficients is not yet incorporated in the first prototype due to the current lack of user profiles. This will be the next addition when the prototype will be further developed. Those prohibitive coefficients are comparatively simple though, so they were not of primary interest for the first tests. Decisions previously taken within the application are not used yet either for the same reason. Before gathering adequate amounts of data through large-scale testing, the vector-based machine learning would not only have been very limited; it also implies a high risk of overfitting the model (Tao et al., 2006).

### 3.3.5 Data Integration into the Application

Once the presented algorithm is implemented in the prototype, the required data sources will be integrated for the various decision criteria, i.e., the factors emissions, costs, and travel duration for the first prototype of EmiLa. That data is retrieved from third parties, such as different regional, national, and international mobility service providers, via an application programming interface (API). Figure 3.2 illustrates this process.

EmiLa retrieves the information from the interfaces of third-party providers, which is then processed within the EmiLa application for route planning. Data on the emission per kilometer of the different available vehicles is stored in an internal database. EmiLa evaluates the resulting recommendations for a requested route by the results of the EmiQ algorithm. Thus, the user can retrieve the result via any Internet-enabled terminal device in



**Fig. 3.1** Operating principle of the application

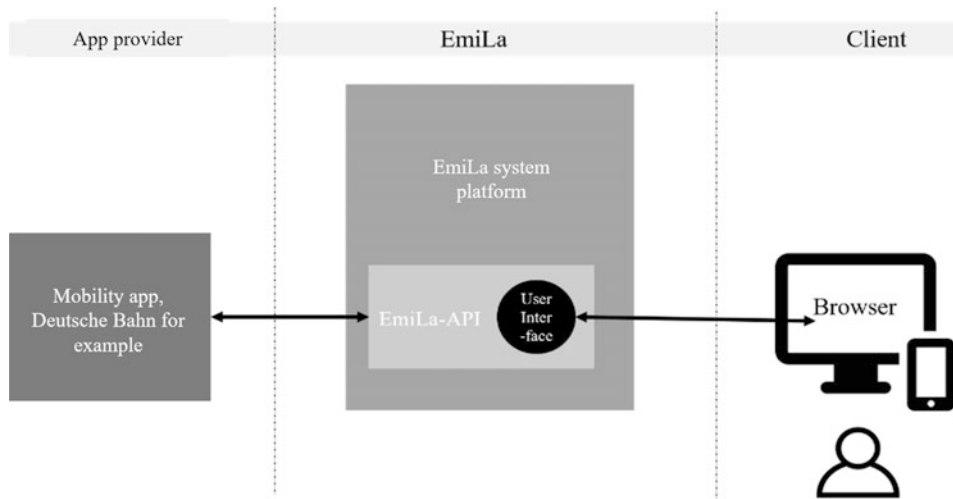


**Fig. 3.2** Integration of third party data through API

any web browser (Ott, 2018). In order to implement the algorithm beyond the first prototype stage, EmiLa primarily needs to integrate information from mobility service providers. Therefore, a wide variety of additional information such as weather data and occupancy information from parking garages will be integrated. Traffic data, availability of charging stations, and many further data sources are also beneficial. Apps for virtual meetings can be another interesting tool to integrate or recommend within EmiLa. This will avoid certain trips entirely and thus save costs, emissions, and travel time. A list of possible interfaces is given in Table 3.1.

### 3.4 Testing of the Algorithm

In order to validate the practicality and usability of the algorithm and its recommendations within an application, the prototype of the routing app EmiLa has been developed and tested based on real-world scenarios. These first tests shall serve as a basis for possible adjustments to the included factors as well as the subsequent expansion of the algorithm and interfaces within the application in iterative loops.

#### 3.4.1 EmiLa Testing Results

First tests were carried out for the travel planning of a selection of hypothetical domestic trips. For international trips, too few mobility service providers have been integrated in the app so far to allow for meaningful tests. Since public transport is shaped by national and



**Table 3.1** Possible API to implement for EmiLa

Provider	Content/data
Google Maps	<ul style="list-style-type: none"> <li>• Navigation</li> <li>• Travel time, distance, and routes by car, by bike, and by foot</li> <li>• Travel time and routes by local public transport</li> <li>• In certain areas, myTaxi and E-scooter-sharing options</li> </ul>
OpenStreetMap	<ul style="list-style-type: none"> <li>• Navigation</li> <li>• Travel time, distance, and routes by car, by bike, and by foot</li> <li>• Slope</li> <li>• Fuel/energy consumption</li> <li>• Road type and properties</li> </ul>
HERE WeGo	<ul style="list-style-type: none"> <li>• Navigation</li> <li>• Travel time, distance, and routes by car, by bike, and by foot</li> <li>• Travel time and routes by local public transport</li> <li>• Carsharing</li> <li>• Taxis</li> </ul>
YouNow (Reach Now, Park Now, Charge Now, Share Now, Free Now)	<ul style="list-style-type: none"> <li>• Navigation</li> <li>• Travel time, distance, and routes by car, by bike, and by foot</li> <li>• Travel time and routes by local public transport</li> <li>• Payment</li> <li>• Ride-hailing</li> <li>• Carsharing.</li> <li>• Availability, reservation, and payment of parking</li> <li>• Charging infrastructure</li> </ul>
Local transport associations, e.g., transport and tariff association, Stuttgart	<ul style="list-style-type: none"> <li>• Travel time and routes by local public transport</li> </ul>
Scooter-Sharing, e.g., lime, Voi, and tier	<ul style="list-style-type: none"> <li>• Availability and cost of shared e-scooter</li> </ul>
Carpool services, e.g., BlaBlaCar, MiFaZ, and Simply Hop	<ul style="list-style-type: none"> <li>• Available carpool or passengers</li> </ul>
Carsharing, e.g., Share Now, Stadtmobil, Flinkster, and local providers	<ul style="list-style-type: none"> <li>• Availability and cost of shared cars</li> </ul>
Bike-sharing, e.g., RegioRad, Smoove, Citybike, Call a Bike, Lidl-Bikes, Deezer, Nextbike, and local providers	<ul style="list-style-type: none"> <li>• Availability and cost of shared (e-) bikes</li> </ul>
Long-distance busses and trains, e.g., FlixBus and FliXTrain	<ul style="list-style-type: none"> <li>• Travel time, distance, costs, and routes</li> </ul>

(continued)

**Table 3.1** (continued)

Provider	Content/data
Car parks, parking spots, e.g., at public transport hubs, Contipark, Deutsche Bahn, and GitHub	• Availability and cost of parking
Weather data providers, e.g., Deutscher Wetterdienst	• Current weather and forecast
Virtual meeting and conference services, e.g., GoToMeeting, Microsoft Teams, and Zoom	• Digital meetings to connect with customers, partners, colleagues, etc.

regional providers, the implemented API of German providers are of little to no use for mobility planning in other countries. Tests will be conducted based on the following scenarios, representing common types of trips over varying distances and for different lengths of stay:

1. Long-distance trip for one person between urban areas with one overnight stay (Munich-Berlin-Munich): arrival on Sunday evening and return on Monday evening.
2. Long-distance trip for one person between a structurally weak region and an urban area without overnight stay (Wittenberg-Stuttgart-Wittenberg): arrival on Tuesday morning and return on Tuesday evening.
3. Medium-distance trip for two people between two rural areas for a whole week (Calw-Radolfzell on Lake Constance-Calw): arrival on Monday morning and return on Friday evening.
4. Short-distance trip for one person between a suburban and an urban area for a workday (Boeblingen-Stuttgart-Boeblingen): arrival on Tuesday morning and return on Tuesday afternoon.
5. Short-distance trip for two people within a village (Dagersheim-Dagersheim): departure Saturday morning and return Saturday morning, about half an hour later.

Figure 3.3 shows an exemplary view of the options recommended by EmiLa as well as the preliminary user interface based on the first trip of the first scenario (departure from Munich to Berlin on a Sunday at 17:45): the best option according to EmiQ is a connection by bus, which takes longer than a connection by train but causes less emissions and costs only about one third compared to the train. The emission values are made comprehensible by a traffic light system since most users have little experience judging emissions based on grams per kilometer. The private car with one passenger scores worst with an overall EmiQ value of 3.67, which is the result of high emissions, the second longest travel time, and the highest costs.

The resulting recommendations for all scenarios and trips are summarized in Table 3.2.

These tests show that the application is generally capable of algorithmically comparing and evaluating travel options with respect to the defined parameters. Travel time and the costs were manually compared to different sources and have proven to be sufficiently accurate. Overall, the recommendations are comprehensible and useful: train, car, and bike

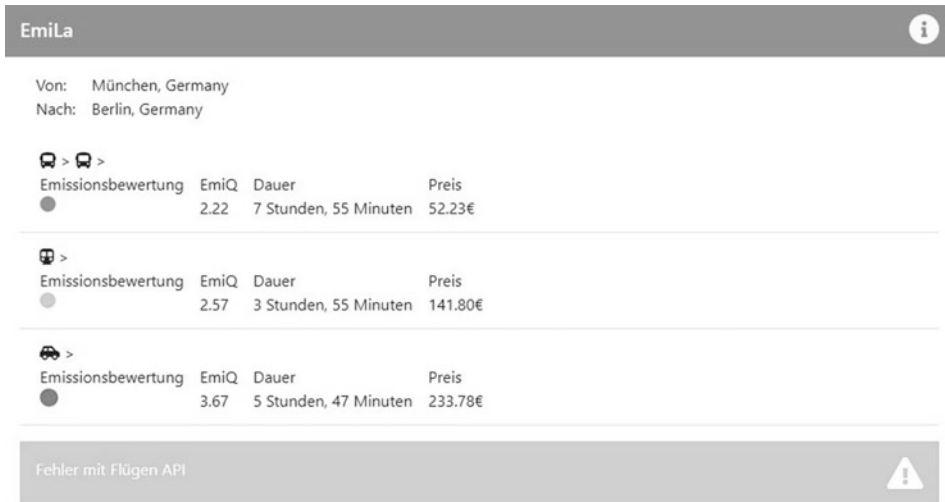


**Fig. 3.3** Route planning for Sunday, 27/09/2020, at 5:45 p.m. from Munich to Berlin

are all recommended in scenarios where they represent the best balance between emissions, costs, and travel duration. In particular, the first rank for the car when traveling with two people between two rural areas reflects the particularities of a well-balanced choice mode of transport. No single mode of transport or in some cases even a car with an internal combustion engine is overall a good choice when public transport is too inefficient along a certain route.

Another observation based on these results is the distinct impact of personal preferences, especially in case of huge differences in duration and costs. An example thereof is the trip from Wittenberg to Stuttgart, where the second option is 27 EUR more expensive but 2 h faster. Depending on the individual situation, the order of the first and second recommendation might just as well be the other way around. Such individual calibrations to the recommendations are possible by individually adapting the coefficients of the factors defining their impact on the overall result on a user-specific level, as has been outlined in the third chapter.

### 3.5 Conclusions

The testing results underline the potential of the developed algorithm and application as a contribution to establishing widespread use of sustainable mobility. With no additional effort required from the user, a balanced recommendation for a mode of transport is made, taking into account emissions, costs, and travel duration. Thus, utilizing more sustainable

**Table 3.2** Resulting recommendations for the testing scenarios (mode of transport for the longest distance is denoted)

Start → destination (day, time of departure)	1st recommendation (factor values)	2nd recommendation (factor values)	3rd recommendation (factor values)
Munich → Berlin (Sunday, 17:45)	High-speed train A (emissions medium, costs 96 EUR, duration 4:59 hours)	High-speed train B (emissions medium, costs 80 EUR, duration 5:20 hours)	Car (emissions high, costs 234 EUR, duration 5:49 hours)
Berlin → Munich (Monday, 17:00)	High-speed train A (emissions medium, costs 40 EUR, duration 4:56 hours)	High-speed train B (emissions medium, costs 67 EUR, duration 4:56 hours)	Car (emissions high, costs 215 EUR, duration 5:51 hours)
Wittenberg → Stuttgart (Tuesday, 6:00)	High-speed train A (emissions medium, costs 40 EUR, duration 7:27 hours)	High-speed train B (emissions medium, costs 67 EUR, duration 5:27 hours)	Car (emissions high, costs 216 EUR, duration 5:26 hours)
Stuttgart → Wittenberg (Tuesday, 18:00)	High-speed train A (emissions medium, costs 40 EUR, duration 6:11 hours)	High-speed train B (emissions medium, costs 40 EUR, duration 6:11 hours)	Car (emissions high, costs 216 EUR, duration 5:26 hours)
Calw → Radolfzell on Lake Constance (Monday, 7:00)	Car (emissions high, costs 30 EUR, duration 1:35 hours)	Long-distance train A (emissions medium, costs 25 EUR, duration 3:25 hours)	Long-distance train B (emissions medium, costs 48 EUR, duration 2:25 hours)
Radolfzell on Lake Constance → Calw (Friday, 17:00)	Car (emissions high, costs 30 EUR, duration 1:35 hours)	Long-distance train A (emissions medium, costs 25 EUR, duration 2:47 hours)	Long-distance train B (emissions medium, costs 45 EUR, duration 2:20 hours)
Boeblingen → Stuttgart (Tuesday, 7:00)	Commuter train A (emissions medium, costs 3 EUR, duration 0:10 hours)	Commuter train B (emissions medium, costs 3 EUR, duration 0:10 hours)	Bike (emissions low, costs 0 EUR, duration 1:04 hours)
Stuttgart → Boeblingen (Tuesday, 16:30)	Commuter train A (emissions medium, costs 3 EUR, duration 0:09 hours)	Commuter train B (emissions medium, costs 3 EUR, duration 0:09 hours)	Bike (emissions low, costs 0 EUR, duration 1:04 hours)
Dagersheim church → Dagersheim supermarket (Saturday, 8:00)	Bike (emissions low, costs 0 EUR, duration 0:05 hours)	Walking (emissions low, costs 0 EUR, duration 0:14 hours)	Car (emissions high, costs 0,5 EUR, duration 0:02 hours)
Dagersheim supermarket → Dagersheim church (Saturday, 9:00)	Bike (emissions low, costs 0 EUR, duration 0:05 hours)	Walking (emissions low, costs 0 EUR, duration 0:14 hours)	Car (emissions high, costs 0,5 EUR, duration 0:02 hours)

mobility without relevant sacrifices in other areas becomes as simple as using any other existing routing app, providing cognitive-rational motives for the users. Additionally, emission-related challenges and gamification features will provide emotive motivation for developing more sustainable habits. Nonetheless, the choice is made by the user and not the app itself. This encourages further testing regarding the influence of the recommendations on the users' decisions, i.e., the effectiveness of the application for encouraging the use of sustainable modes of transport as well as the preferred handling of conflicts between user preferences and rational, sustainable recommendations.

The prototype used for the previously presented testing of the algorithm is still a very limited implementation, especially in regard to individualization and user specificity. Further development of the application will be required in order to verify the practical viability regarding the inclusion of more decision criteria as well as the vector-based user-specific machine learning on the basis of Itskov (2019) and De Mello and Ponti (2018). Data security and privacy protection will become a more defining concern during the necessary storage and utilization of user data. Once these remaining functionalities have been implemented, a large-scale user test could provide the final confirmation of the developed algorithm.

---

## Bibliography

- Brandt, M. (2016): *So nutzen die Deutschen Google*. Statista. Statista GmbH. Zugriff: 17. September 2020. <https://de.statista.com/infografik/6020/nutzung-von-google-diensten-in-deutschland/>
- De Mello, Rodrigo Fernandes; Ponti, Moacir Antonelli (2018): *Machine Learning: A Practical Approach on the Statistical Learning Theory*. Springer Nature Switzerland AG, Cham. <https://doi.org/10.1007/978-3-319-94989-5>
- Draper, Norman; Smith, Harry (1998): *Applied Regression Analysis*. Wiley, New York.
- Itskov, Mikhail (2019): *Tensor Algebra and Tensor Analysis for Engineers with Applications to Continuum Mechanics. Fifth Edition*. Springer Nature Switzerland AG, Cham. <https://doi.org/10.1007/978-3-319-98806-1>
- Kazhamiakin, R. et al (2015): *Using Gamification to Incentivize Sustainable Urban Mobility*. In: 1st IEEE International Smart Cities Conference. <https://doi.org/10.13140/RG.2.1.2622.2166>
- La Rocco, Nicolas (2016): *Stiftung Warentest: Google Maps hat im Test vor TomTom die beste Navigation*. Computer Base, Berlin. <https://www.computerbase.de/impresum/>
- Leicht, Luca (2018): *Smartphones gewinnen, Mercedes und Volvo patzen: Durch vernetzte Autos sollen Staus der Vergangenheit angehören. Wir haben aktuelle Echtzeit-Verkehrsdienste getestet, um zu klären, wer am schnellsten ans Ziel kommt – App oder Navi?* Auto Motor Sport, Stuttgart. <https://www.auto-motor-und-sport.de/verkehr/navi-echtzeit-navigationssysteme-test-stau-service/>
- Ott, M. (2018). *Apps effektiv managen und vermarkten*. Springer Vieweg, Wiesbaden. <https://doi.org/10.1007/978-3-658-22296-3>

- Scholz, D. (2018). *Multikriterielle Optimierung*. In: *Optimierung interaktiv*. Springer Spektrum, Berlin, Heidelberg. [https://doi.org/10.1007/978-3-662-57953-4\\_7](https://doi.org/10.1007/978-3-662-57953-4_7)
- Tao, Dacheng; Li, Xuelong; Wu, Xindong; Hu, Weiming; Maybank, Stephen (2006): *Supervised tensor learning*. In: *Knowledge and Information Systems 2006*. Springer-Verlag, London. <https://doi.org/10.1007/s10115-006-0050-6>

**Open Access** This chapter is licensed under the terms of the Creative Commons Attribution 4.0 International License (<http://creativecommons.org/licenses/by/4.0/>), which permits use, sharing, adaptation, distribution and reproduction in any medium or format, as long as you give appropriate credit to the original author(s) and the source, provide a link to the Creative Commons license and indicate if changes were made.

The images or other third party material in this chapter are included in the chapter's Creative Commons license, unless indicated otherwise in a credit line to the material. If material is not included in the chapter's Creative Commons license and your intended use is not permitted by statutory regulation or exceeds the permitted use, you will need to obtain permission directly from the copyright holder.





# Challenges to Turn Transport Behavior into Emission-Friendly Use of Means of Transport

# 4

Torsten Armstroff and Lutz Gaspers

## Abstract

The target of emission reduction in Germany requires a turn from petrol/diesel motorized private transport toward emission-free transport solutions. Besides electrified cars, bicycles, scooters, and pedelecs become more and more common: easy to finance, easy to use, fast in town, reliable, and emission-free. Hence, many local authorities intend to force bicycle use significantly. Almost every German citizen owns a bicycle; however, **roughly** 50% are used less than once a month or not at all.

Bicycle traffic contributes just 11% to Germany's modal split (amount of moves). Other countries nearby indicate that pedelec movement will become a significant player in people movement. The means of transports are just one side of the medal of the turn to future transport opportunities.

Is it necessary to own vehicles, bicycles, and scooters? There are plenty of scenarios, where private ownership of means of traffic does not solve transport problems and/or lacks of availability at a certain point of need.

How does sharing satisfy local transportation needs? How can sharing of emission-free vehicles contribute to a successful future transportation in Germany? The chapter will focus on a few hints to answer these questions, building on findings of studies and field tests and the view beyond the German horizon.

---

T. Armstroff · L. Gaspers (✉)

Competence Center Mobility and Transport, University of Applied Sciences Stuttgart, Stuttgart, Germany

Hochschule für Technik Stuttgart, Stuttgart, Germany

e-mail: [lutz.gaspers@hft-stuttgart.de](mailto:lutz.gaspers@hft-stuttgart.de)

© The Author(s) 2022

V. Coors et al. (eds.), *iCity. Transformative Research for the Livable, Intelligent, and Sustainable City*,

[https://doi.org/10.1007/978-3-030-92096-8\\_4](https://doi.org/10.1007/978-3-030-92096-8_4)

---

**Keywords**

Sustainable mobility · Modal split · Pedelec · Pedelec sharing · Mobility benchmark

---

## 4.1 Development of Modal Split for Germany

iCity’s workpackage “eBike sharing concept for Stuttgart and Tuttlingen” dealt with criteria definition for the use of pedelec sharing. It focused on the shift from motorized private transport towards emission free transport solutions and took up the question of use vs. ownership.

Looking at the use of means of transport in Germany, there is a slight increase in bicycle use within the time frame 2002–2017. However, the overall modal split distribution of means of transport has been quite stable over a long time period. Nearly 60% of traffic is performed by personal car transport, either as driver or as passenger. Regarding the modal split of kilometers, the usage of the car as driver or as passenger sums up to 75% of all moved kilometers. Public transport contributes to 19%, and transport on foot and by bicycle equals 3% of all moves (Table 4.1).

---

## 4.2 Benchmark View of Modal Split for the Netherlands

In the first instance, research circled on the benchmark question of how other people deal with bike traffic and are there significant options for change. The modal split of the Netherlands (Ministerie 2016) differs significantly from Germany. Despite differences in modal split related to means of transport by up to 30%, bicycle use differs by 245% related to amount of moves. Moreover, the difference related to passenger kilometers sums up to 300% (Figs. 4.1 and 4.2).

What makes the use of the bicycle in the Netherlands so different? There are several indicators (Schweighöfer 2019):

- Topologically, there are just a few hills in the Limburg region of the Netherlands. Most of the country is flat.
- Car drivers are to blame for accidents in any case.

**Table 4.1** Modal split for Germany (Bundesministerium 2017)

Modal split ways (%)	2002	2008	2017
On foot	23	24	22
Bicycle	9	10	11
Car—as driver	44	43	43
Cars—as passenger	16	15	14
Public transport	8	8	10



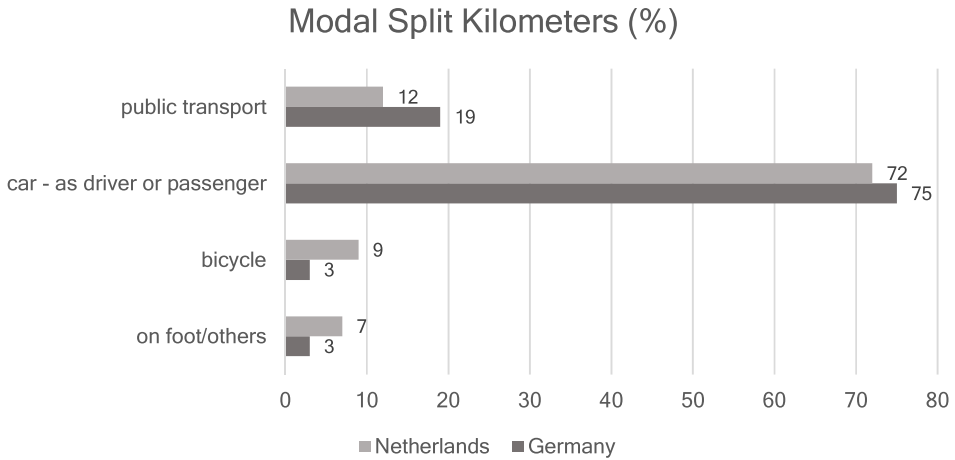


**Fig. 4.1** Modal split kilometers of the Netherlands/Germany (Bundesministerium für Verkehr und digitale Infrastruktur. (2017). Ergebnisbericht Mobilität in Deutschland; Ministerie van Infrastructuur en Milieu. (2026). Mobiliteitsbeeld)

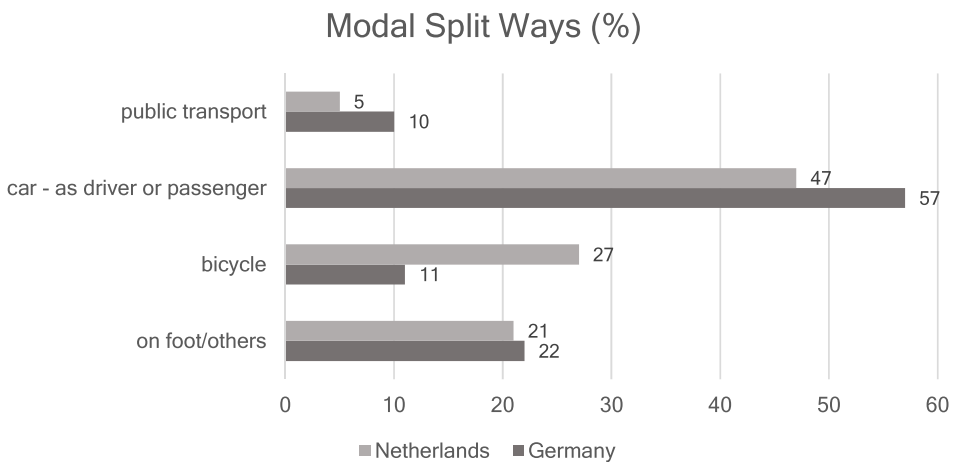


**Fig. 4.2** Modal split ways of the Netherlands/Germany (Bundesministerium für Verkehr und digitale Infrastruktur. (2017). Ergebnisbericht Mobilität in Deutschland; Ministerie van Infrastructuur en Milieu. (2026). Mobiliteitsbeeld)

- Separate roundabouts, tunnels, bridges, traffic lights, and fast tracks are available for bicycles.
- The worldwide biggest bicycle parking garage is located in Utrecht and offers 4500 parking lots, planned to be extended to 20,000, using electronic vacancy guiding system.
- Roughly 40% of the residents use the bike on way to work.

- Every resident owns 1.3 bikes per average.
- Investments in bicycle infrastructure are significantly higher than in Germany (investments in bicycle infrastructure/resident per year: Stuttgart, 5 €; Munich, 2.20 €; Berlin, 4.70 €; Amsterdam, 11 €; Utrecht, 132 €).
- Bicycle routes are marked in different categories (fastest routes, routes through nice areas).
- A country-wide infrastructure program ensures the extension of currently 300 km bicycle fast tracks by additional 600 km (Fietserbond.nl [2020](https://www.fietserbond.nl/)).

The major difference in bicycle use between the Netherlands and Germany are the following pre-conditions that enable bicycle traffic:

- Convenience and safety-related conditions (i.e., it is not mandatory to wear a helmet).
- Broad bicycle routes, consequently separated from car traffic.
- The bicycle belongs to the country’s branding—people identify with bicycles.
- Road construction rules and regulations that support the extension of bicycle traffic—bicycle-focused road construction will enhance bicycle use.
- The influence of mindset related to ecological and health-wise benefits of bicycle use starts at high school.
- Priority for bicycle traffic on the road.
- Integrated design and planning of transport infrastructure taking cross finance solutions for bicycle infrastructure by cities, public transport providers, and the engagement of employers into account.
- Turn minimum amount of car park slots into maximum amount of bicycle slots for office and residential buildings.

---

### **4.3 Sharing as Opportunity to Extend Bicycle and Pedelec Use in Germany**

The use of means of transport is mainly triggered by:

- Its availability and easy-to-use opportunities.
- Target and distance of the route.
- The cost of use.
- The comfort and safety it provides on the defined route.
- Ecological sense of responsibility.

Focusing on the share of means of transport with the target to reduce traffic emissions, it mainly competes with the private owned diesel or petrol engine passenger car—always available, easy to use, safe, and high travel comfort—however, expensive, space-consuming, and not environmental friendly.

Transport time to work, combined with long-term transport behavior patterns, is crucial for the choice of means of transport (Viergutz 2011). Moreover, the means of transport used for the way to work significantly influences the use of means of transport for ways outside of work. Twenty-seven percent of moves are related to way of work or at work. They significantly influence the use of means of transport in leisure time, contributing 28% to the modal mix of moves in Germany.

Moving people to multi- or intermodal use of means of transport requires attractive transport opportunities—close at the spot of use and easy to handle. This includes the reservation and usage processes as well as the transport vehicle itself. The abilities of people of different ages need to be taken into consideration. Bike, scooter, and pedelec may become an important role in supporting public transport by bridging the last mile or, in case the distance fits, to replace the passenger car at all.

Field tests with pedelecs in rural areas in the south of Germany (i.e., region of Tuttlingen) show that pedelecs mainly replace bicycles (54%); however, 30% of the test representatives state that they replaced the passenger car. At the downside, 11% of test people replaced walks by pedelec usage and 3% the public transport (Schiele et al. 2020).

Average speed of bicycle and pedelec rides differed in the field test by just 1 km/h (bicycle 11 km/h, pedelec 12 km/h); however, average distance traveled by bicycle (4 km) was significantly shorter than average distance by pedelec rides (7 km). Hence, pedelecs may support car replacement on distances longer than average bicycle rides.

Discussing the topic ownership vs. share of pedelecs, it became clear that the majority of test representatives would enjoy what pedelec sharing offers. Comparing cost of a pedelec sharing systems for small cities like Tuttlingen with the prices customers are willing to pay, it becomes obvious that a pedelec sharing systems require an immense portion of subvention by public or private authorities. Test representatives stated that they are willing to pay 8 €/average for a 1-day pedelec rental.

Pedelec sharing systems require an adequate business model containing:

- Pedelecs.
- Sharing locations and electrification for loading and parking.
- Locking system.
- Maintenance, cleaning, and repair of pedelec and sharing locations.
- Workshop.
- Redistribution services.
- Administration, marketing, and sales.
- Back-end system.
- Energy cost.

Taking actual cost and willingness to pay for share services into account, pedelec sharing systems may just become an attractive business model in case of significant raising cost of ownership for passenger cars. In addition, reduced accessibility of urban areas of interest for cars may influence bike and pedelec sharing.

Two scenarios of business models for bike/pedelec sharing solutions in the region of Tuttlingen have been calculated. Besides the one-time cost to establish the basic services, annual operation cost appears.

Scenario 1 calculates based on a mixed bicycle/pedelec park of 26 bicycles and 14 pedelecs and 80 parking lots at 10 rental stations (König et al. 2019). The ratio of annual operation cost (based on 0.64 rentals per bike and day) related to the rental revenues is 3.4:1. Rental frequency is defined based on findings of the study “Public bicycle sharing systems—innovative mobility in cities” for cities with 20,000–100,000 inhabitants (Bundesministerium 2014).

Scenario 2 calculates with 50 pedelecs at 7 rental stations. Rental price and rental frequency are based on findings of OBIS (Büttner and Mlasowsky 2011). Findings show the ratio of annual operation cost related to the rental revenues is 2.69:1.

Both scenarios don't include one-time ramp-up efforts and installation cost. Hence, a sustainable acceptance for pedelec sharing can actually just be raised by advertising revenues, public subvention, and subvention of corporate mobility management activities.

The project “Ebike pendeln,” established by the Senate of Berlin, shows that the engagement of companies to make pedelecs and related infrastructure for parking and loading available will significantly reduce car usage and emission (Czowalla 2016). However, the change of long-term mobility behavior requires long time test phases for mobility options in order to convince people for emission-free mobility solutions.

The project “Ebike pendeln” provided 324 persons the opportunity to test pedelec use for way to work in a time frame of 8 weeks. The overall project lasted 2 years.

---

## 4.4 Necessity for Further Research

Our findings suggest that reaching transformation targets for emission-free transport in Germany starts with mindset change. How can transport behavior be significantly changed in short time frame, while it has been stable for decades? This needs to be investigated further besides providing technological and infrastructure improvements to attract emission-free means of transport. Furthermore, business models that attract the economical motivation for installation and use of emission-free means of transport need to be investigated further.

---

## References

- Bundesministerium für Verkehr und digitale Infrastruktur. (2014). Innovative Öffentliche Fahrradverleihsysteme. Ergebnisse der Evaluation und Empfehlungen aus den Modellprojekten  
Bundesministerium für Verkehr und digitale Infrastruktur. (2017). Ergebnisbericht Mobilität in Deutschland

- Fietserbond.nl. (2020). Snelfietsroutes. <https://www.fietzersbond.nl/ons-werk/mobiliteit/snelfietsroutes> (Accessed 24 August 2020)
- J. Büttner, J. Mlasowsky. (2011). Optimising bike sharing in European cities. OBIS
- J. König, J. Weißbeck, D. Creuz. (2019). Entwicklung eines Fahrradverleihsystems für die Stadt Tuttlingen - Auswertung eines Feldversuchs und Ableitung von Handlungsempfehlungen für die Stadt Tuttlingen. Hochschule für Technik Stuttgart.
- L. Czowalla. (2016). EBike Pendeln, Nutzungs- und Akzeptanzkriterien von Elektrofahrrädern im beruflichen Pendelverkehr, Abschlussbericht der wissenschaftlichen Begleitforschung, Hochschule für bildende Künste Braunschweig, Institut für Transportation Design.
- Ministerie van Infrastructuur en Milieu. (2016). Mobiliteitsbeeld. [http://web.miniemen.nl/mob2016/documents/Mobiliteitsbeeld\\_2016.pdf](http://web.miniemen.nl/mob2016/documents/Mobiliteitsbeeld_2016.pdf) (Accessed 24 August 2020)
- P. Schiele, E. Sahin, R. Zellhöfer. (2020). Handlungsempfehlungen für ein Pedelec-Sharing-System in der Stadt Tuttlingen. Hochschule für Technik Stuttgart.
- Schweighöfer, K. (2019). Das Königreich der Radler. Deutschland.de. <https://www.deutschland.de/de/topic/leben/fahrradland-niederlande-warum-das-fahrrad-so-beliebt-ist>. Accessed 21 January 2020.
- Viergutz, D. (2011). Determinanten der Verkehrsmittelwahl. Bachelor Thesis, Technische Universität Dresden.

**Open Access** This chapter is licensed under the terms of the Creative Commons Attribution 4.0 International License (<http://creativecommons.org/licenses/by/4.0/>), which permits use, sharing, adaptation, distribution and reproduction in any medium or format, as long as you give appropriate credit to the original author(s) and the source, provide a link to the Creative Commons license and indicate if changes were made.

The images or other third party material in this chapter are included in the chapter's Creative Commons license, unless indicated otherwise in a credit line to the material. If material is not included in the chapter's Creative Commons license and your intended use is not permitted by statutory regulation or exceeds the permitted use, you will need to obtain permission directly from the copyright holder.





# Positioning of Pedelecs for a Pedelec Sharing System with Free-Floating Bikes

5

Paul Rawiel

## Abstract

For intelligent mobility concepts in growing urban environments, positioning of transportation vehicles and generally moving objects is a fundamental prerequisite. Global Navigation Satellite Systems (GNSS) are commonly used for this purpose, but especially in urban environments under certain conditions, they offer limited accuracy due to buildings, tunnels, etc. that can deviate or mask the satellite signals. The use of existing built-in sensors of the vehicle and the installation of additional sensors can be utilized to describe the movement of the vehicle independently of GNSS. This conforms to the concept of dead reckoning (DR). Both systems (GNSS and DR) can be integrated and prepared to work together since they compensate their respective weaknesses efficiently. In this study, a method to integrate different inertial sensors (gyroscope and accelerometer) and GNSS is investigated. Pedelecs usually do not have many inbuilt additional sensors like it is the case in cars; therefore, additional low-cost sensors have to be used. An extended Kalman filter (EKF) is the base of calculations to perform data integration. Driving tests are realized to check the performance of the integration model. The results show that positioning in situations where GNSS data is not available can be done through dead reckoning for a short period of time. The weak point hereby is the calibration of the accelerometer. Inaccurate accelerometer data cause increasing inaccuracy of the position due to the double integration of the acceleration over time.

---

P. Rawiel (✉)  
Hochschule für Technik Stuttgart, Stuttgart, Germany  
e-mail: [paul.rawiel@hft-stuttgart.de](mailto:paul.rawiel@hft-stuttgart.de)

© The Author(s) 2022  
V. Coors et al. (eds.), *iCity. Transformative Research for the Livable, Intelligent, and Sustainable City*,  
[https://doi.org/10.1007/978-3-030-92096-8\\_5](https://doi.org/10.1007/978-3-030-92096-8_5)

51

---

**Keywords**

GNSS · Dead reckoning · Extended Kalman filter · Vehicle positioning · Sensor integration

---

## 5.1 Introduction

In this paper, the integration of different sensors for the positioning of moving vehicles is presented. Most available positioning solutions use freely available services from Global Navigation Satellite Systems (GNSS). Due to the satellite signals being shadowed or reflected when a vehicle passes through urban canyons or tunnels, its position is falsified or in the worst case cannot be determined at all. A more accurate and reliable position is required for modern mobility concepts like pedelec sharing systems with a free-floating pedelec fleet. If the sharing system shall work with free-floating pedelecs, the positions of the pedelecs have to be stored in the backend of the system when the customer ends the rent. This position is shown to possible following users and staff. Therefore, a minimum position accuracy that enables the finding of the pedelec is required, but not guaranteed by GNSS solutions under certain conditions often occurring in urban environments. The research presents a low-cost system for the enhancement of vehicle positioning by integrating a number of additional low-cost sensors to generate a trajectory that the vehicle has passed through from the moment on when the GNSS position quality is questionable. A focus is set on the accuracy of the accelerometer. The data of this sensor is used to calculate distances in periods of lack of GNSS signals. Due to the double integration of the acceleration, this data accuracy is crucial for the position determination. In order to compensate GNSS limitations in urban environments, dead reckoning (DR) methods based on an on-board multi-sensor system are used in this investigation. The aim of the developed system is to reach an accuracy of 10–15 m for the position, also on sections of the trajectory, where GNSS is not available or strongly falsified. This accuracy of 10–15 m is considered sufficient for users and technical staff of a pedelec sharing system to find the pedelecs.

IMU have been integrated in different multi-sensor platforms for different purposes. However, the drift of IMU sensors results in significant accumulated errors for long-term position and orientation measurement. Different approaches to handle these errors have been presented in many researches. Zhao and Wang (2012) used magnetometers and ultrasonic sensors and integrated these data with the inertial sensor data in a Kalman filter for motion measurement of smaller objects in an indoor environment. Another research for indoor navigation where a Kalman filter was used for the fusion of data of a high-sensitivity GPS receiver, WLAN-based positioning, accelerometer data and a digital compass was presented by Bhuiyan et al. (2012). Kalman filtering is not the only possible way to integrate data of different types of sensors. El-Sheimy, Chiang and Noureldin (2006), Kakinuma and Hashimoto (2012) and Atia, Donnely, Noureldin and Korenberg (2014)

published their researches about navigation using neural networks, SLAM algorithms and landmark detection or particle filters for the integration of multiple sensors into a navigation system.

---

## 5.2 Materials and Methods

Dead reckoning as a navigation method can substitute GNSS positioning for a limited period of time. General principles of dead reckoning can be found in Groves (2007) and Grewal, Andrews and Bartone (2020). The main drawback of this method is that displacement, heading and attitude are subject to cumulative errors over time. The total deviations depend on sensor's accuracy, data quantization errors and temporal frequency of the input data (Groves, 2007, pp. 217–249). Time synchronization of the data of the different sensors is also an issue that has influence on the position accuracy (Ding, Wang, Li, Mumford, & Rizos, 2008).

The multi-sensor platform used in this research consists of a board with a microcontroller on which the following sensors were soldered: As a reference, an Xsens MTi-G-700 with an integrated GNSS antenna was used. As a low-cost system, the sensor unit SMI130 from Bosch was used combined with a GNSS receiver NEO-M8 (u-blox). The sensors were integrated into the telecommunication unit (TCU) that is placed on the cockpit of the pedelec. A Kalman filter (KF) is applied to integrate the data from the sensors and to optimize the results statistically minimizing derived errors. The theoretical background of the sensor integration using a KF can be found in Grewal and Andrews (2001), Grewal, Weill and Andrews (2007) and Groves (2007). The MATLAB toolbox NaveGo (Gonzales, Giribet, & Patiño, An approach to benchmarking of loosely coupled low-cost navigation systems, 2015a) (Gonzales, Giribet, & Patiño, NaveGo: a simulation framework for low-cost integrated navigation systems, 2015b) was used to integrate the data of the different sensors in a loosely coupled system using an extended Kalman filter. The MATLAB toolbox NaveGo allows to analyse the quality of a low-cost IMU using the Allan variance, to process the sensor data in a strapdown algorithm and to integrate them with GNSS measurements. Furthermore, the toolbox allows to simulate errors in the sensor data. The MATLAB scripts are available as open source over the platform GitHub (Gonzales, Giribet, & Patiño, NaveGo: a simulation framework for low-cost integrated navigation systems, 2015b).

The general workflow presented in Fig. 5.1 was followed to obtain the results presented in the subsequent section:

The global coordinate system into which the data of each sensor have to be transformed is the UTM coordinate system. Deeper information about coordinate systems and transformations especially for navigation purposes can be found in Grewal, Weill and Andrews (2007); Grewal, Andrews and Bartone (2020); and Yang, Snyder and Tobler (1999). Diebel (2006) describes the necessary concepts to understand the mathematical principles involved in the definition of the orientation of a rigid body in a three-dimensional



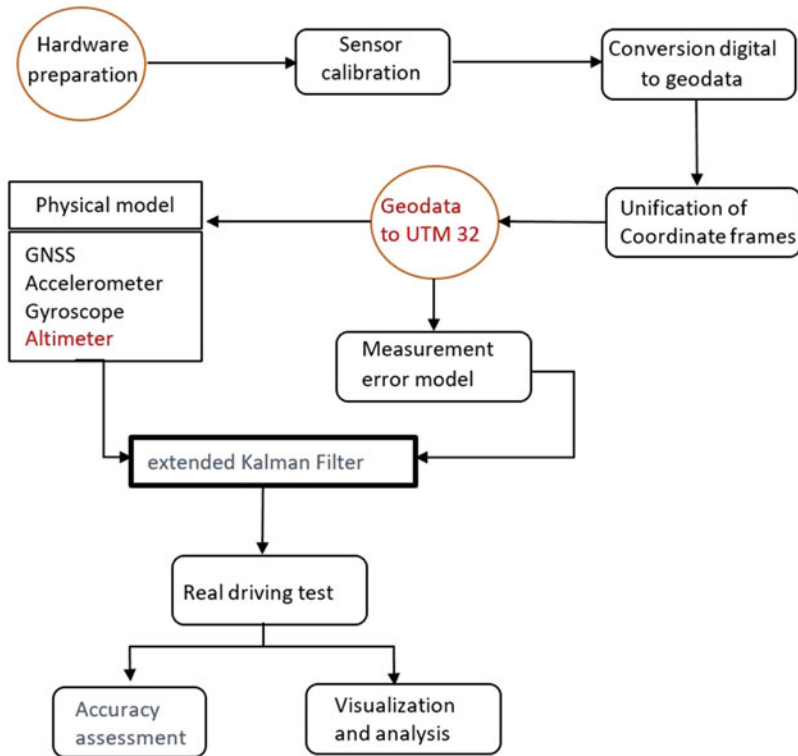


**Fig. 5.1** Methodology and general workflow

space by means of Euler angles and cosine orientation matrix. For the theoretical background of the projection of the three-dimensional coordinates to plane UTM coordinates, please refer to Snyder (1987).

## 5.3 Sensor Tests

In this chapter, some sensor tests that were performed will be described to show the error behaviour of the sensors.

### 5.3.1 The Influence of Temperature

To investigate the behaviour of the gyroscope under changing temperature, Vallejo Orti (2015) used a similar sensor setup and performed several experiments introducing the gyroscope in a temperature-controlled space and recording the measurements of the gyroscope for this theoretical zero rate angle status (the device remained totally

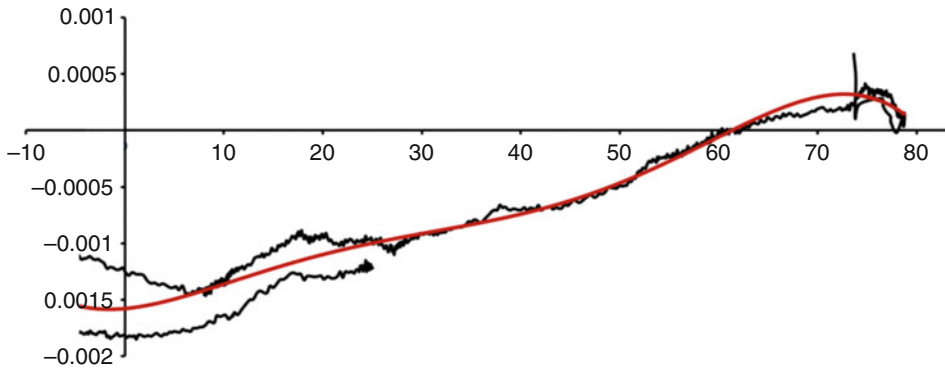


**Fig. 5.2** Experimental results for Temperature-Offset calibration (black) and corresponding adjusted curve (red) for Yaw angular velocity ( $\omega\Psi$ ) (Vallejo, 2015)

motionless). The output data derived from these experiments can be used to create a statistical adjustment based on *least squares method* (Tennissen, 2003). The best fit to the determined offset curve is a fifth-order polynomial function. Adjustment result and measured zero rate curves for the yaw angle are shown in Fig. 5.2.

### 5.3.2 Variation of the Total Acceleration in Relation to the Inclination of the Sensor

Several series of measurements under different inclinations were taken. The following figure shows how the total gravitation as the square root of the sum of the squares of the acceleration measured on each of the three axes of the accelerometer changes with the inclination (Rossknecht, 2019). The results are shown in the Fig. 5.3.

## 5.4 Sensor Calibration and Alignment

As the inertial measurement unit with its accelerometer and gyroscope has its own coordinate system, the three axes of the accelerometer as well as the gyroscope must be aligned to the axes of the navigation coordinate system. The data of the gyroscope can be falsified by the drift as described in Sect. 5.3.1. This drift can be determined each time when the sensor is without motion. In this situation, the angle velocities measured by the sensor correspond to the drift. So the measurements can be easily corrected. For longer periods of the sensor in motion, a predefined calibration curve as described above can be helpful to improve the data.

The accelerometer always measures the earth acceleration that is approximately  $9.81 \text{ m/s}^2$  in direction of the force of gravity. This can be used to align the z-axes of the

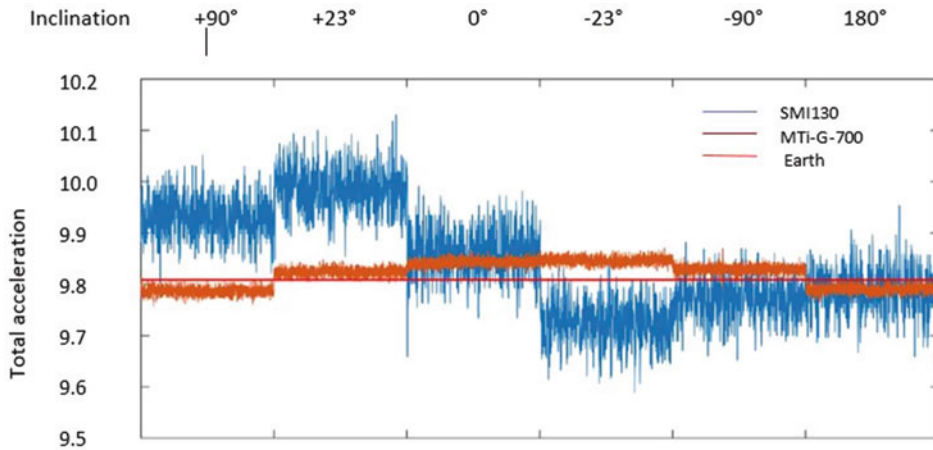


**Fig. 5.3** Total acceleration in relation to the roll angle of the sensor unit (Rossknecht, 2019)

**Table 5.1** Results of the accelerometer calibration

Axes	Bias	Scale
$X$	-0.01935202	1.00006765
$Y$	-0.01358702	0.99970273
$Z$	0.03754575	1.00018655

accelerometer to the direction of gravity when the sensor is without motion. For further processing of the data in the Kalman filter, the earth acceleration must be eliminated in order to use only accelerations that cause a movement of the vehicle. The raw data of the accelerometer can include a bias and a scale factor that cause errors in the data. In Grewal, Weill and Andrews (2007), a method is proposed to determine this bias and scale. For the sensor data used in this research, the following results were obtained:

The following figure shows that the calibration data is not stable over time. For the data shown in this figure, the sensor remained without motion for a certain time, then was accelerated in direction of the  $x$ -axes of the sensor and then remained without motion again. In the upper graphics of the figure, one can see that in the initial motionless period, the acceleration values that were corrected with the calibration data shown in Table 5.1 correspond to the expected value of zero in the motionless state. After the acceleration, when sensor was without motion again, the bias changed that leads to acceleration values slightly below zero. In the lower graphics of the Fig. 5.4, the effect on the velocity calculation is shown. The sensor does not move, but the continuously slightly negative values of the acceleration lead to an increasing absolute value of the velocity that results in a fast-growing error of the position calculation.

In a former work at the HFT Stuttgart (Vallejo Orti, 2015), this problem was already encountered but not further investigated. In that work, the sensor was placed into a car,

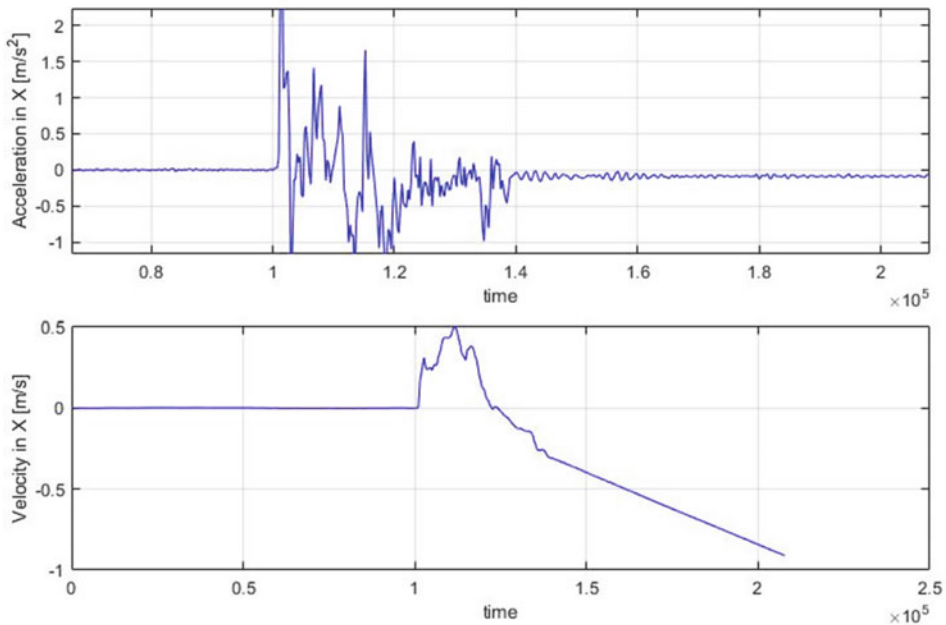


**Fig. 5.4** Instability of calibration data

where the wheel ticks sensor was used to precisely determine a driven distance. The driving direction was derived from the data of the gyroscope, and the accelerometer data did not contribute anymore to the calculation of the position. In the current research with pedelecs, there is also wheel ticks sensor that could be used, but with a single wheel tick per wheel rotation, it is much less accurate and reliable than for a car, where on each wheel, 42 wheel ticks for a complete wheel rotation are detected.

---

## 5.5 Kalman Filter

The Kaman filter is widely used for the integration of GNSS data with inertial and other sensors (Grewal, Andrews, & Bartone, 2020). The main idea of the Kalman filter is to describe a system in motion with its kinematic equations that allows a prediction of the system state that can then be compared to measurements related to the position during the movement. That way a position can be recursively determined out of a system description and a stream of measurements. The system parameters are adjusted permanently based on an assumption for the noise of the system process on one hand and a covariance matrix for the accuracy description of the measured observations on the other hand.

The state  $x$  of a system for any point  $k$  in time can be described with the following state equations:

$$x_{k+1} = \Phi_k x_k + w_k.$$

with the state transition matrix  $\Phi_k$  and the system noise  $w_k$  (Grewal et al., 2020).

With the help of the corresponding measurement model,

$$z_k = H_k x_k + v_k$$

The measurements are linked to the system state with the matrix  $H_k$  describing the relation between the measurements and the state parameters. In  $v_k$ , the noise of the measurements is modelled. The system noise as well as the measurement noise is assumed as unbiased, normal distributed white noise. With the covariance matrices  $Q_k$  and  $R_k$ , it applies:

$$w_k \tilde{N}(0, Q_k) \quad \text{resp.} \quad v_k \tilde{N}(0, R_k)$$

The Kalman equations consist of a prediction of a system state and its corresponding covariance matrix at time  $k$  based on the previous system state at time  $k-1$  (predictor) and a measurement update (corrector).

Time update (predictor):

$$x_{k(-)} = \Phi_k \hat{x}_{k-1(+)}$$

$$P_{k(-)} = \Phi_k P_{k-1(+)} \Phi_k^T + Q_k$$

Measurement update (corrector):

$$K_k = P_{k(-)} H_k^T (H_k P_{k(-)} H_k^T + R_k)^{-1}$$

$$\hat{x}_{k(+)} = \hat{x}_{k(-)} + K_k (z_k - H_k \hat{x}_{k(-)})$$

$$P_{k(+)} = P_{k(-)} - K_k H_k P_{k(-)}$$

Here  $K_k$  is the Kalman gain matrix. It can be interpreted as a weight matrix applied to the difference between the  $k$ th measurement  $z_k$  and the *expected measurement*  $H_k \hat{x}_{k(-)}$  based on the a priori estimate  $\hat{x}_{k(-)}$ .

$\hat{x}_{k(-)}$  and  $P_{k(-)}$  are the a priori values for the state vector and its covariance matrix before the information in the measurements is used.  $\hat{x}_{k(+)}$  and  $P_{k(+)}$  are the corresponding a posteriori values after the measurements have been used.

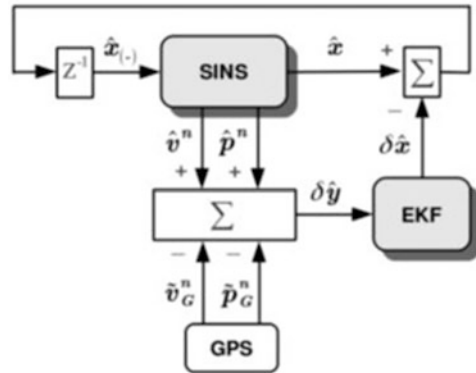
### 5.6 Findings and Results

During several driving tests (Rossknecht, 2019), data with the previously described sensors were collected and processed using the NaveGo fusion algorithm ((Gonzales, Giribet, & Patiño, An approach to benchmarking of loosely coupled low-cost navigation systems, 2015a), (Gonzales, Giribet, & Patiño, NaveGo: a simulation framework for low-cost integrated navigation systems, 2015b)). This algorithm realizes a sensor integration in a loosely coupled system. The navigation solutions of the INS calculated in a strapdown inertial navigation system (SINS) and the GNSS positions are integrated in an extended Kalman filter (EKF). The following Fig. 5.5 shows how SINS, GNSS and EKF work together.

The calculated navigation solution was exported to a KML file to be visualized in Google Earth. The navigation solution of the low-cost sensors carried by the TCU of the pedelec can thus be compared to the navigation solution provided by the sensor unit of Xsens MTi-G-700.

It can be seen that in open area where GNSS signals are not significantly delimited, the two algorithms produce mainly the same results. In regions where GNSS data reception is critical, differences become visible. In the upper left part of the image, it can be seen that the NaveGo solution deviates from the street where the real trajectory led through. In underground passages (lower right part of the image), differences between the two algorithms can be observed as well. In this test, the Xsens fusion algorithm (that is not published by Xsens) in combination with the Xsens sensor data produces a better

**Fig. 5.5** Diagram of SINS, GNSS and EKF integration (Gonzales, Giribet, & Patiño, NaveGo: a simulation framework for low-cost integrated navigation systems, 2015b)



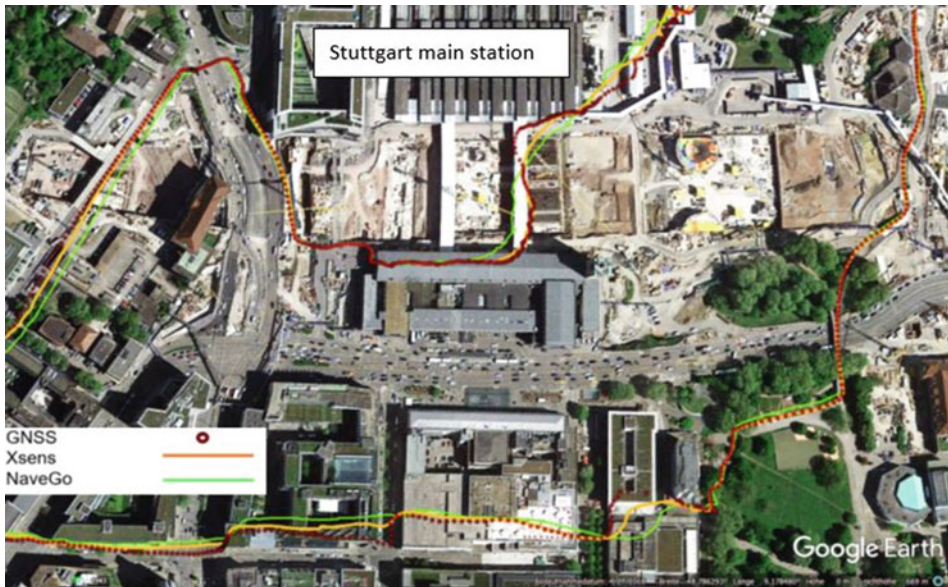


**Fig. 5.6** Comparison of the solutions of the sensor fusion using the Xsens algorithm (orange) and the NaveGo algorithm (green) (Rossknecht, 2019)

navigation solution than the low-cost sensors combined with the NaveGo algorithm (Rossknecht, 2019).

The main goal of the research was to improve the positions that can be obtained with a GNSS antenna in situations when GNSS signals are disturbed or not available at all. To test GNSS reception failure, the pedelec was driven into an underground car park. Both the GNSS antenna of the TCU and the GNSS of the Xsens MTi-G-700 still delivered data after entering the underground car park. The GNSS signals in this case can reach the antenna only through being reflected and thus inevitably produce erroneous positions. Due to the high weight that is applied to the GNSS data in both algorithms, the GNSS data dominates in the calculation of the position that can be seen in the Fig. 5.6.

The yellow line is the reference trajectory where the pedelec has been driven. The left image shows the solution of the low-cost sensor data processed in the NaveGo algorithm. The image in the middle shows the solution of the MTi-G-700 data processed with the NaveGo algorithm, while the image to the right shows the trajectory produced by the Xsens algorithm using the MTi-G-700 data. It can be seen that the solutions differ from each other but no solution succeeded in approximating the real trajectory (Rossknecht, 2019) (Fig. 5.7).

The next test shows the result of a simulated outage of GNSS signals for a certain period of time (Fig. 5.8).

The yellow line represents the reference trajectory that was followed with the pedelec. The blue dots are GNSS positions. In the centre of the image, this line of GNSS positions is

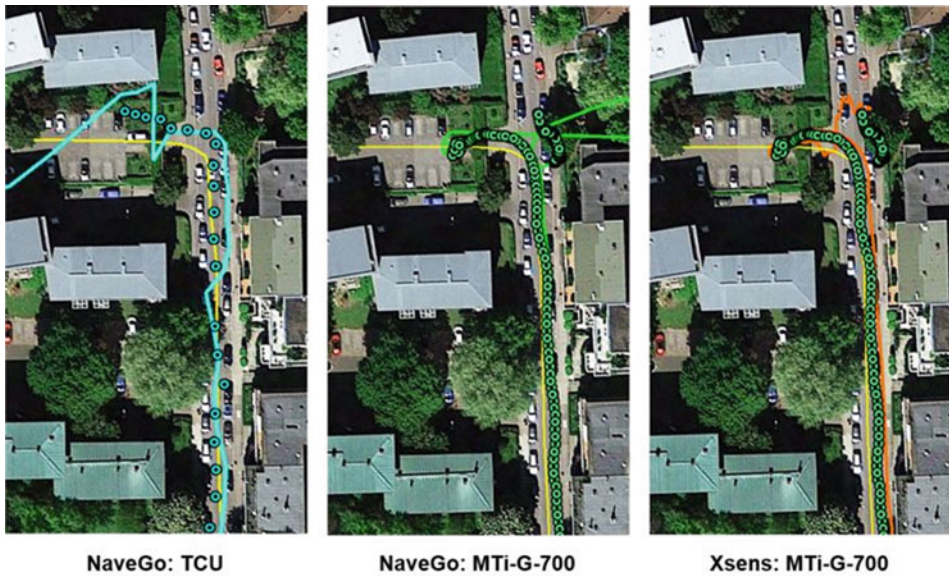


**Fig. 5.7** Comparison of the sensor fusion solutions (Rossknecht, 2019) (Underlying map: Google 2018)

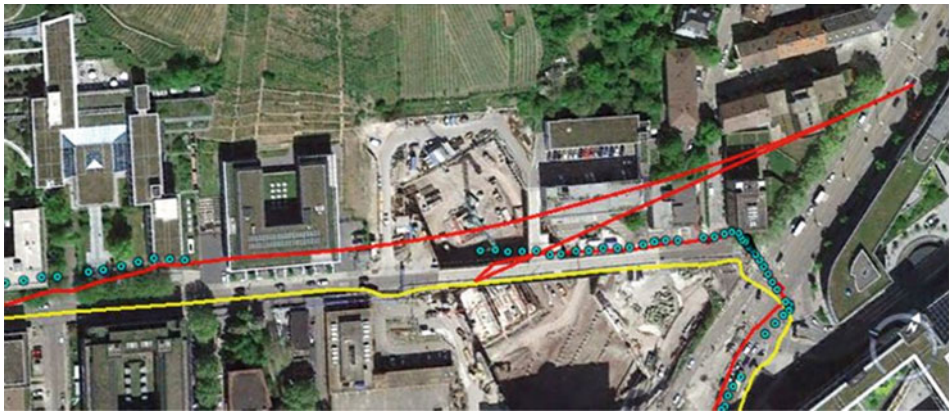


**Fig. 5.8** Simulated GNSS outage for 20 s (Rossknecht, 2019)

interrupted, and the algorithm uses only INS data to calculate positions. The red line represents the trajectory as calculated by the NaveGo algorithm through integration of all available sensor data. It can be seen that during the GNSS outage, the positions drift away from the reference trajectory until GNSS signal is back again after 20 s and the calculated positions snap back more close to the reference trajectory.



This result is not satisfactory for a significant improvement of positioning of pedelec for a sharing system using an additional inertial measurement unit. The reason of the fast drift away from the reference trajectory can be mainly found in the lack of calibration of the accelerometer as described at the beginning of this article. Further research is needed to improve the sensor data by finding ways to calibrate the accelerometer on the fly.

---

## 5.7 Necessity for Further Research

As mentioned above, the result of the use of a low-cost IMU integrated with a GNSS is not satisfactory according to the needs of a pedelec sharing system with free-floating pedelecs.

In Sect. 5.3, some error sources in the IMU data already have been described. Some tests laid open that the data as measured by the IMU lead to fast increasing position errors that make the calculated positions unusable after a short period of time.

Different approaches can be followed to improve the determination of the positions. One possible way of improvement could be to introduce a bias and a scale for the accelerometer into the Kalman filter state vector as unknown parameters and thus estimate these calibration parameters on the fly by the algorithm in time periods when GNSS signals are available.

Another approach is to determine calibration parameters for the accelerometer and the gyroscope in advance based on certain measurements that can be done in a laboratory. Under laboratory conditions, precise calibration parameters can be determined. But as mentioned in Sect. 5.3, the calibration parameters are not stable over time. So methods for recalibration on the fly should be investigated. Such a recalculation of calibration parameters can be done when the sensor is without motion. In such a situation, e.g. the bias of the gyroscope is simply the values of the angle rates that are measured for the three rotation axes. For the accelerometer, it is more complicated due to the fact that earth acceleration is always measured and has to be extracted from the data. If the  $z$ -axis of the accelerometer is not aligned to the direction of gravity force, the earth acceleration influences the measurements on all three axes of the accelerometer. This makes the calculation more complex but not impossible. The main issue is the detection of motionless time periods. In a car, this can be done easily using the wheel ticks sensor. On a pedelec, it will be more difficult to reliably detect a motionless time period. Even if there is no forward motion, e.g. during a stop due to a red signal, the pedelec may be inclined to the left and right. A stopping pedelec is due to the two wheels only much less stable than a car. So, in this field, further research is needed to improve the positioning of pedelecs.

A different approach to improve the position is to use the information of a digital map. In this approach, the form of the driven trajectory is used to match this form with possible trajectories on a map. A promising work about a map matching algorithm has been developed by Fill (2015). Further information about map matching can be found in Alt, Efrat, Rote and Wenk (2003) and Quddus, Ochieng and Noland (2007).

## References

- Alt, H., Efrat, A., Rote, G., & Wenk, C. (2003). Matching planar maps. *Journal of Algorithms* (49), pp. 262-283.
- Atia, M., Donnelly, C., Noureldin, A., & Korenberg, M. (2014). A novel systems integration approach for multi-sensor integrated navigation systems. *2014 IEEE International Systems Conference Proceedings*, pp. 554-558.
- Bhuiyan, M. Z., Kuusniemi, H., Chen, L., Ruotsalainen, L., Pei, L., Guinness, R., & Chen, R. (2012, 06). Utilizing Building Layout for Performance Optimization of a Multi-Sensor Fusion Model in Indoor Navigation. *2012 International Conference on Localization and GNSS, ICL-GNSS 2012*, pp. 1-6.
- Diebel, J. (2006). *Representing Attitude: Euler Angles, Unit Quaternions, and Rotation Vectors*. California: Stanford University.
- Ding, W., Wang, J., Li, Y., Mumford, P., & Rizos, C. (2008, February). Time Synchronization Error and Calibration in Integrated GPS/INS Systems. *ETRI Journal*, 30(1).
- El-Sheimy, N., Chiang, K.-W., & Noureldin, A. (2006, 11). The Utilization of Artificial Neural Networks for Multisensor System Integration in Navigation and Positioning Instruments. *Instrumentation and Measurement, IEEE Transactions on Vol. 55*, pp. 1606 - 1615.
- Fill, K. (2015). *Entwicklung und Untersuchung eines Map-Matching-Algorithmus zur unterstützenden Ortung von Fahrzeugen in Stadtgebieten*. Stuttgart: Bachelor-Arbeit, HFT Stuttgart, unpublished.
- Gonzales, R., Giribet, J., & Patiño, H. (2015a). An approach to benchmarking of loosely coupled low-cost navigation systems. *Mathematical and Computer Modelling of Dynamical Systems*, 21(3), pp. 272-287.
- Gonzales, R., Giribet, J., & Patiño, H. (2015b). NaveGo: a simulation framework for low-cost integrated navigation systems. *Journal of Control Engineering and Applied Informatics*, 2015(17), pp. 110-120.
- Grewal, M., & Andrews, A. (2001). *Kalman filtering: theory and practice using MATLAB* (2 ed.). New York: John Wiley & Sons Ltd.
- Grewal, M., Andrews, A., & Bartone, C. (2020). *Global Navigation Satellite Systems, Inertial Navigation and Integration, fourth edition*. Wiley.
- Grewal, M., Weill, L., & Andrews, A. (2007). *Global Positioning Systems, Inertial Navigation, and Integration* (2 ed.). John Wiley & Sons Ltd.
- Groves, P. (2007). *GNSS, Inertial and Multisensor Integrated Navigation Systems* (2 ed.). Boston, London: Artech House.
- Kakinuma, K., & Hashimoto, M. T. (2012, 12). A novel systems integration approach for multi-sensor integrated navigation systems. *2012 IEEE/SICE International Symposium on System Integration, SII 2012*, pp. 422-427.
- Quddus, M., Ochieng, W., & Noland, R. (2007). Current map-matching algorithms for transport applications: State-of-the art and future research directions. *Transportation Research Part C: Emerging Technologies*, 15(5), pp. 312 - 328.
- Rossknecht, M. (2019). *Integration von GNSS und INS zur Positionsbestimmung von E-Bikes*. Stuttgart: Bachelor-Arbeit, HFT Stuttgart, unpublished.
- Snyder, J. P. (1987). *Map Projections - A Working Manual*. Washington D.C.: U.S. Government Printing Office.
- Teunissen, P. (2003). *Adjustment Theory: an introduction, Series on Mathematical Geodesy and Positioning*. Delft: Delft University Press.
- Vallejo Orti, M. (2015). *Integration and Synchronization of different sensors for the positioning of moving vehicles*. Stuttgart: Master-Thesis HFT Stuttgart, unpublished.

- Yang, Q., Snyder, J., & Tobler, W. (1999). *Map Projection Transformation: Principles and Applications*. CRC Press.
- Zhao, H., & Wang, Z. (2012, 05). Motion Measurement Using Inertial Sensors, Ultrasonic Sensors, and Magnetometers With Extended Kalman Filter for Data Fusion. *IEEE Sensors Journal - IEEE SENS J, Vol. 12*, pp. 943-953. doi:<https://doi.org/10.1109/JSEN.2011.2166066>

**Open Access** This chapter is licensed under the terms of the Creative Commons Attribution 4.0 International License (<http://creativecommons.org/licenses/by/4.0/>), which permits use, sharing, adaptation, distribution and reproduction in any medium or format, as long as you give appropriate credit to the original author(s) and the source, provide a link to the Creative Commons license and indicate if changes were made.

The images or other third party material in this chapter are included in the chapter's Creative Commons license, unless indicated otherwise in a credit line to the material. If material is not included in the chapter's Creative Commons license and your intended use is not permitted by statutory regulation or exceeds the permitted use, you will need to obtain permission directly from the copyright holder.





# Behavioural Development of University Graduates in the Area of Work-Related Mobility: A Study Conducted for the University of Applied Sciences, Stuttgart

Joschua Weißbeck and Lutz Gaspers

## Abstract

Work-related mobility currently makes up the biggest share of the total transport volume in passenger transport and is dominated by private motorized vehicles. The paper is based on research about environmentally friendly modes of transportation performed by students on their way to the University of Applied Sciences, Stuttgart, and whether it has an influence on the mobility behaviour of graduates in work and business traffic or not. Another goal was to find out whether or not one's sustainable mobility behaviour would be maintained throughout the rest of one's professional life. For this, an online survey was conducted with graduates of the University of Applied Sciences, Stuttgart. The results of the survey confirm a very high sustainability in the field of work-related mobility. Previous studies have only looked at education- and work-related mobility behaviour separately and did not research how or if the former has effects on the latter. The comparison of results from those studies with the information provided by the graduates on their behaviour in occupational mobility also confirms an above-average sustainability.

## Keywords

Sustainable mobility · Mobility behaviour · Public transportation · Work-related mobility

---

J. Weißbeck (✉)  
Stadt Waiblingen, Waiblingen, Germany  
e-mail: [joschua.weissbeck@waiblingen.de](mailto:joschua.weissbeck@waiblingen.de)

L. Gaspers  
Hochschule für Technik Stuttgart, Stuttgart, Germany

## 6.1 Introduction

### 6.1.1 Problem Definition

Sustainability is becoming increasingly important in all mobility-related areas. Measures are increasingly taken to reduce pollutant emissions. New forms of sustainable mobility arise extending the range of options. The German Sustainability Strategy stipulates that final energy consumption in passenger transport is to be reduced by 15–20% by 2030 compared to 2005 (Becker and Hoffmann 2018). However, it did not lead to a significant change in final energy consumption so far. This can be explained by the fact that the total amount of passenger transport has risen continuously since 2005 and that the share of motorized private mobility in total transport volume has also risen slightly over the same period (Nobis et al. 2019).

The proportion of traffic generated by travels to the workplace or additional business trips has increased even more in comparison. Business traffic in particular has almost doubled in recent years in terms of the number of trips. Combined work and business traffics currently account for the largest share of total transport volume (Follmer and Gruschwitz 2019). This should be viewed critically, especially regarding the choice of transport mode. Almost two thirds of all trips by full-time workers are carried out by motorized private modes of transportation. This figure is even higher for business purposes (Nobis et al. 2019).

On the other hand, for university students, a much greater flexibility and sustainability in mobility behaviour are becoming apparent. Nobis et al. (2019) found that the share of motorized private mobility among students for transfer to and from university was only 14% in 2017 and has decreased steadily in recent years. The shares of the carbon neutral modes of transportation such as public transportation, bicycle and on foot are much larger here as opposed to people who work full time. Public transport, in particular, has considerably higher shares (Nobis et al. 2019).

The goal of this study is to find out if the choice of carbon neutral means of transportation during the years of study leads to a noticeably higher usage of sustainable mobility in the years after finishing the degree. This would suggest a link between students' mobility behaviour on the way to university and their behaviour later in their careers.

### 6.1.2 Research Definition

There has been hardly any research on the relationship between mobility behaviour during the study period and later working life which is the focus of this study conducted with graduates of the University of Applied Sciences, Stuttgart. The university is located in the city centre of Stuttgart and is close to a multitude of bus stops and train stations. This makes the use of public transportation especially appealing as an alternative to private motorized vehicles. The basis for this research project was earlier studies on the choice of transport

and mobility behaviour of students, which were carried out at the Competence Centre Mobility and Transport (MoVe) of the University of Applied Sciences, Stuttgart, and other institutes (Heckmann 2019; Berghoff and Hachmeister 2018). The study results clearly show that the proportion of students at the University of Applied Sciences, Stuttgart, using sustainable transport for educational purposes is far above the state and national average. Their share of public transport in the total traffic volume is particularly high, and use of motorized private mobility is also correspondingly low. However, it is not possible to say whether and to what extent this sustainability exists in the long term after entering working life. This is the main motivation behind conducting this study.

---

## 6.2 Research Methodology

Due to the fact that the target group consists exclusively of graduates of the University of Applied Sciences, Stuttgart, the best method to collect data was to pursue an online survey, as this would reach almost all potential participants. The exact target group were graduates from the study courses “Infrastructure Management” and “Traffic Infrastructure Management” who have finished their studies within 2011 and 2020. The surveyed graduates were all asked to fill out the entire questionnaire, which means all of the collected data stems from one static group of people. It should also be noted that the surveys’ design allowed for skipping irrelevant questions, e.g. a graduate who has not worked since finishing their studies was not shown any survey questions relating to their mobility behaviour for their way to work. Thus, slightly varying sample sizes for different questions (see Chap. 6.3) were a result of this.

The questionnaire itself was divided into five sections or blocks. The first block included questions about mobility-related behaviours during college. This was followed by questions relating to the professional and occupational mobility of the participants at the beginning of their working lives. In the third section, questions were asked about current behaviour for work-related mobility. The first three sections mainly concentrated on values on the availability and use of modes of transportation, choice of main modes of transportation, selection factors for the choice of modes of transportation, frequency of use, duration and length of trips as well as frequency of business trips that were determined.

The fourth block included general questions on attitudes towards sustainable mobility, followed by questions on personal and socio-demographic characteristics. Many of the questions within the first three blocks were repeatedly asked, as these act as a timeline and thus allow comparability between the different sections. The survey was designed so that both quantitative and qualitative parameters were queried in order to obtain a comprehensive data set.

### 6.3 Data Evaluation

The collected data was comprehensively analysed, and the most important results are presented for the purpose of this paper. The survey data was compared with other studies. In addition, the evaluations of the first three question blocks of the graduate survey were compared to show the development of the participants' mobility behaviour over time.

Roughly 370 people were asked to complete the survey, 91 of which were completed. This is a high response rate of about 25%. Out of those, 70 have started working since their graduation and were also asked to complete the second section of the survey pertaining to work-related mobility behaviour focusing on the first 6 months after being employed. Sixty-eight out of the remaining 70 participants have at least been working for more than 1 year since graduation and were also asked to fill out the third block of questions, which were primarily about their mobility behaviour for their way to work within the last 6 months at the time of taking the survey.

At the time of the survey, most participants were between 20 and 30 years old (74%). Twenty-four per cent were between 31 and 35 years old. There were no significant differences in the answer schemes probably due to the relatively small age range of the two groups. So age differences are not a relevant signifier regarding the following data evaluation, which is a first finding of this study.

#### 6.3.1 Evaluation of Education-Related Mobility Behaviour

Public transport is the main mode of transport used by participants to get to college (see Fig. 6.1). A total of 77% of the respondents stated that they mainly used public transportation. In comparison, the amount of graduates who indicated using a bicycle as their main mode of transportation was 7.7%. For car users, this figure is only 3.3%.

Especially in comparison with the results of the educational commuter survey of the microcensus, there is a clear tendency to show that public transport and sustainable mobility in general were used far more frequently by the surveyed graduates of the University of Applied Sciences, Stuttgart, and that only very few preferred the priority use of cars (Statistisches Bundesamt 2016).

The very strong use of public transport by students for their way to the University of Applied Sciences, Stuttgart, which was already established by previous studies conducted by the university itself, was able to be confirmed to a similar extent in this survey (Heckmann 2019). In a further evaluation, it is now to be examined whether the service provided by public transportation has been met with satisfaction among the participants. Of all survey participants who stated that they used public transport to get to university, 78.6% were satisfied or very satisfied with the service. This figure is slightly above the average value determined for metropolitan areas in the MiD (Mobilität in Deutschland) study (Follmer and Gruschwitz 2019). Likewise, only very few respondents were unsatisfied with the public transport situation for educational purposes (see Fig. 6.2). This means that

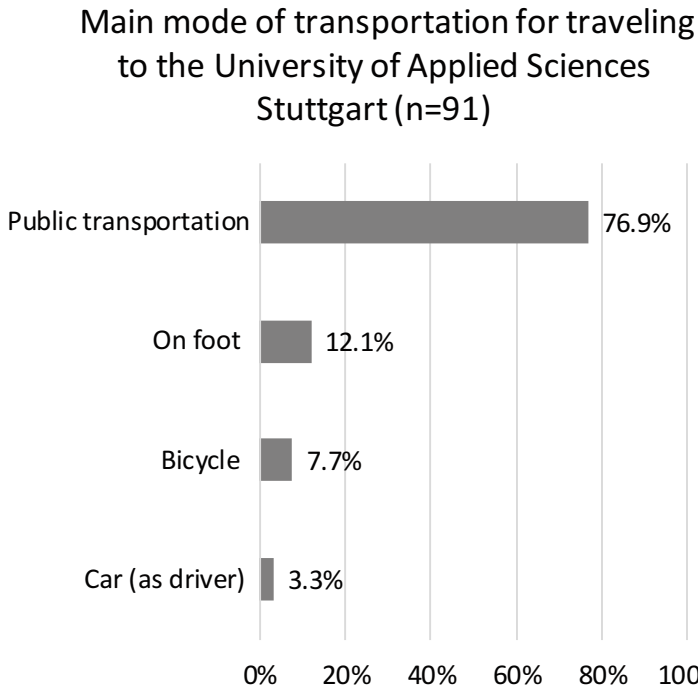


**Fig. 6.1** Main mode of transportation used by the surveyed graduates for traveling to the University of Applied Sciences Stuttgart

the quality of public transport in Stuttgart is generally good, which indicates that the use of this mode of transportation was not adversely affected during the course of study.

Furthermore, the efficiency of public transport in comparison to motorized private mobility for the trip to college was examined. For this purpose, values for mobility time (in minutes) and transport volume (in passenger kilometres) were determined for the various modes of transportation by means of information on route lengths and durations. This made it possible to form efficiency parameters that indicate the number of passenger kilometres per minute. This corresponds to 0.6 passenger kilometres per minute for public transport. The parameter for cars is 0.59 pkm/min. Thus, the use of a car for the way to the University of Applied Sciences, Stuttgart, cannot be classified as more efficient than public transportation. This means that, on average, the survey participants did not lose any time if they chose public transport instead of motorized private vehicles. This creates a better basis for the willingness to also choose sustainable mobility in later professional life.



### Level of satisfaction with public transportation for traveling to the University of Applied Sciences Stuttgart (n=84)

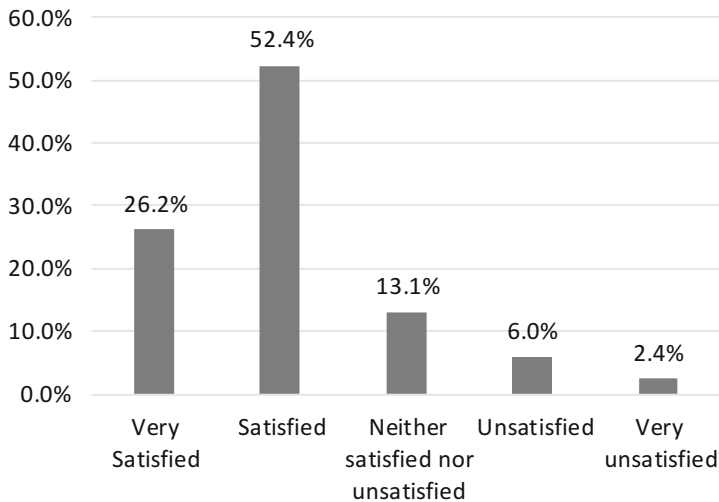


**Fig. 6.2** Level of satisfaction of the surveyed graduates with public transportation for traveling to the University of Applied Sciences Stuttgart

### 6.3.2 Evaluation of Work-Related Mobility Behaviour After Graduation

Public transportation receives an overall share of about 43% of participants who use the said mode of transportation for most of their trips to work. This also means that the mode of transportation was most frequently used by the respondents at the start of their working lives (see Fig. 6.3). Although there is a clear decline compared to the education-related mobility, the figure recorded for commuting to work can still be regarded as very high. Motorized private mobility receives a total of 41.5%, almost a third of which is accounted for by company or business cars. The share of bicycle traffic has also increased slightly. The assumption that the results of this survey could be an indication of a more sustainable mobility behaviour of the graduates is made clear by a comparison with previous studies. The share of public transport is about three times higher than in the microcensus or the MiD study (Statistisches Bundesamt 2016; Nobis et al. 2019). At the same time, the use of motorized private vehicles decreases by about 25% in comparison to those studies. The share of bicycle traffic is roughly the same in all studies.

In order to check the influence of population density or type of environment, evaluations were carried out on the basis of the information provided by the survey participants. First of all, the location of the workplace is considered. Almost half of the respondents worked in a

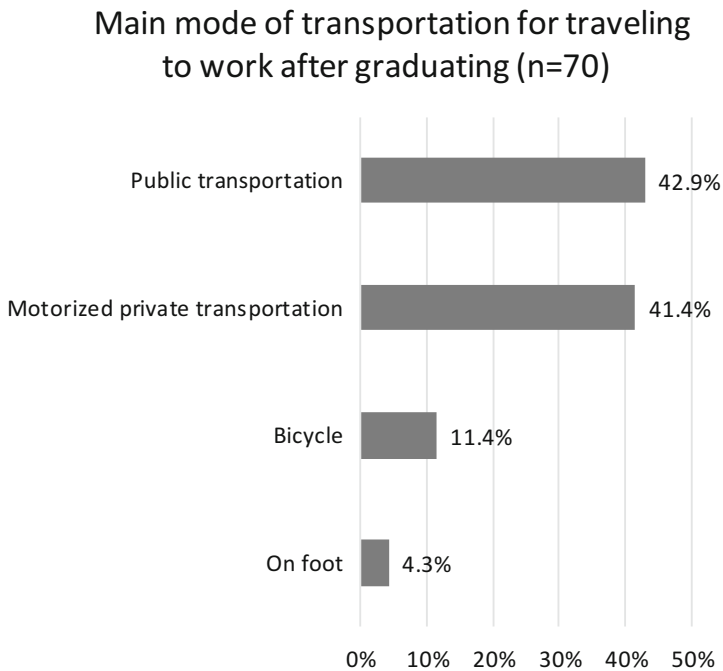


**Fig. 6.3** Main mode of transportation used by the surveyed participants for traveling to work after graduating

city with over 500,000 inhabitants after completing the study. An additional 20% had a workplace in towns with over 100,000 to 500,000 inhabitants. The remaining third worked in places with a smaller population. Half of the said third even worked in very rural areas with a population of less than 10,000.

In order to identify possible correlations, the main mode of transportation was considered in relation to the number of inhabitants (see Fig. 6.4). This confirms that the participants almost exclusively use motorized private mobility as their main mode of transportation for trips to work in towns with fewer than 10,000 inhabitants. Car use decreases with increasing population. At the same time, the use of public transportation in particular increases. In cities with more than 500,000 inhabitants, more than half of the participants used public transportation to get to work. Similarly, cycling and walking in urban areas are more likely to be considered for work-related mobility. This is mainly due to the fact that more respondents have to travel shorter distances to reach their workplace and that the use of these modes of transportation is therefore a reasonable option. All in all, a higher degree of sustainability in the context of commuting can thus be observed among the surveyed graduates, particularly when living and working in urban areas. The efficiency of public transportation in those areas is comparable to that of motorized private vehicles. In most cases, the mobility behaviour from education-related mobility can be continued

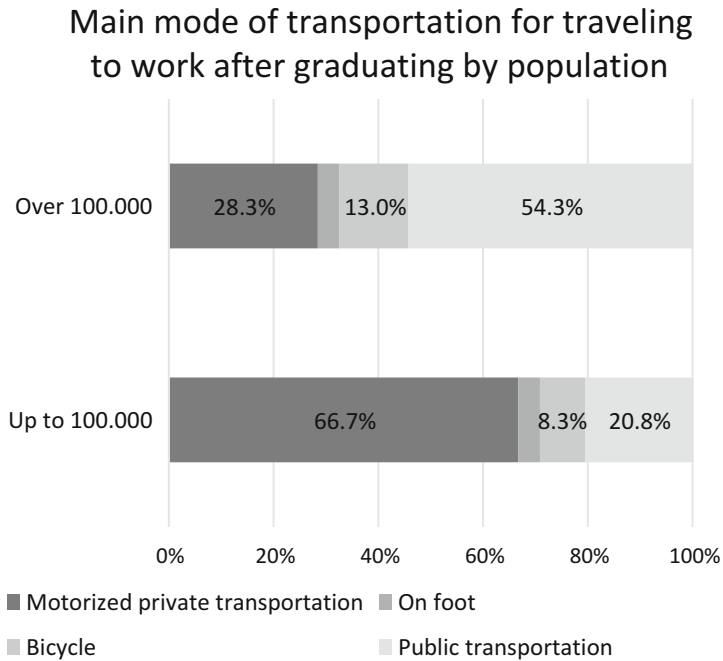


**Fig. 6.4** Main mode of transportation used by the surveyed participants for traveling to work after graduating by population

without additional obstacles. The shorter average commuting distances also mean that using a bicycle or walking is a realistic option for more respondents. In rural regions or places with low population, private motorized transport is almost exclusively seen as the only sensible option, as public transport is associated with high losses of time and flexibility.

### 6.3.3 Evaluation of Current Work-Related Mobility Behaviour

The surveyed graduates chose a car more often as the main mode of transportation later in their career than at the beginning of their employment (see Figs. 6.3 and 6.5). Both the share for private and company car usage has increased. Overall, public transportation sees a decrease of about 5%, although the overall share of 38.3% is still well above the average values of the microcensus or the MiD study. Even now environmentally friendly mobility is still primarily chosen by slightly more than half of the respondents for commuting to work and thus, despite the decline, represents a much higher proportion compared to the microcensus or MiD, in which it accounts for only about one third. As public transportation in particular has lost shares, one reason for this could be a greater regional shift of

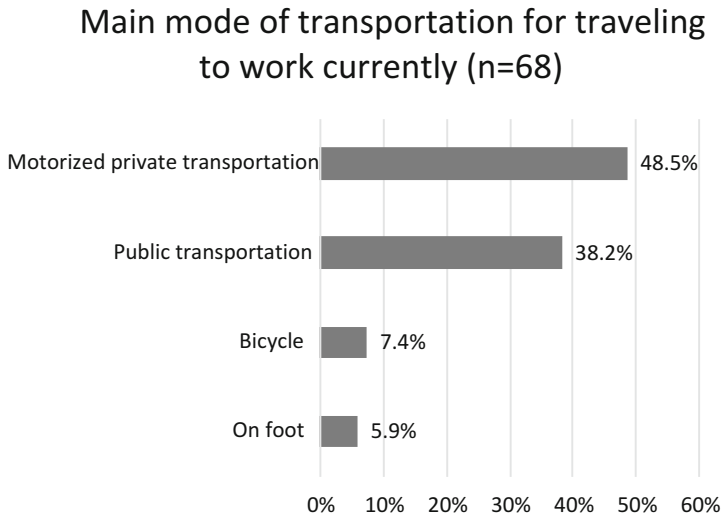


**Fig. 6.5** Main mode of transportation used by the surveyed graduates for traveling to work currently

participants to places with more rural structures. Here it is more likely that cars will be chosen as the main mode of transportation.

Over the period under study, respondents have increasingly moved to cities with populations of less than 500,000. In the year of the study conduct 2020, the majority of the surveyed graduates work or live in cities with up to 100,000 inhabitants. Thus, over the period under study, more graduates have moved to rural or suburban areas. This migration could explain why motorized private mobility is used more in the current occupational situation, especially if both workplace and a participant's home are outside of a large city. In this case, the probability of using a mode of transportation other than a car for commuting to work decreases significantly.

The evaluation of the choice of main mode of transportation by population segments validates the assumption of increased relevance of motorized private vehicles outside large cities (see Fig. 6.6). Regarding all categories of less than 10,000 to 100,000 inhabitants, more respondents, both in terms of pure number and proportionately, used the car more often as their main means of work-related mobility. As a result, public transportation is becoming even less important in these segments and is being considered even less frequently. A very high usage of sustainable transport can be observed for the group of participants whose place of work has a population of more than 100,000. Here, environmentally friendly means of transport are used by the surveyed university graduates just as much as at the beginning of their working lives.

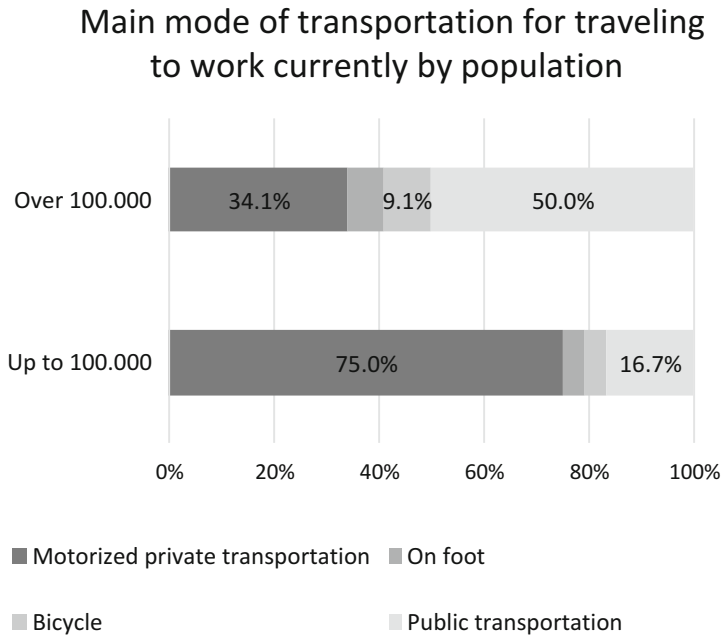


**Fig. 6.6** Main mode of transportation used by the surveyed graduates for traveling to work currently by population

## 6.4 Conclusion

In comparison to other studies, sustainable mobility is used much more often at the beginning of employment to get to work than is generally the case for employed people.

The study shows that the very high use of public transport during college also leads to an increase in usage of public transportation for commuting to work. This development remains the same throughout the career.

However, other factors such as measures of company mobility management and the regional structures in which workplace and homes are located shape work-related mobility behaviour of graduates. This spurs or limits the influences created over the course of their studies.

The study shows that mobility behaviour during studies will be continued after graduation. Paving the way for more use of sustainable transport during college time will lead to a more conscious choice of mode of transportation in the long run. A sustainable design of mobility in the context of transportation for the purpose of education can significantly influence and improve the establishment of more environmentally friendly behaviour in work-related mobility.

## References

- Becker, H., Hoffmann, J. (2018). Nachhaltige Entwicklung in Deutschland – Indikatorenbericht 2018, Statistisches Bundesamt, Wiesbaden
- Berghoff, Sonja; Hachmeister, Cort-Denis (2018): Verkehrsmittel für den Weg zur Hochschule: Wie Studierende ihre Hochschule erreichen - gestern und heute, Centrum für Hochschulentwicklung, Gütersloh
- Follmer, R., Gruschwitz, D. (2019). Mobilität in Deutschland – MiD Kurzreport Ausgabe 4.0. Studie von infas, DLR, IVT und infas 360 in Auftrag des Bundesministers für Verkehr und digitale Infrastruktur, Bonn; Berlin
- Heckmann, R. (2019). Analyse des Mobilitätsverhaltens an innerstädtischen Hochschulen am Beispiel der Hochschule für Technik Stuttgart, Stuttgart
- Nobis, C., Kuhnimhof, T., Follmer, R., Bäumer, M. (2019). Mobilität in Deutschland – Zeitreihenbericht 2002 – 2008 – 2017. Studie von infas, DLR, IVT und infas 360 in Auftrag des Bundesministers für Verkehr und digitale Infrastruktur, Bonn; Berlin
- Website statistisches Bundesamt (Bildungspendler Mikrozensus) (2016): <https://www.destatis.de/DE/Themen/Arbeit/Arbeitsmarkt/Erwerbstaetigkeit/Tabellen/pendler2.html>

**Open Access** This chapter is licensed under the terms of the Creative Commons Attribution 4.0 International License (<http://creativecommons.org/licenses/by/4.0/>), which permits use, sharing, adaptation, distribution and reproduction in any medium or format, as long as you give appropriate credit to the original author(s) and the source, provide a link to the Creative Commons license and indicate if changes were made.

The images or other third party material in this chapter are included in the chapter's Creative Commons license, unless indicated otherwise in a credit line to the material. If material is not included in the chapter's Creative Commons license and your intended use is not permitted by statutory regulation or exceeds the permitted use, you will need to obtain permission directly from the copyright holder.





# Cargo-Hitching in Long-Distance Bus Transit: An Acceptance Analysis

# 7

Vanessa Meyer, Sarah Lang, and Payam Dehdari

## Abstract

The combination of freight transport and mobility—also known as cargo-hitching—is a form of delivery that has been implemented in various modes of transport. This concept is already widely used in Europe, Africa and North America in long-distance bus transport and ensures parcel delivery via the cargo compartment of long-distance buses. This paper aims to investigate the acceptance of cargo-hitching in long-distance bus transport in Germany. For this purpose, first the term cargo-hitching is defined, and an overview of cargo-hitching concepts in long-distance bus transport worldwide is given. In the following, the principles of attitudinal acceptance are explained. A modified version of the UTAUT2 model was used as the basis for an empirical study in the form of a quantitative online survey ( $n = 245$ ). The results provide information about factors influencing acceptance as well as wishes and requirements of potential users. Parts of the UTAUT2 model were verified by regression analysis. It was shown that the variables' habit, price value, hedonic motivation, performance expectancy and social influence predict the behavioural intention to use cargo-hitching in our sample significantly ( $p < 0.05$ ). Furthermore, risks, benefits and willingness to pay were determined, which could contribute to the development of a business model. These included measures to improve transparency, security and information flow of the cargo-hitching process.

---

V. Meyer (✉) · S. Lang · P. Dehdari  
University of Applied Sciences Stuttgart, Stuttgart, Germany  
e-mail: [02meva1mul@hft-stuttgart.de](mailto:02meva1mul@hft-stuttgart.de)

© The Author(s) 2022  
V. Coors et al. (eds.), *iCity. Transformative Research for the Livable, Intelligent, and Sustainable City*,  
[https://doi.org/10.1007/978-3-030-92096-8\\_7](https://doi.org/10.1007/978-3-030-92096-8_7)

77

---

**Keywords**Cargo-hitching · Urbanization · Metropolitan area · Acceptance · Mobility

---

## 7.1 Introduction

Particularly noteworthy is the transport of parcels by bus, as it is already established in countries such as Sweden, the USA and Canada (Bussgods 2020; Greyhound Freight 2020; Maritime Bus 2020). This system enables same-day delivery between different bus stops and leads to a concentration of packages on routes that are already in use (Arvidsson et al. 2016). In Germany, however, despite a well-developed long-distance bus network maintained by the provider FlixBus, which is the biggest far-distance bus operator in Germany, several field trials of similar parcel transport systems have failed, and no comprehensive business model has been established (Deutsche Verkehrs-Zeitung 2015). Stakeholders should be involved in the development of a new business model to guarantee its success (Van Duin et al. 2019; Bektaş et al. 2017). In the field of logistics, critics have observed that only the ideas of companies are properly taken into account in the development of new concepts, while the needs and wishes of customers are hardly considered (Wang et al. 2018). A successful business model maximizes adoption of a new concept by meeting identified customer needs, wishes and demands (Ram 1989). However, as far as known, no study thus far has explicitly addressed customer wishes in connection with parcel transport by long-distance buses.

This paper aims to close this gap with an empirical study and to examine minimum requirements that are set by consumers for a potential cargo-hitching concept for FlixBus, which served as a fictitious example for a potential cargo-hitching process in Germany. Above all, acceptance should be perceived as the overriding goal.

---

## 7.2 Cargo-Hitching as an Alternative Delivery Concept

### 7.2.1 Definition

Cargo-hitching is generally classified as an extended form of crowdsourced delivery, as its main goal is to reduce freight flows by integrating them into existing passenger flows (Aleo Horcas 2019; Faulin et al. 2018). In the case of crowdsourced delivery, logistics flows are reduced by private individuals taking shipments with them. Cargo-hitching, on the other hand, uses existing vehicle movements to transport parcels together with people (Giret et al. 2018). Bektaş et al. (2017) have described the cargo-hitching concept as a combination of passenger and freight flows, whereby the cargo spaces of public transport vehicles such as buses, trains and trams are to be used for parcel transport. Taxis have also been deemed suitable for cargo-hitching (Faulin et al. 2018). Van Duin et al. (2019) have described the goal of cargo-hitching as the “[...] use of the unused capacity of public



transport passenger vehicles for freight and parcel transport". Mazzarino and Rubini (2019) have used cargo-hitching to describe a mix of passenger and freight transport as well.

### **Overview of Existing Concepts**

The Swedish long-distance bus company Bussgods has been mentioned in several publications as an example of cargo-hitching in long-distance bus transport. Bussgods delivers parcels within Sweden by bus. Customers can drop off and pick up parcels at service points. It is also possible to track parcels via the website (Van Duin et al. 2019; Arvidsson et al. 2016). In Germany, there have been a number of field trials in long-distance bus transport. One example is the company Postbus, which offered the first long-distance parcel transport by bus within Germany in 2015. The test service was limited to the route between Berlin and Hamburg; expansion to other cities was planned but never implemented (Bauer 2015). A further keyword search on the Internet revealed five other bus companies and two bus station services worldwide that offer a service similar to that of Bussgods. An investigation of the services given by these bus companies provided first indications, which were used to create a demonstrative example for the subsequent online survey. In order to make this example more tangible, the German long-distance bus company FlixBus was also examined more closely in the following. Insights from the findings were also taken into account in the creation of the concept.

### **FlixBus as Cargo-Hitching Carrier**

As the buses of FlixBus operate 7 days per week and several times per day on many routes, same-day delivery and delivery on Sundays and holidays are possible (FlixBus 2020a). The official FlixBus ticket shops are also open on Sundays and public holidays so that delivery and collection of packages can be guaranteed (FlixBus 2020b). The synergistic effect of combining mobility and logistics is expected to reduce emissions, as no additional bus lines are used. This expectation is additionally supported by research on the CO<sub>2</sub> emissions of FlixBus buses. The Institute for Energy and Environmental Research in Heidelberg has determined that the long-distance bus service of FlixBus is the most environmentally friendly means of transport, ahead of even Deutsche Bahn, with CO<sub>2</sub> emissions of 23 g per passenger kilometre (pkm), compared to 35 g/pkm for the German railways' long-distance service. The lower emissions result from a higher capacity utilization rate of the FlixBus buses (average capacity utilization of 62%) compared to the long-distance service of Deutsche Bahn (capacity utilization of 52%). The higher emissions for long-distance railway are explained by the provision of electricity. The comparison of emissions of the transport modes published by the German Umweltbundesamt is based on the average electricity mix in Germany (Institut für Energie und Umweltforschung Heidelberg 2017; Umweltbundesamt 2018).

Furthermore, it must be taken into account that same-day deliveries in particular leave a disproportionately large CO<sub>2</sub> footprint (Paazl n.d.). However, it is necessary to consider both pre- and post-carriage, which depend on the choice of transport mode—if one drives to a stop by car, the emissions are higher than with public transport (Brown 2019). The

parcel is registered online by the shipper via the website or the app so that the parcel can be registered in the system in time. As with Bussgods (2020), the next possible bus departure times are then displayed. As a rule, the parcel must be dropped off 30–60 min before departure at a FlixBus ticket shop which serves as collection points. Alternatively, partner shops are to be established in cities without an official ticket shop. This principle is based on the parcel shop partner contracts used by Hermes and DPD. These partner contracts could be extended to petrol stations, kiosks and smaller retailers in the vicinity of FlixBus bus stops (Bretzke 2014). As all buses are already equipped with live GPS tracking for passengers, parcels may also be tracked with the same system (FlixBus 2020c). Service staff give parcels to the bus driver, who stows the parcels in the cargo compartment. As soon as the parcel arrives, the recipient is notified and can pick it up on presentation of valid identification. A pictorial representation of the described process is shown in Fig. 7.1. To be able to investigate the created model in a subsequent empirical study, a theoretical insight into customer acceptance is required.

---

### 7.3 Adapting an Underlying Acceptance Model

This paper focuses on attitudinal acceptance, which can be defined as a fundamental willingness to use an innovation (Reichwald 1978). Attitudinal acceptance occurs before an innovation is purchased or used. In this phase, the potential users learn about the offered innovation for the first time (*awareness*), the *interest* is formed, and the users consider whether the offered innovation can offer a benefit to them (*expectation*) (Kollmann 1998).

The empirical study of this thesis uses an acceptance model that takes into account aspects of customers' attitudinal acceptance. For this, the UTAUT2 model was chosen, as it is designed to determine the usage intention of customers as well as the use behaviour (Venkatesh et al. 2012). As this paper deals with attitudinal acceptance, use behaviour is not considered. Instead, only the effect on behavioural intention is examined, which is defined as "an individual's positive or negative feelings about performing the target behaviour" (Venkatesh et al. 2003). The UTAUT2 (2012) model has been used in many studies on the acceptance of technology and innovations as a basis for the determination of acceptance factors. The model consists of seven independent variables, which predict behavioural intention: performance expectancy, effort expectancy, social influence, facilitating conditions, hedonic motivation, price value and habit. In addition, the study by Sonneberg et al. (2019) should be mentioned, as it dealt with the acceptance of alternative last-mile delivery options. In this study, sustainable expectancy (SE) was applied for the first time as an extension of the UTAUT2 model (Sonneberg et al. 2019). This variable indicates whether the perception of sustainability has an impact on behavioural intention. Consequently, sustainable expectancy was integrated as an additional variable into the model. Figure 7.2 illustrates the UTAUT2 model and the connections between each variable.

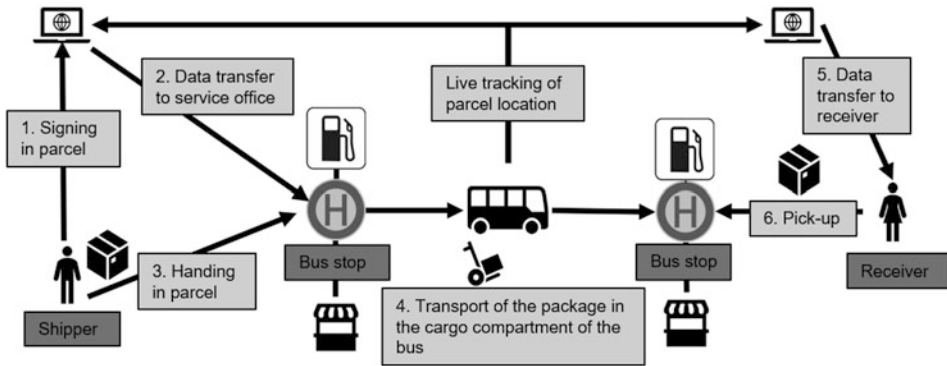


**Fig. 7.1** Cargo-hitching process via FlixBus

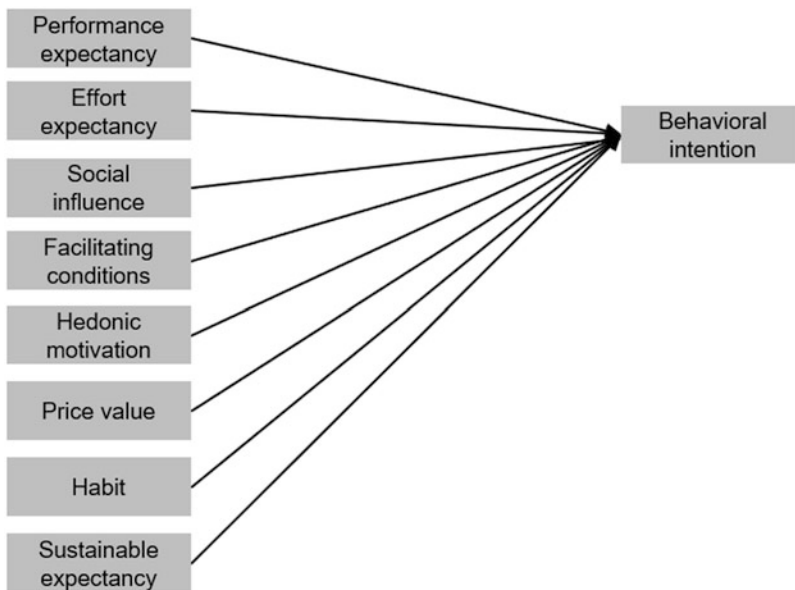


**Fig. 7.2** Modified UTAUT2 model

## 7.4 Methodology: Acceptance Analysis of a Cargo-Hitching Model

Two central research questions were raised:

1. What factors influence the acceptance of cargo-hitching by FlixBus for delivery within Germany?

## 2. What requirements do consumers have for cargo-hitching by FlixBus for delivery within Germany?

The hypotheses were derived from the UTAUT2 model (2012) and the study by Sonneberg et al. (2019). It was assumed that the independent variables have a positive influence on the dependent variable behavioural intention. Accordingly, identical hypotheses were formulated for each variable.

*Hypothesis 01:* Performance expectancy of cargo-hitching via FlixBus has a positive influence on behavioural intention to use cargo-hitching via FlixBus.

*Hypothesis 02:* Effort expectancy of cargo-hitching via FlixBus has a positive influence on behavioural intention to use cargo-hitching via FlixBus.

*Hypothesis 03:* Social influence of cargo-hitching via FlixBus has a positive influence on behavioural intention to use cargo-hitching via FlixBus.

*Hypothesis 04:* Facilitating conditions of cargo-hitching via FlixBus have a positive influence on behavioural intention to use cargo-hitching via FlixBus.

*Hypothesis 05:* Hedonic motivation regarding cargo-hitching via FlixBus has a positive influence on behavioural intention to use cargo-hitching via FlixBus.

*Hypothesis 06:* Price value on cargo-hitching via FlixBus has a positive influence on behavioural intention to use cargo-hitching via FlixBus.

*Hypothesis 07:* Habit regarding cargo-hitching via FlixBus has a positive influence on behavioural intention to use cargo-hitching via FlixBus.

*Hypothesis 08:* Sustainable expectancy of cargo-hitching via FlixBus has a positive influence on behavioural intention to use cargo-hitching via FlixBus.

In answering the second research question, the requirements and wishes of potential users were necessarily determined. The requirements were determined via an evaluation of the perceived advantages and disadvantages by the respondents. The factors of risk, costs and benefits played a role.

- Which services are important to the users?
- How much are users willing to pay?
- What risks are perceived?

### 7.4.1 Method

A quantitative online survey was used as a study method, partly supplemented by qualitative questions. The survey was open to responses from 19 April to 26 April 2020. In total, the questionnaire was divided into four categories. First, the cargo-hitching concept was presented. The model set out in Sect. 7.2 served to explain to the respondents how cargo-hitching by FlixBus works.

The second section of the questionnaire was devoted to the first research question. The modified UTAUT2 model elucidated in Sect. 7.3 served as a basis. The individual

independent and dependent variables were presented as factors, of which the independent variables performance expectancy, effort expectancy, social influence, facilitating conditions and sustainable expectancy were stored with multiple items (two to three items). For hedonic motivation, price value and habit, one item each was selected to measure the respective superordinate factors. The individual factors were operationalized by using items already validated by Venkatesh et al. (2003, 2012). However, the content of these items was adapted to the FlixBus concept, translated from English in German and also reformulated in the subjunctive, since only behavioural intention was to be measured. To determine behavioural intention, the respondents evaluated the thesis “I intend to use the package delivery by FlixBus in the future”. Participants answered the questions on a 5-point Likert scale (from 1 = *Do not apply* to 5 = *Apply*).

In the third part of the questionnaire, possible requirements and wishes of the respondents for cargo-hitching by FlixBus were determined. Here, a distinction was made between the views of the sender and the recipient in order to obtain more information. The questions focused on the reasons why cargo-hitching could be used and what concerns the respondents had with respect to cargo-hitching. To answer these questions, the respondents chose from several possible answers. To obtain a broader spectrum, respondents were offered the possibility of adding further information by filling out an available text field. In addition, various questions on intended use were presented to the respondents. Again, a 5-step Likert scale was used and provided with probability indicators (from 1 = *Do not apply* to 5 = *Apply*). Furthermore, this part of the questionnaire addressed price sensitivity. Questions were asked about the respondents’ willingness to pay in two different cases. Case 1 concerned the price of a 2 kg parcel that was dropped off at a FlixBus stop and was in turn picked up by the recipient at the destination stop. The delivery took place on the same day and was also possible on Sundays and holidays. As a price comparison, an express delivery on the next working day by DHL of 14.00 € was indicated (DHL 2020). The same applied for Case 2: a delivery by FlixBus in combination with a door-to-door delivery was specified. The delivery was to take place within one to three business days. The online price for the same form of delivery by DHL was indicated as 5.49 € (DHL 2020).

In the fourth section of the questionnaire, socio-demographic data was collected by means of questions on age, gender, population of main residence and current profession.

---

## 7.5 Results

### 7.5.1 Sample

Ultimately, 245 people completed the questionnaire ( $n = 245$ ). 59.18% of the respondents were female, 39.59% were male, and 2 persons (0.82%) indicated their gender as diverse. One person did not indicate their gender. On average, the subjects were 27 years old ( $SD = 8.62$ ). Accordingly, 61.63% of all subjects stated that they were students, followed

by 26.53% who were in full-time employment. When asked about the population of their main residence, 37.14% stated that they live in a big city with at least 500,000 inhabitants; 24.90% said they live in a small town with a population between 5000 and 19,999 people. 9.80% stated that they live in rural areas with a population of less than 5000; 15.92% live in a medium-sized city with a population between 20,000 and 99,999. 12.24% live in large cities (100,000–499,999 inhabitants).

### 7.5.2 Answering the First Research Question: The UTAUT2 Model

To determine the most influential factors on behavioural intention within UTAUT2, a multiple regression was carried out. Performance expectancy (PE), effort expectancy (EE), facilitating conditions (FC), habit (HT), price value (PV), hedonic motivation (HM), social influence (SI) and sustainable expectancy (SE) served as independent variables, while behavioural intention (BI) served as dependent variable. Cronbach's alpha values provided information on the reliability of the individual scales of the items (Fig. 7.3). Cronbach's alpha of 0.60 and higher is considered reliable (Ursachi et al. 2015). Variables with Cronbach's alpha below 0.60 were not considered further, namely, facilitating conditions ( $\alpha = 0.469$ ) and effort expectancy ( $\alpha = 0.570$ ) were not considered in further analysis.

Descriptive data of the behavioural intention showed that 18.4% disagreed with the statement "I intend to use parcel delivery by FlixBus in the future"; 23.3% partially disagreed, 29.4% were undecided, 22.9% partially agreed, and 6.1% agreed with the statement.

Figure 7.4 provides an overview of the coefficients of the regression analysis. Results of the multiple regression revealed a significant overall effect, whereby the 6 independent variables explained 54.70% of the variance ( $R^2 = 0.54$ ,  $F(6; 237) = 50.00$ ,  $p < 0.001$ ). The following variables predicted BI significantly: HT ( $b = 0.347$ ,  $p < 0.001$ ), PV ( $b = 0.244$ ,  $p < 0.001$ ), HM ( $b = 0.170$ ,  $p < 0.01$ ), PE ( $b = 0.127$ ,  $p < 0.05$ ) and SI ( $b = 0.110$ ,  $p < 0.05$ ). SE did not predict BI significantly ( $b = -0.032$ ,  $p > 0.05$ ). Overall, hypotheses *H01*, *H03*, *H05*, *H06* and *H07* were supported. On the other hand, hypotheses *H02*, *H04* and *H08* were invalidated because the independent variables EE and FC proved to be unreliable; furthermore, SE proved to be insignificant.

### 7.5.3 Answering the Second Research Question: Wishes and Requirements of Potential Users

The second research question dealt with the determination of requirements and wishes of potential users in order to optimize the later acceptance of use through a customer-oriented approach. When asked about their first reaction to parcel delivery by FlixBus, the majority of the respondents indicated good or very good (72.70%), 7.70% indicated bad or not good, and the remainder gave a neutral opinion (19.60%). Figure 7.5 depicts the frequency

Variable	Number of Items	Cronbach's Alpha
Performance Expectancy (PE)	2	.675
Effort Expectancy (EE)	2	.570
Social Influence (SI)	2	.892
Facilitating Conditions (FC)	3	.469
Habit (HT)	2	.646
Sustainable Expectancy (SE)	3	.797

**Fig. 7.3** Cronbach's alpha values

Influence on Behavioral Intention			
Variable	Unstandardized	Standardized	Std. Error
Constant	-.772*		.296
Performance expectancy (PE)	.167*	.127*	.076
Social influence (SI)	.155*	.110*	.076
Hedonic motivation (HM)	.198**	.170**	.062
Price value (PV)	.276***	.244***	.064
Habit (HT)	.427***	.347***	.073
Sustainable expectancy (SE)	-.047	-.032	.080
R <sup>2</sup>	.559		
adj. R <sup>2</sup>	.547		
F (df=2; 49)	50.002***		

\*p < .05; \*\*p < .01; \*\*\*p < .001

**Fig. 7.4** Coefficients of regression analysis

distribution. The respondents were asked specifically to identify reasons for and reasons against using cargo-hitching via FlixBus. The results indicate that the respondents most frequently named delivery on Sundays as the decisive factor (73.90%), followed by delivery on public holidays (71.00%) and overall fast delivery (63.70%). On the other hand, 71.00% of the respondents were concerned by the distance to FlixBus stops. The unpunctuality of the buses and damage to the parcels were causes for concern for 53.10% of the respondents, closely followed by theft of parcels from the cargo compartment with 52.70%.

Furthermore, the respondents were able to name additional service features that were at least rather important to them in an open-ended question. The answers ( $n = 42$ ) were provided with content codes and clustered. This resulted in three topics, *Information*, *Safety*

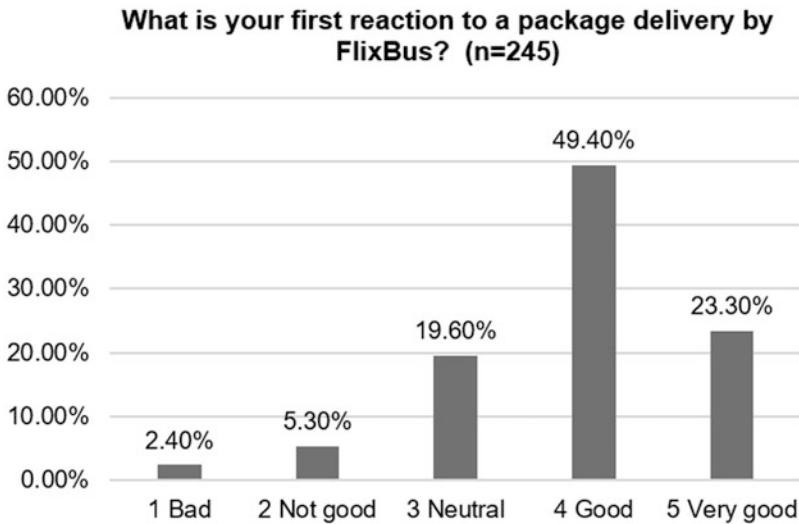


**Fig. 7.5** First reaction to cargo-hitching via FlixBus

and *Flexibility*, to which most of the answers could be assigned. The remaining answers were generally mentioned only once and are therefore not explained in detail. Ten answers were assigned to the category *Information*. Topics such as transparency, tracking and tracing and an app with a notification function were mentioned (“App or online portal, in which you specify when you want to send something where and when you want to send it [...]”; “Online Support Q&A as the concept is new (what happens in case of loss, damage, etc.)”). Seven answers could be assigned to the category *Safety*. Concerns about theft protection were mentioned, and solutions such as separate or lockable compartments in the cargo area (“Separate parcel compartments for theft prevention”) were suggested. In this context, transport insurance and guarantees for punctual deliveries were also specified (“A guarantee that the parcel will arrive undamaged and will not be stolen”). *Flexibility* was assigned to six answers. Flexible delivery and collection times as well as packing stations were mentioned (“Delivery and collection at flexible times. Late in the evening for example. Drop-off and pick-up point nearby”).

The respondents were willing to pay on average 10.87 € ( $SD = 5.47$ ) for a delivery to the bus stop. On average, the respondents stated a maximum amount of 5.51 € ( $SD = 3.21$ ) for a door-to-door delivery.

---

## 7.6 Discussion and Outlook

Cargo-hitching in long-distance bus transit is an innovation that has not yet been introduced nationwide in Germany. This form of delivery offers a number of advantages such as faster and more efficient delivery. It was also found that this form of delivery—



under certain conditions as discussed in Sect. 7.2—could have a positive effect on the environment, as freight transport and mobility could be combined, thus reducing the number of CEP vehicles. Although UTAUT2 could not be fully applied, factors influencing the behavioural intention were identified. Although it was recognized that certain factors can increase the intention of use and thus the acceptance of cargo-hitching, it can be generally criticized that the model does not provide any explanations or concrete recommendations for action to increase acceptance (Niklas 2015). However, the knowledge gained can be used for a follow-up study. Furthermore, the overall opinion on cargo-hitching via FlixBus was positive, although behavioural intention was not particularly high. It is clear that although delivery is seen as positive, this perception does not automatically result in a behavioural intention to use it, which could be due to specific concerns.

Risks in the areas of security and flexibility were identified, which must be proactively mitigated. From the question on the importance of the individual service features, it became clear that transparency was particularly important to the subjects. Tracking and tracing were considered to be very important. In addition, the open-ended question revealed wishes for a continuous flow of information. Few of the bus companies that have implemented cargo-hitching either have transport insurance included in their prices or offer insurance for additional costs. However, it is also necessary to work proactively on security. Lockable or separated freight compartments were suggested as a means of preventing theft. With regard to the unpunctuality of buses, the urgency of the parcel is important. There is evidence of frequent unpunctuality of FlixBus buses. Specifically, every second bus is late, and an average delay of 30 min must be expected (Hain 2020). Although these delays would generally not hamper a same-day delivery, a delivery timed to the minute would be unlikely.

In particular, the price sensitivity reveals that customers are on average not willing to pay more than the prices charged by DHL. This could be related to the fact that this is a new provider competing against long-established companies such as DHL and Hermes, and trust must therefore be earned. These stated maximum costs may provide an anchor for the customers' willingness to pay when establishing a business model. By taking these findings into account, attitudinal acceptance can be established, and the basis for overall acceptance can be created. Finally, it must be borne in mind that this form of delivery is a niche for particularly fast deliveries to private individuals.

---

## References

- Aleo Horcas, D. (2019). Social Transport Status Quo (Bachelor Thesis).
- Arvidsson, N., Givoni, M., & Woxenius, J. (2016). Exploring Last Mile Synergies in Passenger and Freight Transport. *Built Environment*, 42(4), 590–604. <https://doi.org/10.2148/benv.42.4.523>
- Bauer, M. (2015, December 8). Deutsche Post DHL: Postbus wird zum Kurier. Retrieved April 14, 2020, from <https://www.eurotransport.de/artikel/deutsche-post-dhl-postbus-wird-zum-kurier-6809825.html>

- Bektaş, T., Crainic, T. G., & Van Woensel, T. (2017). From Managing Urban Freight to Smart City Logistics Networks. *Series on Computers and Operations Research*, 143–188. [https://doi.org/10.1142/9789813200012\\_0007](https://doi.org/10.1142/9789813200012_0007)
- Bretzke, W. R. (2014). *Nachhaltige Logistik - Zukunftsfähige Netzwerk- und Prozessmodelle* (3rd ed.). Berlin, Germany: Springer.
- Brown, L. (2019, March 29). How green is your parcel? Retrieved April 30, 2020, from <https://www.bbc.com/news/science-environment-47654950>
- Bussgods. (2020). Skicka paket inom Sverige - Bussgods Sverigefrakt. Retrieved May 1, 2020, from <https://www.bussgods.se/>
- Deutsche Verkehrs-Zeitung. (2015, October 28). Start-Up befördert Pakete per Fernbus. *Deutsche Verkehrs-Zeitung*. Retrieved from <https://www.dvz.de>
- DHL. (2020). Preise und Produkte für Ihren nationalen Versand | DHL. Retrieved April 16, 2020, from <https://www.dhl.de/de/privatkunden/pakete-versenden/deutschlandweit-versenden/preise-national.html>
- Faulin, J., Grasman, S., Juan, A., & Hirsch, P. (2018). *Sustainable Transportation and Smart Logistics* (1st ed.). Maarssen, Netherlands: Elsevier.
- FlixBus. (2020a). FlixBus. Retrieved April 23, 2020, from <https://www.flixbus.de>
- FlixBus. (2020b). FlixBus und FlixTrain Tickets bei offiziellen Ticketverkäufern. Retrieved May 15, 2020, from <https://www.flixbus.de/service/ticketverkaufsstellen>
- FlixBus. (2020c). Sicherheit im Fernbus → FlixBus. Retrieved May 15, 2020, from <https://www.flixbus.de/unternehmen/sicherheit>
- Giret, A., Carrascosa, C., Julian, V., Rebollo, M., & Botti, V. (2018). A Crowdsourcing Approach for Sustainable Last Mile Delivery. *Sustainability*, 10(12), 4563. <https://doi.org/10.3390/su10124563>
- Greyhound Freight. (2020). Freight & Parcel Delivery. Retrieved April 25, 2020, from <https://www.greyhound.com.au/freight>
- Hain, A. (2020, February 1). Fernbusse in Deutschland: Jeder zweite Flixbus zu spät. Retrieved December 19, 2019, from <https://www.tagesschau.de/inland/flixbus-fernbusse-101.html>
- Institut Für Energie- Und Umweltforschung Heidelberg. (2017, October 26). Umweltbilanzierung Fernlinienbus. Retrieved May 12, 2020, from [https://www.ifeu.de/wp-content/uploads/20171026\\_Ergebnisse\\_Fernlinienbus\\_Final.pdf](https://www.ifeu.de/wp-content/uploads/20171026_Ergebnisse_Fernlinienbus_Final.pdf)
- Kollmann, T. (1998). *Akzeptanz innovativer Nutzungsgüter und -systeme*. Wiesbaden, Germany: Springer Fachmedien.
- Maritime Bus. (2020). Parcel Express. Retrieved May 2, 2020, from <https://maritimebus.com/en/services/parcel-express>
- Mazzarino, M., & Rubini, L. (2019). Smart Urban Planning: Evaluating Urban Logistics Performance of Innovative Solutions and Sustainable Policies in the Venice Lagoon—the Results of a Case Study. *Sustainability*, 11(17), 1–27. <https://doi.org/10.3390/su11174580>
- Niklas, S. (2015). *Akzeptanz und Nutzung mobiler Applikationen*. Wiesbaden, Germany: Springer Gabler.
- Paazl. (n.d.). Delivery Sustainability - When shipping get serious. Retrieved May 12, 2020, from <https://www.retailinsiders.nl/docs/826a7f1d-11c0-4bd7-9d8f-beacbb0c4092.pdf>
- Ram, S. (1989). Successful Innovation Using Strategies to Reduce Consumer Resistance An Empirical Test. *Journal of Product Innovation Management*, 6(1), 20–34. <https://doi.org/10.1111/1540-5885.610020>
- Reichwald, R. (Ed.). (1978). *Die Akzeptanz neuer Bürotechnologie: Zur Notwendigkeit der Akzeptanzforschung bei der Entwicklung neuer Systeme der Bürotechnik* (Vol. 1). Munich, Germany: Hochschule der Bundeswehr München.
- Sonneberg, M.-O., Werth, O., Kohzadi, H., Kraft, M., Neels, B., & Breitner, M. H. (2019). Customer Acceptance of Urban Logistics Delivery Concepts. *IWI Discussion Paper Series, (# 91)*, 1–90.

- Retrieved from [https://www.iwi.uni-hannover.de/en/forschung/iwi-diskussionspapiere/?tx\\_t3luhpublications\\_publications%5Bpublication%5D=2259&tx\\_t3luhpublications\\_publications%5Baction%5D=show&tx\\_t3luhpublications\\_publications%5Bcontroller%5D=Publication](https://www.iwi.uni-hannover.de/en/forschung/iwi-diskussionspapiere/?tx_t3luhpublications_publications%5Bpublication%5D=2259&tx_t3luhpublications_publications%5Baction%5D=show&tx_t3luhpublications_publications%5Bcontroller%5D=Publication)
- Umweltbundesamt. (2018). Vergleich der durchschnittlichen Emissionen einzelner Verkehrsmittel. <https://www.umweltbundesamt.de/bild/vergleich-der-durchschnittlichen-emissionen-0>
- Ursachi, G., Horodnic, I. A., & Zait, A. (2015). How Reliable are Measurement Scales? External Factors with Indirect Influence on Reliability Estimators. *Procedia Economics and Finance*, 20, 679–686. [https://doi.org/10.1016/s2212-5671\(15\)00123-9](https://doi.org/10.1016/s2212-5671(15)00123-9)
- Van Duin, R., Wiegmans, B., Tavasszy, L., Hendriks, B., & He, Y. (2019). Evaluating new participative city logistics concepts: The case of cargo hitching. *Transportation Research Procedia*, 39, 565–575. <https://doi.org/10.1016/j.trpro.2019.06.058>
- Venkatesh, V., Moris, M. G., Davis, G. B., & Davis, F. D. (2003). User Acceptance of Information Technology: Toward a Unified View. *MIS Quarterly*, 27(3), 425–478. Retrieved from [http://www.vvenkatesh.com/wp-content/uploads/2015/11/2003\(3\)\\_MISQ\\_Venkatesh\\_etal.pdf](http://www.vvenkatesh.com/wp-content/uploads/2015/11/2003(3)_MISQ_Venkatesh_etal.pdf)
- Venkatesh, V., Thong, J. Y. L., & Xu, X. (2012). Consumer Acceptance and Use of Information Technology: Extending the Unified Theory of Acceptance and Use of Technology. *MIS Quarterly*, 36(1), 157–178. Retrieved from <https://pdfs.semanticscholar.org/6256/0e2001480fd1f22558ce4d34ac93776af3e6.pdf>
- Wang, X., Yuen, K. F., Wong, Y. D., & Teo, C. C. (2018). An innovation diffusion perspective of e-consumers' initial adoption of self-collection service via automated parcel station. *The International Journal of Logistics Management*, 29(1), 237–260. <https://doi.org/10.1108/ijlm-12-2016-0302>

**Open Access** This chapter is licensed under the terms of the Creative Commons Attribution 4.0 International License (<http://creativecommons.org/licenses/by/4.0/>), which permits use, sharing, adaptation, distribution and reproduction in any medium or format, as long as you give appropriate credit to the original author(s) and the source, provide a link to the Creative Commons license and indicate if changes were made.

The images or other third party material in this chapter are included in the chapter's Creative Commons license, unless indicated otherwise in a credit line to the material. If material is not included in the chapter's Creative Commons license and your intended use is not permitted by statutory regulation or exceeds the permitted use, you will need to obtain permission directly from the copyright holder.





# Promoting Zero-Emission Urban Logistics: Efficient Use of Electric Trucks Through Intelligent Range Estimation

8

Sebastian Stütz, Andreas Gade, and Daniela Kirsch

## Abstract

Critical success factors for the efficient use of electric trucks are the operational range and the total costs of ownership. For both range and efficient use, power consumption is the key factor. Increasing precision in forecasting power consumption and, hence, maximum range will pave the way for efficient vehicle deployment. However, not only electric trucks are scarce, but also is knowledge with respect to what these vehicles are actually technically capable of. Therefore, this article focuses on power consumption and range of electric vehicles. Following a discussion on how current research handles the mileage of electric vehicles, the article illustrates how to find simple yet robust and precise models to predict power consumption and range by using basic parameters from transport planning only. In the paper, we argue that the precision of range and consumption estimates can be substantially improved compared to common approaches which usually posit a proportional relationship between energy consumption and travel distance and require substantial safety buffers.

## Keywords

Electric trucks · Power consumption · Range estimation · LASSO regression

S. Stütz (✉) · A. Gade · D. Kirsch  
IU International University of Applied Sciences, Dortmund, Germany  
e-mail: [sebastian.stuetz@iu.org](mailto:sebastian.stuetz@iu.org)

© The Author(s) 2022  
V. Coors et al. (eds.), *iCity. Transformative Research for the Livable, Intelligent, and Sustainable City*,  
[https://doi.org/10.1007/978-3-030-92096-8\\_8](https://doi.org/10.1007/978-3-030-92096-8_8)

## 8.1 Introduction

Research on electrified delivery has gained substantial momentum over the past decade as companies from various industries try to reduce their carbon footprint in transport. Urban logistics seems like a perfect field of application for electric trucks since it allows delivery runs without causing tailpipe nitrogen oxides or particulate matter emissions and helps to curb the problem of traffic noise (Pelletier, Jabali, and Laporte 2016). From a business perspective, it also makes perfect sense to deploy electric trucks in urban areas since usual delivery runs are both rather predictable and short enough to allow the use of range-limited vehicles (Quak and Nesterova 2018; Teoh 2018). Range is acknowledged as the dominant limiting factor for electric vehicles, and several sophisticated models on this topic have been proposed (Zhou, Ravey, and Péra 2019). But since applying the latter requires a plethora of different input variables, the continuous availability of fine granular data or even both (Tseng and Chau 2017), this article takes a different perspective on this issue. Instead, it is investigated to which degree basic information from vehicle dispatching can be used for range prediction with higher precision than widespread naïve approaches assuming a direct proportional relationship between energy consumption and travel distance.

This contribution is organized as follows: As a first step, the relevance of precise range estimations for fleet and operation managers and why range/energy consumption belongs to the key variables to promote electric vehicles are illustrated. A subsequent literature overview shows how energy consumption and vehicle range are usually handled, respectively. It is argued that there is a strong need of range estimation models for which input data is easily available. These models have to be usable by decision-makers with access to basic route optimization tools and allow a more precise estimate than the frequently used simple albeit imprecise rule of three. Using real-world data from the research project “EN-WIN” of Fraunhofer IML combined with a regression approach, different consumption/range estimation models are discussed and benchmarked with the widespread naïve approach.

Funded by the German Federal Ministry of the Environment, Nature Conservation and Nuclear Safety, grant no. 16EM3118, the EN-WIN consortium consisting of Technical University of Berlin, Fulda University of Applied Sciences, Florida-Eis Manufaktur GmbH, Ludwig Meyer GmbH & Co. KG, BPW Bergische Achsen KG and Fraunhofer Institute for Material Flow and Logistics (lead) assessed options to facilitate and improve the deployment of electric trucks using real-world energy consumption data.

---

## 8.2 The Need for Precise Energy Consumption and Range Estimation

As profit-oriented entities, companies are inclined to electrify substantial parts of their fleets only if two preconditions are met:

- There is an electric vehicle which is technically capable to substitute the currently used combustion-powered vehicle, especially in terms of range and payload (Felipe, Ortuño, Righini, and Tirado 2014).
- The expected total costs of ownership (TCO) for the electric vehicle are lower than the TCO for the currently used combustion-powered vehicle (Camilleri and Dablanc 2017).

In case a fleet manager agrees to both aspects and acquires and deploys a certain electric truck, two important operational questions arise in addition: “How to make sure that the vehicle actually provides an ongoing advantage in total ownership costs?” and “How to make sure route planning does not exceed the electric range?”

It is evident that detailed and reliable knowledge about realistic vehicle ranges is decisive for the adoption and ongoing (i.e. economically viable) use of electric trucks (Erdelić and Carić 2019). As Fig. 8.1 illustrates, logistics companies have strict requirements when it comes to vehicle payload and range.

Vehicle batteries are a payload reducing factor, while, at the same time, they represent a key determinant of vehicle range (Pelletier, Jabali, and Laporte 2016). Range, however, does not only depend on battery capacity alone but also on the actual use case (typical routes, road network, stop frequency, ambient temperature, etc.) which makes it questionable to posit a proportionality of energy consumption and trip length. Therefore, a fleet manager must carefully consider the trade-offs between payload and range requirements (Stütz, Taefi, and Fink 2018). While payload is *ex ante* known from specification documents, consumption, and consequentially range, is not. When companies consider the purchase of electric vehicles, they need to assess their economic potential. For the latter, the expected electricity consumption is a key TCO driver and is depending on the actual use case. This illustrates that oversimplified or imprecise information concerning the

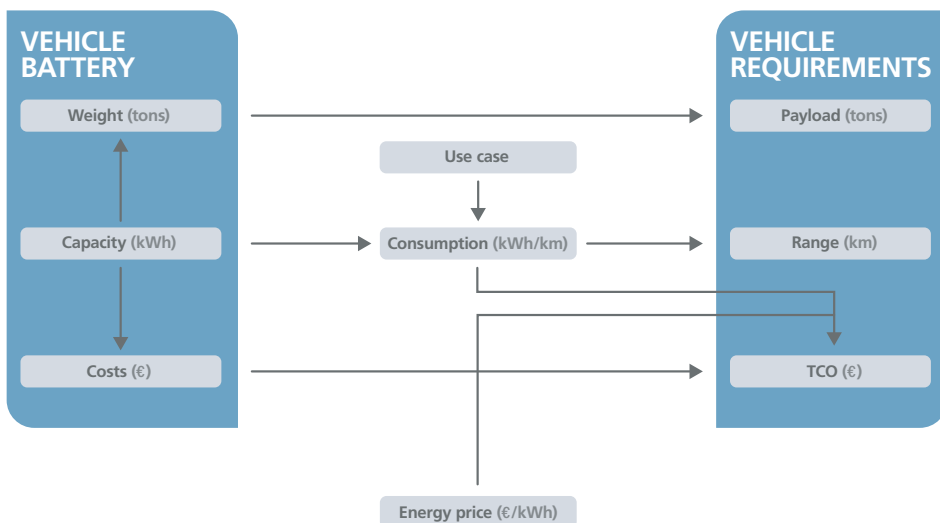


**Fig. 8.1** Interrelationships between vehicle battery, vehicle requirements, use-case, and TCO

efficiency of an electric truck will directly affect business case considerations in various ways (cf. Fig. 8.2).

- On the *tactical level*, fleet managers can overestimate vehicle range, thereby paving the way for overambitious electrification in that sense that the organization has not yet acquired the necessary knowledge and experience to use the electric trucks. Opposite, too low efficiency estimates will lead to an exclusion of suitable vehicles. From a cost perspective, imprecise consumption figures will, likewise, lead to a situation in which cost-effective vehicle will appear as uneconomical and vice versa (Taefi, Fink, and Stütz 2016).
- On the *operational level*, imprecision will either lead to over- or underestimation of vehicle range. Either case has negative business impacts as vehicles actually run out of energy while en route or regularly return to the depot with a substantial battery charge remaining, thus wasting parts of their potential to reduce operational costs (Stütz et al. 2016).

This illustrates that reliable use case-specific and credible knowledge about real-world power consumption and range is one of the most critical issues to address in order to promote the broad adoption of electric vehicles. Literature is following different paths to integrate this crucial variable.

- (a) *Power consumption is regarded as a set of given values taken from external sources.* This seems expedient when the actual consumption and vehicle performance are not the focus of research, for example, when extending vehicle routing models (VRP) to integrate the specific properties of electric vehicles. However, when these models are parameterized and solved, the context-specific and route-dependent consumption becomes an issue (Erdelić and Carić 2019; Erdoğan and Miller-Hooks 2012).
- (b) *Relative power consumption is regarded as a given value,* usually as kWh per kilometre, while proportionality between total power consumption per journey and distance travelled is assumed (Moll, Plötz, Hadwich, and Wietschel 2020; Felipe, Ortuño, Righini, and Tirado 2014). Alternatively, positing a certain *maximum vehicle range*, relative consumption can implicitly be set as a fixed value (Alp, Tan, and Udenio 2019). In either case, consumption is static and not a characteristic of the actual vehicle context (like distance travelled or ambient conditions) (Granada-Echeverri, Cubides, and Bustamante 2020; Wang, Lim, Tseng, and Yang 2018).
- (c) *Power consumption is calculated using physical simulation.* This usually involves sophisticated modelling and calculations of the vehicle's kinetic energy requiring detailed technical parameters but allows to integrate various influencing factors, such as drag, rolling friction to acceleration or brake energy recovery (Lin, Zhou

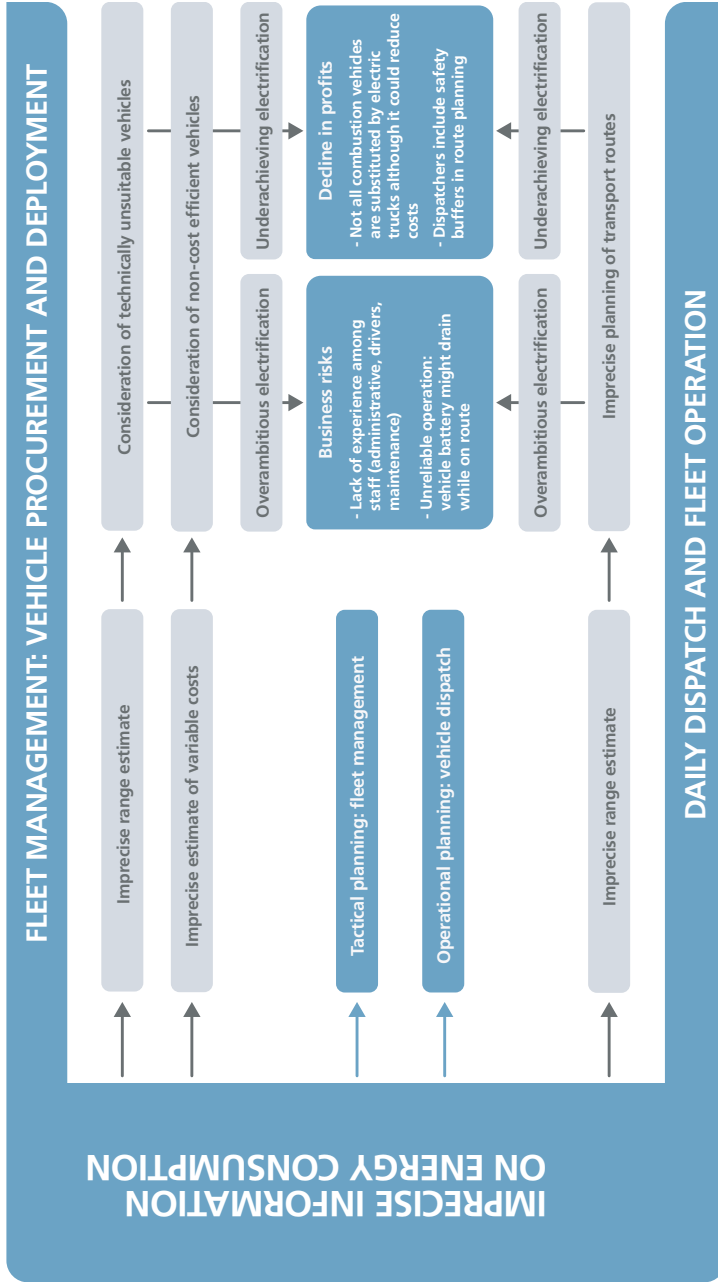


**Fig. 8.2** Negative effects of imprecise range estimates on tactical and operational planning



and Wolfson 2016; Goeke and Schneider 2015; Helms, Pehnt, Lambrecht and Liebich 2010).

- (d) Total power consumption is *calculated using an estimation function* that goes beyond a mere proportionality between distance travelled and energy consumed (Liimatainen, van Vliet, and Aplyn 2019; Davis and Figliozzi 2013).

All four approaches require specific input data in order to serve as a data source for electric power consumption. Typically, three different data sources can be distinguished:

- (a) *Assumptions*, for example, the assumption that range assured by the manufacturer can be used to derive the vehicle's relative consumption or that the values from one trial can be used for calculations related to another trial involving the same type of vehicle.
- (b) *Standardized values*, for example, values from vehicle surveys as included in the Handbook Emission Factors for Road Transport (HBEFA) (Helms, Pehnt, Lambrecht and Liebich 2010) or derived from standardized driving cycles (Camilleri and Dablanc 2017; Lee, Thomas, and Brown 2013).
- (c) *Context-specific real-world values*, i.e. real-world data gathered from the very use case for which consumption data is needed, for example, a case in which data from one electrified package delivery van is taken to plan the delivery round trips of the same van or a different van of the same type operating from the same depot (Taefi, Stütz, and Fink 2017).

It is apparent that either current approaches for range estimation rely on sophisticated simulation models requiring meticulous calibration and precise information about the intended routes, including road gradients, or they require access to precise data from similar use cases as well as the capabilities to process that data. It can be doubted that both are easily available to companies involved in urban logistics, especially since the majority of those companies are small- or medium-sized enterprises, and that the respective requirements can rarely be met on a daily basis (Osypchuk 2019; Oberhofer and Fürst 2013). In practice, companies rely on a planning method assuming a proportionality between range and distance combined with a substantial safety buffer leading to inefficient vehicle use (Stütz et al. 2016).

---

### 8.3 Towards an Intelligent Method for Range Prediction

To overcome this gap between theoretically applicable estimations based on multiple variables and, hence, inducing substantial effort for data acquisition and the other extreme of range-driving-distance proportionality (Stütz, Fink, Taefi 2018), Fraunhofer IML conceived the research project "EN-WIN". One objective of this project was to assess the possible increase of range prediction quality when only basic route characteristics (like the number of delivery stops) are considered.

**Table 8.1** Overview of data collected from 18-ton trucks during the course of the “EN-WIN” project

Total days of operation	Total driving distance (km)	Total power consumption (kWh)
420	49,220	58,418

**Table 8.2** Linear models used for range prediction

Model no.	Variables used			
	Travel distance	Ambient temperature	Number of delivery stops	Payload
1	X			
2	X	X		
3	X		X	
4	X			X
5	X	X	X	
6	X	X		X
7	X		X	X
8	X	X	X	X

When it comes to data acquisition, it can be safely assumed that this data is definitely available for dispatchers, even in SMEs, as they are elementary results of route planning (Oberhofer and Fürst 2013). Moreover, the project considered ambient temperature as an additional variable and produced a method to collect this data more efficiently (Jerratsch, Herzlieb and Marker 2018). The researchers involved used an extensive trial between 2017 and 2020 to collect data from eight electric trucks of various sizes (4.25 tons to 40 tons) using tracking devices. This article puts the focus on the data collected from the journeys of the 18-ton trucks to address the question whether basic information from vehicle dispatch allows more precise range prediction than just assuming a proportional relationship between energy consumption and travel distance. After data sanitization, a total of 420 days of vehicle operation remained for analysis (cf. Table 8.1).

As a first step, it is safe to assume that a dispatcher has access to the following basic set of information since they directly trace back to transport orders and customers (Seiler 2012):

- Travel distance: length of entire round trip starting and finishing at the depot.
- Number of delivery stops: total number of customers on the delivery route.
- Payload: shipment weight at the beginning of the round trip.

Additionally, using data from public sources, it is also safe to assume that a dispatcher is able to include ambient temperature (at least the average daily temperature recorded at depot location). As a next step, the dominant drivers of energy consumption of these should be included in a range prediction model. With travel distance already considered as a main driver for energy consumption, eight different models each using (a subset of) the aforementioned variables (cf. Table 8.2) could be derived.

A classic least-square model is not sufficient for the present case since it will definitely result in non-zero beta weights for any covariate. Instead, it is desired that the model selects

the best variables to accurately predict energy consumption and range, respectively, while avoiding overfitting. The LASSO (least absolute shrinkage and selection operator) method seemed expedient for that purpose (Tibshirani 1996). Basically, it extends the least-square approach by the concept of penalizing high values for regression coefficients. Since the LASSO may shrink least-square estimators to zero (in contrast to ridge regression), it also performs variable selection and helps us to focus on main drivers of energy consumption (Tibshirani 2011). LASSO is defined as follows:

$$\hat{\beta}_{\text{Lasso}} = \arg \min_{\beta} \left[ |y - X\beta|^2 + \lambda \sum_{j=1}^p |\beta_j| \right]$$

In each of our eight models,  $y$  is, of course, energy consumption, while the vector  $X$  represents the respective set of explanatory variables (Table 8.2), and  $\beta$  is the vector of regression coefficients. The regularization parameter  $\lambda$  is determined using a tenfold cross-validation. This means our database of 420 days of operation is partitioned into 10 segments of 42 randomly selected days with 9 segments being used to calibrate the model and 1 to test it. The calibration and test procedure is carried out ten times so that each set of 42 days has served exactly once for quality testing. Overall precision of the model is calculated over the ten test runs as an average mean square error over all three iterations.

## 8.4 Results and Discussion

The reported results along with the breadth of the database are detailed in Table 8.3. Prediction quality is provided as a mean absolute percentage error (MAPE) and the goodness of fit as the adjusted coefficient of determination (adjusted  $R^2$ ). Note that the number of records used for each model may deviate due to different availability of input

**Table 8.3** Linear models, database breadth, model fitness and prediction quality

Model no.	Independent variables	Number of records	Adjusted $R^2$	MAPE (%)
1	Distance	416	0.801	11.32
2	Distance, temperature	416	0.869	9.01
3	Distance, stops	406	0.825	9.35
4	Distance, payload	60	0.529	18.59
5	Distance, temperature, stops	406	0.882	7.49
6	Distance, temperature, payload	60	0.532	17.66
7	Distance, stops, payload	57	0.517	17.71
8	Distance, temperature, stops, payload	57	0.498	18.63

data. For instance, the lower number of records for models involving payload traces back to the poor reliability of the data recorded by the vehicle-integrated weighing system.

The results suggest that the simple rule of three approach (model 1) can substantially be improved both in terms of model fitness and prediction quality when the model is extended to include ambient temperature and the number of stops (models 2, 3 and 5). Assuming that dispatchers use a safety buffer based on the MAPE when designing round trips, higher precision (lower MAPE) directly translates into more planning flexibility since assumed vehicle range grows. For this purpose, model 5 offers both the highest precision and best model fit. As an unexpected result, including payload (as defined above) as an explanatory variable did not add to the range prediction's precision. A possible explanation could be that during a delivery route, payload changes with each stop requiring a closer look at the respective stops, their sequence and the change in payload. Mere kinetic considerations make it seem worthwhile to consider other options to integrate payload. Results from model 8 suggest that temperature, after all, could play a minor role compared to the other variables as LASSO eliminates it in this model.

---

## 8.5 Conclusion

Predicting energy consumption and, thereby, range for electric trucks are key tasks for fleet managers and dispatchers alike. However, common approaches of range estimation often focus on sophisticated models and methods implicitly assuming continuous availability of different kinds of data. Moreover, it can be expected that, in practice, neither the technical competencies to collect and process data nor the required data to work with those models are available in a company. Therefore, this article illustrated that there is actually a possibility to improve the simple rule of three approach for range estimation by only using data which any logistics planner deals with on a daily basis:

- *Travel distance* which can directly be calculated, even manually, when a dispatcher has decided how to serve the respective customer orders.
- *Number of delivery stops* which is known when the dispatcher has decided which customer orders are allocated to a specific vehicle.
- *Ambient temperature* which can be drawn from public statistics or weather forecasts.

All models discussed are rather simple linear models with few variables, allowing range estimation to be integrated easily into route planning, even in manual procedures. As a first subsequent step, it seems natural to apply similar models to the other vehicle classed from EN-WIN's field trials.

In model 5, adding only average daily temperature and number of customer stops to the planned travel distance showed promising results, reducing the MAPE to 7.49% from 11.32%. This improvement directly increases route flexibility and reliability of route planning for electric vehicles as observations in the field regularly show substantial safety

buffers with respect to expected range. Given the mere physical importance of gross weight (and, hence, payload) for the kinetic energy involved in transport, it is a surprise to see a decrease in estimation quality when including weight/payload. It has to be considered that the number of datasets with data about vehicle weight is particularly small (57 days, cf. Table 8.3). Models not including payload can make use of about 400 round trips, so it can be assumed that either the mere quantity of records too small or considering the initial payload as a parameter is not expedient since payload lowers or at least changes with each delivery stop (Table 8.3). In this context, it might also be important that no model considered the actual stop sequence and their impact on vehicle payload.

Further research directions are, therefore, targeted at practical methods to increase the number of valid records including payload or gross vehicle weight providing a broader database. Exploring the impact of weight on power consumption is particularly important for urban logistics. Companies able to determine the expected range of a certain vehicle based on actual shipment weights and distances can avoid purchasing vehicles based on exaggerated range expectations which, due to large batteries, may offer a sufficient maximum range but are lacking payload.

When it comes to estimation models, it seems worthwhile to refine the approach and disintegrate each round trip into individual legs for which partial energy consumption is estimated and finally summed up to consumption and maximum range per trip, respectively. This kind of model would allow to consider:

- Stop sequence, i.e. including the actual order size and the respective weight to be unloaded at a specific customer site.
- Trip structure, i.e. the actual distances covered between stops and from or to the depot.

Such kind of approach still requires no further data than currently known to vehicle dispatchers but may (at least for routes with numerous stops) entail a substantial increase in effort to calculate ranges. Possible trade-offs between precision of range estimate and dispatcher's working hours could, therefore, move into the focus as well.

**Author Notes and Acknowledgements** The authors welcome correspondence concerning this article and regarding electrified transport in general: Fraunhofer IML, Joseph-von-Fraunhofer-Str. 2–4, 44,227 Dortmund, Germany.

Dr. Sebastian Stütz, Researcher, Team Urban Logistics and Electromobility, sebastian.stuetz@iml.fraunhofer.de; Andreas Gade, Researcher, Team Urban Logistics and Electromobility, andreas.gade@iml.fraunhofer.de; and Daniela Kirsch, Research Team Leader, Team Urban Logistics and Electromobility, daniela.kirsch@iml.fraunhofer.de.

The authors would like to thank all data-contributing businesses and research partners and in particular the German Federal Ministry for the Environment, Nature Conservation and Nuclear Safety (BMU) for the research grant (no. 16EM3118), without which the project “EN-WIN” could not have been realized. The authors are indebted to Mrs. Carolin Drenda and Mr. Robin Drabon for their constructive feedback on the manuscript.

## References

- Alp, O., Tan, T., & Udenio, M. (2019). Adoption of Electric Trucks in Freight Transportation. Research Paper University of Calgary
- Davis, B. A., & Figliozzi, M. A. (2013). A methodology to evaluate the competitiveness of electric delivery trucks. *Transportation Research Part E: Logistics and Transportation Review*, 49(1), 8–23
- Camilleri, P., & Dablanc, L. (2017). A Methodology For Assessing The Potential Of Electric Vehicles 1 With French Commercial Vans As A Case Study 2 (No. 17-00980)
- Erdelić, T., & Carić, T. (2019). A Survey on the Electric Vehicle Routing Problem: Variants and Solution Approaches, *Journal of Advanced Transportation*, Vol. 2019, 1-48
- Erdoğan, S., & Miller-Hooks, E. (2012). A green vehicle routing problem. *Transportation research part E: logistics and transportation review* 48(1), 100-114
- Felipe, Á., Ortuño, M. T., Righini, G., & Tirado, G. (2014). A heuristic approach for the green vehicle routing problem with multiple technologies and partial recharges. *Transportation Research Part E: Logistics and Transportation Review*, 71, 111-128
- Helms, H., Pehnt, M., Lambrecht, U., & Liebich, A. (2010). Electric vehicle and plug-in hybrid energy efficiency and life cycle emissions. In 18th International Symposium Transport and Air Pollution, Session, Vol. 3, p. 113
- Jerratsch, J. O., Herzlieb, T., & Marker, S. (2018). Using Secondary Data To Reduce Measuring Efforts In Naturalistic Driving Observation. In Conference on Future Automotive Technology.
- Goeke, D., & Schneider, M. (2015). Routing a mixed fleet of electric and conventional vehicles. *European Journal of Operational Research* 245.1 (2015), 81-99
- Granada-Echeverri, M., Cubides, L., & Bustamante, J. (2020): The electric vehicle routing problem with backhauls. *International Journal of Industrial Engineering Computations* 11.1 (2020), 131-152.
- Lin, J., Zhou, W., & Wolfson, O. (2016). Electric vehicle routing problem. *Transportation Research Procedia* 12. Supplement C, 508-521
- Lee, D. Y., Thomas, V. M., & Brown, M. A. (2013). Electric urban delivery trucks: Energy use, greenhouse gas emissions, and cost-effectiveness. *Environmental science & technology*, 47(14), 8022-8030
- Liimatainen, H., van Vliet, O., & Aplyn, D. (2019). The potential of electric trucks – An international commodity level analysis. *Applied Energy*, 236, 804-814.
- Moll, C., Plötz, P., Hadwich, K., & Wietschel, M. (2020). Are Battery-Electric Trucks for 24-Hour Delivery the Future of City Logistics? A German Case Study. *World Electric Vehicle Journal*, 11(1), 16
- Oberhofer, P., & Fürst, E. (2013). Sustainable development in the transport sector: influencing environmental behaviour and performance. *Business Strategy and the Environment*, 22(6), 374-389
- Ospychuk, O. (2019). The possibilities of using IT platforms for urban freight distribution in transport SMEs from the West Pomeranian region. *Transportation Research Procedia*, 39, 381-388
- Pelletier, S., Jabali, O., & Laporte, G. (2016). 50th anniversary invited article—goods distribution with electric vehicles: review and research perspectives. *Transportation Science*, 50(1), 3-22
- Quak, H. J., & Nesterova, N. N. (2018). Zero emission city logistics. The possibilities of battery electric reight vehicles-now and in the future. Conference: HVTT15. International Symposium on Heavy Vehicle Transport Technology, At Rotterdam, 1-12
- Seiler, T. (2012). Operative transportation planning: solutions in consumer goods supply chains (Doctoral dissertation TU Berlin)

- Stütz, S., Bernsmann, A., Baltzer, T., Hentschel, N., Pommerenke, K., Rogmann, B., & Wunderlin, P. (2016). Elmo - Elektromobile urbane Wirtschaftsverkehre. Final Report. <https://doi.org/10.2314/GBV:867815116>
- Stütz, S., Fink, A., & Taefi, T. T. (2018). Insights into Real-World Energy Consumption of Medium-Duty Electric Vehicles, EVS30 Symposium, Stuttgart, Germany, October 9-11, 2017
- Taefi, T. T., Fink, A., & Stütz, S. (2016). Increasing the Mileage of Battery Electric Medium-Duty Vehicles: A Recipe for Competitiveness? Research paper University of Hamburg
- Taefi, T. T., Stütz, S., & Fink, A. (2017). Assessing the cost-optimal mileage of medium-duty electric vehicles with a numeric simulation approach. *Transportation Research Part D: Transport and Environment*, 56, 271-285
- Teoh, T. G. H. (2018). Suitability of battery electric vehicles and opportunity charging for urban freight transport: an evaluation framework (Doctoral dissertation Nanyang Technological University Singapore)
- Tibshirani, R. (1996). Regression shrinkage and selection via the lasso. *Journal of the Royal Statistical Society: Series B (Methodological)*, 58(1), 267-288
- Tibshirani, R. (2011). Regression shrinkage and selection via the lasso: a retrospective. *Journal of the Royal Statistical Society: Series B (Statistical Methodology)*, 73(3), 273-282
- Tseng, C. M., & Chau, C. K. (2017). Personalized prediction of vehicle energy consumption based on participatory sensing. *IEEE Transactions on Intelligent Transportation Systems*, 18(11), 3103-3113
- Wang, J., Lim, M.K., Tseng, M.L., Yang, Y. (2018): Promoting Low Carbon Agenda in the Urban Logistics Network Distribution System, *Journal of Cleaner Production*, 211, 146-160
- Zhou, Y., Ravey, A., Péra, M.-C. (2019): A survey on driving prediction techniques for predictive energy management of plug-in hybrid electric vehicles. *Journal of Power Sources*, 2019, 412,480-495

**Open Access** This chapter is licensed under the terms of the Creative Commons Attribution 4.0 International License (<http://creativecommons.org/licenses/by/4.0/>), which permits use, sharing, adaptation, distribution and reproduction in any medium or format, as long as you give appropriate credit to the original author(s) and the source, provide a link to the Creative Commons license and indicate if changes were made.

The images or other third party material in this chapter are included in the chapter's Creative Commons license, unless indicated otherwise in a credit line to the material. If material is not included in the chapter's Creative Commons license and your intended use is not permitted by statutory regulation or exceeds the permitted use, you will need to obtain permission directly from the copyright holder.



---

**Part II**  
**Energy**





# Increased Efficiency Through Intelligent Networking of Producers and Consumers in Commercial Areas Using the Example of Robert Bosch GmbH

Andreas Biesinger, Ruben Pesch, Mariela Cotrado, and Dirk Pietruschka

## Abstract

Energy-efficient heating and cooling systems as well as intelligent systems for energy distribution are urgently required in order to be able to meet the ambitious goals of the European Union to reduce greenhouse gas emissions. The present article is intended to show that intelligent system extensions for the area of heating, cooling and electricity production for the industrial sector can lead to significant increase in efficiency. For this purpose, a simulation study for the expansion of a combined heat and power (CHP) plant with 2 MW thermal output using a 1.4 MW absorption chiller has been carried out. This shows that a heat-controlled CHP unit can significantly increase its running time. A system model was created for the initial situation and validated with existing measurement data. In the second step, this model was expanded to include the ACM module. The simulation was able to prove that in the event of a system expansion, the run time of the CHP unit can be increased by 35%. In addition to then increase of energy efficiency in the supply system, the analysis also focuses on the efficiency of the energy distribution via thermal networks in an industrial environment. The presented paper therefore also highlights the optimization potentials in the operation of thermal supply networks for industrial applications. For this purpose, a mathematical model has been developed which in addition to the components of the thermal network itself also comprises the producers

A. Biesinger (✉) · R. Pesch · M. Cotrado  
Hochschule für Technik Stuttgart, Stuttgart, Germany  
e-mail: [Andreas.biesinger@hft-stuttgart.de](mailto:Andreas.biesinger@hft-stuttgart.de)

D. Pietruschka  
Institute for Applied Research, University of Applied Sciences Stuttgart, Stuttgart, Baden-Württemberg, Germany

and consumers. The specific construction of thermal networks for the supply of industrial properties requires adapted solutions for the simulation of such systems. Therefore, amongst other things, in the paper, solutions are shown for the modelling of direct flow local heating networks as well as for the operation of a cascade-controlled pump group.

---

**Keywords**

District heating network · Simulation · Combined heat and power plant (CHP) · Absorption chiller (ACM) · Combined cooling · Heat and power system (CCHP) · Digital twin · Heating network transition · Decentralized feed-in · Low return line temperatures · Parallel primary/secondary piping (direct flow local heating networks) · Virtual heat exchanger

---

## 9.1 Introduction

In order to achieve the ambitious goals of the European Union (EU) of reducing greenhouse gas emissions by 80% below the 1990 level by 2050 (European Commission, 2011), the efficiency of energy generation and its distribution must be significantly improved. Around half of the EU's total final energy consumption is used for heating and cooling buildings and the use of thermal energy in industrial environments (European Commission, 2016). The cooling of office buildings and industrial processes is responsible for a significant part of the total electricity consumption. This proportion is expected to increase further in the coming years (RESCUE, 2015). Special weather situations such as persistent heat waves are putting considerable strain on the power grid already (ENTSOE, 2017).

In addition to efficient cooling, intelligent heat generation and in particular heat distribution are equally important. This also includes a sensible combination of different forms of energy, for example, through combined heat and power. The operation of thermal networks is changing. The endeavour to lower the flow temperature in heating networks as much as possible and in return to increase it in cold water networks poses new challenges for planners and operators. The flexibilization of thermal networks is therefore an important factor in achieving the goals set by 2050.

Against this background, the iCity project deals within the sub-project 3.1, "Increasing efficiency through intelligent networking of producers and consumers in commercial areas using the example of Robert Bosch GmbH at the Schwieberdingen location", with various questions about increasing the efficiency of an industrial site. Robert Bosch GmbH's Schwieberdingen industrial site serves as a case study for the development and testing of general approaches.

Two main topics are dealt with in the present work. On the one hand, this is the development of a simulation tool for calculating thermal networks. The specific requirements of the heating network of the present case study must be considered. On the other hand, the increase in efficiency of the operation of an industrial combined heat and power plant (CHP) through the establishment of a combined cooling, heat and power

system (CCHP) is considered. It has been shown that CHP plants in Europe get a very useful extension to combined cooling, heating and power systems by combining them with absorption chillers (ACM) (Haider, M., et al., 7/2005a). With modern absorption chillers and an intelligent control concept, the running times of a CHP unit can be significantly extended (Albers, J. et al., 2017). To analyse the combined operation and to evaluate the optimal sizing, a detailed dynamic simulation model has been developed in TRNSYS. Monitoring data collected for the heating and cooling supply of the whole site has been used as a basis for the simulations.

## 9.2 Case Study Description

The Schwieberdingen location has been operated by Robert Bosch GmbH as a development centre since 1968 and currently employs around 6800 people. The site covers more than 45 hectares, with currently around 60 buildings. Figure 9.1 shows an aerial photo of the industrial site from 2018.

The structure of the industrial site is in constant change. Ongoing construction projects continuously change both the building landscape and the building use. The location has an independent heating and cooling supply. The required thermal heating and cooling energy is generated in two energy centres and distributed to the consumers via the on-site networks. Figure 9.2 shows the two energy centres 509 (central 1) and 307 (central 2) beside the buildings of the industrial site.

Through the iCity project, a comprehensive measurement data recording of all energy flows is being set up for the Bosch Schwieberdingen industrial area. The energetic data of



**Fig. 9.1** Industrial site Schwieberdingen of Robert Bosch GmbH

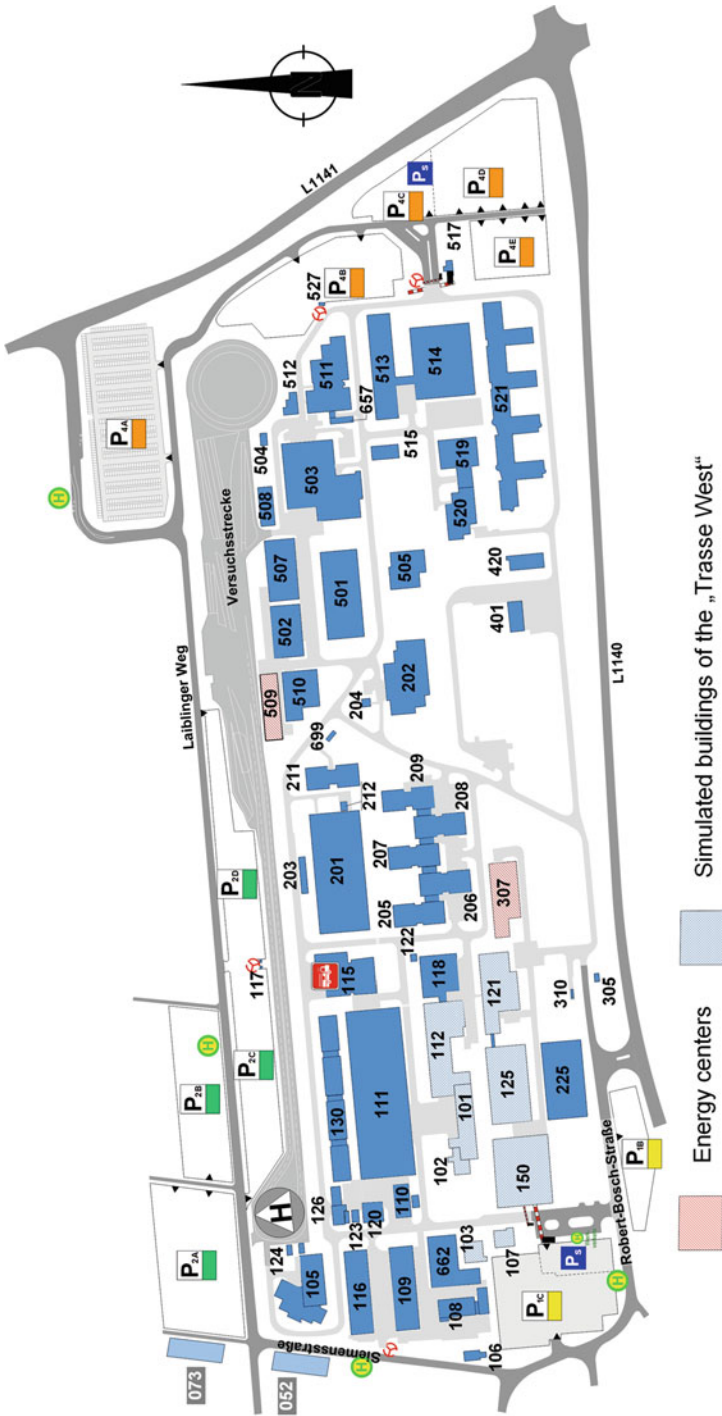


**Fig. 9.2** Location scheme of the Bosch Schwieberdingen industrial site with the two energy centres 509 (central 1) and 307 (central 2), as well as the buildings on the supply “Trasse West” (Robert Bosch GmbH)

all thermal generators and the distribution of the generated energy via the heating or cooling network at the location are recorded using measurement technology. The cross-system measurement data are recorded centrally via the building management system at the site and historized in databases. With the “EmTool”, a software developed at Stuttgart Technology University of Applied Sciences, these databases are summarized and continuously updated. The EmTool is able to generate synchronized time series across all systems, which enables a detailed analysis of the measurement data. For the present work, time series as input data for simulations and their validation are generated with the EmTool.

The heating energy consumption of approx. 20 GWh per year and the cooling energy consumption of approx. 40 GWh per year of the entire industrial site are covered by two heating and cooling centrals and distributed through heating and cooling networks. In case of the cooling, some additional decentralized chillers are used in buildings which are not connected to the cooling grid. To cover the high energy demand, the total installed heating capacity in the two energy centres is approx. 23 MW and is provided by natural gas boilers and a heat pump for the low-temperature heating distribution. Part of the heating energy is generated by a combined heat and power plant, which varies between 8 and 10 GWh per year. The total installed cooling capacity at the location is approx. 21 MW and is mainly covered by compression chillers with dry or hybrid air coolers and wet cooling towers. The property’s annual electricity consumption is around 65 GWh (including electricity for cooling). At the site, seven photovoltaic systems and the CHP unit are currently operated to generate their proper electricity. In-house power generation for 2019 (CHP and five PV systems) was around 8 GWh. Figure 9.3 shows the measured data of the site for the electrical energy demand, heating and cooling energy demand as well as the property’s own energy production for heat and electricity by the CHP and photovoltaics.

Figure 9.4 shows the thermal networks for supplying the industrial site with the required heating and cooling. A 7°/13° cooling network and two heating networks with different temperature levels are operated via the two energy centres. In addition to the 90°/70° high-temperature network from central 2, a 60°/40° low-temperature network is operated for the eastern part of the site via a heat pump in central 1.

---

## 9.3 Study to Increase the Run Time of a CHP by an Absorption Chiller

### 9.3.1 Initial Status Analysis

The following sections deal with analyses on the operation of the above-mentioned CHP plant in the industrial environment. The gas-fired combined heat and power plant has a thermal capacity of 2 MW. The electrical capacity is thereby approximately 1.6 MW. The co-generation unit is located in the central 2 heating and cooling centres, where the majority of the heating energy for the site is generated. In the central 1, however, most of the cooling energy is provided. The location of the two power stations is shown in

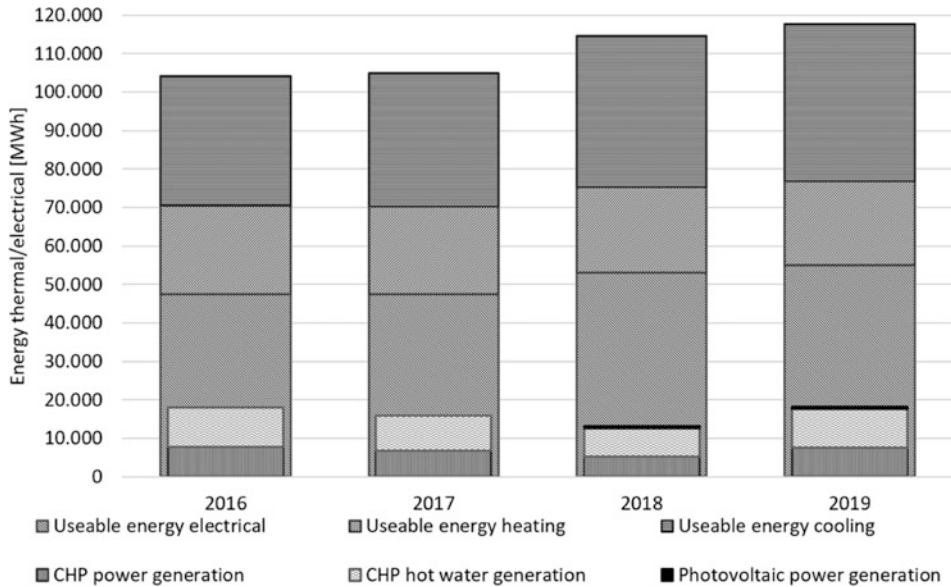


**Fig. 9.3** Energy consumption data as well as own production at the site by CHP and photovoltaics

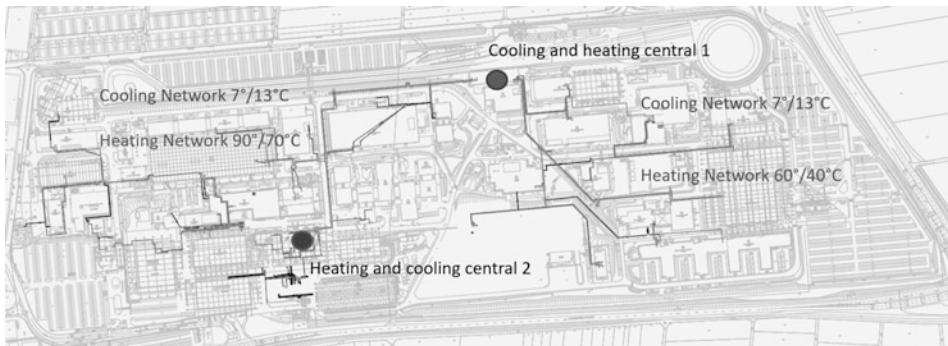


**Fig. 9.4** Heating and cooling networks at the industrial site (Robert Bosch GmbH)

Fig. 9.4 (in the context of heating and cooling network) and Fig. 9.2 (in the context of the site buildings).

The CHP is heat-controlled, i.e. operation depends on the seasonally fluctuating heat load at the site. Bosch's decision to operate the CHP unit heat-controlled is based on ecological considerations. The CHP unit couples the heat generated into the heating network all year round, thus covering the base load of the heating requirement. However, in summer or during off-peak periods, the load in the heating network regularly falls below the thermal part load operation of the CHP unit, which leads to power modulations and a clocked operation. Figure 9.5 shows the typical course of CHP operation on two exemplary

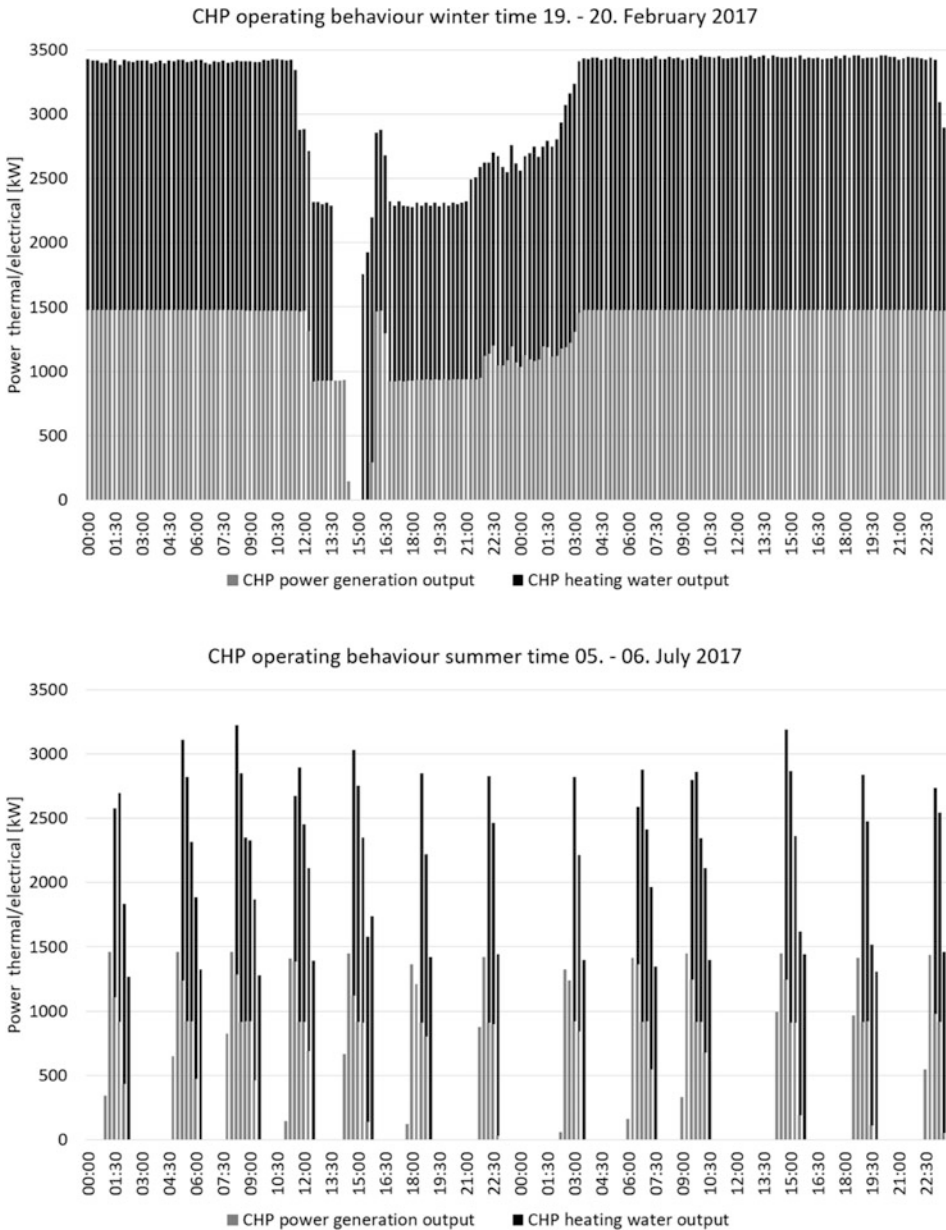


**Fig. 9.5** Typical behavior of the CHP operation for two exemplary days in winter and in summer

days in winter and in summer 2017. The diagram below clearly shows the fluctuating operation of the CHP in summer. This results from the high heat output of the CHP unit with simultaneous low network consumption. In winter, on the other hand, the CHP unit is

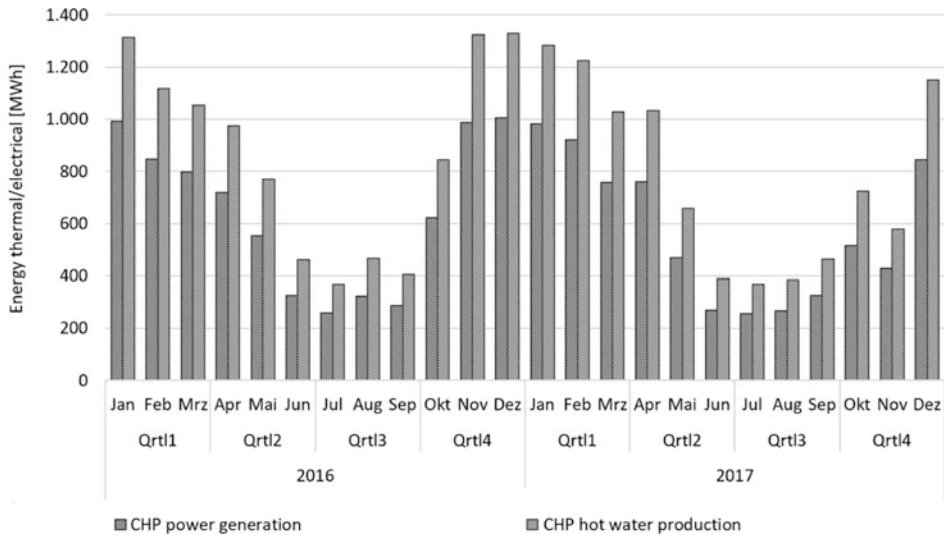


**Fig. 9.6** Monthly net electricity and hot water generation of the CHP for the years 2016 and 2017

operated at full load for long periods, which is usually only interrupted briefly, as can be seen in the upper of the two diagrams.

Due to the clocked operation of the CHP in summer, the theoretically possible running times of the plant are not achieved. The diagram in Fig. 9.6 shows that electricity and heat generation in the summer months is significantly lower than in the winter months. The present study aims to investigate the possibilities of increasing the running time of the CHP.

All considerations regarding the optimization of running time assume that the CHP unit continues to be operated in a heat-controlled manner. This requirement means that a solution must be worked out, from which the additionally generated heat can be used under energetically, ecologically and economically sensible aspects. Initial considerations in this regard included a concept to supply heat in excess of the plant's own requirements to a residential area close to the site via a district heating connection. After initial studies, however, this concept had to be rejected. Further scenarios aimed at storing the excess heat in long-term storage facilities. Within the framework of the project, extensive studies were carried out on the so-called seasonal storage systems. Projects that have already been implemented but are also still in the planning stage were examined for their applicability to the case study. As an example for the concept implementation of seasonal storage, a project in Friedrichshafen Wiggenshausen (Morgenbrodt, L. 2008) can be mentioned, which is one of the largest in Germany. The parameters of the storage facility and its characteristics provide an overview of the potential applications of this technology. The seasonal storage facility has a volume of 12,000 m<sup>3</sup> with a storage capacity of 675 MWh. The planned construction costs of the project were estimated at about 1.35 million euros. Irrespective of



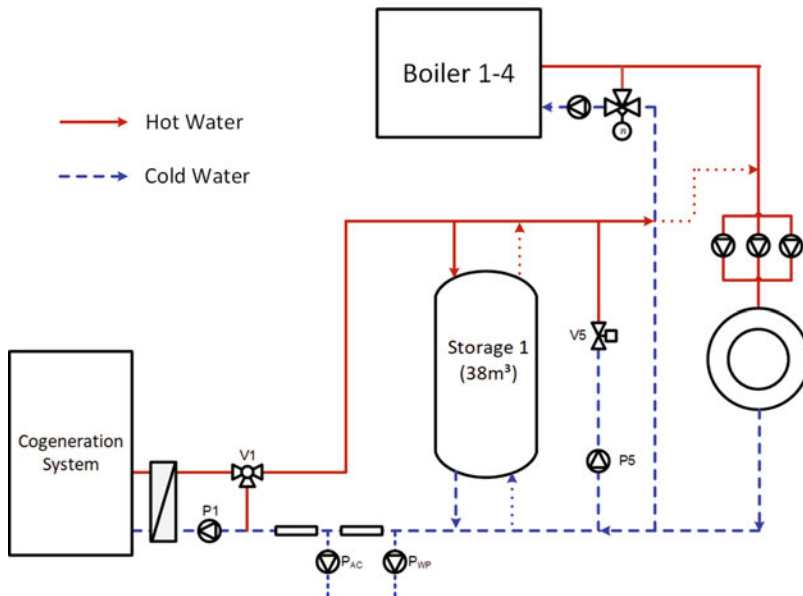


**Fig. 9.7** Simplified scheme of the heating center central 2

the above-mentioned costs, implementation cannot be considered reasonable from a technical point of view. With a storage capacity of 675 MWh, the co-generation plant will be extended by just under a month in summer. Therefore, such a solution is not reasonable from an economic point of view.

Another promising idea was to extend the operating time of the CHP by means of a combined cooling, heat and power system. For this purpose, it should be investigated whether the integration of an absorption chiller, which is operated by means of the heat generated by the CHP unit into the energy production process, can be realized. This concept was generally considered to be promising and should therefore be investigated in more detail in this study.

Figure 9.7 shows a very simplified scheme for heat generation in the central 2 by the CHP. A 38 m<sup>3</sup> hot water tank is located between the CHP unit and the hot water network. This is dynamically loaded when the heat load on the hot water network falls below the minimum output of the CHP unit. The CHP is operated in two stages. Normal operation corresponds to the nominal thermal output of 2 MW, and in partial load operation, the CHP unit achieves an output of 1.5 MW. In the summer months, the CHP unit starts about six times within 24 h with a respective running time of about 75 min per cycle. This means that the CHP unit starts up almost 1000 times during the summer months because it is heat-controlled. During the summer months, the entire heating load of the site is carried by the CHP. In the winter months, the gas boilers 1–4 are dynamically switched on according to the existing heating load. The economic efficiency of CCHP plants depends significantly on the utilization period of the units (annual full load utilization hours) (Haider, M., et al.,

8/2005b). Due to the different operating conditions, a precise analysis of the load curves for electricity demand, heating demand and cooling demand at the industrial site is essential.

The diagram in Fig. 9.8 shows the total monthly heat energy provided by the CHP and the gas boilers in central 2 for the year 2017. During the summer months, the heat demand of the industrial site drops under 500 MWh, which is about 1000 MWh less than the monthly heat production of the CHP. Accordingly, during the summer months, nearly 1000 MWh more could be produced via the CHP. From this, a theoretical (maximum) heat potential for the operation of the CHP unit can be determined from a static point of view. This is the difference between the amount of heat required, i.e. the existing load profile, and the heat that can theoretically be generated by the CHP unit. In the diagram, this potential is represented by the line with the circle symbols. For the year 2017, this value is approx. 8750 MWh.

With this purely static approach, however, it is not possible to examine the extent to which the operation of an ACM can be integrated into the energy supply of an industrial site in terms of systems technology.

In the present study, therefore, the operating mode of a planned system is examined in detail with the aid of dynamic simulation. For this simulation study, the existing load curves and system-related boundary conditions of the case study are to be considered. Thus, an exemplary operation of the CHP can be investigated based on realistic data. The results obtained in this way can be used for further considerations such as a CO<sub>2</sub> balance, an economic analysis or an operation optimization. Furthermore, the scenario developed can be used for planning and implementation at other industrial sites.

### 9.3.2 Simulation Study

For the creation of the simulation models mentioned here, the software TRNSYS in version 18 was used. First, the basic methodology is explained. In the following, the created simulation model is explained in detail. Finally, the results are presented and discussed.

#### Methodology

A numerical model of the existing CHP plant was created as a basis for the simulation study on combined heat and power generation. In a first step, the basic model was validated with the measurement data available on site. The aim of this fundamental work was to obtain a basic model of the CHP system validated with load curve data available at the site, which could be extended in the second part of the study by the module of the absorption chiller. For the CHP base model, the CHP and the associated 38 m<sup>3</sup> storage tank were considered, as shown in Fig. 9.7 in simplified form. The gas boilers 1–4 as further heat generators were not yet part of this model.

For the simulation study, an extended model was created in the next step. For this, the basic model had to be extended by the module of the absorption chiller. This system includes the ACM itself, three cooling towers for recooling the chiller and a significant

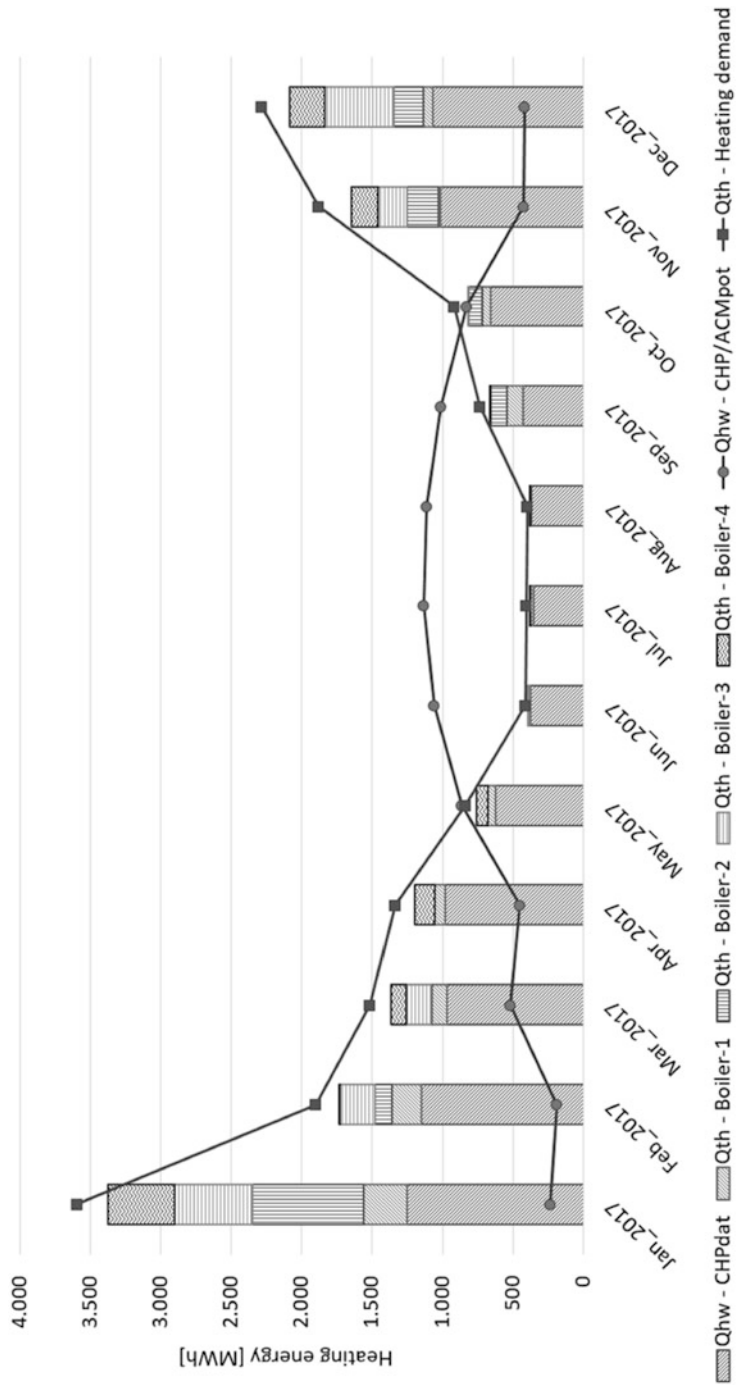


**Fig. 9.8** Theoretical heat potential for the operation of an ACM through extended running times of the CHP

buffer storage expansion in the form of a second tank with a volume of 160 m<sup>3</sup>. For the study, the technically possible maximum storage size for the site was used. This is a result of the maximum size of the storage components that can still be transported on normal traffic routes. With these components, a simple system was created with a focus on functionality. First of all, this model was to be used to investigate the basic feasibility as well as an expected extension of the operating time of the CHP. For the study, a lithium bromide absorption chiller with a nominal cooling capacity of 1.4 MW and a hot water-side power consumption of 2 MW at a temperature spread of 90/55 °C was selected. In order to be able to take the dynamic heating and cooling load of the case study into account in the model, it had to be extended with the components of heat and cold generation. Therefore, in the last step of the modelling, the gas boilers as heat generators and the compression chillers with the associated recooling as cooling generators were implemented into the overall model. In addition to the thermal simulation, the parameters of the electrical generators and consumers were also included in the model. Figure 9.9 shows a simplified schematic of all components that are part of the simulation model, with the exception of the gas boilers. In the illustration, the components of the absorption chiller module are outlined with a dashed line.

### Model Description

As mentioned at the beginning, the simulation model was developed in TRNSYS 18. In the following, some basic information on the most important modules of the model is explained.

The central CHP model was created with the Type 907 “IC Engine Generator”. Water is used as heat transfer medium. Its density and specific heat capacity are considered in the model depending on the temperature. The heat exchanger is calculated with Type 5b, and the heat transfer of exhaust gas and heat pump (cabin cooling) is calculated with TEES Type 682 “Heating and Cooling Loads Imposed on a Flow Stream” (Tess Library, TESS 2017). The pipe connections for fluid transport are made with Type 31. Type 2d (*On/Off* differential controller) was used to model the pumps. The two heat accumulators were modelled with Type 158. The absorption chiller was modelled with the TRNSYS Type 107, and for the three cooling towers of the recooling system, the Type 162b was used. The three compression chillers used in the central 2 energy centre differ in their design and performance. The smaller plant with a cooling capacity of 1 MW was modelled with TESS Type 666 (Tess Library, TESS 2017), and the two larger 2.5 MW plants were modelled with TESS Type 668.

### Control Strategies

A control concept for dynamic simulation was developed for the basic model of CHP operation. For this purpose, the control concept of the existing plant had to be divided into defined operating states with the respective parameters. For the final model, with ACM, further operating states were defined according to this procedure. The relevant parameters

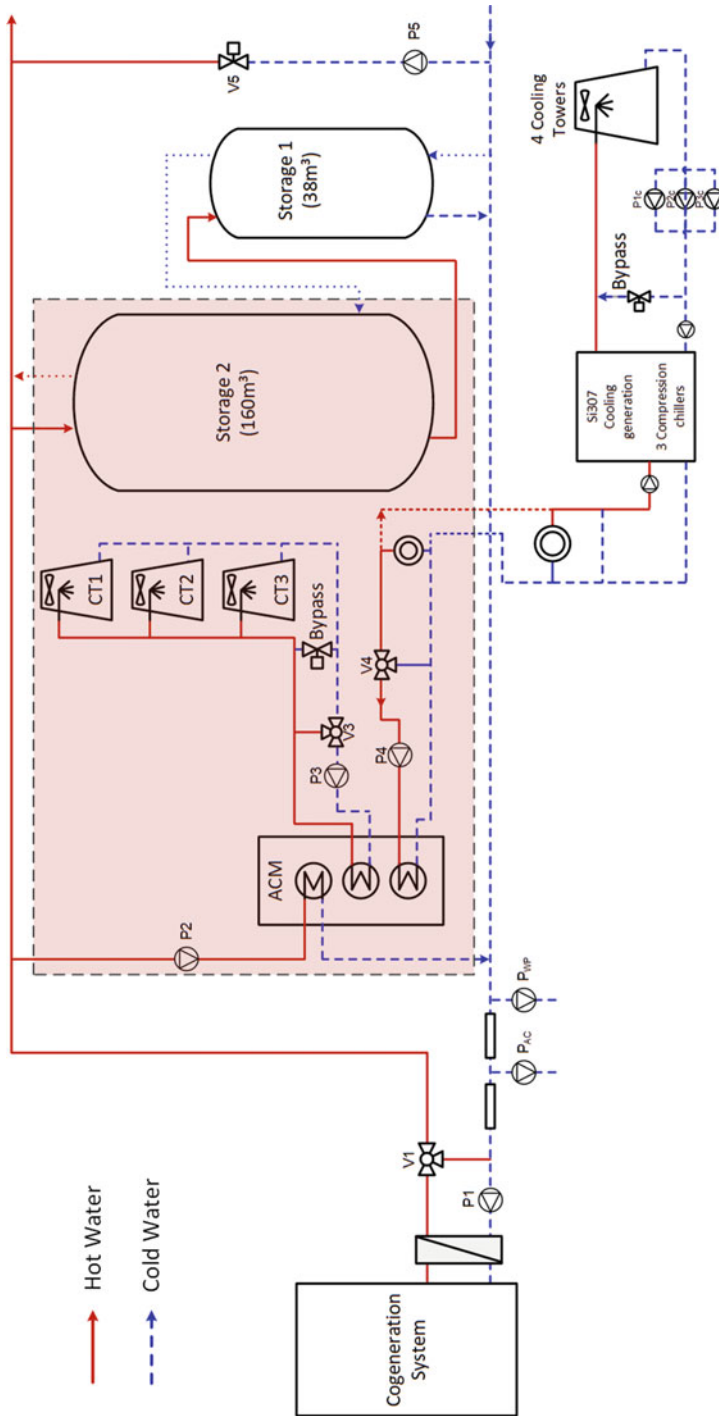


**Fig. 9.9** Simplified scheme for the integration of an ACM into the existing CHP plant system

**Table 9.1** Operating states from which the control strategy is defined

Status	CHP	ACM	Storage	Hot water network	Cold water network
1	ON (full power)	OFF	Partial loading	Demand	Demand
2	ON (partial power)	OFF	Partial loading	Demand	Demand
3	OFF	OFF	Unloading	Demand	NO demand
4	ON (full power)	ON	Partial loading	Demand	Demand
4.1	ON (full power)	ON	Partial unloading	Demand	Demand
5	ON (full power)	OFF	OFF	Demand	NO demand

for plant control are anchored in the respective states. A total of six states were thus defined with which the entire plant operation can be represented.

Table 9.1 shows in a simple matrix the respective states of the plant operation considered for the study. States 1 to 4.1 represent the transition months and the summer. State 5 is pure winter operation. Although there is also a cooling requirement here due to the test stands operated all year round at the site, the heat produced by the CHP unit is completely fed into the heating network and not used for the operation of the ACM. However, during the winter months, the refrigeration required for this purpose is provided entirely by central 1.

For the operation of the gas boilers and the compression refrigeration machines, operating states were also defined and implemented in a control matrix. These states are downstream of the respective superordinate state from the overall model.

## Simulation Results

The two scenarios—(1) initial state with a pure CHP operation and (2) plant extension with an absorption chiller—were simulated with input data from the case study for the period April 2018 to March 2019. For a comparability of the two cases, they must be based on the same data of the thermal energy supply. Therefore, the measured load curve data for heat and cold production in the period under consideration were used as input data for the simulations. A time step of 5 min was chosen for the simulation. The system limit for the following considerations was set at the central 2 energy centre.

The diagram in Fig. 9.10 shows a summary of the central results from both scenarios. The “cooling generation of central 2” is the amount of cooling energy distributed from energy central 2 via the cooling network to the connected consumers. This amounts to 6214 MWh in the period considered and is generated conventionally via the existing compression chillers. Not listed here is the part of the cooling generation that comes from energy central 1. Central 1 also supplies the site with the required cooling energy during the winter months.

For the simulation of the second scenario, the already explained control scheme was applied. The parameters used were selected in such a way that operation of the complex

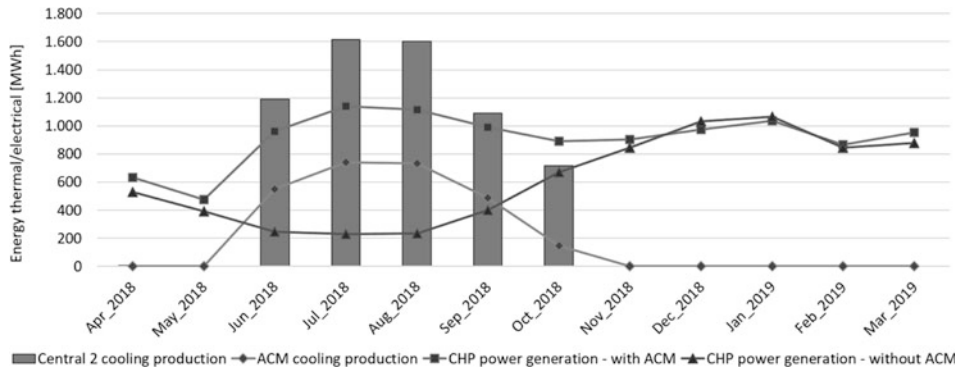


**Fig. 9.10** Electricity and cold production to be expected through the combined heat and power generation

plant network is ensured. The focus here is on extending the operating time of the CHP. Accordingly, the scenario does not yet represent the optimal ACM operation. From this point of view, the cooling quantity produced by ACM is 2658 MWh. This means that approx. 43% of the total cooling demand, which must be covered by the central 2 energy centre, can be produced via the ACM.

The diagram also shows the electricity production achieved by the CHP for both scenarios. As expected, the ACM operation significantly increases the operating time of the CHP unit in summer and thus also the electricity production. In this scenario, an additional production of electrical energy for the site of 3570 MWh can be achieved for the period under review. This corresponds to an increase in CHP electricity production of around 49%.

Ideally, the increase in the site's own electricity production takes place during the period when demand in the energy centre is at its highest. In the summer months, the electricity consumption for energy production is highest over the year as the compression chillers are increasingly in operation during this period. The diagrams in Fig. 9.11 compare the simulation results for electricity consumption and electricity production for the two scenarios. The diagram on top shows the initial situation. Here it becomes clear that the low level of CHP electricity production in the summer months cannot cover the needs of the energy centre. This is divided into three groups: electricity consumption by the CHP (in the diagram below electricity consumption\_CHP-ACM), electricity consumption by the heat generators and electricity consumption for conventional cooling, which accounts for the largest share. The consumption of the generating plants themselves and the auxiliary energy consumption that can be allocated, such as that caused by pumps, are taken into account here. In comparison to the initial scenario, this scenario with ACM shows that the total electricity demand for refrigeration is decreasing. Although the electricity demand for the CHP-ACM system increases, the demand for conventional refrigeration decreases at the same time. Due to the longer running time of the CHP, the own power production

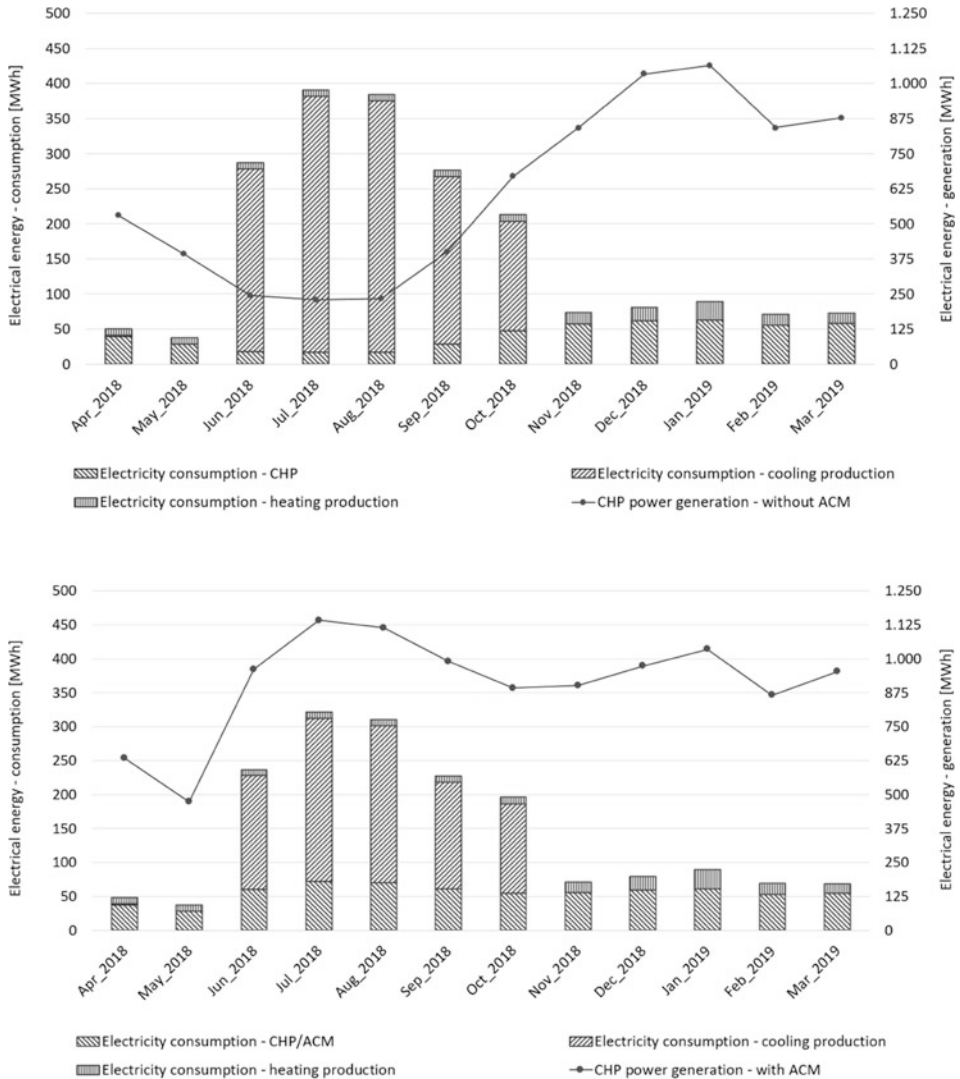


**Fig. 9.11** Power consumption and power production for the cases with (bottom) and without (top) absorption chiller

increases, as already shown, so that the demand can be covered by the central 2 energy centre.

Figure 9.11 shows the impact of the plant expansion on electricity production and consumption. The diagrams in Fig. 9.12 show the comparison for thermal energy. The red line on the diagram on top shows the heat requirement of the energy centre during the period under consideration and how this is covered by the CHP and gas boilers. In the period under consideration, from April 2018 to March 2019, the heat requirement is



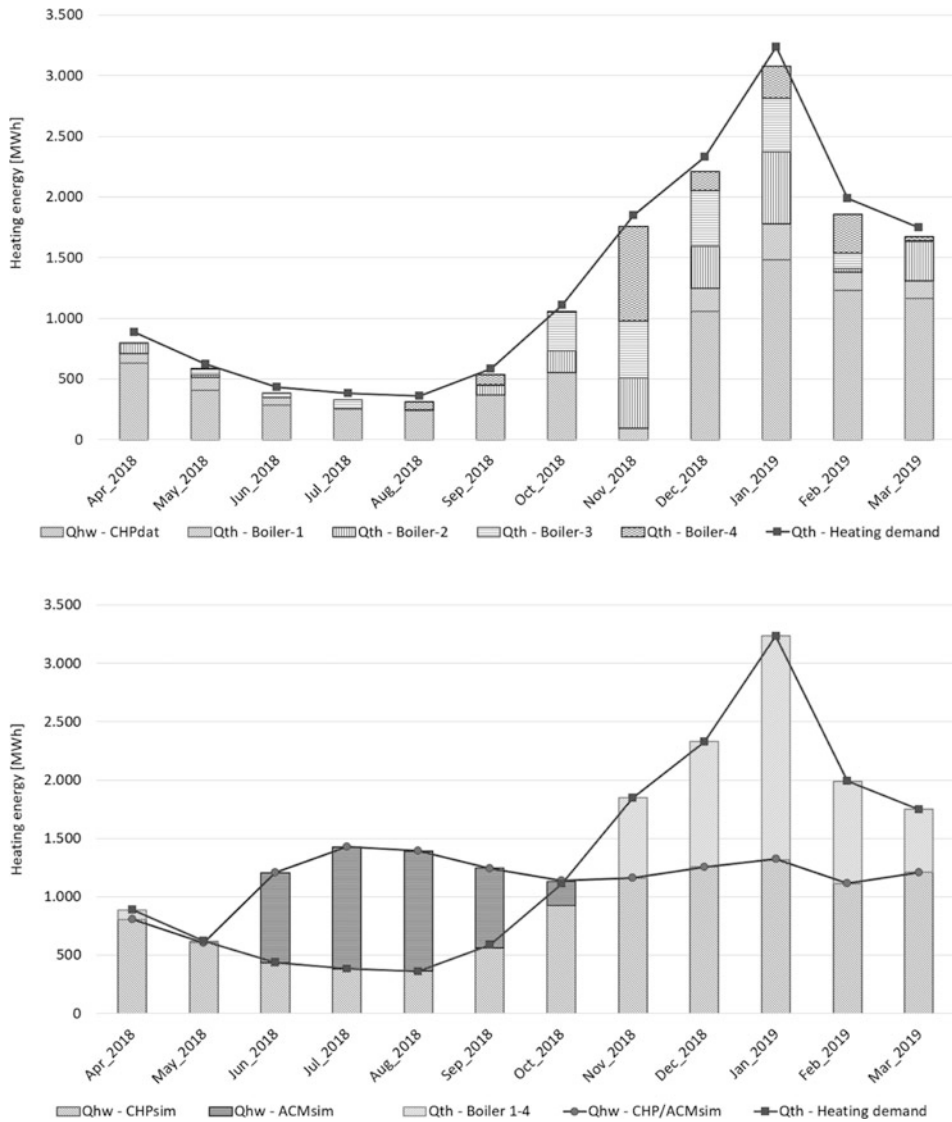


**Fig. 9.12** Thermal comparison of CHP operation with (bottom) and without (top) absorption chiller

15,465 MWh, of which 7672 MWh is covered by the heat production of the CHP unit. Due to the heat supply of the CHP unit, this diagram again shows the low running time of the CHP unit in the summer months. The potential heat production for the CHP unit due to the maximum expected running time is 9848 MWh for this period. The diagram below in Fig. 9.12 shows the results for the simulation of the CCHP system. For the simulation, the real load curves of central 2 for heating and cooling are used. The heat production by the CHP unit is divided into the share for covering the heating demand (Qhw - CHPsim) and

the share of heat production for the ACM operation ( $Q_{hw} - ACM_{sim}$ ). In total, the heat production by the CHP unit in this scenario amounts to 13,885 MWh, which is shown in the diagram with the line  $Q_{hw} - CHP/ACM_{sim}$ . Thus, an increase of 6213 MWh is achieved for the CHP unit through the additional use of the ACM which results in 3570 MWh additional electricity generation. The first simulations for a combined heat and cooling system thus show that the theoretically possible potential can thus be exploited to a good 60%.

The operation of absorption chillers depends on various factors. One limiting factor is the load curve of the cooling demand of the site. If the mass flow of the cold water network at the evaporator of the ACM is too low, the ACM switches to shutdown mode due to the lack of storage facilities for the cold produced. In addition, the heat requirement influences the running times of the ACM. To show this, it is necessary to consider the mass flows. The diagram in Fig. 9.13 shows the simulated mass flows for a selected period in the summer. The summer operation of the heating network at the site is usually characterized by domestic hot water (DHW) preparation. The heating energy required for this is provided exclusively by the CHP. The DHW preparation is given priority over the ACM operation. In real operation, this prioritization is solved purely hydraulically. If the heating demand increases, the CHP unit decreases the lateral mass flow for charging the storage tank and is, however, directly fed into the hot water network. Additional heat demand is covered by the hot water stored in the tank. This has the consequence that the hot water level in the storage tank drops during the ACM operation. If there is an increased demand from the hot water network over a longer period, the storage tank temperature drops below the critical value for ACM operation, and the absorber goes into shutdown mode. The diagram in Fig. 9.13 shows these relationships between mass flows and storage temperatures. The periods in which the mass flow<sub>ACM</sub> (line with circles) goes to zero mark the standstill times of the absorption chiller. These periods are marked in the diagram for clarification.

### 9.3.3 Conclusions

The present contribution shows the results of a simulation study which analyses the CHP operation and its extension to a combined cooling, heating and power systems by combining them with absorption chillers. The plant concept and measurement data from the case study “Entwicklungszentrum Robert Bosch GmbH Standort Schwieberdingen” were used. The CHP plant considered in the study has a thermal capacity of 2 MW, and the electrical capacity is 1.6 MW. The cooling capacity of the extension plant is 1.4 MW. The measurement data available in detail in the case study show that in the years 2016–2019, the CHP unit was able to produce an average of 9000 MWh of heat and 6800 MWh of electricity per year. This means that the CHP unit achieves a capacity utilization of a good 52% of the maximum possible capacity utilization in continuous operation. The reason for this is that the CHP unit is operated on a purely heat-controlled basis for ecological reasons of the site operator. As a result, the CHP unit has an extremely low capacity utilization in the summer

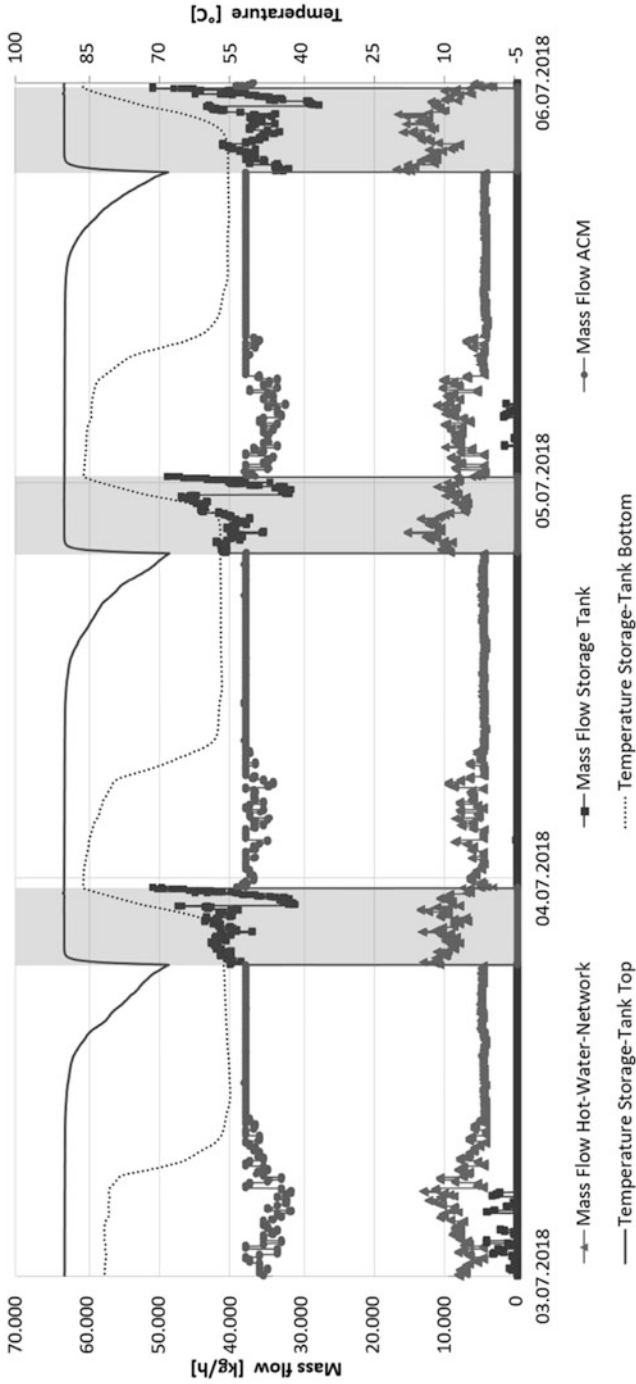


**Fig. 9.13** Distribution of the hot water mass flows that are generated by the CHP plant

months. This study therefore analyses the extent to which longer plant operating times can be achieved by adding an absorption chiller to the CHP unit. The present work investigates the operation of this overall system based on a detailed plant simulation in TRNSYS. The dynamic simulation provides information on how the CHP-ACM operation fits into the energetic overall operation of the case study.

The simulation results show that a significant increase in the operating times of the CHP unit can be expected with the additional absorption chiller. For the simulation, a defined period from April 2018 to March 2019 was considered. For this period, there was an increase from 44% to 79% of the maximum possible heat production by the CHP unit and thus also its capacity utilization. Downtimes due to maintenance work or revisions of the CHP and ACM are not included in this consideration. A detailed analysis of the complex plant operation shows that for ACM operation, downtimes are to be expected for certain boundary conditions even in the summer months.

The work presented here shows that for complex plant systems, such as those presented here, a static consideration can only provide approximate results. The detailed plant model for the simulation of the overall system provides valuable operating information at this point and represents a basis for plant planning and later system optimization. The chosen approach can be transferred to similar constellations in other real estate operations. The findings on modelling gained here will simplify this for future applications. However, the simulation of complex systems, such as the plant available here, is always comparatively time-consuming. For the validation of the basic model, a database that is as consistent as possible is also required.

---

## **9.4 Development of a Simulation Programme for Modelling and Calculation of a Thermal Local Heat Supply**

### **9.4.1 Initial Status Analysis**

The previous part of this article deals with increasing the efficiency of power generation and its supply in an industrial context. Just as important as an energetically optimized energy production is the efficient transport of energy to the respective consumer. Terms such as lowering the supply temperature (Leoni, 2020 or Tol, 2021), decentralized feed-in (Monsalvete, 2017 or Paulick, 2018) or generation change (Haoran Li, 2018) in the field of thermal networks characterize the current developments in this sector. In this chapter, the energy distribution, here in particular the heating distribution by means of a district heating network on an industrial scale, is analysed.

One of the main topics of the present iCity sub-project is the analysis of the heating network at the Schwieberdingen site. The production of heat and cold is divided into two energy centres, which are connected to the properties at the site via two separate distribution networks. In the following, the subject of the analysis is a sub-area of the Schwieberdingen heating network (“Trasse West”). This area needs a simulation model

representing the hydraulic and thermal conditions as accurately as possible. In Fig. 9.2, the buildings along the supply route “Trasse West” are marked with light-grey hatched pattern. Due to the numerous measuring points for temperature, pressure and volume flows within the heating network, the simulated values can be compared with the measured values. With a calibrated model of the heat distribution of the supply route “Trasse West”, scenarios are simulated to find opportunities to reduce the return temperatures of the heating network. Lower return line temperatures mean a higher spread between supply flow and return flow temperature. Through a higher temperature spread, electricity for the operation of the circulation pumps can be saved even though the supplied heating energy remains the same. There are also reduced thermal losses of the network to the environment (media channels or soil). So the lower return temperature saves thermal and electrical energy during the operation of the network. In comparable studies, a saving potential in the order of 0.15 euro/(K\*MWh) was realized (Köfinger, 2017).

Using the example of the “Trasse West”, it will also be analysed to what extent it is possible to reduce the supply temperature without endangering the thermal comfort within the buildings. As a practical implementation measure, the area is examined for possibilities of cascaded connections of consumers (Köfinger 2017). As a criterion for a cascaded connection, the return temperature of the buildings will also be used. However, the focus of this investigation is on finding the highest possible return temperatures that could satisfy a nearby consumer as a supply temperature.

### 9.4.2 Simulation Study of “Trasse West”

The graphical programming software INSEL, which was co-developed at Stuttgart Technology University of Applied Sciences, was chosen as the simulation tool for the investigation of the “Trasse West”. INSEL is a modular programming language similar to TRNSYS. In INSEL, different plant configurations can be displayed on a graphical user interface by interconnecting blocks. The “blocks” in INSEL correspond in functionality and semantics to the “types” in TRNSYS. INSEL is open for the integration of experimental user blocks via dynamic link libraries (“.dll”), which allows the simulation of more complex plant components. The user block “spHeat” described in the following is a block developed at the University for the simulation of thermal networks in INSEL.

## Methodology

### Network Types and Their Representability in “spHeat”

“spHeat” is a simulation tool for mapping the hydraulic and thermal properties of first- to third-generation district heating networks (see Fig. 9.14). For first-generation heating networks, usually only one central heat generator is provided, which is connected to consumers by means of a distribution network. Networks of the second generation include

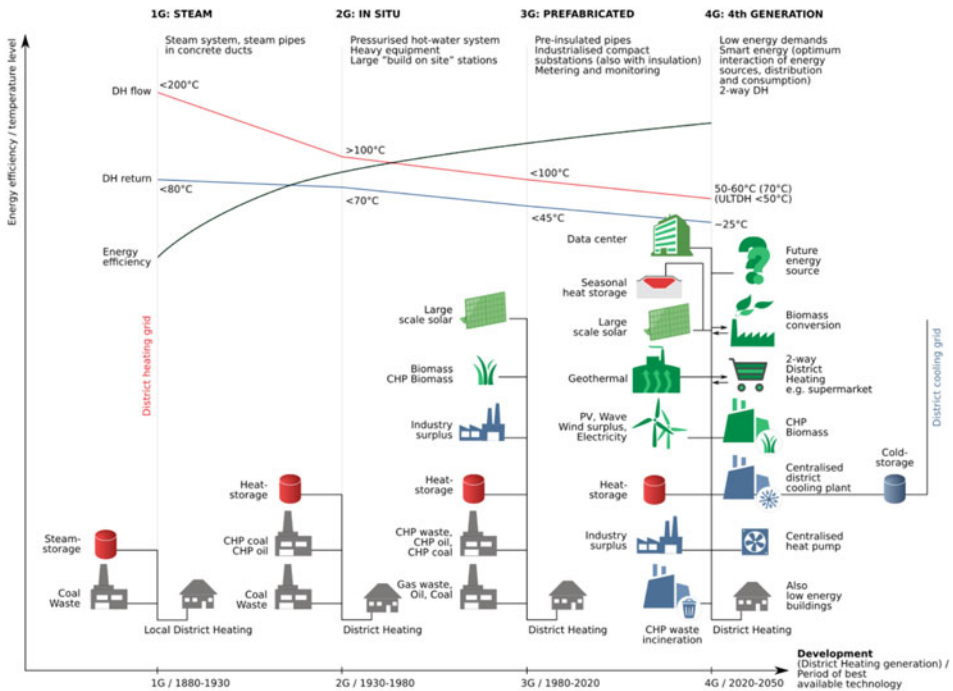


**Fig. 9.14** Evolution in the system development of district heating networks (1st–3rd generation with central circulation pump at the heating plant, decentralised feed-in only planned from third generation). [https://de.wikipedia.org/wiki/Fernw%C3%A4rme#/media/Datei:Generations\\_of\\_district\\_heating\\_systems\\_DE.svg](https://de.wikipedia.org/wiki/Fernw%C3%A4rme#/media/Datei:Generations_of_district_heating_systems_DE.svg). Based on Ashreeta Prasanna et al.: Optimisation of a district energy system with a low temperature network. In: *Energy* and Henrik Lund et al.: fourth Generation District Heating (4GDH)

additional heat generators in the network structure, and the flow temperatures are usually lower.

In third-generation networks, the flow temperature of the networks is further reduced. As a result of this development, it will be possible for the first time to integrate heat from renewable sources in these network types. Possible energy sources include biogenic fuels (biogas, wood chips, etc.) with high combustion temperatures and heat from solar collectors (Heymann, 2018). When selecting the renewable energy sources, it must be ensured that the temperature requirements of the networks of approx.  $70^{\circ}\text{C}$  are achieved (valid for supply line or supply line feed-in). For return temperature increases in pure heating networks, without combined heat and power generation, energy sources with lower source temperatures can also be considered. Common to both types of feed-in is the central connection of the renewable heat. In these network architectures, decentralized feed-in is not provided for and is therefore not supported by the standard version of “spHeat”.

**Fig. 9.15** Network tree with 6 nodes and 5 edges. [https://en.wikipedia.org/wiki/Tree\\_\(graph\\_theory\)](https://en.wikipedia.org/wiki/Tree_(graph_theory)) call 20.10.2020 14:00 h

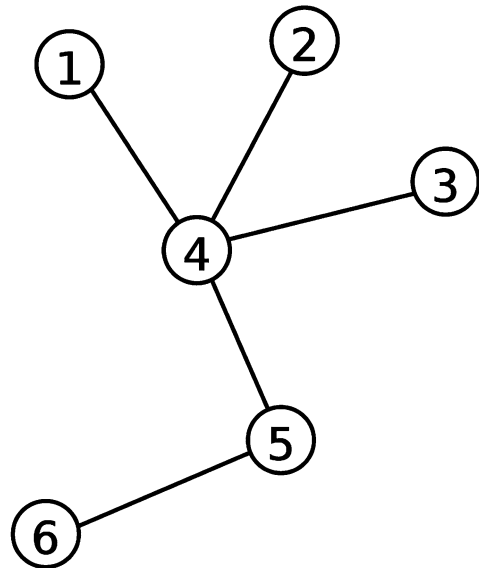


### Image of the Topography of a Network in “spHeat”

Decisive physical parameters for the description of a thermal network are the pressure distribution in the network and the resulting mass flows as well as the flow and return temperatures of the heat transfer medium. The mathematical equivalent of the real network is realized by a subdivision into network nodes and the edges in between (Fig. 9.15).

A network node can represent, e.g. a simple valve, a pipe diameter change, a consumer with a transfer station or a change of direction of the line in the locality. Network edges generally represent pipe sections with constant diameter and constant material and without additional installations. Once the pressure conditions in the network have been calculated and the heat extraction in the case of consumers or the heat input in the case of a decentralized heat generator is known, the temperatures at the network nodes can be calculated by energy balances.

### Programme Sequence for the Calculation of the Variable Sizes of a Mesh in “spHeat”

A quasi-dynamic approach is used to determine the different pressures in the network. The flow and pressure are calculated with the help of a static flow model in the subprogramme “spHydro”. Since the relationship between flow resistance and resulting mass flow is not linear, a numerical approximation method must be used for the calculation (Newton iteration). The temperature, however, is calculated dynamically in “spThermo” depending on the flow velocity and various boundary conditions such as soil and ambient temperature. To solve the differential equations of heat transfer along the pipes, the backward differential method is implemented. In “spHeat”, the network is divided into flow and return flow plane. Both subnetworks are calculated separately (Fig. 9.16).

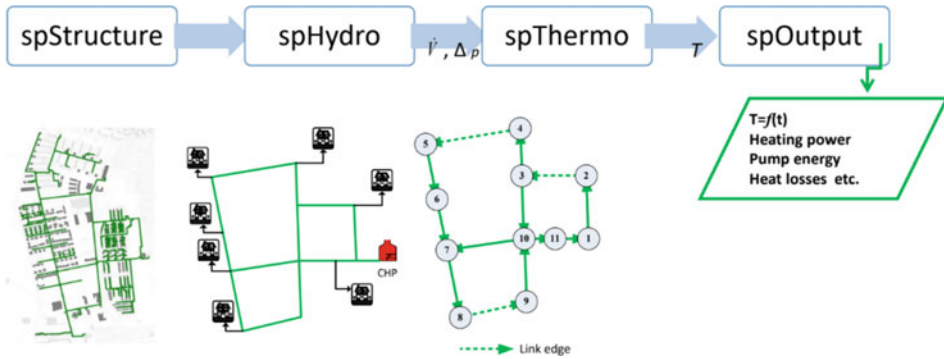


**Fig. 9.16** Program flow diagram of “spHeat” with hand over of variables from program sections

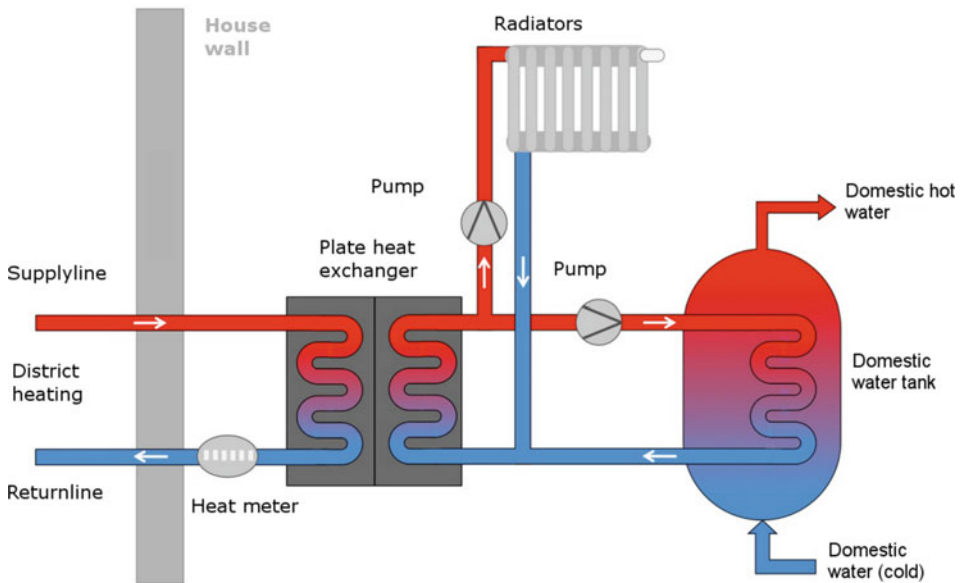


**Fig. 9.17** District heat connection with transfer station (left primary circuit, right secondary circuit). Source <https://www.energiepfad.ch/wiki/fernwaermeuebergabestation/> Call 06.10.2020 16:30 h. (Verein Energiepfad Grabs/FirstMedia Solutions GmbH St. Gallen)

## Model Description

### Hydraulically Separated Systems (Normal Case) or Direct Flow District Heating Networks

A basic assumption made in the simulation with “spHeat” is the division of the network into primary and secondary side and the coupling of both by heat exchangers in the transfer stations (see Fig. 9.17).



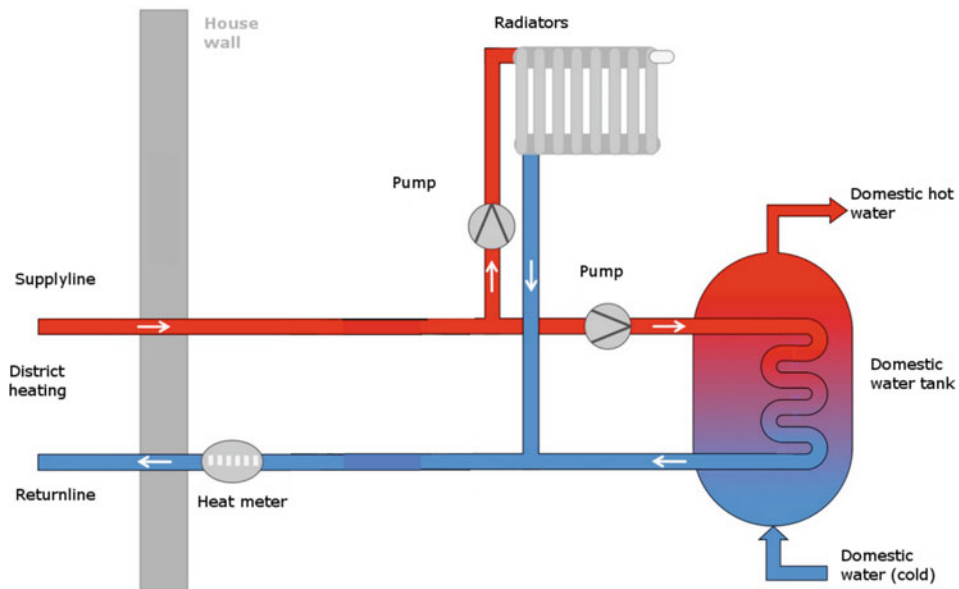


**Fig. 9.18** Local heating connection without transfer station (Situation local heating network Bosch Schwieberdingen). (Originally: Verein Energiepfad Grabs/FirstMedia Solutions GmbH St. Gallen)

Thus, the simulation assumes two hydraulically separated circuits, the district heating network on the primary side and the internal heating circuit on the secondary side. The block “spHeat” only calculates the primary circuit.

In order to be able to map the network of the Schwieberdingen site mathematically, an adaptation of the source code of “spHeat” is necessary, because the primary and secondary circuit is not separated in the Schwieberdingen plant (see Fig. 9.18). Rather, there is only one circuit whose heat transfer medium (water) flows directly through the radiators in the properties and the water heaters in the energy centre Si307. This special feature of the system has far-reaching consequences for the calculation of the flow conditions on the primary side.

In classical heating networks with hydraulic separation between primary and secondary circuit, the change of flow conditions on the secondary side, e.g. by opening radiator valves, has no hydraulic effect on the primary side. But here these flow changes would have a considerable effect on the flow resistance of the entire system.

To prevent this flow-related influence of “building services components” on the hydraulics of the distribution network of the “Trasse West”, decentralized circulation pumps are used at the Schwieberdingen site (see Fig. 9.18). These are dimensioned and controlled in such a way that a constant differential pressure between flow and return can be maintained at the heating distributor.

To simulate the heating network in Schwieberdingen as a direct flow network with the existing software, a virtual heat exchanger as a new interface (see section “Creating the

Simulation Model in the INSEL-GUT”) had to be created for “spHeat”. This interface allows the mapping of dynamic change of the flow conditions due to the radiator regulation and the calculation of the hydraulics on the primary side.

### Circulation Pumps (Single Pump or Pump Phalanx)

During the original development of the “spHeat” programme, certain system components were mapped in a simplified form. The modelling depth of these components had to be adapted to the existing conditions in Schwieberdingen. One example is the internal mapping of circulating pumps for the primary circuit.

“spHeat” calculates the coefficients of the quadratic pump characteristic curve based on three operating points of a pump, defined by the delivery head in metres above the volume flow (Fig. 9.19 light-grey sloping curve).

Single pumps can be modelled with this method. When using two or more pumps in parallel operation, this method is insufficient.

The heat network in Schwieberdingen is operated with a pump phalanx with one, two or three pumps of the same type running in parallel. The starting and stopping of pumps is controlled by the differential pressure and depends on the actual flow rate.

The integration of the control of the pump phalanx in “spHeat” was not considered to be the best solution, but the opposite way to extract the calculation algorithm for the

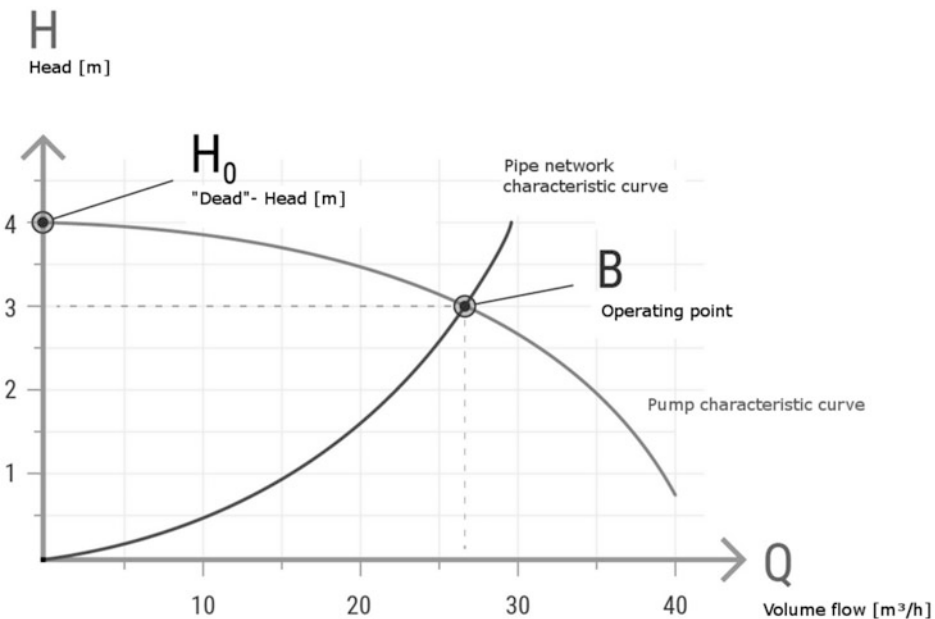


**Fig. 9.19** Pump characteristic curve (light-grey sloping curve) meets pipe network characteristic curve (dark-grey rising curve) at operating point B source: <https://heizung.de/> call 20.10.2020 14:30 h. (Viessmann Climate Solutions Berlin GmbH)

characteristic curve determination from “spHeat” and transfer it into a separate INSEL block. The interfaces between the pump modelling and “spHeat” are then no longer the operating points of the feed pump (delivery head and volume flow) but the coefficients of the quadratic equation.

Advantages of this solution are the increased flexibility in the modelling of pump components and the simplification of the “spHeat” source code. Also, this deconcentration of the programme routine of “spHeat” leads to the possibility to model decentralized supply by the so-called prosumers (consumers that can also supply heat to the network) with their own pumps.

The parameters the programme routine uses to distinguish between a consumer (without pump) and a prosumer (with pump) are the coefficients of the square pump curve ( $cA$ ,  $cB$ ,  $cC$ ), which are all set to zero, in the case of a consumer. The pressure difference at a given operating point of the pump (given volume flow) is calculated as follows:

$$\Delta p = cA * \dot{V}^2 + cB * \dot{V} + cC$$

$\Delta p$ : pressure difference in metres of pump head (m).

$cA$ : quadratic coefficient of pump pressure equation ( $\text{m}/(\text{m}^3/\text{s})^2$ ).

$cB$ : linear coefficient of pump pressure equation ( $\text{m}/(\text{m}^3/\text{s})$ ).

$cC$ : offset of pump pressure equation (m).

$\dot{V}$ : volume flow ( $\text{m}^3/\text{s}$ ).

### Image of the Pump Control in Si307

The pump control is shown in detail in Fig. 9.20. On the left side, you can see the input files of the pump control separately for operating modes “one pump”, “two pumps in parallel” or “three pumps in parallel”. For the continuous simulation of the “Trasse West”, a seamless switching of the operating modes during the simulation run is essential. The simulation blocks on the right side of Fig. 9.20 allow exactly this.

To get an idea of the variable pump control modes, Fig. 9.21 shows the pump characteristics for a single pump (solid line with diamond marking) and the operation of two pumps in parallel (solid line with triangle marking) or three pumps in parallel (solid line with square marking).

While the maximum head is nearly identical for all curves, the three operating modes differ considerably in the achievable flow rates at a fixed pressure difference. The changes of the pump line coefficients  $cA$ ,  $cB$  and  $cC$  during the simulation run are shown in Fig. 9.22. This figure shows how these quantities change as a function of time. During the simulation run, the jump functions of  $cA$ ,  $cB$  and  $cC$  represent the switching from operation with one pump 100% (solid line with diamond marking) to two pumps in parallel operation also 100% (solid line with triangle marking (Fig. 9.21)).

For clarification, the switching of two operating states was chosen, which would not follow each other in real operation, because in the chosen example, a speed control of the

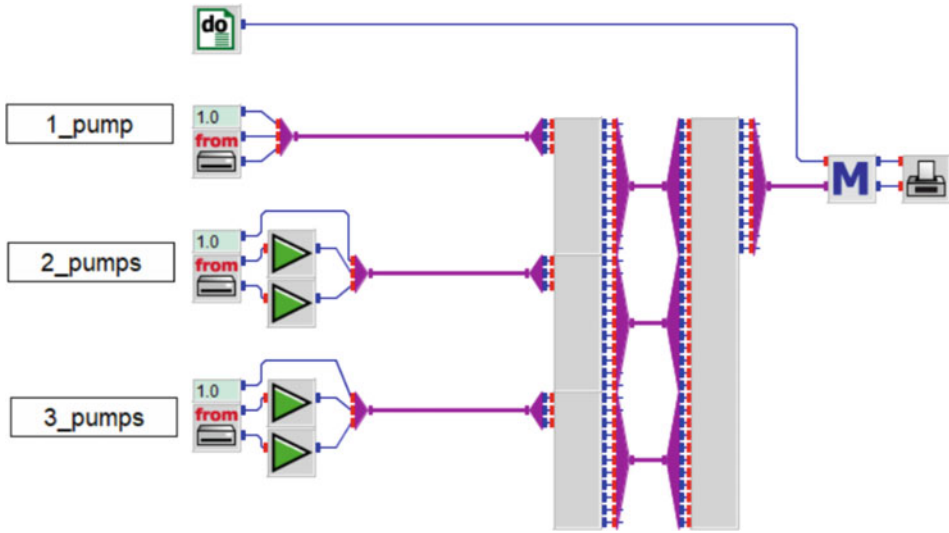


**Fig. 9.20** Pump control from the INSEL model for the “Trasse West” (left, the READ blocks for reading in the pump control signal differential pressure and volume flow; centre, pump blocks with calculation algorithm of cA, cB and cC; right, output files and plot block)

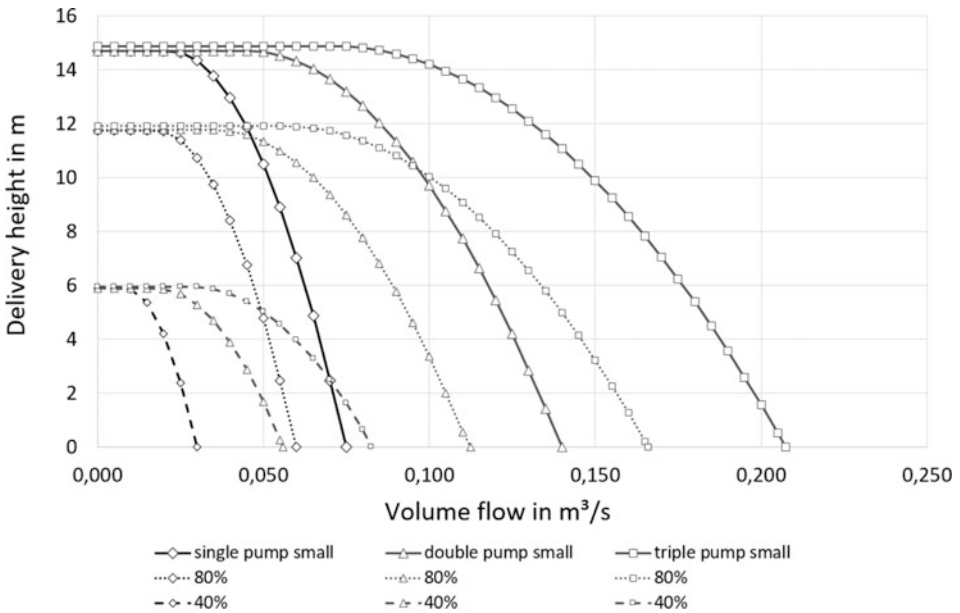


**Fig. 9.21** Pump curves for a single small type pump, two small pumps in parallel and three small parallel pumps in operating modes 100%, 80% and 40% of pump speed

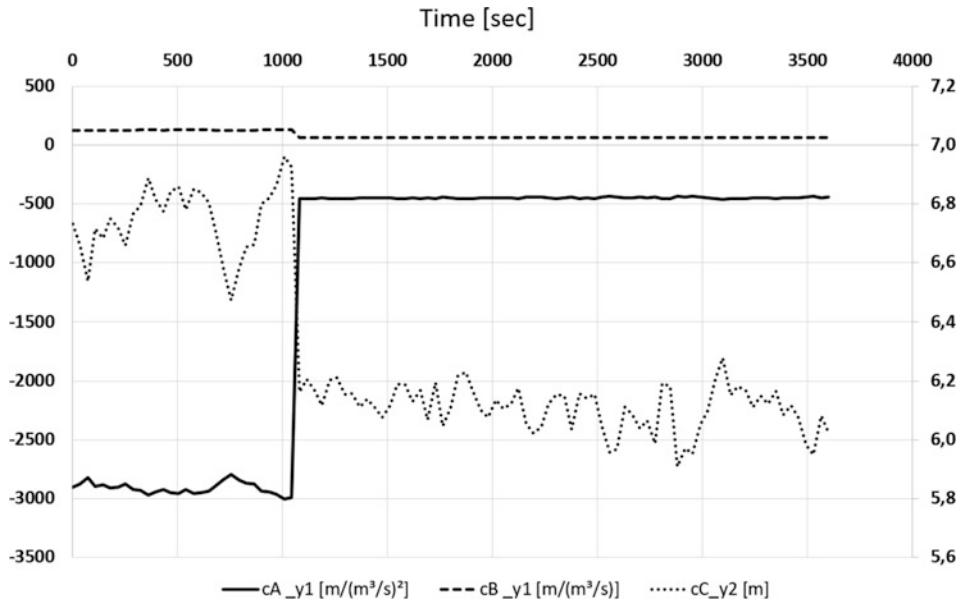


**Fig. 9.22** The pump parameter coefficients  $c_A$ ,  $c_B$  and  $c_C$  as variables depending on the switching on and off of individual pumps (representation of the time course in January for approx. 2 operating hours, switching from 100% single pump to 100% double pump)

pumps was left out (dotted curves (Fig. 9.21)). The adaption of the pump speed would be the first try to match the requirement of a fixed pressure difference between supply line (SL) and return line (RL) within the district heating. In this case, the change of the pump coefficients  $c_A$ ,  $c_B$  and  $c_C$  would be continuous instead of forming a step function as shown in Fig. 9.22.

## Creating the Simulation Model in the INSEL-GUI

### Topology of the “Trasse West”

The simulation model for the “Trasse West” is to be divided thematically into the heat distribution and consumption via the “Trasse West” and its connected consumers and the heat generation in the energy centre Si307. The special features of the plant in Schwieberdingen require changes at the simulation block “spHeat” for a congruent modelling in INSEL.

### Heat Distribution and Consumption

#### *Definition of a “Virtual Heat Exchanger”*

Since the “spHeat” routine assumes hydraulically separated circuits (primary and secondary circuit), the variable flow resistance of the “virtual heat exchanger” must be updated from time step to time step. For this purpose, the measured differential pressure

between supply and return flow at the heating manifolds is converted into an additional flow resistance, which is added to the values from the pressure loss calculation of the pipe network. In this way, the hydraulic changes can be transferred to the primary circuit by opening and closing the valves, without having to make changes to the architecture of two separate circuits defined for “spHeat”. The thermal boundary conditions for the “virtual heat exchanger” can also be determined from the measured variables at the heating manifolds (measured SL/RL temperature, measured volume flow). These values can be used to balance the thermal power that is delivered to the “virtual secondary side”.

### **Validation of Image of Pump Control and “Virtual Heat Exchanger”**

Figure 9.23 shows the structure of the simulation model for testing the virtual heat exchanger and the pump phalanx on the reliability of the representation of the real conditions. The core of the modelling is the combination of all connected consumers of the local heating system of the Bosch site in Schwieberdingen into one (“2\_Big\_Consumer”). In order to determine the hydraulic resistance of the entire network, it is necessary to calculate the pressure loss from the differential pressure between the supply and return line at the Si307 energy centre (“1\_Producer”). This variable, supplemented by the time step values for the pump characteristics cA, cB and cC, is the input variable for modelling the network hydraulics (“spHeat” block in the centre of the GUI).

Simulation results of this setup are compared to measured data to prove the correct modelling of the hydraulic conditions of the network.

The comparison between the values of the simulated and measured volume flow for the hour 0–5 on September 1, 2020, is shown in Fig. 9.24. The two curves match almost identical during the analysed period. The comparison of the two values over a 5-day period is shown in Fig. 9.25. Also, in this period the results of the simulation match with the measured data at the Schwieberdingen site.

Figure 9.26 shows the deviation of each simulated value compared to the measured value for the 5-day period (dots). The maximum deviation between the two values is +7 or –8% which only occurs at very few data points.

Most of the data lies within the standard deviation of 0 to +2% which is a confirmation that the simulation performance is very adequate in comparison to the real circumstances. With this deviation, the detail of the big heat consumer can be raised in the next step of the investigation.

## **Heat Generation**

### *Layout of the Distribution Circuits in the Heating System Si307*

#### *Layout of Manifold Heating System Si307*

The “Trasse West” is a distribution network of the heating circuits supplied by the Si307 energy centre (see Fig. 9.27). Further connected distribution circuits are the branch for the planned “Trasse Süd”, the heating centre Si307 itself (own consumption “Si307\_consumer”) as well as the consumer “Si121” and the “Trasse Ost”. All circuits

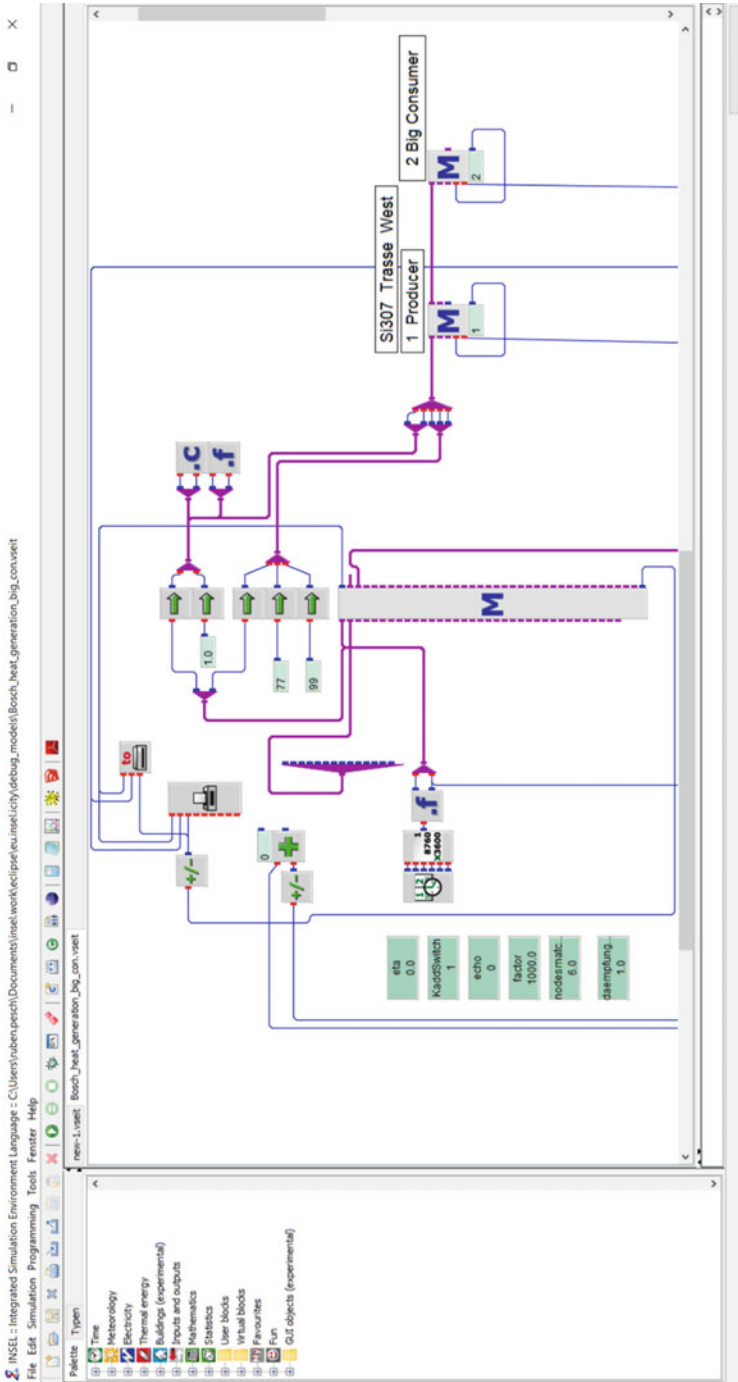


**Fig. 9.23** Scheme of a simplified model for the DH in Schwieberdingen. The whole network is simulated as one virtual consumer (named here as “Big\_Consumer”)

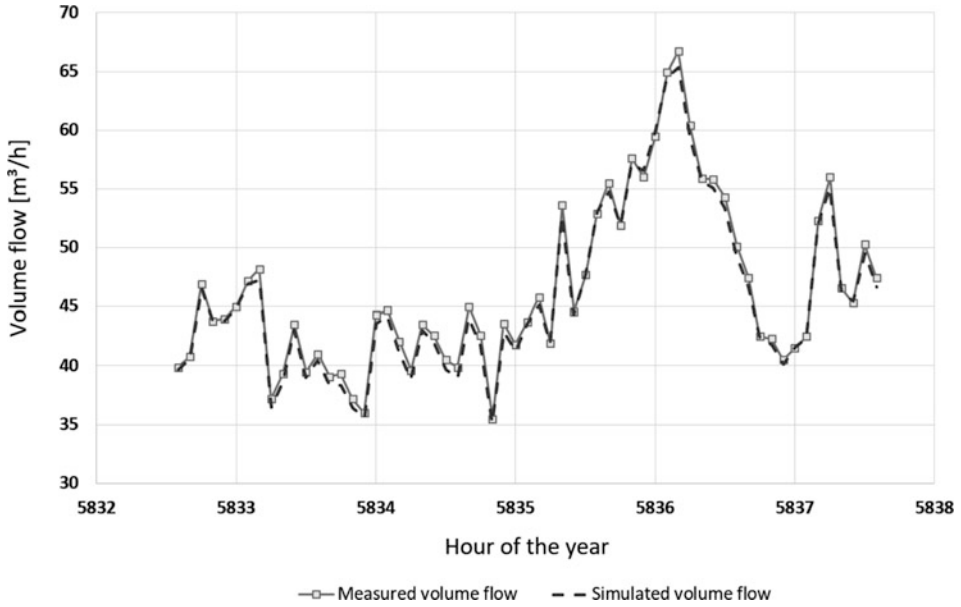


**Fig. 9.24** Match of calculated and measured value of total mass flow for the DH in Schwieberdingen (here hour 0–5 of September 1, 2020)

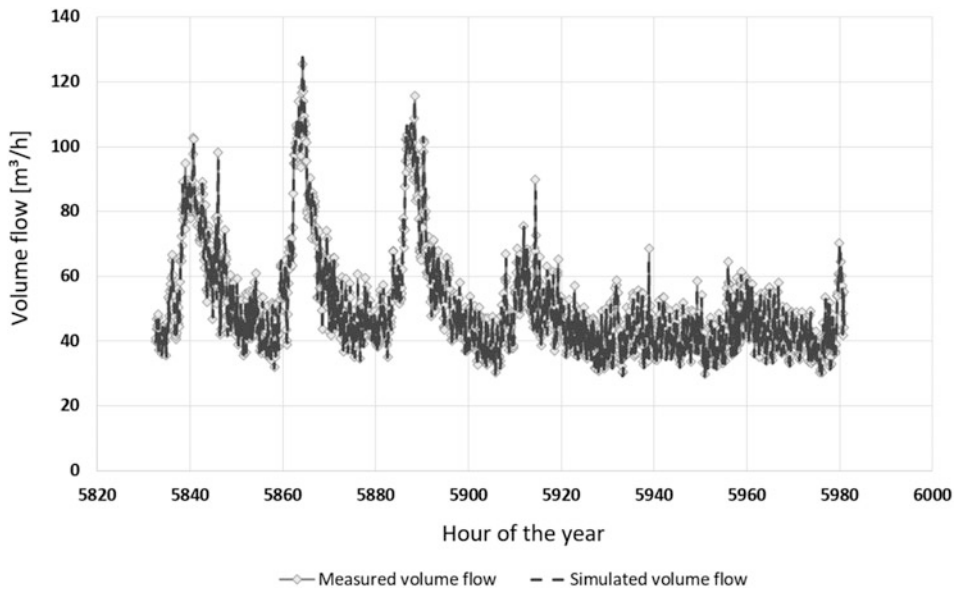


**Fig. 9.25** Match of calculated and measured value of total mass flow for the DH in Schwieberdingen (here September 1–5, 2020)



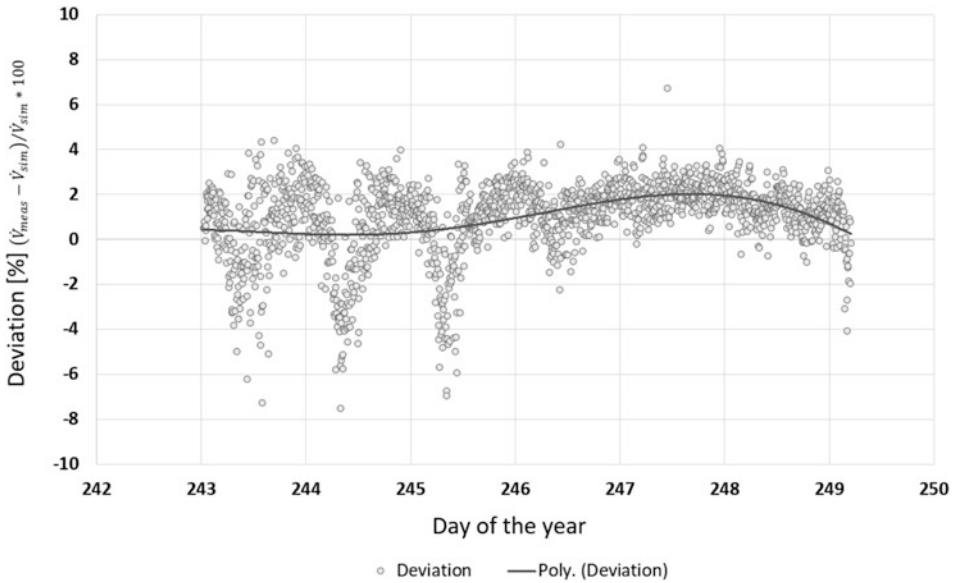


**Fig. 9.26** Deviation of simulated values for total mass flow compared to measured ones (September 1–5, 2020)

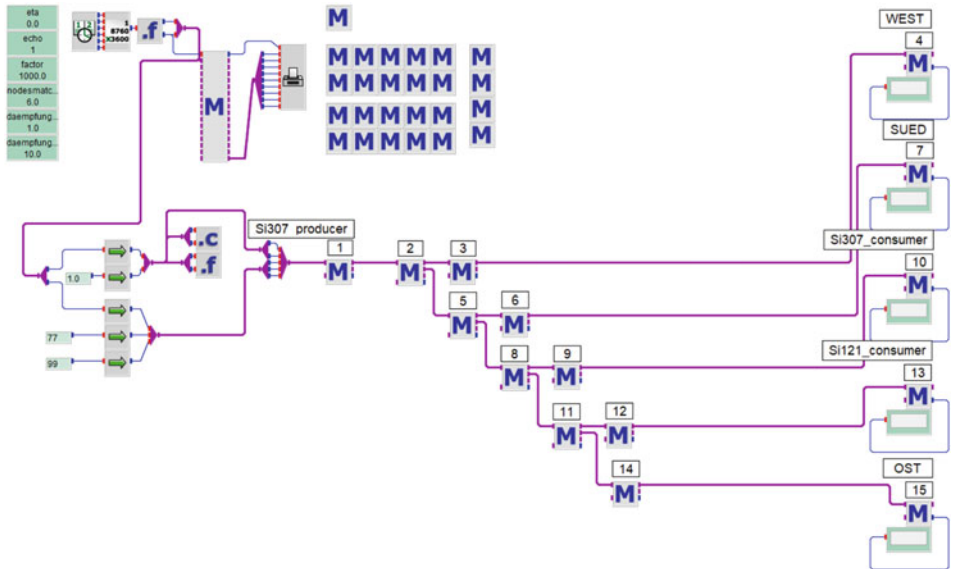


**Fig. 9.27** Heating distributor in the Si307 energy centre (to simulate the “Trasse West”, it is necessary to model the other consumers with load data, as the circulation pumps and pressure maintenance include all connected consumers)

are connected via the main manifold in Fig. 9.27 with the node numbers 2–3, 5–6, 8–9, 11–12 and 14 marked with the pump phalanx and the water heaters of the energy centre (node 1).

Since the pump phalanx with up to three pumps is connected to the manifold in parallel operation and directly supplies all connected distribution circuits without hydraulic switches, the flow conditions in all distribution circuits must be considered in the hydraulic and thermal balancing of the “Trasse West”.

The principle of the “virtual heat exchanger” is also used here to represent the other outlets of the heating circuit distributor. Except for the “Trasse West”, the hydraulic resistances of all outlets (“Trasse Süd”, “Si307\_consumer”, etc.) are modelled via the differential pressure at the respective flow and return lines at the heating manifold (for the “Trasse Süd” at node 5, for “Si307\_consumer” at node 8, etc.). From the measured volume flow and the SL/RL temperatures, the thermal boundary conditions of these balance limits can be determined for the simulation model.

#### *Layout of “Trasse West”*

From the metrologically recorded values at the heating distributors of the buildings (the location is shown in Fig. 9.28 in the centre of the buildings), the necessary calculations can be made, which allow the modelling of a “virtual heat exchanger”.

At the “virtual heat exchanger” interface, the flow temperature (SLsim) calculated by the “spHeat” block is reduced by the amount of thermal power transferred to a return temperature (RLsim), which is then compared with the measured values of the building’s return temperature. If both return temperatures match within the error tolerance, the simulation model is brought into agreement with the measured data.

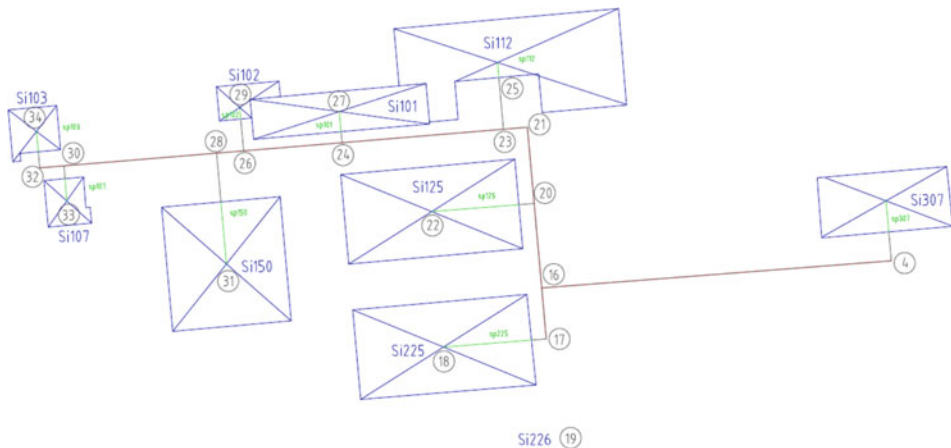


**Fig. 9.28** Topology of the “Trasse West” of the heating network in Schwieberdingen (the main pipeline network with DN 300, the service pipes to the heating distributors, diameter varying depending on the connected load)

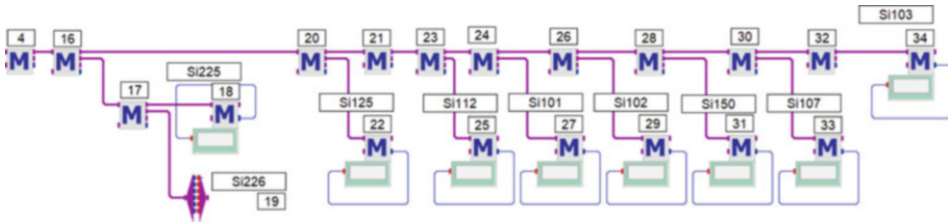


**Fig. 9.29** Mathematical model of the “Trasse West” in the graphic programming language INSEL (with corresponding designation of the network nodes in the block diagram; see Fig. 9.12)

### Calculation Routine of “spHeat”

Starting from a flow rate for the “Trasse West” (node “4” in Figs. 9.28 and 9.29) at the Si307 heating system, the actual mass flows are determined iteratively by calculating the pressure loss along the network’s pipelines.

The Newton iteration method is used, because hydraulic resistances (unlike, e.g. electrical resistances) are not linearly related to the driving force but are measured in a quadratic relationship. Consequently, the relevant systems of equations for the description of the pressure distribution or the flow velocities cannot be solved analytically but can be approximated exclusively by numerical means. The iteration loop is aborted if the deviation of the calculated total mass flow to the preset mass flow (measured at the heating system Si307) is within the set error limits. If there is no convergence between the two quantities after several iteration steps specified by the user, the simulation is aborted with an error message.

In the case of convergence, the iteration loop has been passed successfully. The mass flows of all network edges and the differential pressures between forward and return flow at all network nodes (nodes 16–34 in Fig. 9.28 or Fig. 9.29) were determined.

In a further step, all temperatures of the network nodes are defined by balancing the thermal losses of the pipe network in connection with load data for the extraction of heat by the consumers (nodes 18, 19, 22, 25, etc. in Fig. 9.29).

Thus, the continuous simulation is based purely on the input values at the outlet of the “Trasse West” in the heating system (node 4 in Fig. 9.29) and the load data of the consumers (“Si225”, “Si226”, “Si125”, etc.). The distribution network in between (shown in Fig. 9.29 with thick dark-grey line) is clearly defined due to the material properties and input variables determined by the user.

### Input Data from Measured Values

The available input data for network simulation is shown in Fig. 9.30. Measured values for the Si225 building are available for supply and return temperatures, flow rate, differential pressures and thermal output at the heating manifold “building-specific” and with high temporal resolution. Not all metres of the properties of the “Trasse West” record as completely as in the example building Si225. In close cooperation with the facility management of the Bosch site in Schwieberdingen, schedules for metre replacement and

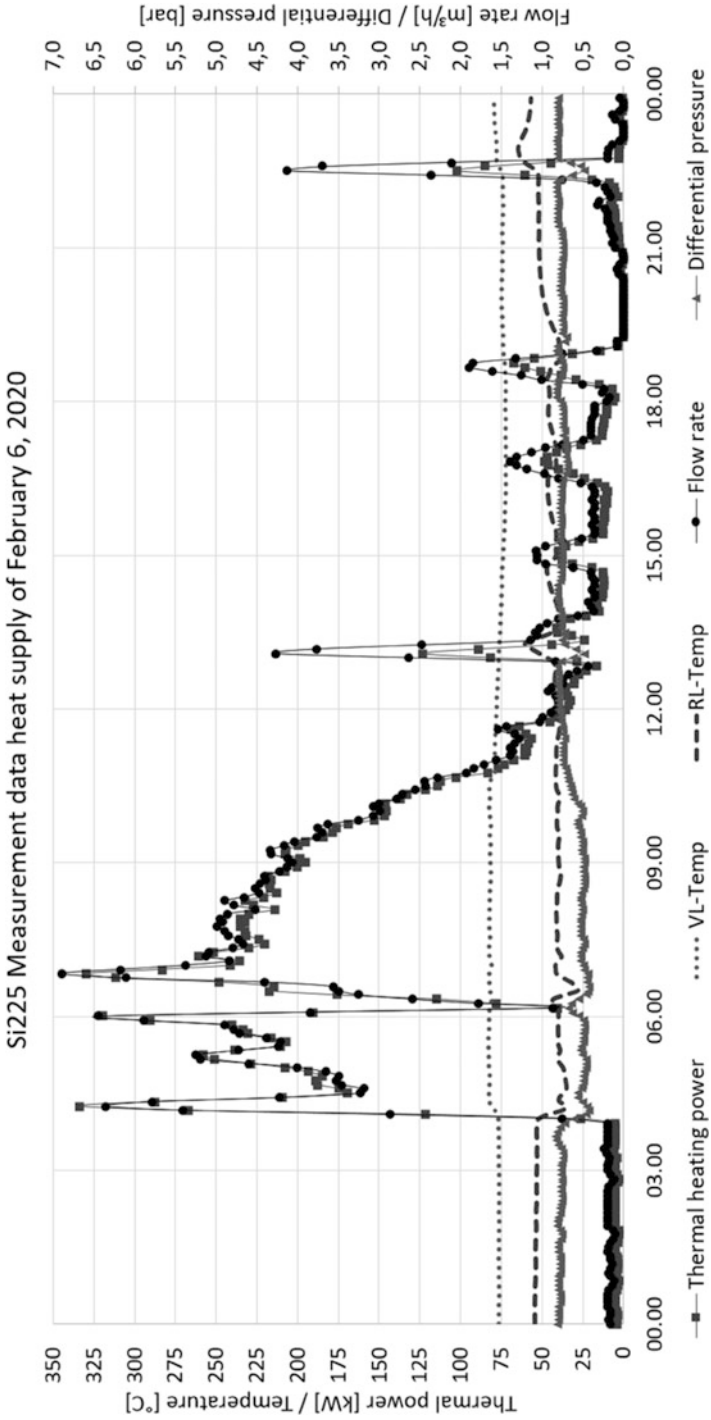


**Fig. 9.30** Course of the input data of “spHeat” in building Si225 for an exemplary day

improvements in data management are being developed. The aim is to record the properties of the “Trasse West” for a sufficiently long period (4–6 weeks minimum) in order to validate the INSEL model with this complete data set.

### 9.4.3 Summary and Outlook

With the changes to the “spHeat” calculation routine, a calculation programme that can map district heating networks of the first to third generation with hydraulic separation between the primary and secondary circuit has been enhanced to emulate networks with direct heating circuit flow.

This required the considerations discussed with the umbrella term “virtual heat exchanger”. The technical changes for the implementation of “virtual heat exchangers” in the INSEL block “spHeat” were successfully integrated, so that the software can simulate considerably more flexible district heating networks with and without hydraulic separation between primary and secondary circuit beyond the concrete application in Schwieberdingen.

The further procedure for the application case Schwieberdingen can be outlined as follows:

After checking and calibrating the two separate simulation sections (heat generation and heat distribution/consumption) with measured values, the two sections are merged into a holistic simulation model of the “Trasse West”. With this holistic simulation model, which is often referred to as “digital twin”, investigations with different boundary conditions are possible.

At the current stage of network expansion, the properties of the “Trasse West” are supplied with a minimum flow temperature of approx. 70 °C for a large part of the existing buildings. The level of the flow temperature, which was chosen when the site was first built in 1968 (the original dimensioning was 120 °C for the SL), is too high for the supply of buildings with current building shells and heating technology.

Since a mix of buildings constructed during the last five decades is supplied with the district heating network at the Schwieberdingen location, especially on the “Trasse West”, the supply temperature of the network cannot be lowered without endangering the supply security of the older buildings or the water heaters in the newer buildings.

With the simulation model, however, scenarios can be calculated without interfering with the ongoing operation, such as how the return temperature of the “Trasse West” could be further reduced by a cascade connection.

A basic requirement for a cascade connection is a high return temperature of one building, combined with a low requirement for the supply temperature level of a second building in the immediate vicinity. A further prerequisite is that the heating capacities of these two buildings allow a cascade connection. If both conditions are fulfilled, the building with a low supply temperature requirement can be connected to the return flow of the

building with a high return temperature and thus cool down a return flow which is, e.g. approx. 55 °C to 25 °C.

The advantages of this type of connection are both savings of thermal energy due to lower thermal losses of the pipe network and an increase in the spread between flow and return temperature and the associated savings of electrical drive energy for the pump phalanx.

Further scenarios in which the buildings of the “Trasse West” are also integrated as single zone building models in the calculation model are conceivable. If this modelling depth is reached, statements about the thermal comfort in the buildings would then be possible when the total supply temperature is lowered.

---

## References

- ENTSOE, 2017. 2017 Summer Outlook - Winter Review 2016–17 - 1 June 2017. European Network of Transmission System Operators.
- European Commission, 2011. EU Energy Roadmap 2050. European Union.
- European Commission, 2016. An EU Strategy on Heating and Cooling. European Union. <https://ec.europa.eu/energy/en/topics/energy-efficiency/heating-and-cooling>
- Albers, J., Lanser, W., Paitazoglou, Ch., Petersen, S. (2017). Was können modern Absorptionskältemaschinen leisten? In BTGA-Almanach 2017 (pp. 34-39). Bundesindustrieverband Technische Gebäudeausrüstung e.V. STROBEL VERLAG GmbH & Co. KG, Arnsberg 2017
- Haider, M., Luedeking, G. (7/2005a). Auslegung und Wirtschaftlichkeit von KWKK-Anlagen Teil 1. In KI Luft- und Kältetechnik 7/2005 (pp. 267-271). Hüting GmbH, Mediengruppe Süddeutscher Verlag, Heidelberg 2005
- Haider, M., Luedeking, G. (8/2005b). Auslegung und Wirtschaftlichkeit von KWKK-Anlagen Teil 2. In KI Luft- und Kältetechnik 8/2005 (pp. 308-311). Hüting GmbH, Mediengruppe Süddeutscher Verlag, Heidelberg 2005
- Morgenbrodt, L. (2008). Pilotprojekt Solarstadt Wiggenshausen-Süd Solare Nahwärme. Technische Werke Friedrichshafen GmbH (<https://www.baubiologie.de/downloads/wug/solarstadt.pdf>). Friedrichshafen 2008.
- Haoran Li et al., 2018. Transition to the 4th generation district heating - possibilities, bottlenecks, and challenges. Energy Procedia 149. Page 483–498
- Heymann et al., 2018. Concept and Measurement Results of two Decentralized Solar Thermal Feed-in Substations. Energy Procedia 149. Page 363-372.
- Köfinger et al., 2017. Reduction of return temperatures in urban district heating systems by the implementation of energy-cascades. Energy Procedia 116. Page 438–451
- Leoni et al. (2020). Developing innovative business models for reducing return temperatures in district heating systems: Approach and first results, Energy 195
- Monsalvete Álvarez de Urbarri et al., 2017. Energy performance of decentralized solar thermal feed-in to district heating networks. Energy Procedia 116. Page 285–296
- Paulick et al., 2018. Resulting Effects On Decentralized Feed-In Into District Heating Networks – A Simulation Study. Energy Procedia 149. Page 49–58
- RESCUE, 2015. EU District Cooling Market and Trends - Renewable Smart Cooling for Urban Europe. European Union.

TESS, 2017. TRNSYS component models developed by the engineering consulting company TESS <http://www.trnsys.com/tess-libraries/> (Retrieved: 20/10/2017).

Tol et al., 2021. A novel demand-responsive control strategy for district heating systems, featuring return temperature reduction *Energy and Built Environment* 2. Page 105–125

**Open Access** This chapter is licensed under the terms of the Creative Commons Attribution 4.0 International License (<http://creativecommons.org/licenses/by/4.0/>), which permits use, sharing, adaptation, distribution and reproduction in any medium or format, as long as you give appropriate credit to the original author(s) and the source, provide a link to the Creative Commons license and indicate if changes were made.

The images or other third party material in this chapter are included in the chapter's Creative Commons license, unless indicated otherwise in a credit line to the material. If material is not included in the chapter's Creative Commons license and your intended use is not permitted by statutory regulation or exceeds the permitted use, you will need to obtain permission directly from the copyright holder.





# Case Study of a Hydrogen-Based District Heating in a Rural Area: Modeling and Evaluation of Prediction and Optimization Methodologies

# 10

Daniel Lust, Marcus Brennenstuhl, Robert Otto, Tobias Erhart, Dietrich Schneider, and Dirk Pietruschka

## Abstract

Buildings are accountable for about one third of the greenhouse gas emissions in Germany. An important step toward the reduction of greenhouse gases is to decarbonize the power productions and heating systems. However, in an energy system with a high share of renewable energy sources, large shares of energy have to be stored in summer for the winter season. Chemical energy storages, in this case hydrogen, can provide these qualities and offer diverse opportunities for coupling different sectors.

In this work, a simulation model is introduced which combines a PEM electrolyzer, a hydrogen compression, a high-pressure storage, and a PEM fuel cell for power and heat production. Applied on a building cluster in a rural area with existing PV modules, this system is optimized for operation as a district heating system based on measured and forecasted data. Evolutionary algorithms were used to determine the optimized system parameters.

The investigated system achieves an overall heat demand coverage of 63%. However, the local hydrogen production is not sufficient to meet the fuel cell demand. Several refills of the storage tanks with delivered hydrogen would be necessary within the year studied.

---

D. Lust (✉) · M. Brennenstuhl · R. Otto · T. Erhart · D. Schneider  
Hochschule für Technik Stuttgart, Stuttgart, Germany  
e-mail: [daniel.lust@hft-stuttgart.de](mailto:daniel.lust@hft-stuttgart.de)

D. Pietruschka  
Institute for Applied Research, University of Applied Sciences Stuttgart, Stuttgart, Baden-Württemberg, Germany



---

**Keywords**

Water electrolysis · Hydrogen storage · Fuel cell · Hydrogen system model · District heating · Evolutionary algorithms · Machine learning · Random forest · Decision tree · Gradient boosting

**Abbreviations**

ANN	Artificial neural network
CHP	Combined heat and power
DEAP	Distributed evolutionary algorithms in python
DTR	Decision tree regression
GB	Gradient boosting
LOHC	Liquid organic hydrogen carrier
MAE	Mean absolute error
MAPE	Mean absolute percentage error
OCV	Open cell voltage
OP	Operating point
PEM	Proton exchange membrane
PV	Photovoltaic
$R^2$	Coefficient of determination
RF	Random forest
SOC	State of charge
SOFC	Solid oxide fuel cell

---

**10.1 Introduction****The Role of Hydrogen for Energy Storage**

To reach the goals of reducing carbon dioxide emissions in Europe set out by the Paris Climate Agreement (keep global warming beneath 2 °C (United Nations Climate Change, 2020)) and the European Green Deal (no net greenhouse gas emissions in Europe until 2050 (European Commission, 2020)), hydrogen will play a significant role in the future energy system. If the installed power of highly fluctuating renewable power generators rises, the need to store surplus electrical energy is obvious. In addition to battery storage systems and pumped storage, the generation of green hydrogen via electrolysis will be essential.

Hydrogen is a versatile energy carrier, which could be used for several sectors:

- Industry, for instance, steel production.
- Mobility, such as fuel cell vehicles or further processed to liquid hydrocarbons (Fischer-Tropsch synthesis).
- Residential and commercial buildings, for instance, combined heat and power generation with stationary fuel cells.

In June 2020, the German federal government released a framework for action concerning hydrogen technologies, the “National Hydrogen Strategy” (BMW, 2020). The 38 measures include the installation of 5 GW hydrogen generation capacity until 2035 and the extended funding of fuel cell heating systems.

This paper presents the results of a case study that focuses on the heat generation for a rural residential district with a fuel cell combined heat and power (CHP) unit. In this sector, the use of hydrogen should not be considered as a competitive technology to direct electrification via heat pumps and batteries, but rather as a useful supplement with the ability of large-scale seasonal storage and sector coupling.

---

## 10.2 Related Work/State of the Art: Research

### Hydrogen Production, Storage, and Use in Residential Districts

In the case study, hydrogen is stored as compressed gas. Other possibilities to locally store large amounts of hydrogen over seasonal durations include its conversion to organic molecule, such as liquid organic hydrogen carriers (LOHC) (Teichmann et al., 2012) and formic acid or formate, respectively (Lust et al., 2019).

### Fuel Cell CHP

Several research papers deal with the usage of fuel cells as CHP units and the optimization of the operation to reduce primary energy demand. Similar conclusions of different research activities suggest that the design of the fuel cell CHP (stack size, auxiliary systems) and the control strategy must be carefully evaluated for each specific use case.

In their review article, Dodds et al. (2015) highlight that in the UK (and other cold climate locations), the peak thermal demand of residential buildings matches with the national peak electrical demand. Thus, the use of fuel cell CHPs offers an additional value to the energy system and complements heat pumps.

Windeknecht and Tzscheuschler (2015) describe a fuel cell CHP (SOFC) for a single-family household fueled by natural gas. They state that lowering the storage temperature from 60 °C to 35 °C increases the heat output of the fuel cell but requires additional systems. The temperature level of fuel cell-based heating systems must therefore be carefully evaluated, taking various factors into account.

There are different options for the heat recovery of solid oxide fuel cell (SOFC) and proton exchange membrane fuel cell (PEMFC) CHPs, including the possibility of an afterburner, to generate additional heat from unreacted hydrogen at the anode exhaust gases (Adam, Fraga, & Brett, 2015). Also, the concept of a complete self-sufficient public building with power generation (PV, wind), electrolysis, and fuel cells is described by Marino, Nucara, Pietrafesa, and Pudano (2013).

### Realized Project

A currently realized project with water electrolysis and hydrogen use in a residential area is the “Neue Weststadt” project in the city of Esslingen east of Stuttgart (Energiewendebauen,

2020). In this project, power is generated with 220 kW<sub>p</sub> PV and used in an alkaline electrolyzer (500 kW) to produce hydrogen on site with waste heat utilization to supply the district with heat. The produced hydrogen is not stored but rather injected into the natural gas grid. In a later project phase, hydrogen is filled into trailers, and a refueling station for fuel cell vehicles is planned (Marx, 2020).

### Control of Fuel Cell CHPs

To optimize the control strategy of a fuel cell CHP, Cappa, Facci, and Ubertini (2015) suggest to minimize a cost function, including the costs of the fuel ( $C_s$ ), maintenance ( $C_m$ ), cold start ( $C_s$ ), and electricity export. Compared to a reference scenario (electricity from grid, heat from gas fueled boiler), this optimized control strategy of the fuel cell CHPs allows to reduce the annual net expenditure of 47% (40% with thermal driven control). In the past, incentives for CHP systems in Germany have been granted for heat-led systems only or in some cases with feed-in bonus for heat-led systems. The aim of this incentive strategy was to avoid excessive heat rejection and waste of fuel (Erhart, 2015). Especially for city quarters with district heating systems, the main purpose of the CHP was to provide thermal energy, with electricity as by-product. In the past few years, the share of electric heating systems and power-to-heat systems has increased (Agora Energiewende, 2017). With higher envelope standards, specific heat demand for houses decreases (Günther et al., 2020). Furthermore, the number of heat pumps installed per year over the last 18 years increased by a factor of around 10 (BWP, 2020). Therefore, electricity as main energy thermal source for heating homes is becoming more and more central.

### Application of Forecasting Models Based on Machine Learning in the Field of Energy Management

Several research companies have dealt with the question of load curve prediction. The method of artificial neural networks (ANNs) is often used for this purpose, which also includes the multiple layer perceptron (MLP) model (A. S. Ahmad et al., 2014). However, far fewer projects have dealt with the application of decision trees or ensembles with decision trees (random forest, gradient boosting) (M. W. Ahmad, Mourshed, & Rezgui, 2017). In those projects in which the random forest (RF) or gradient boosting (GB) model is applied, the results are quite comparable to those of ANNs (M. W. Ahmad et al., 2017; Moon, Kim, Son, & Hwang, 2018; Robinson et al., 2017).

Moon et al. (2018) use a hybrid model consisting of a multiple layer perceptron and a random forest for the prediction of load profiles. For this purpose, the electrical demand data of a Korean university are used. The patterns are also used to allocate the different electrical load profiles. These data are then fed into the hybrid model, which is trained by this information.

In the work of M. W. Ahmad et al. (2017), the models ANN and RF are explicitly compared, and the results are contrasted. For this purpose, a 5-min resolved HVAC data set of a hotel in Madrid is used. Also, daily bookings and weather data are determined. The results of this work show that the artificial neural network prevails over the random forest but that the results for both systems are highly satisfactory. The random forest can show a

coefficient of determination of 0.92 compared to 0.95 for the artificial neural network. This corresponds to a very good prediction performance for both models.

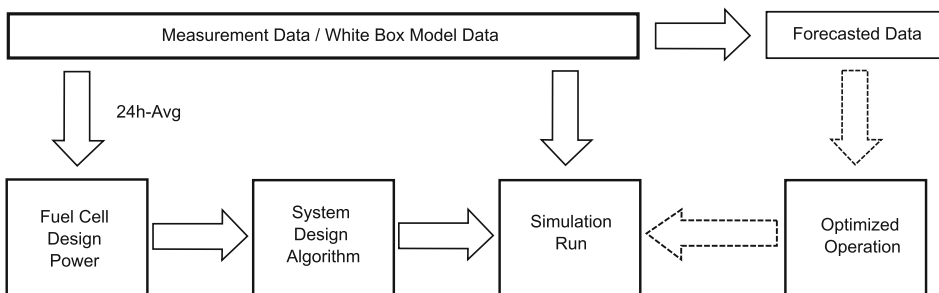
### 10.3 Methodology

Figure 10.1 depicts the procedure of this work. Measurement data (24 h-averaged) and white-box model data are used to set the fuel cell heating power. On that basis, all other system parameters are determined by evaluating a target function with evolutionary algorithms. The unaveraged (1-min time step) measured and white-box data is used to calculate the system performance with the optimized parameters. Besides, forecasting algorithms are trained on the measured and white-box data. In the long run, these algorithms should replace the white-box data for faster computation. The forecasted data could be used to optimize the system operation on a minute-based time scale.

#### Simulation Environment

INSEL is an acronym for the Integrated Simulation Environment Language of doppelintegral GmbH, a graphical programming language for the creation and execution of simulation applications mainly used in the renewable energy sector. INSEL comprises a graphical model editor (JAVA) with calculation sub-routines written in C++ or Fortran. INSEL has a large variety of predefined functions, the so-called blocks, for different domains (solar, electric, chemical, thermal, meteorological).

The workflow of the simulation is shown in Fig. 10.2. Load curves for the generated power and the heat demand must be provided via prior simulations or measurement data. A Python script specifies the system's parameters and generates an executable INSEL file from a template. The INSEL runtime environment is started from the Python script. After the simulation run finishes, an output file is generated from INSEL and processed in Python. Finally, the simulation results are visualized using GNUplot scripts. This workflow also allows the implementation of forecast and optimization algorithms with Python as a common programming interface.



**Fig. 10.1** Methodology—flow diagram

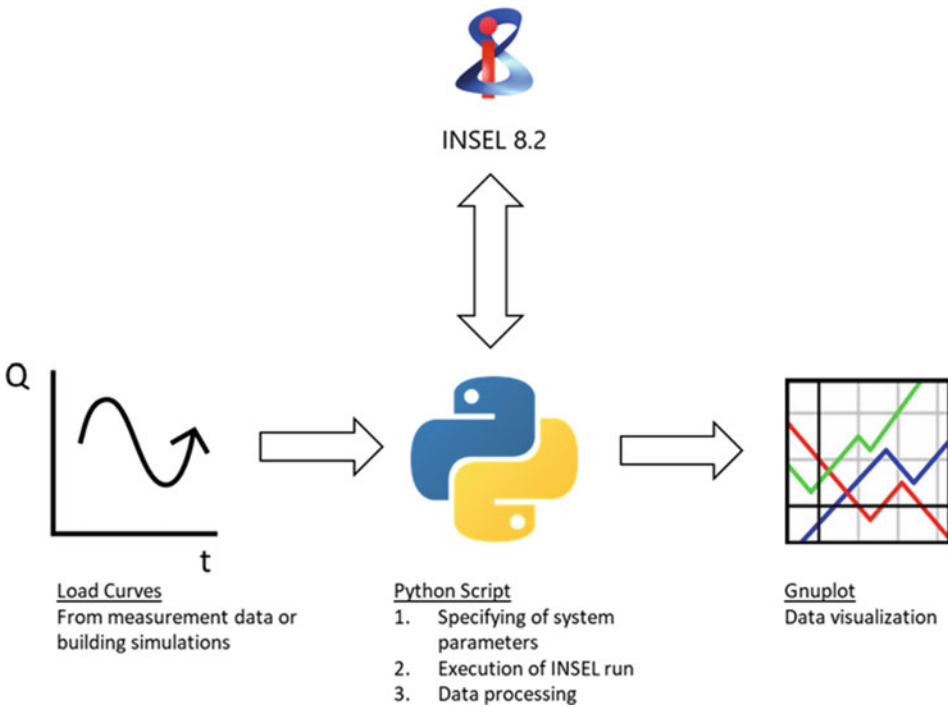


**Fig. 10.2** Simulation workflow

### Optimization

To determine the optimal size of the system components, a genetic algorithm was applied to the system model, varying the size of the electrolyzer, the battery, and the storage tank. This was realized in Python via the DEAP toolbox (Distributed Evolutionary Algorithms in Python (DEAP, 2021)). Thereby, the optimization is based on the following target function:

$$f = P_{El} \cdot c_{El} + E_{BAT} \cdot c_{Bat} + V_{tank} \cdot c_{tank} + (0.8 + N_{refill}) \cdot c_{H2} \cdot \frac{V_{tank} \cdot P_{tank}}{R_s \cdot T}$$

This economic optimization aims at identifying the local hydrogen production and the amount of needed external hydrogen refills. In this scenario, the size of the fuel cell and hence the cumulated hydrogen demand is fixed.

For the economic optimization, the EAC (equivalent annual cost), which represents the annual cost of owning, operating, and maintaining the different system components, was calculated based on the annuity method according to the guideline VDI 2067 “Economic efficiency of building services systems” (Verein Deutscher Ingenieure, 2012). Furthermore, to take into account inflation, a procedure according to Hessisches Umweltministerium (1999) was used, assuming the specific investment costs according

**Table 10.1** Target function parameters

Component	Symbol	Specific investment costs	EAC	Lower/upper limit	Sources
Electrolyzer	$c_{EI}$	1200 €/kW	122 €/kW*a	10/200	Götz et al. (2016)
Battery	$c_{BAT}$	275 €/kWh	28 €/kW*a	10/200	Multiple sources, e.g., US Department of Energy (2019)
Storage	$c_{tank}$	2693 €/m <sup>3</sup>	274 €/kW*a	10/200	<a href="http://www.linde-gas.de">www.linde-gas.de</a>
Hydrogen refill	$c_{H2}$	11.4 €/kg	–	–	Based on hydrogen market price and assumed delivery costs

to Table 10.1. They resulted in corresponding annual costs with the assumption of a lifetime of 20 years.

Assumptions:

- Battery costs depend on the battery capacity, not on the power.
- All costs scale linear.
- Type I (steel cylinder) hydrogen tanks fulfill safety issues for stationary outdoor storage.
- Hydrogen refills via trailers are logistically feasible.
- Hydrogen costs consist of market price (9.5 €/kg) + 20% delivery costs (initial hydrogen fill without delivery costs  $\rightarrow (0.8 + N_{refill}) \cdot c_{H2}$ ).
- Lifetime of electrolyzer, battery, and storage tanks: 20 years.
- All parameters are bounded to keep the component design within reasonable limits.

### Forecast Models

*Scikit-Learn: A Toolbox for Developing Forecast Models in the Field of Machine Learning*

Scikit-Learn is an open-source project, in which different tools of machine learning are offered. The project is constantly being developed, and the range of models and tools to be used is constantly increasing. For example, support vector machines or neural networks based on the multi-layer perceptron can be created and applied simply by configuring and adjusting the hyperparameters (Pedregosa et al., 2011). This toolbox is applicable in the popular programming language Python and thus allows an easy use of models from the field of statistics as well as machine learning (Müller & Guido, 2015).

*Scikit-Learn: Decision Tree, Random Forest, and Gradient Boosting*

The Scikit-Learn library has some models for the application of decision trees and their ensembles which can be used for classification as well as regression. In this work, the classical (decision tree regressor) as well as the random forest and gradient boosting of the Scikit-Learn library are used. Grid search and cross-validation are used to discuss the best models (Geron, 2017; Ng & Soo, 2018).

### *Statistical Tools for the Evaluation of the Models*

In this work, the statistical evaluation of the forecast is done with three tools. These are the coefficient of determination ( $R^2$ ), the mean absolute percentage error (MAPE), and the mean absolute error (MAE). They are often used in the field of machine learning (A. S. Ahmad et al., 2014; M. W. Ahmad, Mourshed, Yuce, & Rezgui, 2016; Geron, 2017).

### *Application of the Forecasting Model*

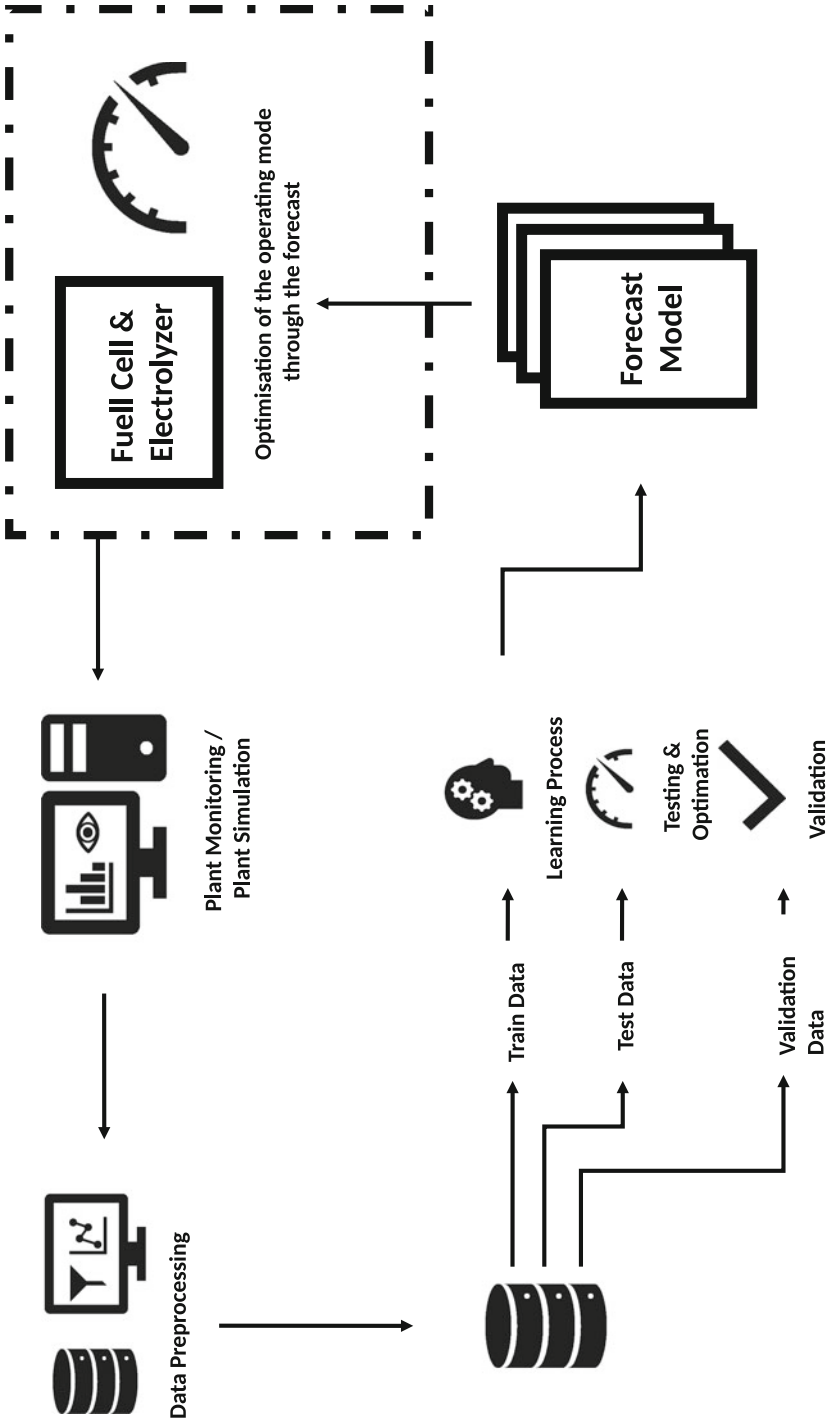
The application of machine learning in this work makes it possible to predict the energetic user behavior in order to optimize building services equipment and its operation. For this purpose, measured values from the past are often used to train a model (M. W. Ahmad et al., 2016; Jain, Smith, Culligan, & Taylor, 2014; Zhang, Grolinger, Capretz, & Seewald, 2019). Since there are no consistent measured data of the buildings in the investigated area over longer periods (1 year or more), the simulation results, based on previously calibrated white-box models (Brennenstuhl et al., 2019; Brennenstuhl, Lust, Pietruschka, & Schneider, 2021), of 5 years were used to train the model. Weather data from the year 2019 is used for the forecast. The optimization of the building services engineering is further the subject of the research and is not addressed in this paper.

Figure 10.3 shows the process of the forecast. First, the data is provided by monitoring or simulation. In this case, the data are initially simulation data. These must be pre-processed. This means that errors have to be detected and filtered, the format has to be adapted, and features have to be added or reduced. Since measured values or simulations usually do not have a stratified data set, it still has to be re-sorted. This ensures that when the data set is divided into training, test, and validation data, all possible constellations of characteristics and output values are equally distributed. The trained model is checked for its performance using the test data set. Particularly strong models are checked for overfitting to the test data set using the cross-validation procedure and the validation data set. During the cross-validation, the test data set as well as the training data set is completely changed once. If the prediction quality remains more or less constant, a well-generalized model can be assumed.

Another test is the application of a validation data set. It is removed from the entire data set in advance and is usually used for final testing. If the qualitative values of this application are similar to those of the previous tests, the model is valid and can be used for the forecast.

Table 10.2 shows the used features. The temporal characteristics are generated using Unix time. The ambient temperature and the global radiation are taken from the respective data set. Floating point numbers are limited to two decimal places to reduce variation. Not all features are applied to the respective models. For example, it has been shown that electricity demand can be better predicted without the ambient temperature and global radiation. However, these two characteristics play an important role in the prediction of heat demand.

In order to generate the best output, the hyperparameters of each model must be adjusted. It can be done automatically with a grid search, which either already contains a



**Fig. 10.3** Process of the forecast



**Table 10.2** Used features

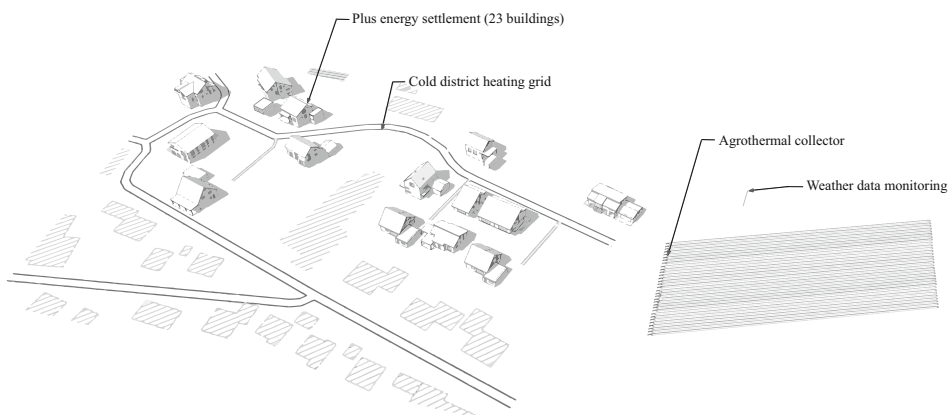
Input feature	MOY	DOW	HOD	MOD	Tamb	I_RAD
Description of the used input feature	Month of the year: Represents the actual month as a feature of the time	Day of the week: Represents the actual weekday as a feature of the time	Hour of the day: Represents the actual hour (24 h) as a feature of the time	Minute of the day: Represents the actual minute as a feature of the time	Ambient temperature: Represents an environmental value as a physical feature	Global radiation: Represents an environmental value as a physical feature

cost function and thus determines the best value itself or determines hyperparameters by random range hyperparameter and thus scans a certain range. In this work, the grid search was performed by a random range of values (Geron, 2017; Müller & Guido, 2015). The training of the procedure is done with minute data. The output or the forecast can be in minute values, quarter hours, and hourly values. In this case, the output is in hours, because errors are averaged and the curve is smoother. Because of this smoothing to hours, the results of the forecast are better than with minute values.

### Case Study: Building Cluster in the Municipality of Wüstenrot

The case study described within this paper focuses on the rural municipality Wüstenrot in Baden-Württemberg and in detail on a newly built plus energy district called “Vordere Viehweide.” Wüstenrot is not connected to a natural gas grid, and thus, many of the existing buildings are heated by oil-fired boilers. To counteract this, measures to increase the share of renewable energy (RE) in the community’s heat and electricity supply were developed as part of the EnVisaGe research project (Municipality of Wüstenrot, 2018), which was carried out between 2012 and 2016. This included the development of several local heating networks and the realization of a new plus energy district. The latter consists of 23 residential buildings with high-energy standard (see Fig. 10.4). All buildings are equipped with decentral heat pumps that are supplied by a cold district heating grid that is connected to a large-scale low-depth geothermal system (“Agrothermie”). All buildings have PV systems installed with a peak power output between 6 kW<sub>p</sub> and 29 kW<sub>p</sub> (overall, 97.39 kW<sub>p</sub>). Within six buildings, all thermal and electrical energy flows and temperatures are monitored in detail. The energy flows of six additional buildings are measured. This monitoring data is accessible via a cloud-based monitoring and control system.

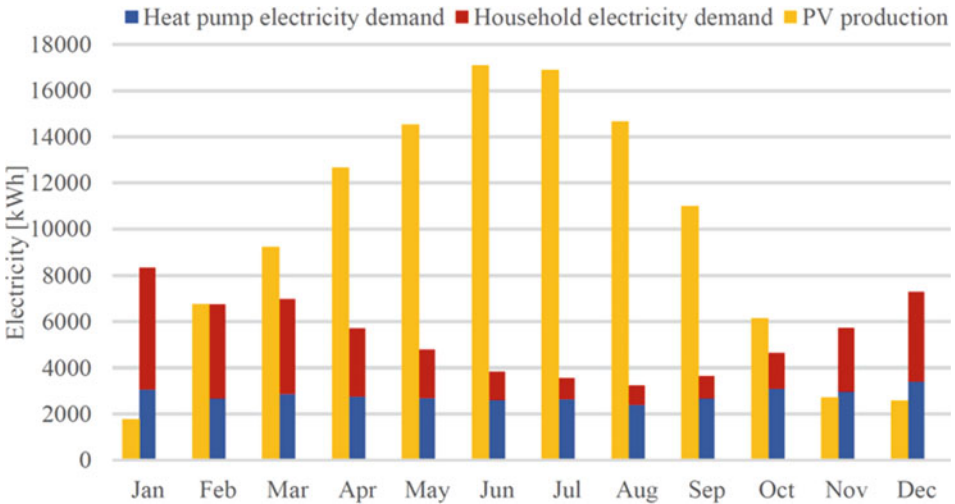
As Table 10.3 and Fig. 10.7 indicate, more PV electricity is produced than consumed by the households and heat pumps. In addition, larger differences occur due to the imbalance of heating demand and PV production on a seasonal level (see Fig. 10.5) but also on a daily



**Fig. 10.4** The Plus Energy Settlement “Vordere Viehweide”

**Table 10.3** The plus energy settlement's energy balance

Yearly thermal heat demand (kWh)	134,542.7 kWh
Yearly electrical heat pump demand (kWh)	30,757.8 kWh
Yearly electrical household demand (kWh)	33,855.7 kWh
Yearly PV power production (kWh)	116,165.2 kWh
Yearly surplus electrical power (kWh)	51,551.8 kWh

**Fig. 10.5** Case study monthly electricity balance for 10 Buildings (Simulation Output According to Metrological Data from 2019)

basis. In this context, short- and long-term storage solutions are beneficial to reduce electrical grid stress. Short-term storage solutions could be battery storages, and long-term seasonal storage could be provided by hydrogen-based systems. The heating power demand of the building cluster during the course of 1 year is shown in Fig. 10.6 (Fig. 10.7).

## 10.4 Hydrogen System: Modeling, Design, and Control

In this study, the existing heating system with decentral heat pumps is replaced by a central hydrogen-based energy system. The investigated hydrogen system consists of a central unit with a PEM electrolyzer and a buffer battery, electrically connected to the building cluster and the power grid. The hydrogen produced by the electrolyzer is compressed to 25 MPa and locally stored, whereas the produced oxygen is not further utilized. A PEM fuel cell is used to generate heat and power from hydrogen. The produced heat is distributed via a heating network to the building cluster (see Fig. 10.8).

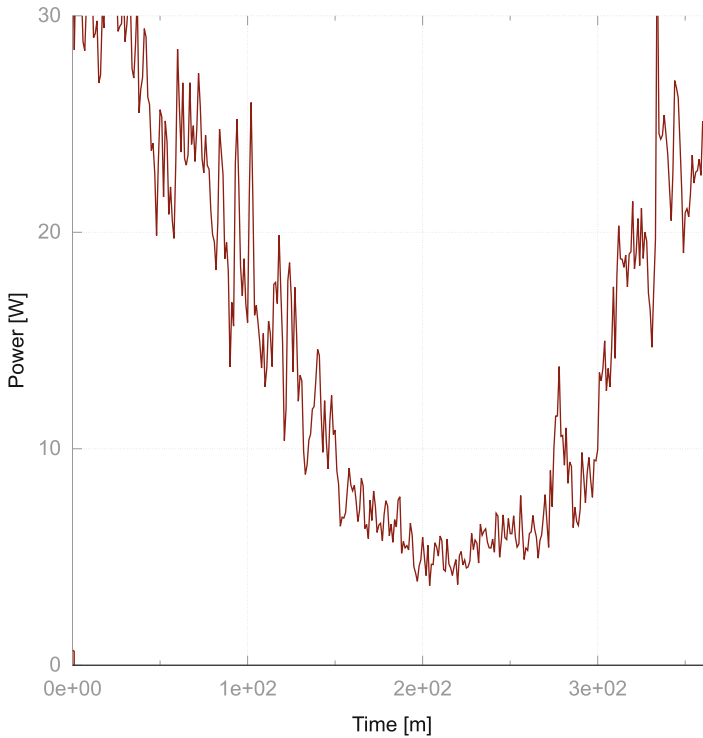


**Fig. 10.6** Heating power demand of the building cluster

### Simulation Models

The models of the individual components of the hydrogen system are described in the subsequent section. All models are written in C++ and compiled as INSEL blocks.

#### *PEM Electrolyzer*

At the anode of a PEM electrolyzer, water molecules are split to protons, electrons, and oxygen. The membrane is permeable for protons, which at the cathode combine with electrons to form hydrogen. Overall, one molecule of hydrogen and half a molecule of oxygen are formed per converted water molecule.

Anode:	$\text{H}_2\text{O} \rightarrow 2 \text{H}^+ + 2 \text{e}^- + 0.5 \text{O}_2$
Cathode:	$2 \text{H}^+ + 2\text{e}^- \rightarrow \text{H}_2$
Overall:	$\text{H}_2\text{O} \rightarrow \text{H}_2 + 0.5 \text{O}_2$

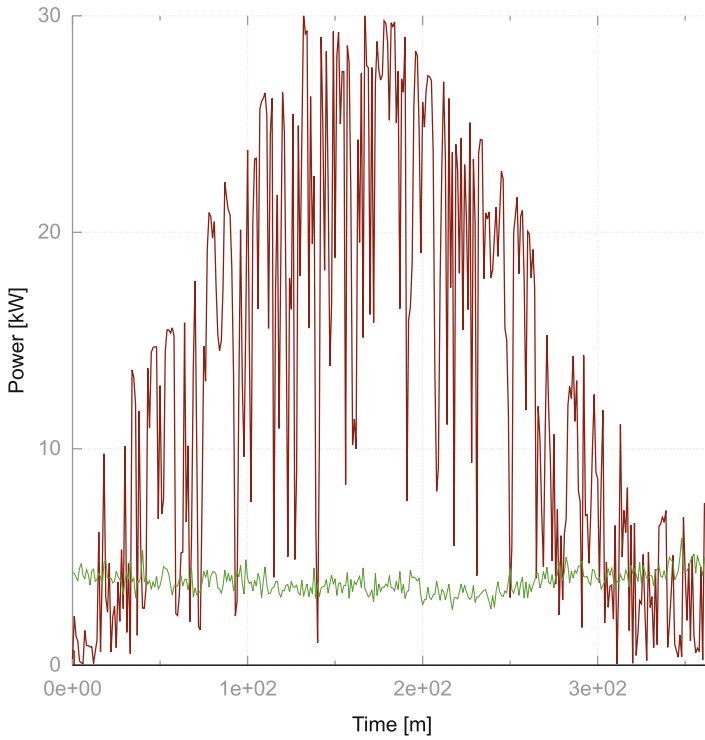


**Fig. 10.7** PV power production and domestic electricity demand

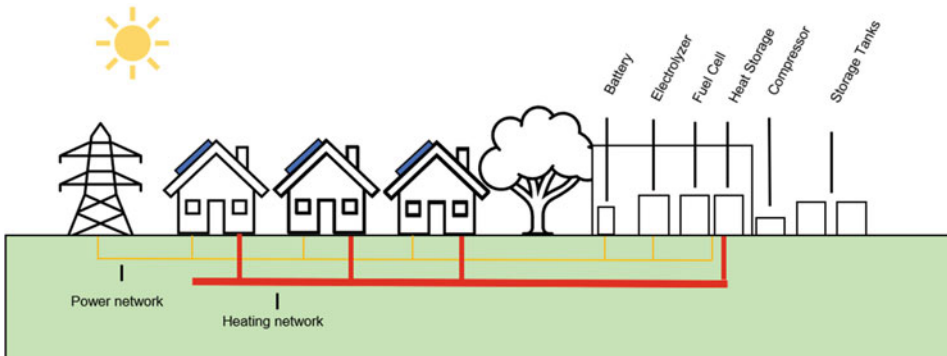


**Fig. 10.8** Schematic representation of the investigated hydrogen system

For a detailed description of PEM electrolyzer modeling, see Carmo, Fritz, Mergel, and Stolten (2013).

#### *Compressor*

The hydrogen compression process is modeled as isothermal (approximately true for multi-stage compressors) and hydrogen treated as an ideal gas<sup>1</sup> corrected with a compressibility factor  $Z$  (from empirical equations (see Lemmon, Huber, and Leachman (2008) and Zheng et al. (2016)) or interpolated from table data).

The power needed for the compression calculates as follows:

$$P_0 = \frac{\dot{m}}{dt} \cdot R_s \cdot T \cdot Z \cdot \ln \left( \frac{P_{\text{storage}}}{P_{\text{in}}} \right) \quad (10.1)$$

If the efficiency of the compressor is considered, the power consumption of the compressor results from Eq. (10.2).

$$P = \frac{P_0}{\eta} \quad (10.2)$$

#### *Storage Cylinder*

To determine the pressure in the storage tank, the net hydrogen mass flow is calculated by the currently occurring inflow from the electrolyzer and outflow requested by the fuel cell (Eq. 10.3).

$$\dot{m}_{H_2} = \dot{m}_{H_2, \text{inflow}} - \dot{m}_{H_2, \text{outflow}} \quad (10.3)$$

With the net mass flow and the amount of hydrogen present in the previous time step results the overall mass of hydrogen in the storage device (Eq. 10.4).

$$m_{H_2} = \int \dot{m}_{H_2} \cdot dt \quad (10.4)$$

In real compressed gas storage situations, the heating of the gas due to compression and the opposite effect, cooling due to relaxation (Joule-Thomson effect), must be considered, as this effect lowers the storage capability. This is especially observed in fast filling processes (e.g., filling stations). In this case, these effects are neglected (in Eq. 10.5,  $T_{\text{gas}} = T_{\text{amb}}$ ) because the incoming hydrogen mass flow is low compared to the storage capacity. The pressure in the storage tank (in Pa) is calculated with the ideal gas law (Eq. 10.5).

---

<sup>1</sup>If hydrogen is compressed at higher pressures, e.g., >70 MPa, for filling stations, other gas models should be taken.

**Table 10.4** Fuel cell parameters

24 h-averaged minimal heat demand	3.67 kW
FC thermal power design point	15 kW
FC assumed efficiency	0.6
FC net power design point	37 kW

$$p_{\text{storage}}(t) = \frac{m_{\text{H}_2}(t) \cdot R_S \cdot T_{\text{gas}}}{V} \quad (10.5)$$

### PEM Fuel Cell

As an electrochemical device with similarities to PEM electrolyzers, the model of the fuel cell is at this point not further described. A profound introduction into PEM fuel cell modeling is, e.g., given by Spiegel (2008).

### Fuel Cell Design

In this scenario, the fuel cell was designed so that the minimal occurring part load represents 25% of the fuel cells' nominal thermal power. This design point was chosen to minimize the on-off cycles of the fuel cell. The minimal occurring part load was determined from the 24 h-averaged heat demand of the building cluster. The resulting parameters for the fuel cell are summarized in Table 10.4.

Figure 10.9 shows the load duration curve of the annual heat demand and the fuel cell thermal power (15 kW).

### Control

**Input Power Distribution Algorithm:** The surplus electrical power<sup>2</sup> generated by the PV devices is divided between the electrolyzer, the battery, and the power grid, according to the algorithm shown in Fig. 10.10.

To keep the electrolysis power within the operating boundaries of the electrolyzer, the two parameters  $P_{\text{el, min}}$  and  $P_{\text{el, max}}$  are determined in the controller. It is tried to ensure the minimal electrolysis power if possible, by using the energy stored in the buffer battery. This control strategy avoids standby phases for the electrolyzer.

In this scenario, the minimal electrolysis power  $P_{\text{el, min}}$  is determined by the battery power. In further studies, this value should be optimized according to the specific system design (battery power compared to electrolyzer power) and the characteristics of the electrolyzer (warm-up time, part load capability).

**Electrolyzer Temperature Control:** Besides the input power of the electrolyzer, as shown above, also the cell temperature is controlled with a PID controller (only cooling, no heating). The temperature setpoint is set to 80 °C.

<sup>2</sup>PV power minus building load.

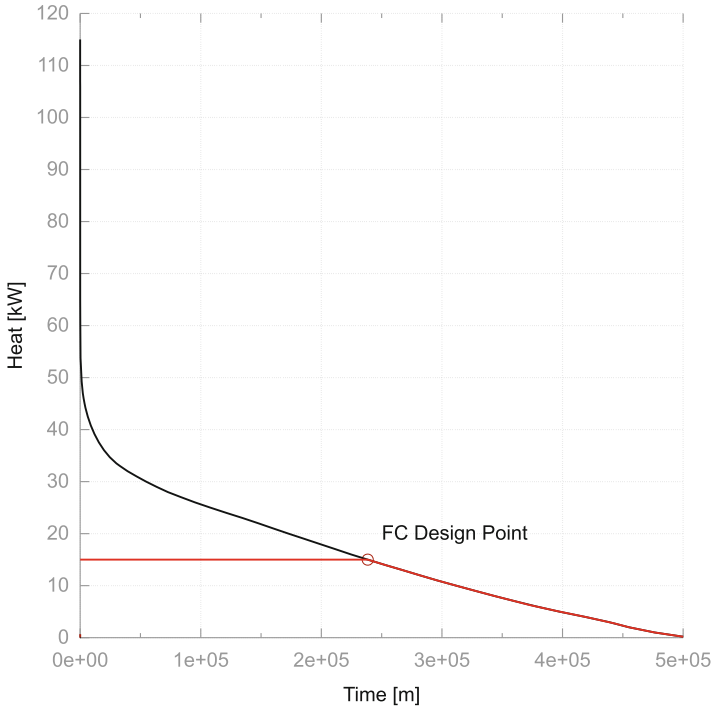


**Fig. 10.9** Load duration curve—heat demand

**Fuel Cell Control:** In this scenario, the fuel cell is operated as a thermal driven CHP device. For the operation of the fuel cell, setpoints for the heat demand and the cell temperature are specified. The regulating variable for the heat demand is the current  $I$ , which affects the hydrogen consumption rate. To keep the cell temperature at the setpoint, the mass flow of a cooling loop is adjustable (see Fig. 10.11).

The upper limit for the current controller is determined by the operating point (OP) at which the cell power density is maximized. It is recognizable from Fig. 10.12 that the maximal power density of the fuel cell is achieved at a current density of about 80% ( $0.88 \text{ A/cm}^2$ ) of the limiting power density ( $1.1 \text{ A/cm}^2$ ). The voltage-current-characteristic of the fuel cell is shown in Fig. 10.13.<sup>3</sup>

## 10.5 Simulation Results and Discussion

### Evaluation of Prediction Algorithms

For the grid search, the random forest model has proven to be the best for the data sets. Not only the output quality is better but also the training time of the model with the RF method

<sup>3</sup>The curves are generated with the fuel cell INSEL model.



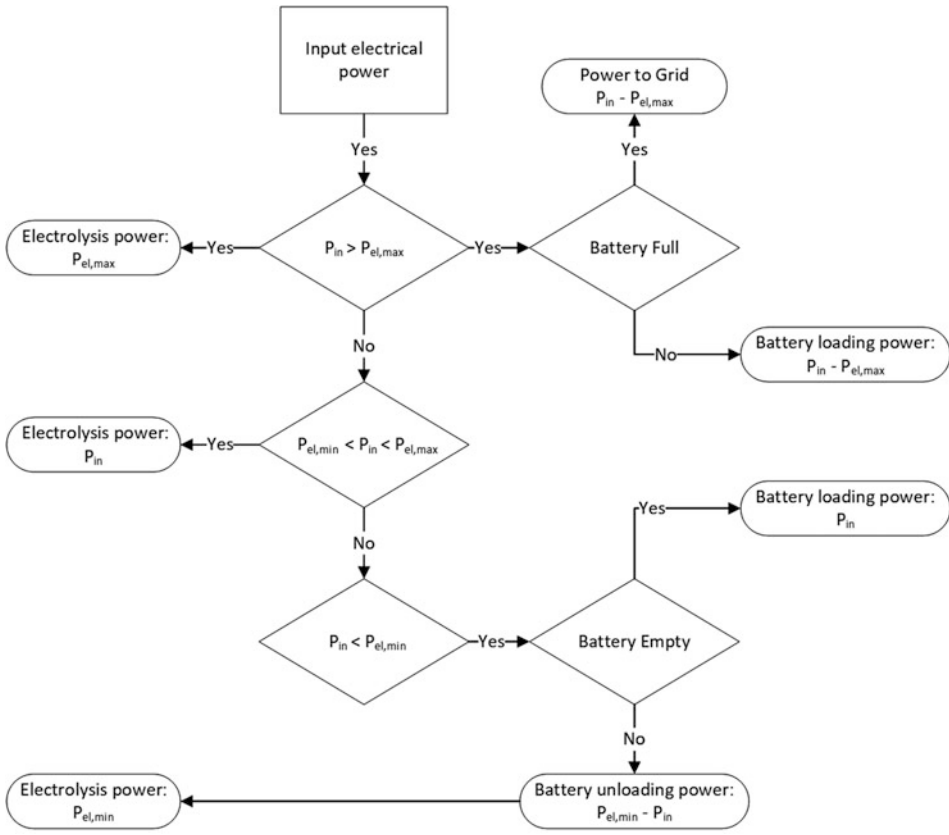


**Fig. 10.10** Power distribution algorithm

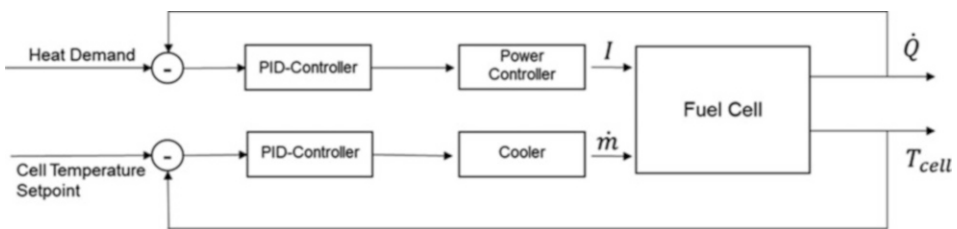


**Fig. 10.11** FC control scheme

is significantly faster than that of the gradient boosting or the DTR. With a training data set size of 6 times 2,628,000,000 features and an output, this is, among other things, an essential feature.

Table 10.5 shows the results of the grid search. It can be seen that the RF method has a much better coefficient of determination and MAPE for both outputs (heat demand and

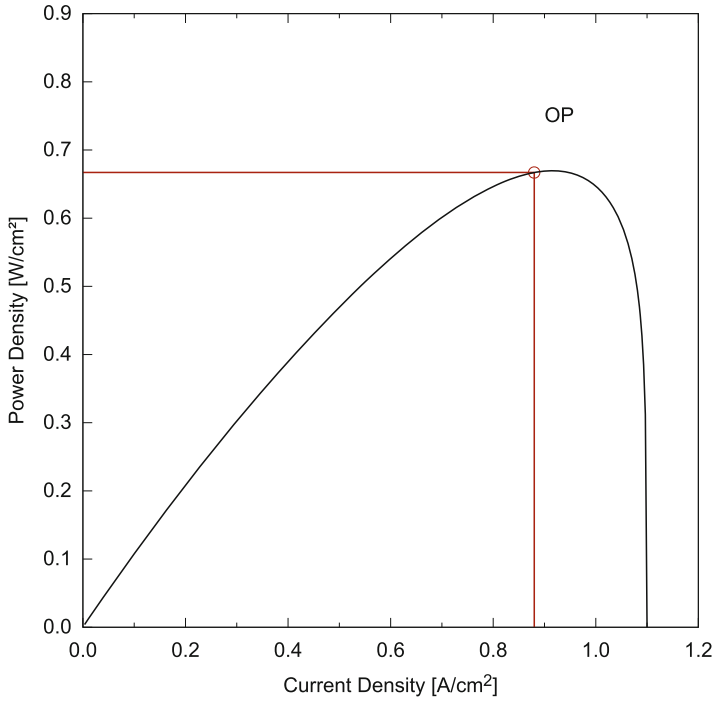


**Fig. 10.12** FC current–power–density characteristics

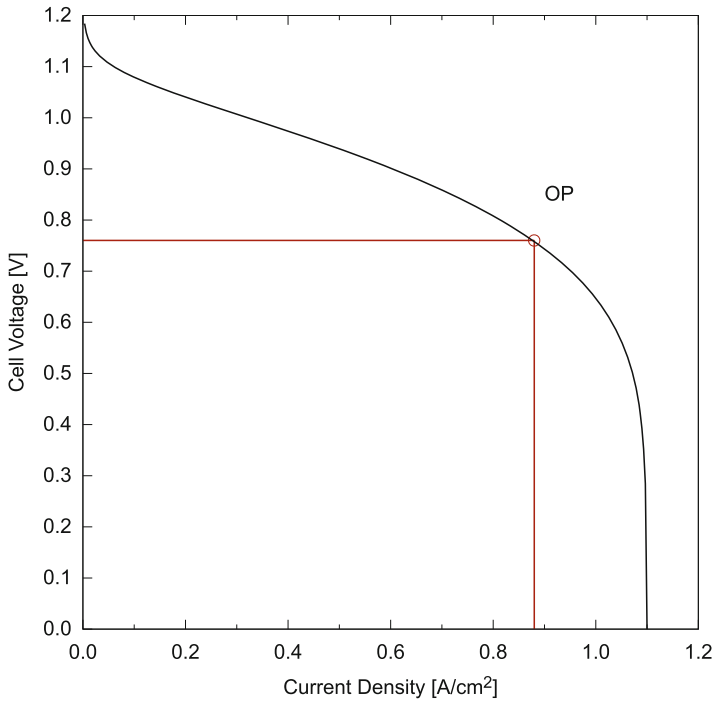


**Fig. 10.13** FC current–density–voltage characteristics

**Table 10.5** Grid search for the best hyperparameters and the best output results

Grid search for the best model			
Model	Best $R^2$	Best MAPE	Best MAE
<i>Minutely data: Prediction of electrical energy demand</i>			
Decision tree	69%	24.35%	0.9 kW
Random forest	79%	20.65%	0.11 kW
Gradient boosting	52%	20.41%	0.17 kW
<i>Minutely data: Prediction of heat energy demand</i>			
Decision tree	84%	5.83%	0.49 kW
Random forest	95%	5.83%	0.28 kW
Gradient boosting	84%	8.87%	0.48 kW

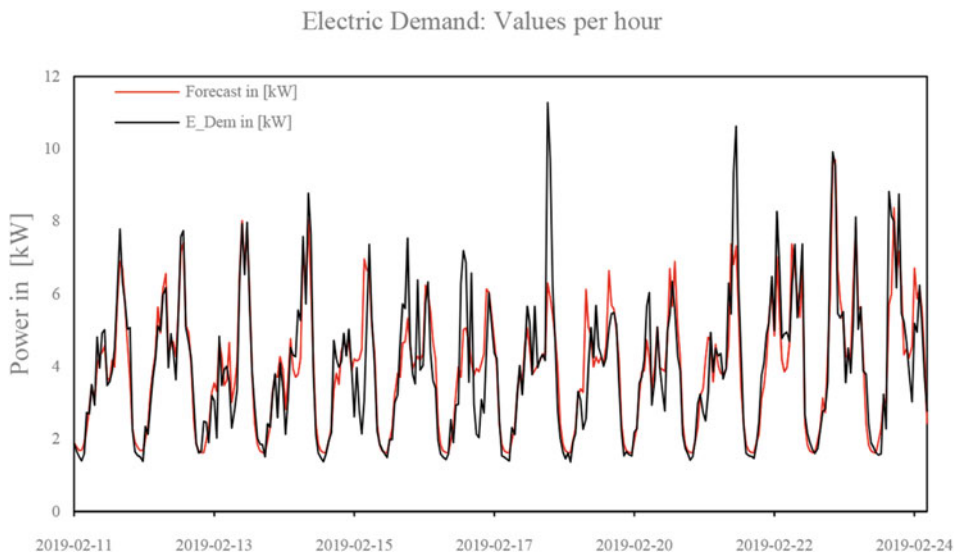


**Fig. 10.14** Forecast of the electricity demand

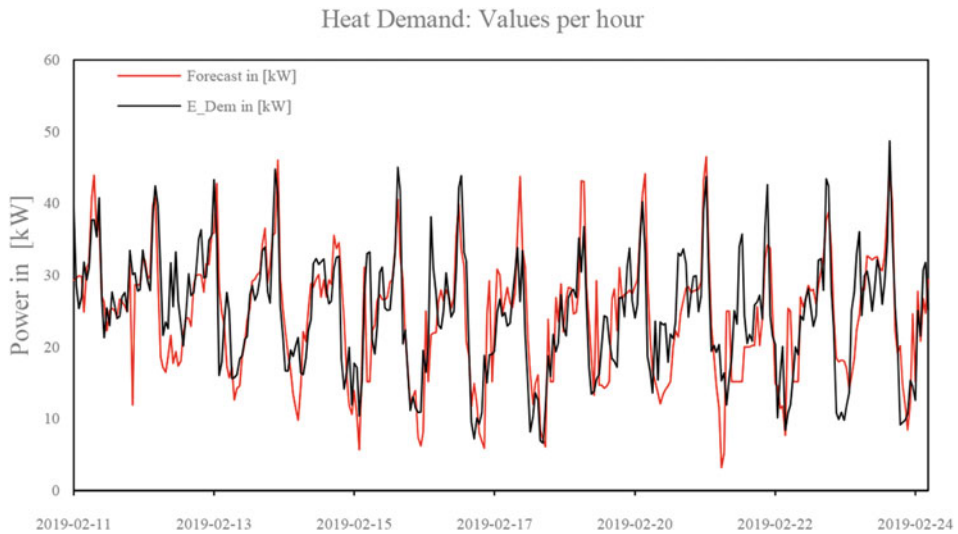
household electricity demand). The MAE is also much lower in the RF method than in the other methods. The RF method is therefore used for the forecasts. The output of the data is in the form of hourly values.

Figure 10.14 shows a section of the household power demand by the “Vordere Viehweide” in Wüstenrot (black) and the corresponding forecast (red). The course of the day is described very well by the model. The hyperparameters were determined by grid search (see under random forest) and amount to 23 estimators and 7834 leaves. Combined with the 2019 weather data, the model achieves a determination rate of 82% with a MAPE of 9.12%. The MAE is 0.44 kW (see also Table 10.6).

Figure 10.15 shows a section (February 13 to February 23) of the heat demand for the year 2019 (black) and the associated forecast. The forecast was trained with the best model

**Table 10.6** Statistic results of the forecasts

Results of the hourly energy forecast			
Model	Best $R^2$	Best MAPE	Best MAE
<i>Prediction of electrical energy demand</i>			
Random forest	82%	9.12%	0.44 kW
<i>Prediction of heat energy demand</i>			
Random forest	75%	41.9%	3.95 kW

**Fig. 10.15** Forecast of the heat demand

that was found by the grid search and created with the input data of the year 2019. The hyperparameters for the model consist of 22 estimators and 7314 leaves. Table 10.6 shows the statistical results. In the model for the heat demand, a determination of 75% is reached with a MAPE of 41.9%. The MAE corresponds to 3.95 kW.

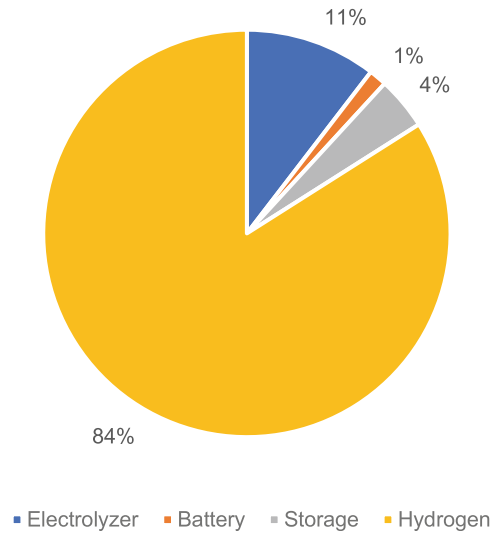
The results (Table 10.6) with the prediction by the RF should be viewed critically, since these are synthetic load curves and thus exclude the user dynamics in many respects. Furthermore, the grid search does not provide all the possibilities of the best hyperparameters due to the systematic nature of the search, so it cannot be automatically said that these hyperparameters provide the best results. However, this investigation has the potential to predict the course of a load profile to a certain degree and thus possibly optimize the control of the system.

### Optimization Results

The optimization loop was executed with 200 generations and 40 populations with results shown in Table 10.7.

**Table 10.7** Optimized system parameters

Component	Optimization result
Electrolyzer rated power	56 kW
Storage size	10 m <sup>3</sup>
Battery size	33 kWh
Battery power	14 kW
Best target function result	-65,689.37 €
External hydrogen refills	23

**Fig. 10.16** Cost distribution

These system parameters lead to 23 necessary refills ( $N_{\text{refill}} = 23$ ) and to a best target function result of -65,689.37 €. The distribution of the costs of the individual items is shown in Fig. 10.17. Eighty-four percent of the system costs are caused by the necessary external refills of the hydrogen tank. However, the market price of hydrogen will most likely decrease with additional global and national production capacity. An independency of hydrogen imports could be achieved by the installation of more electricity production capacity (additional PV or supplementary wind turbines) and more electrolysis power, combined with a bigger hydrogen storage capacity (Fig. 10.16).

Figure 10.17 indicates that 93% of the annual surplus electrical energy (PV production minus household demand) is directly utilized in the electrolyzer to produce hydrogen. Another 5% is temporarily stored in the battery and utilized in the electrolyzer if the input power is lower than minimal operating power of the electrolyzer. Only 2% (1862 kWh) of the surplus power could not be used directly and is fed into the electricity grid.

Monthly heat demand and production (Fig. 10.18) and monthly power demand and production (Fig. 10.19) show that the deficits of the heat coverage in the winter months go

**Fig. 10.17** Surplus electrical energy distribution

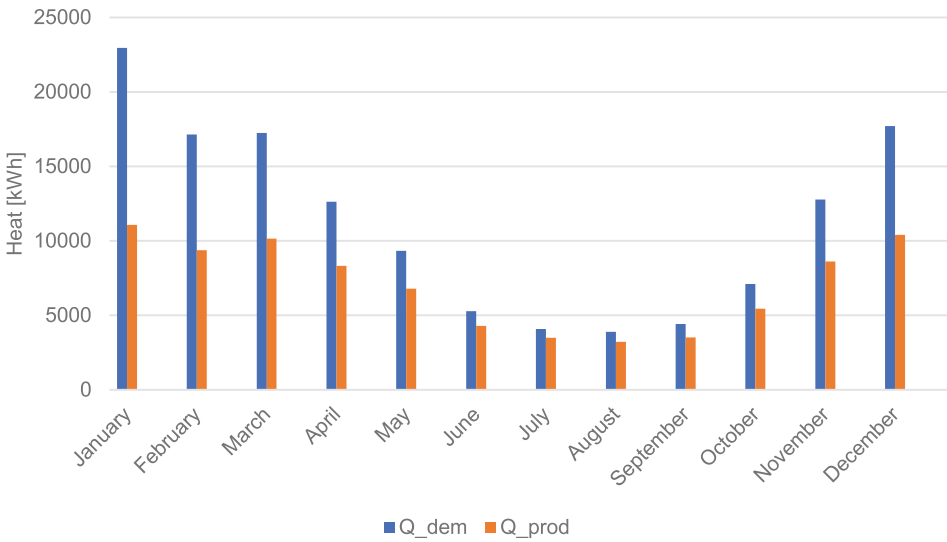
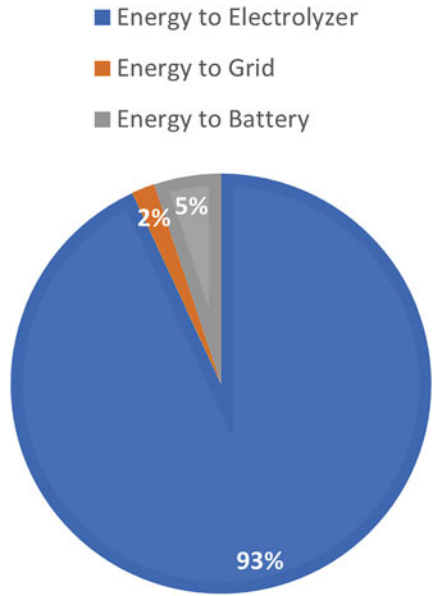


**Fig. 10.18** Monthly heat demand and production

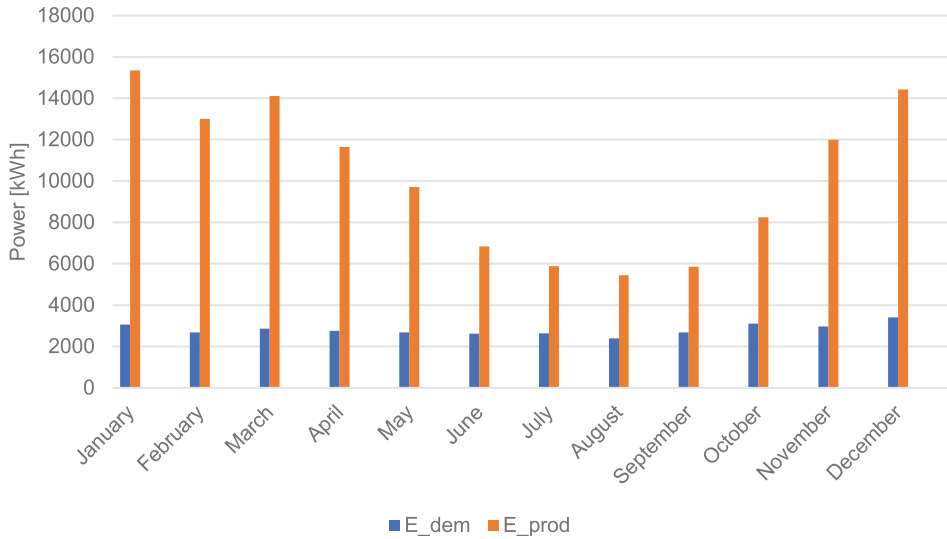


**Fig. 10.19** Monthly power demand and production

along with a high excess of electrical energy, which could be used to produce additional heat via heat pumps.

The following sections will discuss the results for the individual components.

### Electrolyzer

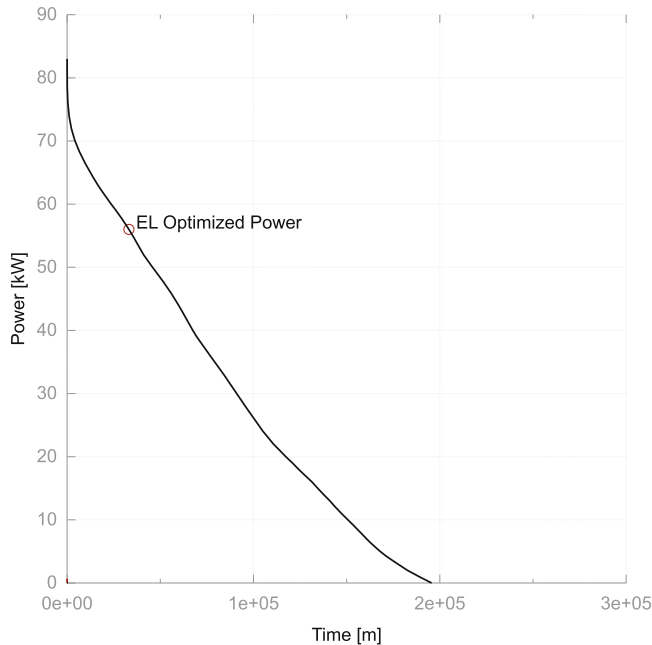
The optimized electrolyzer results in a rated electrolysis power of 56 kW meaning 64 cells in series with a cell area of 300 cm<sup>2</sup>.

Figure 10.20 shows the annual load duration curve of the building cluster's surplus power. With an installed PV power of about 97 kW<sub>p</sub>, the optimized electrolysis power is about 58% of the electricity production capacity.

A rated electrolysis power of 56 kW in combination with a 33 kWh, 14 kW battery leads to 613 full-load hours (7% of the year) and 5818 standby hours (66.4%) of the electrolyzer. This setup leads to 5343 off-on switches (see Table 10.8).

Although PEM electrolyzers are known for short start-up times and good part load behavior, a future optimization goal could be the reduction of standby hours which mostly occur during the winter season (see Fig. 10.21). A significant reduction of the standby hours could be achieved with an installation of wind turbines.

The temperature of the electrolyzer during the year is shown in Fig. 10.22. As the temperature setpoint is at 80 °C, the electrolyzer is cooled, if the temperature rises above this value. The waste heat could potentially be used to raise the overall system efficiency. However, in this setup, the setpoint temperature is not reached.



**Fig. 10.20** Load duration curve of surplus power

**Table 10.8** Simulation results—electrolyzer

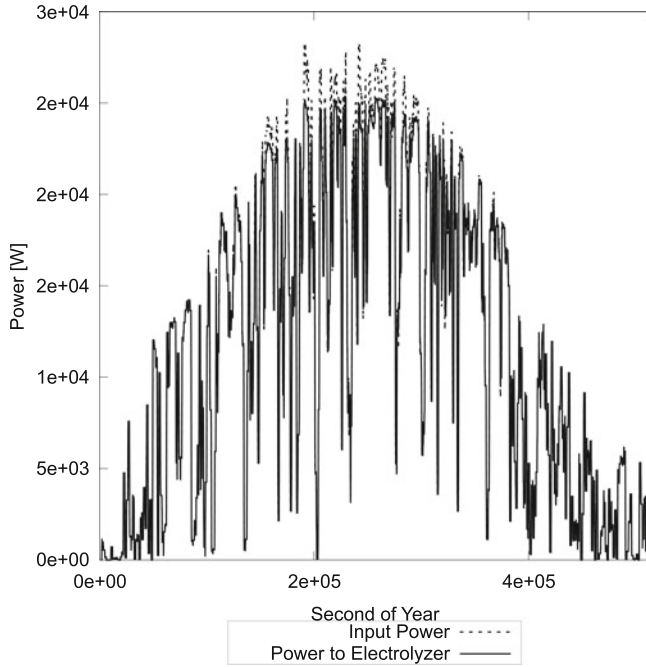
	56 kW rated power
Electrolyzer full-load hours	613 h (7%)
Electrolyzer standby hours	5818 h (66.4%)
Electrolyzer off-on switches	5343
Peak hydrogen production rate	1.07 kg/h
Peak current	450 A

The hydrogen production rate of the electrolysis process is proportional to the electrolysis current (see Eq. 10.9). Thus, Figs. 10.23 and 10.24 show similar curves with peak hydrogen production and current in the middle of the simulation run (summer months with high PV loads). The voltage also follows the rise of the electrolysis current due to higher voltage losses. A maximal hydrogen production rate of 1.07 kg/h is achieved.

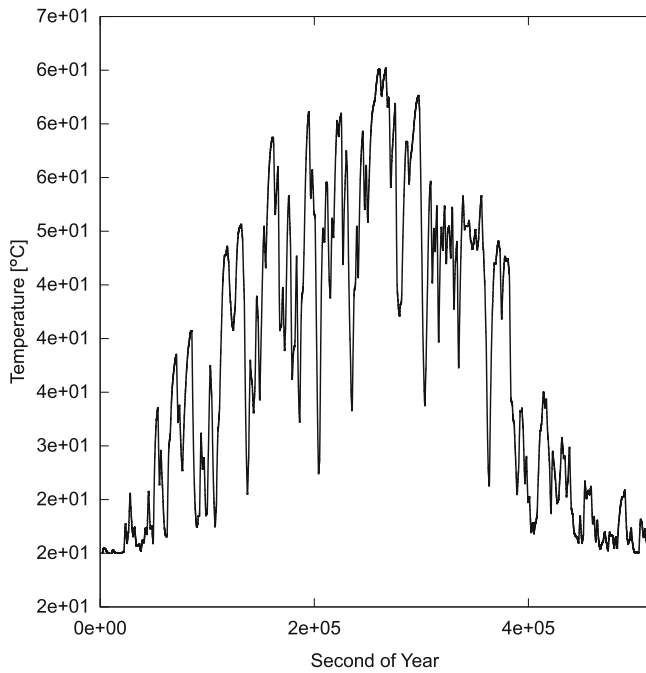
### Fuel Cell

In this scenario, the fuel cell produces 84,696 kWh of heat per year with a maximum thermal power of 14.9 kW. This amount covers 63% of the overall heat demand (Table 10.9). Additionally, 122,507 kWh of electrical power is produced with a maximal electrical power of 22.5 kW, which could be fed into the electrical grid or utilized to produce additional heat.

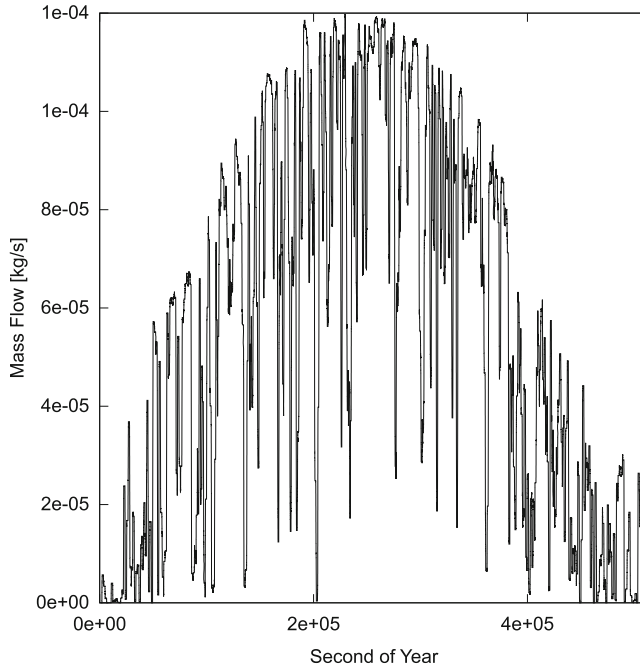




**Fig. 10.21** Electrolysis power (24 h-Avg)



**Fig. 10.22** Electrolyzer temperature



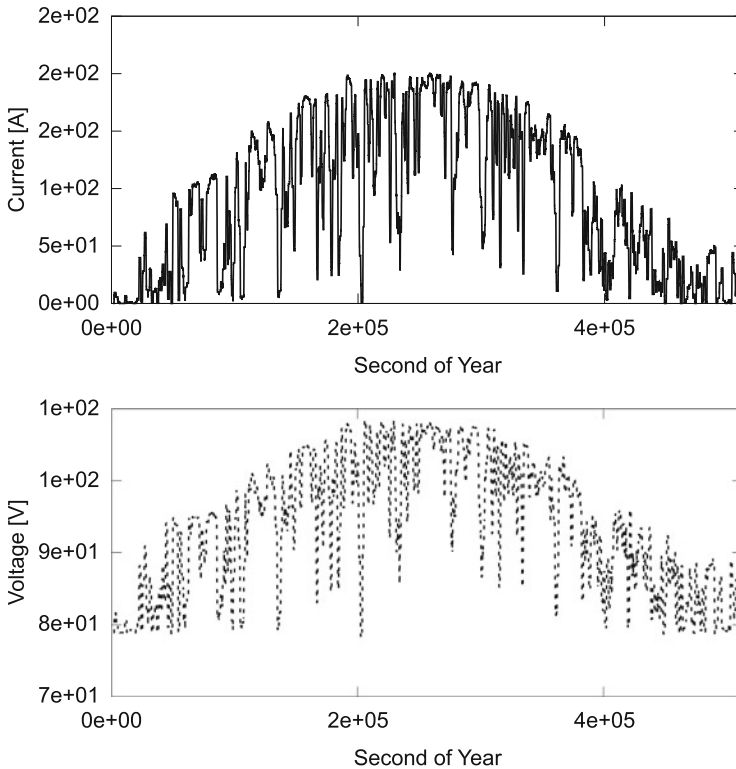
**Fig. 10.23** Hydrogen production rate (24 h-Avg)

Figure 10.25 shows that especially at the beginning and the end of the year (heating period), the heating capacity of the fuel cell is not sufficient to cover the heating demand. Hence, the investigated system could not be operated independently and must be complemented by other heating technologies (afterburner, heat pumps, boilers) and heat storages. As expected from the characteristic electrical behavior of galvanic cells, the voltage of the fuel cell drops, if high currents are removed (see Fig. 10.26). In a heat-driven mode, the current corresponds to the demanded heat generation.

Figures 10.27 and 10.28 show the temperature and the electrical power output of the fuel cell. It is high at the beginning and the end of the simulation run, which matches with higher electrical demand in these periods of the year and is good to be used to generate additional heat via heat pumps. Hence, it closes the gap of the heat demand and the generated heat of the fuel cell.

### Storage

The hydrogen storage device in this scenario starts with filled hydrogen tanks ( $10 \text{ m}^3$  at 25 MPa). In the course of the year, 23 refills with delivered hydrogen are needed (see Fig. 10.29). It is also visible from this figure that the amount of produced hydrogen in the summer is not sufficient to fill the storage. In fact, only the emptying of the storage tank is slowed down.



**Fig. 10.24** Electrolyzer Current and Voltage (24 h-Avg)

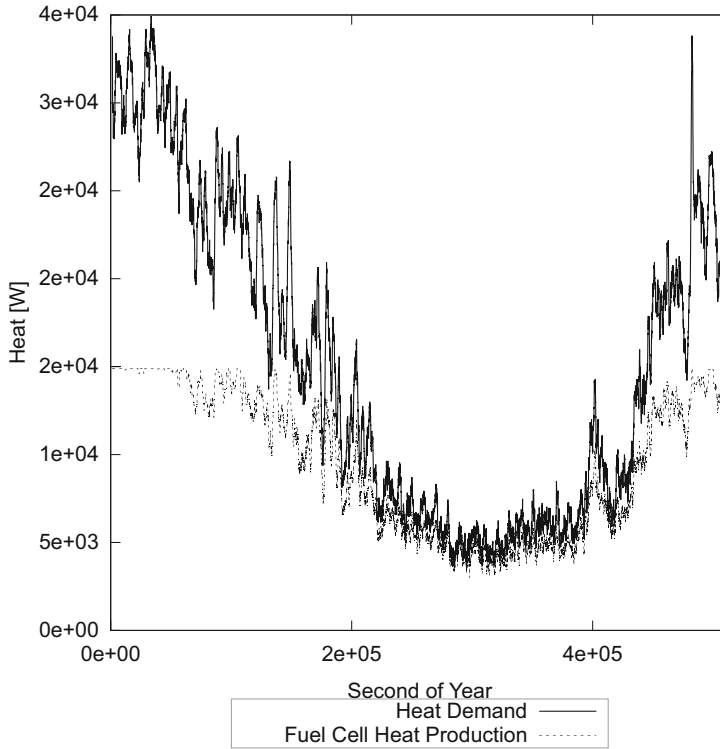
**Table 10.9** Simulation results—fuel cell

Yearly heat production (kWh)	84,696
Heat coverage	63%
Yearly FC power production (kWh)	122,507
Maximum thermal power (kW)	14.9
Maximum electrical power (kW)	22.5

With standard gas cylinder packages ( $12 \times 50$  l), 17 packages are necessary to achieve a storage capacity of  $10 \text{ m}^3$ . This number of packages would cover an area of about  $15.4 \text{ m}^2$  (see Fig. 10.30). The storage setup with individual cylinder packages enables a straightforward adjustment of the overall storage capacity depending on the given system setup.

### Battery and Compressor

The net power flow in and from the battery and the battery state of charge are shown in Fig. 10.31. The curve points to high fluctuations of the battery load, which might decrease the battery performance and lifetime.



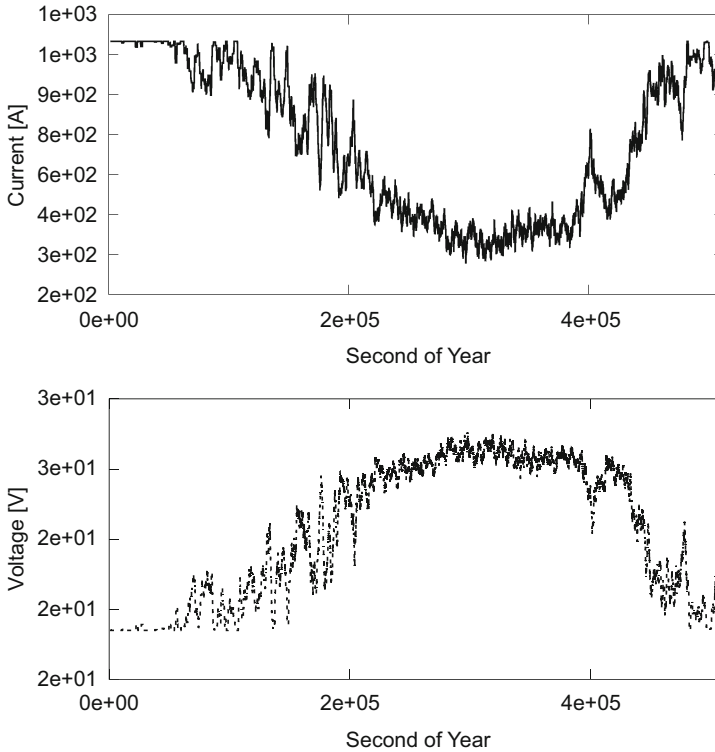
**Fig. 10.25** Heat demand and production (24 h-Avg)

Figure 10.32 displays the power demand of the hydrogen compressor with 24 h-averaged values. High loads occur in the summer month, where the hydrogen production rate from the electrolyzer maximizes. Overall, the yearly energy demand of the compressor is 3859 kWh with a peak load of 2574 W.

## 10.6 Conclusions

The main steps and results of this study are summarized here:

- A model for a hydrogen-based district heating system was introduced.
- The model was applied on a building cluster with PV in a rural area with a combination of measured and white-box model data for heat demand and power generation.
- The fuel cell was designed with 15 kW thermal power and 37 kW overall rated power.
- Evolutionary algorithms were used to determine the size of an electrolyzer, a battery, and a hydrogen storage based on a target function with economic assumptions.



**Fig. 10.26** FC current and voltage rate (24 h-Avg)

- An electrolyzer rated power of 56 kW was found to be optimal for this scenario (58% of the installed PV power). With this setup, 93% of the surplus power is directly used in the electrolyzer, and 2% is fed into the power grid (5% is temporarily stored in the battery).
- The fuel cell covers 63% of the annual heat demand. The generated surplus of electrical power could be used for further heat production.
- The optimized storage size of 10 m<sup>3</sup> is not sufficient to match the hydrogen demand of the fuel cell without external hydrogen deliveries which are responsible for 84% of the overall annual costs.
- By RF prediction, a coefficient of determination for household electricity demand of 82% can be achieved, and a MAPE of 9.12% can be achieved.
- The prediction by RF for the heat demand reaches a coefficient of determination of 75% and a MAPE of 41.9%.

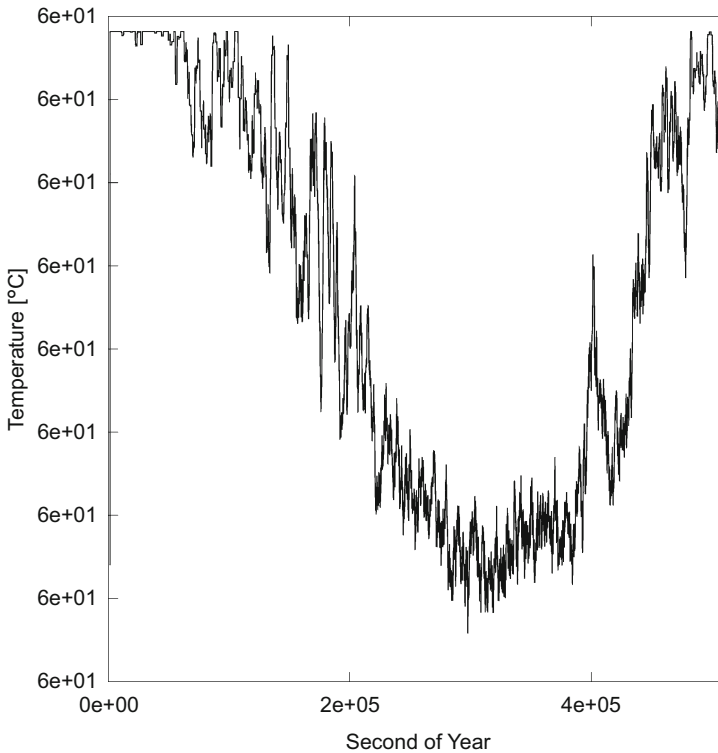


**Fig. 10.27** FC temperature (24 h-Avg)

## 10.7 Outlook

Studies following this work have to aim at rising the overall heat demand coverage of the system by integrating a central heat pump, which consumes the electrical power produced by the fuel cell. Another step would be to additionally utilize the waste heat of the electrolyzer. Wind turbines will be integrated into the system model in order to achieve independency of external hydrogen deliveries.

Furthermore, the forecasting tool based on the RF will be integrated into the work process. The forecast serves to optimize the work process and represents an optimizer in this respect. In addition, it will also be investigated how this optimizer can affect a real plant engineering.

Next steps:

- Model validation and improvement with measurement data from a hydrogen test rig.
- Dynamic coupling of the hydrogen system model with the building and the PV models.

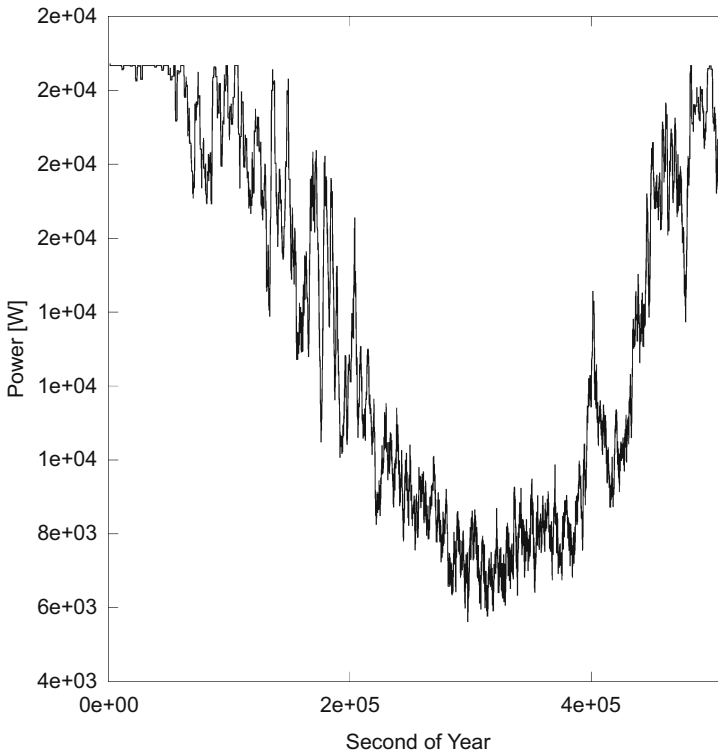


**Fig. 10.28** FC electrical power output

- Integration of a central heat pump, wind turbines, a heating network, and thermal storage in the system model.
- Evaluation of other hydrogen storage technologies, for instance, hydrogen storage as formic acid.
- Integration of the RF prediction tool with a self-learning component.
- Optimization of the hydrogen system operation based on a prediction tool.

**Acknowledgments** The results of this work were partially generated at the Hochschule für Technik Stuttgart, within the research project NEQModPlus (EnEff:Stadt, 03ET1618B) at Locasys GmbH and within the Joint Graduate Research Training Group Windy Cities.<sup>4</sup>

<sup>4</sup><http://windycities.de/>

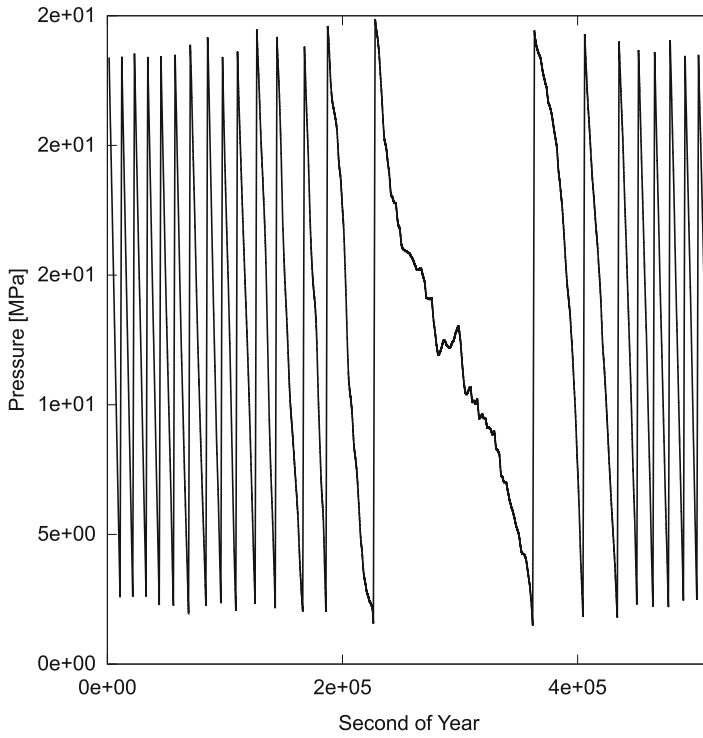


**Fig. 10.29** Storage pressure

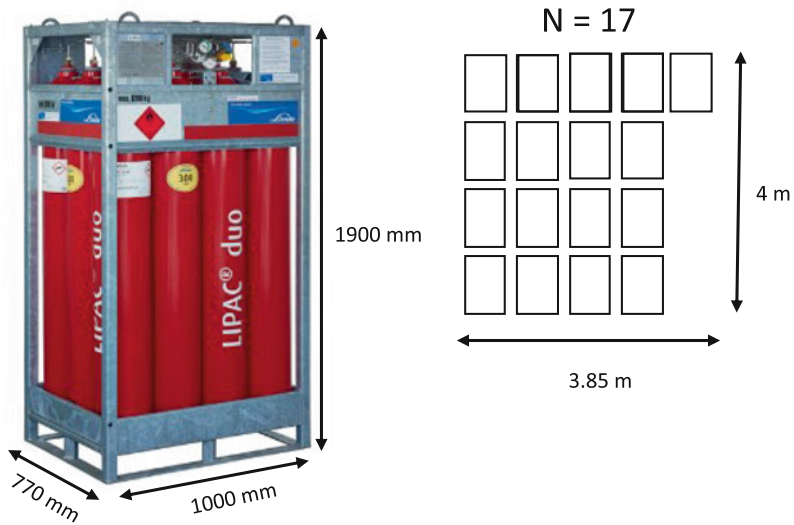


**Fig. 10.30** Hydrogen storage dimensions



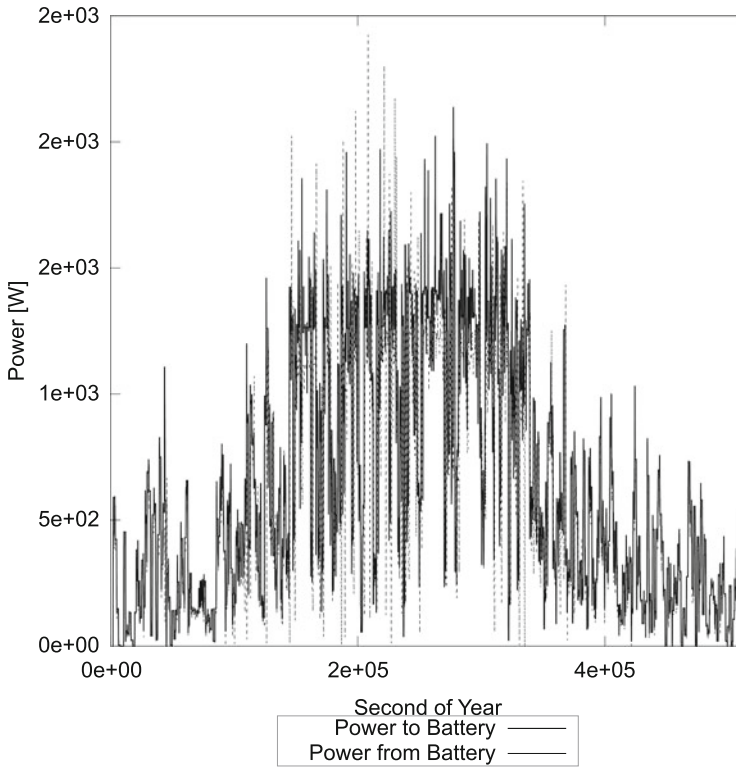


**Fig. 10.31** Battery power flow (24 h-Avg)

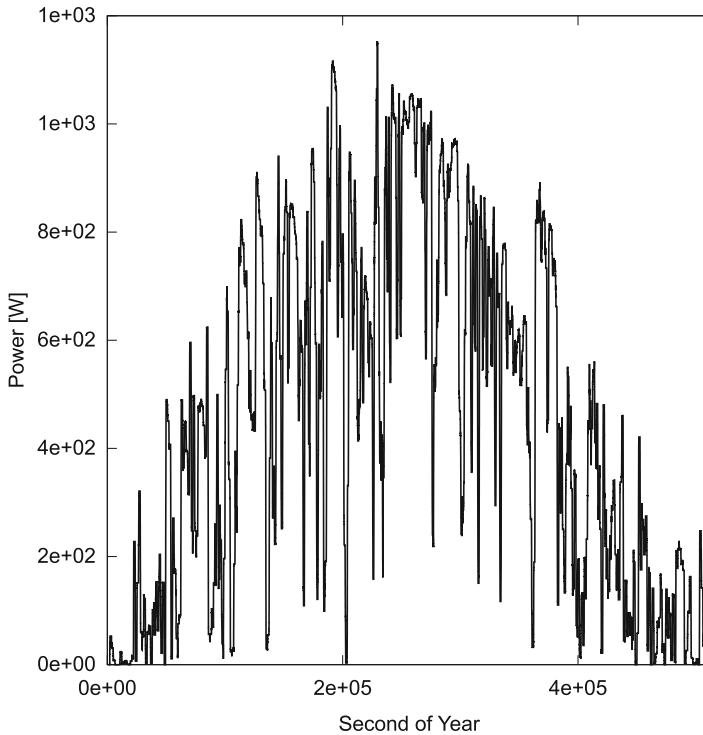


**Fig. 10.32** Compressor power

## References

- Adam, A., Fraga, E. S., & Brett, D. J. L. (2015). Options for residential building services design using fuel cell based micro-CHP and the potential for heat integration. *Applied Energy*, 138, 685–694. <https://doi.org/10.1016/j.apenergy.2014.11.005>
- Agora Energiewende. (2017). W, (107/01).
- Ahmad, A. S., Hassan, M. Y., Abdullah, M. P., Rahman, H. A., Hussin, F., Abdullah, H., & Saidur, R. (2014). A review on applications of ANN and SVM for building electrical energy consumption forecasting. *Renewable and Sustainable Energy Reviews*. <https://doi.org/10.1016/j.rser.2014.01.069>
- Ahmad, M. W., Mourshed, M., & Rezgui, Y. (2017). Trees vs Neurons: Comparison between random forest and ANN for high-resolution prediction of building energy consumption. *Energy and Buildings*. <https://doi.org/10.1016/j.enbuild.2017.04.038>
- Ahmad, M. W., Mourshed, M., Yuce, B., & Rezgui, Y. (2016). Computational intelligence techniques for HVAC systems: A review. *Building Simulation*, 9(4), 359–398. <https://doi.org/10.1007/s12273-016-0285-4>
- BMWi. (2020). The National Hydrogen Strategy.
- BWP Bundesverband Wärmepumpe e.V. (2020). BWP-Branchenstudie 2021. <https://www.waermepumpe.de/presse/zahlen-daten/>

- Brennenstuhl, M., Lust, D., Pietruschka, D., & Schneider, D. (2021). Demand Side Management Based Power-to-Heat and Power-to-Gas Optimization Strategies for PV and Wind Self-Consumption in a Residential Building Cluster. *Energies*, 14(20). <https://doi.org/10.3390/en14206712>
- Brennenstuhl, M., Zeh, R., Otto, R., Pesch, R., Stockinger, V., & Pietruschka, D. (2019). Report on a Plus-Energy District with Low-Temperature DHC Network, Novel Agrothermal Heat Source, and Applied Demand Response. *Applied Sciences*.
- Cappa, F., Facci, A. L., & Ubertaini, S. (2015). Proton exchange membrane fuel cell for cooperating households: A convenient combined heat and power solution for residential applications. *Energy*, 90, 1229–1238. <https://doi.org/10.1016/j.energy.2015.06.092>
- Carmo, M., Fritz, D. L., Mergel, J., & Stolten, D. (2013). A comprehensive review on PEM water electrolysis. *International Journal of Hydrogen Energy*, 38(12), 4901–4934. <https://doi.org/10.1016/j.ijhydene.2013.01.151>
- DEAP. (2021). DEAP - Distributed Evolutionary Algorithms in Python. Retrieved July 22, 2021, from <https://deap.readthedocs.io/en/master/>
- Dodds, P. E., Staffell, I., Hawkes, A. D., Li, F., Grünewald, P., McDowall, W., & Ekins, P. (2015). Hydrogen and fuel cell technologies for heating: A review. *International Journal of Hydrogen Energy*, 40(5), 2065–2083. <https://doi.org/10.1016/j.ijhydene.2014.11.059>
- Energieverbände. (2020). Esslingen District Setting Up its Own Hydrogen Production.
- European Commission. (2020). A European Green Deal.
- Erhart, T.G. (2015). Improvement of heat-led CHPs based upon ORC-technology. University of Strathclyde, Glasgow. Institute of Electric and Electronic Engineering
- Gemeinde Wüstenrot. (2018). EnVisaGe - Wüstenrot auf dem Weg zur Plusenergiegemeinde. Retrieved August 30, 2018, from <http://www.envisage-wuestenrot.de/>
- Geron, A. (2017). *Hands-On Machine Learning With Scikit-Learn & Tensor Flow*. *Hands-on Machine Learning with Scikit-Learn and TensorFlow*. <https://doi.org/10.3389/fninf.2014.00014>
- Götz, M., Lefebvre, J., Mörs, F., McDaniel Koch, A., Graf, F., Bajohr, S., ... Kolb, T. (2016). Renewable Power-to-Gas: A technological and economic review. *Renewable Energy*, 85, 1371–1390. <https://doi.org/10.1016/j.renene.2015.07.066>
- Günther, D., Wapler, J., Langner, R., Helmling, S., Miara, M., Fischer, D., ... Wille-Hausmann, B. (2020). *Wärmepumpen in Bestandsgebäuden*. Freiburg.
- Hessisches Umweltministerium. (1999). *Heizenergie im Hochbau - Leitfaden energiebewußte Gebäudeplanung*. Wiesbaden.
- Jain, R. K., Smith, K. M., Culligan, P. J., & Taylor, J. E. (2014). Forecasting energy consumption of multi-family residential buildings using support vector regression: Investigating the impact of temporal and spatial monitoring granularity on performance accuracy. *Applied Energy*. <https://doi.org/10.1016/j.apenergy.2014.02.057>
- Lemmon, E. W., Huber, M. L., & Leachman, J. W. (2008). Revised Standardized Equation for Hydrogen Gas Densities for Fuel Consumption Applications. *Journal of Research of the National Institute of Standards and Technology*, 113(6), 341–350.
- Lust, D., Rößner, P., Brennenstuhl, M., Klemm, E., Plietker, B., & Eicker, U. (2019). Decentralized city district hydrogen storage system based on the electrochemical reduction of carbon dioxide to formate, 4(Ires), 137–144. <https://doi.org/10.2991/i-res-19.2019.17>
- Marino, C., Nucara, A., Pietrafesa, M., & Pudano, A. (2013). An energy self-sufficient public building using integrated renewable sources and hydrogen storage. *Energy*, 57(2013), 95–105. <https://doi.org/10.1016/j.energy.2013.01.053>
- Marx, S. (2020). Klimaquartier - Neue Weststadt Esslingen. Stuttgart.
- Moon, J., Kim, Y., Son, M., & Hwang, E. (2018). Hybrid short-term load forecasting scheme using random forest and multilayer perceptron. *Energies*. <https://doi.org/10.3390/en11123283>

- Müller, A. C., & Guido, S. (2015). *Introduction to Machine Learning with Python and Scikit-Learn*. O'Reilly Media, Inc.
- Ng, A., & Soo, K. (2018). *Data Science – was ist das eigentlich?! Data Science – was ist das eigentlich?!* <https://doi.org/10.1007/978-3-662-56776-0>
- Pedregosa, F., Varoquaux, G., Gramfort, A., Michel, V., Thirion, B., Grisel, O., . . . Duchesnay, É. (2011). Scikit-learn: Machine learning in Python. *Journal of Machine Learning Research*.
- Robinson, C., Dilkina, B., Hubbs, J., Zhang, W., Guhathakurta, S., Brown, M. A., & Pendyala, R. M. (2017). Machine learning approaches for estimating commercial building energy consumption. *Applied Energy*. <https://doi.org/10.1016/j.apenergy.2017.09.060>
- Spiegel, C. (2008). *PEM Fuel Cell: Modeling and Simulation using MATLAB*. <https://doi.org/10.1016/B978-012374259-9.50006-9>
- Teichmann, D., Stark, K., Müller, K., Zöttl, G., Wasserscheid, P., & Arlt, W. (2012). Energy storage in residential and commercial buildings via Liquid Organic Hydrogen Carriers (LOHC). *Energy and Environmental Science*, 5(10), 9044–9054. <https://doi.org/10.1039/c2ee22070a>
- U.S. Department of Energy. (2019). *Energy Storage Technology and Cost Characterization Report*.
- United Nations Climate Change. (2020). The Paris Agreement.
- Verein Deutscher Ingenieure. (2012). *VDI 2067 - Economic efficiency of building installations. Fundamentals and economic calculation*.
- Windeknecht, M., & Tzscheuschler, P. (2015). Optimization of the heat output of high temperature fuel cell micro-CHP in single family homes. *Energy Procedia*, 78, 2160–2165. <https://doi.org/10.1016/j.egypro.2015.11.306>
- Zhang, X. M., Grolinger, K., Capretz, M. A. M., & Seewald, L. (2019). Forecasting Residential Energy Consumption: Single Household Perspective. In *Proceedings - 17th IEEE International Conference on Machine Learning and Applications, ICMLA 2018*. <https://doi.org/10.1109/ICMLA.2018.00024>
- Zheng, J., Zhang, X., Xu, P., Gu, C., Wu, B., & Hou, Y. (2016). Standardized equation for hydrogen gas compressibility factor for fuel consumption applications. *International Journal of Hydrogen Energy*. <https://doi.org/10.1016/j.ijhydene.2016.03.004>

**Open Access** This chapter is licensed under the terms of the Creative Commons Attribution 4.0 International License (<http://creativecommons.org/licenses/by/4.0/>), which permits use, sharing, adaptation, distribution and reproduction in any medium or format, as long as you give appropriate credit to the original author(s) and the source, provide a link to the Creative Commons license and indicate if changes were made.

The images or other third party material in this chapter are included in the chapter's Creative Commons license, unless indicated otherwise in a credit line to the material. If material is not included in the chapter's Creative Commons license and your intended use is not permitted by statutory regulation or exceeds the permitted use, you will need to obtain permission directly from the copyright holder.





# Parking and Charging: New Concepts for the Use of Intelligent Charging Infrastructure in Car Parks

# 11

Esther Herrlich, Elisabeth Schaich, Stephanie Wagner,  
and Dieter Uckelmann

## Abstract

A reliable charging infrastructure for electric vehicles used in individual transport including availability and accessibility is necessary because it contributes highly to the decision of purchasing a BEV (battery electric vehicle). In Germany, charging is mainly done at home; however, parking spots in car parks have the potential to densify charging infrastructure in semi-public spaces. Intelligent car parks represent further developments which add a variety of technologies, energy management tools and value-added services to parking in general. The article addresses the question of technical maturity of charging infrastructures used in intelligent car parks and their marketability. Examples are charging methods such as conductive and inductive charging or various payment options. Pilot projects are described, and possible concepts of charging in intelligent car parks are explained, thereby addressing a growing interest in the subject.

## Keywords

e-Mobility · Charging infrastructure · Intelligent car parks · Big data · Artificial intelligence (AI)

E. Herrlich · E. Schaich · S. Wagner · D. Uckelmann (✉)  
Hochschule für Technik Stuttgart, Stuttgart, Germany  
e-mail: [dieter.uckelmann@hft-stuttgart.de](mailto:dieter.uckelmann@hft-stuttgart.de)

© The Author(s) 2022  
V. Coors et al. (eds.), *iCity. Transformative Research for the Livable, Intelligent, and Sustainable City*,  
[https://doi.org/10.1007/978-3-030-92096-8\\_11](https://doi.org/10.1007/978-3-030-92096-8_11)

183

## 11.1 Introduction

In this article, a literature overview on the state of the art in e-mobility, charging infrastructure and various charging technologies is conducted. Use cases and pilot projects related to car parks are presented. An expert survey has been pursued, and its results are published for the first time. Finally, an outlay of future technologies that can be used in intelligent car parks is given.

### Climate Change and Mobility

Although greenhouse gas emissions have risen continuously since the beginning of industrialization, the recent acceleration of climate change currently poses one of the most pressing global challenges. Addressing this issue, 197 countries signed the Paris Agreement in 2015 to limit global warming to a maximum of 1.5 °C by 2050. To achieve this agreement, the reduction of greenhouse gas emissions had to be readjusted. Therefore, the EU agreed to reduce carbon emissions by 55% until 2030 compared to 1990 (DW 2020). By 2050, greenhouse gas neutrality is targeted. Road transport contributed 21% of the total EU CO<sub>2</sub> emissions in 2017. To achieve climate neutrality by 2050, rapid changes and measures for limitation are necessary (BMU 2019: 8–9). e-Mobility has the potential to contribute highly to the reduction of greenhouse gas emissions. Based on latest knowledge, the mandatory targets can only be reached by using battery electric vehicles (BEVs). From an environmental policy point of view, the end of combustion engines by 2050 is unavoidable (Clausen 2018: 14–15).

### State of the Art of BEV

In Germany, the BEV market is still relatively small. Nonetheless, it is highly dynamic and presumably will grow exponentially. Out of the approximately 140 models offered in Germany in 2020, 70 models are produced by German car manufacturers. Government incentives are supporting the market and the transition to e-mobility (VDE 2020).

Major drivers for the BEV market in Germany are the expansion of charging infrastructure, an improved range of the vehicles, affordable pricing of charging and subsidies by the government (Mehta et al. 2019: 3). Significant barriers of e-mobility are the high purchase price, the limited range and the lack of a nationwide battery charging infrastructure (Clausen 2018: 13; Mehta et al. 2019: 3). From 2016 to 2019, the buying interest in BEV in Germany has doubled to 55% (Aral AG 2019). Experts predict an expansion of the charging infrastructure from 2025 until 2040. Furthermore, the vehicle's range will be optimized, and the number of BEV owners will increase (Mehta et al.: 6–9). In order to achieve the EU targets for 2030, the demand of six million electric vehicles must be met in 2019 (Cornet et al. 2019: 35).

The number of charging stations in Germany grows linearly and has reached more than 21,000 units in Q4/2020 (Chargemap SAS 2020). On average, users of electric vehicles in Germany charge 65–70% at home, 15% at public charging stations and 7% at charging stations at the workplace (BDEW 2019: 6–8). Charging stations are often located in urban

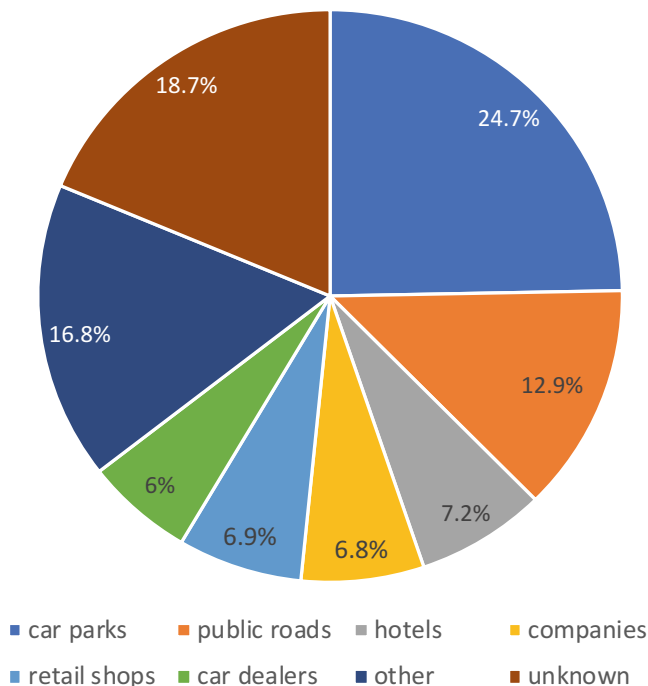


**Fig. 11.1** Location of charging stations in Germany (May 2020), own figure, data based on Chargemap SAS 2020

areas. One-quarter of all charging stations listed in Chargemap is located at parking spaces. In German cities, there is one charging station available for three electric vehicles on average (Chargemap SAS 2020; Oberst 2018: 1–3).

Deficiencies of charging stations include the varying payment system, the insufficient transparency of charging costs and the need for a special registration to operate the charging process (Clausen 2018: 13; Oberst 2018: 1–3). A nationwide charging infrastructure is an essential prerequisite. However, its expansion faces a problem as sales in charging do not cover investment costs and refinancing takes several years. Thus, there is an interdependency between the market development of BEVs and the charging infrastructure (Oberst 2018: 1–3) (Fig. 11.1).

### The Role of Parking in Mobility

Parking is an essential component of mobility since it marks the beginning and the end of each driving process and covers as much as 23 h per day on average. In large cities, space for car parking can cover up to 40% of the total traffic area. Most parking spaces are located in the city centre, mainly close to shopping centres. The demand for parking depends on the number of cars and further on the number of retail shops and commuter traffics (Quantum Immobilien 2018).

## 11.2 State of the Art

### Charging Technologies

Currently, there are four different charging systems in use: cable-bound (also called cable-bound charging or the so-called plug and charge) is a conductive charging system, whereas wireless charging is an inductive charging system. Furthermore, there is battery swap and finally the so-called redox flow principle. In Germany, only cable-bound charging technology is in use. There are two kinds of conductive charging methods: alternating current charge (AC) and direct current charge (DC). Cable-free charging is currently being tested in pilot projects as another technology, for example, for cabs (Universität Duisburg-Essen 2019). Battery replacement has not been standardized and is rarely used (VDE FNN et al. 2020: 8).

For cable-bound charging, there are different charging modes, which are defined in the standard DIN EN 61851-1 (VDE 0122-1): charging processes with an output of max. 22 kW are considered “normal charging” and represent the modes 1–3 of AC charging. Higher powers (e.g., 50 kW) are called “fast charging” and are considered DC charging mode 4. This is stated in the EU Directive 2014/94/EU. For both conductive charging technologies, communication between infrastructure and BEV operates via cable. For AC charging, communication in accordance with ISO 15118 is optional; for DC charging, communication is mandatory and operates via charging cable that is permanently integrated in the charging station. Information on energy requirements, planned duration of the charging process and information on pricing and billing are exchanged during communication (VDE FNN et al. 2020: 9–11). The DC fast-charging infrastructure is expanded to ensure a wide coverage along the motorways and main traffic axes and to supply a new generation of BEVs with higher ranges. The Combined Charging System (CCS) is used to ensure the compatibility of different generations of charging infrastructures (NPE 2020).

### Charging Infrastructure and Legal Requirements of Maintenance and Handling

When selecting charging infrastructures for parking garages with a floor space of 100 m<sup>2</sup> or more, the garage regulation of the respective federal state must be considered, and identification and safety obligations must be fulfilled. VDE 100-722 must be followed, and the infrastructure is supposed to be designed for mode 3 or 4 (NPE 2020; VDE FNN et al. 2020: 19–20). It is necessary to analyse the type and number of BEVs expected at the location. Furthermore, data of considered charging capacities, duration of parking and charging behaviour of the vehicle owners need to be estimated. Since charging infrastructure demands much electrical power for several hours, supply lines and distributors must be designed generously, also considering the fast-growing market of BEV leading to increasing requirements. There is an obligation to notify the network operator if power levels exceed between 3.7 and 12 kVA to avoid unnoticed network overload. Above 12 kVA, the network operator has to be asked for approval (VDE FNN et al. 2020: 14–17).



Measures for monitoring, evaluating and billing of charging processes need to be considered in the planning process of the public charging infrastructure. The facilities for these measures are called *back-end system*. Suitable interfaces between charging stations and back-end are required. Relevant standards for the development of charging infrastructures are currently progressing. For example, it is important to position the charging station in the immediate proximity of the parking space and without affecting the other users of the parking space. Operators of charging stations must ensure that fire and data protection criteria are confirmed. The intuitive operation of the charging station in a well-lighted environment must be ensured. According to the charging station ordinance, charging stations in public spaces must be usable for charging without prior conclusion of a contract. DIN IEC 63119-1:2018-04 stipulates that the operators of different charging infrastructures must conclude contracts with each other for shared use, i.e., “roaming” by customers (VDE FNN et al. 2020: 23–25). The charging stations are exposed to environmental factors such as weather, temperature fluctuations and vandalism.

For easy handling across manufacturers, the plug and charge system is being pursued. This system enables immediate charging once the cable is plugged in. The payment process is initiated automatically. This requires a standardized and secure communication between BEV and charging station, guaranteed by ISO 15118. In a strategic collaboration between Hubject and Electrify America, the introduction of the system in North America has started at the end of 2020 (Werwitzke 2020).

An argument against the plug and charge system is that the situational electricity costs, network load and battery charge level are not considered. The charging method per kWh may be more expensive than other charging systems (Torres-Sanz et al. 2018: 22875–22888). The utilization and amortization period of public charging points can be seen critically. Although customers are willing to pay for DC charging, subsidies are required to convince charging point manufacturers to provide the overly scaled number demanded by policy makers (Wirges 2016: 131–133).

Further, the expansion of public fast-charging stations is planned. Until 2023, 1000 locations are identified for DC fast-charging networks. These charging stations will supply electric power of more than 150 kW. In addition, it is planned to expand the number of normal and fast-charging stations to 72,000 (BMVI 2020).

This article mainly focuses on charging infrastructure in public car parks. However, one should consider the public funds of private charging stations since charging at home is still preferred by around 65% in 2019 (BDEW 2019: 8). The purchase of private charging points is funded with 900 € by the Federal Ministry of Transport and Digital Infrastructure. It includes private homes, residential buildings and any other non-public construction of charging points. This, for example, could lead to increasing sales of wall boxes (BMVI 2020).

### **Grid Integration**

A conflict of objectives arises between the permanent supply of energy and the three attributes cheap, efficient and environmentally friendly (Gemsjäger, Monscheidt 2020). If

electric vehicles demand electricity in an uncontrolled and uncoordinated manner, high loads occur at peak times, which endangers the stability of the electricity grid. Due to the expansion of renewable energies and the use of small generators, the electricity supply is more volatile anyway (Linnhoff-Popien et al. 2015: 52). Energy producers, storage facilities and consumers organize their operations efficiently in smart grids, considering the demand and supply situation (VDE FNN et al. 2020: 33). Parking and charging time is decoupled in this intelligent charging management. Factors such as the current grid load, battery capacity and BEV demand are considered. The charging quantity is also calculated under these paradigms (Gemsjäger, Monscheidt 2020).

Grid stability is supported by bidirectional charging which is defined as charging at times of low demand and feeding into the grid at peak times. For stakeholder satisfaction, the collection and evaluation of Big Data using artificial intelligence (AI) is useful. Thus, an energy management system can be operated in real time, which allocates the available resources using AI (BDI e.V 2018). As the expansion of e-mobility continues, parking lot operators are invoked to provide more charging points.

---

### 11.3 Pilot Projects

Daily business of parking lot operators may be expanded to real-time charging load management in the future. The integration of charging as an added service during parking could possibly be profitable for car park operators. Since demand in charging stations increases, their availability at parking spots might become important (Wirges 2016: 236). Charging is already possible in selected car parks of the operator APCOA—the biggest European parking-space provider—in German cities but is limited to a few charging points (APCOA PARKING n.d.).

The *project AUTOPLES* (automated parking and charging of electric vehicle systems) was performed from January 2013 to June 2015, and it was funded by the German Federal Ministry of Education and Research, BMBF. The goal was the development of a parking and charging system in the car park Hofdienergarage in Stuttgart. The research focused on an intelligent charging infrastructure. The concept seeks to be technically feasible, economical and marketable. It is possible to gradually expand the 16 charging points, which are integrated in the car park infrastructure. The parking spots need to be booked and reserved in advance via app. Since several vehicles can be charged simultaneously, the planning of energy demand is important. The reservation system contributes to a better demand forecast. The conductive charging process could be further automated when using a robot which finds the charging socket independently without human intervention. The user can monitor the charging status via app during the parking process (FZI 2015).

The *V-Charge project* of Volkswagen AG in cooperation with Robert Bosch GmbH, the Swiss Federal Institute of Technology Zurich, the Technical University of Braunschweig, the University of Parma and the University of Oxford was funded by the European Commission within the “Europe 2020” programme. Reservation and booking of a parking

spot are operated via app. A status check is carried out, whereby the demand of the vehicles' energy and the parking time are queried (Furgale et al. 2013: 809, 811). The charging is operated inductively (Pudenz 2015). Big Data regarding the expected parking time, the current battery level and the planned travel distance are required to distribute the energy capacities according to the demand of all charging vehicles (Furgale et al. 2013: 811).

A different approach was taken by the project of Volkswagen AG's "CarLa" loading robot in 2018 (Volkswagen AG 2018). Mobile robots equipped with a battery pack approach the vehicle and charge it independently without human intervention. The robot's gripper arm detects the position of the charging socket and identifies the plug type. Smartphone, robot and vehicle communicate with each other exchanging information and data. Relevant data includes the type of vehicle, type of plug, position of the plug and energy demand. These robots act intelligently and decide in which order they approach and charge the vehicles based on communicated data (Walzel et al. 2016: 110–111).

It can be deduced that the technical maturity and marketability of intelligent car parks varies and that a wide range of technical feasibility studies of intelligent car parks has been conducted. In the following section, several technologies will be evaluated and discussed based on the literature review and the expert's opinions.

---

## 11.4 Technologies in Intelligent Car Parks

During the research of this paper, the authors have interviewed eight experts on the topic of intelligent car parks. The results serve as a basis for further discussions of the technology maturity state and the expected marketability of intelligent car parks. In summer 2020, a questionnaire was handed out to stakeholders such as parking spot operators, energy suppliers, companies operating in charging infrastructure, associations and state agencies. The time to marketability is given in years (Fig. 11.2). The technology maturity state is depicted by a scale from 0 (low) to 10 (high).

According to the experts, the expansion of the DC fast-charging infrastructure will benefit the use of DC technology to a high degree. However, there are different opinions about the time until its implementation. Although DC is already a standard for BEV, its penetration for plug-in hybrids (PHEV) will still take time. One expert sees DC charging stations as a niche solution in car parks. Fast charging is predicted to be possible as an additional service with a higher price. Fast inductive charging will complement conductive charging in 5–10 years.

In general, there is a high interest in research about *autonomous driving*. Due to this, it is included in the survey. In six of seven answers, autonomous driving is categorized in terms of the technology maturity state with a low to medium degree, and the time horizon to marketability is seen in the range of 5–10 years.

Payment via app is a valid solution. According to the eight experts, this *payment option* has a high level of technology maturity and is already marketable, no later than within

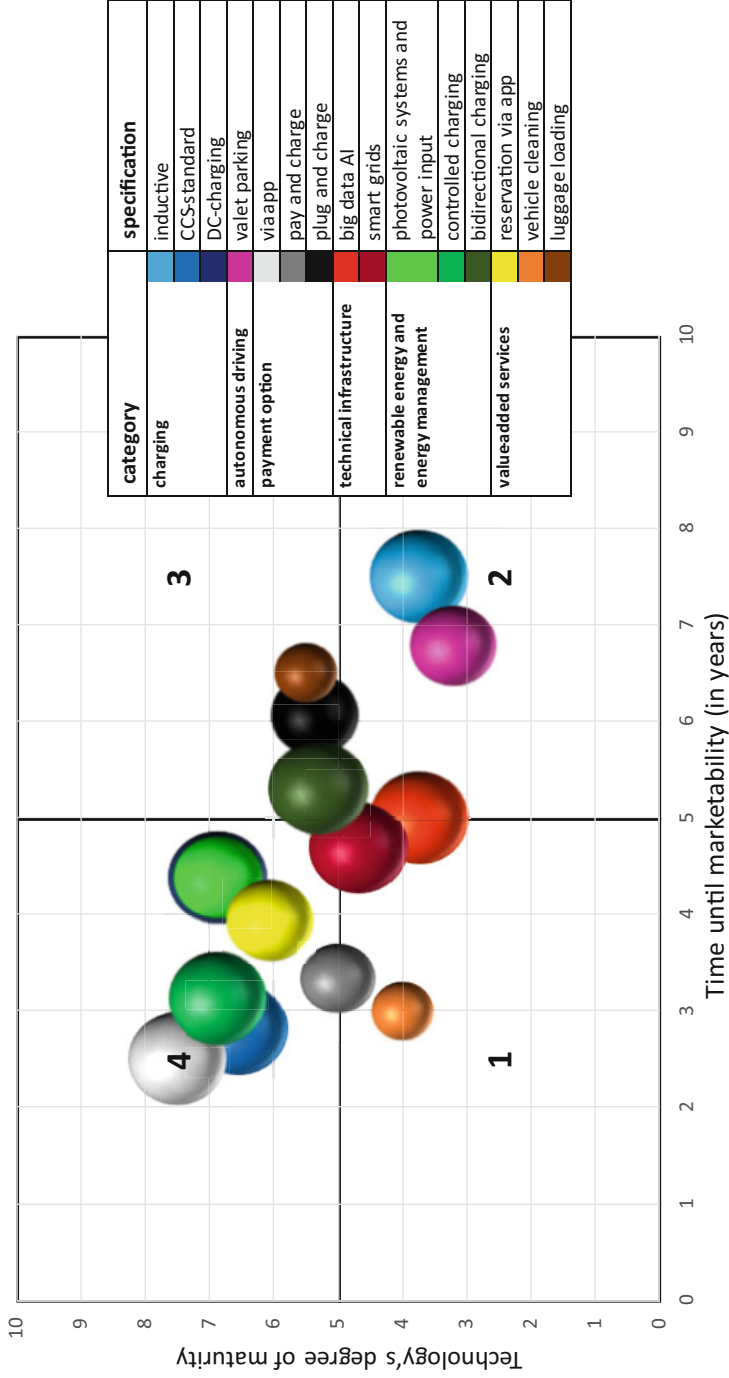


**Fig. 11.2** Survey results of technologies in car parks

5 years. Opinions regarding pay and charge payments differ. Nearly half of the answers are in matrix quadrant four, indicating a medium to high technology maturity. Two answers suggest a timely deployment within the next 5 years and a low to medium maturity level. The marketability of plug and charge depends on the ISO 15118 standard, which is essential for charging and the payment process. Currently, so far only few electric vehicles support the ISO 15118 standard. This leads to a lower market attractiveness of this payment possibility. Starting from 2025, a nationwide implementation seems realistic, although the technology's maturity is considered to be on a medium to high level.

The usage of Big Data and AI in the category of *technical infrastructure* is an essential component of intelligent car parks. Big Data and AI is already used in internal route planning of vehicles, although its expansion to other potential use cases takes more time. The current technology maturity level is estimated to be low by three-quarters of the experts. Further, the marketability is expected within the next 6–10 years. Smart grid technologies are already applied in individual applications. However, their legal integration is not established yet. The grid operation and energy supply contracts still need to be revised for a practical application, and the relevant markets need to grow. The marketability of smart grid technologies is expected in 5–6 years, while the technology maturity is perceived on a medium level. As long as a smart grid is not implemented, the missing load balancing needs to be compensated by higher standby energy generators or energy storage.

According to the experts, technical conditions for the use of photovoltaic systems in car parks and their integration in the charging infrastructure are on a high level. There is disagreement about the time required for the implementation of *renewable energy management* like photovoltaic systems. Car park operators cast doubt on the willingness to invest in an own photovoltaic system. However, several car park operators already use it. Controlled charging defines a controlled and coordinated electricity supply for electric vehicles within the charging environment. This is technically already possible, and the experts assess an implementation within the next 5 years. Estimations regarding the technology maturity level of bidirectional loading differ; however, three-quarters of the experts assume that a technical solution is implemented in the next 5 years. The lack of a policy framework/legislation and high investment costs endanger the large-scale implementation and influence the time for marketability. According to one expert, energy storage devices (e.g., batteries) will be used in public parking spots during peaks of energy demand. Further, an integration in the energy management is easier and less complex. According to the experts' assessment, the use of intelligent controlled charging will be implemented in the next few years. Bidirectional charging is a further development towards an integrated energy management. Due to the lack of a legislation framework, it probably will take longer.

As described in the pilot projects, reservation via app as a *value-added service* is already possible; however, it is not used frequently so far. The marketability of this service is expected within the next 5 years, and the technology maturity level is rated high by three-quarters of the experts. Vehicle cleaning during parking is expected to be implemented until 2025. However, due to the expected high price, the involvement of a third-party

company and the legal complexity, a general low demand for this service is presumed. The service of luggage loading in a vehicle operated by a third party has a medium technology maturity level, while the marketability of the service is considered in 5–10 years. However, there are obstacles regarding the customer acceptance since a high level of trust is required for this.

---

## 11.5 Conclusion and Outlook

Due to the increasing demand for electric vehicles, the expansion of charging infrastructure meets high interest. It is estimated that parking spots in car parks have a high potential to increase the number of charging stations. In this article, the state of the art of e-mobility in relation to the charging infrastructure is presented. It can be deduced that the technical implementation of charging infrastructure in car parks is not an issue. Rather, the establishment of legal standards is a far greater challenge. However, standardization of charging points is urgently required to support the growth of e-mobility.

In August 2020, the national central office for charging infrastructure in Germany published a position paper on the “User Journey” of charging electric vehicles. It is explained that charging electric vehicles differs from refuelling a conventional car and, therefore, is a new experience for users. Results show that high user-friendliness and an integration of the charging process in daily routine are essential for a good experience (Nationale Leitstelle Ladeinfrastruktur 2020: 4–5).

Therefore, these issues need to be solved fast in order to meet customer demands. In Germany, the automotive industry will play an important role in establishing harmonized or competing charging infrastructures. Standardization helps to reduce investment risks for the stakeholders. The number of electric vehicles increases continuously, and therefore, the demand for charging infrastructure in public places will rise. To increase the number of BEVs in Germany and to support the car manufacturing industry, the German government decided to extend the subsidies to buy or lease BEVs from 2021 to 2025. Since the implementation of charging infrastructure is a competitive advantage, car operators should already prepare for this. e-Mobility is currently subsidized, which supports investments of car park operators. However, sustainable business models are needed in the future.

Further, in the position paper of the national central office for charging infrastructure, it is discussed that there will not be one universally valid concept for charging. Still, until 2025, the plug and charge technology will mainly be more important since the ISO standard 15,118 will be developed (Nationale Leitstelle Ladeinfrastruktur 2020: 26).

In a long-term perspective, more international cooperation and standardization would be beneficial but is hindered by competition. In an alliance with the Chinese Electricity Council, the Japanese CHAdeMO Consortium develops its own fast-charging standard by the end of 2020, which is implemented in Japan and China. It is supported by Asian car

manufacturers. Technically, it is ahead of the in Europe prioritized CCS standard. Charging capacities exceed 500 kW, and the charging time can be reduced to a few minutes. Thus, the introduction of this new fast-charging system could lead to a gain in German and possibly worldwide market leadership for Japan and China (Holzer, Kirchbeck 2018).

---

## References

- Aral AG. (2019). Aral Studie - Trends beim Autokauf 2019. <https://www.aral.de/content/dam/aral/business-si-tes/de/global/retail/presse/broschueren/aral-studie-trends-beim-autokauf-2019.pdf>. Accessed 20 April 2020.
- APCOA PARKING. (n.d.). E-Fahrzeuge laden. <https://www.apcoa.de/parkprodukte/e-fahrzeuge-laden/> Accessed 29 April 2020.
- Bundesministerium für Umwelt, Naturschutz und nukleare Sicherheit (BMU). (2019). Eckpunkte für das Klimaschutzprogramm 2030. <https://www.bundesregierung.de/resource/blob/975232/1673502/768b67ba939c098c994b71c0b7d6e636/2019-09-20-klimaschutzprogramm-data.pdf?download=1>. Accessed 15 June 2020.
- Bundesministerium für Verkehr und digitale Infrastruktur (BMVI) (2020). Startschuss für Wallbox-Förderung / Masterplan Ladeinfrastruktur wird konsequent umgesetzt. <https://www.bmvi.de/SharedDocs/DE/Pressemitteilungen/2020/065-scheuer-startschuss-fuer-wallbox-foerderung.html>. Accessed 17 December 2020.
- Bundesverband der Deutschen Industrie (BDI) e.V. (2018). Internet der Energie – Künstliche Intelligenz aus der Sicht von Energie und Klima 2018. <https://bdi.eu/publikation/news/internet-der-energie-kuenstliche-intelligenz-aus-der-sicht-von-energie-und-klima/>. Accessed 10 June 2020.
- Bundesverband der Energie und Wasserwirtschaft (BDEW) e.V. (2019). Meinungsbild E-Mobilität. [https://www.bdew.de/media/documents/Awh\\_20190527\\_Fakten-und-Argumente-Meinungsbild-E-Mobilitaet.pdf](https://www.bdew.de/media/documents/Awh_20190527_Fakten-und-Argumente-Meinungsbild-E-Mobilitaet.pdf). Accessed 20 April 2020.
- Chargemap SAS. (2020). Anzahl der Ladestationen in Deutschland. <https://de.chargemap.com/about/stats/deutschland>. Accessed 19 April 2020.
- Clausen, J. (2018). Roadmap Elektromobilität Deutschland. Ziele, Chancen, Risiken, notwendige Maßnahmen und politische Initiativen. <https://nachhaltigeswirtschaften-soef.de/sites/default/files/Borderstep31-1-18Roadmap-E-Mobilitaet.pdf>. Accessed 15 June 2020.
- Cornet, A., Deubener, H., Dhawan, R., Möller, T., Padhi, A., Schaufuss, P. Tschiesner, A. (2019). Race 2050 – A Vision for the European Automotive Industry. <https://www.mckinsey.com/~media/mckinsey/industries/automotive%20and%20assembly/our%20insights/a%20long%20term%20vision%20for%20the%20european%20automotive%20industry/race-2050-a-vision-for-the-european-automotive-industry.ashx>. Accessed 20 April 2020.
- DW (2020). EU agrees on tougher climate goals for 2030. <https://www.dw.com/en/eu-agrees-on-tougher-climate-goals-for-2030/a-55901612>. Accessed 11 December 2020.
- E-mobil BW GmbH. (n.d.). Autoples. <https://www.emobil-sw.de/autoples> Accessed 4 May 2020.
- Furgale, P. et al. (2013). Toward auto-mated driving in cities using close-to-market sensors: An overview of the V-Charge Project. 2013 IEEE Intelligent Vehicles Symposium (IV). <https://doi.org/10.1109/IVS.2013.6629566>.

- FZI. (2015). Modern E-Parking & Charging: Automatisches Parken und Laden in der Stuttgarter Innenstadt. <https://www.fzi.de/aktuelles/news/detail/artikel/modern-e-parking-charging-automatisches-parken-und-laden-in-der-stuttgarter-innenstadt/> Accessed 5 April 2020.
- Gemsjäger, B., Monscheidt, J. (2020). Stresstest Elektromobilität – Simulationsbasierte Analyse von Anforderungen und Maßnahmen zur optimierten Netzintegration von Ladeinfrastruktur. In Doleski, O. (eds.) *Realisierung Utility 4.0* Band 2. (pp. 733–757). Wiesbaden: Springer Fachmedien Wiesbaden.
- Holzer, H., Kirchbeck, B. (2018). Angriff auf CCS-Stecker – China und Japan entwickeln Schnelllader. <https://www.next-mobility.news/angriff-auf-ccs-stecker-china-und-japan-entwickeln-schnelllader-a-749777/>. Accessed 30 May 2020.
- Linnhoff-Popien, C., Zaddach, M., & Grahl, A. (2015). Marktplätze im Umbruch: Entwicklungen im Zeitalter des mobilen Internets. In *Marktplätze im Umbruch* (pp. 21–33). Springer Vieweg, Berlin, Heidelberg.
- Mehta, D., Hamke, A-K., Sapun, P. (2019). Expert opinion on eMobility report 2019. Statista Mobility Market Outlook. <https://www.statista.com/study/66755/expert-opinion-on-emobility-in-germany-report/>. Accessed 19 April 2020.
- Nationale Leitstelle Ladeinfrastruktur (2020). Thesenpapier: Einfach laden. Das Ladeerlebnis als User Journey an öffentlichen Ladestationen für Elektrofahrzeuge jetzt und 2025. <https://nationale-leitstelle.de/wp-content/pdf/thesenpapier-einfach-laden-web.pdf>. Accessed 17 December 2020.
- Nationale Plattform Elektromobilität (NPE). (2020). Elektromobilität: So funktioniert's. High Power Charging: Wie schnell ist künftig schnell? <http://nationale-plattform-elektromobilitaet.de/anwendung/high-power-charging/>. Accessed 30 May 2020.
- Oberst, C. (2018). Ladesäulen für Elektroautos: Ein Henne-Ei-Problem. [https://www.iwkoeln.de/fileadmin/user\\_upload/Studien/Kurzberichte/PDF/2018/IW-Kurzbericht\\_2018-49\\_Lades%C3%A4ulen.pdf](https://www.iwkoeln.de/fileadmin/user_upload/Studien/Kurzberichte/PDF/2018/IW-Kurzbericht_2018-49_Lades%C3%A4ulen.pdf). Accessed 20 April 2020.
- Pudenz, K. (2015). V-Charge: automatisiertes Parken und Aufladen von E-Fahrzeugen. <https://www.springerprofessional.de/automobil%2D%2D-motoren/v-charge-automatisiertes-parken-und-aufladen-von-e-fahrzeugen/6586856> Accessed 29 April 2020.
- Quantum Immobilien AG. (2018). Parken 2020 – Szenarien für die Entwicklung des Parkraums in Deutschland, In *Quantum Fokus* 2 2012.
- Torres-Sanz, V., Sanguesa, J. A., Martinez, F. J., Garrido, P., Marquez-Barja, J. M. (2018). Enhancing the Charging Process of Electric Vehicles at Residential Homes. In *IEEE Access* 6 (pp. 22875–22888).
- Universität Duisburg-Essen. (2019). Taxi-Lade-Konzept für den öffentlichen Raum (TALAKO). <https://www.uni-due.de/iam/talako.php>. Accessed 30 May 2020.
- VDE FNN, BDEW, DKE, ZVEH, ZVEI. (2020). Technischer Leitfaden Ladeinfrastruktur Elektromobilität. Version 3. <https://www.vde.com/resource/blob/988408/a2b8e484994d628b515b56376f809e28/technischer-leitfaden-ladeinfrastruktur-elektromobilitaet%2D%2D-version-3-data.pdf>. Accessed 30 May 2020.
- Volkswagen AG. (2018). CarLa lädt das Auto auf. <https://www.volkswagenag.com/de/news/stories/2018/03/karla-charges-the-car.html#> Accessed 5 Dezember 2020.
- Walzel, B. et al. (2016). Automated robot-based charging system for electric vehicles, p. 101–113. In: 16. Internationales Stuttgarter Symposium. Wiesbaden: Springer Fachmedien Wiesbaden.
- Werwitzke, C. (2020). Initiative zur Fortentwicklung von Plug&Charge. <https://www.electrive.net/2020/03/24/initiative-zur-fortentwicklung-von-plugcharge/> Accessed 30 May 2020.



Wirges, J. (2016). Planning the charging infrastructure for electric vehicles in cities and regions. Dissertation. Karlsruher Institut für Technologie (KIT), Karlsruhe. <https://doi.org/10.5445/KSP/1000053253>. (pp. 131-133, 236).

**Open Access** This chapter is licensed under the terms of the Creative Commons Attribution 4.0 International License (<http://creativecommons.org/licenses/by/4.0/>), which permits use, sharing, adaptation, distribution and reproduction in any medium or format, as long as you give appropriate credit to the original author(s) and the source, provide a link to the Creative Commons license and indicate if changes were made.

The images or other third party material in this chapter are included in the chapter's Creative Commons license, unless indicated otherwise in a credit line to the material. If material is not included in the chapter's Creative Commons license and your intended use is not permitted by statutory regulation or exceeds the permitted use, you will need to obtain permission directly from the copyright holder.



---

## Part III

# Simulation and Data



# ARaaS: Context-Aware Optimal Charging Distribution Using Deep Reinforcement Learning

# 12

Muddsair Sharif, Charitha Buddhika Heendeniya, and Gero Lückemeyer

## Abstract

Electromobility has profound economic and ecological impacts on human society. Much of the mobility sector's transformation is catalyzed by digitalization, enabling many stakeholders, such as vehicle users and infrastructure owners, to interact with each other in real time. This article presents a new concept based on deep reinforcement learning to optimize agent interactions and decision-making in a smart mobility ecosystem. The algorithm performs context-aware, constrained optimization that fulfills on-demand requests from each agent. The algorithm can learn from the surrounding environment until the agent interactions reach an optimal equilibrium point in a given context. The methodology implements an automatic template-based approach via a continuous integration and delivery (CI/CD) framework using a GitLab runner and transfers highly computationally intensive tasks over a high-performance computing cluster automatically without manual intervention.

## Keywords

Continuous integration and delivery (CI/CD) · Electric vehicles (EVs) · Autonomous vehicles (AS) · Deep reinforcement learning (DRL) · Charging station (CS) · Context-aware (CA)

M. Sharif · G. Lückemeyer  
Hochschule für Technik Stuttgart, Stuttgart, Germany

C. B. Heendeniya (✉)  
Scuola universitaria professionale della Svizzera italiana, Manno, Switzerland  
e-mail: [charitha.heendeniya@supsi.ch](mailto:charitha.heendeniya@supsi.ch)

## 12.1 Introduction

Over the past decade, the penetration of non-gasoline vehicles such as electric, hybrid, and plug-in hybrid vehicles in Germany has multiplied (Fig. 12.1). At present, there are close to 240,000 registered electric and plug-in hybrid vehicles in Germany. Moreover, according to the German Association of Energy and Water Industries (BDEW), as of March 2020, there are 27,730 publicly available charging stations to serve the electric and plug-in hybrid vehicle fleet of Germany VDA (2020). Today, the vast majority of electricity-powered vehicles in Germany are private cars. As the German government has ambitious plans to encourage electric mobility in Germany in the coming years, the penetration of electricity-powered vehicles should grow steadily.

Electrification has profound economic and ecological impacts on the future of the mobility sector. New business models arise based on the provision of different mobility services and shared economy. Moreover, we see the emergence of a complete ecosystem around mobility due to the converging trends of the physical and digital domains and the innovation and business models (Dia, 2019; Barreto et al., 2020).

This article focuses on the digital domain, which provides the playing field for the stakeholders, e.g., electric vehicles (EVs), autonomous vehicles (AS), charging stations, smart grid, and fleet management, to interact seamlessly. The efficiency of these complex interactions between the stakeholders determines the optimality of the outcome received by each participating stakeholder. This article presents an application based on deep reinforcement learning to optimize agent interactions and decision-making in an IoT-enabled smart

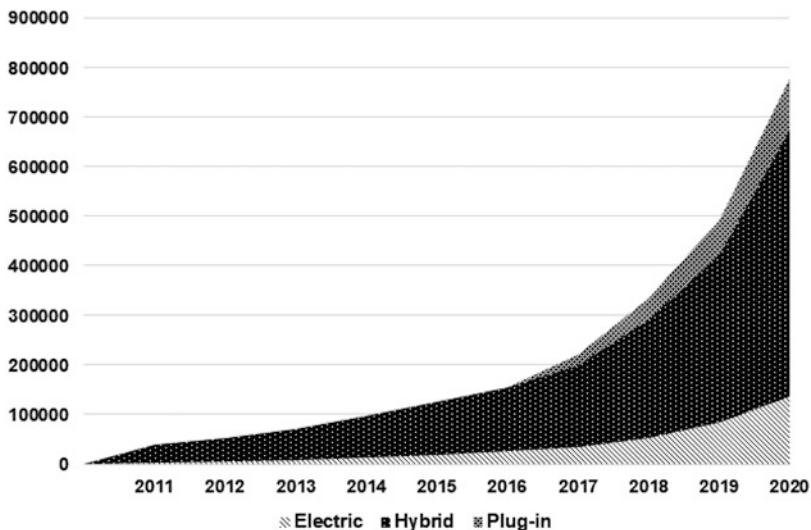


**Fig. 12.1** The growth of electric, hybrid, and plug-in hybrid vehicle penetration in Germany from 2011 to 2020. (Data: Kraftfahrt-Bundesamt)

mobility ecosystem. The optimization objective of agent interactions is the aggregate utility of all interacting agents described using the weighted sum approach. The algorithm also defines a set of soft and hard constraints. The hard constraints must always be adhered to by the agents; however, the soft constraints may be violated conditionally under extreme circumstances. The methodology adheres to the automatic template-based approach via CI/CD framework using GitLab runner.

Previous research work has addressed specific aspects of optimal agent interactions in a smart mobility landscape. For example, Lin et al. (2016) present a linear programming model of an optimal routing problem that takes into consideration charging station location and the cost. Chen et al. (2018) present a weighted sum multi-objective optimization model that takes into account the different preferences of the user. The mixed-integer quadratic programming model presented in this study is solved using a commercial optimizer such as CPLEX or Gurobi. Bessler and Grønþæk (2012) use a heuristic-based approach. The algorithm evaluates the optimal routing plan for EVs by considering the distance to the charging stations in the vicinity, the traffic situation, and the feasible charging patterns. However, to our understanding, the simultaneous consideration of multiple stakeholder perspectives has not been done in the past.

---

## 12.2 Architecture

The overall objective in this section is to describe the proposed architecture in detail with the addition of continuous integration or a continuous deployment (CI/CD)-based approach (Sharif et al. 2020b). We also explain how the algorithm processes contextual information to meet the necessary optimality conditions for each of the stakeholders. Moreover, four types of stakeholders are identified while keeping the concept of smart mobility in mind. These four types of stakeholders are EV end-user, grid operator, fleet operator, and charging station maintainer which have been explained thoroughly in our previous publication (Sharif et al. 2020a). Two of them, i.e., EV end-user and grid operator, are in the focus of the smart mobility use case in this article.

As shown on the left-hand side of Fig. 12.2 of the proposed architecture, each stakeholder provides a set of individual inputs ( $X_i, X_j \dots X_m$ ) which are “daily travel activities, routing suggestion(s), car-battery, and environment” with associated actions ( $A_i, A_j \dots A_m$ ). The rewards ( $R_i, R_j \dots R_m$ ) are the computed output(s) such as “charging type, the distance towards charging station, charging cost, etc.” Furthermore, there might be a probability that few of the inputs are mutually equivalent in more than one stakeholder with dissimilar priorities as well as constraints.

$$Q(s, a) = r + \gamma \max_a' Q(s' + a')$$

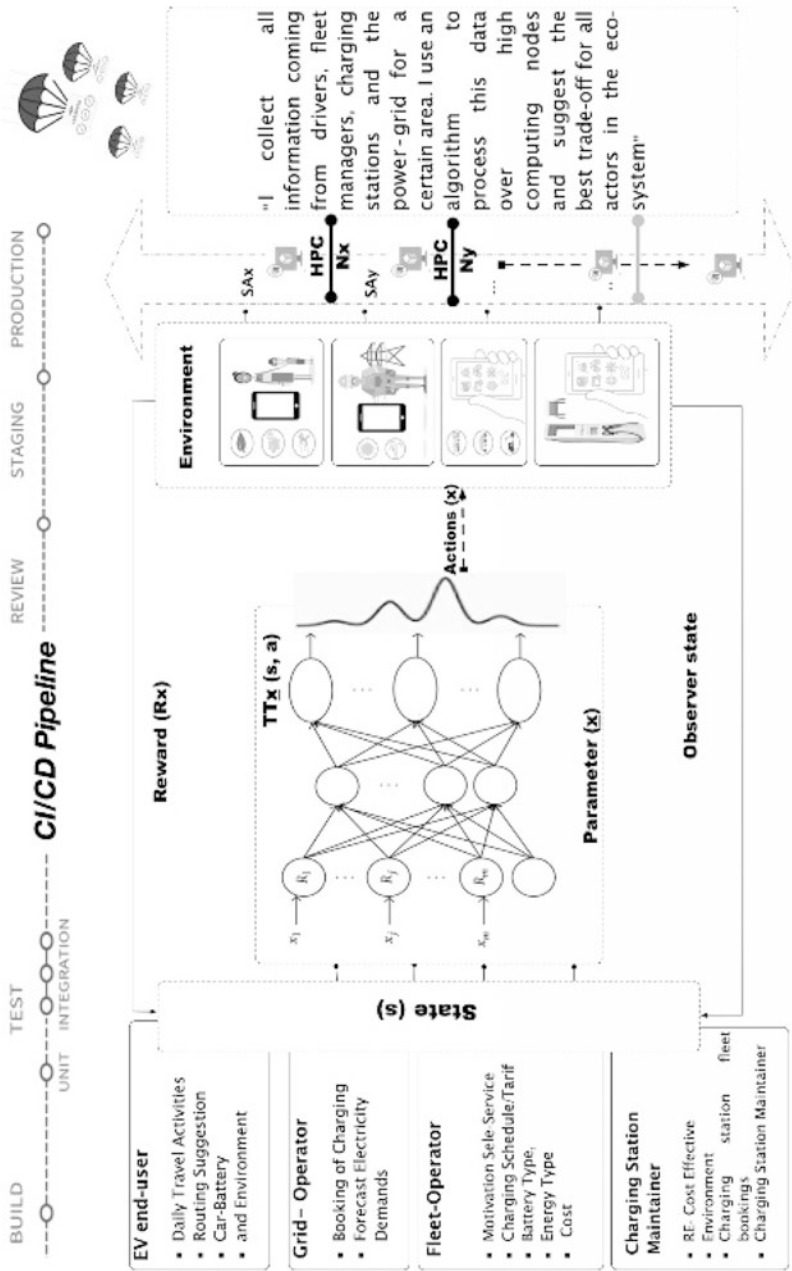


Fig. 12.2 ARaaS: a deep reinforcement learning base architecture

After this, these sets of information are processed via a state-of-the-art approach using a deep reinforcement learning-based algorithm via a Bellman equation, in which the system learns from the  $Q$ -value of state  $s$  and action  $a$  as inputs:  $(Q(s, a))$  must be equivalent to the instantaneous reward  $r$  acquired as a result of that action and additionally the  $Q$ -value of the finest feasible next action  $a'$  taken from the next state  $s'$ , which is multiplied by a given discount factor. Moreover, this is a value with premises range  $\in (0,1]$  which is a hyper-parameter.

We further need to decide how much weight to assign to the impurity for the short-term and long-term rewards (Tang et al., 2020; Nguyen et al., 2020a; François-Lavet et al., 2018). The right-hand side of Fig. 12.2 shows a specific output generated for different environments. For example, the EV end-user will acquire the best schedule and routing selection bestowing toward the needs of the car's battery and the environment with appropriate personal convenience. Grid operators will acquire the demand forecasts of electricity of a specific region according to the reservation of the charging stations, which decreases the fluctuation of the electric. The system will continuously learn from its environment and observe state(s) by interpolating weights, etc. (Li et al., 2020; Nguyen et al., 2020b; Wang et al., 2013).

The core functionality is exposed as a component to stakeholders from other domains with a distinct objective over a self-developed middleware-as-a-service component (see the right-hand side of Fig. 12.2). This extension leads us to prove the performance of our model at the urban scale level where high-dimensional data and scalability of models are required. For example, "Stakeholder 'X' would like to collect information coming from EV end-users, fleet-managers, charging stations, and the power-grid for a certain area. Use an algorithm to process this data over high computing nodes and suggest the best trade-off for all actors in the eco-system." To fulfill such a type of user scenario, we develop our electro-vehicle middleware where we promote a smart mobility use case established on the interaction between the stakeholders as depicted in Fig. 12.2, where stakeholders from different domains exchange information according to their objective. The middleware-as-a-service utility provides a set of services for each application (app. SAx, SAy, SAz, etc.) to handshake with high-performance computing nodes such as Nx, Ny, and so on. Each of these services requires high-performance computation nodes to execute their service request, and finally, the results calculated by the algorithm are assigned back to the respective app (Sharif et al., 2017; Amogh Vardhan et al., 2019; Espenholt et al., 2018; Jiang et al., 2019). The initial objective of the algorithm is to find the optimal trade-off scenario for EV charging by considering a set of conflicting interests of multiple stakeholders acting in the smart mobility ecosystem (Fig. 12.2).

Suppose that the City Council of Stuttgart, Germany, would like to organize an event where people from all over the country are expected to participate. We continue with the same set of stakeholders. Due to the popularity of the electric car, the event organizer expects many people from neighboring cities will participate via personal transportation, i.e., often EV. The event organizer needs to distribute resources optimally in terms of

mobility, which will be a very challenging task (Alyousef et al., 2018). To fulfill this extent of expectation, organizers require frequent and timely updates of the resource distribution.

We proposed an automation-based service mobility which keeps running algorithm (s) using a GitLab CI/CD runner to pass computation-intensive tasks over to a high-performance computing cluster and find the best trade-off for all actors in the ecosystem. In the next section, we present a user scenario that promotes the proposed methodology.

### 12.3 User Scenario

Tina lives in Tübingen and owns an electric car. She drives her car to Stuttgart regularly, where she spends much of the time working and networking. Once, on the way to Stuttgart, she observes that her battery is low on charge, and she would like to locate a charging station near her current location  $P(x, y)$ . She finds the charging stations  $CS1(x', y')$ ,  $CS2(x', y')$ ,  $CS3(x', y')$ , and  $CS4(x', y')$ , each of which has different charging options (i.e., fast charging or slow charging) at different charging costs. The price of charging the EV (in EUR/kWh) at the four charging stations are  $a1(t)$ – $a4(t)$  (see Fig. 12.3). Note that charging prices are given as a function of time to accommodate for time-varying electricity prices. To locate the optimal charging location that matches her requirements, she uses the algorithm proposed in this paper. Optimality is a perception that merely depends on the user’s primacies to a set of conflicting interests.

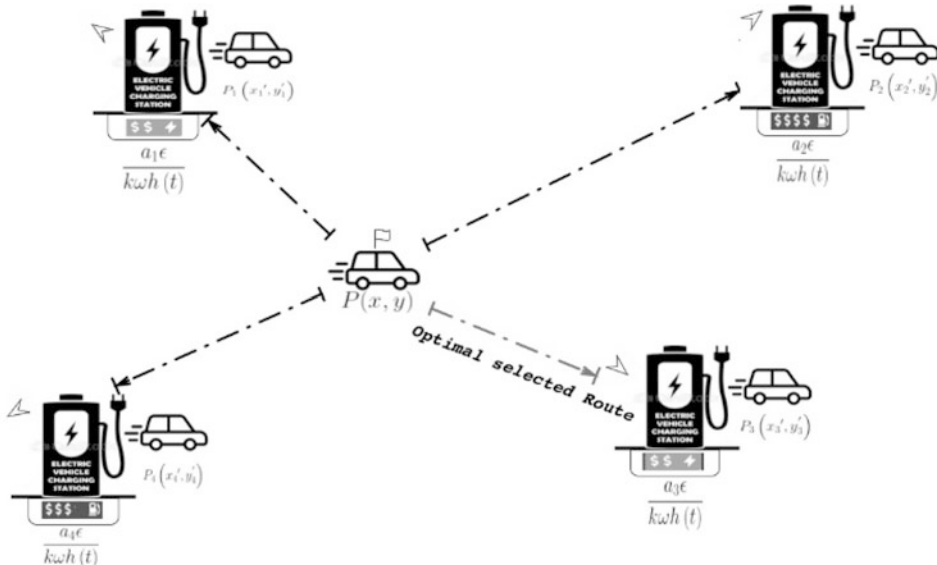


**Fig. 12.3** The optimal charging station’s route selection



In this example, Tina has a high priority to requirements such as the charging station availability, charging price, distance to the charging station, charging time, and potential service disruptions. Once Tina chooses her priorities, the algorithm processes her requirement and recommends her the most appropriate charging location that fits her requirements. Moreover, the algorithm can compare the charging station of choice with the other charging stations in the vicinity. The application allows her to make an informed decision about the best charging station that fits her need and also gives her the option to reserve a charging point ahead of time to confirm availability. Once the reservation is complete, the application ensures that the charging point remains available at the specified time (see Fig. 12.4).

On the other hand, the local grid operator monitors the electricity demand forecast, i.e.,  $Obj_y$  in Fig. 12.3, variation due to EV charging requirements. For example, Wolfgang works for the local grid operator and is responsible for the uninterrupted electricity supply in his control area. Due to the rapid adoption of EVs and many public charging stations set up to serve those vehicles, he knows that there can be peak times when electricity demand can suddenly increase. He has several strategies to deal with such peak demands; for example, he can activate reserve power supplies or activate a demand response plan. However, without an accurate forecast or a warning in advance, the activation of demand response or reserve power can be more expensive.

The application can provide the grid operator with a forecast of the electricity demand due to vehicle charging the next 15–60 minutes' period. Note that the forecast has more likelihood to be precise for 15 minutes' forecast period rather than for 60 minutes' forecast period due to uncertainty, which the application takes into account. Based on the grid operator's constraints, the application can also highlight where the potential demand-supply bottlenecks can occur. This information helps Wolfgang to plan the best course of action to ensure the reliability of the electricity supply in advance. With our application's service, now Wolfgang also has an additional action that he can take to mitigate supply bottlenecks, which is to advise charging station owners to interrupt their services for the incoming service requests. In other words, the service availability status of a charging station can be updated by request from the grid operator that serves as a "proactive" demand response strategy. Activation of demand response, either passive or proactive, incurs a cost to the grid operator and a loss of utility to vehicle owners whose services are denied.

---

## 12.4 Simulation Environment

The system evaluation is assessed with respect to an EV end-user objective such as optimal cost and with respect to a grid operator objective such as energy demand or charging station availability, on behalf of the event organizer, i.e., the City Council. The event organizer would like to take a closer look at the resource demand and supply distribution optimally in between the event's participants.

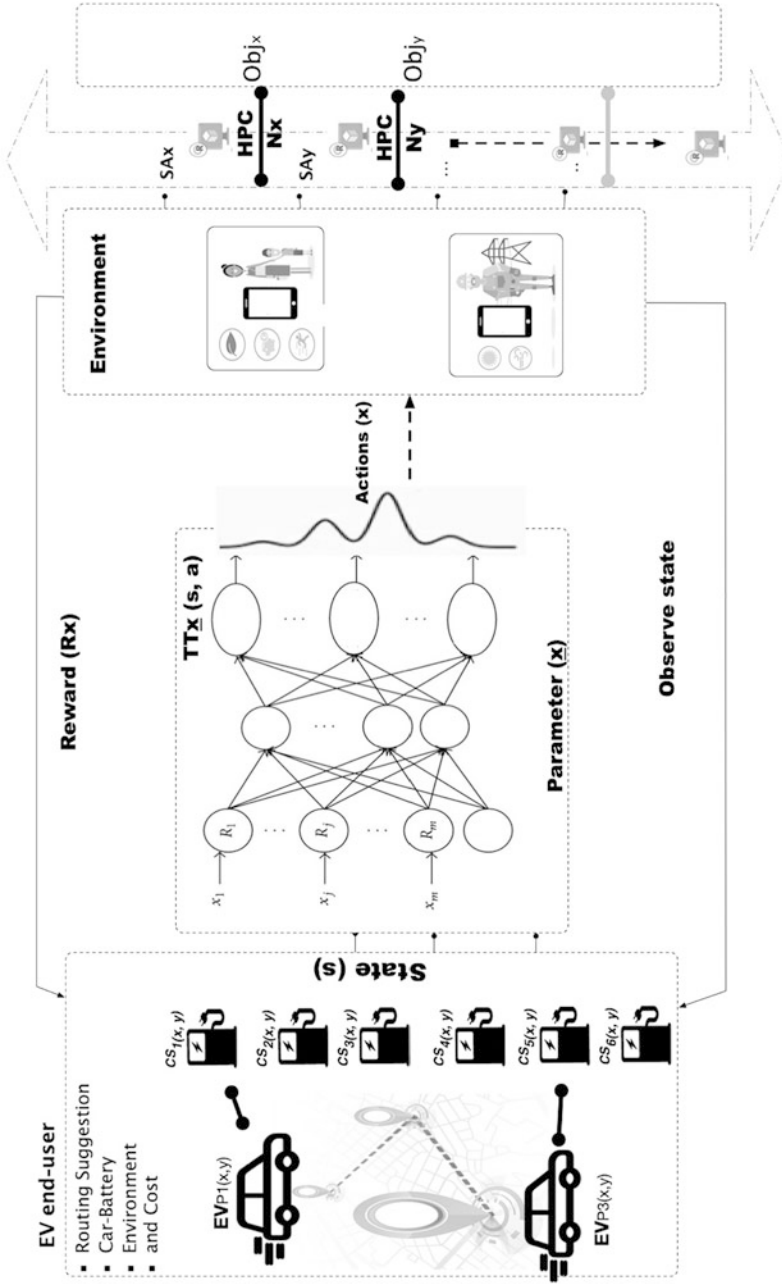
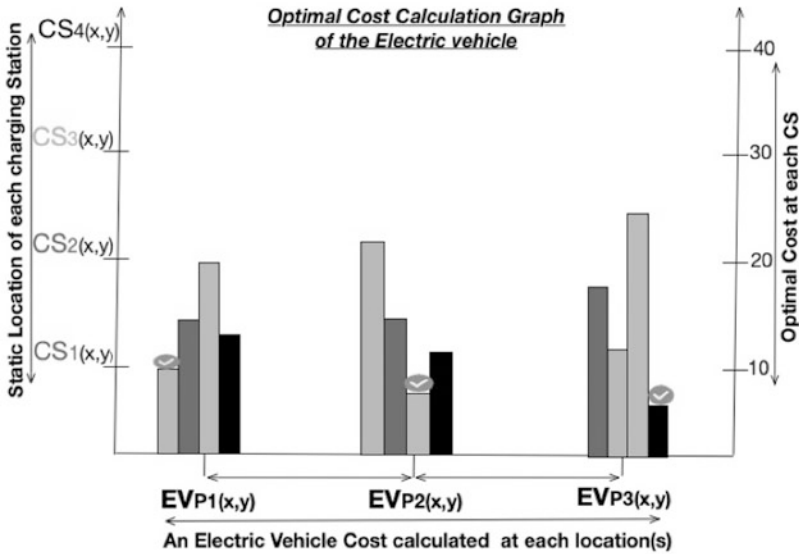


Fig. 12.4 Use case elaboration as per stakeholder's perspective



**Fig. 12.5** (a) Optimal cost calculation graph of the EV. (b) A 30-min electricity demand forecast for one charging station. The uncertainty of the forecast increases for longer prediction horizons

Revisiting the end-user from the use case example (see Sect. 12.3), Tina's car has a usable battery capacity of 120 Ah, and it is compatible with both slow- (maximum charging rate of 11 kW) and fast-charging (maximum charging rate of 50 kW) connectors. When Tina decides to look for a charging station, the state of charge of the battery has already degraded to 10%.

Figure 12.4 shows a graphical overview of the use case. The EV drives past four different charging stations CS1–CS4. Tina may decide to check for a charging location at any random point along the route denoted by P1–P3, and the optimizer yields a different objective value depending on the context related to that point. Figure 12.5 shows the optimal objective function value calculated for the EV at different locations on the driving route. The different colors represent the different charging stations. In this example, the optimal objective value is also the minimum cost, which, however, is not always true when multiple contradicting concerns and end-user priorities are taken into consideration when evaluating the objective function.

## 12.5 Conclusion and Future Work

Presently, we have only picked up one scenario with a smaller time-stamp, i.e., EV end-user and grid operator, in our simulation environment. Moreover, the simulated use case in a static environment that predicts the maturity of the system with multiple

stakeholder participation. Therefore, the current simulation environment does not include time-varying contexts such as variable pricing and power distribution forecasts. From the software architecture point of view, the service app middleware layer is already presented in another paper.

The dynamic coupling between the optimal charging resource distribution and electricity network models enables us to define the network capacity as a finite resource in the resource distribution algorithm and observe the state and impacts of the local distribution network during the smart charging process. This future extension enables us to simulate optimal EV charging resource distribution scenarios in combination with other distributed loads and generators in a city. Furthermore, this will be a significant step forward in the field of integrated urban energy system planning.

---

## References

- Alyousef, A., Danner, D., Kupzog, F., and de Meer, H. (2018). Design and validation of a smart charging algorithm for power quality control in electrical distribution systems. In *Proceedings of the Ninth International Conference on Future Energy Systems, e-Energy '18*, page 380–382, New York, NY, USA. Association for Computing Machinery.
- Amogh Vardhan, K., Jakaraddi, M. G. D., Shetty, J., Chala, A., and Camper, D. (2019). Design and development of IoT plugin for hpc systems. In *2019 IEEE 4th International Conference on Big Data Analytics (ICBDA)*, pages 158–162.
- Barreto, L., Amaral, A., and Baltazar, S. (2020). Mobility in the Era of Digitalization: Thinking Mobility as a Service (MaaS). In *Jardim-Goncalves, R., Sgurev, V., Jotsov, V., and Kacprzyk, J., editors, Intelligent Systems: Theory, Research and Innovation in Applications*, pages 275–293. Springer International Publishing, Cham.
- Bessler, S. and Grønbaek, J. (2012). Routing ev users towards an optimal charging plan. *World Electric Vehicle Journal*, 5(3):688–695.
- Chen, T., Zhang, B., Pourbabak, H., Kavousi-Fard, A., and Su, W. (2018). Optimal routing and charging of an electric vehicle fleet for high-efficiency dynamic transit systems. *IEEE Transactions on Smart Grid*, 9(4):3563–3572.
- Dia, H. (2019). *Rethinking Urban Mobility: Unlocking the Benefits of Vehicle Electrification*, pages 83–98. Springer Singapore, Singapore.
- Espeholt, L., Soyer, H., Munos, R., Simonyan, K., Mnih, V., Ward, T., Doron, Y., Firoiu, V., Harley, T., Dunning, I., Legg, S., and Kavukcuoglu, K. (2018). Impala: Scalable distributed deep-rl with importance weighted actor-learner architectures.
- François-Lavet, V., Henderson, P., Islam, R., Bellemare, M. G., and Pineau, J. (2018). An introduction to deep reinforcement learning. *Foundations and Trends® in Machine Learning*, 11(3-4): 219–354.
- Jiang, Z., Gao, W., Wang, L., Xiong, X., Zhang, Y., Wen, X., Luo, C., Ye, H., Zhang, Y., Feng, S., Li, K., Xu, W., and Zhan, J. (2019). Hpc ai500: A benchmark suite for hpc ai systems. *Kraftfahrt-Bundesamt (2020). Fahrzeuge*.
- Li, K., Zhang, T., and Wang, R. (2020). Deep reinforcement learning for multiobjective optimization. *IEEE Transactions on Cybernetics*, page 1–12.

- Lin, J., Zhou, W., and Wolfson, O. (2016). Electric vehicle routing problem. *Transportation Research Procedia*, 12:508–521. Tenth International Conference on City Logistics 17-19 June 2015, Tenerife, Spain.
- Nguyen, N. D., Nguyen, T. T., Nguyen, H., and Nahavandi, S. (2020a). Review, analyze, and design a comprehensive deep reinforcement learning framework. *CoRR*, abs/2002.11883.
- Nguyen, T. T., Nguyen, N. D., Vamplew, P., Nahavandi, S., Dazeley, R., and Lim, C. P. (2020b). A multi-objective deep reinforcement learning framework. *Engineering Applications of Artificial Intelligence*, 96:103915
- Sharif, M., Heendeniya, C. B., Muhammad, A. S., and Lückemeyer, G. (2020a). Context-aware optimal charging distribution using deep reinforcement learning. In *Proceedings of the 2020 the 4th International Conference on Big Data and Internet of Things, BDIOT 2020*, page 64–68, New York, NY, USA. Association for Computing Machinery.
- Sharif, M., Janto, S., and Lueckemeyer, G. (2020b). Coaas: Continuous integration and delivery framework for hpc using gitlab-runner. In *Proceedings of the 2020 the 4th International Conference on Big Data and Internet of Things, BDIOT2020*, page 54–58, New York, NY, USA. Association for Computing Machinery.
- Sharif, M., Mercelis, S., Van Den Bergh, W., and Hellinckx, P. (2017). Towards real-time smart road construction: Efficient process management through the implementation of internet of things. In *Proceedings of the International Conference on Big Data and Internet of Thing, BDIOT2017*, page 174–180, New York, NY, USA. Association for Computing Machinery.
- Tang, Y., Agrawal, S., and Faenza, Y. (2020). Reinforcement learning for integer programming: Learning to cut. *VDA (2020). Electric Mobility: Electric Mobility in Germany*
- Wang, G., Xu, Z., Wen, F., and Wong, K. (2013). Traffic-constrained multiobjective planning of electric-vehicle charging stations. *IEEE Transactions on Power Delivery*, 28(4):2363–2372.

**Open Access** This chapter is licensed under the terms of the Creative Commons Attribution 4.0 International License (<http://creativecommons.org/licenses/by/4.0/>), which permits use, sharing, adaptation, distribution and reproduction in any medium or format, as long as you give appropriate credit to the original author(s) and the source, provide a link to the Creative Commons license and indicate if changes were made.

The images or other third party material in this chapter are included in the chapter's Creative Commons license, unless indicated otherwise in a credit line to the material. If material is not included in the chapter's Creative Commons license and your intended use is not permitted by statutory regulation or exceeds the permitted use, you will need to obtain permission directly from the copyright holder.





# A Multi-camera Mobile System for Tunnel Inspection

# 13

Fatemeh Alidoost, Gerrit Austen, and Michael Hahn

## Abstract

The safety, proper maintenance, and renovation of tunnel structures have become a critical problem for urban management in view of the aging of tunnels. Tunnel inspection and inventory are regulated by construction laws and must be carried out at regular intervals. Advances in digitalization and machine vision technologies enable the development of an automated and BIM-based system to collect data from tunnel surfaces. In this study, a tunnel inspection system using vision-based systems and the related principles are introduced to measure the tunnel surfaces efficiently. In addition, the main components and requirements for subsystems are presented, and different challenges in data acquisition and point cloud generation are explained based on investigations during initial experiments.

## Keywords

Machine vision · LED · Multi-camera · BIM · 3D models · Photogrammetry

---

F. Alidoost (✉) · G. Austen · M. Hahn  
Hochschule für Technik Stuttgart, Stuttgart, Germany  
e-mail: [fatemeh.alidoost@hft-stuttgart.de](mailto:fatemeh.alidoost@hft-stuttgart.de)

© The Author(s) 2022  
V. Coors et al. (eds.), *iCity. Transformative Research for the Livable, Intelligent, and Sustainable City*,  
[https://doi.org/10.1007/978-3-030-92096-8\\_13](https://doi.org/10.1007/978-3-030-92096-8_13)

211

### 13.1 Introduction

The inventory and monitoring of transport structures, such as tunnel and bridge constructions, are essential to improve the mobility in urban areas. Tunnels are mostly underground constructions which serve to pass under obstacles such as mountains or hills, waterways, or other traffic routes. In cities, they protect residents from road or rail traffic noise. Mobility systems and infrastructure and their consequences for the people living in a city are a key topic of the iCity project, to which this paper contributes with the development of a system for 3D tunnel inspection.

Tunnel inspection includes monitoring and mapping of the tunnel surfaces to generate 3D models and to detect anomalies as well as localizing tunnel objects, e.g., technical equipment, for building information modeling (BIM) applications. This results in a significant total workload and makes it necessary to develop optimum and intelligent solutions in a digitalized manner. Traditionally, tunnel inspection methods are accomplished by local visual inspection and the use of adapted devices, which usually require on-site installation and interaction with the surface of the tunnel. Despite being time-consuming and cumbersome, manual measurements of the tunnels by operators require quite expensive equipment and a lot of working hours. Moreover, a tunnel blocking for several hours or even days is usually necessary to reduce the risk areas for operators.

To improve the automation level and efficiency of inspection systems, advanced and intelligent technologies are necessary. The current approaches can be divided into two main groups, namely, laser-based and image-based techniques. Laser scanners are one of the state-of-the-art sensors for 3D mapping and can be deployed on terrestrial stations or mobile mapping vehicles to accurately capture dense point cloud data of the tunnel surface (Chen et al. 2015; Wang et al. 2014). However, a mobile system with a typical laser scanner is very cost-intensive and even today costs much more than several \$50,000 (O'Neill, 2020).

With recent advances in multi-view image processing and high-speed image capturing techniques, a practical and inexpensive solution for automatic tunnel inspections with image-based systems has become feasible. This technique involves a set of industrial cameras installed in a specific ring to cover the entire area of the tunnel, as well as light sources to provide sufficient illumination for image capturing. However, there are distinct hardware components and data processing challenges and considerations that directly affect the accuracy of the final results. This study aims to address those challenges and to investigate optimal solutions to develop a cost-effective system for the automated and BIM-compatible inspection of tunnels.

---

### 13.2 Related Work

BIM technology is widely used to present the digital model-based process of planning, designing, constructing, operating, and managing for the infrastructures such as buildings, roads, bridges, and tunnels over the entire life cycle of the project (Ehrbar et al. 2019;

Fargnoli et al. 2019). The procedure of inspection and maintenance of tunnels and collected 3D information and geo-data of underground structures can support BIM systems (Chen et al. 2019; Yin et al. 2020).

With the advances in photogrammetric and computer vision algorithms, the interest in developing automatic and inexpensive approaches for tunnel inspection is rapidly increasing. In an early study, Gavilán et al. (2013) developed a mobile inspection system that includes six linear cameras and six laser-based projectors for tunnel surveys at speeds up to 30 km/h and with a depth accuracy of 0.5 mm. Similar to this study, Zhan et al. (2015) presented an inspection system that includes seven linear cameras and structured-light projectors and can operate at a speed of about 60 km/h. A challenge of tunnel inspection is to detect damages with mm to sub-mm accuracy. To this end, Stent et al. (2015) proposed a low-cost system to inspect 0.3 mm cracks using two consumer-grade digital cameras installed on a robotic rotating arm. One of the advanced mapping systems in GNSS-denied areas, proposed by Chapman et al. (2016), includes an array of 16 cameras and light sources to monitor the roadway tunnels. They reported an average positioning error of about 0.34 m. For subway tunnel inspection, Huang et al. (2017) developed a small vision-based system including line-scan cameras and light sources. The inspection equipment is designed to achieve a resolution of 0.3 mm/pixel at a speed of 5 km/h. In another study, an inspection system, proposed by Attard et al. (2018), includes one consumer-grade digital camera and light sources to capture high-resolution images from tunnel walls. This system achieves an average accuracy of 81.4% for change detection. However, it needs a robotic arm and special installations on walls to move through the tunnel which is not applicable for road tunnels. To monitor defects such as cracks in roadway tunnels, Jiang et al. (2019) developed a high-speed system including line-scan cameras and near-infrared (NIR) illumination which can guarantee to achieve a photographing speed of up to 100 km/h.

Following the existing approaches, an image-based inspection system for tunnel mapping consists of different hardware and software components which should be selected and assembled based on the project requirements such as the speed of monitoring, the tunnel conditions, the total cost, the total size and weight of the system, the carrying vehicle type, and the final deliveries.

---

### 13.3 Proposed Method

This study aims to examine the main parameters and challenges of a cost-effective mobile system for roadway tunnel inspection. The intended operating speed of the proposed system is about 60–65 km/h which is suitable for traffic flows and fast monitoring of long tunnels. The main components are machine vision (MV) cameras, light sources, a synchronization unit, and a mobile platform, as shown in Fig. 13.1. The outputs are raw RGB images of the entire tunnel area which can be further processed for generating 3D colorful point clouds, damage detection, and object recognition maps. The project should



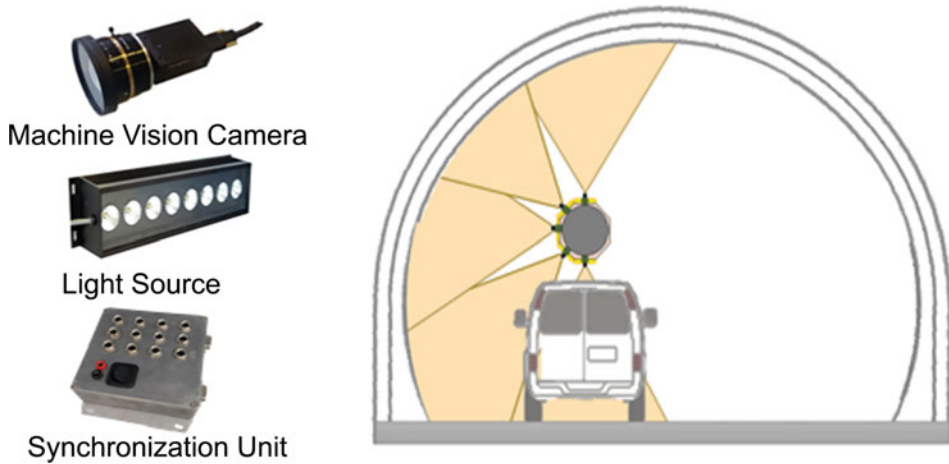


**Fig. 13.1** Main components of the tunnel inspection system

strive for a relative accuracy of about 2 cm for 3D models and a surface resolution of about 3–5 mm for images.

### 13.3.1 Camera Selection

The performance of the camera can directly affect the accuracy of the final results for tunnel inspection. The main features of a camera are listed in Table 13.1. According to previous studies, two different types of cameras can be used for image capturing, i.e., digital cameras and machine vision (MV) cameras. While digital cameras are cheaper and can acquire high-resolution images, the total speed of scanning cannot be fast due to their limited exposure time (ET) in order to avoid motion blur. On the other hand, MV cameras are available as line-scan and area-scan sensors. The line-scan cameras are the best option in high-speed processing or fast-moving applications. However, the image acquisition with linear cameras generally requires to continuously record the rotational and transitional movements, e.g., by an inertial measurement unit. In addition, perspective distortion can be expected because of the limited field of view (FOV) of linear sensors (Attard et al. 2018; Teledyne Dalsa 2014). Also, the line-scan cameras usually need high-power illuminator, unlike area-scan cameras (Attard et al. 2018; Huang et al. 2017). On the other hand, the area-scan cameras have a standard interface, easier setup, and alignment.

For area-scan cameras, a global shutter should be used, instead of a rolling shutter, to reduce the motion blur as well as noise in images. In this case, the scene will be *frozen* at a certain point in time and there is no motion blur. Another important parameter of the camera is the interface of the camera such as USB2, USB3, and GigE. Among different interfaces, USB3 is the fastest interface (e.g., 400 MB/s), and it uses the least amount of

**Table 13.1** Camera features

Items	Features	Pros	Cons
Model	Digital	High resolution (e.g., >12 megapixels), cheap (e.g., <\$1000)	Large ET (e.g., >250 $\mu$ s), Heavy (e.g., >100 gr)
	Machine vision	Small exposure time (e.g., <10 $\mu$ s), Light (e.g., <100 gr)	Low resolution (e.g., <15 megapixels), expensive (e.g., >\$2000)
Sensor	Line scan	High-speed capturing	Small field of view, image distortion
	Area scan	Easy and standard, large field of view	Not as fast as line cameras
Shutter	Global	No motion blur, no noise	Expensive ( $\sim 3\times$ of the rolling shutter's cost)
	Rolling	Cheaper	Motion blur, including a switch noise effect
Interface	USB3	400 megabytes/s, excellent for multi-camera application	4.5 m cable length
	GigE	Good for multi-camera, 10 m cable length	100 megabytes/s

computer processor power. Therefore, it is ideal for high-resolution and high-speed imaging (VisionCamera 2019).

### 13.3.2 Light Selection

Light sources play a major role in vision-based inspection systems by providing enough lighting to capture blur-free images. LED (light-emitting diode) technology is widely used for lighting in machine vision applications because it can provide high performance, stability, high intensity, as well as cost-efficiency.

LEDs can be operated in three modes, i.e., continuous, switch, and flash operations. In order to scan at a speed up to 65 km/h, the required light for the camera should be provided for a very short time interval (e.g., about 10 microseconds) to ensure that there is no motion blur in the images. This is only possible using flash LEDs. Ideally, the selected LED should be able to produce strobe pulses with a pulse width that corresponds to the camera exposure time (Eq. 13.6). Other important features for an LED are the flash rate and the working distance. Recent LED technologies can provide more than 50 kHz flash strobe. However, the normal working distances of LEDs are less than 1 meter which is not perfect for many tunnels. Therefore, the irradiance of the selected LED should be sufficient to provide powerful light for bigger distances of several meters (e.g., 3–8 m working distances). The relation between the irradiance ( $E$ ) and working distance ( $R$ ) is given in Eq. (13.1).

$$E \text{ [W/m}^2\text{]} = E_o \text{ [W/m}^2\text{]} \times \left( \frac{R_o \text{ [m]}}{R \text{ [m]}} \right)^2 \quad (13.1)$$

where  $E_o$  is the irradiance of the LED at the distance of  $R_o$ , provided by the manufacturer.

### 13.3.3 System Design

One of the crucial parameters for the total costs of the final system is the number of cameras required for covering an entire ring of the tunnel. The number of cameras is also defined by the desired overlap of the images within a ring. Although the overlap between two consecutive images along the moving direction (i.e., the horizontal overlap) should be 80% or more for the image alignment and stereo matching algorithms, the overlap between two adjacent cameras (i.e., the vertical overlap) can be less than 50%, e.g., only 10% as illustrated in Fig. 13.2. Since most tunnels can be passed in two opposite directions, five cameras are sufficient in our case to scan each side of the tunnel during one pass (Fig. 13.2). In this case, the angle between the camera axes of adjacent cameras ( $\alpha$ ) is 45 degrees and the vertical overlap is determined by Eq. (13.2).

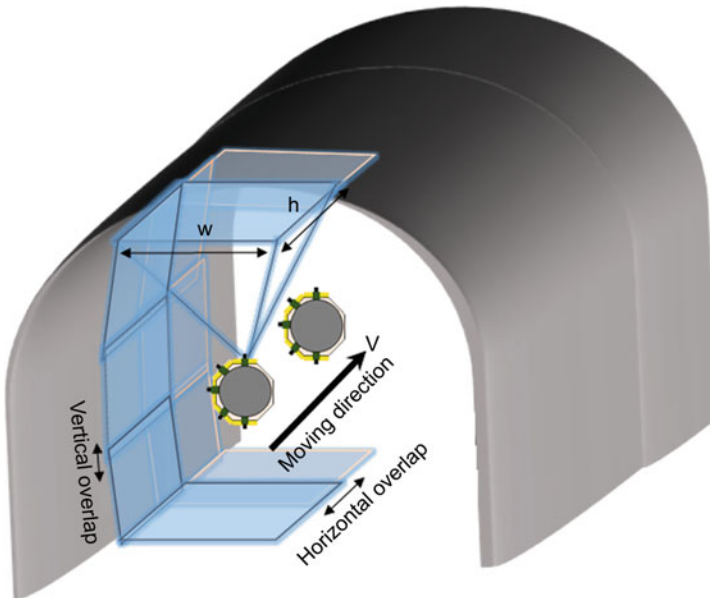


**Fig. 13.2** Schematic sketch of the multi-camera mobile system

$$\text{VerticalOverlap} [\%] = \left( 1 - \frac{\alpha[\text{deg}]}{\text{FOV}_w[\text{deg}]} \right) \times 100 \quad (13.2)$$

Half of the vertical overlap applies to each of the two neighboring images.  $\text{FOV}_w$  is the field of view, corresponding to the sensor's width  $w$ , given by Eq. (13.3).

$$\text{FOV}_w [\text{deg}] = 2 \times \arctan \left( \frac{w[\text{mm}]}{2 \times f[\text{mm}]} \right) \times 180 [\text{deg}]/\pi \quad (13.3)$$

The sensor size is given by  $w$  and  $h$  in mm. The parameter  $f$  is the camera's focal length. The horizontal overlap between two consecutive images depends on the speed of the vehicle ( $V$ ), the capturing rate ( $\text{FPS}$ ), and the working distance ( $D$ ) and is given by Eq. (13.4).

$$\text{HorizontalOverlap} [\%] = \left( 1 - \frac{V[\text{m/s}] \times f[\text{mm}]}{\text{FPS}[\text{Hz}] \times h[\text{mm}] \times D[\text{m}]} \right) \times 100 \quad (13.4)$$

To calculate the required capturing rate for each camera ( $\text{FPS}$ ), the bandwidth of the USB3 interface should be considered, as shown in Eq. (13.5).

$$\text{FPS} [\text{Hz}] = \frac{\text{Bandwidth} [\text{Mb/s}] \times 1000000}{W [\text{px}] \times H [\text{px}] \times \text{BPP}} \quad (13.5)$$

where  $W$  and  $H$  are the sensor sizes in pixels and the  $\text{BPP}$  is bytes per pixel which is 1.5 for a 12-bit RGB image. Another important parameter for designing the proposed system is the exposure time of the camera which is related to the motion blur ( $B$ ) as well as the LED's pulse width. In our design, the allowed amount of motion blur in an image should not exceed 0.2 pixels. A blurring above this threshold can affect the 3D model and final results. Based on the speed of the vehicle ( $V$ ), and the size of the pixel ( $PS$ ), the required exposure time ( $ET$ ) can be calculated according to Eq. (13.6).

$$\text{ET} [s] = \frac{(D[\text{m}] \times B [\text{px}] \times PS [\text{mm}])/f[\text{mm}]}{V[\text{m/s}]} \quad (13.6)$$

### 13.3.4 Time Synchronization

In tunnel inspection using multi-cameras and multi-LEDs, the vital task is synchronizing the light system and the image acquisition system. The synchronization parameters are the

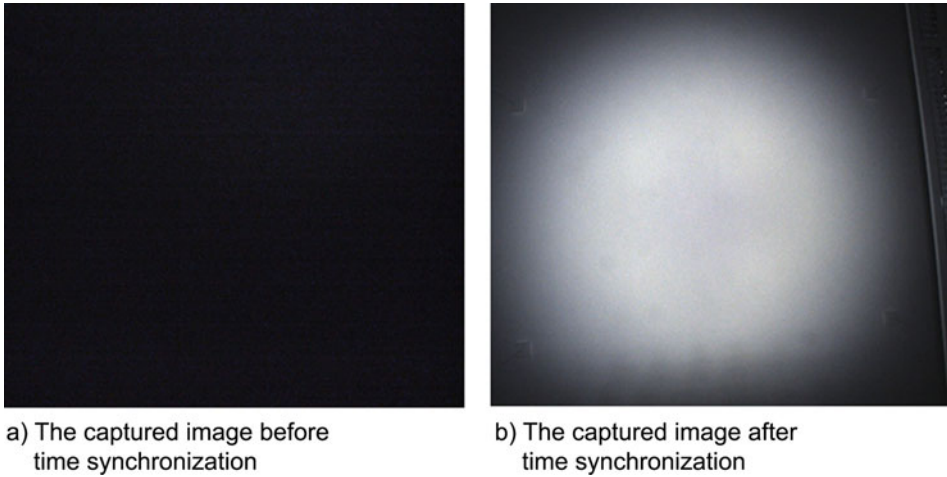


**Fig. 13.3** Camera and LED synchronization for a 50- $\mu$ s exposure time

trigger rate and pulse width of the trigger signal which are calculated for the primary camera. The trigger rate is equal to the required acquisition rate for each camera and is calculated by Eq. (13.5). The pulse width of the signal is chosen so that it corresponds to the required exposure time of the camera (see Eq. 13.6). As shown in Fig. 13.1, at the present project stage, a self-made synchronization unit is used to connect cameras and LEDs based on internal input and output pins. As shown in Fig. 13.3, the dark image will be captured for a short exposure time (e.g., 50 microseconds) if the LED and camera are not properly synchronized.

### 13.3.5 Tunnel Conditions

The system is to be developed for the roadway tunnels with different shapes like circular or rectangular tunnels. The working distance is 3–8 m and the light conditions in the tunnel are low. Therefore, high-power LEDs are selected to provide sufficient illuminations even in absolute darkness conditions. Moreover, the extraneous light interference is prevented due to the short exposure time of the camera (see Eq. 13.6). The system can be installed on a normal car like a kombi van (Volkswagen, 2020), and the intended operating speed of the vehicle is about 60–65 km/h which is suitable for traffic flows and fast monitoring of long tunnels with a minimum motion blur in the final images.

### 13.3.6 Image Processing Challenges

The generation of point clouds from the tunnel images offers challenges that are not found in many other close-range or UAV-based applications. Special features are often poorly textured environments, low lighting, noisy images, and little vertical overlap between the images. In addition, many images are captured in a long tunnel, and the limited computing capacity often prevents all images from being processed in one go. To address these issues, different scenarios are proposed in this study.

The first scenario is to coarsely estimate the exterior orientations (EOs) of the cameras in a local auxiliary coordinate system and use them as initial values for the image alignment algorithm. The EOs can be calculated based on the tunnel dimensions as well as the camera's installation angles in relation to the auxiliary coordinate system, as illustrated in Fig. 13.4. Figure 13.5 shows the first experiment with a test block of 1600 images. The alignment algorithm benefits from the coarsely determined EOs, and the semi-global matching algorithm produces a more complete point cloud.

The second scenario is to process the images of a long tunnel by dividing the image set into several overlapping image blocks, generate a point cloud for each block, and then fuse point clouds using a point-based registration technique. The experimental result for this scenario is shown in Fig. 13.6. The mean error and standard deviation of differences between the fused point cloud and the original point cloud are 0.07 m and 0.08 m, respectively. The merging of the point clouds of the three blocks worked well as long as the overlap between the blocks did not fall below 20% of the length of one of the blocks.

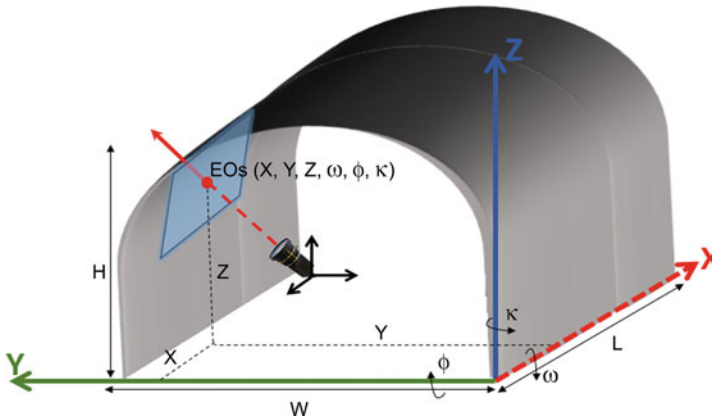


**Fig. 13.4** Exterior orientations and the local auxiliary coordinate system

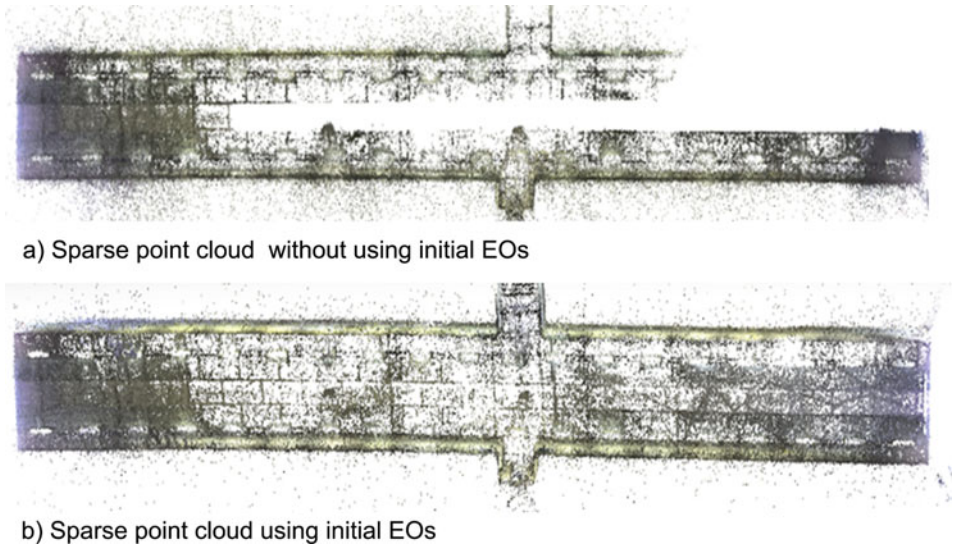


**Fig. 13.5** Point cloud generation

---

## 13.4 Conclusion

This article discusses the most important components of a multi-camera system for tunnel inspection including cameras, LEDs, and the synchronization unit. Based on the project requirements for ground pixel resolution, point cloud density and accuracy, the speed of scanning, the tunnel dimensions, and the total costs, each component should be selected to guarantee the performance and automation of the final system. Therefore, different possible options for each component are discussed, and the best possible solution is proposed to design and develop the inspection system, as shown in Table 13.2. Supported by initial experimental tests, image processing challenges are addressed in order to generate 3D models of the tunnel. We will report in the future on the system assembling with Metaphase LEDs, Gardasoft controllers, and Grasshopper cameras and on our experiments with data recording in tunnels and data processing for object recognition and damage detection using deep learning algorithms.

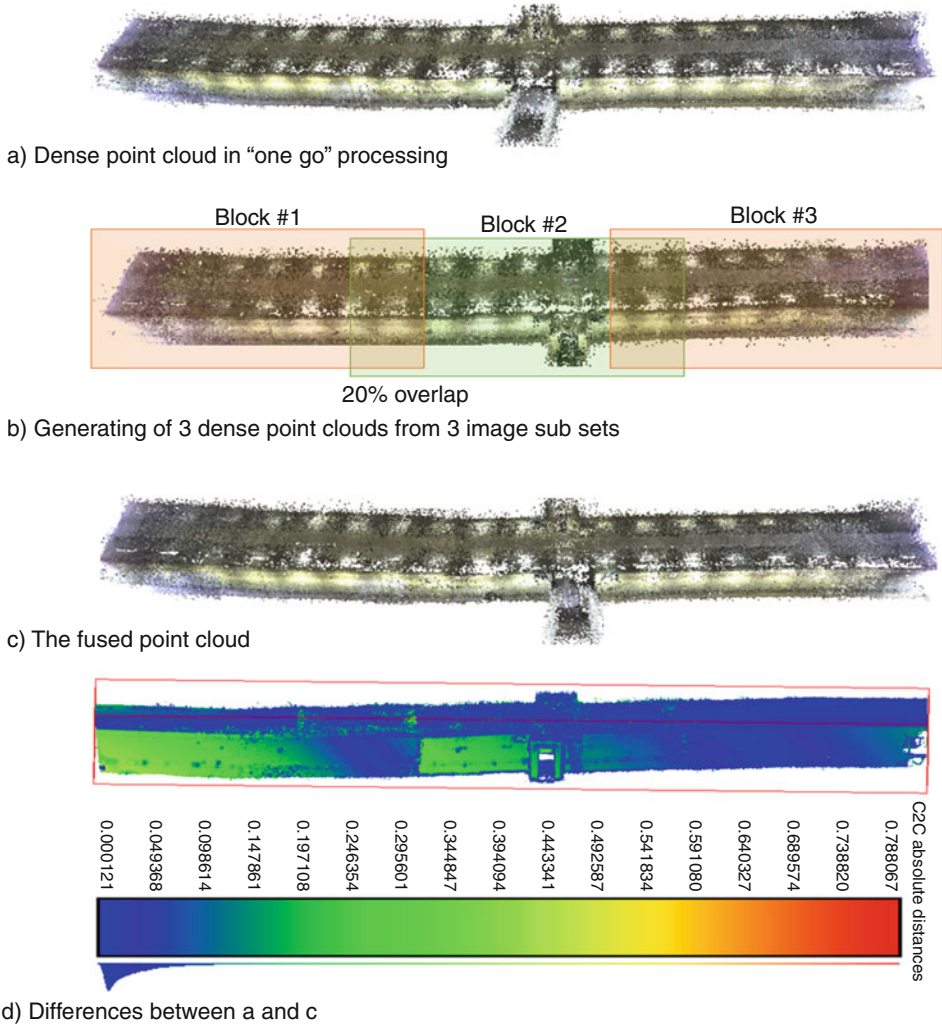


**Fig. 13.6** Block-wise point cloud generation



**Table 13.2** The proposed setup for the project

Parameters	Items	Values
Camera parameters	Sensor	CMOS, area scan
	Resolution	5 MP
	Pixel size	3.45 $\mu\text{m}$
	Sensor size	2448 $\times$ 2048 pix
	Focal length (lens)	6 mm
	Shutter	Global
	Image rate	>5 Hz
	Interface	USB 3.0 (400 MB/s)
	Pixel bit depth	12 bits
	Chroma	Color
	Shutter speed	>6 $\mu\text{s}$
	Price range	\$1500–3000
LED parameters	LED shape	Area based
	Operation mode	Flash
	Wavelength	White
	Flash pulse width	>20 $\mu\text{s}$
	Flash rate	>5 Hz
	Working distance	>3 m
	Irradiance at 2 m	878 $\text{W}/\text{m}^2$
	Price range	\$1000–2000
Default parameters	The intended speed	60 km/h
	Working distance	5 m
	Installation angle	45°
Calculated parameters according to the equations	Irradiance at 5 m	140 $\text{W}/\text{m}^2$
	$\text{FOV}_w \times \text{FOV}_h$	70° $\times$ 60°
	Vertical overlap	~35%
	Horizontal overlap	~84%
	FPS	~17 Hz
	Exposure time	~35 $\mu\text{s}$

**Acknowledgments** This research is funded by the Federal Ministry for Economic Affairs and Energy (BMWi) as part of the ZiM project ABOUT. The project partner is Viscan Solutions GmbH.

## References

Attard, L., Debono, C. J., Valentino, G., & Di Castro, M. (2018). Vision-based change detection for inspection of tunnel liners. *Automation in Construction*, 91, 142–154. <https://doi.org/10.1016/j.autcon.2018.03.020>

- Chapman, M. A., Min, C., & Zhang, D. (2016). Continuous mapping of tunnel walls in a GNSS-denied environment. In *International Archives of the Photogrammetry, Remote Sensing and Spatial Information Sciences - ISPRS Archives* (Vol. 41, pp. 481–485). <https://doi.org/10.5194/isprsarchives-XLI-B3-481-2016>
- Chen, H. M., Uliyanov, C., & Shaltout, R. (2015). 3D laser scanning technique for the inspection and monitoring of railway tunnels. In *RailNewcastle conference 2015* (pp. 73–84). <https://doi.org/10.21307/tp-2015-063>
- Chen, L., Lu, S., & Zhao, Q. (2019). Research on BIM-Based highway tunnel design, construction and maintenance management platform. In *IOP Conference Series: Earth and Environmental Science* (Vol. 218). <https://doi.org/10.1088/1755-1315/218/1/012124>
- Ehrbar, H., Braun, M., Fentzlof, W., Franz, S., Rahm, T., Scheffer, M., & Weiner, T. (2019). *Digital Design, Building and Operation of Underground Structures, BIM in Tunnelling*. Cologne: Deutscher Ausschuss für unterirdisches Bauen e. V. (DAUB).
- Fargnoli, M., Lleshaj, A., Lombardi, M., Sciarretta, N., & Di Gravio, G. (2019). A BIM-based PSS approach for the management of maintenance operations of building equipment. *Buildings*, 9(6). <https://doi.org/10.3390/buildings9060139>
- Gavilán, M., Sánchez, F., Ramos, J. A., & Marcos, O. (2013). Mobile Inspection System for High-Resolution Assessment of Tunnels. In *The 6th International Conference on Structural Health Monitoring of Intelligent Infrastructure*. Hong Kong 1.
- Huang, H., Sun, Y., Xue, Y., & Wang, F. (2017). Inspection equipment study for subway tunnel defects by grey-scale image processing. *Advanced Engineering Informatics*, 32, 188–201. <https://doi.org/10.1016/j.aei.2017.03.003>
- Jiang, Y., Zhang, X., & Taniguchi, T. (2019). Quantitative condition inspection and assessment of tunnel lining. *Automation in Construction*, 102, 258–269. <https://doi.org/10.1016/j.autcon.2019.03.001>
- O'Neill, B. (2020). Terrestrial laser scanners (TLS): guide and product selection. Retrieved from <https://www.aniwaa.com/buyers-guide/3d-scanners/terrestrial-laser-scanners-long-range/>
- Stent, S. A. I., Girerd, C., Long, P. J. G., & Cipolla, R. (2015). A low-cost robotic system for the efficient visual inspection of tunnels. *32nd International Symposium on Automation and Robotics in Construction and Mining: Connected to the Future, Proceedings*. <https://doi.org/10.22260/isar2015/0070>
- Teledyne Dalsa. (2014). *Understanding Line Scan Camera Applications*. Retrieved from <https://www.inspect-online.com/file/track/7757/1>
- VisionCamera. (2019). HOW TO SELECT A MACHINE VISION CAMERA INTERFACE (USB3 / GIGE / 5GIGE / 10GIGE VISION)? Retrieved from <https://www.vision-camera.nl/How-to-select-a-machine-vision-camera-interface-USB3-GigE-5GigE-10GigE-Vision>
- Volkswagen. (2020). The Transporter 6.1 Kombi. Retrieved from <https://www.volkswagen-nutzfahrzeuge.de/de/modelle>
- Wang, W., Zhao, W., Huang, L., Vimarlund, V., & Wang, Z. (2014). Applications of terrestrial laser scanning for tunnels: a review. *Journal of Traffic and Transportation Engineering (English Edition)*, 1(5), 325–337. [https://doi.org/10.1016/S2095-7564\(15\)30279-8](https://doi.org/10.1016/S2095-7564(15)30279-8)
- Yin, X., Liu, H., Chen, Y., Wang, Y., & Al-Hussein, M. (2020). A BIM-based framework for operation and maintenance of utility tunnels. *Tunnelling and Underground Space Technology*, 97. <https://doi.org/10.1016/j.tust.2019.103252>
- Zhan, D., Yu, L., Xiao, J., & Chen, T. (2015). Multi-camera and structured-light vision system (MSVS) for dynamic high-accuracy 3D measurements of railway tunnels. *Sensors (Switzerland)*, 15(4), 8664–8684. <https://doi.org/10.3390/s150408664>

**Open Access** This chapter is licensed under the terms of the Creative Commons Attribution 4.0 International License (<http://creativecommons.org/licenses/by/4.0/>), which permits use, sharing, adaptation, distribution and reproduction in any medium or format, as long as you give appropriate credit to the original author(s) and the source, provide a link to the Creative Commons license and indicate if changes were made.

The images or other third party material in this chapter are included in the chapter's Creative Commons license, unless indicated otherwise in a credit line to the material. If material is not included in the chapter's Creative Commons license and your intended use is not permitted by statutory regulation or exceeds the permitted use, you will need to obtain permission directly from the copyright holder.





# Evaluation of Crowd-Sourced PM<sub>2.5</sub> Measurements from Low-Cost Sensors for Air Quality Mapping in Stuttgart City

# 14

Joseph Gitahi and Michael Hahn

## Abstract

Exposure to particulate matter (PM) pollution poses a major risk to the environment and human health. Monitoring PM pollution is thus crucial to understand particle distribution and mitigation. There has been rapid development of low-cost PM sensors and advancement in the field of Internet of Things (IoT) that has led to the deployment of the sensors by technology-aware people in cities. In this study, we evaluate the stability and accuracy of PM measurements from low-cost sensors crowd-sourced from a citizen science project in Stuttgart. Long-term measurements from the sensors show a strong correlation with measurements from reference stations with most of the selected sensors achieving Pearson correlation coefficients of  $r > 0.7$ . We investigate the stability of the sensors for reproducibility of measurements using five sensors installed at different height levels and horizontal distances. They exhibit minor variations with low correlation of variation (CV) values of between 10 and 14%. A CV of  $\leq 10\%$  is recommended for low-cost sensors. In a dense network, the sensors enable extraction pollution patterns and trends. We analyse PM measurements from 2 years using space-time pattern analysis and generate two clusters of sensors that have similar trends. The clustering shows the relationship between traffic and pollution with most sensors near major roads being in the same cluster.

## Keywords

Particulate matter · Low-cost sensors · Crowd-sourced air quality data · Citizen science

J. Gitahi (✉) · M. Hahn  
Hochschule für Technik Stuttgart, Stuttgart, Germany  
e-mail: [joseph.gitahi@hft-stuttgart.de](mailto:joseph.gitahi@hft-stuttgart.de)

## 14.1 Introduction

Ambient air pollution poses a crucial environmental risk to human health globally. This applies especially to urban centres which are characterized by high population densities, heavy vehicle traffic and high concentration of industries. Fine dust particles also referred to as particulate matter (PM) are a major component of air pollution whose sources include dust; combustion particles from power plants, vehicles and industries; and reactions of chemicals such as  $\text{SO}_2$  and  $\text{NO}_x$ . They are categorized as  $\text{PM}_{10}$  and  $\text{PM}_{2.5}$  for particles with a diameter of less than or equal to  $10\ \mu\text{m}$  and  $2.5\ \mu\text{m}$ , respectively.  $\text{PM}_{2.5}$  passes through the respiratory system with ease due to the smaller size, thus presenting a higher risk to human health. To reduce health impacts, the World Health Organization (WHO) has recommended  $\text{PM}_{2.5}$  concentration thresholds of 10 and  $25\ \mu\text{g}/\text{m}^3$  for annual and daily averages, respectively (WHO, 2016).

Two major sources of data are used for air quality monitoring, satellite remote sensing products and ground-based sensors. Columnar aerosol optical depth (AOD), a by-product of atmospheric correction of optical satellite images, is retrieved based on the inversion of radiative transfer (RT) equations which model the scattering and absorption of solar radiation by aerosols, gas and water molecules in the atmosphere. Readily available satellite AOD include the Moderate Resolution Imaging Spectroradiometer (MODIS) product MOD04 providing a high temporal resolution AOD for daily-based monitoring at 3 km (MOD04\_3K) and 10 km (MOD04\_L2) spatial resolution suited for global and regional scales. Under European Space Agency's (ESA) Copernicus programme, Sentinel-3 provides AOD at 300 m spatial resolution with a revisit time of 1–2 days.

Besides land monitoring satellites, satellite missions dedicated to air quality monitoring like ESA's Sentinel-5P measure gaseous and aerosol pollutants. Sentinel-5P continuously measures gaseous pollutants and aerosol index at a spatial resolution of  $7\ \text{km} \times 3.5\ \text{km}$  with daily global coverage. While satellite remote sensing products have the inherent advantage of extensive spatial coverage, their spatial-temporal resolutions are not capable of mapping spatial-temporal air quality variations in detail. Ground-based air quality sensors such as reference monitoring stations, operated by environmental agencies and institutions, are highly accurate and reliable. However, due to their high installation costs, only a few reference stations are in use. Low-cost sensors present an opportunity to create dense air quality monitoring networks.

Air pollution in urban environments has large spatial and temporal variations which require a dense network of sensors for adequate monitoring. High-quality and accurate air quality monitoring stations are costly to install in large numbers. Citizen science initiatives have embarked on installing low-cost sensors for civic engagement in monitoring and controlling air pollution. Some of the initiatives in Europe include CITI-SENSE ([www.citi-sense.eu](http://www.citi-sense.eu)), hackAIR ([www.hackair.eu](http://www.hackair.eu)) and OK Lab Stuttgart ([www.luftdaten.info](http://www.luftdaten.info)). These sensors create a dense network which can supplement air quality data from the few reference stations. The sensors provide relative and indicative air quality measurements but at lower accuracies than required for regulatory purposes. They are prone to erroneous

measurements due to sensor faults, wrong handling by users and interference from meteorological parameters such as temperature and humidity. The measurements also have substantial data gaps hindering continuous air quality monitoring. Evaluation of the sensors is thus necessary before using them for mapping spatial and temporal variations of air pollution.

European countries are required to comply with EU air quality monitoring directives—Directive (AQD) 2008/50/EC on Air Quality (EU, 2008). The AQD outlines the criteria and reference measurement methods by member countries using fixed monitoring stations for legislative purposes. However, the directive also allows for supplementary indicative measurements from low-cost sensor platforms provided they meet the defined data quality objective (DQO). The DQO, a measure of the acceptable uncertainty of measurements, allows uncertainties of up to 50% for PM<sub>10</sub> and PM<sub>2.5</sub> measurements.

Most of the low-cost PM sensors in the market detect the number and size of dust particles in the air based on the light-scattering principle. For these sensors, accumulation of dust particles in the measuring chamber and extreme weather conditions, especially high humidity, are some of the factors affecting data quality (Castell et al., 2017; Badura et al., 2018; Bulot et al., 2020). The sensors are evaluated on several aspects: stability and accuracy of measurements, and their precision. The operational stability is crucial to determine sensors' performance over long-term measurement campaigns. They are assessed for stability and accuracy by comparing with measurements of co-located reference stations, while precision is determined by testing the reproducibility of data from different units of the same sensor model. The precision of sensors is evaluated using the coefficient of variation (CV) which is a ratio of the standard deviation and mean of measurements. A CV of zero shows a perfect agreement, and a CV of  $\leq 10\%$  is acceptable for PM monitoring using low-cost sensors (Sousan et al., 2016; Bulot et al., 2020).

Different models of commercially available low-cost PM sensors have been subjected to tests in several studies to ascertain their accuracy and precision. The SDS011 sensor by Nova Fitness is a popular choice due to its low cost (<20 €), low energy requirement and relatively stable performance. Badura et al. (2018) compared multiple units of four low-cost sensor models with a TEOM 1400a reference station for 6 months. Multiple units of SDS011 sensors were assessed for reproducibility where they scored a CV of 7% indicating good precision. The sensors also exhibited good agreement with the reference station with  $R^2$  values of between 0.79 and 0.86. In another study, Liu et al. (2019) evaluated three SDS011 sensors co-located with a reference station over 4 months in Oslo. PM<sub>2.5</sub> measurements from the sensors were highly correlated with the reference station having correlation values  $r$  of  $>0.97$ . On accuracy assessment, the sensors achieved good linearity with the reference station attaining  $R^2$  values of between 0.55 and 0.71, and low RMSE values of  $<6 \mu\text{g}/\text{m}^3$ .

In this study, we evaluate the suitability of PM<sub>2.5</sub> measurements from a low-cost sensor network for spatial-temporal mapping of air quality in Stuttgart city. The sensors are evaluated on three aspects. Firstly, we perform an inter-sensor comparison by placing the sensors with different vertical and horizontal distances in the same location to determine

the influence of sensor's placement on performance. Secondly, we assess the stability and correlation of selected SDS011 sensors with the nearest reference station using a long-term dataset spanning over 1 year. Lastly, the dense network of sensors is analysed to identify PM distribution and patterns in a spatial-temporal context.

---

## 14.2 Methodology

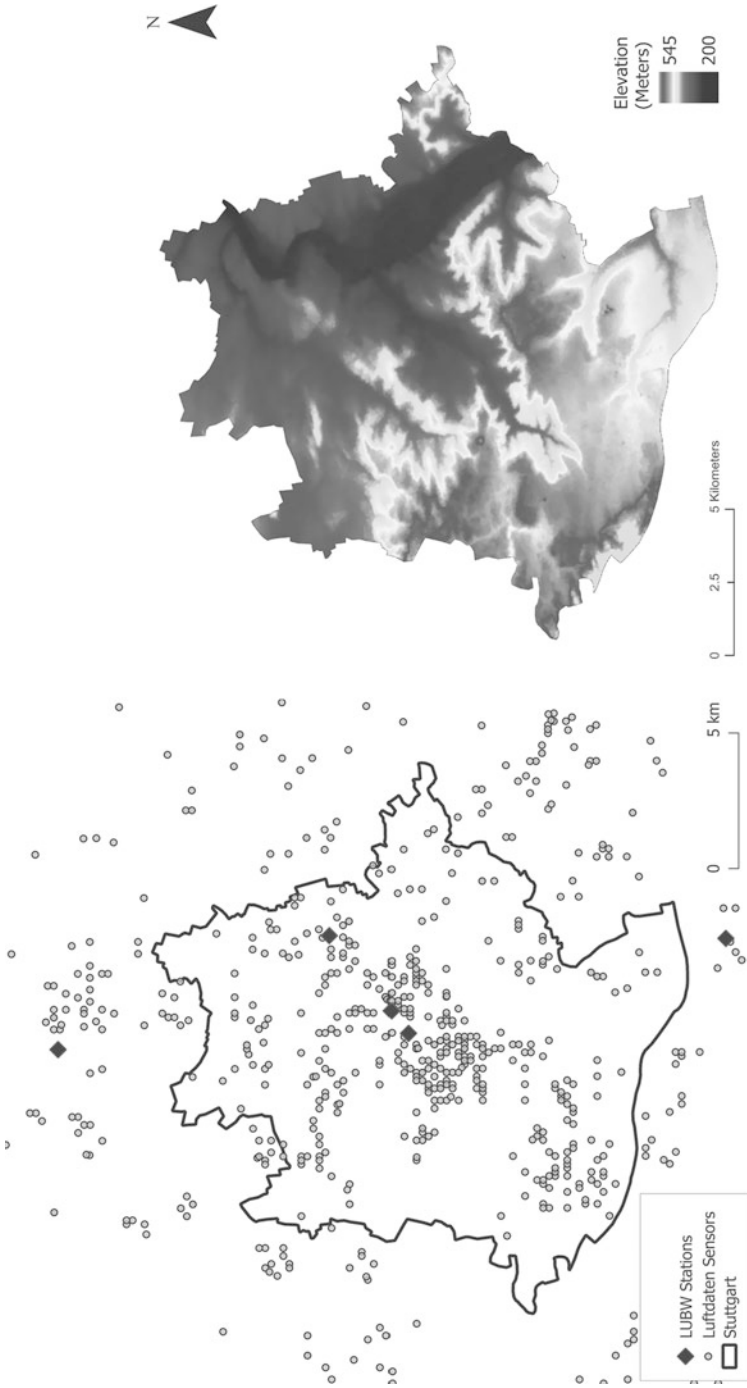
### 14.2.1 Study Area

The city of Stuttgart suffers from high pollution; PM levels have in the past exceeded the thresholds set by WHO which attributed to high traffic and industrial activities. Geographically, the city centre and main industrial areas are in a valley which affects air pollution transport and dispersion (Fig. 14.1).

### 14.2.2 Datasets

In the study, we use two PM<sub>2.5</sub> datasets. The first dataset is from five traffic and background air quality monitoring stations operated by the state institute for environment, Landesanstalt für Umwelt Baden-Württemberg (LUBW). The stations are distributed within and outside the city boundary and are used as reference stations in this study. From these reference stations, we obtain three PM measurements: PM<sub>10</sub> gravimetry, PM<sub>2.5</sub> gravimetry and PM<sub>10</sub> photometry. The photometric measurements are available in real time for public information, while the more accurate gravimetric measurements are available after 10 days. Hourly averages of PM<sub>2.5</sub> g gravimetric measurements are retrieved from LUBW API and stored in a spatial database. We use a dataset of measurements from June 2019 to June 2020.

The second dataset is from Luftdaten network of low-cost sensors by OK Lab Stuttgart ([www.luftdaten.info](http://www.luftdaten.info)) with approximately 200–350 operational sensors in the city at any given time. The primary sensor used in this network is the Nova PM sensor SDS011 which uses light scattering to measure the number and diameter of dust particles passing through the detector. OK Lab Stuttgart provides users with a list of components required to build the sensor as well as firmware and the configuration needed to set up the sensor and to upload recorded data to a central portal. The components include a micro-controller unit, SDS011 module, an optional temperature and humidity module and a pipe casing. The cost of the setup ranges from 25 € to 30 €. The sensors upload PM measurements every 2.5 min to the Luftdaten portal that is accessible via an API. We use scheduled scripts to retrieve and store measurements every 15 min. This dataset is available from August 2018 to August 2020 for sensors inside and near the city boundary. Table 14.1 shows the sensor specifications (Nova Fitness, 2015).

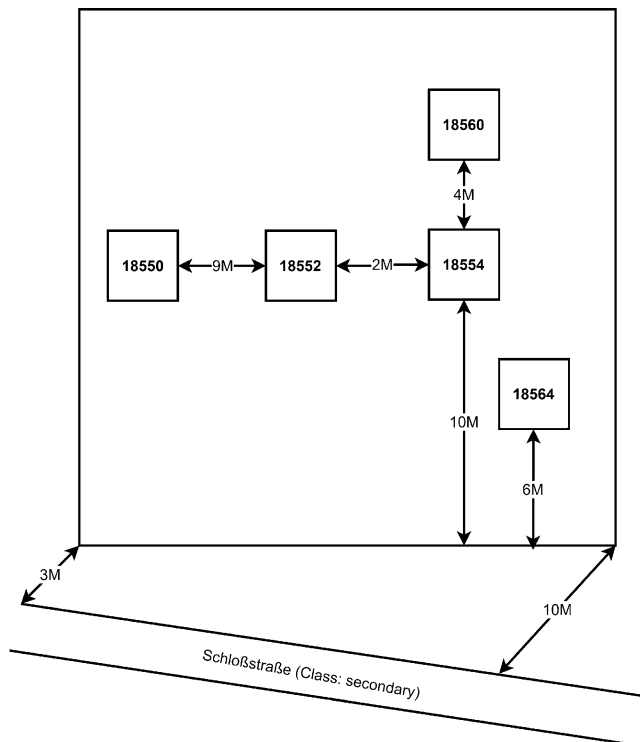


**Fig. 14.1** A map (left) showing the location of low-cost sensors and reference monitoring stations by the state environmental authority. The map on the right shows an elevation map of the greater Stuttgart city region. The city centre and most industries are situated in the valley region



**Table 14.1** Nova SDS011 PM sensor specifications

Item	Specification
Measuring parameters	PM <sub>2.5</sub> , PM <sub>10</sub>
Measuring range	0.0–999.9 µg/m <sup>3</sup>
Minimum resolution of dust particles	0.3 µm
Response time	< 10 seconds
Relative error	Maximum of ±15% and ± 10 µg/m <sup>3</sup> at 25 °C and 50% RH
Temperature range	–20–50 °C
Humidity range	0–70% relative humidity (RH)
Service life	8000 h

**Fig. 14.2** Installation of low-cost sensors at different points on the wall of building in University of Applied Sciences, Stuttgart. The building is adjacent to a secondary-class road

In Stuttgart University of Applied Sciences, we installed five SDS011 sensors for further investigations on their stability when placed at different heights and horizontal distances. They were installed on the facet of a building which is approximately 3–10 m adjacent to a secondary-class road. The placement of the sensors is shown in Fig. 14.2.

Since most of the sensors do not have a weather module, we use weather data from the OpenWeatherMap service. The data includes temperature, relative humidity, atmospheric pressure, wind direction and speed from 23 locations in the study area. An alternative weather dataset from Deutscher Wetterdienst (DWD) is available but has only one measurement location in the study area. This data is retrieved from the API at 15-min interval and is available from June 2019 to June 2020.

### 14.2.3 Data Preparation

In the first step, PM observations from the low-cost sensors are aggregated to hourly averages followed by removing measurements that lie outside the measuring range. The hourly aggregates are calculated to match the reference stations' sampling rate. We then create a new dataset by combining hourly PM measurements from the sensors and the reference stations, and the weather data. This fused dataset is created by spatially joining the low-cost PM measurements to the nearest weather and LUBW stations. Since the LUBW stations are few and sparsely distributed, a field containing the spatial distance in metres is calculated to allow analysis of low-cost sensors that are only within a specific distance from the high-quality stations. This combined dataset ranges from June 2019 to June 2020.

### 14.2.4 Low-Cost Sensors' Evaluation

Repeatability of PM measurements is crucial when using low-cost sensors for air quality monitoring. The coefficient of variation (CV) is calculated for hourly average PM<sub>2.5</sub> measurements to assess sensors' precision for the sensors installed in the university building as shown in Eq. (14.1). Temporary CV is calculated for corresponding hourly average measurements and a final CV determined as an average of all temporary CVs. Two sets of sensors were compared: sensors placed at the same height but varying horizontal distances and sensors placed at different heights on the building.

$$CV_t = \frac{\sigma_t}{\mu_t} \cdot 100 \quad (14.1)$$

where  $CV_t$  is the coefficient of variation at time  $t$  and  $\sigma_t$  and  $\mu_t$  are the standard deviation and mean at time  $t$ , respectively.

The sensors' performance is further assessed by comparing with the LUBW reference stations by calculating the Pearson correlation coefficient ( $r$ ) and the root mean square error (RMSE). In this assessment, PM<sub>2.5</sub> measurements from low-cost sensors that are within 1 km radius of the reference stations and within the operating range of 0–70% RH are selected for analysis. To further examine the quality of the low-cost sensors'

measurements, we select one low-cost sensor for each reference station with the highest correlation and perform multilinear regression. In the linear fitting, reference station  $PM_{2.5}$  is the dependent variable, and low-cost sensors  $PM_{2.5}$ , temperature and humidity are the independent variables as shown in Eq. (14.2). The relationships are evaluated using coefficients of determination ( $R^2$ ) and RMSE.

$$y = \beta_0 + \beta_x + \beta_{RH} + \beta_T \quad (14.2)$$

Multilinear regression fitting where  $y$  is the reference station  $PM_{2.5}$ ,  $x$  is the low-cost sensor  $PM$ ,  $RH$  is the relative humidity and  $T$  is the temperature.

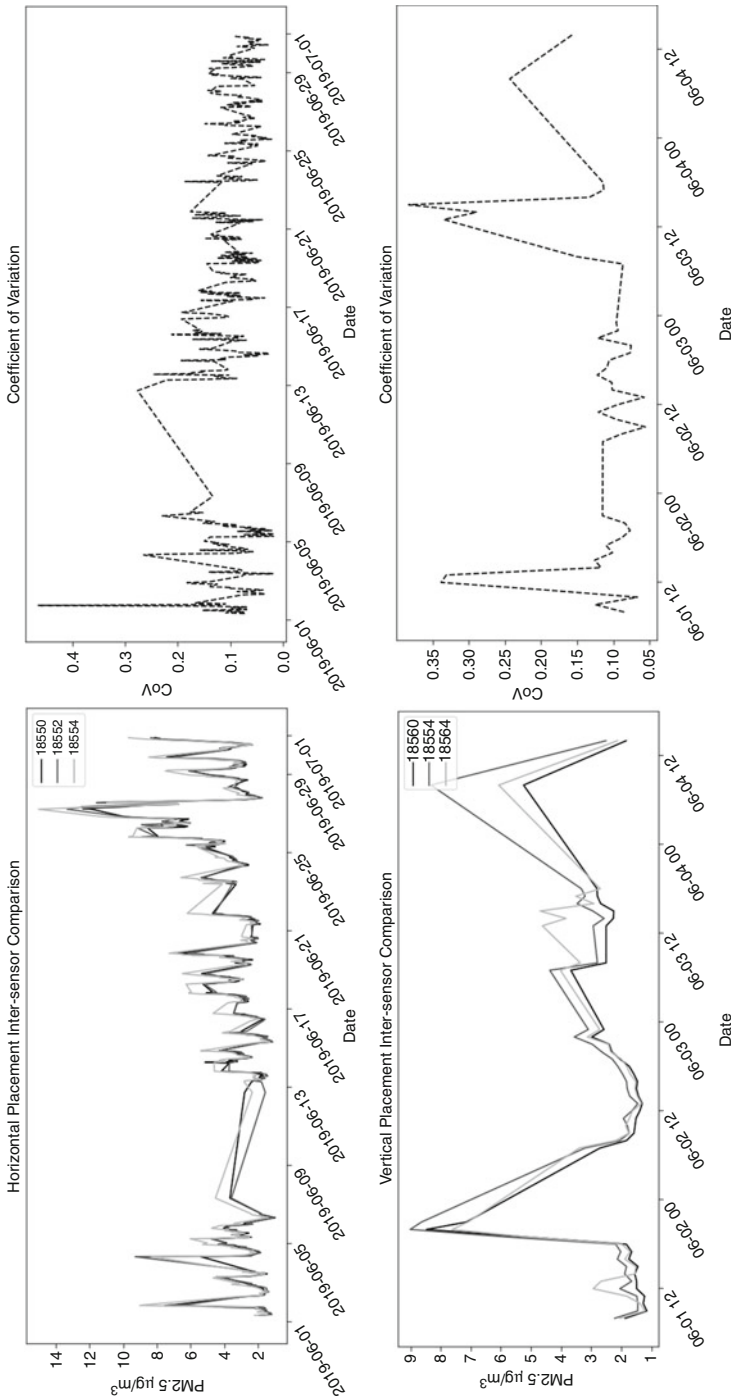
A dense network of sensors provides a chance to extract underlying air pollution spatial patterns using long-term measurements. We use ArcGIS Pro Space-Time Pattern Mining toolbox to analyse  $PM_{2.5}$  distribution and patterns in space and time. First, we create space-time bins by aggregating  $PM_{2.5}$  measurements into daily averages per sensor location. Data gaps due to sensor malfunction and transmission issues are filled by interpolating values based on the temporal trend of  $PM_{2.5}$  values for each sensor. The space-time cubes are then used to analyse  $PM$  concentrations using the time series clustering technique. In this technique, similar sensors are grouped based on either similar  $PM_{2.5}$  values, increase and decrease of values at the same time or having similar repeating patterns. We extract cluster patterns based on  $PM_{2.5}$  values using the long-term dataset from August 2018 to August 2020.

---

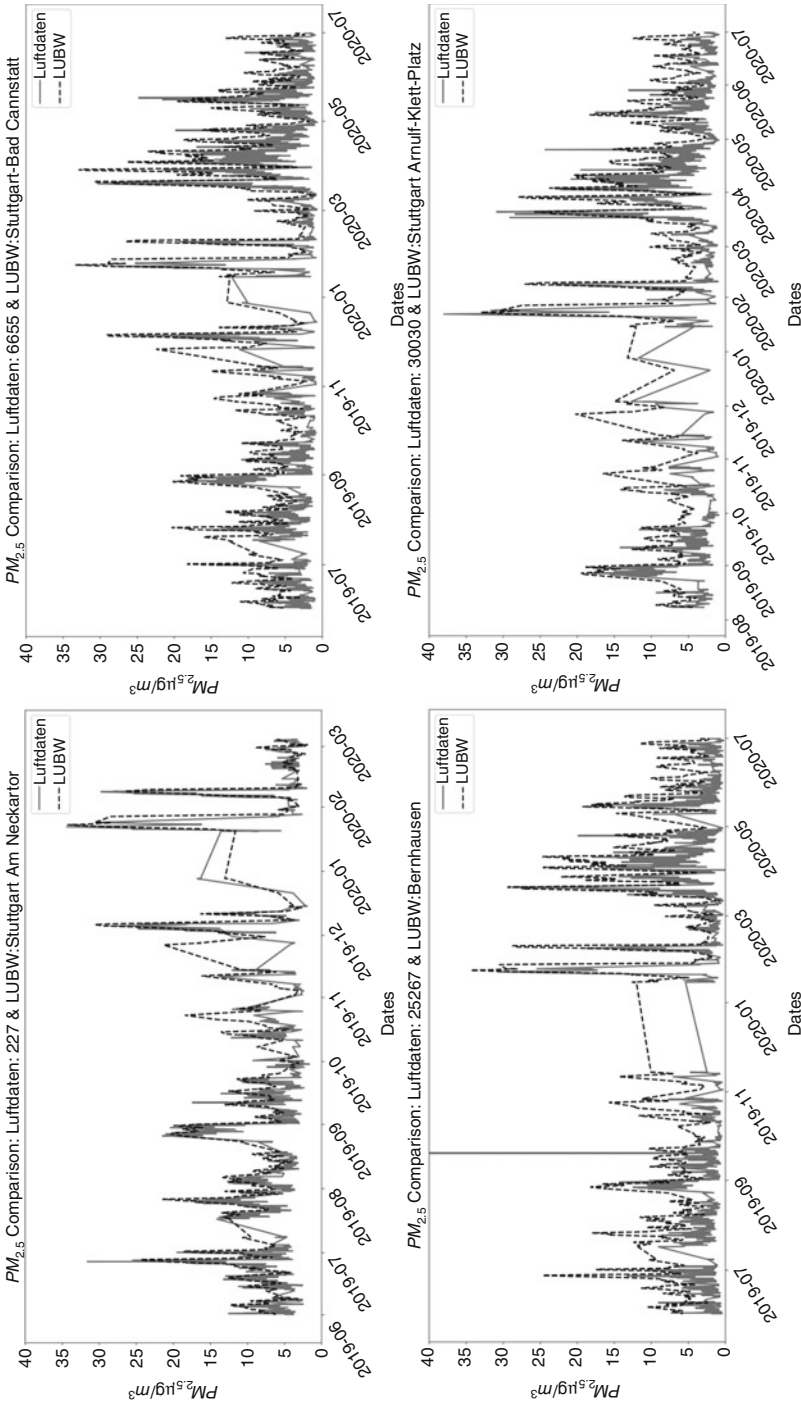
### 14.3 Results and Discussion

Figure 14.3 represents the results of  $PM_{2.5}$  measurements from five sensors placed at varying horizontal and vertical distances. Three sensors placed at the same height of 10 m and short horizontal distances of 2, 9 and 11 m from each other had stable measurements throughout the 1-month testing period. There were no significant variations and the sensors showed good precision with a mean CV of 10%. For the vertical assessment on sensors placed at different heights of 6, 10 and 14 m, the measurements followed a similar trend but with minor variations and a mean CV of 14%. Sensor 18,560 at 14 m generally has slightly lower values compared to the other two, but sensor 18,554 at 10 m has slightly higher values than the sensor at 6 m.

A trend analysis of  $PM_{2.5}$  measurements by the sensors over 1 year shows a good correlation with the reference stations. Out of the 52 sensors selected, 23 had a correlation coefficient  $r$  values of  $>0.7$ , and only 13 had  $r$  values of  $<0.5$ . In both urban and suburban settings, most of the sensors were able to detect peaks recorded by the reference stations with minor variances. The higher variations are observed in cold months starting from October to March as seen in Fig. 14.4. In the 1 km radius, distance from the reference station has little influence on the correlation, but the location of sensors has a greater impact. In the city centre map shown in Fig. 14.5, sensors in similar settings as the



**Fig. 14.3** PM<sub>2.5</sub> measurements and coefficients of variations from an inter-sensor comparison exercise on sensors placed at varying horizontal and vertical distances



**Fig. 14.4** A comparison of low-cost sensors' (solid line) and LUBW reference stations' (dashed line)  $PM_{2.5}$  measurements. The four plots are from low-cost sensors that have the highest correlation with the respective nearest reference station measurements

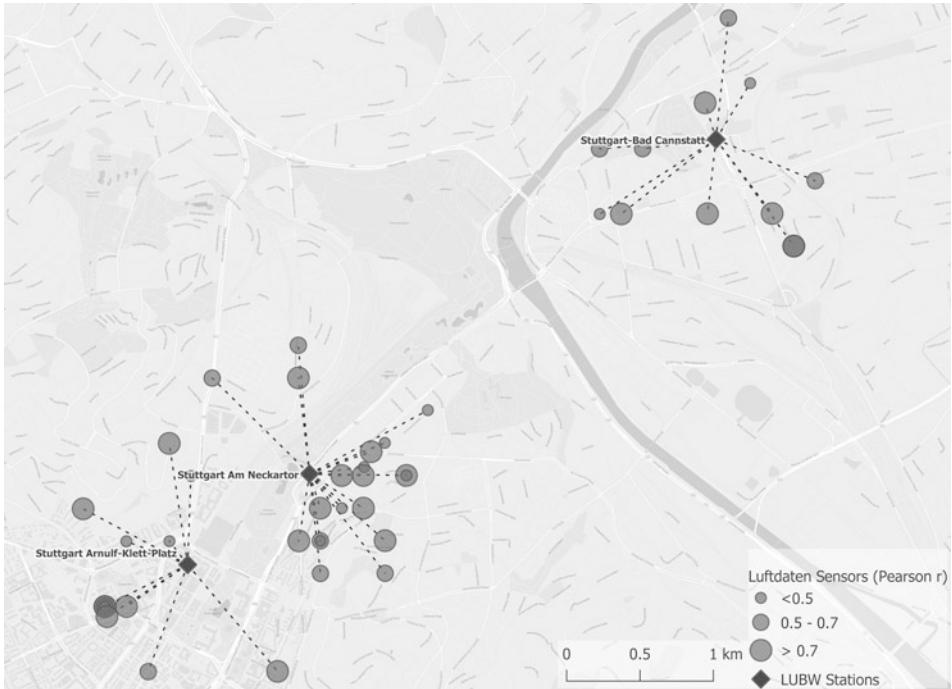


**Fig. 14.5** A map of Stuttgart city centre showing Luftdaten low-cost sensors that are within 1 km radius of LUBW sensors. The symbol size represents the Pearson correlation coefficient ( $r$ ) of PM<sub>2.5</sub> measurements recorded between June 2019 and June 2020

reference stations are highly correlated regardless of the distance. In such an urban environment, the sensors are influenced by the distance to the road network and the type of roads in the vicinity (Table 14.2).

We select the highest correlated sensors for each reference station and fit the measurements using multilinear regression shown in Eq. (14.2). We examine the relationship between the sensors in Table 14.3 and reference stations for the period June 2019–June 2020, summer months June–September 2019 and winter months December 2019–March 2020. The sensors showed good linear correlation over the whole period ( $R^2$  values 0.52–0.64) but lower correlations during winter ( $R^2$  values 0.38–0.58) as seen in the comparison charts in Fig. 14.6. This is due to SDS011 sensors not having a heating mechanism to eliminate water droplets in the measuring chamber which negatively affects their performance. The best results are the warmer period with  $R^2$  values ranging from 0.62 to 0.71. The scatterplots of the multilinear fittings are shown in Fig. 14.7.

A space-time cube created using ArcGIS pro with data aggregated to daily averages shows that for the period between August 2018 and August 2020, there were 758 unique sensors in the study area. However, all the sensors had data gaps, and 47% of the

**Table 14.2** Long PM<sub>2.5</sub> measurement comparison for low-cost sensors within a 1 km radius of each LUBW reference station

Reference station	Bernhausen	Ludwigsburg	Stuttgart Am Neckartor	Stuttgart Arnulf-Klett-Platz	Stuttgart-Bad Cannstatt	
<i>Code</i>	<i>DEBW042</i>	<i>DEBW024</i>	<i>DEBW118</i>	<i>DEBW099</i>	<i>DEBW013</i>	
<i>Type</i>	<i>Background</i>	<i>Background</i>	<i>Traffic</i>	<i>Traffic</i>	<i>Background</i>	
<i>Setting</i>	<i>Suburban</i>	<i>Suburban</i>	<i>Urban</i>	<i>Urban</i>	<i>Urban</i>	
Low-cost sensors within 1 km radius	3	2	20	15	12	
Pearson <i>r</i>	MIN	0.22	0.69	0.13	-0.15	0.18
	MEAN	0.45	0.72	0.57	0.52	0.64
	MAX	0.68	0.75	0.77	0.76	0.78
RMSE	MIN	6.04	6.09	4.14	5.50	4.55
	MEAN	39.25	7.06	16.01	6.77	6.76
	MAX	104.76	8.03	121.01	9.46	15.23

**Table 14.3** Low-cost sensors with the highest correlation for each reference station

Reference station	Bernhausen	Ludwigsburg	Stuttgart Am Neckartor	Stuttgart Arnulf-Klett-Platz	Stuttgart-Bad Cannstatt
<i>Type</i>	<i>Background</i>	<i>Background</i>	<i>Traffic</i>	<i>Traffic</i>	<i>Background</i>
<i>Setting</i>	<i>Suburban</i>	<i>Suburban</i>	<i>Urban</i>	<i>Urban</i>	<i>Urban</i>
<i>Luftdaten sensor ID</i>	<b>25,267</b>	<b>34,589</b>	<b>227</b>	<b>30,030</b>	<b>6655</b>
<i>Distance (metres)</i>	204	920	246	506	510
Pearson <i>r</i>	0.68	0.75	0.77	0.76	0.78
RMSE	6.95	6.09	4.14	5.50	6.06
No. of observations	2994	1245	1746	2507	3206

observations had to be estimated by interpolating values based on the temporal trend of each sensor. Out of the 758 sensors, only 452 sensors were transmitting data as of August 2020. This could indicate a high failure rate of the sensors or mishandling by users. A different number of clusters were evaluated to extract patterns in the dataset with two clusters giving the optimum results. From the time series clustering results in Fig. 14.8, sensors that are near major roads, Cluster 2, have similar trends with higher values than sensors in the background. Leveraging on the large number of sensors shows potential in mapping pollution trends in space and time. For example, in Fig. 14.9 the sensors in Cluster 2 were able to detect lower PM<sub>2.5</sub> concentration levels during the lockdown period (March–August 2020) due to Covid-19 compared to the same period in 2019.

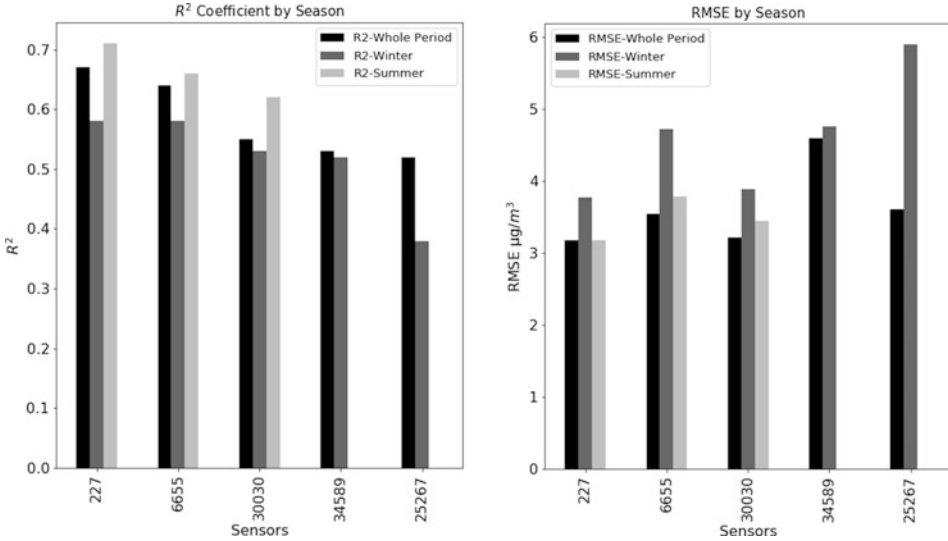


**Fig. 14.6** Seasonal comparison of  $R^2$  and RMSE statistics

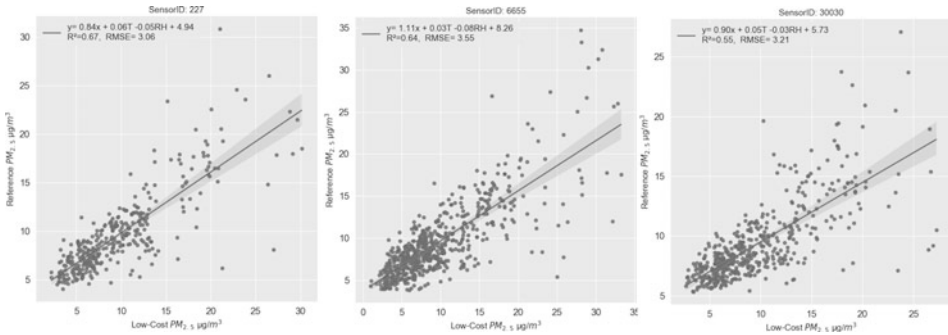


**Fig. 14.7** Multilinear fitting results of hourly average reference and PM<sub>2.5</sub> measurements after correcting for relative humidity and temperature effects

## 14.4 Conclusions

Low-cost sensors have the potential to improve spatial-temporal monitoring of PM pollution and supplement information from the costlier reference monitoring stations. The sensors exhibit stability and high correlation to reference measurements with varying degrees of accuracy. Whereas the sensors have lower accuracies and data gaps, using them in a dense network provides a wide coverage necessary for analysing pollution patterns and trends. One major challenge is outlier detection since it is hard to separate high pollution events from erroneous recordings due to the sensor’s fault. In a crowd-



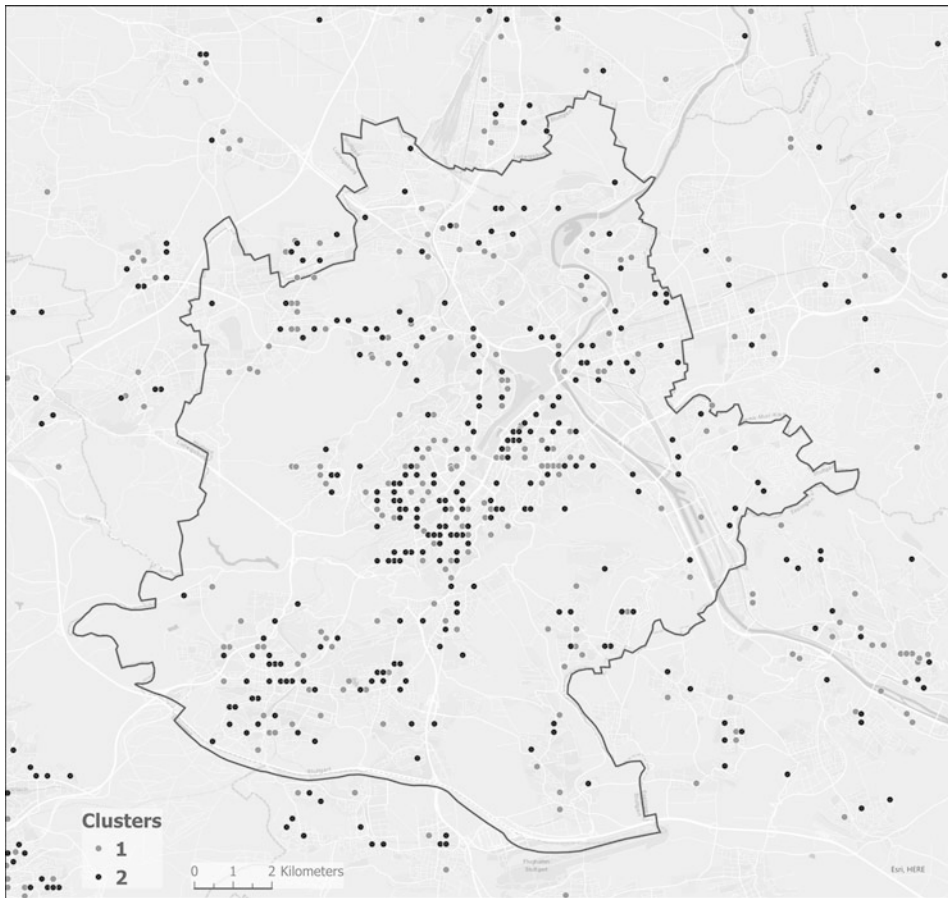


**Fig. 14.8** A map showing the sensors clustered based on  $PM_{2.5}$  values trends over 2 years from August 2018 to August 2020

sourced project like OK Lab Stuttgart, sensor installation and placement by the users is not standardized leading to measurements that are not representative of the location. For more accurate data collection, extensive sensor calibration, testing and robust outlier detection and removal techniques should be applied. Machine learning techniques could also be used to predict and fill in data gaps.

**Acknowledgement** The project “iCcity: intelligent city” is sponsored by the Federal Ministry of Education and Research (BMBF) under the promotion code 13FH9I011A and supervised by the project executing organization VDI Technologiezentrum GmbH for the BMBF.

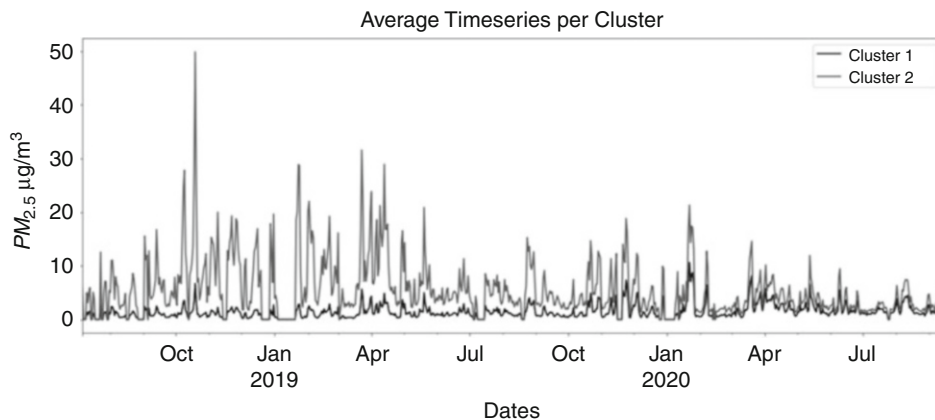


**Fig. 14.9** Time series plot showing the average PM<sub>2.5</sub> values for each cluster

## References

- Badura, M., Batog, P., Drzeniecka-Osiadacz, A. and Modzel, P. (2018), “Evaluation of Low-Cost Sensors for Ambient PM 2.5 Monitoring”, *Journal of Sensors*, 2018, 1-16, *Journal of Sensors*, Vol. 2018, pp. 1–16.
- Bulot, F.M.J., Russell, H.S., Rezaei, M., Johnson, M.S., Ossont, S.J.J., Morris, A.K.R., Basford, P.J., Easton, N.H.C., Foster, G.L., Loxham, M. and Cox, S.J. (2020), “Laboratory Comparison of Low-Cost Particulate Matter Sensors to Measure Transient Events of Pollution”, *Sensors (Basel, Switzerland)*, Vol. 20 No. 8.
- Castell, N., Dauge, F.R., Schneider, P., Vogt, M., Lerner, U., Fishbain, B., Broday, D. and Bartonova, A. (2017), “Can commercial low-cost sensor platforms contribute to air quality monitoring and exposure estimates?”, *Environment international*, Vol. 99, pp. 293–302.
- EU (2008), “Directive 2008/50/EC of the European Parliament and of the Council of 21 May 2008 on ambient air quality and cleaner air for Europe”, *Official Journal of the European Union*.
- Liu, H.-Y., Schneider, P., Haugen, R. and Vogt, M. (2019), “Performance Assessment of a Low-Cost PM<sub>2.5</sub> Sensor for a near Four-Month Period in Oslo, Norway”, *Atmosphere*, 10(2), 41, *Atmosphere*, Vol. 10 No. 2, p. 41.
- Nova Fitness (2015), “Laser PM<sub>2.5</sub> Sensor specification. Product Model: SDS011” (accessed 10 October 2020).
- Sousan, S., Koehler, K., Thomas, G., Park, J.H., Hillman, M., Halterman, A. and Peters, T.M. (2016), “Inter-comparison of Low-cost Sensors for Measuring the Mass Concentration of Occupational Aerosols”, *Aerosol science and technology the journal of the American Association for Aerosol Research*, Vol. 50 No. 5, pp. 462–473.
- WHO (2016), *Ambient air pollution: A global assessment of exposure and burden of disease*, Geneva, Switzerland.

**Open Access** This chapter is licensed under the terms of the Creative Commons Attribution 4.0 International License (<http://creativecommons.org/licenses/by/4.0/>), which permits use, sharing, adaptation, distribution and reproduction in any medium or format, as long as you give appropriate credit to the original author(s) and the source, provide a link to the Creative Commons license and indicate if changes were made.

The images or other third party material in this chapter are included in the chapter's Creative Commons license, unless indicated otherwise in a credit line to the material. If material is not included in the chapter's Creative Commons license and your intended use is not permitted by statutory regulation or exceeds the permitted use, you will need to obtain permission directly from the copyright holder.





# Augmented Reality for Windy Cities: 3D Visualization of Future Wind Nature Analysis in City Planning

# 15

Shubhi Harbola, Martin Storz, and Volker Coors

## Abstract

Effective government management, convenient public services, and sustainable industrial development are achieved by the thorough utilization and management of green, renewable resources. The research and the study of meteorological data and its effect on devising renewable solutions as a replacement for nonrenewable ones is the motive of researchers and city planners. Sources of energy like wind and solar are free, green, and popularly being integrated into sustainable development and city planning to preserve environmental quality. Sensor networks have become a convenient tool for environmental monitoring. Wind energy generated through the use and maintenance of wind turbines requires knowledge of wind parameters such as speed and direction for proper maintenance. An augmented reality (AR) tool for interactive visualization and exploration of future wind nature analyses for experts is still missing. Existing solutions are limited to graphs, tabular data, two-dimensional space (2D) maps, globe view, and GIS tool designed for the desktop and not adapted with AR for easy, interactive mobile use. This work aims to provide a novel AR-based mobile supported application (App) that

---

S. Harbola (✉)

University of Stuttgart, Stuttgart, Germany

e-mail: [Shubhi.Harbola@hft-stuttgart.de](mailto:Shubhi.Harbola@hft-stuttgart.de); [ShubhiHarbola@gmail.com](mailto:ShubhiHarbola@gmail.com)

M. Storz

University of Applied Science, Stuttgart, Germany

e-mail: [Martin.Storz@hft-stuttgart.de](mailto:Martin.Storz@hft-stuttgart.de)

V. Coors

Institute for Applied Research, University of Applied Sciences Stuttgart, Stuttgart, Baden-Württemberg, Germany

e-mail: [Volker.Coors@hft-stuttgart.de](mailto:Volker.Coors@hft-stuttgart.de)

© The Author(s) 2022

V. Coors et al. (eds.), *iCity. Transformative Research for the Livable, Intelligent, and Sustainable City*,

[https://doi.org/10.1007/978-3-030-92096-8\\_15](https://doi.org/10.1007/978-3-030-92096-8_15)

241

serves as a bridge between three-dimensional space (3D) temporal wind dataset visualization and predictive analysis through machine learning (ML). The proposed development is a dynamic application of AR supported with ML. It provides a user interactive designed approach, presenting a multilayered infrastructure process accessed through a mobile AR platform that supports 3D visualization of temporal wind data through future wind analysis. Thus, a novel AR visualization App with the prediction of wind nature using ML algorithms would provide city planners with advanced knowledge of wind conditions and help in easy decision-making with interactive 3D visualization.

---

**Keywords**

Wind speed · 3D visualization · Predictive models · Augmented reality · Green energy · Machine learning · Meteorological data · Mobile App · Planning cities · Wind forecasting

---

## 15.1 Introduction

The usage of environmental monitoring system accumulates data that extend our knowledge about the current status of the environment. The progressing interconnection of sensors with the quality and quantity of meteorological data has led to an increase in techniques and methods that support interactive visualization and analysis of temporal data (Hart, 2006; Bogue, 2008). Today, environmental scientists and city planners now prefer improved interactive visualization capabilities not only for the historical dataset but also for predictive analyses. There is a gap between the observed environment and its three-dimensional space (3D) digital representation in the user-specified time frame for interactive analysis of temporal wind data. Thus, there is still a dissociation that the planner likely needs to solve for comprehending the situation. The scientific temporal data visualizations are frequently used in support of interactive visual analytics and are well-accepted within the geoinformatics disciplines. The data variety, diversity, and volume have brought forward an impressively large number of methods to deal with various issues related to spatial and temporal aspects, dynamic interactions, and different view types in multiple ways of connecting data with two-dimensional space (2D) maps or 3D globes (Harbola and Coors, 2018). The characteristics of data, voluminous data, multidimensionality, and high spatial distribution contribute to make situation assessment one of the most demanding tasks, both for the user and the platform (Thomas and Cook, 2005). Numerous studies have stressed on the importance of spatial reference of data, while others focus more on the temporal aspect. Depending on user requirements and the nature of the target audience, there are different levels of experience and interests that are amenable to scientific time data (Nocke et al., 2008). It could be standard 2D presentation techniques, both scalar- and vector-based 3D data representations, and mobile GIS combined with handheld software (ESRI, 2004; Lin and Loftin, 1998). Combining the augmented reality (AR) for temporal geoscientific visualization is still yet to be explored. There are studies that deal with unconventional visualizations of urban pollution levels using mobile AR or tripod-

mounted AR system to visualize GIS data designed and developed on a range of human factor studies (White, 2017; King et al., 2005). Mobile visualization offers a solution in that it directly places heterogeneous datasets at different spatiotemporal scales in their accurate spatial and temporal context. AR, while coordinated with ML, is an advantage that speeds up the process and comes up with new good implemented cases that remains a challenge.

In contrast to these works, this paper proposes a combination of visual analysis platform with spatial, temporal, and future prediction information for the user-defined time frame. It comes along as an AR mobile Application (App) for quick, advance, and easy interface. Moreover, mobile display, combined with AR, proposes a natural way to relate abstract content to the physical world through graphic overlays. Interactive 3D visualizations of future prediction methods (which work on the original wind data by taking into consideration the noise) are still required. In this regard, the current study:

- (i) Introduces the concept of mobile environmental monitoring using handheld AR.
- (ii) Analyzes and describes its associated workflow following an iterative user-centered design (UCD) process.

The proposed AR mobile supported App provides an innovative infrastructure. It enables access to wind datasets for both future and historical data for user-desired time frame in interactive 3D visualization. It enables near real-time data access. The developed App will provide forecast of wind nature and helps to select good sites for wind analysis-related projects. This 3D visualization will devise smart utilization of renewable energy for safe and better city planning. This can help to manage and develop the city's resources. The remaining paper is organized as follows: The proposed methods and datasets used are discussed in Sect. 15.2 and Sect. 15.3, respectively, and the results are discussed in Sect. 15.4, followed by a conclusion in Sect. 15.5.

---

## 15.2 Methodology

The proposed method is a technique to visualize the historical as well as future temporal wind datasets interactively. The developed 3D visualization AR mobile supported App is called WindAR (Fig. 15.1). The WindAR supported 3D visualization of the data makes it easy to connect with the temporal wind dataset accompanied by spatial and future prediction information. The WindAR starts with an interactive selection dashboard that provides the user with an interactive way of selecting the location of a sensor. The App offers the possibility to select data of the sensor at the respective location via the name of the sensor from a predefined list or by specifying the coordinates of the sensor. The location is displayed in 3D in the WindAR. The user then selects the desired time frame (day, month, year). The detailed information in terms of 3D temporal wind flow is displayed for the selected time frame. Then, the user could perform the intermediate reset for the input of the section in the dashboard and compare other desired cases visually. This period could be in the past, which is already available in the App database, or in the future. Here, future



**Fig. 15.1** 3D visualisation of the sensor's location in WindAR App

values are obtained by predicting wind parameters for very short term (a few hours in the future). 1D Multiple CNN (1DMCNN) (Harbola and Coors, 2019) is used as a regression method to predict wind parameters. The 1DMCNN architecture consists of five individual CNN, each of which has its own input layer and is connected to the two common fully connected layers, followed by the output layer. The output layer uses a linear activation function, while hidden layers use the exponential linear unit (ELU), a nonlinear activation function. The output layer has nine neurons to predict the regression output. Each neuron in the output layer corresponds to an epoch. The 3D visualization of the temporal wind flow supported by AR is created using Unity's real-time development framework. Unity offers many tools to create 3D applications. It supports all relevant AR platforms (such as Android, iOS, HoloLens) with the same codebase. Unity's ability to render mesh-based 3D or 2D graphics very quickly makes it an incredibly capable engine for creating proposed spatial, temporal, and user interactive significant mobile AR App WindAR.

### 15.3 Dataset

Stuttgart wind datasets are used in this study. In the corner of Hauptstaetter Strasse 70173 Stuttgart, the historical data of 1987 to 2017 is taken from Stuttgart station sensor.<sup>1</sup> This dataset contains the wind speed and direction with temporal information attached in a 30-minute interval. The temporal meteorological dataset is organized with past data first

<sup>1</sup> <https://www.stadtklima-stuttgart.de>

**Fig. 15.2** Running WindAR App in mobile (top view)



followed by the latest data. It helps to predict wind speed and direction for interactive selection of time frame in 3D WindAR.

---

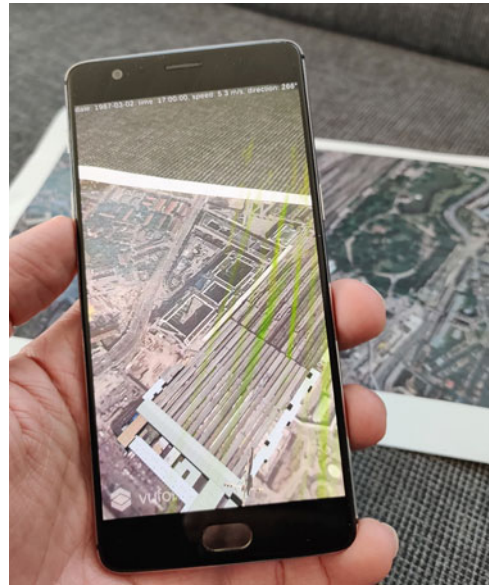
## 15.4 Results

The proposed algorithms were implemented using Python and executed with four cores on Intel® Core™ i7-4770 CPU @3.40 GHz. Stuttgart's 30-year historical data was used to train and test the regression-based prediction model 1DMCNN, thereby forecasting the wind speed and direction. The interactive WindAR App is a platform to visualize the sensors' dataset with spatial and temporal information attached, as shown in Figs. 15.1 and 15.2.

In this first version of running AR mobile App WindAR (Fig. 15.3), the .csv files of temporal wind datasets are included in the App itself. During the initialization of this App (starting up), the .csv files are parsed line per line, and useful information is extracted into



**Fig. 15.3** Setting-up the WindAR App in user's mobile



two lists of each selected parameter. The first list was a collection of all unique dates without the time in the file, to make user-desired time frame date selection possible. The second more extensive list contains all data entries from the list, including date, time, wind speed, and direction. Once during the run time, the desired time range has been selected. A temporary array with all the required information is generated and visualized in 3D with AR using WindAR. The time complexity of loading and parsing the dataset is given by  $O(n)$ . The extracted geometry (and background) of the sensor location and the environment are linked to the App using the Vuforia image targets method (Inc., 2011).

3D visualization is done by using Unity's physical wind system in combination with a particle system. The wind flow is represented by dust particles' flowing speed according to the magnitude and direction of the real-world temporal.

wind flow sensor measurements. The 3D visualization of temporal wind flow over the sensor location is accompanied by a played wind sound that uses pitches that depend on the strength of the wind. In order to provide close to real 3D visualization in AR platform, the wind flow particles are color-coded depending on the wind strength (blue (less than 2 m/s)→green (2–4 m/s)→yellow (4–6 m/s)→red (above than 6 m/s)) accompanied with the wind flow motion, thus leaving a trail behind (as shown in Figs. 15.4 and 15.5). In Figs. 15.6, 15.7, 15.8 and 15.9 the wind flow particles are color-coded depending on the wind strength accompanied by the wind flow motion leaving a trail behind, as discussed above. Besides, there is a weathercock, which is rotated to show the wind direction purely at the sensor's location Figs. 15.6.

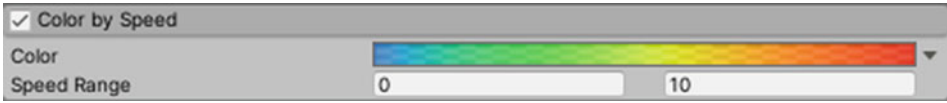


**Fig. 15.4** Wind flow visualisation color (strength) assignment scheme

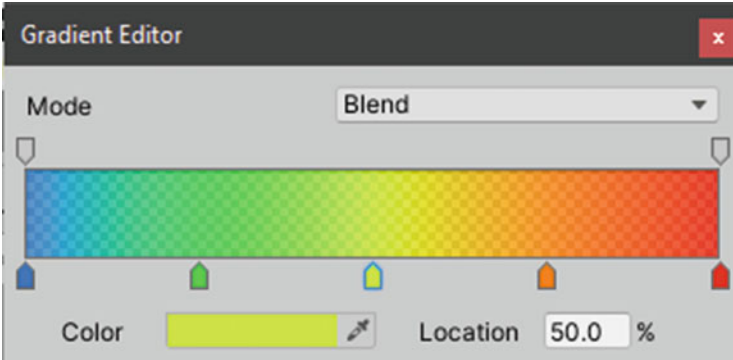


**Fig. 15.5** Wind flow color coding scheme ranges

**Fig. 15.6** Wind flow with 3D geometry visualisation accompanied in the WindAR App

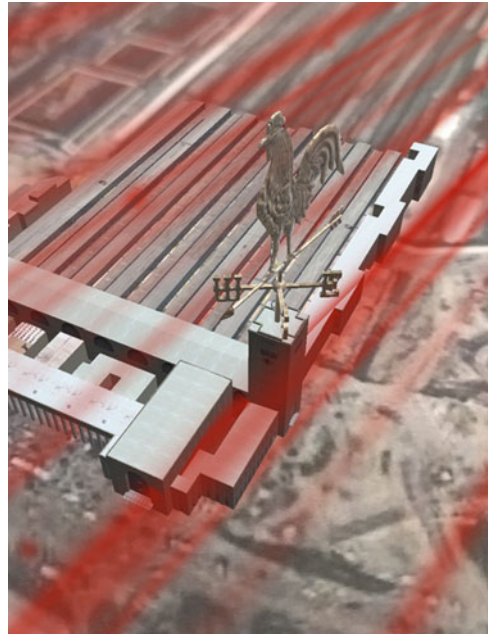


**Fig. 15.7** Wind flow particles trail visualisation in the WindAR App (side view)

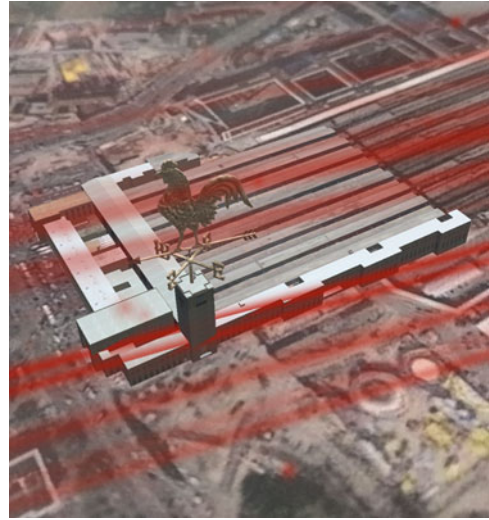
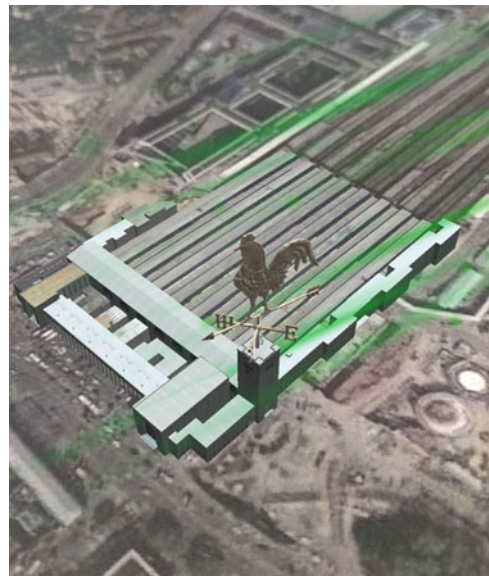


**Fig. 15.8** Wind color coded flow visualisation in the WindAR App



### 15.4.1 Discussion

The proposed WindAR App is an easy and interactive AR technique in which users could scan the sensor spatial location. The user automatically gets detailed information about the sensor's recording parameters and measurements with respect to the time of the year. AR mobile supported App allows for close to real-time data access. The developed App provides forecast of the wind in a given area, thereby helping in the proper selection of

**Fig. 15.9** Wind color coded flow visualisation in the WindAR App (top view)



sites for wind analysis-related projects. The AR-based 3D visualization enables information on renewable energy use for competent management, safe and better city planning, and development of the city's energy resources.

---

## 15.5 Conclusion

The study of meteorological parameters and their effects has been the attention of researchers in smart city planning to enable thorough use and management of resources that would contribute to convenient public services and sustainable industrial development. Using renewable energy supply would provide a healthy and amiable city, and increased welfare in more general terms. To ensure incorporation into the planning process, the renovation of the existing planning is indeed the most promising field for climate-related intervention. In this paper, we have presented an AR mobile App with quick, advance, and easy interface. It consists of a unique interactive visual analysis platform that combines spatial, temporal, and future prediction information for the user-defined time frame. The authors have stressed the need to include energy-conscious strategies to improve environmental quality. The integration of new knowledge and innovative technologies in sustainable transformation is the motive of this proposed work. The AR-based 3D visualization proposed here could be further improved in combination with a web service that loads the dataset directly into the App from the web server without using .csv files. The authors' future focus is on fully automatic identification and location detection of these sensors in real time, with sensor data displayed interactively in WindAR App. Meanwhile, the predicted speed and direction has the potential to select a feasible location for the wind sensor installation, and the developed interactive visual analysis of the AR application facilitates the selection. In addition, since the output of the wind turbines is highly dependent on the wind speed and direction, WindAR would provide a foresight for better planning.

**Acknowledgments** The Stuttgart wind dataset is downloaded from the History of the Section of Urban Climatology within the Office for Environmental Protection of the City of Stuttgart (DEPUC) website. Shubhi Harbola has received funding within the Joint Graduate Research Training Group Windy.

Cities. This research program (funding number: 31-7635.65-16) is supported by the Ministry of Science, Research and Art of Baden-Württemberg, Germany. Martin Storz extends his gratitude for the financial support within the SensAR project. The Carl-Zeiss-Stiftung funds SensAR.

---

## References

- Bogue, R., 2008. Environmental sensing: strategies, technologies and applications. *Earth-Science Reviews* 28, pp. 275–282.
- ESRI, 2004. ArcPad: Mobile GIS. Technical report.
- Harbola, S. and Coors, V., 2018. Geo-visualization and visual analytics for smart cities: A survey. *International Archives of the Photogrammetry, Remote Sensing and Spatial Information Sciences*.
- Harbola, S. and Coors, V., 2019. One dimensional convolutional neural network architectures for wind prediction. *Energy Conversion and Management* 195, pp. 70–75.
- Hart, J., K., 2006. Environmental sensor networks: a revolution in the earth system science? *Earth-Science Reviews*.
- Inc., P., 2011. Vuforia development library. Last accessed 16 April 2020.
- King, G. R., Piekarski, W. and Thomas, B. H., 2005. Arvino—outdoor augmented reality visualization of viticulture gis data. In: *IEEE Computer Society Proceedings of the 4th IEEE/ACM international symposium on mixed and augmented reality*, Vol. 123, p. 52–55.
- Lin, C. R. and Loftin, R. B., 1998. Application of virtual reality in the interpretation of geoscience data. In: *Proceedings of the ACM symposium on virtual reality software and technology 1998 VRST 98*, Vol. 98, p. 187–194.
- Nocke, T., Sterzel, T., Boettinger, M. and Wrobel, M., 2008. Visualization of climate and climate change data: an overview. In: Ehlers EEA et al. (eds) *Digital earth summit on geoinformatics 2008 tools for global change research* pp. 226–232.
- Thomas, J., and Cook, K. A., 2005. Illuminating the path: the research and development agenda for visual analytics. *IEEE*.
- White, S., 2017. Sitelens: situated visualization techniques for urban site visits. p. 1117–1120.

**Open Access** This chapter is licensed under the terms of the Creative Commons Attribution 4.0 International License (<http://creativecommons.org/licenses/by/4.0/>), which permits use, sharing, adaptation, distribution and reproduction in any medium or format, as long as you give appropriate credit to the original author(s) and the source, provide a link to the Creative Commons license and indicate if changes were made.

The images or other third party material in this chapter are included in the chapter's Creative Commons license, unless indicated otherwise in a credit line to the material. If material is not included in the chapter's Creative Commons license and your intended use is not permitted by statutory regulation or exceeds the permitted use, you will need to obtain permission directly from the copyright holder.





# Storing and Visualising Dynamic Data in the Context of Energy Analysis in the Smart Cities

# 16

Thunyathep Santhanavanich, Rosanny Sihombing,  
Pithon Macharia Kabiro, Patrick Würstle, and Sabo Kwado Sini

## Abstract

There is increased activity in developing workflows and implementations in the context of urban energy analysis simulation based on 3D city models in smart cities. At the University of Applied Sciences Stuttgart (HFT Stuttgart), an urban energy simulation platform called ‘SimStadt’ has successfully been developed. It uses the CityGML 3D city model to simulate the heat demand, photovoltaic potential, and other scenarios that provide dynamic simulation results in both space and time dimensions. Accordingly, a tool for managing dynamic data of the CityGML models is required. Earlier, the CityGML Application Domain Extension (ADE) had been proposed to support additional attributes of the CityGML model; however, there is still a lack of open-source tools and platforms to manage and distribute the CityGML ADE data efficiently. This article evaluates and compares alternative methods to manage dynamic simulation results of the 3D city model and visualise these data on the 3D web-based smart city application, including the use of SimStadt web services, databases, and OGC SensorThings API standard.

## Keywords

Urban energy analysis · 3D building model · CityGML · 3D tiles · SensorThings · Smart cities · SimStadt

T. Santhanavanich (✉) · R. Sihombing · P. M. Kabiro · P. Würstle · S. K. Sini  
Center for Geodesy and Geoinformatics, Hochschule für Technik Stuttgart, Stuttgart, Germany  
e-mail: [thunyathep.santhanavanich@hft-stuttgart.de](mailto:thunyathep.santhanavanich@hft-stuttgart.de)

© The Author(s) 2022

V. Coors et al. (eds.), *iCity. Transformative Research for the Livable, Intelligent, and Sustainable City*,

[https://doi.org/10.1007/978-3-030-92096-8\\_16](https://doi.org/10.1007/978-3-030-92096-8_16)

251

## Abbreviation

3DCityDB	3D City Databases
HFT Stuttgart	Hochschule für Technik Stuttgart (de) or University of Applied Sciences Stuttgart (en)
HTML	HyperText Markup Language
INSPIRE	Infrastructure for Spatial Information in the European Community
NPM	Node Package Manager
OGC	Open Geospatial Consortium
PV	Photovoltaic
REST	Representational state transfer
STA	SensorThings API
UML	Unified Modeling Language
XML	Extensible Markup Language

---

### 16.1 Introduction

As cities continue the implementation of smart city concepts around the world, a smart city has been defined as a way of continuously optimising traditional services and networks by taking advantage of developments in Information and Communications Technology (ICT) to become more efficient to benefit its inhabitants (European Commission 2020). Smart cities are often associated with the intelligent network of connected objects and machines that continuously transmit data using sensors technology and the cloud (Jawhar et al. 2018). At the same time, the virtual 3D city model has been used predominantly in the past for visualisation (Biljecki et al. 2015). There is a need to visualise and analyse city data alongside the 3D virtual city model since the 3D city model could also contain essential datasets related to individual buildings that can altogether be used in helping municipalities, enterprises, and citizens make better decisions that improve the quality of life in their cities.

While different standards are used to model and manage 3D city models, having a common standard eases the exchange of this data between various partners, thereby making these data reusable. To have a standard definition of the basic entities, attributes, and relationships of a 3D city model, the Open Geospatial Consortium (OGC) CityGML was developed to enable not just the visualisation of the virtual 3D city model but also the management and sharing of these models (Gröger et al. 2012). As one of the popular standards, CityGML has been widely accepted and used for modelling and sharing the 3D city model (Arroyo Ohori et al. 2018).

With CityGML models used to store building energy-related information like building function and year of construction which are vital for building energy simulation, various energy simulation platforms like SimStadt (Schumacher 2020) have adopted CityGML as a

definitive source for 3D city model information as data input for performing energy simulations such as energy demand and solar energy potential. These simulation results are usually represented by the visualisation platform as it makes data more comfortable for the human to understand and makes it easier to detect patterns, trends, and outliers in groups of data (Yi et al. 2008). Furthermore, city administrators and agencies can, therefore, use these data visualisations to make important decisions concerning their cities and make changes where needed to improve efficiency.

However, the various data simulation results from CityGML-based building models could lead to the complexity and heterogeneity of the data model. Therefore, a proper way of managing and visualising this information is necessary and needed to trace patterns and place meaning within the data being integrated. In the past, the Application Domain Extension (ADE) had been developed for extending and managing a specific group of environmental data such as energy-related building data to be modelled in connection to CityGML (Biljecki et al. 2018). Still, ADE has some limitations as it needs layers of data conversion, structures, and tools to access, deliver, and visualise on the web client (Lim et al. 2020).

In this article, we study and evaluate alternative approaches for managing energy-related building information with a particular focus on how the 3D city model can be used for collecting, computing, and visualising energy simulations using the following methods: (1) computing and visualising the simulated energy data of 3D building models on-the-fly, (2) using the PostgreSQL database as a datastore for simulated energy data, and (3) using SensorThings for managing the simulated energy data. These methods are, however, not the only methods available, but we intend to compare them to find out which is more efficient when it comes to managing and visualising energy-related building information such as photovoltaic (PV) energy generation potential, heat demand, etc. from CityGML models.

---

## 16.2 Background

### 16.2.1 Energy Data Simulation of the 3D Building Models

SimStadt is a simulation software developed at HFT Stuttgart. This software is based on the modules from the INSEL block diagram simulation system (Schumacher 2020). It is used to create workflows to simulate the dynamic energy-related attributes in the 3D city models in CityGML format (Monsalvete et al. 2015). CityGML is an OGC standard format to store and exchange city models based on the Extensible Markup Language (XML) format, which contains 3D urban geometry description and other metadata.

An example of a workflow from the SimStadt simulation platform is the heating demand workflow, which is based on the monthly energy balance. This workflow requires three building parameters extracted from the input CityGML data: geometric data, building physics attributes, and building usage attributes. To calculate the building physics



attributes, information from the CityGML attributes *yearOfConstruction* and *function* are required. These two sets of information are then used to categorise buildings based on their type and age (Nouvel et al. 2015). Information about the age of a building is used in calculating the thermal transmittance of walls, roofs, floors, and ceiling surfaces (Agugiaro 2016; Zirak et al. 2020).

## 16.2.2 Energy Data Management

### CityGML Application Domain Extension

The possibility for CityGML to be extended through the ADE mechanism enables other information to be modelled along with the already existing real-world 3D model. Since the availability of this possibility, several pieces of information have been modelled, which includes Energy ADE and Utility Network ADE (Kolbe et al. 2011). Energy ADE extends the CityGML standard by features and properties, which are necessary to perform energy simulation and for storing the corresponding results (Gröger et al. 2012). With the objectives of managing and storing data required for calculating building energy simulation and results, Energy ADE provides a holistic approach for managing energy-related information. It can also be used not just for a detailed single-building energy simulation but also for city-wide, bottom-up energy assessments, focusing specifically on the buildings sector (Agugiaro et al. 2018). There are several applications for exploring a CityGML dataset, but most use cases have to convert the CityGML to another format such as glTF, 3D Tiles, or i3s for web visualisation. After the conversion process, the data and information linked to CityGML ADE are lost. For example, the 3D City Database (3DCityDB) has implemented ADE support into its database. However, users have to develop their mapping script for reading the ADE contents from the database and matching these datasets to the viewer format (Yao et al. 2018).

In 2015, research on storing and exchanging sensor or time-series data in the CityGML model had been conducted with a concept referred to as ‘Dynamizer’ as one of the CityGML ADE (Chaturvedi et al. 2015). It is used to model and implement the dynamic properties for semantic 3D city models. It allows representing dynamic and time-varying attributes directly in the 3D city model in CityGML format. It supports encodings of the dynamic data by Domain-Range encoding and by Time-Value pair encoding in XML format. Each CityGML model can contain several representation encodings of the dynamic data. Example use cases of using Dynamizers had been implemented to connect the dynamic properties of the building, such as heat demand or energy generation from the attached solar panels. However, there are still limitations to the use of the Dynamizers concept. For example, the data manager must have access to the 3D city model, which may prove difficult when the city model data and simulated data are managed by different parties or organisations. Also, tools for parsing supporting encoding types of the Dynamizers written in XML are needed to access the dynamic contents. The data conversion and data structures still have to be implemented in order to utilise the data efficiently.

### SensorThings API (STA)

The SensorThings API is one of the OGC standards of a protocol that unifies ways to interconnect the Internet of Things (IoT) devices, data, and applications over the web. SensorThings has two main parts which are Sensing and Tasking. The Sensing part provides an easy-to-use representational state transfer (REST) application programming interface (API) for managing the heterogeneous data. These operations include HTTP *POST*, *GET*, *PATCH*, and *DELETE* to create, read, update, and delete the sensor data and metadata, respectively (Liang et al. 2016). Recently, SensorThings API has been used by several domains. For example, SensorThings has been used as a service for managing heterogeneous air quality sensor data in the European Union Infrastructure for Spatial Information in the European Community (INSPIRE) (Kotsev et al. 2018) and managing COVID-19 statistics (Santhanavanich et al. 2020). Additionally, the SensorThings API is expandable to manage dynamic time-series datasets in the CityGML 3D city models; the systematic study on this topic was conducted by Santhanavanich and Coors (2021).

#### 16.2.3 3D Data Visualisation (Digital Globe)

The development of web applications for visualisation of 3D objects is built upon the foundation of the web technologies HTML5 and WebGL. HTML5 introduced the *canvas* element, which, when coupled with JavaScript, allows graphics to be drawn by web browsers while taking advantage of the multi-threading capability of modern browsers. WebGL extends the *canvas* element and allows for the rendering of 3D graphics without the need for plugins and extensions (Chaturvedi et al. 2015). The Cesium JavaScript library has been developed with this vision of the ‘digital earth’ in mind; it supports 3D data natively, it is able to portray massive amounts of data, and it allows users to combine heterogeneous datasets (Moore, 2018). From a technical perspective, Cesium may be described as an imperative high-level JavaScript library built on top of WebGL that provides a mapping API that is considered a suitable replacement for the now deprecated Google Earth API (Hoetmer 2014; Krämer and Gutbell 2015). In recent research, Würstle et al. (2020) have shown a proof of concept for visualising the 3D city models with the simulated energy data from SimStadt in the CesiumJS WebGL framework.

---

## 16.3 Concept

This section explains our concept for managing the simulated energy data of 3D building models using the SimStadt simulation software. Several approaches had been implemented and these are compared and evaluated in turn. These approaches include (1) computing and visualising the simulated data on the fly, (2) using the PostgreSQL database as a datastore

for the simulated energy data of 3D building models, and (3) using SensorThings for managing the simulated energy data of 3D building models.

### **16.3.1 Computing and Visualising the Simulated Energy Data of 3D Building Models on-the-Fly**

This approach uses SimStadt web service to run energy simulations using only a web browser and network connection. Therefore, this approach makes the energy analysis available through a network regardless of the operating system of the running devices. The end users on this approach define the input parameter values on an HTML (HyperText Markup Language) form and then submit them to SimStadt to run the energy analysis. SimStadt will receive these values as a request to run an energy analysis. If the process is successful, SimStadt will respond to the energy analysis request with the analysis result data in JSON format. Afterwards, the analysis result data must be extracted and mapped to fit the 3D Tiles colouring scheme so that each building in the 3D building model can be coloured based on its corresponding analysis result for the geovisualisation purpose. Mapping the result data to the 3D Tiles should be done as many times as the number of data categories for the 3D geovisualisation. In this approach, there is no mechanism to store the result data once the users stop the web-based application by closing the web browser. Therefore, in a new web session, the whole process must be repeated when a user runs an energy simulation process, even though the result for the selected building or area might be the same as the previous energy simulation request.

### **16.3.2 Using the PostgreSQL Database as a Datastore for the Simulated Energy Data of 3D Building Models**

The main aspect of this approach is the use of the database for managing the energy data and building relevant information. The 3DCityDB has an implementation for PostgreSQL, which in this approach, is used to store the 3D city models in the CityGML format. The database functions as an anchor point for the SimStadt simulation software. The SimStadt platform requires building information from the CityGML model to run its workflows. This approach allows us to keep everything up to date in a centralised way where not every file needs to be updated if it is used solely for visualisation purposes. The connection between the database and the simulation software is bidirectional. The database provides the input data to the simulation software, and the software stores its output in the database. Through the visualisation, users can update values in the database for the simulation.

### 16.3.3 Using SensorThings for Managing the Simulated Energy Data of 3D Building Models

This approach is based on the CityThings from our previous work (Santhanavanich and Coors 2021), which uses the SensorThings as a standardised specification API for managing the dynamic energy data in the 3D city models. The concept of this approach is to precalculate the energy-related data of the 3D city models with SimStadt. Then, the JSON result from SimStadt is constructed to conform with the SensorThings and its entities' specification. The produced JSON result is then added or updated to the SensorThings server with the HTTP *POST* or *PATCH* operations, respectively. On the client-side, users can directly request the energy data of each 3D building in JSON format from the SensorThings server with the HTTP *GET* request. This result of energy data is used to map to the 3D city models for the data visualisation.

---

## 16.4 Implementation

The implementations of this research are based on the 3D city models in the CityGML format. First, the building simulations were performed in the SimStadt simulation platform based on these CityGML building models (see Sect. 16.4.1). Second, three different approaches for managing the energy-related result from SimStadt and distributing to the web clients were conducted (see Sect. 16.4.2). Finally, the 3D building models with energy data were visualised on the web-based clients for each data management approach. The implementations of each approach in this paper are described in Fig. 16.1.

After servers had been implemented according to the three mentioned approaches, a 3D web application had been developed to present the result data by colouring the building roofs using the data and also showing them in an informative table (see Fig. 16.2). This table is displayed when users select a particular roof in the application. The building roofs are symbolised in different colours based on six different result data, where users can switch between to have a more intuitive result, which should help users to interpret the result data. These result data are PV potential yield, PV specific yield, levelised cost of electricity, total investment, discounted payback period, and financial feasibility.

### 16.4.1 Energy Simulation of the 3D Building Models with SimStadt Software

This study uses SimStadt to simulate the buildings' PV potential and heat demand analysis to demonstrate the management of the dynamic data from a building energy analysis. The 3D building model is the basis of the calculation in SimStadt. SimStadt extracts the geometric and semantic data from the CityGML of the observed area for the simulation process. Furthermore, it also requires the local weather data of the observed area on an

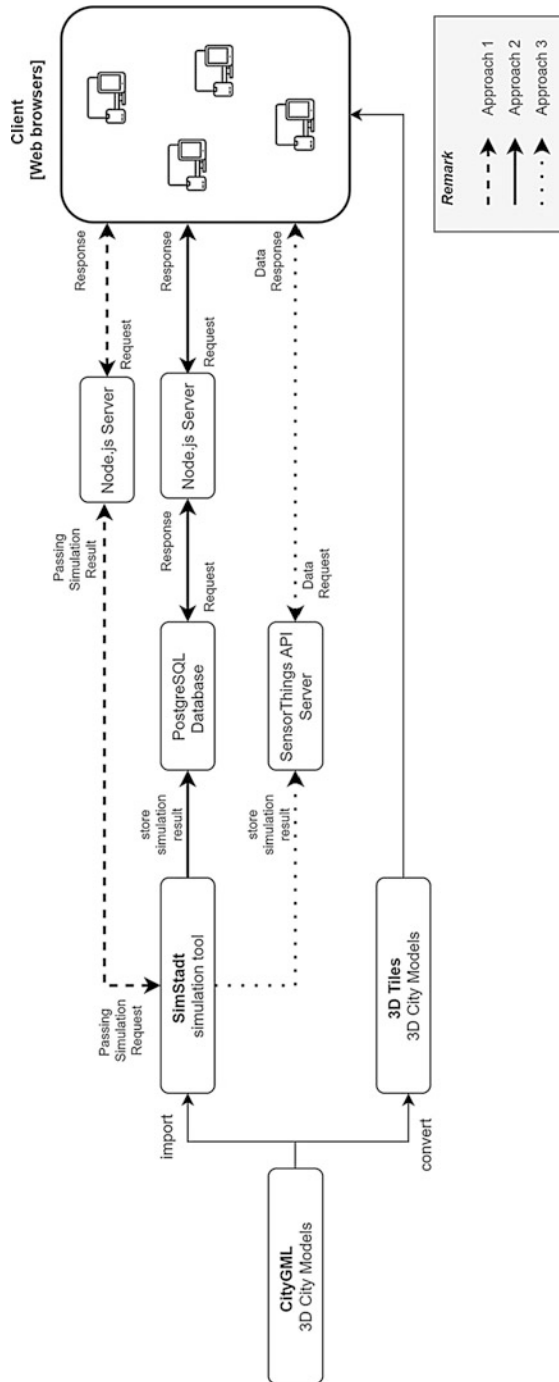
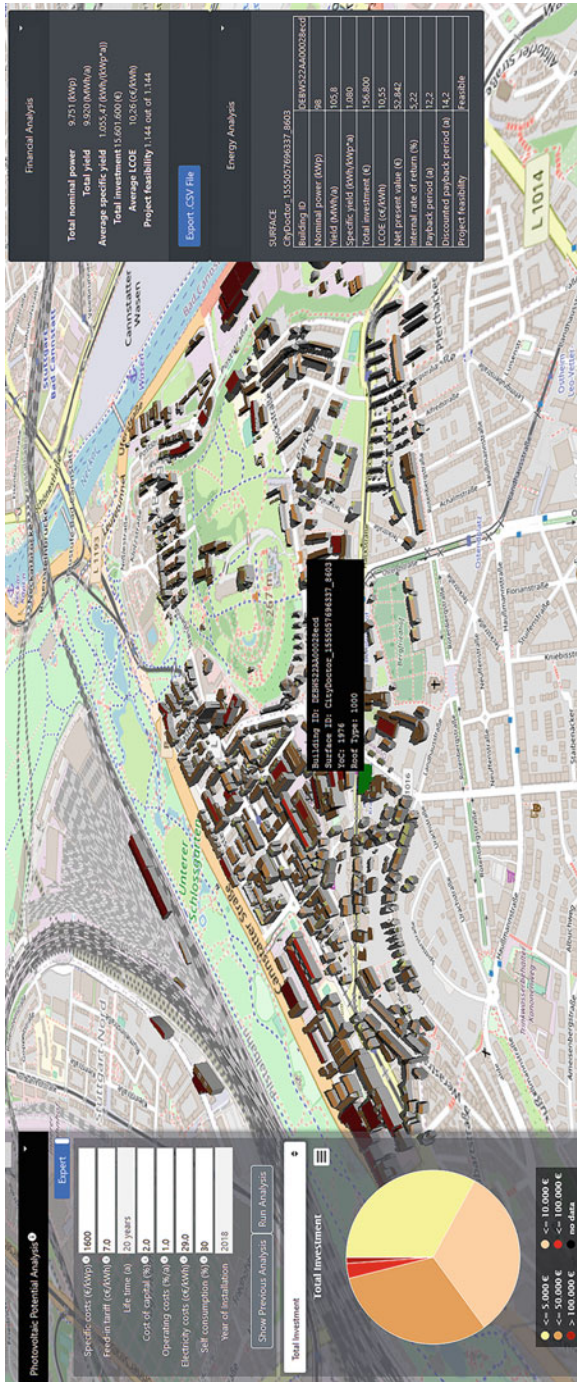


Fig. 16.1 Overall system architecture



**Fig. 16.2** A 3D web application for visualising the 3D building models in the area of Stöckach, Stuttgart with the simulated total investment cost to install PV system using SimStadt simulation API

hourly and monthly basis, including ambient temperature, relative humidity, horizontal global, and diffuse radiations, which can be imported from a third-party data provider (e.g. PVGIS, Insel) or weather data files (Meteonorm). In the on-the-fly approach (see Sect. 16.3.1) and the SensorThings approach (see Sect. 16.3.3), we simulated buildings' PV potential and the financial feasibility of the photovoltaic system in Stöckach, a city quarter of Stuttgart, Germany. We implemented the approach with database (see Sect. 16.3.2) by simulating buildings' heat demand of Ludwigsburg, Germany.

## 16.4.2 Managing Simulated Energy Data of 3D Building Models

### Approach 1: Managing Simulated Energy Data of 3D Building Models on-the-Fly

In this approach, users are asked to define the mandatory input parameters on the 3D web platform. Afterwards, the system translates the user-defined input values into a web service request to SimStadt to perform a PV potential and feasibility simulation based on the user-defined input values. Upon a successful simulation process, SimStadt sends back the simulation result data in JSON format. This result consists of 125 roof surfaces, and each surface has 38 name/value pairs consisting the roof details, such as building ID, surface ID, coordinate, azimuth, tilt, and PV potential and feasibility analysis-related details, such as PV potential yield, irradiance on roof plane from January until December, total investment, maintenance costs, and financial feasibility.

### Approach 2: Managing Simulated Energy Data of 3D Building Models Using a Database

This approach uses three main components. The main part of this approach is the database which is a PostgreSQL implementation as illustrated in Fig. 16.1. The 3DCityDB can import CityGML building models to the database using a 3DCityDB Importer tool. A tool was created to add the energy-related data to the database. The supported SimStadt workflows for this approach are solar potential and energy demand. The energy demand workflow consists of six individual modules. To connect from SimStadt to the database, the workflow needs to be extended. The third module in this workflow is a preprocessing step where the model is prepared for the further calculations which are done in the following modules. The specifically programmed extension is used after the last preprocessing step and before the first calculation step.

### Approach 3: Managing Simulated Energy Data of 3D Building Models Using OGC SensorThings API

This approach uses SensorThings as a standard interface to manage and distribute the simulated energy data of 3D building models. This includes the installation of the SensorThings on the server following by the data modelling based on the entities model of the SensorThings standard specification. Then, the data and metadata of the simulation

tool and simulation result are stored to the SensorThings with the SensorThings Manager tool (STA Manager). Finally, the testing is conducted before sharing and connecting the SensorThings to the clients.

The simulation result from the SensorThings can be requested by any client through the HTTP *GET* request according to the SensorThings standard specification in the standard document (Liang et al. 2016) with the CityThings concept (Santhanavanich and Coors 2019). For the visualisation, the 3D city models in 3D Tiles format were loaded in the CesiumJS-based application. These 3D Tiles models preserved the *gml\_id* attributes as identification of each building. Accordingly, clients can request for all dynamic contents of each building by specifying the *gml\_id* of the CityGML building model.

---

## 16.5 Evaluation

This research evaluates and compares three different approaches for managing the energy-related data of the 3D city models including (1) managing building simulation data on-the-fly (via simulation API), (2) managing building simulation data using a database, and (3) managing building simulation data using OGC SensorThings API standard. Several features in aspects of data visualisation on the web client and data organisation had been conducted (see Table 16.1).

In the first approach, the simulation is done on-the-fly in real time. The main advantage of this approach over other approaches is that users can input the parameters for the building energy simulation every time they use the application. However, as the simulated data is not stored anywhere, the energy simulation process is always triggered every time users visualise the energy data, which costs the server computation and user payload.

In the second approach, the regular database is used for storing and distributing the energy-related data of the building models. This provides an advantage when storing large-scale building data. Also, the simulation data can be loaded to the client in a very short time as the simulation data is pre-calculated on the server-side. However, as there is no interface to get the data from the database, it needs a programming tool to connect a client to the database level, which this process has to be repeated when applying to a new use case. Another obvious drawback is that users cannot input the parameters to calculate specified simulation scenarios on-the-fly. To deal with this, several simulation scenarios can be pre-calculated with a trade-off for the storage requirement on the database.

In the last approach, the SensorThings API specification is implemented on the server-side for managing the energy-related data of the building models in which each *Thing* entity is linked to the particular CityGML part by the CityThings concept (Santhanavanich and Coors 2021). As the backend of the SensorThings server is the database, it supports large-scale building energy data transaction. In this approach, users can request, add, update, or delete energy data of the building models from the database through the SensorThings interface, which is a standardised specification from OGC (Liang et al. 2016). Accordingly, the data managed by SensorThings can be distributed widely for



**Table 16.1** The overview feature comparison of three different approaches for organising the building simulation data

Data management Features		Managing simulated energy data of 3D building models on-the-fly	Managing simulated energy data of 3D building models using a database	Managing simulated energy data of 3D building models using OGC SensorThings API
Data visualisation visualization	User interface for visualising building simulation on the web client	Users can input any parameters or scenarios on-the-fly	Users can only select pre-simulated scenarios	Users can only select pre-simulated scenarios
	User loading time for visualising building simulation	~20–30 s per 100 buildings	~1 to 2 s per 100 buildings	~1 to 2 s per 100 buildings
Data organisation	Support data storage in the database	–	Supported	Supported
	Management of the multiple building simulation scenarios in the database	–	Manually manage with an additional application layer, e.g. node.js server	Organised by SensorThings data model in the <i>Datastream</i> entity
	Role-based data access to the simulation data	–	Accessible only to the database administrators. Role-based access control can be extended	Different authentication roles can be given to users (read, write, update, delete, and admin)
	Interface to access, add, update, and delete the data in the database	–	Manually manage with an additional application layer, e.g. Node.js server	Users with appropriate roles can access, add, update, and delete data through the REST-based protocol
	Building simulation data distribution	–	The API to allow data access can be extended. The API document must be added	The data can be access through SensorThings interface. The standard API document is provided by OGC

several client applications with the SensorThings interface without the need for the dynamic web server to access the database. Although it lacks flexibility for user's specified parameters, several simulation scenarios can be performed and updated to the SensorThings server effectively through the HTTP *POST* method. Compared to the CityGML ADE, SensorThings manages the energy data independently, and there is no need for modifying the existing CityGML XML schema for the energy data. Moreover, the SensorThings has the JSON-based encoding, and its interface supports queries through the HTTP *GET* request, which includes result sorting, result filtering, and geolocation filtering. Still, the data modelling of the energy data to the SensorThings schema is not straightforward, since the characteristic of dynamic data from an energy simulation is different from the ones from IoT devices. Therefore, the mapping must be carefully designed in order to reach optimal usage.

---

## 16.6 Conclusion

CityGML models are used in several domains and locations around the world. In the context of the building energy demand and PV potential simulation, the CityGML ADE had been developed to handle the simulation result. However, there is still a lack of open-source tools and platforms to manage and distribute data efficiently. In this article, we present a way to bridge these gaps by evaluating and comparing three alternative approaches for managing the building energy simulation data, including (1) managing simulation data on-the-fly (via simulation API), (2) managing simulation data using a database, and (3) managing simulation data using OGC SensorThings API standard. The three implementations were assessed comparatively in the use cases of heat demand and PV potential analysis in cities in Germany, including Stöckach-Stuttgart, Ludwigsburg, and Grünbühl. The evaluation of these three approaches is discussed in Chap. 5. In summary, each approach discussed in this research has advantages and disadvantages that can effectively influence which approach will be selected by researchers or application developers.

The first approach would give users the flexibility to simulate the building energy demand and potential with user-specified parameters in which the high-performance computation power is needed on the server-side. However, in the second and third approaches, the database is used to store the simulated result in advance, in which high disk space on the server is required to store several simulation scenarios. Comparing the regular database and the SensorThings for storing the simulated result, the SensorThings shows advantages of flexibility, allowing users with multiple roles to read, add, update, and delete the data with the standardised request protocol. Accordingly, using SensorThings is more efficient and effective in terms of data management and data distribution. In conclusion, the integration of the SimStadt API service for simulating results on-the-fly and the SensorThings API for managing pre-simulated results is recommended to enable most benefits to store and visualise the energy analysed data in the smart cities' application.

## References

- Agugiaro, G., Benner, J., Cipriano, P., & Nouvel, R. (2018). The Energy Application Domain Extension for CityGML: enhancing interoperability for urban energy simulations. *Open Geospatial Data, Software and Standards*, 3(1). <https://doi.org/10.1186/s40965-018-0042-y>
- Arroyo Ohori, K., Biljecki, F., Kumar, K., Ledoux, H., & Stoter, J. (2018). Modeling Cities and Landscapes in 3D with CityGML. In A. Borrmann, M. König, C. Koch, & J. Beetz (Eds.), *Building Information Modeling* (pp. 199–215). Springer International Publishing. [https://doi.org/10.1007/978-3-319-92862-3\\_11](https://doi.org/10.1007/978-3-319-92862-3_11).
- Biljecki, F., Stoter, J., Ledoux, H., Zlatanova, S., & Çöltekin, A. (2015). Applications of 3D City Models: State of the Art Review. *ISPRS International Journal of Geo-Information*, 4(4), 2842–2889. <https://doi.org/10.3390/ijgi4042842>.
- Biljecki, F., Kumar, K., & Nagel, C. (2018). CityGML Application Domain Extension (ADE): overview of developments. *Open Geospatial Data, Software and Standards*, 3(1). <https://doi.org/10.1186/s40965-018-0055-6>.
- Agugiaro, G. (2016). Energy planning tools and CityGML-based 3D virtual city models: experiences from Trento (Italy). *Applied Geomatics*, 8(1), 41–56. <https://doi.org/10.1007/s12518-015-0163-2>.
- Chaturvedi, K., Yao, Z., & Kolbe, T. H. (2015). Web-based Exploration of and interaction with large and deeply structured semantic 3D city models using HTML5 and WebGL. In *Bridging Scales-Skalenübergreifende Nah-und Fernerkundungsmethoden*, 35. Wissenschaftlich-Technische Jahrestagung der DGPF.
- European Commission. (2020). Smart cities: Cities using technological solutions to improve the management and efficiency of the urban environment. [https://ec.europa.eu/info/eu-regional-and-urban-development/topics/cities-and-urban-development/city-initiatives/smart-cities\\_en](https://ec.europa.eu/info/eu-regional-and-urban-development/topics/cities-and-urban-development/city-initiatives/smart-cities_en). Accessed 14 September 2020.
- Gröger, G., Kolbe, T.H., Nagel, C. & Häfele, K.-H. (2012). OGC City Geography Markup Language (CityGML) Encoding Standard. Version:2.0.0. OGC 12-019. <http://www.opengis.net/spec/citygml/2.0>. Accessed 2 Nov. 2018.
- Hoetmer, K. (2014) *Announcing deprecation of the Google Earth API*. <https://mapsplatform.googleblog.com/2014/12/announcing-deprecation-of-google-earth.html>. Accessed 14 September 2020.
- Jawhar, I., Mohamed, N., & Al-Jaroodi, J. (2018). Networking architectures and protocols for smart city systems. *Journal of Internet Services and Applications*, 9(1). <https://doi.org/10.1186/s13174-018-0097-0>.
- Kolbe, T. H., König, G., & Nagel, C. (Eds.). (2011). *Lecture Notes in Geoinformation and Cartography. Advances in 3D Geo-Information Sciences*. Springer Berlin Heidelberg. <https://doi.org/10.1007/978-3-642-12670-3>
- Kotsev, A., Schleidt, K., Liang, S., van der Schaaf, H., Khalafbeigi, T., Grellet, S., Lutz, M., Jirka, S., & Beaufils, M. (2018). Extending INSPIRE to the Internet of Things through SensorThings API. *Geosciences*, 8(6), 221. <https://doi.org/10.3390/geosciences8060221>.
- Krämer, M., & Gutbell, R. (2015). A case study on 3D geospatial applications in the web using state-of-the-art WebGL frameworks. In *Proceedings of the 20th international conference on 3d web technology* (pp. 189–197). <https://doi.org/10.1145/2775292.2775303>.
- Liang, S., Huang, C. & Khalafbeigi, T. (2016). OGC SensorThings API Part 1: Sensing. <http://www.opengis.net/doc/is/sensorthings/1.0>. Accessed 11 August 2020.
- Lim, J., Janssen, P., & Biljecki, F. (2020). VISUALISING DETAILED CITYGML AND ADE AT THE BUILDING SCALE. *ISPRS - International Archives of the Photogrammetry, Remote Sensing and Spatial Information Sciences*, XLIV-4/W1-2020, 83–90. <https://doi.org/10.5194/isprs-archives-XLIV-4-W1-2020-83-2020>.

- Monsalvete, P., Robinson, D., & Eicker, U. (2015). Dynamic Simulation Methodologies for Urban Energy Demand. *Energy Procedia*, 78, 3360–3365. <https://doi.org/10.1016/j.egypro.2015.11.751>.
- Moore, V. (2018). Revisiting The Digital Earth. <https://cesium.com/blog/2018/01/31/digital-earth-revisited/> Accessed 14 September 2020.
- Nouvel, R., Brassel, K. H., Bruse, M., Duminil, E., Coors, V., Eicker, U., & Robinson, D. (2015). SimStadt, a new workflow-driven urban energy simulation platform for CityGML city models. In *Proceedings of International Conference CISBAT 2015 Future Buildings and Districts Sustainability from Nano to Urban Scale* (pp. 889–894).
- Schumacher, J. (2020). INSEL 8: Software for simulation, monitoring, and visualisation of energy systems. <https://www.insel.eu/en/what-is-insel.html>. Accessed 17 August 2020.
- T., Santhanavanich C., Kim V., Coors (2020) INTEGRATION OF HETEROGENEOUS CORONAVIRUS DISEASE COVID-19 DATA SOURCES USING OGC SENSORTHINGS API. *ISPRS Annals of the Photogrammetry Remote Sensing and Spatial Information Sciences VI-4/W2-2020*135-141 10.5194/isprs-annals-VI-4-W2-2020-135-2020
- Thunyathep, Santhanavanich Volker, Coors (2021) CityThings: An integration of the dynamic sensor data to the 3D city model. *Environment and Planning B: Urban Analytics and City Science* 48(3) 417-432 10.1177/2399808320983000
- Würstle, P., Santhanavanich, T., Padsala, R., & Coors, V. (2020). The Conception of an Urban Energy Dashboard using 3D City Models. In *Proceedings of the Eleventh ACM International Conference on Future Energy Systems* (pp. 523–527). ACM. <https://doi.org/10.1145/3396851.3402650>.
- Yao, Z., Nagel, C., Kunde, F., Hudra, G., Willkomm, P., Donaubaauer, A., Adolphi, T., & Kolbe, T. H. (2018). 3DCityDB - a 3D geodatabase solution for the management, analysis, and visualisation of semantic 3D city models based on CityGML. *Open Geospatial Data, Software and Standards*, 3(1). <https://doi.org/10.1186/s40965-018-0046-7>.
- Yi, J. S., Kang, Y. A., Stasko, J. T., & Jacko, J. A. (2008). Understanding and Characterising Insights: How do people gain insights using information visualisation?. In *Proceedings of the 2008 Workshop on BEyond time and errors: novel evaluation methods for Information Visualization* (pp. 1-6).
- Zirak, M., Weiler, V., Hein, M., & Eicker, U. (2020). Urban models enrichment for energy applications: Challenges in energy simulation using different data sources for building age information. *Energy*, 190, 116292. <https://doi.org/10.1016/j.energy.2019.116292>.

**Open Access** This chapter is licensed under the terms of the Creative Commons Attribution 4.0 International License (<http://creativecommons.org/licenses/by/4.0/>), which permits use, sharing, adaptation, distribution and reproduction in any medium or format, as long as you give appropriate credit to the original author(s) and the source, provide a link to the Creative Commons license and indicate if changes were made.

The images or other third party material in this chapter are included in the chapter's Creative Commons license, unless indicated otherwise in a credit line to the material. If material is not included in the chapter's Creative Commons license and your intended use is not permitted by statutory regulation or exceeds the permitted use, you will need to obtain permission directly from the copyright holder.





# Deep Learning Methods for Extracting Object-Oriented Models of Building Interiors from Images

# 17

Lars Obrock and Eberhard Gülch

## Abstract

In this chapter, we present an approach of enriching photogrammetric point clouds with semantic information extracted from images of digital cameras or smartphones to enable a later automation of BIM modelling with object-oriented models. Based on the DeepLabv3+ architecture, we extract building components and objects of interiors in full 3D. During the photogrammetric reconstruction, we project the segmented categories derived from the images into the point cloud. Based on the semantic information, we align the point cloud, correct the scale and extract further information. The combined extraction of geometric and semantic information yields a high potential for automated BIM model reconstruction.

## Keywords

Semantic modelling · BIM · Point clouds

## 17.1 Introduction

The digitalisation of the building sector is progressing steadily. Object-oriented models in BIM (building information modelling) are the central elements and represent the entire life cycle of a building, from planning and operation to demolition. In addition to the 3D

---

L. Obrock (✉) · E. Gülch  
Hochschule für Technik Stuttgart, Stuttgart, Germany  
e-mail: [lars.obrock@hft-stuttgart.de](mailto:lars.obrock@hft-stuttgart.de)

© The Author(s) 2022  
V. Coors et al. (eds.), *iCity. Transformative Research for the Livable, Intelligent, and Sustainable City*,  
[https://doi.org/10.1007/978-3-030-92096-8\\_17](https://doi.org/10.1007/978-3-030-92096-8_17)

267

component and object geometries, they also contain all relevant semantic information. However, the introduction of BIM is currently taking place almost only in the planning of new buildings (greenfield). Due to the very high complexity of manual data acquisition and processing, the recording of already existing buildings (brownfield) as BIM models has been a minor topic so far. Developing an automatic extraction of the necessary information yields a high potential at simplifying the creation of such “As-Build” or “As-Is” models and thus the possibility to make them widely available. Creating these models requires three-dimensional data. We consider photogrammetry as a very suitable method to not only capture and reconstruct buildings as point clouds of high quality but also to extract further semantic information out of these images. Image information is acquired indoor and outdoor and can be merged with point cloud data from mobile laser scanning devices.

We present our general workflow for modelling interior and exterior parts of a building to derive 3D geometries and semantic information. Then we focus on details of our developed theory and the implemented approach to provide both semantic and geometric information for the case of interior rooms. The results in real-world scenes are analysed and an outlook for further developments is given.

---

## 17.2 Related Work

Building information modelling is a major focus of the digital transformation of the building sector. With the *Stufenplan Digitales Planen und Bauen*, the Federal Ministry of Transport and Digital Infrastructure gradually introduced the BIM method into the planning processes of public infrastructure (Bramann et al., 2015a). In Germany, its implementation is taking place supported by guidelines and investigation mainly focusing on its introduction and execution in various disciplines, e.g. Egger et al. (2013), Eschenbruch et al. (2014), Kaden et al. (2019) and Bramann et al. (2015b).

A reconstruction of existing buildings as three-dimensional BIM models is possible using measurements of geodetic instruments (Borrmann et al., 2015) or (Clemen and Ehrich, 2014). The increased demand of geometric three-dimensional data and additional semantic information of a BIM model is mostly ignored. In consequence, the acquisition and modelling of measurement data is highly complex and requires a large expenditure of time and money.

The whole field of deep learning has become a major focus of research in recent years. Especially computer vision based on convolutional neural networks progressed a lot since Krizhevsky et al. (2012) were able to achieve great improvements in image classification. Many approaches aim at further development and improvement of reached accuracies, e.g. Szegedy et al. (2015), Simonyan and Zisserman (2015) and Huang et al. (2017). In addition to the pure classification of entire images, the idea of localising the detected class in the image also gained a lot of interest. Two different approaches have emerged for this purpose. Object detection, as presented in Ren et al. (2015), uses bounding boxes to locate and classify objects. Even more precise, the semantic segmentation classifies every pixel of

an image. As the resolution of the input images is retained, this method is very well suited to project the extracted semantic information into a point cloud.

One of the first popular networks was by Long et al. (2015), which was named fully convolutional network (FCN). In Obrock and Gülch (2018), our first approach to automatically generate a semantically enriched point cloud from mobile sensors was based on the application of deep learning for segmentation of eight interior building components and objects using an FCN. In Gülch and Obrock (2020), we were able to verify that the combination of photogrammetry and deep learning is a solid approach to generate a semantically enriched point cloud of interiors now using DeepLabv3+ (Chen et al., 2018). In consequence, the components and objects can be differentiated very well in the point cloud.

In this contribution, we relate our recent developments in this approach to our overall designed framework and show updated results with further improved quality.

---

## 17.3 Methodology

### 17.3.1 Overview

Images are the main component of our approach because of the massive amount of information contained in them. They are the input for the photogrammetric point cloud generation and the extraction of objects based on deep learning methods. In addition, we include point clouds from low-cost mobile laser scanning devices in interior rooms to provide point cloud information in areas where walls and room parts are very homogeneous and do not allow reliable point cloud derivation from imagery. For exterior parts, we rely on photogrammetry only, as low-cost mobile laser scanning devices have limited range of acquisition. We have developed a strategy as shown in Fig. 17.1 to combine interior and exterior parts of a building to, e.g. estimate wall dimensions. To link exterior and interior, we focus on doors and windows and have developed acquisition strategies for the different building parts using different sensors. We integrate point clouds and align them to get the geometric 3D information. We derive semantic information from imagery and point clouds, and we basically use the same methods for interior and exterior parts; however, the type of classes and thus object parts differ. In this contribution, we will only concentrate on the semantic segmentation of interior rooms.

### 17.3.2 Workflow for Reconstructing Interior Rooms Based on Image Data and Deep Learning

Details of our approach of interior rooms are given in Fig. 17.2. We use DeepLabv3+ as the architecture of our neural network to segment components and objects of interiors visible in

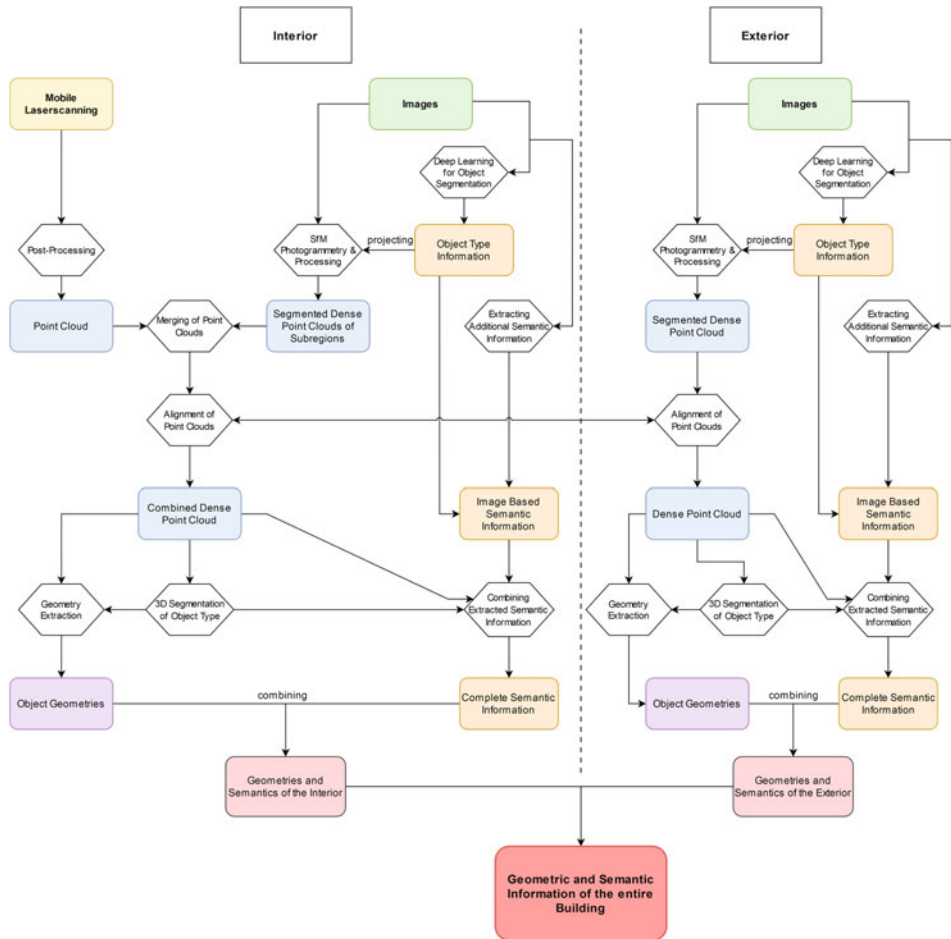


**Fig. 17.1** Methodology to acquire geometric and semantic information for interior and exterior parts of a building using images from cameras and point clouds from mobile laser scanning

the images at pixel level. And network backbone xception 65 is used. The training of the model is conducted using manually segmented ground truth data.

The trained model then is used for inference on the images of an exemplary room. The images also are used to generate a point cloud using photogrammetry. Afterwards, the category information stored in the RGB values of the segmented images is transferred in the point cloud by projection based on the determined camera parameters. Ideally, the result would be a classified point cloud, but because of interpolation, the points cannot be clearly assigned to the categories. Therefore, an additional step is taken to reclassify them. By using the clearly classified point cloud as input for further post-processing, we are able



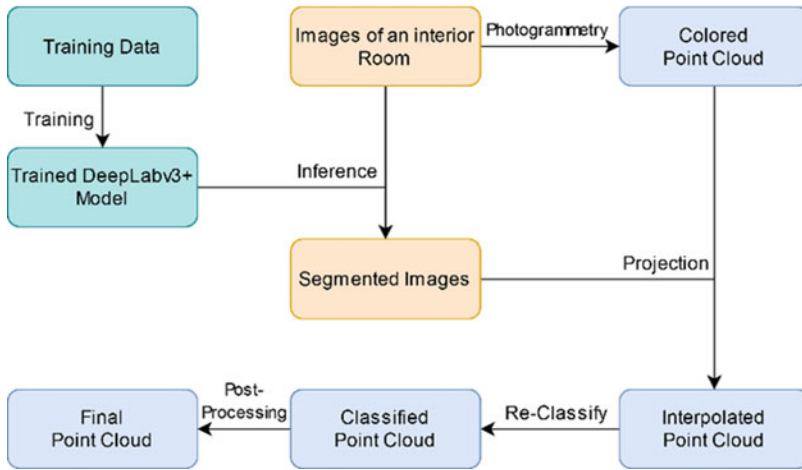


**Fig. 17.2** Detailed workflow for semantic and geometric generation of interior rooms

to automatically correct the rotation and scale, as well as extract additional information like floor, ceiling and wall planes.

We are testing our approach on two rooms, an office and a computer laboratory.

## 17.4 Semantic Segmentation of Interiors

A comprehensive and high-quality segmentation of all the important building components and objects visible in the images is our basic source of information. It is of essential importance for a complete reconstruction of an existing building. The current object categories include 25 components and objects important for a great variety of interiors (Table 17.1). Because the category “Wall” had to be excluded due to negative effects on the segmentation quality, the model was trained for extracting 24 categories and a “Background” class of unclassified objects.

An extensive training data set was created for training the neural network. It is based on nearly 300 images and the corresponding manually segmented ground truth annotations and was expanded to almost 18,000 unique images using data augmentation.

Based on a pre-trained model, the training was conducted using fine-tuning.

The resulting trained neural network is used for inferencing the images of the two rooms. In an additional post-processing step, some small, random areas, which are partially present in the segmentations but do not relate to any real object, are filtered out.

As shown in Fig. 17.3, we can obtain rather good results, despite the complexity of the categories. Some of the categories, especially the ones covering large areas, have a high consensus. Errors are occurring where objects resemble each other too closely, like the feet of the “Table” and “Chair”. It is also noticeable that unique objects are segmented more

**Table 17.1** Overview over 25 object categories of interiors

Room forming components	Connecting components	Fixed objects of interest		Movable objects of interest
Floor	Door	Light switch	Socket	Poster
(Wall)	Window	Lamp	Pillar	Bookshelf
Ceiling		Heater	Pipe	Carpet
		Stairs	Railing	Cabinet
		Sink	Toilet	Chair
		Cable trunking	Fire alarm	Table
		Fire alarm siren		Fire extinguisher

Our model was trained for 24 classes plus a “Background” class of unidentified objects. The category “Wall” was excluded from training

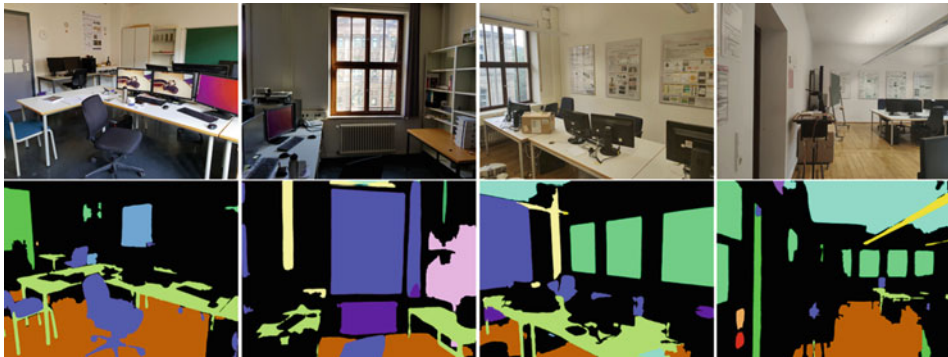


**Fig. 17.3** Exemplary results of our trained DeepLabv3+ model inferring the images of the office room (2× upper left) and the laboratory (2× upper right) captured using one camera each. The bottom row shows the segmented categories of each image

precisely than plain and uniform areas like “Ceiling”, in which some holes occur. Small objects like “Light switch” and “Socket” are mostly well segmented depending on the angle and distance at which they are imaged.

## 17.5 Classified Point Cloud

With BIM models as our target, we need to transfer the two-dimensional semantic information from the images into three dimensions. Using photogrammetry and digital image matching, the original images of both rooms build the basis to create three-dimensional, semantically enriched point clouds using Agisoft Metashape (Agisoft, 2020).

To project the category information stored in the RGB value combinations of the segmented images into the point clouds, the determined camera position and rotation are used.

The resulting point clouds are proofing the feasibility of our concept of an automatic generation and category projection. Despite the visible noise of the point clouds, the rooms are captured rather good. However, there are missing areas, often at the large and uniform components like walls and especially the ceiling, where the point cloud generation was problematic.

---

## 17.6 Reclassifying the Point Cloud

The colour values of the individual points are derived by interpolation of the overlapping values in the individual images (cf. Fig. 17.4). If their camera orientations in three-dimensional space are inaccurate or if the segmentations do not match, the interpolation results in erroneous values in the generated points (e.g. at the door).

To get a clear assignment of the categories, a reclassification of the point cloud is carried out by looking at the colours of the individual points in three-dimensional space and determining their Euclidean distance to the colour values of the individual categories. Additionally, the distances of the colour values of a point to those colour values are calculated, which result from the interpolation of a category with “Background” points as the most common class. If the distances to one of these are smaller than a threshold value, a direct assignment to the corresponding category is made.

In case that these criteria are not fulfilled, the neighbourhood of the points is examined for the assignment of the categories. If still no categories can be determined by distance and neighbourhood investigations, they are listed as an undefined “Background” point. The point clouds resulting from this step now contain clearly assigned categories for each point as shown in Fig. 17.5.

Due to the overlapping of many segmented images, individual segmentation errors rarely influence the final classification of the point cloud. Incorrect category assignments mostly occur if there are systematic errors in the segmented images, the camera positions and rotations are inaccurate or the point cloud has deficiencies.

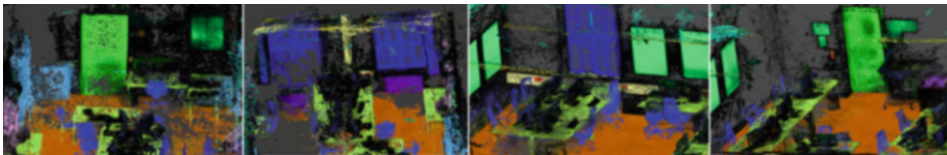


**Fig. 17.4** Different views of the generated point clouds after the projection. There is no clear distinction of categories possible, as the colours changed through interpolation

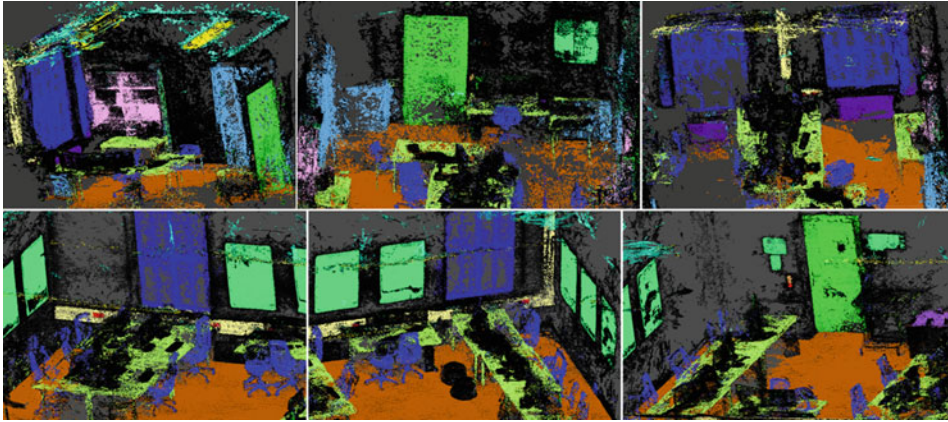


**Fig. 17.5** Different views of the reclassified point clouds. A sharp distinction between categories is now visible

## 17.7 Quality Analysis of the Point Clouds

In Table 17.2 the quality results are shown. They are based on the comparison with manually segmented copies of each point cloud and enable us to extract data about the accuracy (ratio of correctly classified points of each category) and mean intersection over union (mIoU) of the categories present in both rooms. The overall good quality of the classification is confirmed by the mIoU with a value of 54.2%. This also applies for the calculated mean accuracy of 62.3%, which is showing a high consensus of the ground truth points.

Individual IoU numbers range from low values of “Light switch” to high values of “Door”. Especially bigger objects seem to be classified very good. The categories of “Socket” with 19.3% and “Light switch” with 6.5%, which represent very small objects, only achieve a low IoU in the point cloud. Partly contrary to this, the accuracy of “Light switch” is reaching a much better value with 48.9%. This is due to a comparatively high amount of interpolated and then wrongly assigned colours which belonged to points of the floor. Because the number of actual points of “Light switch” is small, these wrongly assigned points have a huge influence on the IoU.

Despite these minor effects, it is clearly visible that through projection and reclassification of the categories in the point clouds, a high quality of classification is reached.

**Table 17.2** Calculated intersection over union (IoU) and accuracy of the objects present in the rooms

	Mean	Background	Floor	Door	Window	Light switch	Socket	Lamp	Heater	Poster	Cable trunking	Cabinet	Ceiling	Bookshelf	Table	Chair
IoU	<b>54.2</b>	62.8	77.9	78.5	77.4	6.5	19.3	52.3	64.3	74.6	40.7	67.7	55.9	38.4	42.9	53.5
Accuracy	<b>62.3</b>	93.9	79.7	84.9	88.7	48.9	19.7	54.5	68.6	76.4	42.1	70.4	57.6	38.8	48.5	61.4

## 17.8 Automated Post-processing

To relate our reclassified point clouds to the real world, we need a post-processing step. Since the point cloud was generated fully automatically and without the use of control points, neither its rotation in space nor its scale correspond to the real conditions. Extracting these is, however, possible based on our generated semantic information.

The points segmented as ground are used as basis and incorrectly classified points are filtered out. From the remaining selected points, the ground plane is derived. Then the point cloud is shifted to the origin and rotated in an iterative process until the ground plane is aligned horizontally. Next, the ceiling plane is determined from the corresponding points segmented as ceiling.

Subsequently, wall planes and wall points are extracted from the point cloud as they could not be considered in the segmentation. This is achieved based on a top view heat map created from the unclassified “Background” points of the point cloud, where the pixel values are based on the numbers of existing points of a grid. When viewed in two dimensions, an accumulation of points is to be expected especially on walls, as they are the vertically limiting elements of the rooms (Fig. 17.6).

The probable angles of the walls are extracted based on the most prominent lines determined by a Hough transform algorithm and then transferred into three-dimensional planes. Previously uncategorised points close to these are classified as wall and their actual best-fit planes are determined.

To achieve a correct scale for the point clouds, the dimensions of an object in the real world and a segmented object in the point cloud have to be adjusted. As an object of comparison, especially doors have proven to be well suited. Because the point clouds are correctly aligned, the height of objects can easily be extracted from its minimum and maximum values and is therefore used for comparison. The resulting scale is used to adjust the point cloud (Fig. 17.7).

When using the scaled point cloud for comparison, the extracted distances are matching the measured real distances often pretty well as shown in Table 17.3.

The extracted walls, floor and ceiling planes, automatically derived entirely from data, represent the room geometry in its basic features.

With our investigations and the solutions based on them, we have taken further important steps to enable automated BIM-compliant modelling of existing buildings.

---

## 17.9 Conclusions

In this paper, we present our methodology for automating BIM model generation from images and mobile laser scanning. We were able to verify that the combination of photogrammetry and deep learning is a solid approach to generate semantically enriched point clouds of interiors. The combined extraction of geometric and semantic information based on segmentation with DeepLabv3+ and projection into the photogrammetric point

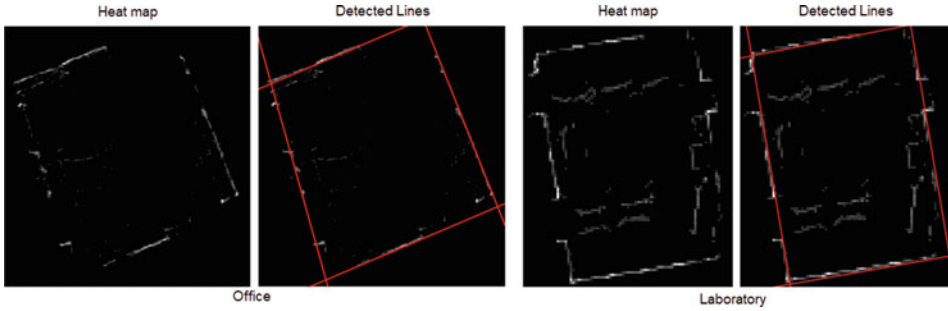


**Fig. 17.6** Derived heat maps of both rooms used to extract the most prominent lines using Hough transform algorithm

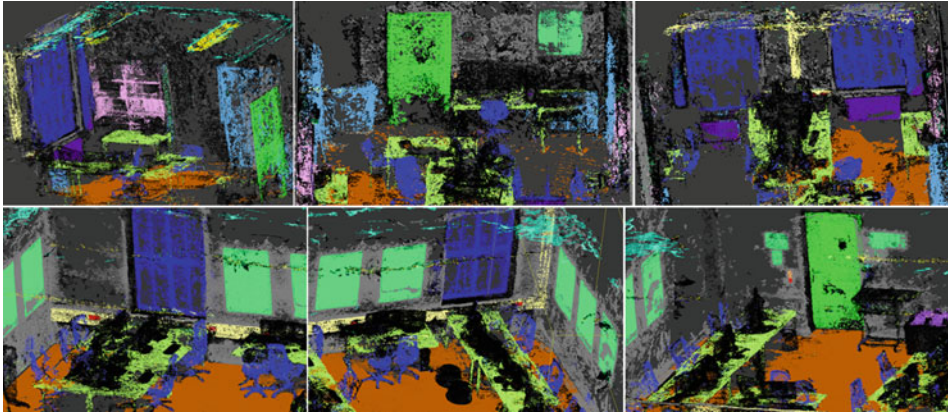


**Fig. 17.7** Different views of the post-processed final point cloud. Rotation and scale are corrected. Extracted wall point is visible in the point cloud in light grey colour

**Table 17.3** Comparison of measurements of objects in the real world to their counterparts in the scaled point cloud

		Real world (cm)	Point cloud (cm)
Office	Height table	72.3	72.1
	Width cabinet	110.0	108.9
Laboratory	Width poster	85.5	84.6
	Height window	201.2	196.9

clouds achieves good results. In consequence, the components and objects can be differentiated very well in the point clouds. The reached mIoU of 54.2% for the classified point cloud confirms the good quality of this approach. Additional important information essential for a BIM model can be extracted by analysing and post-processing the point cloud.

As shown in the methodology, it is planned to extend this approach to the combination and joint processing of several rooms as well as including mobile laser scanners. With the methods presented here, we have created a solid basis for the acquisition and modelling of semantic and geometric information of interiors for BIM models towards their automated reconstruction.

**Acknowledgements** The project “iCity: BIM-konforme Gebäudeerfassung” is sponsored by the Federal Ministry of Education and Research (BMBF) under the promotion code 13FH9E01IA and supervised by the project executing organisation VDI Technologiezentrum GmbH for the BMBF. The responsibility for the content lies with the authors.

---

## References

- Agisoft, 2020. Agisoft Metashape. <http://www.agisoft.com/> (30 September 2020).
- Borrmann, A., König, M. Koch, C., Beetz, J., 2015. Building Information Modeling - Technologische Grundlagen und industrielle Praxis. VDI-Buch, Springer Vieweg, Wiesbaden, 343-361.
- Bramann, H., May, I. and planen-bauen 4.0 – Gesellschaft zur Digitalisierung des Planens, Bauens und Betriebens mbH, 2015a. Stufenplan Digitales Planen und Bauen. [https://www.bmvi.de/SharedDocs/DE/Publikationen/DG/stufenplan-digitales-bauen.pdf?\\_\\_blob=publicationFile](https://www.bmvi.de/SharedDocs/DE/Publikationen/DG/stufenplan-digitales-bauen.pdf?__blob=publicationFile) (31 March 2020).
- Bramann, H., May, I. and planen-bauen 4.0 – Gesellschaft zur Digitalisierung des Planens, Bauens und Betriebens mbH, 2015b. Konzept zur schrittweisen Einführung moderner, IT-gestützter Prozesse und Technologien bei Planung, Bau und Betrieb von Bauwerken – Stufenplan zur Einführung von BIM. [https://www.bmvi.de/SharedDocs/DE/Anlage/DG/Digitales/bim-stufenplan-endbericht.pdf?\\_\\_blob=publicationFile](https://www.bmvi.de/SharedDocs/DE/Anlage/DG/Digitales/bim-stufenplan-endbericht.pdf?__blob=publicationFile) (31 March 2020).
- Chen, L.-C., Zhu, Y., Papandreou, G., Schroff, F., Adam, H., 2018. Encoder-Decoder with Atrous Separable Convolution for Semantic Image Segmentation. Proceedings of the European conference on computer vision (ECCV), 801-818.
- Clemen, C., Ehrich, R., 2014. Geodesy goes BIM. In: allgemeine vermessungs-nachrichten. (avn) 121 (6). <https://gispoint.de/artikelarchiv/avn/2014/avn-ausgabe-62014/2552-geodesy-goes-bim.html> (31 March 2020).
- Egger, M., Hausknecht, K., Liebich, T., Przybylo, J., 2013. BIM-Leitfaden für Deutschland. [https://www.bmvi.de/SharedDocs/DE/Anlage/DG/Digitales/bim-leitfaden-deu.pdf?\\_\\_blob=publicationFile](https://www.bmvi.de/SharedDocs/DE/Anlage/DG/Digitales/bim-leitfaden-deu.pdf?__blob=publicationFile) (31 March 2020).
- Eschenbruch, K., Malkwitz, A., Grüner, J., Poloczek, A., Karl, C. K., 2014. Maßnahmenkatalog zur Nutzung von BIM in der öffentlichen Bauverwaltung unter Berücksichtigung der rechtlichen und ordnungspolitischen Rahmenbedingungen – Gutachten zur BIM-Umsetzung –. [https://www.bmvi.de/SharedDocs/DE/Anlage/DG/Digitales/bim-massnahmenkatalog.pdf?\\_\\_blob=publicationFile](https://www.bmvi.de/SharedDocs/DE/Anlage/DG/Digitales/bim-massnahmenkatalog.pdf?__blob=publicationFile) (31 March 2020).
- Gülch, E. and Obrock, L., 2020: Automated semantic modelling of building interiors from images and derived point clouds based on Deep Learning, Int. Arch. Photogramm. Remote Sens. Spatial Inf. Sci., XLIII-B2-2020, 421–426, <https://doi.org/10.5194/isprs-archives-XLIII-B2-2020-421-2020>, 2020.
- Huang, G., Liu, Z., van der Maaten, L., Weinberger, K. Q., 2017. Densely Connected Convolutional Networks. 2017 IEEE Conference on Computer Vision and Pattern Recognition (CVPR), 2261-2269.



- Kaden, R., Clemen, C., Seuß, R., Blankenbach, J., Becker, R., Eichhorn, A., Donaubaue, A., Kolbe, T. H., Guber, U., DVW – Gesellschaft für Geodäsie, Geoinformation und Landmanagement e. V., Runder Tisch GIS e.V., 2019. Leitfaden Geodäsie und BIM Version 2.0 (2019). [https://rundertischgis.de/images/2\\_publicationen/leitfaeden/GeoundBIM/Leitfaden%20Geod%C3%A4sie%20und%20BIM\\_Onlineversion.pdf](https://rundertischgis.de/images/2_publicationen/leitfaeden/GeoundBIM/Leitfaden%20Geod%C3%A4sie%20und%20BIM_Onlineversion.pdf) (31 March 2020).
- Krizhevsky, A., Sutskever, I., Hinton, G. E., 2012. ImageNet Classification with Deep Convolutional Neural Networks. *Advances in Neural Information Processing Systems (NIPS 2012)*, 1097 - 1105.
- Long, J., Shelhamer, E., Darrell, T., 2015. Fully Convolutional Networks for Semantic Segmentation. *2015 IEEE Conference on Computer Vision and Pattern Recognition (CVPR)*, 3431-3440.
- Obrock, L. S., Gülch, E., 2018. First Steps to Automated Interior Reconstruction from Semantically Enriched Point Clouds and Imagery. *Int. Arch. Photogramm. Remote Sens. Spatial Inf. Sci.*, XLII-2, 781-787.
- Ren, S., He, K., Girshick, R., Sun, J., 2015. Faster R-CNN: Towards Real-Time Object Detection with Region Proposal Networks. *Advances in Neural Information Processing Systems (NIPS 2015)*, 91-99.
- Simonyan, K., Zisserman, A., 2015 Very Deep Convolutional Networks for Large-Scale Image Recognition. *3rd International Conference on Learning Representations (ICLR2015)*.
- Szegedy, C., Liu, W., Jia, Y., Sermanet, P., Reed, S., Anguelov, D., Erhan, D., Vanhoucke, V., Rabinovich, A., 2015. Going deeper with convolutions. *2015 IEEE Conference on Computer Vision and Pattern Recognition (CVPR)*, 1-9.

**Open Access** This chapter is licensed under the terms of the Creative Commons Attribution 4.0 International License (<http://creativecommons.org/licenses/by/4.0/>), which permits use, sharing, adaptation, distribution and reproduction in any medium or format, as long as you give appropriate credit to the original author(s) and the source, provide a link to the Creative Commons license and indicate if changes were made.

The images or other third party material in this chapter are included in the chapter's Creative Commons license, unless indicated otherwise in a credit line to the material. If material is not included in the chapter's Creative Commons license and your intended use is not permitted by statutory regulation or exceeds the permitted use, you will need to obtain permission directly from the copyright holder.



---

**Part IV**

**Urban Planning and Buildings**



# Cooperative Planning Strategies in Urban Development Processes

# 18

## The Example Common Space 'Österreichischer Platz' in Stuttgart

Carolin Lahode and Elisabeth Schaumann

### Abstract

Cities face a variety of challenges today. To react on these challenges, especially the design of public space as a space of encounter and negotiation is important. In this context, cooperative planning processes are gaining more and more popularity, as cooperation seems to offer the chance to produce solutions for a diverse urban coexistence and a collective understanding of the common good.

Despite the frequent use of the term, there is yet no clear definition of cooperative planning processes. In this regard, the article analyses the development process of the 'Österreichischer Platz' in Stuttgart. The project strategy included an open-ended experimental process over the course of 2 years with a multiplicity of stakeholders. The innovative cooperation of various initiatives, the civil population and representatives of the city administration and politics defines the project as a lighthouse project for urban development in Stuttgart.

### Keywords

Cooperative planning · Public space · Participation · Urban development · Planning process

---

C. Lahode (✉) · E. Schaumann  
University of Applied Sciences Stuttgart, Stuttgart, Germany  
e-mail: [Carolin.lahode@hft-stuttgart.de](mailto:Carolin.lahode@hft-stuttgart.de)

© The Author(s) 2022  
V. Coors et al. (eds.), *iCity. Transformative Research for the Livable, Intelligent, and Sustainable City*,  
[https://doi.org/10.1007/978-3-030-92096-8\\_18](https://doi.org/10.1007/978-3-030-92096-8_18)

283

## 18.1 Introduction

Cities face a variety of challenges today. These challenges include structural change in the retail sector, climate change and the necessary climate adaptation measures associated with it (Frauns & Scheuven 2010; Kalandides et al. 2016; Lüscher 2015). In addition, increasing social polarization and a lack of social cohesion, as well as a lack of individuality and neglected public space, are current issues confronting urban development (Fahle & Burg 2014; Frauns & Scheuven 2010; Trommer 2015). This development is also reflected in the UN's Sustainable Development Goals, which include making cities and human settlements inclusive, safe, resilient and sustainable (DSDG 2019).

Public space is the space where the public is formed and as such a place of social action of any kind (Brendgens 2005; Wolf & Mahaffey 2016). The design of public space as a meeting place for urban society and as a source of identity is particularly central. Therefore, an attractive design that meets the diverse demands of the residents is necessary (BBSR 2019).

Currently, participation culture in Germany rarely allows active participation and co-creation in planning processes in public space. However, in order to meet the diverse needs, new activation and participation formats are needed, as well as a rethinking of planning processes. 'Participation is [thus] not only an instrumental enrichment of planning, but also a path to creative spatial development' (Ipsen 2010 p. 237). Ultimately, sustainable urban development is also a social process of different actors, which is thus characterized by cooperation and communication (Kagan, Kirchfeld & Weisenfeld 2019).

This article examines cooperative planning as a strategy for opening up planning processes to different stakeholders of the city and a mode of active co-production of space. The public space project 'Österreichischer Platz' is used as a current example for cooperative urban development. In the absence of an up-to-date and accurate definition of cooperative planning processes, an initial attempt at definition is based on this case study.

---

## 18.2 Participation in Urban Planning Processes

### 18.2.1 Fundamentals and Legal Framework

Since the 1980s, openly kept participation processes have become established in urban planning, as they often lead to an improvement in the content and concept of planning (Bodenschatz & Polinna 2010; Häussermann, Holm & Zunzer 2002; Healey 2012; Selle 2013).

In formal planning processes (e.g. municipal urban land use planning), formal participation of the public and of the bodies responsible for public affairs is required in accordance with §§3,4 BauGB, meaning public information about the planning and opportunity for expression of opinion must be given. With this type of participation, planning law aims to avoid impairments or disturbances by third parties (Selle 2018), but not to empower people to take part in the development of these plans.

Today, informal integrated urban development complements formal planning processes in order to comprehensively meet the multitude of challenges of urban development. Integrated urban development concepts aim, for example, to work out future guiding principles for the development of a city or neighbourhood together with local actors based on an analysis of the current situation. Recommendations for action are also part of these strategies. They rely on active cooperation between citizens, municipalities and economic actors (Krappweis 2020; Beckmann 2018; Frank & Strauss 2010; Wékel 2018).

The German urban renewal strategy (Art. 104b GG and §§136-171e BauGB) also offers participation possibilities. Thereafter, cities can apply for urban development funding. Residents and other stakeholders are then given the opportunity to participate, e.g. through open discussions, surveys or workshops. They can get a direct say by being able to implement smaller measures by themselves, financed by a disposal fund ('Verfügungsfond') (BBSR 2018; BMVBS 2012). Furthermore, it is possible for the citizens to discuss the renewal processes in a neighbourhood management with a direct contact person (BBSR 2018).

Despite these long-standing approaches, opportunities for participation and co-determination in urban planning processes for civil actors remain limited. Recently, the political-administrative planning apparatus is opening up to alternative, experimental and more cooperative participation, in the form of temporary interventions (Schaumann & Simon-Philipp 2018) and civic commitment (Humann & Polinna 2020). The interest in and promotion of cooperative planning is reflected not least in the recently launched federal award 'Koop. Stadt', which honours successful examples of cooperation between municipalities and civil actors.

### 18.2.2 Cooperative Planning as a Theoretical Practice

Although cooperative planning seems to be a quite popular term recently, a more precise or descriptive definition of this term is still lacking. In an attempt to theoretically delimit cooperative planning processes, this article refers to aspects of cooperation, collaborative planning and co-production to form a temporary definition.

Cooperation itself is defined as a strategic and temporary teamwork on clearly defined areas of cooperation between equals to achieve a goal that one party alone can either not accomplish at all or at least as well (BBSR 2020). According to Sennett (2019), cooperation is a craft that requires the ability to listen, empathize and dialogue and dialogic cooperation therefore the highest goal (Sennett 2019, p. 17). Successful cooperation also involves curiosity, appreciation and mutual trust of all parties involved (BBSR 2020).

Referring to these characteristics of cooperation, conclusive similarities to collaborative planning and coproduction can be drawn. Collaborative planning is deemed as an 'inclusive dialogic approach to shaping social space' (Brand & Gaffikin 2007, p. 283) by constant reflection and undistorted debate. This kind of continuous negotiation contributes to a sustainable development of neighbourhoods, cities and regions and thus strengthens

societal cohesion (BBSR 2020, p. 8). However, if one takes collaboration as a term for ideational working together on a topic, it seems to differ from Sennett's understanding of cooperation as craft in so far. Critics further note that collaborative planning is relying too much on consensus and commonality to represent a diversity of opinions. Thus, a demand for a more agonistic approach is emerging (Brand & Gaffikin 2007).

Cooperative planning seems to coincide with the definition of co-production as given by Wolf and Mahaffey (2016) of 'a non-hierarchical methodology, an indirect approach to problem solving that embraces complexity, multiplicity of actors, processes, ideas and solutions' (p. 64). Yet, while participants in co-productive processes collaborate on a common task, in cooperative planning, parties are working parallel on individual areas (BBSR 2020).

Due to their dialogic character, cooperative processes need to be open-ended (Selle 2018). An experimental approach supports the dialogue and negotiation of different needs (Sennett 2019). In this way, the planning homogeneity that often prevails today is counteracted and spaces of potentiality are co-produced (Wolf & Mahaffey 2016).

To illustrate as well as to prove these found criteria for cooperative planning processes, this article analyses the development of the 'Österreichischer Platz' in Stuttgart as a practice example.

---

## 18.3 Case Study 'Österreichischer Platz'

### 18.3.1 General Context

The 'Österreichischer Platz' is a multistorey traffic structure in Stuttgart. This 'square' is situated in the very centre of the city and consists of a traffic circle with an adjoining bridge, a parking area underneath and an adjacent federal road. As a relic of the car-friendly city, the traffic structure and its surrounding area have been on the agenda of local urban planning authorities for a long time. Due to the difficult traffic situation and a complex variety of stakeholders, no conclusive plan has been developed (Fig. 18.1).

The association Stadtlücken e.V.<sup>1</sup> initiated an intervention in 2016 that asked for alternative uses for the parking area, thereby a cooperative development of this actually public space was stimulated. Politics, city administration, civil initiatives and citizens were working together on a common vision.

---

<sup>1</sup> Association based in Stuttgart that aims at raising the awareness of the importance of public space ([www.stadtluecken.de](http://www.stadtluecken.de))



**Fig. 18.1** View of the traffic structure with the parking space beneath the traffic circle

### 18.3.2 Strategy for Spatial Activation

After the success of their initial activities in 2016, the municipality asked Stadtlücken to hand in a proposal for the development of the parking space. Their strategy included an open-ended experimental process over the course of 2 years (period of municipal budget), involving various initiatives and the civil population. The city council approved the strategy and provided a subsidy for the implementation of the project.

The experimental field ‘Österreichischer Platz’ was set up in the front area of the parking space. To get a better understanding of the area and its needs, different usage scenarios were tried out throughout the 2-year project phase. The ideas for potential usages, generated by Stadtlücken and other civil actors, ranged from housing (with a tiny house exhibition), public cinema, concerts and a children’s playground to flea markets. Openly formulated social and democratic values were set up as a scope of action. While the space was still clearly recognizable as a former parking lot, a floor graphic and a few seating facilities formed the design framework for further civic engagement (Fig. 18.2).

Especially in the beginning, members of Stadtlücken took care of the place and organized activities. The activation of the parking space through the idea of an open construction site and the events generated a lot of attention with neighbours and passers-



**Fig. 18.2** View of the location during the preparations for the opening

by. The project's further publicity strategy included a constantly updated calendar of events online<sup>2</sup> and on site as well as an Instagram channel.

After the first year of intense experimentation, Stadtlücken as curators evaluated the first trials and adapted the usage concept. Regarding noise complaints by neighbours, some of the suggested ideas for the site were either cast off or adapted. Furthermore, a weekly café was installed as an open meeting point for the neighbourhood with one association member as a permanent contact person, who was also needed.

### 18.3.3 Cooperative Process Development

The implementation of such an urban development process required the cooperation of the city administration, civil actors and politicians. At the very beginning of the project, a round table was set up to exchange information and quickly solve problems. This table brought together Stadtlücken (as site and project manager), the Economic Development Agency (as manager of the funding), the Civil Engineering Office (as owner of the parking

<sup>2</sup>Project website: [www.oe-platz.de](http://www.oe-platz.de)



space), the Office for Public Order (as responsible for events) and the Office for Urban Planning as well as other changing offices.

This practice enabled the development of a general event permit for the association. In contrast to the usual 3-month approval period, events could be held at short notice. The installation of a public bouldering facility at the site required an intensive cooperation between civil actors and the administration, as public access in connection with the liability was a major issue.

Throughout the process, Stadtlücken administered and cultivated the space and curated and supervised the various ideas for its use as 'Raumagenten'<sup>3</sup> (BBSR 2020). A call for ideas invited civil actors to submit their ideas. On a simple idea sheet, interested parties were able to write down their concrete idea for use, their individual role description in the implementation process and the support they needed to proceed. This procedure should lead the participants to recognize their own responsibility and design possibilities in the project. To further involve the neighbourhood and adjacent businesses in the project, the association initiated several neighbourhood meetings. The topics and concerns collected during those meetings were passed on to the round tables with the authorities.

Together with the minimal spatial design and the technical infrastructure, which was built up over time, the idea sheets and the neighbourhood meetings completed the framework for civic participation and co-production. At the end of the 2-year period, the 'Österreichischer Platz' counted around 175 single events. In a preliminary evaluation process, certain key findings, such as a need for space for the common good, culture, encounter, exercise and experiments, were established for the further development of the site (Fig. 18.3).

In a more advanced strategy, Stadtlücken and the administration together proposed the development of a cooperative urban space for the new funding period. The elaborated vision envisaged a cooperative consisting of honorary associations and initiatives. The initiatives would use the space itself and manage and provide the space for the general public in cooperation with the city council and administration. The 'Österreichischer Platz' would thereby not only include public space but also studios, workshops and co-working spaces. This concept was again approved by the municipal council.

---

<sup>3</sup>'Raumagenten' 'take over a mediating function between initiatives and the city administration or Urban policy in terms of access to space, obtaining permits, and participation in political decision-making processes' (BBSR 2020, p. 123).



**Fig. 18.3** The ‘Österreichischer Platz’ as a place of negotiation for different actors and uses

## 18.4 Assessment

To classify the experimental planning process of the ‘Österreichischer Platz’ as cooperative, this article refers to the identified characteristics of cooperation, co-production and collaborative planning processes as described above. Assessing the characteristics of the development process, many aspects of participatory cooperative planning were met.

Cooperation between the individual actors took place in parallel sub-areas while collaborating on a common task. Personal contact at the round tables established a base of mutual respect and trust. As a civil initiative, Stadtlücken was given a lot of room for creative leeway by politics and administration. The fact that the project was mainly based on volunteer work thereby certainly played a fundamental role. In the end, the successful cooperation of politicians, administration and civil initiatives made this project possible.

Due to the spatially central location of the project site and the implementation concept, a large cross-section of diverse actors was reached. In addition to representatives from politics and administration, the actors included initiatives, residents and passers-by who all at one point or another were involved in meetings, in activities on site or at events. Since every idea for use directly went into temporary implementation and became apparent in real space, a constant negotiation about common values took place as well. In this sense, direct

communication based on empathy and sympathy was even more important, as not every negotiation necessarily produced a consensus.

As a framework, the idea sheets with their clear allocation of responsibilities and the temporary implementation of ideas in experiments gave equal and low-threshold opportunity to all civil participants to actively take part in the design process and the negotiation of public space. The formulated scope for action gave everybody the same opportunity to submit ideas and implement them and was not tied to social or financial status. Thus, local social fringe groups were also able to participate in the project, and mediation between different social groups could take place on site. Nevertheless, comprehensive online participation formats could have expanded the process.

Since the project was still in an experimental and determination phase of use, there was plenty of leeway for all parties involved. Through the structure of the project, anyone could actively participate in the process of opinion making, as well as the development and implementation process. The experimental and processual character of the project created an urban space as a space of potentiality including plenty of room for productive civic engagement and participation.

---

## 18.5 Conclusion

As the assessment shows, the process characteristics of the ‘Österreichischer Platz’ do qualify as cooperative. A combination of collaborative and co-productive features does in fact apply. The planning process is characterized by the cooperation of different actors individually collaborating on a task and thus co-producing a real common result. In this sense, cooperation actually can be described with Sennett’s words as something craft-like, since it is about the joint creation of something—in this case space.

Successful cooperative planning as collaborative planning is depending on a participation of all relevant stakeholders. However, how do you ensure that all relevant participants actually take part in the process? Although the project was able to reach broad sections of the city society, it is highly likely that not all relevant actors participated in the process. Sufficient time for the negotiation process, direct dialogic communication, increased presence and responsiveness on site would probably allow more reach. An even larger audience could be reached through the increased use of digital and online tools.

In this context, what are the benefits of cooperative planning? First, the experimental approach makes participation in the process equally accessible to everyone, does not require a professional background and as a cooperation of different disciplines produces innovative solutions. Those characteristics are missing in many classic participation models in formal planning. Furthermore, the flexibility vital for experimental implementation can hardly be provided by heavy administrative apparatuses (Kagan et al. 2019). The artisanal character of cooperative planning makes it possible for participants to actively create and produce something instead of just expressing their opinion on already existing plans. However, as the course of the project has shown, most citizens first have to learn to

actively engage with urban space. An understanding of creative work on urban visions and new usage concepts must be developed.

Additionally, the question of competence and responsibility is crucial for the continuation of projects deriving from cooperative planning processes. Municipalities need structures where power sharing and a joint learning process enable civil actors to build their own city. By enabling citizens to actively shape their own urban space, the feeling of ownership and responsibility grows and sustainable, innovative solutions are more likely to develop.

---

## References

- Beckmann, K. J. (2018). Integrierte Stadtentwicklung. In Akademie für Raumforschung und Landesplanung (Hrsg.), *Handwörterbuch der Stadt- und Raumentwicklung*. (p. 1063-1068). Hannover.
- Bodenschatz, H. & Polinna, C. (2010). *Learning from IBA – die IBA 1987 in Berlin*. Berlin.
- Bundesinstitut für Bau-, Stadt- und Raumforschung BBSR. (2018). *Zehn Jahre Aktive Stadt- und Ortsteilzentren: Vierter Statusbericht zum Zentrenprogramm der Städtebauförderung*. Berlin: BBSR.
- Bundesinstitut für Bau-, Stadt- und Raumforschung BBSR. (2019). *Zehn Jahre Aktive Stadt- und Ortsteilzentren – gemeinsam den Wandel gestalten: Dokumentation des Fachkongresses am 20. November 2018 in Berlin*. Retrieved from [https://www.staedtebaufoerderung.info/StBauF/SharedDocs/Publikationen/StBauF/AktiveStadtOrtsteilzentren/Kongress\\_Doku.pdf](https://www.staedtebaufoerderung.info/StBauF/SharedDocs/Publikationen/StBauF/AktiveStadtOrtsteilzentren/Kongress_Doku.pdf).
- Bundesinstitut für Bau-, Stadt- und Raumforschung BBSR. (2020). *Glossar zur gemeinwohlorientierten Stadtentwicklung*. Bonn: BBSR.
- Bundesministerium für Verkehr, Bau und Stadtentwicklung BMVBS. (2012). *Sicherung tragfähiger Strukturen für die Quartiersentwicklung im Programm Soziale Stadt. Forschungen*. 153.
- Brand, R. & Gaffikin, F. (2007). Collaborative Planning in an Uncollaborative World. *Planning Theory* (6, p. 282–313).
- Brendgens, G. (2005). Vom Verlust des öffentlichen Raums. Simulierte Öffentlichkeit in Zeiten des Neoliberalismus. *Utopie kreativ* (182, p. 1088–1097).
- Division for Sustainable Development Goals DSDG. (2019). *Sustainable Development Goals*. Retrieved from <https://www.un.org/sustainabledevelopment/sustainable-development-goals/>
- Fahle, B. & Burg, S. (2014). *Unternehmung Innenstadt, Management der Innenstadtentwicklung von Mittelstädten*. Ludwigsburg: Wüstenrotstiftung.
- Frank, T. & Strauss, W.-C. (2010). Integrierte Stadtentwicklung in deutschen Kommunen: eine Standortbestimmung. In Bundesinstitut für Bau-, Stadt- und Raumforschung (BBSR), *Informationen zur Raumentwicklung* (Heft 4, S. 253-262). Bonn: Bundesamt für Bauwesen und Raumordnung (BBR).
- Frauns, E. & Scheuven, E. (2010). *Positionspapier zur Innenstadt in Nordrhein-Westfalen*. Münster: Netzwerk Innenstadt NRW.
- Häussermann, H., Holm, A. & Zunzer D. (2002). *Stadterneuerung in der Berliner Republik: Modernisierung in Berlin-Prenzlauer Berg*. Wiesbaden: VS Verlag für Sozialwissenschaften.
- Healey, P. (2012). Communicative Planning: Practices, Concepts, and Rhetorics. In S. Bishwapriya, J. Lawrence & C. Rosan (Eds.), *Planning Ideas That Matter* (p. 333-357). Cambridge: The MIT Press.

- Humann, M. & Polinna, C. (2020). Planungsprozesse. In Bundesinstitut für Bau-, Stadt- und Raumforschung BBSR, *Glossar zur gemeinwohlorientierten Stadtentwicklung*. (S. 109-114). Bonn: BBSR.
- Ipsen, D. (2010). Bürgerbeteiligung und konzeptionelle Planung. In E. Becker, E. Gualini, C. Runkel, R. Graf Strachwitz (Ed.), *Stadtentwicklung, Zivilgesellschaft und bürgerschaftliches Engagement* (Vol 6, p. 237-250). Stuttgart: Lucius & Lucius.
- Kagan, S., Kirchberg, V. & Weisenfeld, U. (2019). *Stadt als Möglichkeitsraum: Experimentierfelder einer urbanen Nachhaltigkeit*. Bielefeld: transcript Verlag.
- Kalandides, A., Kather, M. & Köther, P. (2016). *Gute Geschäfte: Was kommt nach dem Einzelhandel?*. Bochum: StadtBauKultur NRW.
- Krappweis, S. (2020). *Formelle und informelle Instrumente der Raumplanung*. Retrieved from [http://planung-tu-berlin.de/Profil/Formelle\\_und\\_Informelle\\_Planungen.htm](http://planung-tu-berlin.de/Profil/Formelle_und_Informelle_Planungen.htm)
- Lüscher, R. (2015). Transforming Cities. In K. Feireiss & O.G. Hamm in co-operation with the Senate Department for Urban Development and the Environment (Ed.), *Transforming Cities. Urban Interventions in Public Space* (p. 22-31), Berlin: jovis.
- Schaumann, E. & Simon-Philipp, C. (2018). Urbane Interventionen im öffentlichen Raum: Transformationspotenziale in Stadtteilzentren. *Forum Stadt, Heft 3*, p. 247-258.
- Selle, K. (2013). "Participation", oder: beteiligen wir uns zu Tode? In K. Selle (Ed.), *Über Beteiligung hinaus*. Dortmund: Rohn Verlag.
- Selle, K. (2018): Stadtplanung und Kommunikation – Gründe, Methoden und Voraussetzungen. In M. Baum, U. Böhm, A. Ley, D. Schönle, B. Hüttenhain & D. Teodorovici (Eds.), *Lehrbausteine Städtebau: Basiswissen für Entwurf und Planung* (9). Stuttgart: Städtebau-Institut, Universität Stuttgart.
- Sennett, R. (2019). *Zusammenarbeit*. Berlin: Hanser Berlin in Carl Hanser Verlag GmbH & Co. KG.
- Trommer, S. (2015). Identität als Katalysator für Stadtentwicklungsprozesse. *vhw FWS*, (1), p. 28–32.
- Wékel, J. (2018). Stadtentwicklungsplanung. In Akademie für Raumforschung und Landesplanung (Hrsg.), *Handwörterbuch der Stadt- und Raumentwicklung*. (p. 2435-2439). Hannover.
- Wolf, G., & Mahaffey, N. (2016). Designing Difference: Co-Production of Spaces of Potentiality. *Urban Planning*, 1(1), p. 59–67.

**Open Access** This chapter is licensed under the terms of the Creative Commons Attribution 4.0 International License (<http://creativecommons.org/licenses/by/4.0/>), which permits use, sharing, adaptation, distribution and reproduction in any medium or format, as long as you give appropriate credit to the original author(s) and the source, provide a link to the Creative Commons license and indicate if changes were made.

The images or other third party material in this chapter are included in the chapter's Creative Commons license, unless indicated otherwise in a credit line to the material. If material is not included in the chapter's Creative Commons license and your intended use is not permitted by statutory regulation or exceeds the permitted use, you will need to obtain permission directly from the copyright holder.





# On the Prospects of the Building Envelope in the Context of Smart Sustainable Cities: A Brief Review

# 19

Heiko Liebhart and Jan Cremers

## Abstract

According to the World Urbanization Prospects of the United Nations (United Nations, Department of Economic and Social Affairs 2018), about 68% of the overall expected world population is going to live in urban areas and cities by the year 2050. The task of transforming modern cities towards a more sustainable and ecological as well as socially likeable environment touches a plethora of disciplines like transportation, energy infrastructure, architecture, building physics, etc. and poses an intricate challenge for architects, engineers, urban planners and social scientist alike. Thanks to the technological evolution, the realization of smart city concepts and solutions has become a viable option to contribute to this goal in a significant manner. The building envelope as an indispensable part of human dwellings and working space has historically mostly taken the classic functionalities of resembling aesthetic expression and providing physical protection. Recent and upcoming technological developments will enable a shift in the role of the building envelope from its mere classical functionalities towards additional contributions to the sustainability and livability of the environment. The prospects of these contributions range from increasing the thermal and visual comfort of the inhabitants and the surrounding environment by adaptive architectural measures towards potential energy saving by energy harvesting devices and synergetic processing and treatment of material flows of the building to provide conditioned air, preprocessed water and even food. In this short essay, we will elaborate on the phenomenon of smart city in general and the role of the building envelope in the context of modern smart city

---

H. Liebhart (✉) · J. Cremers  
Hochschule für Technik Stuttgart, Stuttgart, Germany  
e-mail: [heiko.liebhart@hft-stuttgart.de](mailto:heiko.liebhart@hft-stuttgart.de)

© The Author(s) 2022  
V. Coors et al. (eds.), *iCity. Transformative Research for the Livable, Intelligent,  
and Sustainable City*,  
[https://doi.org/10.1007/978-3-030-92096-8\\_19](https://doi.org/10.1007/978-3-030-92096-8_19)

295

development and its potential on the improvement on different aspects of life and urban environment.

---

**Keywords**

Building envelope · Building simulation · Adaptive architecture · Energy harvesting

---

## 19.1 Emergence of Smart Urban Structures over the Course of Time

Smart/intelligent cities have been fantastic, futuristic concepts for quite some time. But they can also be understood as emergent phenomena, i.e. the consequential outcome of the application of the ongoing technological progress in digitalization, sensor and actuator technology and other fields, to the urban planning and development processes. In this section, we will take a brief excursion to the history of smart city concepts and address how their manifestation as a realistic urban development option has come about in recent years.

The formation of urban structures is a fascinating sophisticated process. Apart from the natural process of emergent growth, driven by the fundamental needs of the inhabitants and bound by the constraints and boundary conditions of the geographical and ecological surroundings, like rivers, ports, market squares and trade routes, urban structures like towns and cities have also been object to selective and purposeful planning and design. These processes of controlled planning and urban development commonly follow certain paradigms and specified goals.

Over the course of time, the paradigms of urban development have undergone several shifts, ranging from royal prestige structures with wide avenues and large squares to the worker neighbourhoods of the industrial production age. It shifted later to the mobility-centred dogma of the traffic-friendly city to spanning new urbanism and more recently developing towards a citizen-friendly synergetic approach, influenced by mostly citizen-driven grassroots movements for reclaiming the common space like the Transition Network (Transition Network 2020), the Critical Mass movement (CriticalMass 2013) or the Occupy movement initiated by Adbusters (Adbusters 2020) and urban gardening aspects (Raskin 2017). In order to achieve certain paradigm-specific goals, certain structures like representative-wide avenues and large squares for prestigious representation, suburban single household settlements, industrial districts, neighbourhoods with affordable housing for workers, malls and parks were actualized in each epoch within the overall urban structure.

While the processes of urban planning and development are mostly locally constrained and operate on the scale of neighbourhoods and single districts, the challenge to design cities as a whole in an holistic approach has also been addressed by several great utopians in the past. The Experimental Prototype Community of Tomorrow (EPCOT), designed by Walt Disney around 1959 (E.P.C.O.T. 2012), resembles one example for the efforts to design attractive cities with high quality of life for its inhabitants while simultaneously utilizing then most recent technological developments, e.g. a monorail transportation

system and agile personal movers within an holistic approach. The geometric circular design of the city complex seemed to be inspired and influenced by the “Radial Garden City” designs of Ebenezer Howard (Howard 1898) and has also found resemblance in predecessors like the Octagon city project (Gambone 1972). Another more recent example for the holistic approach to the development of circular urban structures is the Venus Project, supported by Jacques Fresco and Roxanne Meadows in about 1970 (Fresco 1995). These concepts covered the relevant aspects of functioning city structures like the arrangement of districts for working, recreation and housing and even agriculture as well as providing transportation systems for the inhabitants and for the logistic of goods. The provision of utilities and all relevant maintenance processes were supposed to be coordinated by a central hub, supported by a vast range of sensor data. The Venus Project even aimed for a novel model of a futuristic society expanding on considerations regarding the economic system of the inhabiting society, proposing a resource-based economic model.

Apart from the circular structures, there have also been other futuristic concepts in the past like domed, floating or even walking cities, as presented in 1964 by Ronald James Herron of the seminal English experimental architecture collective Archigram (University of Westminster 2020). These concepts have been mostly addressed within science fiction literature and movies, apart from rather solitary attempts to apply them to real scenarios from bold futurists like Buckminster Fuller with the dome of Manhattan in 1960 (Carlson 2012) and the tetrahedral floating Triton City for Tokyo Bay in 1967 (Hays and Miller 2008) or the domed Eco-City 2020 (evolo 2010), proposed in 2010 by the Russian innovative architectural studio AB Elis Ltd., projected for 100,000-people in the crater of the Mir diamond mine in the Yakutia Republic in Siberia.

Due to technological and organizational restraints, none of these projects were able to be realized on the scale of a functioning entity. The approach to generate a complete city structure from scratch, as appealing it might seem from a conceptual point of view, poses an obstacle since it is not applicable to the transformation of existing metropolitan city structures. Still these efforts can be seen as precursors to the smart city concept arising from an approach of understanding a city as a synergetic life form with manifold data streams to support its metabolism. The increased prevalence of miniaturized interconnectable sensor systems and the general availability of computing capacity and network bandwidth led to a revitalization of the idea of the “intelligent” city in recent years. This reflects, for instance, in the development of the number of publications during the recent years. A brief survey, for the combined key words “smart city”, on the number of publications from the reputable publisher Elsevier at [sciencedirect.com](https://www.sciencedirect.com) illustrates this development. The search returns about 9364 overall publications between the years 1992 and 2020. The number of publications shows a noteworthy increase since about 2010 and a rather steady annual growth by a factor of about 1.4 in the number of publications between 2015 and 2020. On another note, the term circular city, used by Fresco in connection to the spatial configuration of the city and only secondary referring to the underlying resource base economic system (The Venus Project 2020), has recently seen a renaissance in press articles (Wenzel Elsa and GreenBiz 2019), research programmes (BOKU, The University of Natural



Resources and Life Sciences 2018) and scientific literature (Prendeville, Cherim and Bocken 2018) mostly associated not only with smart city concepts but mainly with circular economy aspects. Finally, compilations of recommended procedures for the implementation of smart city concepts have been defined within smart city charts for Germany in 2017 (Günthner, Schweitzer and Jakubowski 2017) and the European Union in 2019 (Wouters, et al. 2019).

---

## 19.2 The Building Envelope: From Skin to Sculpture to Sensor

Since the emphasis of this essay lies on the prospects of the building envelope within the context of the smart city approach, we will not further expand on the various intriguing aspects of smart city concepts but will rather elaborate on the specifics of the building envelope. We will sketch the progression of the building envelope from its static pragmatic nature towards aesthetic and dynamic responsive element.

The building envelope as an indispensable component of the physical building classically constitutes two main functionalities. On the one hand, it covers the rather obvious role of providing shelter and protection from the outer environmental impacts and the control of energy transport including solar radiation and the flow of air between inside and outside. And on the other hand, it resembles the aesthetic vision of its creators and owners. The measures to fulfil the role of physical shelter and protection mostly depend on the available technological and materialistic means, whereas the artistic design is heavily impacted by the predominant spirit of its era. Still these roles are not strictly separable and intertwine to some degree, since available technological measures enable certain aesthetic creations, the necessity to meet certain energetic and comfort goals impact the choice of aesthetic means and the preferences in creative means push certain technological developments. In most functional everyday buildings, these aspects are merged in an amalgamation to a functional equilibrium. A departure from the functional interpretation of the building skin towards the artistic aspects is present in the works of several iconic creators like the masterworks of Jean Prouvé, the wide span lightweight structures of Frei Otto, the sculptural designs by Shigeru Ban or the elaborated structures of Carlo Scarpa accompanied by his interpretation of the building envelope as the third skin of its inhabitants, to just name a few. The general manifestation of the building envelope was mostly that of a static element. This rigid approach was transcended in the early twentieth century by several creators by applying dynamic aspect to the mostly static building and its envelope. In the beginning, the ideas were merely explored in concepts and drawing, for example, by the Russian constructivist architect and graphic designer Chernikhov in 1933 (J. G. Chernichov 1933). The concepts were later picked up and implemented by innovators such as Buckminster Fuller around 1940 (Marks and Fuller 1960), who probably also processed them into the Tensegrity concept (Lalvani 1996). The dynamic approach found application in experimental works, for example, the US Pavilion at Expo 67 in Montreal in 1967 from Buckminster Fuller (Carlson 2012). It took until 1970 for the dynamic concept to gain foothold and be coined

by the term “kinetic architecture” by William Zuk (Zuk and Clark 1970). The application of cybernetic ideas and computational power to the dynamic approach by Negroponte gave rise to the branch of “responsive architecture” (Negroponte 1970) and finally found its youngest manifestation in the concept of “climate adaptive building shells” by Loonen (Loonen, Trčka and Hensen 2011). The integration of modern sensor and actuator technology and control algorithms enables creators to develop buildings towards a vision of a dynamic entity, interacting with its inhabitants and surrounding. Since the establishment and refinement of the ideas of dynamic architecture, a great number of individualistic examples of responsive and climate adaptive buildings have already been built (Loonen 2010).

---

### 19.3 Future Prospects of the Building Envelope: Examples from Research and Commerce

The future of the building envelope within the context of smart/intelligent cities is linked to an increase in its functionality by utilizing state-of-the-art sensor and network technology and several other aspects to adapt its capabilities to the needs of the inhabitants and the impacts of the environment. Some aspects of this extension in functionality can be derived from the concepts of dynamic architecture.

One prevalent goal of climate adaptive building shells is to adjust the impact of radiative heat transfer into the building by dynamic shading. The applied shading mechanisms can be realized by architectural means via kinetic elements or can be integrated into the transparent envelope elements like windows and glass facades. A comprehensive review of various technological shading solutions like electro-, thermo- and photochromic elements in modern window applications is given in the work of Casini (Casini 2016). Novel concepts of combining microfluidic channels and magnetic particle suspension with transparent building elements to achieve switchable shading have also been realized (Heiz, et al. 2017).

Apart from shading, there are also other beneficial aspects that can be addressed by the building envelope. The generation of energy by energy harvesting methods via photovoltaic/photothermic elements has reached technological maturity and can be expected to become more wide spread in the coming years. The term “Building Integrated Photovoltaic/Thermal” (BIPV/T) is already firmly established in the research community. A survey of the term “BIPV” at Elsevier alone returns an overall of 2773 publications for the timespan between 1997 and 2020, with a steady number of 200 to 300 publications per year for the timespan between 2015 and 2020. Commercial PV manufacturers, e.g. Heliatek (Heliatek 2020), have specialized their product portfolio to this application. The application has reached the maturity to fully equip whole building facades with PV elements, e.g. the office building Z3 of the Züblin AG in Stuttgart (Erban, Oman and Popp 2016) and the institute building of the Zentrum für Sonnenenergie- und Wasserstoff-Forschung Baden-Württemberg (ZSW) in Stuttgart (Geuder 2018). The combination of

photovoltaic/photothermal energy harvesting and shading by integrating PV/T elements in shading slats and curtains is subject of research projects like Arkol (Fraunhofer ISE 2020) as well as part of the business concept of startups like SunCurtain (SunCurtain 2020).

The use of fluoropolymer materials like polytetrafluoroethylene (PTFE, colloquially known from the DuPont brand name Teflon)-coated textiles and ethylene tetrafluoroethylene (ETFE) copolymer foil in membrane structures has also seen successful application in the combination with photovoltaic elements (Cremers and Lausch 2008), artificial lighting elements (ETFE 2014), dynamic shading by pressure controlled switching of complementary printing patterns (Gabler, et al. 2010) and low emission coating (Cremers, Palla, et al. 2016). The advancement of these materials for the application in architecture and buildings has been subject to several previous research projects at HFT Stuttgart like MESH (Manara, Beck and Cremers 2012), FMESH (Manara, Kehl, et al. 2018) and FOLLOW-E2 (Hildebrandt, et al. 2019). The combination of fluidic systems and membrane structures has been subject to numerical investigations within research works, for example, at Transsolar Energietechnik GmbH (Ganji Kheybari and Lam 2017).

A vast number of other potential beneficial uses of the building envelop can be unlocked in conjunction with agricultural use by facade greening of curtain walls or compact greening elements integrated into the building skin. The beneficial effects of facade greening range from wastewater treatment (Eisenberg, Ludwig and Well 2020) to regulation of ambient temperature and humidity, air purification with special moss wall elements (Artificial Ecosystems 2020), compensation of carbon dioxide by cultivation of algae (Kerner 2017) and the straightforward provision of edible fruits and leafy greens (Fraunhofer UMSICHT 2011). The biomass produced from algae is versatile in its use and can be processed for food, cosmetics and even fuel. Some of these concepts are closely related to the concepts of vertical farming (Despommier 2010). The incorporation of the roof in conjunction with the synergetic combination of agriculture and fish farming, known as aquaponic, constitutes a highly efficient method and would yield further benefits (Goddek, et al. 2019). Additional benefits arise from a more holistic approach to integrate other streams from the building like air and heat into the system (Windcloud 2020). Another approach is the direct production of hydrogen via solar photoelectrochemical water splitting (May, et al. 2015).

The aspect of air purification by means of special photocatalytic TiO<sub>2</sub> coatings has been addressed by researchers (RWTH Aachen 2018) and even been realized within singular building projects (TDMA 2018). The support of the ventilation system by utilizing natural ventilation phenomena like the chimney effect in conjunction with the well-understood concept of the trombe wall structure is another probable benefit of the additional redirection of the airflow through vortex structures would even enable a separation of airborne particles to support the air purification system.

On a final note, it should also be addressed that the concept of thermal activation of building skin also bears some noteworthy potential for the building envelope beyond its static functionality. Thermal activated building envelope elements have the capability to act

as dynamic heat exchanger and in combination with proper heat pump application enable a reduction of heating and cooling load on the building.

Many of the above concepts and technologies are not exactly novelties. In fact, an overview of many of the mentioned concepts was compiled and presented by Cremers in the past (J. Cremers 2017). Still virtually all of the above-mentioned concepts either will benefit or will only now be efficiently realized through the increased availability of sensor/actuator systems and data-based control algorithms of the smart city concept in its interpretation as a massive IOT entity.

---

## 19.4 Upcoming Investigation Within iCity Phase 2

Within the upcoming phase 2 of the iCity research project, the possibilities and capabilities of different variations of novel building envelope elements and their beneficial impacts for the inhabitants and the environment will be assessed. In phase 1 of the iCity research project, some aspects like optimization of natural ventilation via windows and noise reduction measures in the construction material have already been successfully addressed. The insights from these preceding works will be valuable inputs due to the overlap in the topics since windows are an integral part of the building envelope.

The combination of various solutions in addition to optimized algorithmic control is expected to release additional beneficial synergetic effects. The investigations will be supported by numerical dynamic building simulation in order to quantify the impact on energy balance and environmental parameters like temperature and daylight irradiance. The research will be substantially intensified to identify other main actors in research and commerce on the field and harness interdisciplinary knowledge exchange.

---

## 19.5 Conclusion and Outlook on the Necessity for Further Research

The main takeaway from the presented, somewhat abbreviated, considerations, concerning the role of the building envelope within the context of the smart city concept, is that a shift in the functionality seems to be immanent. The potential for an extension of its functionality and beneficial impact is rather high and diversified. A decent amount of research needs to be done to cover the multitude of aspects and quantify the possible advantages of their application.

## Bibliography

- Adbusters. *Adbusters Media Foundation | Journal of the Mental Environment*. 30 October 2020. <https://www.adbusters.org/> (accessed October 30, 2020).
- Artificial Ecosystems. *Artificial Ecosystems*. 2020. <https://www.artificial-ecosystems.com/> (accessed October 30, 2020).
- BOKU, The University of Natural Resources and Life Sciences. *Circular City*. 2018. <https://circular-city.eu/> (accessed October 30, 2020).
- Carlson, Jen. *The 1960 Plan To Put A Dome Over Midtown Manhattan - Gothamist*. March 8, 2012. <https://gothamist.com/arts-entertainment/the-1960-plan-to-put-a-dome-over-midtown-manchattan> (accessed October 30, 2020).
- Casini, Marco. *Smart Buildings*. Elsevier Science & Technology, 2016.
- Chernichov, Jakov G. [Verfasser/in], ed. *Konstruktion der Architektur und Maschinenformen*. Nachdr. d. Ausg. Leningrad, Verl. der Leningrader Architekten-Ges., 1931. Basel: Birkhäuser, 1991.
- Chernichov, Jakov Georgievic. *101 Architectural Fantasies*. 1933.
- Cremers, J., and F. Lausch. "PV Flexibles - Photovoltaics Integrated in Translucent PTFE-and Transparent ETFE-Membranes Structures." *23rd European Photovoltaic Solar Energy Conference and Exhibition*. WIP-Munich, 2008.
- Cremers, Jan. "The Potential of Building Envelopes to Actively Provide Renewable Energy - a Review and Outlook." Chap. 6, edited by Waclaw Celadyn and Sabina Kuc, 59-70. Kraków: Crakow University of Technology, 2017.
- Cremers, Jan, Nansi Palla, Doris Buck, Andreas Beck, Andreas Biesinger, and Swen Brodtkorb. "Analysis of a Translucent Insulated Triple-layer Membrane Roof for a Sport Centre in Germany." *Procedia Engineering* (Elsevier BV) 155 (2016): 38-46.
- CriticalMass. <http://www.critical-mass.de/>. 24 January 2013. <http://www.critical-mass.de/> (accessed September 30, 2020).
- Despommier, Dickson. *The vertical farm: feeding the world in the 21st century*. Macmillan, 2010.
- Drozdzowski, Ziggy. "The Adaptive Building Initiative: The Functional Aesthetic of Adaptivity." *Architectural Design* (Wiley) 81 (11 2011): 118-123.
- E.P.C.O.T. *The Original E.P.C.O.T.* 2012. <https://sites.google.com/site/theoriginalepcot/home> (accessed October 30, 2020).
- Eisenberg, Bernd, Ferdinand Ludwig, and Friederike Well. *INTERESS-I - Green Technologies in Landscape Architecture*. 2020. <https://www.ar.tum.de/gtla/forschung/interest-i/> (accessed October 30, 2020).
- Erban, Christof, Jens Oman, and Christian Popp. "Neue Z3-Fassade in Stuttgart - Lastabtragend geklebte Photovoltaik-Verbundverglasung." *Stahlbau* (Wiley) 85 (4 2016): 63-74.
- ETFE. *ETFE - Multifunctional Module - Home*. 2014. <https://www.artificial-ecosystems.com/> (accessed October 30, 2020).
- evolo. *Eco-city Inside a One Kilometer Crater in Siberia*. 10 November 2010. <http://www.evolo.us/eco-city-inside-a-one-kilometer-crater-in-siberia/> (accessed October 30, 2020).
- Fraunhofer ISE. *Projekt Arkol: Wärmepotenzial von Fassaden erschließen*. March 25, 2020. <https://www.ise.fraunhofer.de/de/presse-und-medien/presseinformationen/2020/projekt-arkol-waermepotenzial-von-fassaden-erschliessen.html> (accessed October 30, 2020).
- Fraunhofer UMSICHT. *inFARMING | Fraunhofer UMSICHT*. February 23, 2011. <https://www.umsicht.fraunhofer.de/de/presse-medien/pressemitteilungen/2011/infarming.html> (accessed October 30, 2020).
- Fresco, Jacque. *The Venus Project : the redesign of a culture*. Venus, Fla.: Global Cyber-Visions, 1995.

- Gabler, Markus, Jan Cremers, Jan Knippers, and Julian Lienhard. *Atlas Kunststoff + Membranen (DETAIL Konstruktionsatlanten) (German Edition)*. DETAIL, 2010.
- Gambone, Joseph C. "Kansas - A Vegetarian Utopia: The Letters of John Milton Hadley 1855-1856." *Kansas Historical Quarterly* XXXVIII, no. 1 (1972): p. 65-87.
- Ganji Kheybari, Abolfazl, and Jochen Lam. "Building Envelope as Heat Generator: The impact of Water-filled ETFE Cushion on Energy saving and Comfort." Edited by Thomas Auer, Ulrich Knaack and Jens Schneider. *POWERSKIN conference*. Munich: TU Delft Open, 2017.
- Geuder, Thomas. "Institutsgebäude des ZSW, Stuttgart." *Deutsche BauZeitschrift - DBZ*, September 2018.
- Goddek, Simon, Alyssa Joyce, Benz Kotzen, and Gavin M. Burnell. *Aquaponics Food Production Systems: Combined Aquaculture and Hydroponic Production Technologies for the Future*. Springer International Publishing, 2019.
- Gruen, Victor. *The Heart of Our Cities: The Urban Crisis: Diagnosis and Cure*. New York: Simon and Schuster, 1964.
- Günthner, Stephan, Eva Schweitzer, and Peter Jakubowski. *Smart City Charta*. Stand: Mai 2017. Bonn: Bundesinstitut für Bau-, Stadt- und Raumforschung (BBSR) im Bundesamt für Bauwesen und Raumordnung (BBR), 2017.
- Hays, Michael, and Dana Miller. *Buckminster Fuller: Starting with the Universe*. Edited by K. Michael Hays, Dana A. Miller, Antoine Picon, Elizabeth A. T. Smith and Calvin Tomkins. New, Haven: Whitney Museum of American Art in association with Yale University Press, 2008.
- Heiz, Benjamin P. V., Zhiwen Pan, Lingqi Su, Si Thien Le, and Lothar Wondraczek. "A Large-Area Smart Window with Tunable Shading and Solar-Thermal Harvesting Ability Based on Remote Switching of a Magneto-Active Liquid." *Advanced Sustainable Systems* (Wiley) 2 (12 2017): 10.
- Heliatek. *Produkt | Heliatek*. 2020. <https://www.heliatek.com/de/produkt/> (accessed October 30, 2020).
- Hildebrandt, Christina, Hansjörg Zabel, Wolfgang Siefert, Brunhilde Kindle-Hasse, Nina Pfannkuchen, and Jan Cremers. *FOLLOW-E2 - Energiesparende funktionelle Beschichtungen von Polymermaterialien für die Folienarchitektur : Schlussbericht : Berichtszeitraum: 1.3.2017 bis 30.11.2019*. Tech. rep., Herbolzheim: ROWO Coating GmbH, 2019.
- Howard, Ebenezer. *To-morrow: a peaceful path to real reform*. London: Swan Sonnenschein & Co. Ltd., 1898.
- Kerner, Martin. "Anaerobic domestic waste water treatment coupled to a bioreactor facade for the production of biogas, heat and biomass." Edited by Thomas Auer, Ulrich Knaack and Jens Schneider. *POWERSKIN conference*. Munich: TU Delft Open, 2017.
- Kozai, Toyoki, ed. "Smart Plant Factory." Singapore: Springer-Verlag GmbH, 2018.
- Lalvani, Haresh. "Origins Of Tensegrity: Views Of Emmerich, Fuller And Snelson." 11 (1996): 27-27.
- Loonen, R. C. G. M. *Overview of 100 climate adaptive building shells*. Eindhoven University of Technology, 2010.
- Loonen, R. C. G. M., M. Trčka, and J. L. M. Hensen. "Exploring the potential of climate adaptive building shells." *12th International IBPSA Building Simulation Conference (BS 2011), November 14-16, 2011, Sydney, Australia*. 2011.
- Loonen, R. C. G. M., M. Trčka, D. Cóstola, and J. L. M. Hensen. "Climate adaptive building shells: State-of-the-art and future challenges." *Renewable and Sustainable Energy Reviews* (Elsevier BV) 25 (9 2013): 483-493.
- Manara, Jochen, Andreas Beck, and Jan Cremers. *Energieoptimiertes Bauen: Membrankonstruktionen zur energetischen Sanierung von Gebäuden (MESG) - Verbundkoordination : Laufzeit des Vorhabens: 01.11.2008 29.02.2012; Schlussbericht des*

- BMW-geförderten Projekts*. Tech. rep., Bayerisches Zentrum für Angewandte Energieforschung, Würzburg: Bayerisches Zentrum für Angewandte Energieforschung e. V. (ZAE Bayern), 2012.
- Manara, Jochen, et al. *Funktionalisierte Membrankonstruktionen zur energetischen Sanierung von Gebäuden (FMESG) : Schlussbericht des BMW-geförderten Projekts : Laufzeit des Vorhabens: 01.10.2015 - 30.09.2018*. Tech. rep., Bayerisches Zentrum für Angewandte Energieforschung, Wacotech GmbH & Co. KG, VERSEIDAG-INDUTEX GmbH, Renz Solutions GmbH, Hochschule für Technik Stuttgart, Würzburg: Bayerisches Zentrum für Angewandte Energieforschung e.V., 2018.
- Marks, Robert W., and R. Buckminster Fuller. *The Dymaxion world of Buckminster Fuller*. Edited by Robert W. Marks. New York: Reinhold Pub. Corp., 1960.
- May, Matthias M., Hans-Joachim Lewerenz, David Lackner, Frank Dimroth, and Thomas Hannappel. "Efficient direct solar-to-hydrogen conversion by in situ interface transformation of a tandem structure." *Nature Communications* (Springer Science and Business Media LLC) 6 (9 2015).
- Negroponte, Nicholas. *The Architecture Machine*. Cambridge, Mass.: MIT Press, 1970.
- Pettibone, Glen James. "Combined Vertical Farm, Biofuel, Biomass, and Electric Power Generation Process and Facility." Google Patents, 6 2011.
- Pettibone, Glen James. —. "Modular vertical farm cell." Google Patents, 9 2013.
- Prendeville, Sharon, Emma Cherim, and Nancy Bocken. "Circular Cities: Mapping Six Cities in Transition." *Environmental Innovation and Societal Transitions* 26 (2018): 171-194.
- Raskin, Ben. *The Community Gardening Handbook: Plant & Grow*. Leaping Hare Press, 2017.
- Razaz, Zeinab El. "Sustainable vision of kinetic architecture." *Journal of Building Appraisal* (Springer Science and Business Media LLC) 5 (3 2010): 341-356.
- RWTH Aachen. *Aachener Textilfassade verringert Stickoxidbelastung - RWTH Aachen University Institut für Textiltechnik der RWTH Aachen*. 3 August 2018. <https://www.ita.rwth-aachen.de/go/id/reqe> (accessed October 30, 2020).
- Suncurtain. *Das Produkt - SUNCURTAIN*. 2020. <https://www.suncurtain.solar/das-produkt/> (accessed October 30, 2020).
- Sunley, Peter, Ron Martin, and Peter Tyler. "Cities in transition: problems, processes and policies." *Cambridge Journal of Regions, Economy and Society* (Oxford University Press (OUP)) 10 (10 2017): 383-390.
- TDMA. *Gebäude die unsere Luft reinigen - TDMA*. July 3, 2018. <https://tdma.info/de/gebaude-die-unsere-luft-reinigen/#ref-5> (accessed October 30, 2020).
- The Venus Project. *Circular Cities | The Venus Project*. 2020. <https://www.thevenusproject.com/resource-based-economy/environment/circular-city/> (accessed October 30, 2020).
- Transition Network. *Transition Network | Transition Towns | The Circular Economy*. 30 September 2020. <https://transitionnetwork.org/> (accessed September 30, 2020).
- United Nations, Department of Economic and Social Affairs. "<https://population.un.org/>." 2018. <https://population.un.org/wup/DataQuery/> (accessed September 30, 2020).
- University of Westminster. *Walking City - Archigram Archival Project*. 2020. <http://archigram.westminster.ac.uk/project.php?resultpage=2&&id=60&secid=-1> (accessed October 30, 2020).
- Wenzel Elsa and GreenBiz. *A circular city remains a destination of the future, but many are traveling there | Greenbiz*. 25 June 2019. <https://www.greenbiz.com/article/circular-city-remains-destination-future-many-are-traveling-there> (accessed October 30, 2020).
- Windcloud. *Windcloud | Klimafreundliche Cloud und Colocation*. 30 September 2020. <https://windcloud.de/news/100-erneuerbare-energie-und-direkte-abw%C3%A4rmenutzung> (accessed October 30, 2020).

Wouters, Richard, Martin Ander, Miriam Kennet, Petra Kooij, Luuc Ritmeester, and Carlotta Weber. *Eine Charta für die intelligente Stadt*. Green European Foundation, 2019.

Zuk, William and Clark, Roger H. *Kinetic architecture*. New York: Van Nostrand Reinhold, 1970.

**Open Access** This chapter is licensed under the terms of the Creative Commons Attribution 4.0 International License (<http://creativecommons.org/licenses/by/4.0/>), which permits use, sharing, adaptation, distribution and reproduction in any medium or format, as long as you give appropriate credit to the original author(s) and the source, provide a link to the Creative Commons license and indicate if changes were made.

The images or other third party material in this chapter are included in the chapter's Creative Commons license, unless indicated otherwise in a credit line to the material. If material is not included in the chapter's Creative Commons license and your intended use is not permitted by statutory regulation or exceeds the permitted use, you will need to obtain permission directly from the copyright holder.







---

# Monitoring Tool for Improving Indoor Environment Quality and Performance Based on IoT Sensors: State of the Art and Concept

# 20

Salam Traboulsi and Stefan Knauth

---

## Abstract

Indoor temperature is one of the fundamental features of the indoor environment. It can be controlled with distributed IoT sensors, through wireless networks. It affects human indoor environment such as human thermal sensation, productivity at work, buildings' quality, and several syndrome symptoms. In this study, we focus on the effects of the indoor temperature on the human work productivity and thermal sensation. Our research aims to develop an IoT monitoring tool to manage the challenges in smart buildings by extracting and processing relevant data. It proposes data analysis periodically and integrates newly generated data into the analytical cycle that allows improving human indoor environment.

---

## Keywords

Internet of Things · Buildings' performance · Indoor environment management · Workers' productivity

---

S. Traboulsi (✉) · S. Knauth  
Stuttgart University of Applied Sciences, Stuttgart, Germany  
e-mail: [salam.traboulsi@hft-stuttgart.de](mailto:salam.traboulsi@hft-stuttgart.de)

© The Author(s) 2022  
V. Coors et al. (eds.), *iCity. Transformative Research for the Livable, Intelligent, and Sustainable City*,  
[https://doi.org/10.1007/978-3-030-92096-8\\_20](https://doi.org/10.1007/978-3-030-92096-8_20)

307

## 20.1 Introduction

Smart buildings with the introduction of indoor environment management systems are state of the art (Manic et al. 2016). They have integrated monitoring and communication infrastructure that consists of smart devices such as sensors, which are connected to the Internet of Things (IoT). Building management systems (BMS) aim to optimize the energy consumption in buildings, and they manage the critical components such as heating, ventilation, and air conditioning (HVAC), gas, lighting, security system, electricity, and fire system, in communication with IoT distributed devices. However, according to (ASHRAE 2016) studies, the people who work in offices spend about 60–90% of their time indoors in buildings; thus, their comfort and health effects are strongly related to the indoor environment performance and quality evaluations. Since they focus on doing their job and usually don't reflect their energy consumption (Lo et al. 2012; Jia et al. 2019), they may influence the evaluation's performance systems both actively as they adjust thermostats or operate windows and doors and in a passive sense as they optimize indirectly the use of the buildings services, such as HVAC systems, lighting systems, security systems, elevators, water systems, and other building services.

This research provides a concept and design of an ongoing work of monitoring management tool concept and design based on an indoor building performance model, which incorporates fundamental characteristics of the indoor environment, such as indoor temperature and the working peoples' productivity, adopting the agent-based modeling approach. The core of the monitoring tool is the IoT, which consists of sensors collecting a huge amount of data. At present, such IoT monitoring tools are used for improving the energy consumption of buildings via smart HVAC control. In this respect, our challenge is to achieve monitoring workers' behaviors in a minimally intrusive way. That's why we use existing infrastructure in the buildings, where the sensors are integrated and distributed separately, not requiring any disturbance to the working ones, and to develop effective data evaluations improving monitoring management system.

In the following section, we present various strategies and some observations improving our survey. In Sect. 20.3, we introduce the evaluation part by presenting the three actual characteristics of our tool: (1) data visualization, (2) analysis of indoor temperature collected data and predict system behaviors to react beforehand analysis, and (3) thermal sensation analysis in order to improve working peoples' (hereinafter referred to as workers) productivity. Finally, we draw conclusions and recommendations for practice and future research.

This work is realized within the context of the iCity project. It is sponsored by the German Federal Ministry of Education and Research "FH-Impuls 2016" under Contract 13FH9I01IA.

## 20.2 Related Work

Many recent attempts have focused on studying the relation between indoor environment and workers' behaviors in order to improve energy consumption, building's quality, workers' comfort, etc. Thus, various strategies were adopted to represent the essential elements effecting the occupant comfort and the energy consumption performance in the indoor environment. Indeed, researches are distributed in different axes. Some researches (Yang et al. 2013) are based on deterministic data technologies, wherein the data are collected via distributed sensors, sent through networks, and logged. With the support of sensor technologies, other research teams use modeling methodologies based on collected data of the distributed sensors. The modeling methodology is represented, for example, by statistical analysis, which consists of calculating the relationship between occupant behavior and indoor/outdoor environment conditions, electricity usage, or time period, whose results functions return the occupancy state or the probability of studied behaviors. For example, by using weather stations, occupancy sensors and digital photography collect data related to the indoor environment, occupant presence, and position of shading and windows in five office buildings of Austria (Lenoir et al. 2011). They analyzed the relationship between these parameters and deduced that such interactions are difficult to predict at the level of an individual person. However, they concluded that long-term general trends for groups of building occupants can be expressed as a function of indoor and outdoor environmental parameters. Peng et al. (2011) describe occupant behaviors by a quantitative method. They divided occupant behaviors into three types according to the usage with time dedicated, environment dedicated, and random modes. They used environment and user feedback, or probability and time step, to track the behaviors as a function of the above parameters. Finally, they assumed the effect of human behavior on building and energy use. Moreover, others (Jia et al. 2019; Fabi et al. 2014; Klein et al. 2012) integrated methods of statistics and identified indoor environmental factors, and not real-time environment data, that may change the occupant behavior, e.g., window opening or light switch; however, such a behavior may strongly relate to psychological or social conditions. In this sense, today, researchers integrate artificial intelligence (AI) approaches that range from machine learning that correlates behavioral inputs with buildings' collected data to agent-based modeling (ABM). ABM is a computational model for simulation of object interaction with each other and the indoor environment. In our IoT monitoring management tool research, we adopt ABM.

### Observations

According to the existing literature, there are many methodologies used to model the workers' behavior toward improving the energy efficiency of buildings. Therefore, the authors offer here a discussion reflecting their opinion and fortify their line of research.

Some research analyzed the effect of workers' behavior on building energy consumption based only on some hypothetical constraints and not on real measured data. For instance, Peng et al. (2011) supposed the existence of three typical lifestyles of workers without real data source. This research efficiency may be needed to combine occupants' environment real-time data and behavioral tendency data that may be obtained through a monitoring tool. Other researchers, to optimize the energy performance of buildings, have realized the importance of tracking workers' status, i.e., the status of space being occupied or unoccupied. Their aim is to create a worker behavior pattern that integrates the actual operation schedule optimizing indirectly the building services, such as HVAC and lighting systems. However, in addition to the indirect effect, Jia et al. (2019) added the direct effect of the worker behavior on the energy performance of buildings, such as adjusting thermostats or operating windows and doors. In the literature, we found more research that treats the indirect effect, while we believe that a more detailed direct effect study may potentially reduce the energy consumption of buildings. The aforementioned observations show that there is a relationship between workers' behavior and the factors that initiate their actions (or behavior), needless to say, that the collected data are insufficient to offer a complete evaluation. Fabi et al. (2014) aim to show that indoor environment factors that initiate the worker's behavior may result in a high probability of worker behavior change, for example, window opening; however, people mostly seem to act according to an individual decision, sometimes psychological, and rarely according to an environmental factor. To mention that, logically, if a worker behaves according to an environmental factor, this behavior is efficient and performs one or more building services; therefore, it affects and optimizes directly the monitored factors of performance in real time.

---

### 20.3 Setup and Overview of the IoT Monitoring Tool

The IoT monitoring tool is an analytic platform that converts the IoT collected data into insights and simplifies the decision-making process. It uses agent-based modeling (ABM). The IoT monitoring tool should be able to (1) analyze and predict system behavior to react beforehand, (2) share the analysis with the other users by embedding visualizations into a dashboard, (3) and analyze the productivity of office work.

Data were collected using sensor monitoring of a building of Applied Sciences' university in Stuttgart, Germany. Monitoring concerned indoor and outdoor temperature. Parameters were recorded at 5-min intervals and then sent to a local server. Data concerns the outdoor temperature, as well as the indoor temperature average to a different location in the room. Data were collected for the period between January and July 2016. During this monitored period, the outdoor temperature varied between  $-5^{\circ}\text{C}$  and  $38^{\circ}\text{C}$ , while the indoor temperature varied between  $21^{\circ}\text{C}$  and  $33^{\circ}\text{C}$ . The monitoring agents filter data

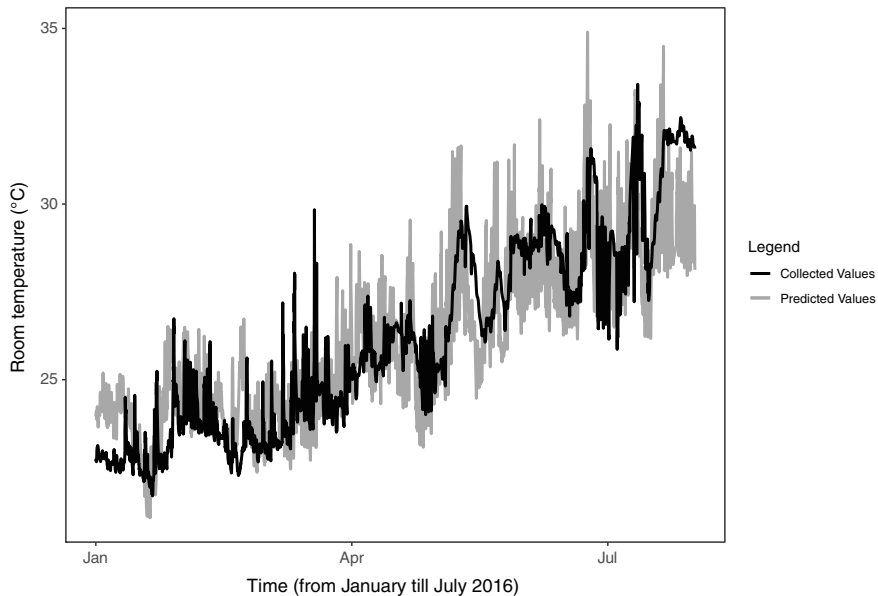


**Fig. 20.1** Simple predicted method

according to conditions, for example, excluding days such as holidays, and/or the greatest similar days.

To visualize into dashboards, and share data analysis with other users, ThingsBoard IoT platform (ThingsBoard 2016) was adopted as IoT technology in our research. ThingsBoard is an open source for data collection, processing, visualization, and device management. IoT monitoring implements few methods for time-series prediction as linear regression used for forecasting the temperature. Figure 20.1 shows a comparison of predicted and recorded indoor temperatures. A good agreement is observed between recorded temperature and linear regression prediction. It has previously been established that indoor environmental quality influences human performance; feeling comfortable at the work office is one of our requirements as workers to improve productivity performance; this performance factor is influenced by many psychological, social, or environmental parameters, and whatever the parameters that can be taken in consideration, all possible parameters vary with time.

Through several studies on performance related to office work, Seppänen et al. (2006) identified a relation between performance and temperature. Various metrics of performance were used in these studies. Field studies used a work task as a metric of performance, in call centers the talk time or using command “regress” in Stata for windows (a program that selects the best fitting linear model of dependent variable on explanatory variables); Seppänen et al. (2006) fit quadratic model to the data for normalized percentage change in performance vs temperature unweighted, weighted by simple size, and weighted by

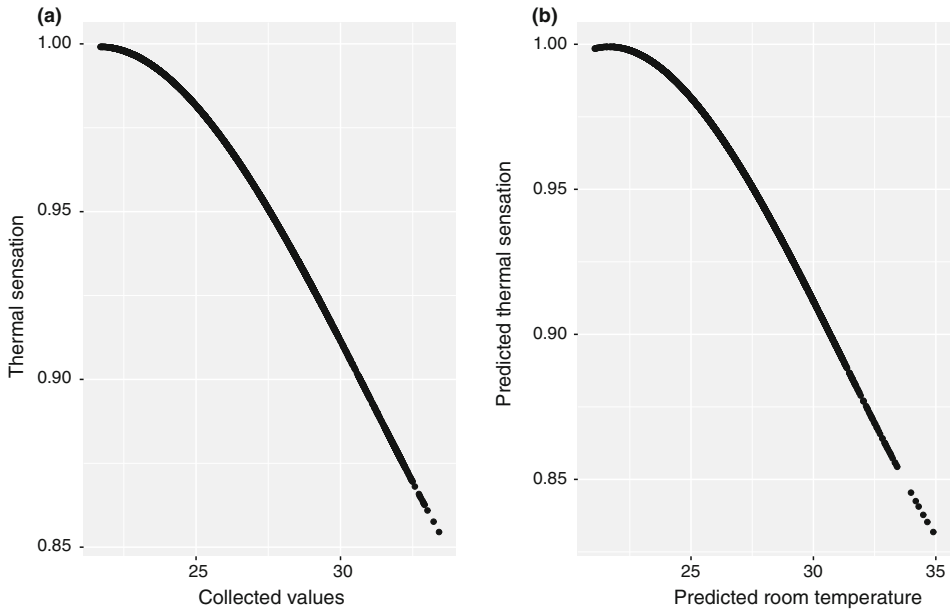


**Fig. 20.2** (a) Normalized performance (thermal sensation) vs room temperature, (b) predicted thermal sensation vs predicted room temperature

combined final weight separately. They deduced this equation for the curve with composite weighting factors:

$$p = 0.1647424 T - 0.0058274 T^2 + 0.0000623 T^3 - 0.4685328$$

where  $p$  is productivity relative to maximum value presenting the worker thermal sensation and  $T$  is indoor temperature, °C. This equation is used for forecasting the workers' productivity considering only the indoor temperature as an input parameter.

Figure 20.2 shows a comparison of real workers' productivity and predicted productivity, (a), according to the collected indoor temperature, and (b), according to regression-based predicted indoor temperature values. A good agreement is observed between recorded and predicted values. Both cases show a consistent decrease in performance of typical office tasks when temperature increases above 26 °C.

This analysis did not include different indoor environment parameters, such as the number of workers, devices, windows, and doors in a room. These parameters could have a significant impact. However, as the next step, the activities that have a significant impact could be monitored and included in the analysis model.

## 20.4 Conclusion

This paper proposes a methodology for the development of a simplified regression-based model for forecasting indoor temperature and predicting the workers' thermal sensation. It shows relevance analysis and leads to a simplified forecasting model with restricted input parameters. Data included outdoor and indoor temperature and humidity. Analyses showed that the indoor temperature and the thermal sensation forecasting could be conducted with good precision using only the indoor temperature history. This result could not be generalized. However, the proposed methodology could be used for improving the indoor quality and the workers' performance. Available data did not include indoor activities. The presence of significant activities should be considered to improve the forecasting model analysis.

---

## References

- ASHRAE. (2016). Guideline 10 provides guidance regarding factors affecting indoor environmental conditions acceptable to the comfort and health of human occupants.
- Fabi, V., Maggiora, V., Corgnati, S. & Andersen, R. (2014). Occupants' behaviour in office buildings: Stochastic models for window opening.
- Jia, M., Srinivasan, R., Ries, R., Weyer, N. & Bharathy, G. (2019). A systematic development and validation approach to a novel agent-based modeling of occupant behaviors in commercial buildings. *Energy and Buildings*. 199. 352-367. <https://doi.org/10.1016/j.enbuild.2019.07.009>.
- Klein, L., Kwak, J., Kavulya, G., Jazizadeh, F., Becerik-Gerber, B., Varakantham, P. & Tambe, M. (2012). Coordinating occupant behavior for building energy and comfort management using multi-agent systems. *Automation in Construction*. 22. <https://doi.org/10.1016/j.autcon.2011.11.012>.
- Lenoir, A., Cory, S., Donn, M. & Garde, F. (2011). Users' Behavior and Energy Performances of Net Zero Energy Buildings. *Energy*. 6. 5-6.
- Lo, S. H., Peters, G. & Kok, G. (2012). Energy-Related Behaviors in Office Buildings: A Qualitative Study on Individual and Organizational Determinants. *Applied Psychology*. 61. 227-249. <https://doi.org/10.1111/j.1464-0597.2011.00464.X>.
- Manic, M., Wijayasekara, D., Amarasinghe, K., & Rodriguez-Andina, J. J. (March 2016). Building Energy Management Systems: The Age of Intelligent and Adaptive Buildings. *IEEE Industrial Electronics Magazine*, 10, 1, (pp. 25-39). doi: <https://doi.org/10.1109/MIE.2015.2513749>.
- Peng, C., Yan, D., Wu, R., Wang, C., Zhou, X. & Jiang, Y. (2011). Quantitative description and simulation of human behavior in residential buildings. *Building Simulation*. 5. <https://doi.org/10.1007/s12273-011-0049-0>.
- Seppänen, O., Fisk, W.J. & Lei, Q.H. (2006). Room Temperature and Productivity in Office Work, eScholarship Repository, Berkeley, California, Lawrence Berkeley National Laboratory, University of California, <http://repositories.cdlib.org/lbnl/LBNL-60952>.

ThingsBoard open-source IoT Platform. ThingsBoard, Inc. is a US corporation founded in (2016) with RnD center in Kyiv, Ukraine. Retrieved from <https://thingsboard.io/>

Yang, Z., Li, N., Becerik-Gerber, B., & Orosz, M. (2013). A systematic approach to occupancy modeling in ambient sensor-rich buildings. Simulation. <https://doi.org/10.1177/0037549713489918>.

**Open Access** This chapter is licensed under the terms of the Creative Commons Attribution 4.0 International License (<http://creativecommons.org/licenses/by/4.0/>), which permits use, sharing, adaptation, distribution and reproduction in any medium or format, as long as you give appropriate credit to the original author(s) and the source, provide a link to the Creative Commons license and indicate if changes were made.

The images or other third party material in this chapter are included in the chapter's Creative Commons license, unless indicated otherwise in a credit line to the material. If material is not included in the chapter's Creative Commons license and your intended use is not permitted by statutory regulation or exceeds the permitted use, you will need to obtain permission directly from the copyright holder.







# Box-Type Windows as Means for Better Air Quality and Acoustic Comfort in Urban Areas

# 21

David Offermatt, Daniel Lust, and Tobias Erhart

## Abstract

Controlled natural ventilation in office buildings can ensure the indoor thermal comfort while reducing the life cycle energy consumption for ventilation, compared to mechanical ventilation systems (e.g. HVAC). Natural ventilation is mostly used in moderate climate zones where air conditioning is not a standard. During intermediate seasons, buildings with HVAC systems can additionally use natural ventilation to reduce energy consumption. However, in dense urban areas, natural ventilation can be problematic in terms of acoustic comfort. Here, a box-type window can serve as a compromise between thermal and acoustic comfort. Due to the more complex handling of the box-type window, an automated (electric driven) novel box-type window approach was developed within the imaF project, a part of the iCity initiative. The following article describes the basics of automated natural ventilation, acoustic characterization as well as architectural integration of this window type and the optimization of the airflow through box-type windows. The results show that the proposed geometry can provide sound insulation while providing an appropriate air exchange rate.

## Keywords

Box-type windows · Controlled natural ventilation · Noise protection · CFD

D. Offermatt · D. Lust · T. Erhart (✉)  
Hochschule für Technik Stuttgart, Stuttgart, Germany  
e-mail: [tobias.erhart@hft-stuttgart.de](mailto:tobias.erhart@hft-stuttgart.de)

© The Author(s) 2022  
V. Coors et al. (eds.), *iCity. Transformative Research for the Livable, Intelligent, and Sustainable City*,  
[https://doi.org/10.1007/978-3-030-92096-8\\_21](https://doi.org/10.1007/978-3-030-92096-8_21)

315

## Nomenclature

ppm	Parts per million
CFD	Computational fluid dynamics
SST	Shear stress transport
Ma	Mach number (Ma)
STL	STereoLithography file format
HVAC	Heating, ventilation, and air conditioning
imaF	intelligentes motorisch angetriebenes Fenster
$G_{\text{FAC}}$	Global irradiation on the facade plane ( $\text{W}/\text{m}^2$ )
$\zeta$	Pressure loss coefficient
$U_{\text{g}}$	U-value glass ( $\text{W}/(\text{m}^2\text{K})$ )
$U_{\text{w}}$	U-value window ( $\text{W}/(\text{m}^2\text{K})$ )
$N_x$	Mesh coordinate/number of cells x-direction
$N_y$	Mesh coordinate/number of cells y-direction
$L_x$	Channel dimension x-direction (m)
$L_y$	Channel dimension y-direction (m)
$k$	Turbulence kinetic energy ( $\text{J}/\text{kg}$ )
$\varepsilon$	Turbulent kinetic energy dissipation rate ( $\text{J}/(\text{kgs})$ )
$w$	Turbulence specific dissipation rate (1/s)
$u_{\text{ref}}$	Flow velocity (m/s)
$C_m$	Model coefficient for the turbulent viscosity (–)
$I$	Turbulence intensity (–)
$n$	Modified turbulence viscosity
$p$	Pressure (Pa)
$\Delta p$	Pressure difference (Pa)
$\rho$	Density ( $\text{kg}/\text{m}^3$ )
$A$	Opening cross ion of windows ( $\text{m}^2$ )
$A_1$	Opening cross section 1 ( $\text{m}^2$ )
$A_2$	Opening cross section 2 ( $\text{m}^2$ )
$A_{\text{eff}}$	Cross-sectional area (m)
$T_{\text{e}}$	Ambient temperature ( $^{\circ}\text{C}$ )
$T_{\text{i}}$	Indoor temperature ( $^{\circ}\text{C}$ )
$\dot{m}$	Mass flow ( $\text{kg}/\text{s}$ )
$R_{\text{w}}$	Sound reduction index (dB)

### 21.1 Introduction

Along with higher energy building standards, the focus in energy saving has been shifting from heat losses by transmission more and more to ventilation heat losses. Whereas in old buildings classic windows naturally leak, the envelope's air tightness increases the demand

of additional air delivered by ventilation systems. Furthermore, higher occupation rates in office rooms lead to a higher sensitivity for appropriate indoor air quality. In many climate zones, the comparably short hot periods do not justify the use of an HVAC system, in particular when the building has a considerable thermal mass. This is the case for most locations in Germany. Nevertheless, there is a worldwide trend towards more air conditioning in urban areas. In Europe alone, an increase of 45% in air conditioning units between 2020 and 2030 is expected (OECD/IEA, 2018).

Analyses within the KonLuft project (Schulze et al., 2016) have shown that life cycle costs (LCC) and life cycle energy consumption of a mechanical ventilation system consume approximately twice the power and resources compared to controlled natural ventilation. The maintenance costs and the complexity level of a building can be significantly reduced by using the natural ventilation principles. During the planning process, engineers must assure that the design of the ventilation concept meets the requirements of the building usage. Often, in commercial buildings, planners prefer mechanical ventilation or HVAC systems over natural ventilation to guarantee the demanded air exchange rates of (DIN EN 13779, 2007) and the former (DIN EN 15251, 2007) or its replacement (DIN EN 16798-3, 2017). The key to robust calculations is the availability of valid discharge coefficients (Gandhi et al., 2015) and the local wind situation (Maas et al., 1991).

Multiple studies in the past reported that natural ventilation can be a reliable and cost-effective alternative. However, in an urban environment, noise pollution causes severe discomfort when windows on street facing facades are opened. During night-time, controlled natural ventilation can reduce the temperature of the room and the building components. For moderate middle European climates, up to  $-5$  K (Erhart et al., 2015) can be achieved. In hot dry climates, natural ventilation achieves up to  $-3$  K to  $-6$  K during one night (Shaviv et al., 2001).

Figure 21.1 shows various influencing factors that need to be taken into account during the planning process. It also shows architectural design guidelines to consider in the first steps of the planning process. The key factors that influence the thermal comfort (see Fig. 21.2) can be assured by rather low-tech approaches through controlled natural ventilation.

The article is divided into the following chapters:

- Controlled Natural Ventilation.
- Box-Type Windows.
- Laboratory Set-Up.
- Airflow Through Box-Type Windows.
- Architectural Integration.
- Acoustic Comfort.
- Conclusion and Outlook.
- Nomenclature

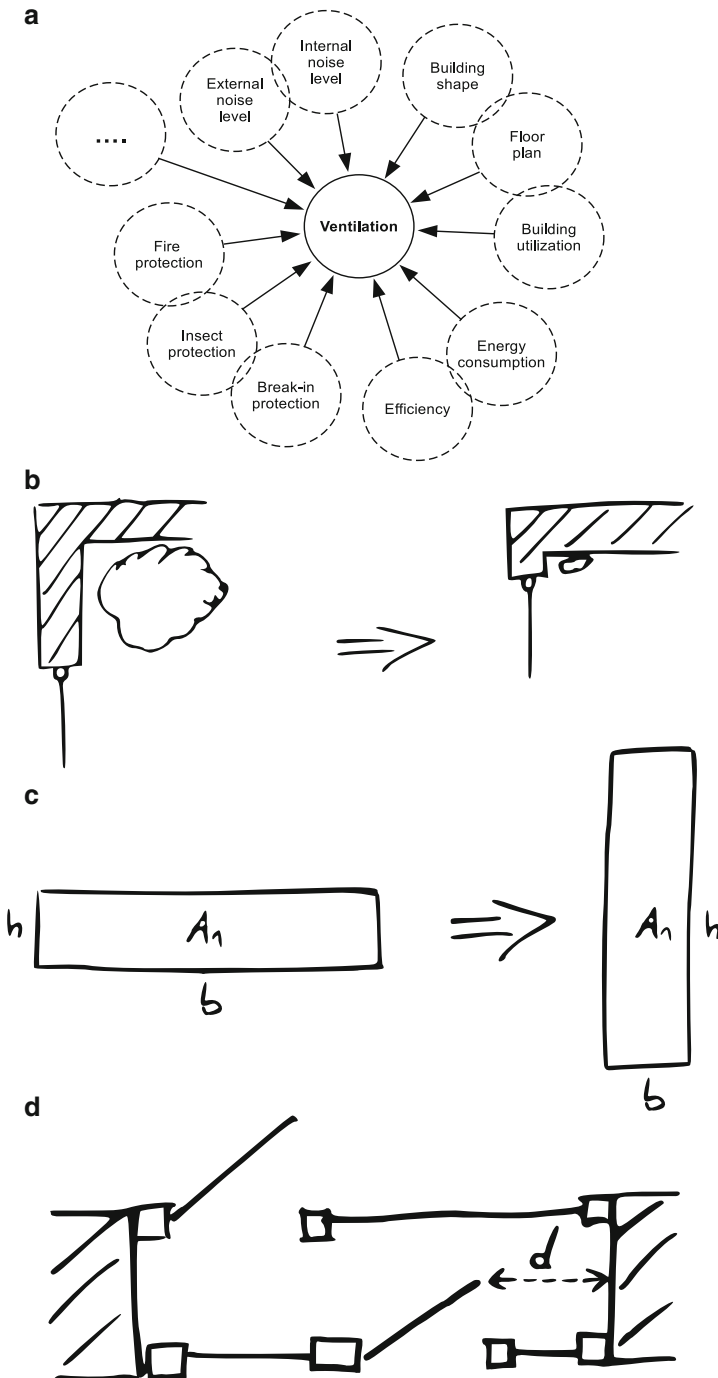


**Fig. 21.1** (a) Parameters that influence ventilation planning. Design. (b, c, d): Design recommendations. Reduction of the window camber. Height instead of width. Position of the opening wing

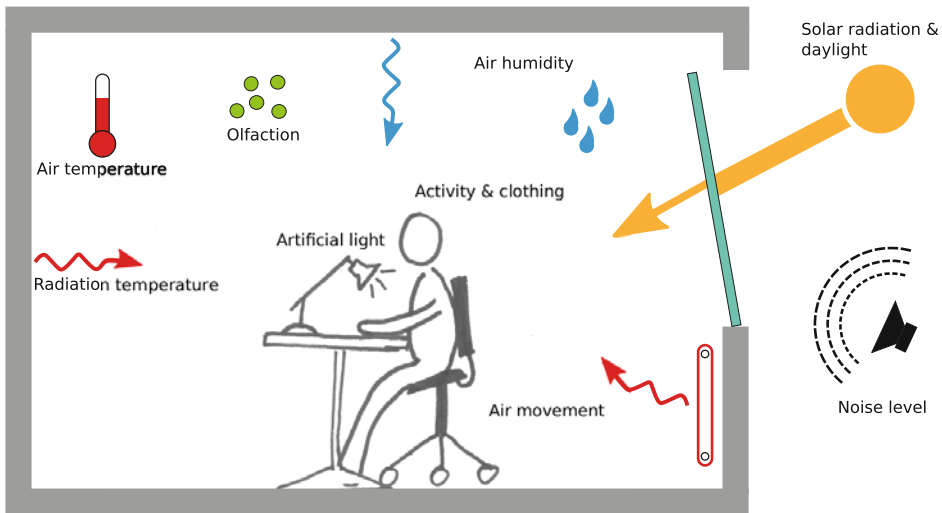


**Fig. 21.2** Ventilation influencing thermal comfort

## 21.2 Controlled Natural Ventilation

For every orifice in a building and each prevailing ambient condition, an associated airflow, or air exchange, can be calculated. The pressure differences between the two sides of the orifice cause an airflow. Differences in temperature, and therefore in density of air, cause the pressure difference through the buoyancy effect. In addition, the wind induces a difference in pressure (Fig. 21.3). Especially in cross-ventilation situations, this case results in significantly higher air exchange rates. However, in urban areas statistically, the thermal regime (temperature difference between internal  $T_i$  and ambient  $T_e$ ) clearly dominates over the wind regime (tangential flow  $U_{Wind}$ ). Consequently, in order to assure the desired air exchange rate, one should configure the windows according to thermal regime properties. While classic natural ventilation depends on the occupants opening the windows, controlled natural ventilation comes with a control system and window drives. The drives today are mainly electric, whereas pneumatic drives have become rare nowadays.

### Control Strategies

One can implement various control strategies for the automation of opening and closing windows. Each of the following strategies can contribute to thermal comfort as a passive solution. The following strategies can be combined or work independently.

- Hysteresis  $CO_2$ : If the  $CO_2$  concentration rises above 1000 ppm, the window opens until the  $CO_2$  concentration drops below 600 ppm.

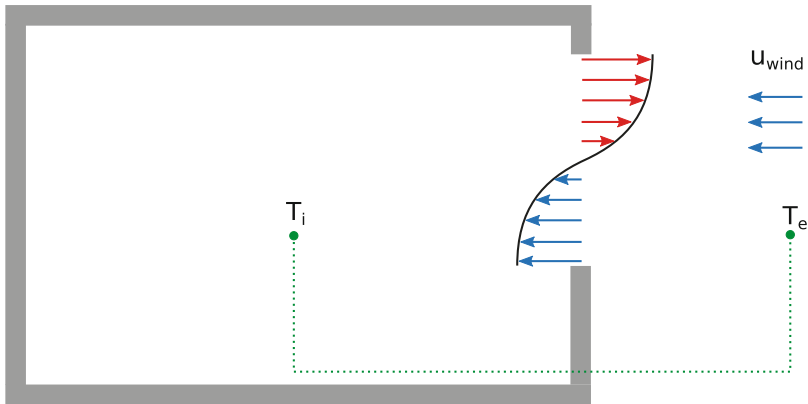


**Fig. 21.3** Impulse for natural ventilation caused by temperature difference or wind. Exemplary for a winter day. Indoor and outdoor temperature and wind velocity

- Hysteresis  $CO_2$  + manual override: A manual mode supplements the described hysteresis  $CO_2$  strategy. This mode allows an interruption by the occupant. During the manual mode, the window is opened or closed via a wall-mounted switch.
- Night cooling: If the ambient temperature ( $T_e$ ) at night is lower than the indoor temperature while the day meets the criteria of a summer day (24-h mean  $T_e \geq 15^\circ C$ ), night cooling mode is enabled.
- A typical combination is night cooling + hysteresis  $CO_2$  + manual mode. This strategy is the best choice to increase hygienic properties of those as basis.
- Increased daytime cooling: If the criterion of a summer day at daytime is met and the inside temperature is higher than the ambient temperature, the window will open.

### 21.3 Box-Type Windows

The historical box-type window consists of two single glazed windows connected with a fix case (box) to one element. It aims to achieve a better heat resistance and an improvement of the sound insulation. In the case at hand, two windows with a size of 1.28 m by 1.45 m and an  $U_w$ -value of  $1.6 \text{ Wm}^{-2} \text{ K}^{-1}$  and  $U_g$ -value of  $1.1 \text{ Wm}^{-2} \text{ K}^{-1}$  (glass 6 | 12 | 4 | 12 | 4) were arranged successively. Two thirds of each window are fixed and one third is an opening segment. The air gap between the windows has a depth of 0.28 m and it has an air volume of  $0.52 \text{ m}^3$ . Figures 21.4a, b show a scheme of the evaluated box-type window and its dimension.

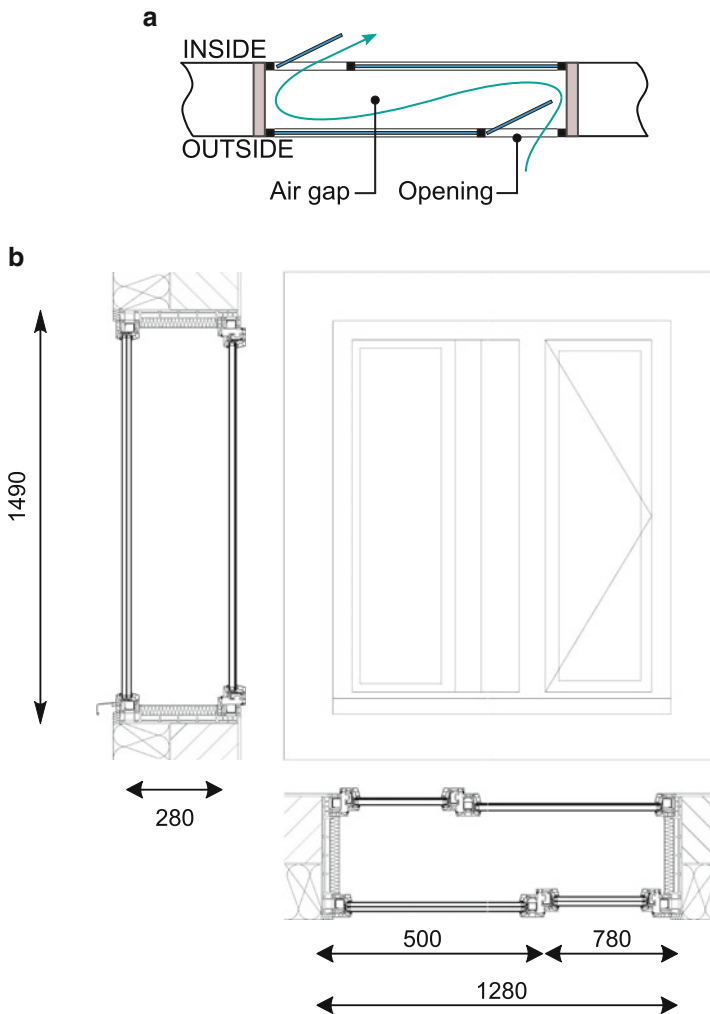


**Fig. 21.4** (a) Scheme and dimensions of the evaluated box-type window. (b) Scheme and dimensions of the evaluated box-type window

## 21.4 Laboratory Set-up

Within the project, an occupied office serves as in situ laboratory. The room measures 4.67 m by 6.47 m, with a height of 3.39 m. The gross volume is 102.4 m<sup>3</sup>; subtracting furniture it results in a ventilated net volume of 98.58 m<sup>3</sup>. The data acquisition system records the following outdoor and indoor thermal properties as well as comfort parameters:

- Indoor air temperature, five sensors equally distributed along the height of the room.
- Indoor radiation temperature at average office clerk head level (sitting position).
- CO<sub>2</sub> measured at the pole in the centre of the room and near to the window.
- Indoor relative humidity.
- Outdoor air temperature (radiation shielded).
- Outdoor relative humidity.
- Wind speed and direction (3D).
- Global irradiation on the outer wall plane.
- Absolute air pressure.

In order to obtain accurate values for the air exchange, multiple tracer gas campaigns were undertaken in the test office using both decay and constant concentration methods with hydrofluorocarbon (HFC) 1,1,1,2-tetrafluoroethane (R134a).

Throughout the measurements, the inside and outside air temperatures and pressures were logged in order to characterize the flow with regard to thermal-induced pressure differences. The experiment was executed with the reference window (opening angle of 15°) and inserted acoustic foam (20 mm).

### **Decay Method**

The decay method starts with a manually initiated constant tracer gas concentration; the room is sealed and the tracer gas is applied. Then, the concentration is measured for approximately 1 h. The event changing the gas equilibrium inside the room, that is, opening the window, is triggered. The latter method is more reliable under the given laboratory set-up as the dosing error for the tracer gas does not go into consideration. More samples can be obtained per time, as the device requires no time for dosing. A downside is the relatively short measuring period. After the tracer gas is below the detection limit, the experiment needs to be paused for the reapplication of tracer gas.

### **The Constant Concentration Method (CC Method)**

The CC method is favourable when data over a long period are needed, for instance, under changing ambient conditions, or to record a full set of day and night data. A dosing unit applies tracer gas according to a control algorithm. The obtained values undergo a Kalman filter.

---

## **21.5 Airflow Through Box-Type Windows**

### **Governing Equations**

The airflow through windows (if wind influences are negligible) is driven by temperature differences between the inside air and the ambient conditions. The pressure resulting from the temperature difference  $\Delta p$  can be approximated according to Eq. (21.1) (with the density  $\rho$ , the free fall acceleration  $g$  and the opening height  $H$ )



$$\Delta p = \rho \cdot \left(1 - \frac{T_i}{T_e}\right) \cdot g \cdot H \quad (21.1)$$

If the pressure loss coefficient  $\zeta$  is known, e.g. from wind channel experiments or from CFD simulations, the corresponding airflow velocity  $u$  can be determined with Eq. (21.2).<sup>1</sup>

$$u = \sqrt{\frac{2 \cdot \Delta p}{\rho \cdot \zeta}} \quad (21.2)$$

The volume flow  $\dot{V}$  could be calculated with the area on which  $\zeta$  refers to (e.g. effective opening area or inlet area of a wind channel) and results as.

$$\dot{V} = u \cdot A \quad (21.3)$$

The actual air exchange rate (ACH) is then defined as shown in Eq. (21.4) with the volume of the investigated room  $V_{\text{room}}$ .

$$\text{ACH} = \frac{\dot{V}}{V_{\text{room}}} \cdot 3600 \frac{\text{s}}{\text{h}} \quad (21.4)$$

ACH is given in changes per hour  $\text{h}^{-1}$ .

### 21.5.1 Airflow Through Box-Type Windows Compared to a Single Window

Compared to single windows with the same opening area, box-type windows show comparably higher pressure losses and hence a lower volume flow at the same inflow conditions (see Fig. 21.5).

With the same boundary conditions, the pressure at windward site of the window more than doubles from 4.67 Pa for the single window to 13.7 Pa for the box-type window. This results from the two sharp airflow deflection at the two opening edges of the box-type window. This effect finally limits the achievable air exchange rates of this window type.

Another limiting factor is the small opening areas resulting from the geometry with the outer window opening to the inside of the encasement. These areas depend on the opening angle (see Fig. 21.6 areas A, A<sub>1</sub> and A<sub>2</sub>). From the characteristic arises an optimal opening angle for every box-type window configuration (see Fig. 21.7).

<sup>1</sup>Note that the velocity calculated with that approach is not necessarily the velocity at the window itself. It depends on which velocity  $\zeta$  refers to. This could be the velocity at the effective opening area, or the inlet velocity of an (artificial) wind channel.

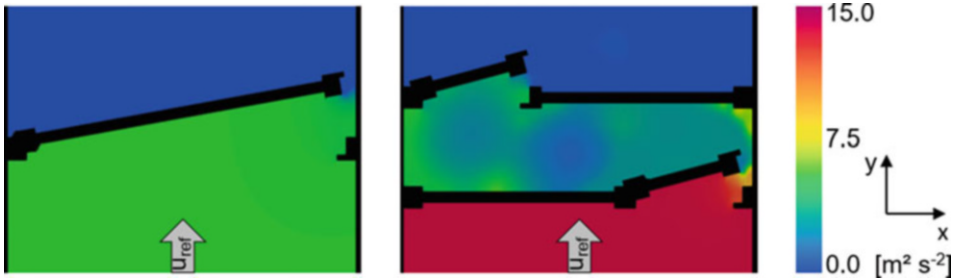
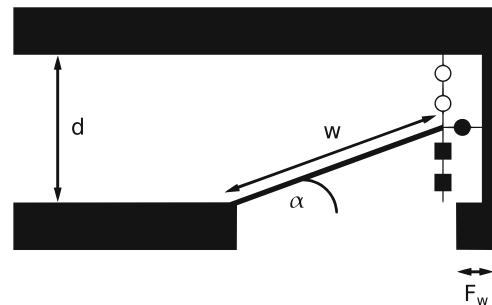


**Fig. 21.5** Comparison of the pressure loss of a single window and the investigated box-type window

**Fig. 21.6** Basic specification to calculate the opening areas



- $d$  Distance between windows
- $w$  Width of opening wing
- $F_w$  Width windowframe
- $\alpha$  Opening angle
- Opening surface  $A$
- Opening surface  $A_1$
- Opening surface  $A_2$

In this specific case ( $d = 0.28$  m,  $w = 0.424$  m,  $F_w = 0.037$  m), the ideal opening angle ( $\alpha$ ) is  $27.5^\circ$ . Up to this angle, the smallest opening area is  $A_2$ . By exceeding an opening angle of  $27.5^\circ$ , surface  $A_1$  becomes the smallest area.

If the inside surfaces of the window box are faced with materials to increase the absorption of sound, these areas may further diminish. Hence, the planning of box-type windows requires a balancing of the acoustic comfort and the ventilation ability.

### 21.5.2 Measurements of the Volume Flow

Figure 21.8 shows the results from tracer gas measurements. The measured air exchange rates over the temperature difference are plotted. This window configuration achieves an ACH up to about 0.5 (shown in Fig. 21.4). Although a trend that ACH increases with rising temperature difference is visible, the measurement points in Fig. 21.8 fluctuate around the

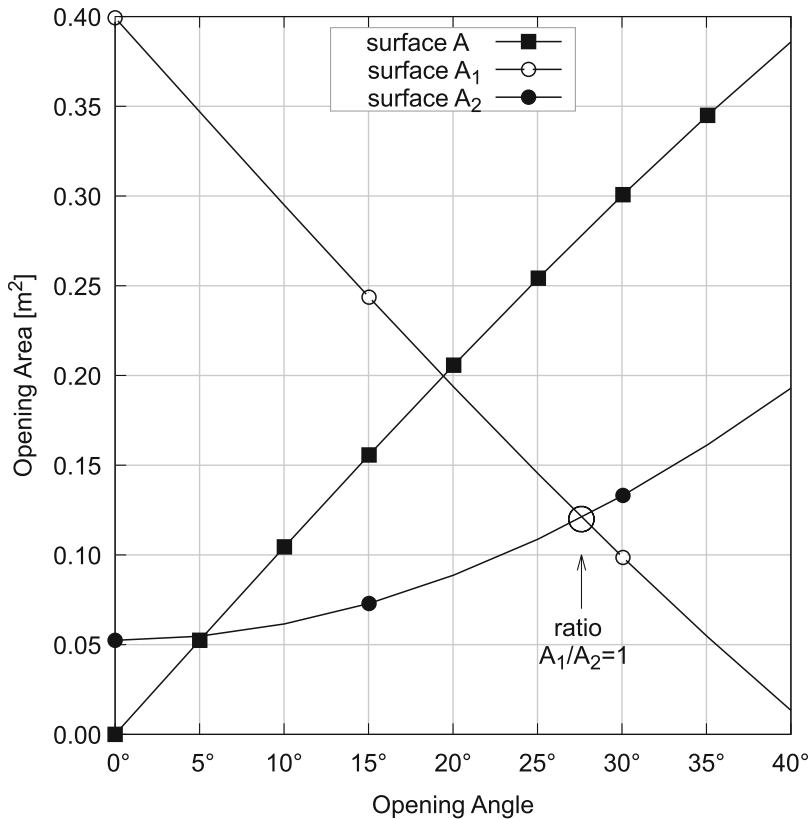


**Fig. 21.7** Behaviour of the different openings of a box-type window,  $A_1/A_2 = 1$  marks the optimum, as the smallest surface reaches its maximum

same temperature differences. This effect might be caused by pressure fluctuations at the building facade due to wind effects like occurring gusts.

Figure 21.9 shows the measured volume flow in comparison to the calculated volume flow (Eqs. 21.1, 21.2 and 21.3) with  $\zeta$  from CFD results versus temperature difference. It is clear from this figure that the calculated volume flow is overestimated compared to the measurement results. This could be caused by several reasons:

- As the window is installed in an occupied office, the measurements were not executed under laboratory conditions. Influences of wind or infiltration could lead to divergent results.
- The pressure loss caused by an installed insect protection mesh was not considered in the CFD calculations.
- Three-dimensional (thermal) airflow effects may be not sufficiently represented in the 2D CFD simulations.

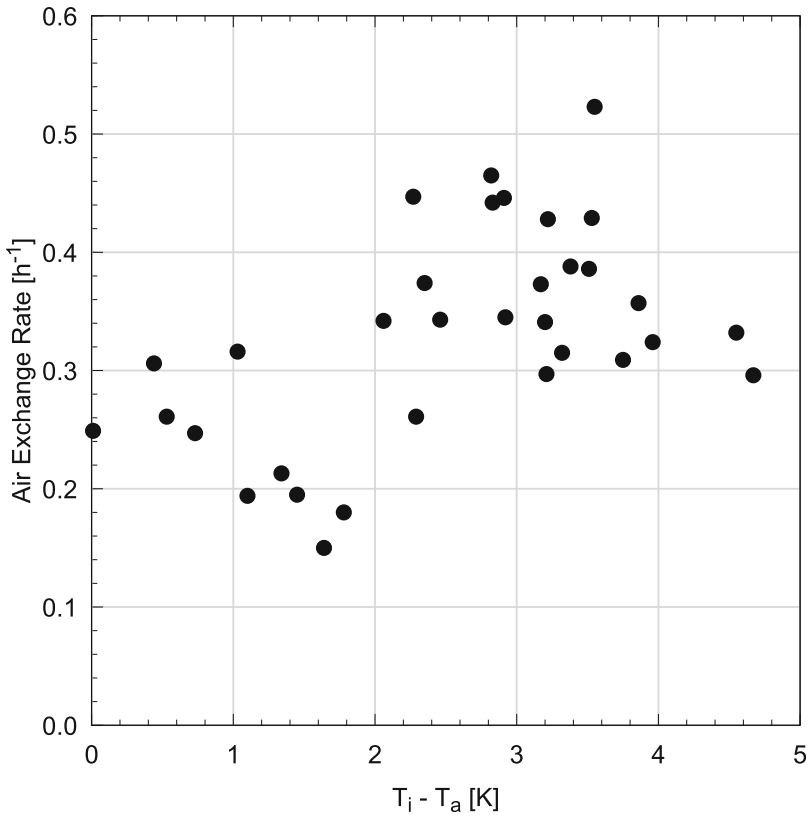


**Fig. 21.8** Tracer gas measurement results

Further experiments must be executed to calibrate the CFD model to the measurement results.

### 21.5.3 Measures to Increase Air Exchange Rates

To increase the volume flow rates through box-type windows, some modifications on the window design are possible. The impact on the actual pressure loss coefficient of three different variants (see Table 21.1; all variants without acoustic foam inlet) is investigated using computational fluid dynamics (CFD<sup>2</sup>).

Table 21.2 shows the resulting pressure loss coefficients for every window variant. Compared to the reference window, the optimization of the opening angle (variant 1) leads to half of the pressure losses. Rounding the corners (variant 2) shows higher pressure losses

<sup>2</sup>OpenFOAM, solver: simpleFoam, turbulence model: k- $\omega$ -SST.

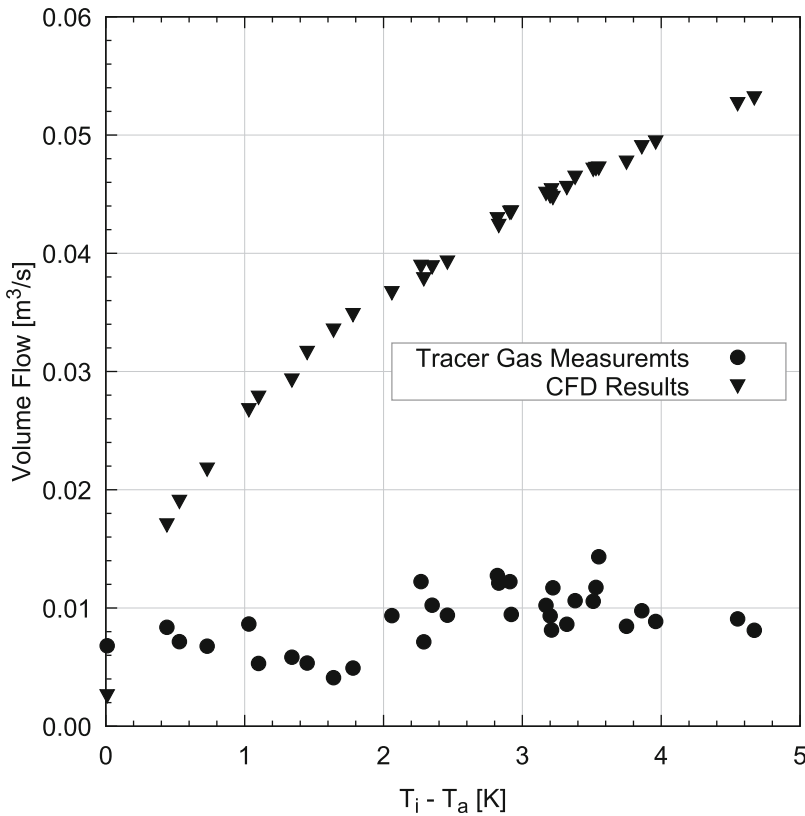


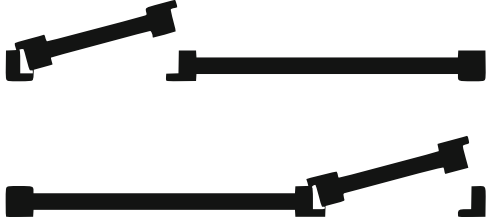
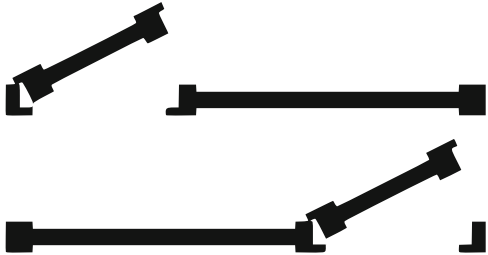
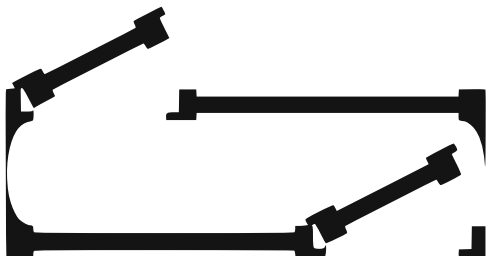
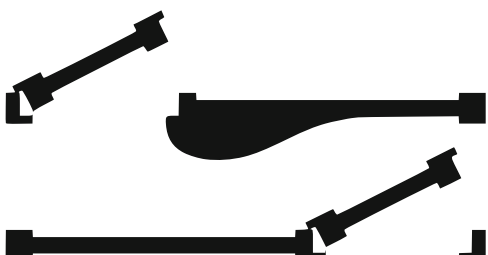
**Fig. 21.9** Measured vs. calculated volume flow

than variant 1, due to the decreased effective opening area (see Table 21.1). By far, variant 3 achieves the highest improvement. The airflow guidance reduces the flow separation at the inner window edge and consequently decreases the occurring velocity significantly. Figure 21.10 depicts this effect, visualizing the flow for every investigated variant.

## 21.6 Architectural Integration

A modular system design supports the construction process and achieves a high degree of prefabrication. To improve the acoustic properties when the windows are closed, two different types of windows have been chosen. Triple glazing in the outer part of the box-type window provides thermal and weather protection. Double glazing with laminated glass serves as basis for the inner part of the box-type window. A surrounding aluminium profile offers space for the control system, cabling and sound absorbing material.

**Table 21.1** Box-type window optimization variants ( $A_{\text{eff}}$  = effective opening area)

Variant	Description	$A_{\text{eff}}$ ( $\text{m}^2$ )	Sketch
Reference	Geometry as installed in the ventilation lab Opening angle: $15^\circ$	0.07	
1	Optimized opening angle (according to Fig. 21.6) Opening angle: $27^\circ$	0.12	
2	Opening angle: $27^\circ$ Rounded corners	0.099	
3	Opening angle: $27^\circ$ Airflow guidance within box	0.12	

**Table 21.2** Resulting pressure loss coefficients for each window variant

Variant	$\Delta p$ (Pa)	$\zeta$	Improvement
Reference	13.65	2236	–
1	6.75	1107	–50.0%
2	7.05	1156	–48.0%
3	3.30	541	–75.8%

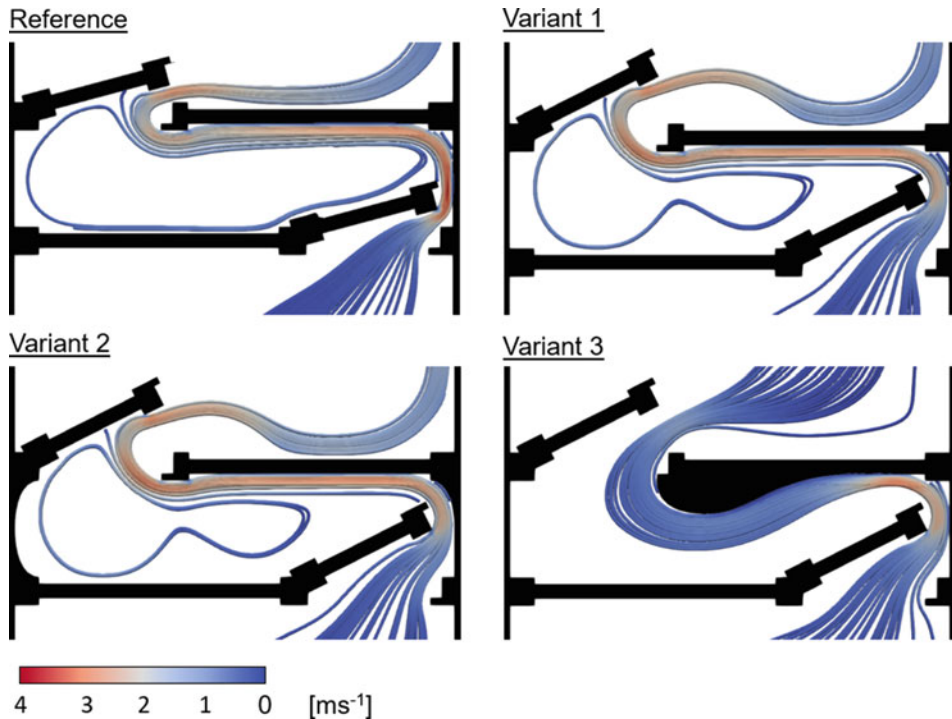


**Fig. 21.10** Airflow through each box-type window variant

Furthermore, the profile supports the element mounting and assures a better construction process. The isometric drawing in Fig. 21.11 depicts the components.

Figure 21.12 shows the architectural integration of the investigated box-type window. With this set-up, only a narrow window frame is visible from the inside. However, with the fixed glazing, maintenance will be more difficult. Figure 21.13 shows a more suitable solution for architectural design and maintenance. A casement window is used as a template. The outer part of the surrounding aluminium profile is enlarged. This offers flexibility in usage of other window types and offers more space for the integrated control as well as sound-absorbing material. To increase air exchange, it also allows the window to be fully opened. Note that the sound insulation is thereby reduced immensely. One can expect a negative effect for the daylight efficiency due to the smaller outer window (see Fig. 21.12). Due to the box principle, the window reveal can be very small despite higher insulation standards from the outside.

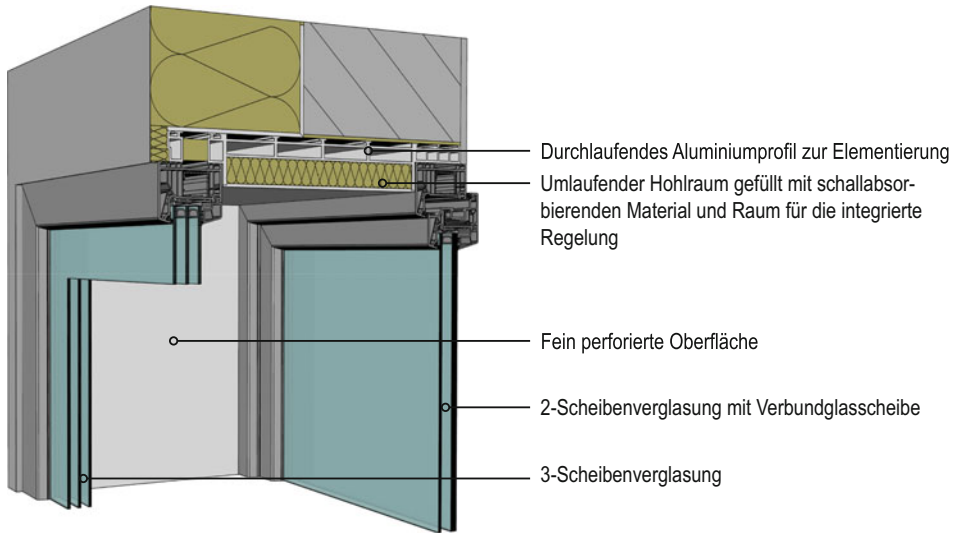


**Fig. 21.11** Structural design of the architectural integrated box-type window

## 21.7 Acoustic Comfort

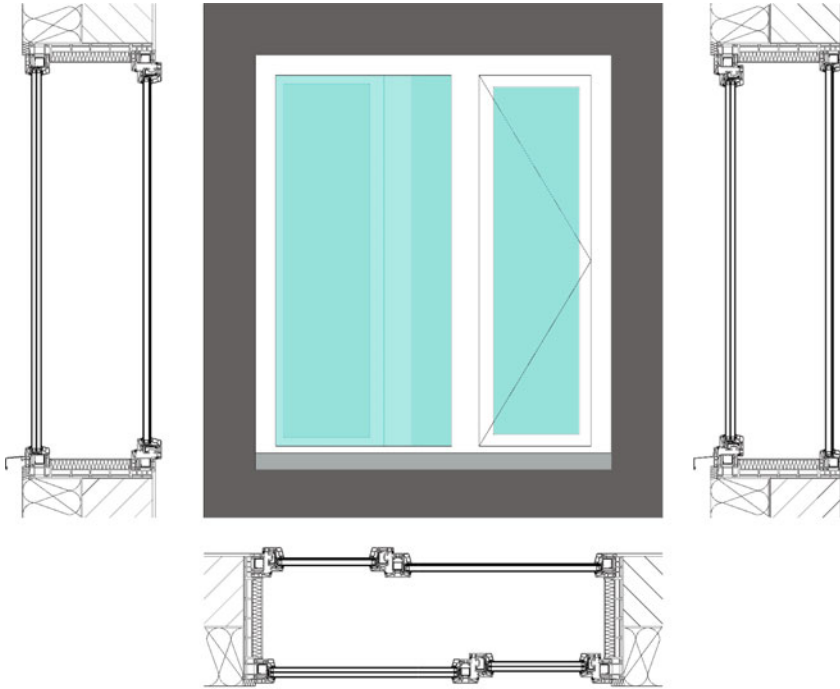
By using a box-type window, the weighted sound reduction index  $R_w$  can be increased around 5 dB in opened and closed states compared to a single window. If the box-type window is additionally equipped with acoustic foam (basotect 20 mm), the sound insulation in closed state again increases by 2 dB.

Without absorbing foam, opening the single and box-type windows 5 cm and 10 cm reduces the weighted sound reduction index by approximately 20 dB to 25 dB, respectively. However, with absorbing foam, the reduction is only 5 dB to 16 dB. Generally, the box-type window without foam has weighted sound reduction index that is 5 dB higher than that of the single window. The box-type window with foam with an opening of 5 cm even outperforms the closed single window by 3 dB and is only 3 dB under the closed box-type window without foam. This option gives the best acoustic results while allowing some sort of natural ventilation (Table 21.3).

## 21.8 Conclusions

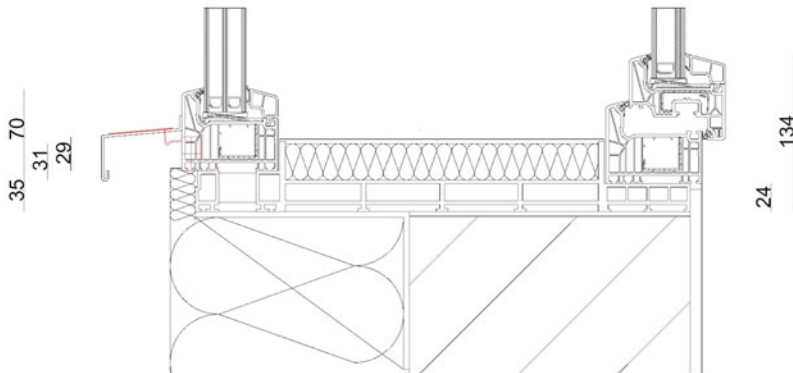
The findings of this work conclude as follows:





M 1:20

	464	
82	280	102
	277	
16	267	16



M 1:5

**Fig. 21.12** Architectural integration of the investigated box-type window\

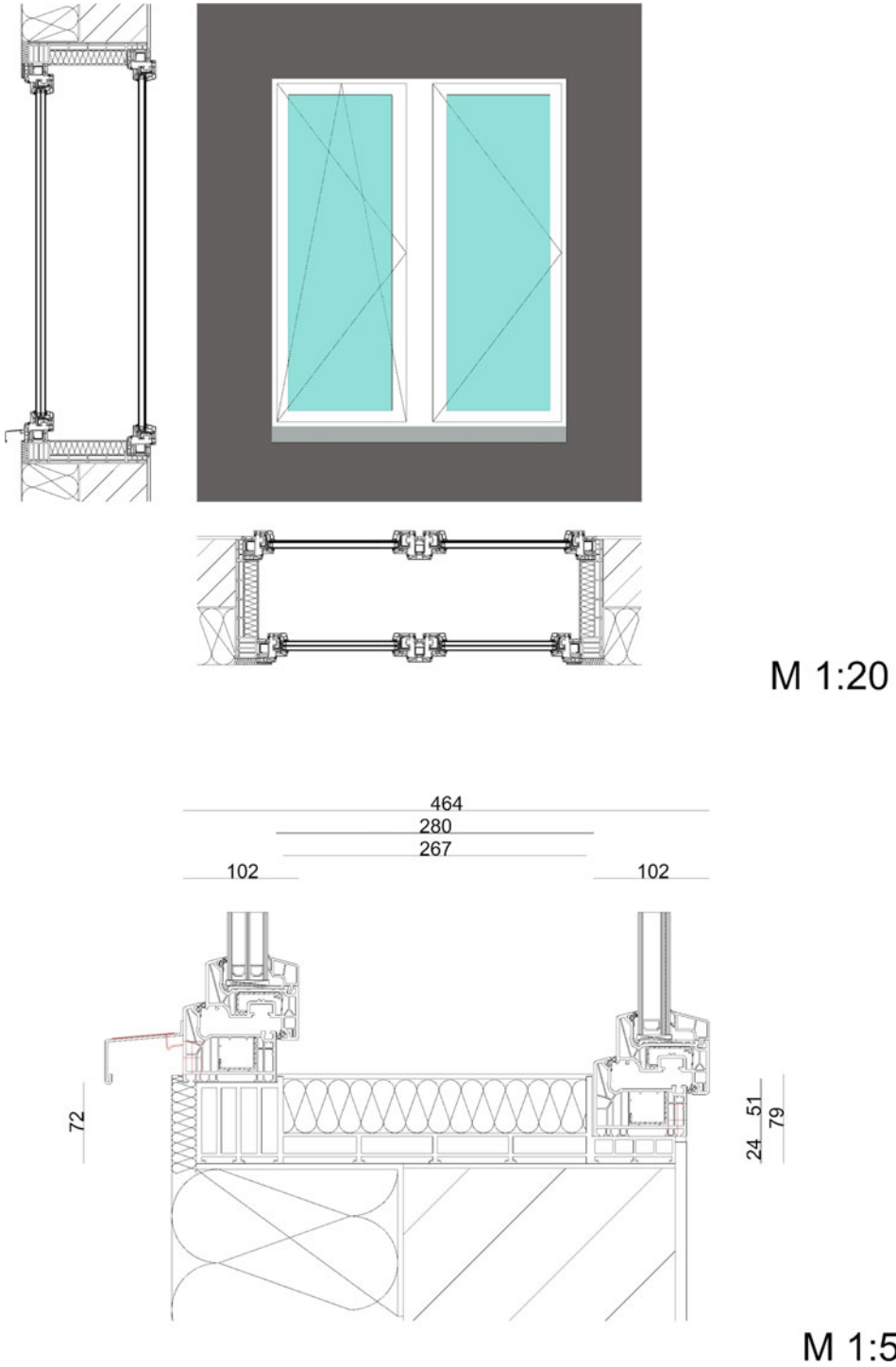


**Fig. 21.13** Alternative for the investigated box-type window, friendly for maintenance and service

**Table 21.3** Expected weighted sound reduction index  $R_w$  of the investigated box-type window

	Single window (dB)	Box-type window (dB)	Box-type window with acoustic foam (dB)
Window closed	34	40	42
Window opened (5 cm)	15	20	37
Window opened (10 cm)	10	16	26

Comparison of a single window, box-type window and the box-type window with acoustic foam

- CFD calculations show that the pressure losses are reduced by approximately 50% by simply optimizing the opening angles of the casements. Further reductions are achievable by guiding the airflow inside the window box.
- The resulting air exchange rate under a mean temperature difference of 3.4 K was around 0.4 1/h (with an infiltration of about 0.14 1/h).
- Despite the relatively small flow cross section, the system provides appropriate air exchange rates. The very low width-to-height-ratio of the window gap (0.0385 m/m) supports higher pressure differences.
- The weighted sound reduction index of an opened box-type window equipped with acoustic foam is around 22 dB higher than an open single window.

---

## 21.9 Outlook

- The 2D CFD simulations will be transferred to 3D simulations which may take buoyancy effects into account better, but come with higher computation costs.
- More detailed calculation approaches must be found and applied to be able to better simulate real airflow conditions, e.g. mounting conditions and wind influences.
- In the future, the more suitable architectural design window will be studied in the laboratory and with CFD simulations.
- Implementation of the algorithm to control the increase of air exchange during the day and subsequent evaluation of the impact on thermal comfort.
- Installation and evaluation of the active noise control in the box-type window.

---

## References

- DIN EN 13779:2007-09; Ventilation for non-residential buildings - Performance requirements for ventilation and room-conditioning systems; German version EN 13779:2007, 2007.
- DIN EN 15251:2012-12; Indoor environmental input parameters for design and assessment of energy performance of buildings addressing indoor air quality, thermal environment, lighting and acoustics; German version EN 15251:2007, 2007.

- DIN EN 16798-3:2017-11; Energy performance of buildings - Ventilation for buildings - Part 3: For non-residential buildings -Performance requirements for ventilation and room-conditioning systems (Modules M5-1, M5-4); German version EN 16798-3:2017, 2017.
- Erhart, T.; Guerlich, D.; Schulze, T.; Eicker, U.; Experimental Validation of Basic Natural Ventilation Air Flow Calculations for different Flow Path and Window Configurations. Energy Procedia 2015, 78, 2838 – 2843. 6th International Building Physics Conference, IBPC 2015, <https://doi.org/10.1016/j.egypro.2015.11.644>, 2015.
- Gandhi, P.; Brager, G.; Dutton, S. A Comparative Study of Mixed Mode Simulation Methods: Approaches in Research and Practice. Proceedings of the Symposium on Simulation for Architecture & Urban Design; Society for Computer Simulation International: San Diego, CA, USA, 2015.
- Maas, J.; Bienfait D.; Vandaele L.; Walker R.; Single sided air movement & ventilation control within buildings, Vol. PAPER 4, 12th AIVC Conference Canada, Ottawa, 1991.
- OECD/IEA. The Future of Cooling, 2018.
- Schulze, T.; Eicker, U.; Haag, M.; Gürlich, D.; Erhart, T.; KonLuft - Energieeffizienz von Gebäuden durch kontrollierte natürliche Lüftung - Abschlussbericht; Hochschule für Technik Stuttgart, Zentralverband Elektrotechnik- und Elektronikindustrie; <https://www.tib.eu/de/suchen/id/TIBKAT%3A872634132>; 2016.
- Shaviv, E.; Yezioro, A.; Capeluto, I.G.; Thermal mass and night ventilation as passive cooling design strategy. Renewable Energy 2001, 24, 445 – 452. [https://doi.org/10.1016/S0960-1481\(01\)00027-1](https://doi.org/10.1016/S0960-1481(01)00027-1), 2001.

**Open Access** This chapter is licensed under the terms of the Creative Commons Attribution 4.0 International License (<http://creativecommons.org/licenses/by/4.0/>), which permits use, sharing, adaptation, distribution and reproduction in any medium or format, as long as you give appropriate credit to the original author(s) and the source, provide a link to the Creative Commons license and indicate if changes were made.

The images or other third party material in this chapter are included in the chapter's Creative Commons license, unless indicated otherwise in a credit line to the material. If material is not included in the chapter's Creative Commons license and your intended use is not permitted by statutory regulation or exceeds the permitted use, you will need to obtain permission directly from the copyright holder.





# Airborne Sound Insulation of Sustainable Building Facades

# 22

Andreas Drechsler, Steffi Reinhold, Andreas Ruff, Martin Schneider,  
and Berndt Zeitler

## Abstract

Two trends are currently leading to an increased risk of indoor noise pollution. Firstly, urban densification causes traffic noise sources to be closer to the building facades which makes them louder at the facades. Secondly, airtightness of buildings, due to energy regulations, leads to the need of natural or mechanical ventilation to ensure a “healthy” indoor air quality, thereby allowing noise to easily pass from outdoors to indoors. In the case of mechanical ventilation, an additional noise source is also created. This study investigates the risk reduction of an indoor noise problem by optimizing the facade elements regarding sound insulation. Noise levels of different transportation noise sources (cars, trucks, trains) are used to calculate the resulting indoor noise levels after passing through the facade elements. The amount of noise transmitted into the indoors is dependent on the frequency spectra of the sources and of the sound reduction properties of the facade elements. Facade elements such as masonry walls, open windows, and ventilators are investigated and modified regarding their sound insulation properties. Through passive means, the weighted sound reduction index of an open window and an open ventilator was increased by 12 dB and 3 dB, respectively. Also, the indoor self-noise of the ventilator was investigated and reduced for different airflow rates.

A. Drechsler · S. Reinhold · A. Ruff · M. Schneider  
Hochschule für Technik Stuttgart, Stuttgart, Germany

B. Zeitler (✉)

Institute for Applied Research, University of Applied Sciences Stuttgart, Stuttgart,  
Baden-Württemberg, Germany  
e-mail: [berndt.zeitler@hft-stuttgart.de](mailto:berndt.zeitler@hft-stuttgart.de)

© The Author(s) 2022

V. Coors et al. (eds.), *iCity. Transformative Research for the Livable, Intelligent,  
and Sustainable City*,

[https://doi.org/10.1007/978-3-030-92096-8\\_22](https://doi.org/10.1007/978-3-030-92096-8_22)

335

---

**Keywords**

Sound insulation · Sound transmission · Indoor noise · Building facade · Traffic noise · Ventilation · Spectrum adaption term

---

## 22.1 Introduction

In order to promote sustainability by saving energy, regulations force new buildings to be constructed more airtightly. To ensure a “healthy” air quality and to reduce the probability of mold growth, ventilation becomes an essential necessity. Furthermore, urban densification leads to buildings being built closer to streets and rail tracks. Both of these factors (ventilation and densification) can lead to higher noise levels and consequently health issues for the inhabitants of these homes.

The resulting indoor noise levels are dependent on the spectra of the outdoor sources and on the spectra of the sound insulation of the facade elements. So firstly, a closer look is taken at the noise spectra of a set of road and rail traffic noise sources, which were captured in the Stuttgart area. To correlate better to the human perception of noise, the A-weighted levels of these noise sources are discussed. The noise levels of a further noise source, namely, the ventilator used for mechanical ventilation, are also presented at different airflow rates.

In a next step, the sound insulation properties of some selected facade elements are viewed and optimized. These elements include a single and double masonry wall, a box-type window with different opening angles, and an (open) ventilator.

The latter two elements allow for necessary natural ventilation through the facade and are optimized by passive means, in other words by changing the impedances of the boundaries. To better understand the sound insulation of the double facade wall, a simple mass-spring-mass model is used to indirectly calculate the effective stiffness between the inner and outer shell of the facade wall.

Finally, the resulting indoor levels of these selected transportation noise sources are compared, and a conclusion is made on which single number values describing the sound insulation of the investigated facade elements best correlate with the reduction of traffic noise through the respective element.

The authors would like to thank the participating industry partners, Siegenia-Aubi KG, Schüco International KG, Aumüller Aumatic GmbH, and Bundesverband Kalksandstein Industrie e.V., as well as the funding organization of the Federal Ministry of Education and Research (BMBF) for supporting this research.

## 22.2 Noise Sources

A selection of noise sources including transportation noise and ventilator noise was chosen for this study. Whereas transportation noises from the sources were simply measured, the radiated noise from the ventilator was optimized through design changes. Both types of noise sources will be discussed for Z-weighted and A-weighted signals. The former is a linear weighting of the frequency components, and the latter simulates the frequency dependency of the average hearing.

### 22.2.1 Transportation

Within a former project by Pietruschka et al. (2011) funded by BWPLUS, average levels of various transportation noises (Truck, Car, City Tram, Regional Train, and Freight Train) were collected in a residential area in Stuttgart according to standard DIN 45642 (2004), however using a dummy head. The shape of the measured levels coincides well with the normative traffic noise levels according to the standard DIN EN ISO 717-1 (2019) and DIN EN 1793-3 (1997). All levels used in this paper (see Fig. 22.1) were recorded in front of the building facades, except for the levels of the Freight Train and the Regional Train, which were recorded at a similar distance from the tracks to the buildings, yet not directly in front of the facades due to organizational issues. The used locations are however expected to give comparable levels to those found in front of the nearby buildings.

Looking at the legend, one can see that the Freight Train has the highest overall levels followed by those of the Truck. Looking at the frequency content, the Truck shows higher levels in the low frequency range, whereas the Freight Train shows higher levels in the high frequency range. The source with the lowest overall level is the City Tram. The levels of the City Tram are also the lowest throughout the whole frequency range and are only undercut by the levels of the Regional Train between approximately 80 and 500 Hz.

Going from Z- to A-weighting, the order of the overall source levels changes only between the Car and the Regional Train (see Table 22.1). Hereby, the latter has higher A-weighted levels due to the more pronounced high frequency components, whereby the former has higher linear weighted levels. The levels going from Z- to A-weighting reduce for the five transportation sources, whereby the Car and Truck show the largest reduction of approximately 7–8 dB due to the strong low frequency component.

### 22.2.2 Ventilator

A further investigated noise source, which also contributes to the indoor noise level, is the ventilator. The sound power radiated (into the building) by a standard quality ventilator built into a wall was measured on the basis of DIN EN ISO 3743-1 (2010) with slight deviations. Drechsler and Ruff (2017) showed that this deviation from the standard

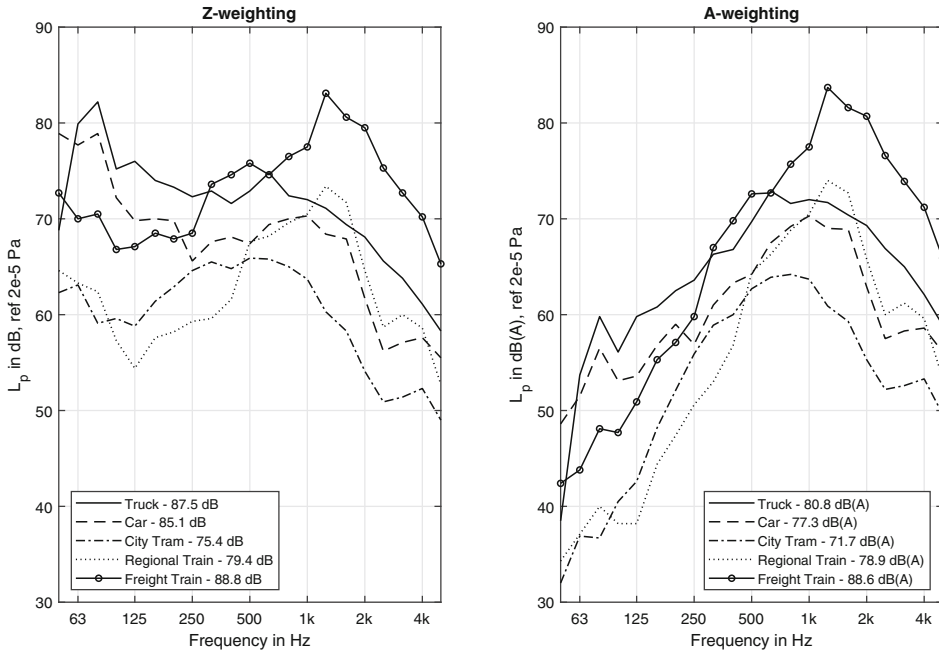


**Fig. 22.1** Outdoor sound pressure levels. Left: linear Z-weighted, right: A-weighted

**Table 22.1** Traffic source levels in dB

Source	Z-weighting	A-weighting	Difference
Truck	87.5	80.8	6.7
Car	85.1	77.3	7.8
City Tram	75.4	71.7	3.7
Regional Train	79.4	78.9	0.5
Freight Train	88.8	88.6	0.2

measurement methods delivers appropriate results. The ventilator was investigated both before (“nor” for normal) and after carrying out some acoustical modifications (“per” for perforation modifications).

In both cases, the ventilator was built into a 150 mm thick calcium silicate brick wall (approximately 350 kg/m<sup>2</sup>) with thin plastering on the inner side and a thermal insulation composite system on the outer side comprised of 200 mm mineral wool with 12.5 mm gypsum board. In the field, plaster is used instead of gypsum board on the outer side, but the acoustical difference is considered negligible. The opening on the inner side was enclosed with a standard plastic covering spaced a few centimeters away with slits on the cover side to allow air exchange. The plastic tube of the ventilator has a diameter of 160 mm and a length of approximately 380 mm. The acoustically modified ventilator tube has the same dimensions, yet an additional effective perforation of approximately 25–30%



**Fig. 22.2** Ventilator tube with 100 mm of perforation at outer end behind ceramic heat exchanger



**Table 22.2** A- and Z-weighted sound power levels  $L_W$  of the ventilator in dB for different airflow rates, directions, and tube types

Tube type	Airflow rate in m <sup>3</sup> /h	Outward direction		Inward direction	
		Z-weighting	A-weighting	Z-weighting	A-weighting
Normal	45	58.1	53.0	57.8	52.5
	32	51.6	46.2	49.7	44.2
	15	38.6	31.6	39.0	32.7
Perforated	45	55.1	51.1	55.3	50.5
	32	48.7	44.1	47.4	42.2
	15	37.0	29.2	38.4	30.9

at the last 100 mm on the outdoor end at the depth of the mineral wool (see Fig. 22.2). More details on the setup can be found in Ruff et al. (2020).

The measured Z-weighted and A-weighted total sound power levels  $L_W$  for different airflow rates (15 m<sup>3</sup>/h, 32 m<sup>3</sup>/h, 45 m<sup>3</sup>/h and different directions (“in” for inward and “out” for outward)) can be seen in Table 22.2. Note, that the levels do not differ much regarding the direction of airflow for both Z- and A-weighted power levels (sums differ by max. 2 dB). Due to adding the perforation (going from “nor” to “per”), the single number values are reduced by 2–3 dB. The modal behavior of the tube is assumed to be the cause and is explained below.

The cut-on frequency of the tube, at which the first radial mode propagates, is  $f_c \approx 2.5$  kHz from  $\lambda = 2\pi r/x_0$ , where  $\lambda$ ,  $r$ , and  $x_0$  are the wavelength, radius of the tube, and zero of the Bessel function (cylindrical function), respectively. The derivation of the Bessel function of zeroth order  $J_0(x_0 = k \cdot r)$ , marking the particle velocity at the boundary of the tube, is zero at  $x_0 = 3.8317$ . Below this cut-on frequency, plane waves propagate in the tube and lead to strong reflections at the ends, as there is an impedance change (plane waves => spherical waves) when exiting the tube. These reflections further lead to resonances with modal shapes that cause higher sound radiation at these frequencies.

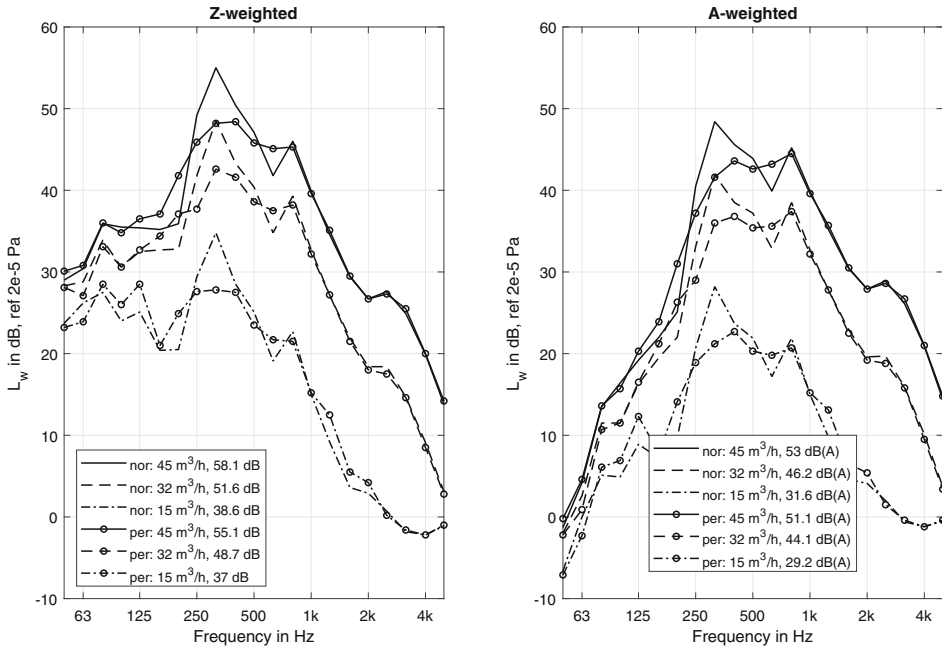


**Fig. 22.3** Sound power levels  $L_W$  in dB and dB(A) of normal and perforated tubes from ventilator at different airflow rates, direction out, solid line: normal tube; dashed line: perforated tube

These resonances can be seen in Fig. 22.3, which also shows that by increasing the airflow rate, the peak in sound power around 315 Hz increases the most, whereas the levels at the low frequencies only rise slightly.

As the peak frequency does not shift by increasing the flow rate, it is believed that this resonance is not caused by the blade passing frequency, yet by the resonance along the tube length itself. This tube resonance is however excited by the noise from the blade passing frequency that lies close by. Being that the one end is somewhat closed (unknown impedance due to the covering) and the other end is relatively open (yet with slats), the resonance should lie somewhere between a quarter wavelength ( $f = 447$  Hz—one end rigid and one end fully open) and a half wavelength ( $f = 223$  Hz—both ends fully open). A resonance frequency at  $f_0 = 315$  Hz would mean that the resonance is at  $0.35 \cdot \lambda \approx 1/3$  ( $>1/4$  and  $<1/2$ ) of a wavelength. A quarter wavelength resonator has its antiresonances and resonances at even and odd multiples of the fundamental frequency, respectively. Being that there is a dip in the levels at approximately double the frequency ( $f_1 = 2 \cdot 315$  Hz), and another local maximum at around three times the frequency  $f_2 = 800$  Hz, supports this theory.

That the latter resonance frequency is slightly lower than three times the frequency is because slightly more than a quarter wavelength fits in this tube as with its not ideally rigid and open ends.

Through the perforation, two things are expected to happen. Firstly, the boundary conditions on the outer side become less defined, thereby spreading out the energy of the resonance to other frequency bands. One can see that the levels are not reduced in all one-third octave bands and even increase at lower frequencies. This supports the assumption that this peak is caused by a tube mode. Secondly, the sound power should get absorbed by the mineral wool. However, the effect is minimal, as otherwise the reduction of the levels at higher frequencies would increase over frequency.

The perforation reduces the peak values for both Z- and A-weighted levels by approximately 6–7 dB for all airflow rates. The overall levels are only reduced by approximately 3 dB. However, being that this peak in the one-third octave band is so high due to the very tonal blade passing frequency, the overall annoyance is reduced by lowering the level at this peak. Tonal sounds are found to be more annoying than stochastic noise according to DIN 45681 (2005).

Depending on the room properties (volume and absorption) and the sound insulation of the facade, these traffic and ventilator noises will be pronounced and disturbing to the occupant.

---

## 22.3 Sound Insulation

The sound insulation most often described by the sound reduction index,  $R_{\text{tot}}$  of the facade, is the energetic sum of the sound insulation of its elements (wall, window, ventilator) weighted by their areas:

$$R_{\text{tot}} = -10 \log \sum_{i=1}^{n=3} 10^{-0.1R_{i,\text{area}}}, \text{ with} \quad (22.1)$$

$$R_{i,\text{area}} = R_i - 10 \log \frac{S_i}{S_{\text{tot}}},$$

where  $S_{\text{tot}}$  is the total area of the facade,  $S_i$  is the area of the element  $i$ , and  $R_{i,\text{area}}$  is the sound reduction index of the element weighted by its area to the total area. In general, the sound reduction index describes ten times the logarithmic ratio of the incident sound power to the radiated power of the element. In this investigation, it was measured according to DIN EN ISO 10140-2 (2020). The total sound reduction index of the facade,  $R_{\text{tot}}$ , will not be discussed much further in this paper, as there exist so many possible permutations of wall, window, and ventilator elements. Yet, in a later section, the sound reduction index,  $R_{i,\text{area}}$ , normalized to the same overall area will be compared between the elements. However, firstly, the sound reduction index,  $R_i$ , of the elements as they were measured is looked at more closely.

**Fig. 22.4** Inner shell of calcium silicate brick wall covered with insulation, anchors (marked with white circles), and first rows of outer shell



### 22.3.1 Wall

Only two of the nine walls that were investigated in the iCity project are presented here. The one wall is a double wall (DW) built of an inner shell (brick wall), cavity (thermal layer), and outer shell (brick wall). The other wall is a single wall (SW) of the same inner shell (brick wall) on its own. They were chosen to demonstrate the effects of the anchors between shells. Due to wind loads, it is important to fasten the outer shell of a facade wall to the inner shell with metal anchors. These anchors, which are set in plastic plugs, however diminish the sound reduction of the wall relative to the same wall without anchors. One goal of this partial study is to find a simple formula to describe the effect of the outer shell fastened by different means and thereby to be able to predict the total sound reduction index before constructing the wall. This will ensure a healthy indoor environment and reduce cost due to over-designed constructions.

The base 175 mm thick calcium silicate brick wall (SW—single wall) has a mass per area of approximately  $340 \text{ kg/m}^2$  (see Fig. 22.4). The other wall system (DW—double wall) is comprised of the base wall, also called inner shell (IS), plus 200 mm of mineral wool cavity insulation, and an external outer shell (OS) constructed of 115 mm thick calcium silicate block bricks with a mass per unit area of approximately  $198 \text{ kg/m}^2$ . Nine anchors per square meter were installed. A more detailed description of the setup can be found in Schneider et al. (2018).

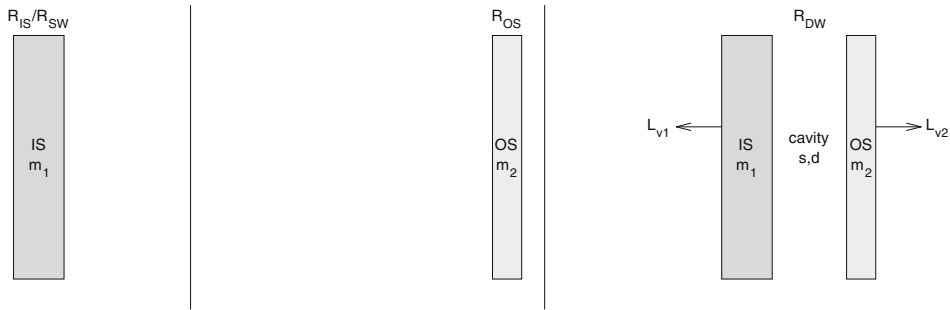


**Fig. 22.5** Sketch of walls defining quantities.  $\Delta R = R_{DW} - R_{SW}$  and  $\Delta L_v = L_{v1} - L_{v2}$ , and equivalent mass ( $m_1$ ,  $m_2$ ), spring ( $s$ ), and damper ( $d$ ) elements

Although the system is quite complex as seen in a modal analysis (not shown here) with coupled modes beginning at 30 Hz, it was decided to firstly model the double wall as a simple mass-spring-mass system. For double walls filled with air or fibrous material, the stiffness of the cavity is well known and predictions of transmission can be made. However, the added anchors complicate matters and at low frequencies add an extra stiffness compared to just air, thereby increasing the mass-spring-mass frequency. The anchors also introduce structure-borne bridges at higher frequencies, which reduce the sound reduction index. The latter effect falsifies the simple estimation using the mass-spring model at higher frequencies.

Although estimates are false at high frequencies, a way was found to extract the effective stiffness of the cavity by comparing the theoretical differences between the sound reduction index of the single wall ( $R_{SW}$ ) and the double wall ( $R_{DW}$ ) utilizing the difference in velocity on the one side, IS, ( $L_{v1}$ ) of the double wall and on the other side, OS, of the wall ( $L_{v2}$ ) (see Fig. 22.5) when exciting the IS with a loudspeaker.

### Mass-Spring-Mass System

How the theoretical quantities of  $R_{DW}$ ,  $R_{SW}$ ,  $L_{v1}$ , and  $L_{v2}$  can be obtained by a simple mass-spring-mass system is shown here. They are all dependent on the impedance of the wall ( $z_w$ ), meaning the ratio of exciting force  $F_1$  and resulting velocity  $v$ . The relationship between the force and velocity of a mass-spring-mass system can be described by the following matrix equation:

$$F = \begin{bmatrix} F_1 \\ 0 \end{bmatrix} = N \cdot \frac{1}{j\omega} \begin{bmatrix} v_1 \\ v_2 \end{bmatrix} \quad (22.2)$$

where  $F_1$  is the force exciting the wall,  $j = \sqrt{-1}$ ,  $\omega$  is the angular frequency, and  $v_1$  and  $v_2$  are the velocities of the inner and outer shells, respectively. The stiffness matrix,  $N$ , is defined as

$$N = \begin{bmatrix} s & -s \\ -s & s \end{bmatrix} + j\omega \begin{bmatrix} d & -d \\ -d & d \end{bmatrix} - \omega^2 \begin{bmatrix} m_1 & 0 \\ 0 & m_2 \end{bmatrix} \quad (22.3)$$

The stiffness and damping of the cavity are described by  $s$  and  $d$ , whereas the masses of the inner and outer shells are defined by  $m_1$  and  $m_2$ .

From this matrix equation, the velocities,  $v_1$  and  $v_2$ , can simply be calculated as

$$v_1 = j\omega F_1 \frac{s + j\omega d - \omega^2 m_2}{\det(N)} \quad (22.4)$$

$$v_2 = j\omega F_1 \frac{s + j\omega d}{\det(N)} \quad (22.5)$$

which can be converted into drive point and transfer impedances dividing by the excitation force,  $F_1$ , respectively.

As the cavity “springs” (air, mineral wool, anchors) are all in parallel, their stiffness per area must be added, leading to a total stiffness of  $s''_{\text{tot}} = s''_{\text{air}} + s''_{\text{mineral}} + s''_{\text{anchor}}$ , with  $s''_{\text{air}} = \rho c^2/d = 1.2 \cdot 340^2/0.2 \text{ N/m}^3$ ,  $s''_{\text{mineral}} = 4.8 \times 10^6 \text{ N/m}^3$ , and  $s''_{\text{anchor}} = E_{\text{an}} \cdot n_{\text{an}} \cdot A_{\text{an}}/l_{\text{an}} = 2 \times 10^{11} \cdot 9 \cdot 2 \cdot \pi \cdot 2 \times 10^{-3} \cdot 0.21 \text{ MN/m}^3$ . Assuming the shells of the wall are limp masses, and neglecting the influence of damping, the resonance frequency of the mass-spring-mass system can be calculated as  $f_0 = 1/(2\pi)\sqrt{s(1/m_1 + 1/m_2)}$ . This means that if the wall had no anchors, the resonance frequency would be lower, as the total stiffness  $s''_{\text{tot}}$  would be lower. A lower resonance frequency is better for the sound insulation, as above it there is an improvement of the sound insulation (see Fig. 22.6). In other words, adding the anchors reduces the performance of the wall, yet they are needed to resist the wind loads. The sound reduction index of this simplified wall can be estimated by

$$R(\varphi) = 20 \log \left| \frac{\frac{z_w}{\cos \varphi} + 2z_p}{2z_p} \right| \quad (22.6)$$

with  $z_w$  being the impedance of the wall and  $z_p = \rho c$  the impedance of a plane wave. For purpose of simplification, a mean incident angle is selected ( $\varphi = 45$  deg) to simulate the outdoor (traffic) noise. The impedance of the single mass wall is  $z_{w1} = j\omega m$  and of the mass-spring-mass wall is  $z_{w12} = F_1/v_2 = \frac{1}{j\omega} \frac{\det(N)}{s+j\omega d}$  (see Eq. 22.5).

The theoretical improvement in sound reduction index by adding the outer shell is  $\Delta R = R(z_{w12}) - R(z_{w1})$ . The expected sound reduction index of the DW can be calculated by adding  $\Delta R$ , and the improvement due to the increase of the total mass ( $\Delta R_{\text{mass}} = 20 \log 10 ((m_{\text{IS}} + m_{\text{OS}})/m_{\text{IS}}) \approx 4 \text{ dB}$ ) to the sound reduction index of measured SW. This leads to the trend seen in the left graph of Fig. 22.6 (dashed line).

Note that the theoretical resonance frequency at 151 Hz (see dip in dashed line of left graph) is higher than measured and that the theoretical improvement with 40 dB/Oct is

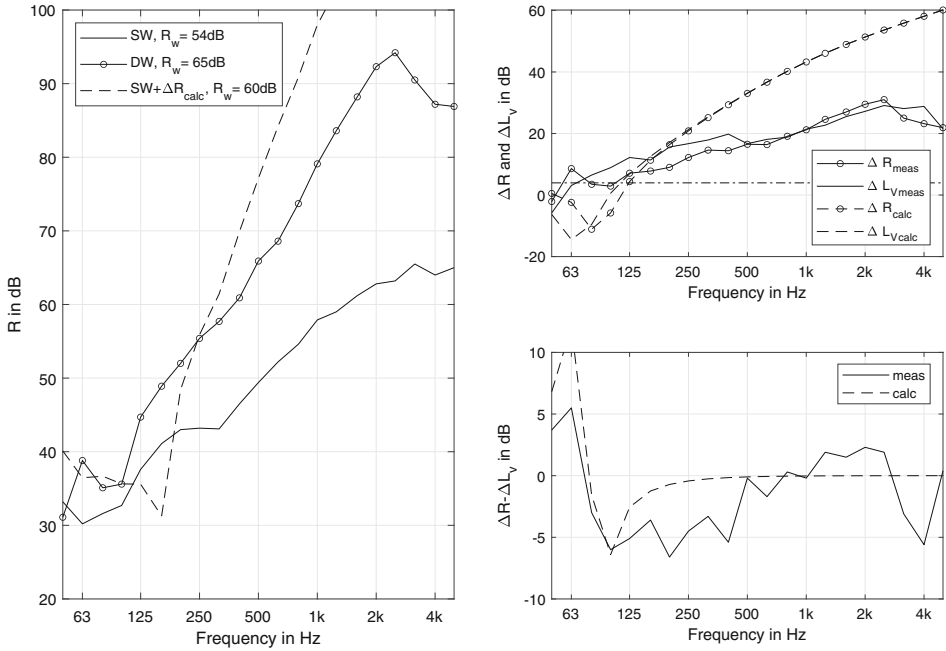


**Fig. 22.6** Left: Sound reduction index, R. Solid—measured, dashed—calculated/predicted from IS-measurement plus improvement from mass-spring-mass approach. Right-top: Improvement of R due to adding OS,  $\Delta R$ , and velocity level difference of both shells,  $\Delta L_v$ . Right-bottom: Difference between  $\Delta R$  and  $\Delta L_v$  for measured (solid) and calculated (dashed) cases

steeper than measured in the high frequencies due to the missing effect of structural bridging. Even though the slope is steeper adding the theoretical improvement, the single number rating is lower than the measured wall due to the resonance dip being too high. The reason for the excessively high resonance frequency is due to the fact that the stiffness of the plastic wall plugs, in which the anchors sit, was not considered.

To find the effective stiffness per area of the cavity including all effects, the velocity level ( $L_v$ ) difference between the IS and OS when exciting the IS was measured and simulated with the same mass-spring-mass system as described above (see right diagrams in Fig. 22.6). In the upper right graph, the measured and predicted improvement in sound reduction index,  $\Delta R$ , and the difference in velocity level,  $\Delta L_v$ , are shown. The predictions unfortunately do not coincide with the measurements. However, if the difference between the deltas  $\Delta R(\text{meas}) - \Delta L_v(\text{meas})$  and  $\Delta R(\text{calc}) - \Delta L_v(\text{calc})$  is calculated (lower right graph), it can be seen that the predicted and measured have the same trend and differ by less than 5 dB throughout the whole frequency range. Note that to achieve these close results, the theoretical effective stiffness per area was reduced to  $s''_{\text{tot}} \approx 37 \text{ MN/m}^3$ . This means that the plastic wall plugs have effectively reduced the  $s''_{\text{tot}}$  from  $113 \text{ MN/m}^3$  to a third and control the stiffness between the shells. As the wall plugs are situated in a different plane

than the other “springs,” the reciprocal of the total stiffness is the sum of the reciprocal stiffnesses, leading to a stiffness of the wall plugs of  $56 \text{ MN/m}^3$ . The total stiffness is lower than the smallest stiffness. Note that the mass-spring-mass resonance frequency thereby reduces from 151 to 87 Hz ( $f = 1/2/\pi\sqrt{s_{\text{tot}}'(1/m_1 + 1/m_2)}$ ).

Overall, it can be said that the OS increases the sound insulation from above 63 Hz starting at 4 dB due to the mass increase (dashed horizontal line). A steady improvement up to 20 dB is achieved until 500 Hz where the slope levels off due to structural bridging. The weighted sound reduction index calculated according to the standard increased by adding the OS  $R_w(\text{SW}) = 54 \text{ dB}$  to  $R_w(\text{DW}) = 65 \text{ dB}$ , a 10 dB increase. If the wall plugs could be made less stiff, a larger increase in sound reduction index would be expected.

### 22.3.2 Ventilator

The setup of the ventilator was already described earlier. In contrast to the wall, the improvement of sound insulation through modifications will be investigated regarding the sound reduction index of small elements using  $D_{n,e}$  instead of R, yet also according to DIN EN ISO 10140-2 (2020).

The dashed-dotted line in Fig. 22.7 depicts the sound insulation of the test wall without a ventilator and hole. The sound insulation drops drastically by incorporating the ventilator, especially around the tube resonance frequency (approximately 250–315 Hz) determined earlier. During times when no ventilation is needed, the tube can be closed upon which the sound insulation increases by approximately 10–15 dB. The improvement due to adding the perforation to the tube, as described earlier, can be seen in the right graph. Unlike the reduction in sound power due to the perforation, the sound insulation also improves at higher frequencies by approximately 2–3 dB. The perforation leads to a similar magnitude in improvement if the tube is open or closed. However, when closed a new peak is introduced at lower frequencies. This supports the earlier assumption that tube modes have the most influence on the radiation and insulation properties. If one side of the tube is closed, the tube acts more like a 1/4 wavelength resonator than a 1/2 wavelength resonator increasing the wavelength at the resonance and reducing its frequency. At these resonance frequencies, the particle velocity at the perforated end has a maximum, whereby through friction much sound energy is transformed to thermal energy increasing the sound insulation.

Comparing the reduction of radiated sound power, one can see that the highest improvement of both is around as much as the first and second resonance frequency of the tube between 250 and 500 Hz.



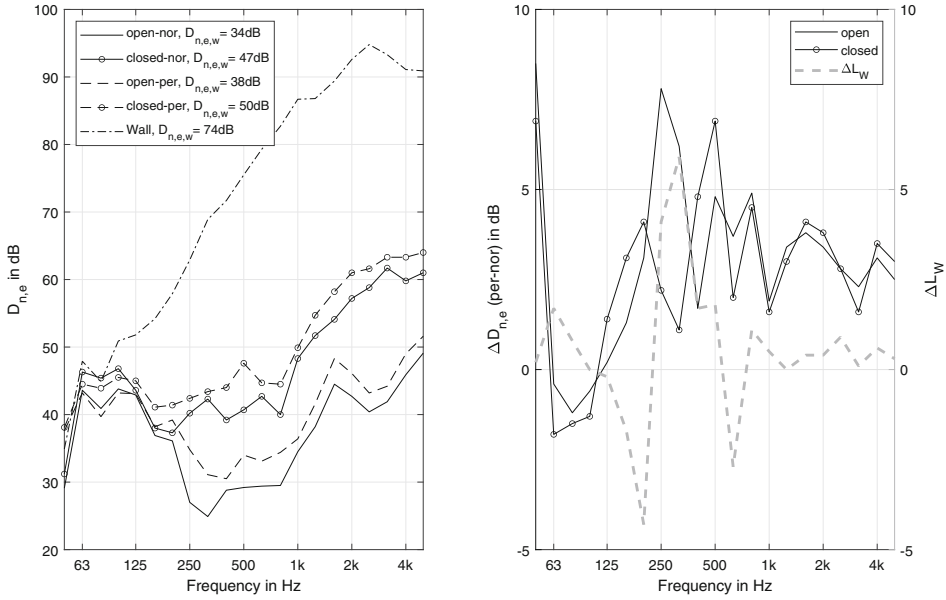


**Fig. 22.7** Left: Sound reduction index of small elements,  $D_n$ . Solid–normal (nor), dashed–perforated (per), o–closed, no marker–open. Right: Improvement due to adding perforation for  $D_n$ , (left axis) and  $L_w$  (right axis)

### 22.3.3 Window

Two different box-type windows were investigated in this iCity project. One was placed in a real office room and studied regarding natural ventilation (Chap. 21) and sound insulation. The other, installed in the acoustic facilities, with a depth of 0.15 m, a height of 1.312 m, and a width of 1.062 m, is discussed in this chapter (see Fig. 22.8) with the focus on sound insulation. A box-type window, such as the “Hamburger Hafencity Fenster,” was chosen because of its high sound insulation in the closed state. It was also chosen to warrant an increased sound insulation when tilted by making the sound enter the one side, in this measurement setup at the top of the box-type window, and travel through the height of the window, before exiting on the bottom half of the other side. For the presented data, the width of opening gaps (upper left and lower right) was always the same (0 mm, 20 mm, 40 mm, or 60 mm).

The measured weighted sound reduction index of the closed window is  $R_w = 51$  dB. However, when tilted open for natural ventilation, the sound reduction reduced to  $R_w = 21$  dB or 24 dB depending on the gap width of the openings (here 60 mm and 20 mm, respectively). The sound reduction index,  $R$ , of the non-treated window can be seen in the left graph of Fig. 22.9. The case with the largest gap has the worst sound insulation. At very low frequencies, the decrease in  $R$  due to opening the windows is approximately 10 dB. The sound waves with very long wavelengths at those frequencies do not “see” the gap in the box-type window and still get reflected strongly. Between 80 and

**Fig. 22.8** Setup of box-type window with Helmholtz absorbers—black circles are openings

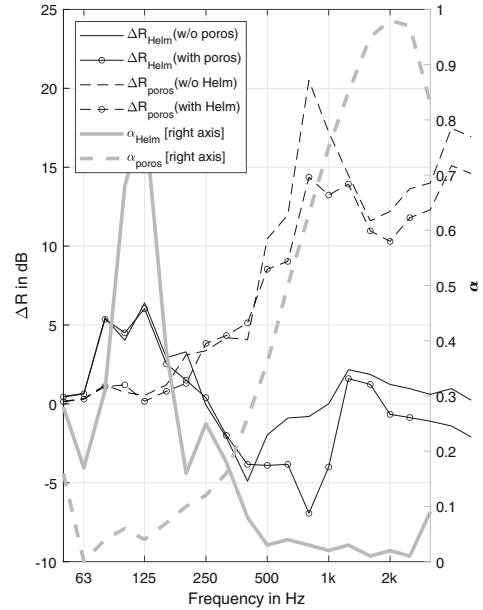
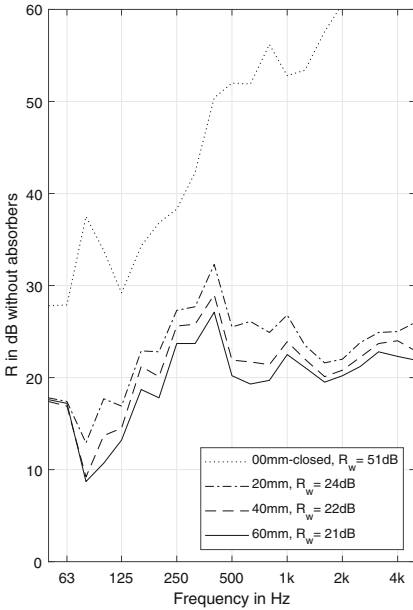


**Fig. 22.9** Left: Sound reduction index of the box-type window,  $R$ , with different gap widths. Right: Average improvement of  $R$  for all gap widths (left axis) and for absorption coefficient (gray–right axis) due to adding Helmholtz and porous absorbers

**Table 22.3** Weighted sound reduction index,  $R_w$ , in dB of windows with various opening gaps and absorber configurations

Gap width in mm	Without porous absorber		With porous absorber	
	Without Helmholtz	With Helmholtz	Without Helmholtz	With Helmholtz
00 (closed)	51	51	52	52
20	24	24	36	36
40	22	23	34	33
60	21	21	33	32

400 Hz, the decrease in  $R$  is approximately 15 dB, and  $R$  runs almost parallel to the case with the closed box-type window. Above 400 Hz, the wavelength gets in the range of the gap length (width of the box-type window), and  $R$  stays almost constant or independent of the frequency and the same amount of sound transmits through the box-type window.

In this project, two similar measures were taken to increase the sound insulation of the tilted box-type window at low and high frequencies by incorporating, first, Helmholtz absorbers (tuned to 125 Hz) and, second, porous absorbers of 40 mm thickness onto the top/bottom and both side window reveals, respectively. The weighted sound reduction index for all four cases (with and w/o Helmholtz absorber and with and w/o porous absorber) is listed for all of the four opening gaps in Table 22.3.

Note that the Helmholtz absorber has little influence on the single number value,  $R_w$ , which rises at most by 1 dB. The porous absorber also has little influence on  $R_w$  for the closed box-type window; however, a large influence of approximately 12 dB when the window is tilted open. The box-type window with a gap of 20 mm and with both Helmholtz and porous absorber has a quite high weighted sound reduction index of  $R_w = 36$  dB. The absorption coefficients of the two absorbers, measured in an impedance tube, can be seen in the right graph (right axis) of Fig. 22.9.

The Helmholtz absorber theoretically tuned to 125 Hz has its maximum of  $\alpha = 0.81$  at 125 Hz. The porous absorber reaches its maximum of  $\alpha = 0.98$  at about the frequency corresponding to a quarter wavelength  $f = c_0/(4 \cdot 0.04 \text{ m}) = 2125$  Hz, where  $c_0 = 340$  m/s is the propagation speed in air.

The Helmholtz absorber does have a larger influence when looking at the sound reduction index,  $R$ . The improvement of sound reduction index,  $\Delta R$ , can be seen in the right graph of Fig. 22.9. At the tuned frequency of 125 Hz, the improvement is approximately 5 dB for both, the case with and w/o porous absorber. At higher frequencies, however, there is a negative improvement with a negative peak at 400 Hz and 800 Hz depending on w/o or with porous absorber, respectively. This suggests that the improvement is not only due to the absorption of sound, but also that the impedance of the box-type window reveals changes now allowing more sound to pass. The worsening of  $R$  at higher frequencies due to the Helmholtz absorber is higher with the additional porous absorber in place. Hence, the improvement of  $R$  due to the porous absorber increases toward higher frequencies as expected.

The improvement for duct acoustics predicted according to Piening found in Möser (2009) and VDI 2081 (2019) is quite a bit lower than measured. Assuming the duct has the full width of the box-type window and the absorbers cover the reveal of the full height of the window, the maximum reduction for the porous absorber is 3.5 dB at 2000 Hz and for the Helmholtz absorber is 2.9 dB at 125 Hz. These values are lower than measured, because Piening only captures the losses along the duct walls and not at the openings at which absorbers are also implemented in these windows. In Fig. 22.9, one can see that the frequency ranges of improvement and high absorption coefficient coincide quite well. At higher frequencies, the improvement due to the porous absorbers declines when half a wavelength fits in the duct depth ( $f_{\text{ray}} = c_0/(0.15 \text{ m}/2) = 1133 \text{ Hz}$ ) due to the sound then traveling more focused as a ray.

## 22.4 Indoor Levels

As the indoor sound pressure levels from the ventilator and traffic sources are dependent on the volume of the room, the equivalent absorption area therein, and the areas of the different facade elements, a facade-room scenario was chosen to allow the comparison between them. As a further simplification, the receiving room will be assumed to have a diffuse sound field (Fig. 22.10).

- Facade width  $w = 5 \text{ m}$ .
- Facade height  $h = 2.5 \text{ m}$
- Facade area  $S = 12.5 \text{ m}^2$
- Ventilator  $S_{\text{vent}} = 0.02 \text{ m}^2$
- Window  $S_{\text{wind}} = 1.56 \text{ m}^2$
- Wall  $S_{\text{wall}} = 10.92 \text{ m}^2$



**Fig. 22.10** Sketch of facade scenario. Wall: dark gray, window: medium gray, ventilator: light gray

- Room depth  $d = 4$  m
- Room volume  $V = 50$  m<sup>3</sup>
- Reverberation time  $T = 0.5$  s (common value for living spaces)

The equivalent absorption area,  $A$ , can be calculated according to Sabine as  $A = 0.163 \cdot V/T = 16.3$  m<sup>2</sup>.

### 22.4.1 Sound Transmission Through Single Elements and Ventilator Levels

As a first step, the element sound reduction index,  $D_{n,e}$ , is converted into a sound reduction index as follows:  $R = D_{n,e} + 10 \log(S_{\text{vent}}/A)$ . Furthermore, the sound reduction indices will be normalized to the chosen scenario by  $R_{i,\text{area}} = R - 10 \log(S_i/S_{\text{tot}})$ . The indoor levels produced by the traffic noise source  $j$  through facade element  $i$  are then approximated by  $L_{ij} = L_{p,j} - R_{i,\text{area}} + 10 \log(S_{\text{tot}}/A)$ , where  $L_{p,j}$  is the level of the source  $j$  measured in front of the facade and  $R_{i,\text{area}}$  is the area of normalized sound reduction index of the facade element  $i$ .

The noise from the ventilation at different speeds and for different modifications can be calculated as  $L_p = L_W - 10 \log(A) - 6$  dB which is also shown in Table 22.4. For a selected set of elements, it can be seen in Fig. 22.11 that the A-weighted indoor levels lie between 10 and 60 dB(A) depending on the facade element (wall, vent, wind) and the traffic source, or they are dependent on the ventilator speed. As the direction of ventilation has little effect on the levels, only levels of inward ventilation are presented.

The WHO-Europe World Health Organization (2018) recommends levels below 40 dB (A) to ensure a healthy night's sleep. Higher levels can cause the occupant to awake constantly, which could lead to a health hazard.

As expected, the indoor dB(A) levels through the wall and through the closed box-type windows are the lowest. More interesting is the fact that the order of loudest to quietest source changes depending on which element the sound transmits through. Outdoors, the sources showed the following order from loudest to quietest:

**Table 22.4** Indoor sound pressure levels,  $L_p$ , of ventilator in dB(A) for normal (nor) and perforated (per) tube for both operating directions outward (out) and inward (in)

Tube type	Airflow rate in m <sup>3</sup> /h	Outward direction	Inward direction
Normal	45	46.9	46.4
	32	40.1	38.1
	15	25.5	26.6
Perforated	45	45.0	44.4
	32	38.0	36.1
	15	23.1	24.8

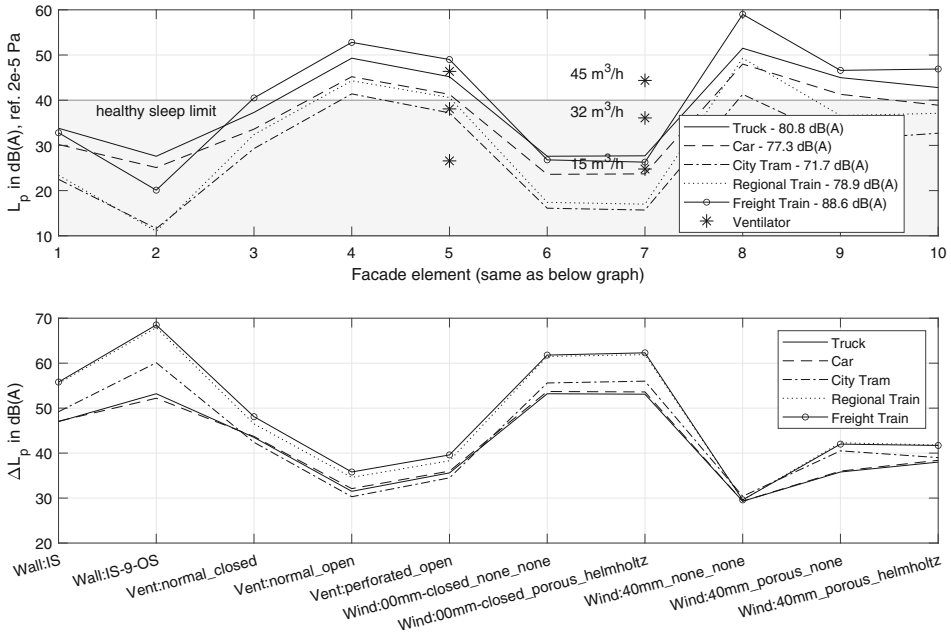


**Fig. 22.11** Top: A-weighted indoor sound levels from ventilator and traffic sources through selected facade elements according to facade and room configuration. Bottom: Reduction of A-weighted levels from outdoor to indoor due to facade elements

1. Freight Train–88.6 dB(A).
2. Truck–80.8 dB(A).
3. Regional Train–78.9 dB(A).
4. Car–77.3 dB(A).
5. City Tram–71.7 dB(A).

Yet, going through the wall (with nine anchors and an outer shell), for example, the order changes to:

1. Truck–27.6 dB(A).
2. Car–25.1 dB(A).
3. Freight Train–20.1 dB(A).
4. City Tram–11.6 dB(A).
5. Regional Train–11.0 dB(A).

This is due to the spectra of the sources and the sound insulation of the elements. The Freight Train level falling from first to third place is because the source has high levels between 1 and 2k Hz (see Fig. 22.1), which are highly attenuated by the wall with an outer shell (see Fig. 22.6).

The dB(A) level of the Car on the other hand is not very strongly attenuated by the wall with the outer shell, because its spectrum has a strong low frequency content (see Fig. 22.1) around the dip in sound insulation of the wall at the mass-spring-mass resonance (see Fig. 22.6), meaning those important frequencies are not reduced.

Furthermore, the top graph in Fig. 22.11 shows that the open windows, even after modifications, lead to the highest indoor levels. It can also be seen that the ventilator produces levels that are lower than all the transportation noises transmitted through the ventilator itself when running with a flow rate below 32 m<sup>3</sup>/h. The transmitted Freight Train noise is even louder than the ventilator at a flow rate of 45 m<sup>3</sup>/h. The ventilator at the middle flow rate produces levels similar to the transmission of the Tram.

To understand the reduction of A-weighted levels due to the facade better, the difference between the out- and indoor levels are plotted for the same element-source pairs in the lower graph of Fig. 22.11. As it was noticed in the upper graph of absolute levels, the wall and closed box-type window achieve the highest reduction in levels of around 60 dB. This corresponds to a subjective perception of  $1/64 = 1/2^{60\text{dB}/10}$  as loud. Again, the reduction depends largely on the spectra of noise source and sound reduction index of the element.

It can be seen that the spread of indoor levels between the different traffic sources is largest for the wall ( $\approx 15$  dB), lower for the closed box-type window ( $\approx 10$  dB), and smallest for the ventilator and open box-type window ( $\approx 5$  dB). The wall shows the largest reduction,  $\Delta L_p$ , for the trains, because the sources have strong higher frequency components, which are strongly attenuated by the wall. The Car and Truck show the lowest reduction by the wall due to the low sound reduction index of the wall at low frequencies and the high levels of the sources at low frequencies. This order of spread can be seen for the other facade elements as well. Adding the Helmholtz resonators to the open box-type window leads to an improvement for the Car and Truck sources, with their low frequency content, and leads to a worsening for the City Tram, because adding the Helmholtz absorber reduced the sound insulation at high frequencies (9), where the City Tram has high levels.

Seeing all this different behavior begs the question, if the weighted sound reduction index, which does not consider the different source spectra, is the proper measure to use for a facade. Please note that this is not a new finding, but has been investigated by many already and is captured, for example, as spectrum adaption terms in the standard DIN EN ISO 717-1 (2019).

## 22.4.2 Which Single Number Value Best Represents dB(A) Reduction?

For this same reason, different single number values (SNV) have been developed, some called spectral adaption terms, which as the name says, make corrections according to the assumed source spectra. Many such SNV have been developed over the years, some through subjective studies as in Hongisto et al. (2018), in which subjects are played back recordings of outdoor noise transmitted to the indoors and asked to rank the signals relative

to their annoyance. As this type of study is out of the scope of this research, it is assumed that the A-weighted indoor levels sufficiently correlate with the human perception of annoyance and comparisons are made between the reduction of A-weighted sound level,  $\Delta L$ , from outdoors to indoors and a selected five of the standard SNV as they exist in DIN EN ISO 717-1 (2019) ( $R_w$ ,  $R_w + C$ ,  $R_w + C_{tr}$ ,  $R_w + C_{50-3150}$ ,  $R_w + C_{tr50-3150}$ ). The latter two will for short be named  $R_w + C_{50}$ ,  $R_w + C_{tr50}$ .

The spectrum adaptation terms  $C$ ,  $C_{tr}$  go from 100 Hz to 3150 Hz in one-third octave bands and put more emphasis on the lower frequencies. The terms with the added 50 Hz do the same, however also considering sounds one octave lower down to the 50 Hz band.

The procedure to calculate the spectrum adaption terms is the same as explained in Sect. 22.4.1, yet now the A-weighted source levels are normalized to zero dB(A) meaning the A-weighted indoor levels and the A-weighted level reductions are the same. Furthermore, the room scenario for the adaption terms is nonexistent, or in other words, the assumption is made that the element surface,  $S_i$ , is the same as the equivalent absorption area in the room,  $A$ . These differences in the calculation methods mean that compared with the level reduction calculated here, there would be an offset even if the same source spectra in both cases would be used.

So, the question addressed here is, which SNVs are most representative to describe the reduction in A-weighted outdoor to indoor levels ( $\Delta L_p$ ) in these studies, with these spectra and these facade elements, and do they coincide with those suggested in the standards? The most appropriate SNVs to use for different traffic situations would be the ones that show the least variation relative to  $\Delta L_p$ . For example, Meier (2021) suggests to use  $R+C$  for outdoor noise and traffic noise outside of built-up areas and  $R+C_{tr}$  within built-up areas.

To give an idea of the variation between the different SNVs, a subset of the elements and sources are displayed in Fig. 22.12. The standard deviations listed in the legend are calculated for all elements presented earlier ( $2 \times$  Walls,  $4 \times$  Vents,  $16 \times$  Windows). This means that because there were many more open box-type window cases, those are weighted more than, for example, the walls. Yet, this is found to be acceptable, because most facades incorporate a window, which often delivers the lowest reduction of A-weighted levels and thereby controls the overall insulation. In the future, it might be more appropriate to select multiple facade variants with different types and sized elements and compare the SNV of the overall sound reduction with the indoor levels on whole  $\Delta SNV = SNV - \Delta L$ .

As mentioned earlier, an offset is expected due to the added room and facade assumptions in this study, meaning that the mean value is not as representative as the standard deviation. As expected, the variation of  $\Delta SNV$  is the largest for the wall with the outer shell regarding both displayed sources. The standard deviations can be found in all sources and SNVs in Table 22.5. For the selected scenarios, the table suggests that  $R_w + C_{50}$  is best suited for the Truck,  $R_w + C_{tr}$  for the Car and Regional Train,  $R_w$  for the City Tram, and  $R_w + C$  for the Freight Train. This would correlate with the normative recommendation, suggesting the use of  $R_w + C$  for the Freight Train and  $R_w + C_{tr}$  for the Car and Truck. The latter only if going down to 50 Hz was not an option.



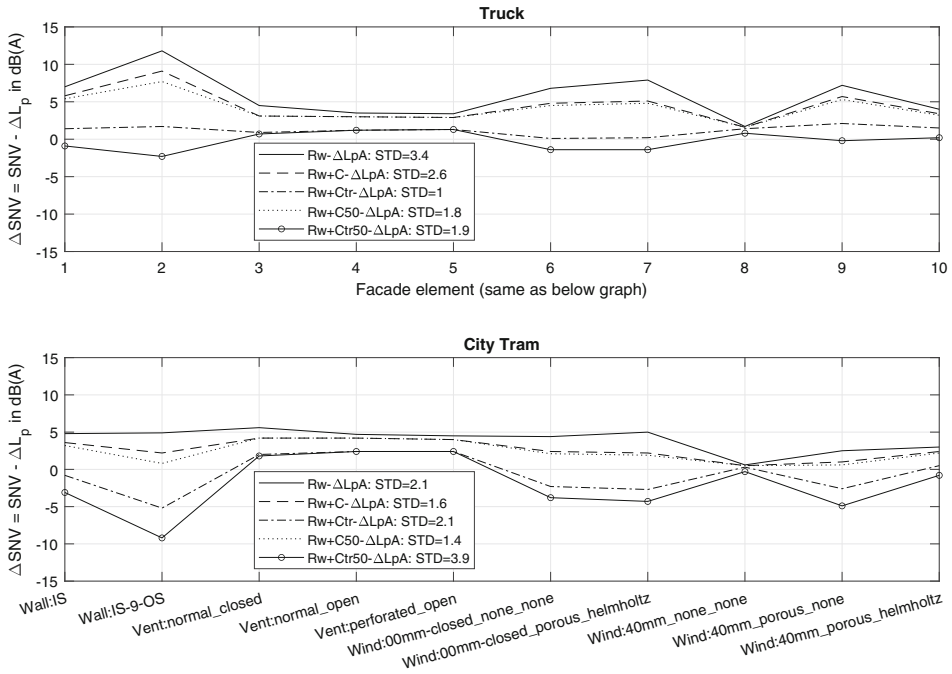


**Fig. 22.12**  $\Delta$ SNV: Difference between single number values (SNV) and A-weighted reduction of sound levels  $\Delta L_p$  for three sources (Truck, Car, and City Tram). Dashed line is mean value and standard deviation is in respective legend

**Table 22.5** Standard deviation of  $\Delta$ SNV: Difference between single number values (rows) and A-weighted reduction of sound levels from outdoors to indoors for all sources (columns)

	$R_w$	$R_w + C$	$R_w + C_{Tr}$	$R_w + C_{50}$	$R_w + C_{Tr50}$
Truck	3.4	4.2	2.1	1.5	1.6
Car	2.6	3.5	1.6	2.1	2.2
City Tram	1.0	1.9	2.1	4.2	4.3
Regional Train	1.8	2.5	1.4	2.5	2.6
Freight Train	1.9	1.1	3.9	5.8	6.0

If only one SNV should be suggested to be used for the rail vehicles, this study would recommend  $R_w$ . One SNV for the Trucks and Cars could be either of these

$$R_w + C_{Tr}, R_w + C_{50}, \text{ or } R_w + C_{Tr50}.$$

## 22.5 Conclusion and Outlook

Within the framework of the iCity research project, the sound insulation of several facade elements was improved by passive means. The weighted sound reduction index of the wall, for example, was improved by 11 dB through adding an outer shell to the inner shell. More importantly, the effective stiffness of attachment anchors was estimated indirectly through vibration and sound insulation measurements, thereby revealing more potential for further improving the walls.

The sound reduction and weighted sound reduction index of the ventilator was improved by 7 dB in one-third octave bands and by 3 dB, respectively, through the simple addition of perforation on the last section of the ventilator tube.

The sound reduction index and weighted sound reduction index of the open box-type window was improved by 6 dB and 1 dB, respectively, by adding Helmholtz absorbers in the box-type window reveals and by 15 dB to 12 dB, respectively, by adding a porous absorber. As shown by others, it was confirmed that the A-weighted indoor levels greatly depend on the spectra of the noise source levels and of the sound reduction index of the facade elements. Although the weighted sound reduction index by adding the Helmholtz absorber only increased by 1 dB, the indoor levels decreased by 3 dB for the Car and Truck sources. The indoor noise level created by the self-noise of the ventilator in the chosen “standard” room was of a similar magnitude as the traffic noise transmitted through it for the medium and high airflow settings.

A multidimensional calculation showed that there exist no correct single number values (SNV) that can be utilized for all scenarios. Even the two SNVs suggested in the standards were not necessarily the best for these noise source-facade element scenarios.

A possible way forward could be to better capture the actual source spectra outdoors for specific areas, for example, through citizen science noise sensors (<https://luftdaten.info/einfuehrung-zum-laermsensor/>), and then select the suitable facade elements to optimize for the overall indoor level in that area.

---

## References

- DIN 45642 (2004). Measurement of traffic noise.
- DIN 45681 (2005). Acoustics – Determination of tonal components of noise and determination of a tone adjustment for the assessment of noise immissions.
- DIN EN 1793-3 (1997). Road traffic noise reducing devices - Test method for determining the acoustic performance - Part 1: Intrinsic characteristics of sound absorption under diffuse sound field conditions.
- DIN EN ISO 10140-2 (2020). Acoustics – Laboratory measurement of sound insulation of building elements - Part 2: Measurement of airborne sound insulation.
- DIN EN ISO 3743-1 (2010). Acoustics - Determination of sound power levels and sound energy levels of noise sources using sound pressure - Engineering methods for small, movable sources in reverberant fields - Part 1: Comparison method for a hard-walled test room.

- DIN EN ISO 717-1 (2019). Acoustics - Rating of sound insulation in buildings and of building elements - Part 1: Airborne sound insulation (iso/dis 717-1:2019).
- Drechsler, A. and Ruff, A. (2017). Schalleistung von Wohnungslüftungsgeräten - Anwendung verschiedener Messmethoden. In Tagungsband DAGA - 43. Jahrestagung für Akustik.
- Hongisto, V., Oliva, D., and Rekola, L. (2018). Subjective and objective rating of the sound insulation of residential building facades against road traffic noise. JASA.
- Meier, A. (2021). Forschungsvorhaben Schallschutz gegen Außenlärm - Anforderungen zum baulichen Schallschutz gegen Außenlärm nach DIN 4109 unter Berücksichtigung des derzeitigen Stands der Technik als Grundlage für bauaufsichtliche Regelungen.
- Möser, M. (2009). Engineering Acoustics - An introduction to noise control. Springer.
- Pietruschka, D., Varga, E., Drechsler, A., Marin, R., Eicker, U., and Fischer, H.-M. (2011). Energetische und akustische Sanierung von Wohngebäuden – Vom Altbau zum akustisch optimierten Passivhaus.
- Ruff, A., Drechsler, A., and Zeitler, B. (2020). Untersuchungen zur Schalleistung und -dämmung eines dezentralen Lüftungsgerätes. In DEGA, Tagungsband DAGA - 46. Jahrestagung für Akustik.
- Schneider, M., Ruff, A., and Zeitler, B. (2018). Sound insulation of double masonry exterior walls. In Euronoise, Proceedings of 11th European Congress and Exposition on Noise Control Engineering.
- VDI 2081 (2019). Air-conditioning - Noise generation and noise reduction.
- World Health Organization (2018). WHO environmental noise guidelines for the European region.

**Open Access** This chapter is licensed under the terms of the Creative Commons Attribution 4.0 International License (<http://creativecommons.org/licenses/by/4.0/>), which permits use, sharing, adaptation, distribution and reproduction in any medium or format, as long as you give appropriate credit to the original author(s) and the source, provide a link to the Creative Commons license and indicate if changes were made.

The images or other third party material in this chapter are included in the chapter's Creative Commons license, unless indicated otherwise in a credit line to the material. If material is not included in the chapter's Creative Commons license and your intended use is not permitted by statutory regulation or exceeds the permitted use, you will need to obtain permission directly from the copyright holder.





# Impact Sound Insulation of Thermally Insulated Balconies

# 23

Lucas Heidemann, Jochen Scheck, and Berndt Zeitler

## Abstract

With the increasing urban densification, balconies are gaining in popularity as they improve the living quality in homes. From a technical point of view, the thermal insulation between balconies and the building's façade is state of the art. In Germany, the most popular balcony construction is a reinforced concrete balcony, separated from the building by a thermal insulation element (TIE), which is meant to reduce the thermal energy loss and thus ensure the sustainability of intelligent buildings. The impact sound transmission from balconies, however, is a problem that has not been addressed enough to date. The paper is based on a project of the same name within the iCity research with the main goal of providing acoustic quantities, e.g. an impact sound pressure level difference, for a TIE that can be used to compare the acoustical quality of products and used to predict the impact sound pressure levels within the building using the standard EN ISO 12354-2. Experimental and numerical studies have been carried out on various ceiling-balcony mock-ups without and with TIEs, e.g. by means of experimental modal analysis and validated finite element models, respectively. These studies showed that even doubling the width of the ceiling-balcony mock-up does not change the results significantly, suggesting that the proposed test set-up is suitable for standard testing. The analysis method and results presented here are for only one test set-up with and without a TIE that underwent constructive modifications during the tests.

---

L. Heidemann (✉) · J. Scheck  
Hochschule für Technik Stuttgart, Stuttgart, Germany  
e-mail: [lucas.heidemann@hft-stuttgart.de](mailto:lucas.heidemann@hft-stuttgart.de)

B. Zeitler  
Institute for Applied Research, University of Applied Sciences Stuttgart, Stuttgart,  
Baden-Württemberg, Germany

The selected TIE shows an effective sound insulation above 400 Hz and achieves a single-number rated impact sound level difference of  $\Delta L_w^* \approx 10$  dB.

---

**Keywords**

Impact sound · Sound insulation · Thermally insulated balconies

---

## 23.1 Introduction

The increase in airborne sound insulation against outdoor noise, achieved by the development of higher quality walls and windows, leads to an increased sensitivity of the inhabitants against noise that is generated by neighbours. This is because the noise levels from the neighbours now emerge above the therefore lower level noise floor from the outdoors. Furthermore, outside areas of flats, such as balconies, are gaining in popularity, leading to more impact sound transmission, which can cause disturbances. These two points were taken into account in 2018, when the German standard of requirements on sound insulation in buildings (DIN 4109:2018-01, 2018) was revised. This standard now contains requirements for balconies on the normalized impact sound pressure level as  $L'_{n,w} \leq 58$  dB. For loggias that are often difficult to differentiate from balconies in modern buildings, the requirement is  $L'_{n,w} \leq 50$  dB. As  $L'_{n,w}$  quantifies the sound pressure level measured in the room when the ceiling or balcony is excited by a standardized tapping machine (Figs. 23.1 and 23.3), a lower level of  $L'_{n,w}$  means better protection from impact noise (e.g. a typical reinforced concrete ceiling without and with a floating floor has levels  $L'_{n,w}$  of around 70 dB and 46 dB, respectively).

In Germany, the most popular balcony construction is a reinforced concrete balcony, separated from the building by a thermal insulation element (TIE) meant to reduce the thermal energy loss. The design of the TIE is primarily based on static requirements. The elements consist of reinforced bars and thrust bearings, sheeted by thermally insulating material like extruded polystyrene. The main goal of the iCity project that is the basis of this paper was to provide characteristic acoustic values for a TIE that can be used for product comparison and used to predict the sound transmission in buildings. A first step to achieve this is to, through measurement and numerical investigations, understand the structure-borne sound transmission through these TIEs.

A not yet fully validated method, suggested by (Blessing, 2018), is to predict the impact sound transmission of balconies in the same fashion as currently done for floors, namely, according to Part 2 of the German standard (DIN 4109:2018-01, 2018) that uses single-number values (in contrast to frequency-dependent values). Yet, currently no standardized laboratory test procedure exists, to determine the “input value”. In other words, the characteristic acoustic values of TIE still need to be defined. The testing procedure shall also provide values for a frequency-dependent prediction following the European standard for building acoustics (EN ISO 12354-2:2017-11, 2017). This chapter describes how this task was tackled and how an approach was developed to predict the impact sound transmission of balconies. Finally, it discusses results of measurements on one laboratory test set-up carried out within this project.

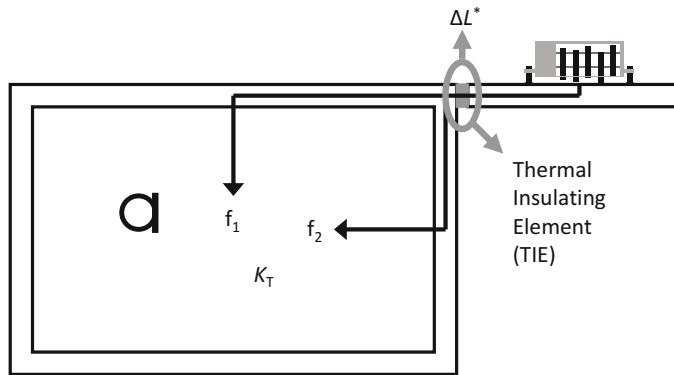


**Fig. 23.1** Diagonal impact sound transmission of a thermally insulated balcony into a receiving room of a neighbouring unit

## 23.2 Structure-Borne Sound Transmission in Buildings

For balconies, the most relevant requirements for impact or structure-borne sound transmission are along the diagonal path into an adjacent room of a second unit as shown in Fig. 23.1. If the balcony is not separated from the building using a TIE, it can be treated as a ceiling. The prediction can then be done according to (DIN 4109:2018-01, 2018), Part 2, taking into account a  $K_T$  value that describes the vibration reduction by the junction formed by ceiling and walls, e.g. with two flanking transmission paths  $f_1$  and  $f_2$  according to (EN ISO 12354-2:2017-11, 2017) from the exited balcony into the receiving room. A prediction with single-number values according to the German standard can be done using Eq. (23.1).

$$L'_{n,w} = L_{n,eq,0,w} - \Delta L_w^* - K_T + \mu_{prog} \text{ in dB} \quad (23.1)$$

with

$L'_{n,w}$  Weighted normalized impact sound pressure level for diagonal transmission

$L_{n,eq,0,w}$  Equivalent weighted normalized impact sound pressure level of the balcony for vertical transmission without flanking elements

$\Delta L_w^*$  Weighted impact sound level difference of the TIE

$K_T$  Correction value for diagonal transmission

$\mu_{prog}$  Safety coefficient;  $\mu_{prog} = 3$  dB for impact sound

The German standard (DIN 4109:2018-01, 2018) does not provide an explicit  $K_T$  value for a transfer situation involving a balcony as shown in Fig. 23.1. In (Blessing, 2018),  $K_T = 5$  dB was used for diagonal transmission from a floor to a room, but if this value is also suitable for balconies is yet to be shown. A lower value would be expected for

balconies, as often large window/door areas at balconies limit the amount of sound energy going into the wall with the windows, redirecting it to the ceiling and walls on the diagonal below. In other words, the large window/door thereby decreases the diagonal vibration reduction at the junction (described by  $K_T$ ) compared to a full heavy wall without window/door that has an assumed  $K_T = 5$  dB.

The quantity  $\Delta L^*$ , termed impact sound level difference, is chosen in analogy to the approach to describe isolating elements for staircases made of reinforced concrete in (DIN 7396:2016-06, 2016). Further information on the development of this method is given in (Maack, Möck, & Scheck, 2020) and (Fichtel & Scheck, 2013).  $\Delta L^*$  quantifies the increase of the impact sound reduction through the insulation element with reference to a rigid connection which describes an insertion loss notated by an asterisk \*. The challenge now is to devise a laboratory test procedure and evaluation that determines  $\Delta L^*$  as close to the real-world situation as possible.

---

### 23.3 Laboratory Test Set-up

In order to define a suitable laboratory test set-up and procedure, the transmission system “thermally insulated balcony” has to be understood thoroughly. Therefore, a laboratory test set-up has been built for experimental studies, consisting of a small ceiling and a thermally insulated balcony similar to test set-ups used by (Schneider & Fischer, 2008). The dimensions of the test set-up and the realization are shown in Figs. 23.2 and 23.3. The larger reinforced concrete slab represents the ceiling in a building and is supported on elastomer strips on two masonry walls. The mass spring system formed by the elastomer strips and balcony and ceiling has a resonance frequency of 25 Hz (Kluth, 2016). The smaller concrete slab represents the balcony. A laboratory set-up was built with a thickness of 18 cm, termed set-up 1a *without* TIE and set-up 1b *with* TIE.

---

### 23.4 Laboratory Test Procedure

The impact sound level difference is determined from velocity level measurements on the ceiling (Figs. 23.3 and 23.4). By Eq. (23.2) the radiated sound pressure level from the ceiling into an (imaginary) receiving room below the ceiling can be calculated.

$$L_p = L_v + 10 \log_{10} \sigma + 6 + 10 \log_{10} \frac{S}{A} \text{ in dB} \quad (23.2)$$

with

$L_p$  Sound pressure level in the receiving room

$L_v$  Spatially averaged velocity level on the ceiling (ref  $5e^{-8}$  m/s)

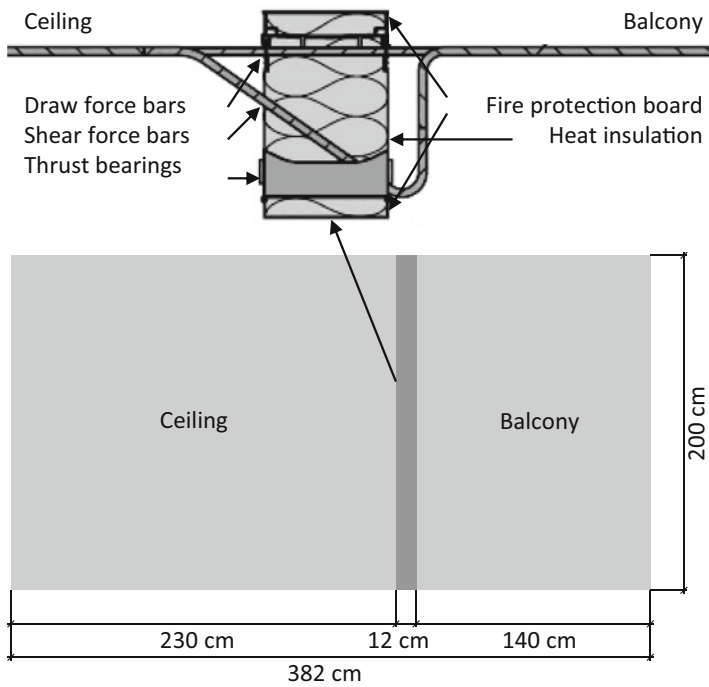


**Fig. 23.2** Dimensions of the laboratory test set-ups; dark grey bar depicts the TIE for set-up 1b with components

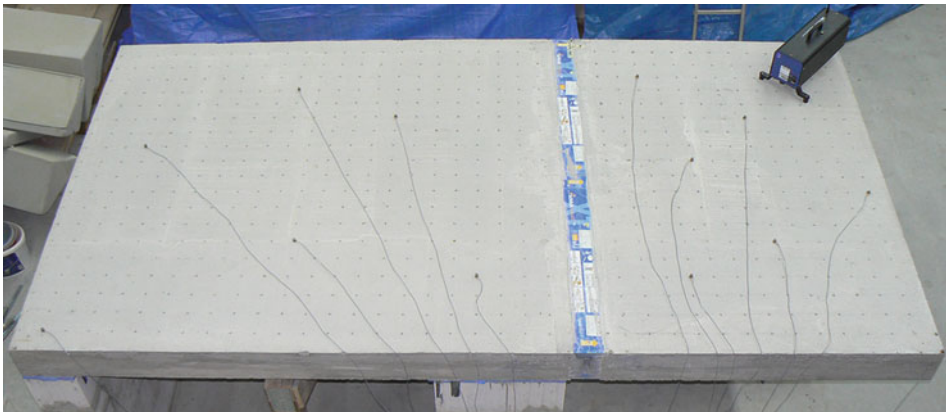


**Fig. 23.3** Laboratory test set-up 1b with ISO tapping machine on the reference excitation position and velocity level measurement positions for determination of the impact sound level difference of the TIE (only those on the ceiling required)



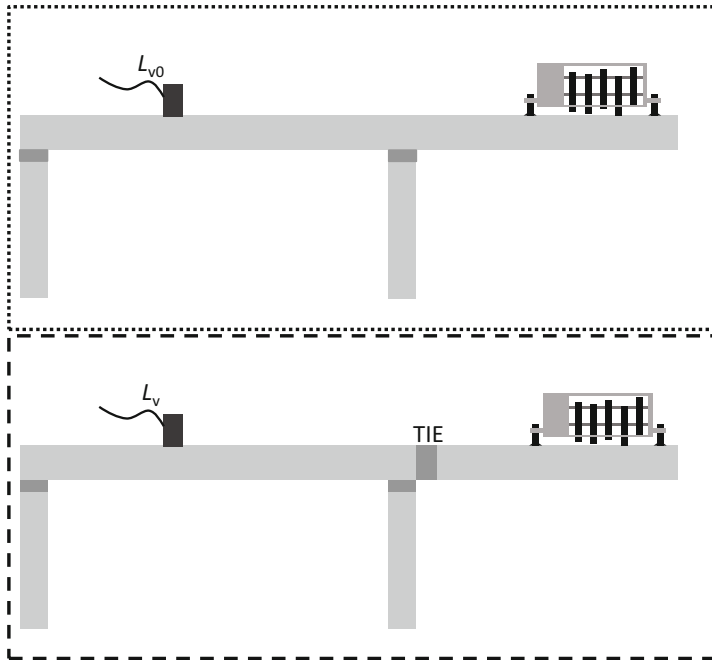


**Fig. 23.4** Side view of the test set-up 1a) without TIE (top) and test set-up 1b) with TIE (bottom)

- $\sigma$  Radiation efficiency; assumption  $\sigma = 1$
- $S$  Area of the ceiling
- $A$  Equivalent sound absorption area in the receiving room

A normalization to the reference absorption area  $A_0 = 10 \text{ m}^2$  results in the normalized impact sound pressure level from velocity level measurements according to Eq. (23.3).

$$L_{n,v} = L_v + 10 \log_{10} \sigma + 6 + 10 \log_{10} \frac{S}{A_0} \text{ in dB} \quad (23.3)$$

The determination of the impact sound level difference  $\Delta L^*$  of the TIE requires measurements on set-up 1a *without* TIE and on set-up 1b *with* TIE (Fig. 23.4).

$$\Delta L^* = L_{n0,v} - L_{n,v} \text{ in dB} \quad (23.4)$$

with

- $\Delta L^*$  Impact sound level difference of the TIE
- $L_{n0,v}$  Normalized impact sound pressure level without TIE
- $L_{n,v}$  Normalized impact sound pressure level with TIE

To determine the *weighted* impact sound level difference  $\Delta L_w^*$  as single-number rating, the procedure according to (DIN EN ISO 717-2:2013-06, 2013) can be used as it is already a standard for floor coverings and isolating elements for heavy stairs.

### 23.5 Experimental Modal Analysis

To analyse the vibration behaviour of the test set-up, an experimental modal analysis was carried out on both set-ups, with and without insulation elements. For the experimental modal analysis, the velocity at each point of interest is measured, while the structure is excited at a reference point with a controlled force signal. The ratio of velocity and force is termed mobility  $Y$ . The term input mobility  $Y_p$  denotes that the force and the velocity are measured at the same point. High mobility values mean that only a little force is necessary to cause a large velocity response and thus peaks in the mobility indicate a resonant behaviour.

The modal analysis can be carried out using the reciprocity principle, by mounting a reference accelerometer at a reference point while exciting every point of interest, e.g. with an impact hammer. This latter method was used here for measurement convenience, as this way only one instead of hundreds of accelerometers needs to be attached to the surface. When visualizing the vibration patterns, the reciprocity once again comes into play and the reference position of the accelerometer becomes the excitation position. The measurement grid with a grid spacing of 10 cm (Fig. 23.3) results in 819 excitation points with the impact hammer. The reference position of the accelerometer was in the corner of the balcony where the highest vibration amplitudes are expected. The input mobilities at the reference position are shown in Fig. 23.5 for set-up 1a (dotted) and set-up 1b (dashed). Examples of vibration shapes at the so-called eigenmodes or intrinsic modes are shown in Fig. 23.6. The

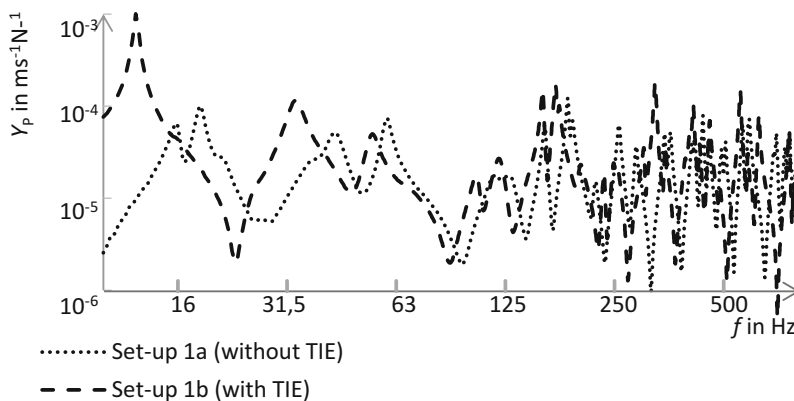


**Fig. 23.5** Input mobilities for set-up 1a and set-up 1b at the reference position for the experimental modal analysis in the corner of the balcony

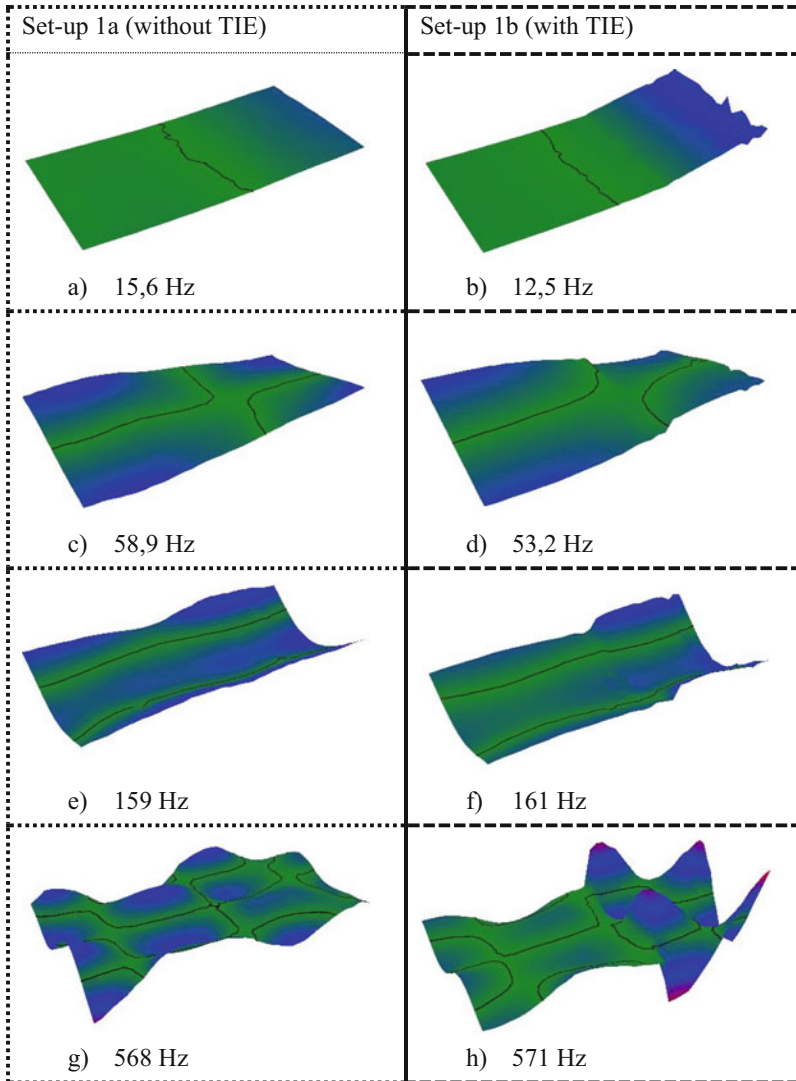


**Fig. 23.6** Vibration shapes of set-up 1a (left) and 1b (right) at selected frequencies

eigenmodes describe the vibration patterns of a system that can vibrate freely, without forced excitation.

The first eigenmode of set-up 1b where the balcony oscillates as a cantilever beam is at about 12 Hz and is determined by the torsion spring stiffness of the TIE and the mass of the balcony. Studies performed by (Kluth, 2016) showed that this vibration is well perceived by a person standing on the balcony and may result in discomfort. For set-up 1a, this problem is not observed as its first resonance is not so pronounced and the frequency is

higher. Investigations based on the finite element method (FEM) also showed that the decoupling of the ceiling and balcony from the masonry walls by the elastomer strips is not yet effective in this low frequency region. This effect was anticipated in the technical design to ensure the following two goals: (1) to be able to measure this cantilever beam vibration as it occurs in buildings in order to get insight into low frequency vibration problems and (2) to be able to measure the structure-borne sound transmission from balcony to ceiling in the common building acoustics frequency range from 50 to 5 kHz without influence of the supporting wall structure.

The vibrations above 50 Hz are dominated by bending modes of the plate(s). Without the TIE, the velocity level amplitudes on the balcony and on the ceiling differ by less than 2 dB. With the TIE, the balcony and the ceiling are effectively coupled in the frequency range from 50 to 400 Hz. Above 400 Hz, the vibration amplitudes on the excited balcony are significantly higher than on the ceiling. Here the TIE partially decouples the balcony from the ceiling.

### 23.6 Impact Sound Level Difference

The impact sound level difference  $\Delta L^*$  is determined from velocity level measurements at the same six positions on the ceiling for set-up 1a and set-up 1b. The ISO tapping machine is positioned diagonally with one hammer at a corner of the balcony (Fig. 23.3) to excite as many eigenmodes as possible and thus to simulate a worst case for the impact sound transmission from balcony to ceiling.

The normalized impact sound levels measured on the ceiling are shown in Fig. 23.7 in 1/3 octave bands from 50 to 5000 Hz. At lower frequencies, both levels with and without TIE follow the same trend with peaks and dips varying around 70 dB. Towards higher

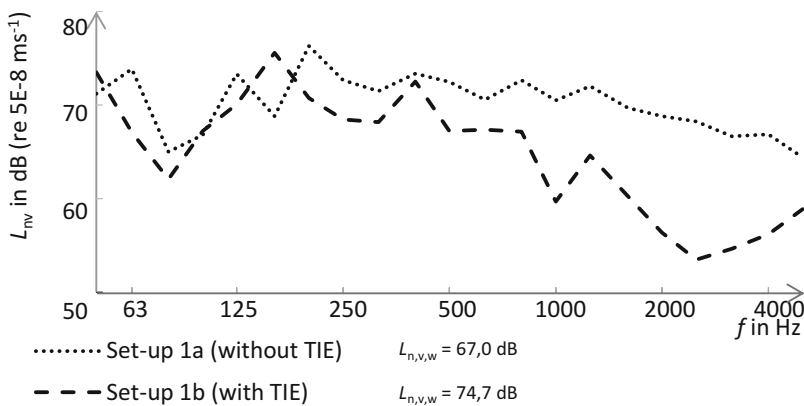


**Fig. 23.7** Normalized impact sound pressure level of set-up 1a and set-up 1b measured on the ceiling

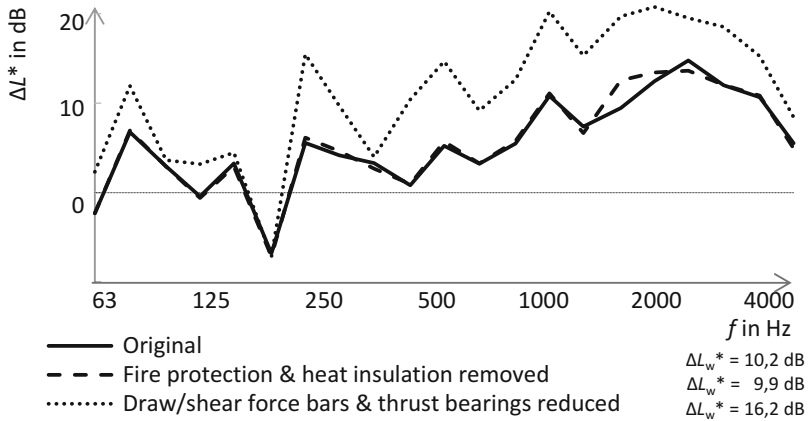


**Fig. 23.8** Impact sound level difference without and with modifications of the TIE

frequencies, they diverge and the levels with TIE sink to values below 60 dB. Figure 23.8 shows the impact sound level difference evaluated from the  $L'_{n,v}$  values shown in Figs. 23.7 and 23.4. As expected from the results of the modal analysis, an effective decoupling of the balcony by the TIE is only given above 400 Hz. Above 400 Hz,  $\Delta L^*$  first increases with frequency as it is typical for isolating elements but then reduces again above 2500 Hz. This is probably due to resonances inside the steel components (Fig. 23.2). The single-number rating of the TIE is  $\Delta L_w^* = 10.2$  dB.

## 23.7 Modification of the TIE

The investigated TIEs consist of statically indispensable tension and shear force bars, thrust bearings, foamed material for thermal insulation and fire protection boards (Fig. 23.2). The influence of each of these components on the impact sound transmission was investigated by modifications after the initial measurements. The fire protection, thermal insulation and load-bearing parts were removed gradually, and the impact sound level was measured for each modification step. After the last modification step, the TIE was reduced to a statically affordable minimum only leaving a few draw force bars, shear force bars and thrust bearings. The exposed area between ceiling and balcony was afterwards filled with concrete to obtain set-up 1a as it is shown in Fig. 23.4 (top). The effect of the fire protection boards and thermal insulation on the sound transmission is negligible. Reducing the tension bars by 67%, shear force bars by 60% and thrust bearings by 38% results in a significant increase of the impact sound level difference.

## 23.8 Finite Element Simulations

The main goal of the finite element simulations was to reduce the measurement effort needed to develop an appropriate laboratory test set-up for TIEs, in particular by defining the dimensions of balcony and ceiling elements. In a first step, the test set-up 1b was modelled in FE. The comparison between measured and simulated input mobility at the reference position at the corner of the balcony of set-up 1b is shown in Fig. 23.9. The agreement is very good in the whole frequency range. The measured and simulated vibration shapes were also drawn upon to further validate the FE simulation model.

In the next step, the velocity levels that result from excitation with the ISO tapping machine were simulated, and from this, the impact sound level reduction was calculated and evaluated. In Fig. 23.10, the impact sound level reduction is shown for set-up 1 as measured and simulated. The agreement across the whole frequency range is within  $\pm 5$  dB, which is similar to the variations in nominally the same buildings and therefore acceptable. Note that the single-number rating only varies by less than 1 dB. In addition, the neglectable influence of the dimensions of the balcony and ceiling elements can be seen in this figure, for which the width of the set-up (length of the TIE) was doubled in the simulation from 200 cm to 400 cm. Again, the agreement across the whole frequency range is within  $\pm 5$  dB, which indicates that the currently proposed set-up (Fig. 23.2) delivers suitable values to characterize TIEs for product labelling and for the prediction of the sound transmission in buildings. Note that the alteration of the FE element dimensions changes the single-number rating by less than 1.5 dB.

## 23.9 Conclusion

For the acoustical characterization of thermal insulation elements of balconies, a laboratory test set-up and method are proposed that can be used for product labelling and to predict the impact sound transmission in buildings. The quantity suggested, the weighted impact

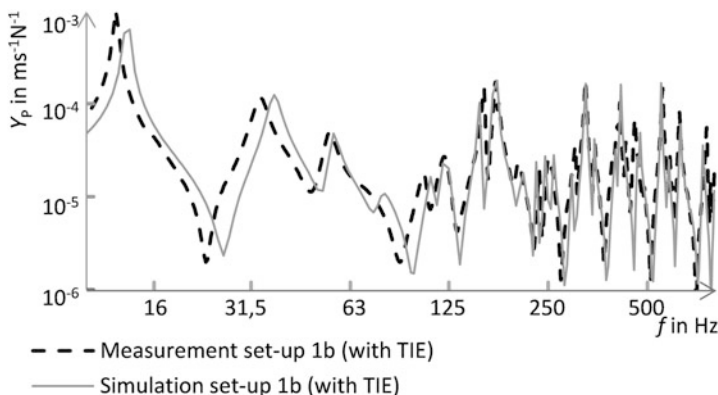


**Fig. 23.9** Input mobility of set-up 1b with TIE measured and simulated

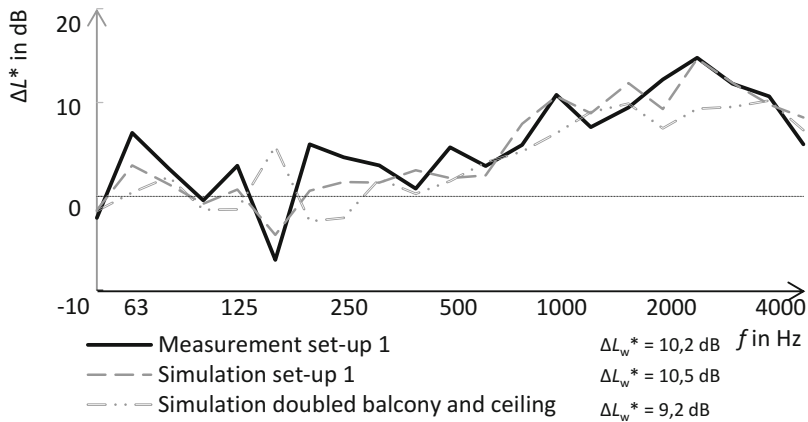


**Fig. 23.10** Impact sound level difference: Measurement and simulation of set-up 1 and simulation of a modified set-up 1 with doubled sizes of balcony, ceiling and TIE

sound level difference ( $\Delta L_w^*$ ), which for the tested TIEs is around  $\Delta L_w^* = 10$  dB, can be determined with velocity level measurements on the laboratory test set-up. For the investigated TIEs, a significant sound insulation between the balcony and the ceiling is observed in the frequency range above 400 Hz. Much trust is placed in the finite element simulations as the measured results on the laboratory test set-ups are in very good agreement with the finite element simulations. Therefore, various studies could be carried out with the FEM such as modifying the size of the laboratory test set-up. It was shown that doubling the width of the set-up (length of the TIE) from 200 cm to 400 cm has no significant effect on the simulated results of  $\Delta L_w^*$ —which is promising for the acceptance of the test set-up.

Further investigations, involving measurements and simulations on various TIEs and measurements in real building situations, will be carried out within the frame of the iCity project in order to further optimize the test set-up and measurement procedure regarding simplicity and accuracy. The building measurements will be used to ensure that the normative prediction models of structure-borne sound transmission in buildings deliver appropriate results with the here proposed “input data”  $\Delta L_w^*$ . Finally, the developed methods will be applied to optimize TIE products regarding the acoustical insulation properties.

## References

- Blessing, S. (2018). Balkone in der DIN 4109. *DAGA*. München.  
 DIN 4109:2018-01. (Januar 2018). Schallschutz im Hochbau. Berlin, Deutschland: Beuth Verlag GmbH.

- DIN 7396:2016-06. (2016). Bauakustische Prüfungen - Prüfverfahren zur akustischen Kennzeichnung von Entkopplungselementen für Massivtreppen. Berlin: Beuth Verlag GmbH.
- DIN EN ISO 717-2:2013-06. (2013). Akustik - Bewertung der Schalldämmung in Gebäuden und von Bauteilen - Teil 2: Trittschalldämmung. Berlin: Beuth Verlag GmbH.
- EN ISO 12354-2:2017-11. (2017). Bauakustik - Berechnung der akustischen Eigenschaften von Gebäuden aus den Bauteileigenschaften - Teil 2: Trittschalldämmung zwischen Räumen. Berlin: Beuth Verlag GmbH.
- Fichtel, C., & Scheck, J. (2013). Prediction of horizontally transmitted Sound from Impacted Lightweight Stairs - Part 2: Proposal for a Standard Test Procedure. *AIA-DAGA*. Meran.
- Kluth, M. S. (Juli 2016). Schwingungsverhalten von thermisch getrennten Balkonplatten. *Bachelorarbeit*. Deutschland: Bachelorarbeit HFT Stuttgart.
- Maack, J., Möck, T., & Scheck, J. (2020). Trittschallschutz. In *Bauphysik Kalender* (S. 235 - 313). Berlin: Ernst & Sohn.
- Schneider, M., & Fischer, H.-M. (2008). Vibration reduction of thermal break balcony connections. *Acoustics '08*. Paris.

**Open Access** This chapter is licensed under the terms of the Creative Commons Attribution 4.0 International License (<http://creativecommons.org/licenses/by/4.0/>), which permits use, sharing, adaptation, distribution and reproduction in any medium or format, as long as you give appropriate credit to the original author(s) and the source, provide a link to the Creative Commons license and indicate if changes were made.

The images or other third party material in this chapter are included in the chapter's Creative Commons license, unless indicated otherwise in a credit line to the material. If material is not included in the chapter's Creative Commons license and your intended use is not permitted by statutory regulation or exceeds the permitted use, you will need to obtain permission directly from the copyright holder.

